Lehrstuhl für Regelungstechnik

Technische Universität München

TECHNISCHE UNIVERSITÄT MÜNCHEN

Lehrstuhl für Regelungstechnik

Constructive Passivity-Based Control of Smooth and Switched Nonlinear Systems

Tobias Kloiber

Vollständiger Abdruck der von der Fakultät für Maschinenwesen der Technischen Universität München zur Erlangung des akademischen Grades eines

Doktor-Ingenieurs

genehmigten Dissertation.

Vorsitzender:	Univ.-Prof. dr. ir. Daniel J. Rixen
Prüfer der Dissertation:	1. Univ.-Prof. Dr.-Ing. habil. Boris Lohmann
	2. Univ.-Prof. Dr.techn. Andreas Kugi, Technische Universität Wien, Österreich

Die Dissertation wurde am 30.04.2014 bei der Technischen Universität München eingereicht und durch die Fakultät für Maschinenwesen am 07.10.2014 angenommen.

For my family.

Acknowledgments

First, I would like to deeply thank my supervisor Prof. Boris Lohmann for giving me the opportunity to join the institute of automatic control and for his support during all stages of this work. The confidence he has shown in me and the freedom he left me in doing my research have layed the foundation for the presented results.

I would like to express my deep gratitude towards Prof. Andreas Kugi for his interest in my work and for being the second examiner for this thesis. I also would like to thank Prof. Daniel J. Rixen for chairing the board of examiners.

I am deeply indebted to Dr. Paul Kotyczka, who is the leader of the energy based modeling and control group at the institute of automatic control, for introducing me to the field of passivity-based control and for his support during all my time at the institute.

Furthermore, I would like to thank my student Andreas Daasch for his valuable contribution to this work.

My deepest thanks go to my colleagues at the institute of automatic control, many of which are not only colleagues but friends. You have been the reason for the excellent atmosphere at the institute that has been a source of motivation and inspiration. I have very much appreciated the helpfulness of you all and I especially would like to deeply thank Sergio Delgado, Klaus Diepold, Dr. Oliver Fritsch, Dr. Heiko Panzer, Dr. Peter Philipp and Dr. Thomas Wolf for the fruitful discussions and constructive comments that have been indispensable for the success of my work. At this point, I also would like to sincerely thank Dr. Guido Koch, who has been the supervisor of my diploma thesis at the institute of automatic control, for introducing me to scientific research and for reinforcing my decision to pursue the doctoral degree. The quality and readability of this thesis has been considerably improved by the careful proofreading of Sergio Delgado, Klaus Diepold, Oliver Fritsch, Guido Koch, Paul Kotyczka and Thulasi Mylvaganam, which is gratefully acknowledged. At least as much as for the scientific discussions I thank you all for the conversations off the job. I have very much enjoyed the coffee and lunch breaks, the after-work beer, the barbecue parties and the evenings with red wine.

A very special acknowledgment goes to my family – especially to my parents Ingrid Kloiber and Konrad Bloier – for all their love, care and support throughout my years of

education and for always being there, when I needed them. Without you this would not have been possible. Special thanks also go to all my friends for their moral support and motivation.

Contents

List of Figures

Glossary

Frequently used mathematical notation

$\lceil \cdot \rceil$	ceiling function
$\mathcal{C}^k$	set of at least k-times continuously differentiable functions
$\frac{d}{dt}(\cdot) = \dot{(\cdot)}$	total time derivative
$\frac{d^k}{dt}(\cdot) = (\cdot)^{(k)}$	kth time derivative
$\nabla_x f(\mathbf{x})$	gradient of a function $f : \mathbb{R}^n \times \mathbb{R}$
$\nabla_x^T f(\mathbf{x}) = (\nabla_x f(\mathbf{x}))^T$	transpose of the gradient
$\nabla_x^2 f(\mathbf{x})$	Hessian of a function $f : \mathbb{R}^n \times \mathbb{R}$
$\frac{\partial}{\partial \mathbf{x}}(\cdot) = (\cdot)'$	Jacobian matrix
$L_f h(\mathbf{x})$	Lie derivative of $h : \mathbb{R}^n \to \mathbb{R}$ along a vector field $\mathbf{f} : \mathbb{R}^n \to \mathbb{R}^n$
$\mathbf{x}(t^-)$ $[\mathbf{x}(t^+)]$	limit of $\mathbf{z}(\tau)$ as $\tau \to t$ from below [above]
$\|F\|^{\mathrm{J}} = \sup_{\mathbf{x}\in \mathrm{J}} \|F(\mathbf{x})\|$	supremum of $F(\mathbf{x})$ on a hyperrectangle J
$F^J_{min} = \min_{\mathbf{x}\in \mathrm{J}} F(\mathbf{x})$	minimum of $F(\mathbf{x})$ on a hyperrectangle J
$F^J_{max} = \max_{\mathbf{x}\in \mathrm{J}} F(\mathbf{x})$	maximum of $F(\mathbf{x})$ on a hyperrectangle J
x_i	ith component of a vector $\mathbf{x}$
m_{ij}	element of a matrix $\mathbf{M}$ in the ith row and the jth column
$[m_{ij}]$	matrix with elements m_{ij}
$\mathrm{diag}\{m_{11}, \ldots, m_{nn}\}$	diagonal matrix with diagonal elements m_{ii}
$\overline{\mathbf{M}}$	conjugate complex of a marix $\mathbf{M}$
$\mathbf{M}^T$	transpose of a matrix $\mathbf{M}$
$\mathbf{M}^*$	conjugate transpose of a matrix $\mathbf{M}$
$\mathbf{M}^{-1}$	inverse pseudoinverse of a matrix $\mathbf{M}$
$\mathbf{M}^\dagger$	pseudoinverse of a matrix $\mathbf{M}$
$\mathbf{M}^{-T}$	transpose of the inverse $\mathbf{M}^{-1}$
$\mathbf{M}^{-*}$	conjugate transpose of the inverse $\mathbf{M}^{-1}$

$\mathcal{N}(\mathbf{M})$	nullspace of a matrix $\mathbf{M}$
$\mathcal{R}(\mathbf{M})$	range of a matrix $\mathbf{M}$
$\det(\mathbf{M})$	determinant of a matrix $\mathbf{M}$
$\mathrm{sym}\{\mathbf{M}\} = \frac{1}{2}(\mathbf{M} + \mathbf{M}^T)$	symmetric portion of a matrix $\mathbf{M}$
$\mathbf{I}_n$	n-dimensional identity matrix
$\mathbf{0}_{n\times m}$	$n \times m$ dimensional zero matrix
$i_+(\mathbf{M})$ $[i^r_+(\mathbf{M})]$	number of [real] eigenvalues of $\mathbf{M}$ in the right half plane
$i_-(\mathbf{M})$ $[i^r_-(\mathbf{M})]$	number of [real] eigenvalues of $\mathbf{M}$ in the left half plane
$i_0(\mathbf{M})$	number of eigenvalues of $\mathbf{M}$ on the imaginary axis
$i^r_0(\mathbf{M})$	number of zero eigenvalues of $\mathbf{M}$
$\dim \Delta$	dimension of a distribution Δ
$\bar{\Delta}$	involutive closure of a distribution Δ
$\partial \mathrm{S}$	boundary of a set S
$\mathrm{int}\,\mathrm{S}$	interior of a set S
$\overline{\mathrm{S}}$	closure of a set S
S^c	complement of a set S
$\|\mathbf{x}\|$	Euclidean norm of a vector $\mathbf{x}$

Frequently used Symbols

Latin Symbols

$\mathrm{A}(\mathbf{x}^*)$	domain of attraction of the equilibrium point $\mathbf{x}^*$
$\mathbf{A}_{cl,p}$	dynamic matrix of the pth closed loop subsystem
$\mathbf{A}_d$	dynamic matrix specifying desired dynamics in LLDA (Section 2.3)
$\mathbf{A}^\alpha$	actuated portion of $\mathbf{A}_d$ [see (2.54)]
$\mathbf{A}^\nu$	unactuated portion of $\mathbf{A}_d$ [see (2.54)]
$\mathbf{A}_p$	dynamic matrix of the pth subsystem
$\underline{B}$ $(\overline{B})$	lower (upper) bound of a function on a hyperrectangle (Section 2.5)
B_R	ball with radius R, i.e., $\mathrm{B}_R = \{\mathbf{x} \in \mathbb{R}^n : \|\mathbf{x}\| \leq R\}$
$\hat{c}$	critical level value (Section 3.1)
$\tilde{c}$	approximation of the critical level value $\hat{c}$
$\mathbf{C}(\mathbf{x})$	matrix describing the relation between $\mathbf{f}^\nu_1$ and $\mathbf{f}^\nu_2$ (Assumption 6.4.1)

$\mathbb{C}$	set of complex numbers
$\hat{d}$	scaled critical level value $\hat{d} = (1 - \epsilon_c)\hat{c}$ with $\epsilon_c > 0$ small
$\mathbf{d}$	disturbance
D	(maximum) set satisfying the conditions of Lemma 3.2.2
$e_y(t)$	output tracking error $e_y = y - y_d$
$\mathbf{e}(t)$	state tracking error $\mathbf{e} = \mathbf{x} - \mathbf{x}_d$
$\mathcal{E}$	set of assignable equilibria of the switched system (6.1), i.e., $\mathcal{E} = \bigcap_{p=1}^{N} \mathcal{E}_p$
$\mathcal{E}_p$	set of assignable equilibria of the pth subsystem of (6.1)
$\mathbf{f}(\mathbf{x}, t)$	vector field
$\mathbf{f}^\alpha(\mathbf{x})$	part of $\mathbf{f}$ corresponding to the actuated portion of (2.49)
$\mathbf{f}_p^\alpha(\mathbf{x})$	part of $\mathbf{f}_p$ corresponding to the actuated portion of (6.23)
$\mathbf{f}^\nu(\mathbf{x})$	part of $\mathbf{f}$ corresponding to the unactuated portion of (2.49)
$\mathbf{f}_p^\nu(\mathbf{x})$	part of $\mathbf{f}_p$ corresponding to the unactuated portion of (6.23)
$\mathbf{f}_p(\mathbf{x}, t)$	drift vector field of the pth subsystem of a switched system (2.67)
$\tilde{\mathbf{f}}_p(\mathbf{z}_1)$	(time-invariant) vector field $\mathbf{f}_p$ in $\mathbf{z}_1$ coordinates (Section 7.2)
$\hat{\mathbf{f}}_p(\mathbf{z}_2)$	(time-invariant) vector field $\mathbf{f}_p$ in $\mathbf{z}_2$ coordinates (Section 7.2)
$\mathbf{f}_{p,d}(\mathbf{x}, y_d^{(r)})$	vector field of the pth subsystem of (7.1) with $u = u_{p,d}$ (Section 7.2.2)
$\tilde{\mathbf{f}}_{p,d}(\mathbf{z}_1, y_d^{(r)})$	vector field $\mathbf{f}_{p,d}$ in $\mathbf{z}_1$ coordinates (Section 7.2.2)
$\hat{\mathbf{f}}_{p,d}(\mathbf{z}_2, y_d^{(r)})$	vector field $\mathbf{f}_{p,d}$ in $\mathbf{z}_2$ coordinates (Section 7.2.2)
$\mathbf{f}^e(\mathbf{e}, t)$	drift vector field of the error system (2.61)
$\mathbf{f}_p^e(\mathbf{e}, t)$	drift vector field of pth subsystem of the error systems (7.105), (7.109)
$\mathbf{f}_{cl,p}^e(\mathbf{e}, t)$	vector field of the pth subsystem of the closed loop error system
$\mathbf{F}(\mathbf{x})$	design matrix $\mathbf{F}(\mathbf{x}) = \mathbf{J}(\mathbf{x}) - \mathbf{R}(\mathbf{x})$
$\mathbf{F}^\alpha(\mathbf{x})$	submatrix of $\mathbf{F}$ associated with the actuated part of (2.49)
$\mathbf{F}_p^\alpha(\mathbf{x})$	submatrix of $\mathbf{F}_p$ associated with the actuated part of (6.23)
$\mathbf{F}^\nu(\mathbf{x})$	submatrix of $\mathbf{F}$ associated with the unactuated part of (2.49)
$\mathbf{F}_p^\nu(\mathbf{x})$	submatrix of $\mathbf{F}_p$ associated with the unactuated part of (6.23)
$\mathbf{F}_p(\mathbf{x})$	design matrix for the pth subsystem $\mathbf{F}_p(\mathbf{x}) = \mathbf{J}_p(\mathbf{x}) - \mathbf{R}_p(\mathbf{x})$
$g_v(\lambda)$	restriction of $H(\mathbf{x})$ to a straight line $g_v(\lambda) = H(\lambda \mathbf{v})$, $\mathbf{v} \in \mathbb{R}^n$
$g_{v,k}(\lambda)$	$g_v(\lambda)$ with $\mathbf{v} = \mathbf{v}_k$
$\mathbf{g}(\mathbf{x}, t)$	input vector
$\mathbf{g}_p(\mathbf{x}, t)$	input vector of the pth subsystem of (7.1)

$\tilde{\mathbf{g}}_p(\mathbf{z}_1)$	(time-invariant) input vector $\mathbf{g}_p$ in $\mathbf{z}_1$ coordinates
$\hat{\mathbf{g}}_p(\mathbf{z}_2)$	(time-invariant) input vector $\mathbf{g}_p$ in $\mathbf{z}_2$ coordinates
$\mathbf{g}^e(\mathbf{e}, t)$	input vector of the error system (2.61)
$\mathbf{g}_p^e(\mathbf{e}, t)$	input vector of the pth subsystem of the error systems (7.105), (7.109)
$\mathbf{G}(\mathbf{x}, t)$	input matrix
$\mathbf{G}^\alpha(\mathbf{x})$	submatrix of $\mathbf{G}$ corresponding to the actuated portion of (2.49)
$\mathbf{G}_p^\alpha(\mathbf{x})$	submatrix of $\mathbf{G}_p$ corresponding to the actuated portion of (6.23)
$\mathbf{G}_p(\mathbf{x}, t)$	input matrix of the pth subsystem of a switched system (2.67)
$\mathbf{G}^\perp(\mathbf{x}, t)$	left annihilator of $\mathbf{G}(\mathbf{x}, t)$
$\mathbf{G}_p^\perp(\mathbf{x}, t)$	left annihilator of $\mathbf{G}_p(\mathbf{x}, t)$
$h_{v,k}(\lambda)$	restriction of $\dot{H}$ to a straight line $h_{v,k}(\lambda) = \dot{H}(\lambda \mathbf{v}_k)$, $\mathbf{v}_k \in \mathbb{R}^n$
$\tilde{h}(\mathbf{z}_1)$	scalar time invariant output function $h(\mathbf{x})$ in $\mathbf{z}_1$ coordinates
$h_p^{(k)}(\cdot)$	kth derivative of $h(\mathbf{x})$ along the trajectories of the pth subsystem
$\tilde{h}_p^{(k)}(\cdot)$	kth derivative of $\tilde{h}(\mathbf{z}_1)$ along the trajectories of the pth subsystem
$\mathbf{h}(\mathbf{x}, t)$	output function $y = \mathbf{h}(\mathbf{x}, t)$
$\mathbf{h}_p(\mathbf{x}, t)$	output function of the pth subsystem of a switched system (2.67)
$\mathbf{h}_p^k(\cdot)$	map subsuming $h_p, \ldots, h_p^{(k-1)}$, i.e., $\mathbf{h}_p^k = [h_p, \ldots, h_p^{(k-1)}]^T$, (Section 7.1)
$\tilde{\mathbf{h}}_p^k(\cdot)$	map subsuming $\tilde{h}_p, \ldots, \tilde{h}_p^{(k-1)}$, i.e., $\tilde{\mathbf{h}}_p^k = [\tilde{h}_p, \ldots, \tilde{h}_p^{(k-1)}]^T$, (Section 7.1)
$H(\mathbf{x})$	storage or energy function
$H_p(\mathbf{x})$	energy function of the pth subsystem of an spH system (6.4)
$\mathbf{J}(\mathbf{x})$	interconnection matrix
$\mathbf{J}_p(\mathbf{x})$	interconnection matrix of the pth subsystem of an spH system (6.4)
$\mathbf{k}_p$	feedback matrix corresponding to the pth subsystem
$\mathbf{K}_I$	integral controller gain (Section 6.6.1)
$\mathbf{K}_z$	estimator gain in the update law (6.77a)
m	dimension of the input vector $\mathbf{u}$ and the output vector $\mathbf{y}$
m_p	dimension of the input vector $\mathbf{u}_p$ of the pth subsystem of (6.1)
M	manifold implicitly defined by $\mathrm{M} = \{\mathbf{x} \mid \nabla^T H(\mathbf{x})\mathbf{x} = 0\}$
n	dimension of the state vector $\mathbf{x}$
n_ξ	number of characteristic coordinates, i.e., dimension of $\boldsymbol{\xi}(\mathbf{x})$
$\mathbb{N}$ ($\mathbb{N}_0$)	set of positive (nonnegative) integers
p	index numbering the subsystems of a switched system (2.67)

$\mathbf{p}_p(\mathbf{x})$	drift vector field of the internal dynamics of the pth subsystem of (7.1)
$\tilde{\mathbf{p}}_p(\mathbf{z}_1)$	vector field $\mathbf{p}_p$ in $\mathbf{z}_1$ coordinates
$\hat{\mathbf{p}}_p(\mathbf{z}_2)$	vector field $\mathbf{p}_p$ in $\mathbf{z}_2$ coordinates
$\mathcal{P}$	index set of a switched system (2.67) (Section 2.4.1)
$\mathbf{q}_p(\mathbf{x})$	input vector of the internal dynamics of the pth subsystem of (7.1)
$\tilde{\mathbf{q}}_p(\mathbf{z}_1)$	input vector $\mathbf{q}_p$ in $\mathbf{z}_1$ coordinates
$\hat{\mathbf{q}}_p(\mathbf{z}_2)$	input vector $\mathbf{q}_p$ in $\mathbf{z}_2$ coordinates
$\mathbf{Q}(\mathbf{x})$	positive semidefinite right hand side of (6.37), (6.38)
$\mathbf{Q}_{ij}$	matrices that form a basis for the set of symmetric matrices $\mathbf{Q}$
r	radius (1st spherical coordinate) (see (3.7))
r_{min}	minimum admissible real part of closed loop eigenvalues (Figure 4.3)
r_{max}	maximum admissible real part of closed loop eigenvalues (Figure 4.3)
r_p	relative degree of the pth subsystem of (7.1)
$\mathbf{r}(\mathbf{x})$	feedback function $\mathbf{u} = \mathbf{r}(\mathbf{x})$
$\mathbf{r}_p(\mathbf{x})$	feedback function associated with the pth subsystem
$\mathbf{R}(\mathbf{x})$	dissipation matrix
$\mathbf{R}_p(\mathbf{x})$	dissipation matrix of the pth subsystem of an spH system (6.4)
$\mathbf{R}_{ij}$	matrices that form a basis for the set of symmetric matrices $\mathbf{R}$
$\mathbb{R}$	set of real numbers
$\mathbb{R}^+$ ($\mathbb{R}_0^+$)	set of positive (nonnegative) real numbers
$\mathbf{s}(\mathbf{x})$	right hand side of a PDE (2.26), (6.16)
S_c^V	sublevel set $\{\mathbf{x} \in \mathbb{R}^n \vert V(\mathbf{x}) < c\}$ of a function V with level value c
$\mathrm{S}_c^V(\mathbf{x}^*)$	connected component of S_c^V that contains $\mathbf{x}^*$
$\mathbb{S}^n$	n-dimensional unit sphere
$\mathcal{S}$	set of admissible switching signals (see p. 42)
$\mathcal{S}_{pc}$	set of piecewise constant switching signals
t	time
t_0	initial time
t_i	switching times
$t_{i,d}$	discontinuities of σ_d (see Section 7.3)
$\mathbf{t}(\mathbf{A})$	tangent vector induced by a matrix $\mathbf{A}$ [see (4.8)-(4.10)]
$\widetilde{\mathbf{T}}_p$	transformation matrix from $\mathbf{z}_1$ to $\mathbf{z}_p$ coordinates

$\widetilde{\mathbf{T}}_{p,\xi}$	first r_p rows of $\widetilde{\mathbf{T}}_p$
$\widetilde{\mathbf{T}}_{p,\eta}$	last $n - r_p$ rows of $\widetilde{\mathbf{T}}_p$
$\widetilde{\mathbf{T}}_{2,\xi}^{-1}$	first r_1 rows of $\widetilde{\mathbf{T}}_2^{-1}$
$\widetilde{\mathbf{T}}_{2,\eta}^{-1}$	last $n - r_1$ rows of $\widetilde{\mathbf{T}}_2^{-1}$
$\mathcal{T}$	discretization of a time interval $[0, T]$
$u_d(t)$	feedforward control corresponding to $y_d(t)$
$u_{p,d}(\mathbf{x}, y_d^{(r_p)})$	feedforward control corresponding to y_d for the pth subsystem of (7.1)
$\tilde{u}_{p,d}(\mathbf{z}_1, y_d^{(r_p)})$	function $u_{p,d}$ in $\mathbf{z}_1$ coordinates
$\hat{u}_{p,d}(\mathbf{z}_2, y_d^{(r_p)})$	function $u_{p,d}$ in $\mathbf{z}_2$ coordinates
$\mathbf{u}(t)$	control input
$\mathbf{u}_p(t)$	input vector of the pth subsystem of the switched system (6.1)
$\mathbf{u}^*$	stationary control input associated with $\mathbf{x}^*$
$\mathbf{U}^k(t)$	vector containing $u, \dots, u^{(k-1)}$, i.e., $\mathbf{U}^k = [u, u^{(1)}, \dots, u^{(k-1)}]^T$
$\mathbf{U}_d^k(t)$	vector containing $u_d, \dots, u_d^{(k-1)}$, i.e., $\mathbf{U}_d^k = [u_d, u_d^{(1)}, \dots, u_d^{(k-1)}]^T$
$\mathbf{v}(t)$	new input after an input transformation
$V(\mathbf{x}, t)$	Lyapunov function
$V_{\hat{d}}$	volume of the set $\mathrm{S}_{\hat{d}}(\mathbf{0})$
$\mathcal{V}$	discretization of the $(n-1)$-dimensional unit sphere
$W_i(\mathbf{x})$	time-invariant positive definite bounds for $V(\mathbf{x}, t)$ and $-\dot{V}(\mathbf{x}, t)$
$\mathbf{W}(\mathbf{x})$	matrix with coefficient functions of a PDE (2.26), (6.16)
$\mathbf{x}(t)$	state vector
$\mathbf{x}^\alpha$	actuated coordinates
$\mathbf{x}^\nu$	unactuated coordinates
$\mathbf{x}(t; \mathbf{x}_0, t_0)$	solution of (2.7) or (2.72) starting from $\mathbf{x}_0$ at t_0
$\mathbf{x}_d(t)$	desired state trajectory
$\mathbf{x}^*$	(desired) equilibrium point
$\mathbf{x}_0$	initial state $\mathbf{x}_0 = \mathbf{x}(t_0)$
$\hat{\mathbf{x}}$	point corresponding to $\hat{c}$ (Section 3.2)
$\hat{\mathbf{x}}_d$	point corresponding to $\hat{d}$ (Section 3.3)
$\mathbf{X}(\mathbf{x})$	unknown in the matrix equations (6.37), (6.38)
$\mathbf{X}^h(\mathbf{x})$	homogeneous solution of (6.37), (6.38)
$\mathbf{X}^p(\mathbf{x})$	particular solution of (6.37), (6.38)

$\mathbf{X}_{ij}^{p}(\mathbf{x})$	particular solution of (6.38) for the right hand side $\mathbf{Q}_{ij}$
$\mathbf{y}(t)$	output of a dynamical system
$y_d(t)$	desired (scalar) output trajectory
$\mathbf{Y}^k(t)$	vector containing $y, \dots, y^{(k-1)}$, i.e., $\mathbf{Y}^k = [y, y^{(1)}, \dots, y^{(k-1)}]^T$
$\mathbf{Y}_d^k(t)$	vector containing $y_d, \dots, y_d^{(k-1)}$, i.e., $\mathbf{Y}_d^k = [y_d, y_d^{(1)}, \dots, y_d^{(k-1)}]^T$
$\mathbf{z}$	spherical coordinates [see (3.7)]
$\mathbf{z}_p$	input-output coordinates of the pth subsystem of (7.1) (Section 7.2)
$\mathbf{z}_{p,d}(t)$	desired trajectory of $\mathbf{z}_p$

Greek Symbols

$\alpha_{ij}(\mathbf{x})$ $[\alpha_{p,ij}(\mathbf{x})]$	elements of $\mathbf{F}^{\alpha}(\mathbf{x})$ $[\mathbf{F}_p^{\alpha}(\mathbf{x})]$
$\tilde{\alpha}_1(\mathbf{z}_1)$	see (7.13)
$\hat{\alpha}_2(\mathbf{z}_2)$	see (7.16)
$\tilde{\beta}_1(\mathbf{z}_1)$	see (7.13)
$\hat{\beta}_2(\mathbf{z}_2)$	see (7.16)
δ_{min}	accuracy with which M is approximated (Section 3.4)
$\Delta(\mathbf{x})$	distribution
$\Delta_{F,p}(\mathbf{x})$	distribution spanned by the rows of $\mathbf{F}_p^{\nu}(\mathbf{x})$
$\Delta_W(\mathbf{x})$	distribution spanned by the rows of $\mathbf{W}(\mathbf{x})$
$\Delta_{W,s}(\mathbf{x})$	distribution spanned by the rows of $[\mathbf{W}(\mathbf{x}),\ \mathbf{s}(\mathbf{x})]$
$\Delta\lambda^{min}$	minimum distance between adjacent points in $\mathcal{V}$
$\Delta\lambda^{max}$	maximum distance between adjacent points in $\mathcal{V}$
$\boldsymbol{\eta}_p(t)$	vector of internal dynamics states of the pth subsystem of (7.1)
$\boldsymbol{\eta}_{p,d}(t)$	desired trajectory of $\boldsymbol{\eta}_p$
θ_i	angles in the spherical coordinate system [see (3.7)]
$\boldsymbol{\theta}$	parametric uncertainty (Section 6.6.2)
λ	variable of $g_{v,k}(\lambda)$ and $h_{v,k}(\lambda)$ (Section 3.2)
λ_k^{min}	initial estimate of $\rho_{\bar{D}}(\mathbf{v}_k)$ (Section 3.3)
$\nu_{ij}(\mathbf{x})$ $[\nu_{p,ij}(\mathbf{x})]$	elements of $\mathbf{F}^{\nu}(\mathbf{x})$ $[\mathbf{F}_p^{\nu}(\mathbf{x})]$
$\boldsymbol{\xi}(\mathbf{x})$	characteristic coordinates of a PDE (2.26), (6.16)
$\boldsymbol{\xi}_p(t)$	vector of input-output dynamics states of the pth subsystem of (7.1)
$\boldsymbol{\xi}_{p,d}(t)$	desired trajectory of $\boldsymbol{\xi}_p$

$\rho_D(\cdot)$	radial function of a set D associated with the origin [see e.g. (3.3)]
$\sigma(t)$	switching signal
$\sigma_d(t)$	switching signal corresponding to $\mathbf{x}_d$ and u_d (see Section 7.3)
$\sigma^e(t)$	switching signal of the error system (7.109)
$\phi(\boldsymbol{\xi}(\mathbf{x}))$	homogeneous solution of a PDE (2.26), (6.16)
$\varphi(\mathbf{x},\mathbf{u})$	function implicitly defining $\partial\chi$ by $\partial\chi = \{(\mathbf{x},\mathbf{u})\|\varphi(\mathbf{x},\mathbf{u}) = \mathbf{0}\}$
$\tilde{\varphi}(\mathbf{z}_1,\mathbf{u})$	function φ in $\mathbf{z}_1$ coordinates
$\hat{\varphi}(\mathbf{z}_2,\mathbf{u})$	function φ in $\mathbf{z}_2$ coordinates
$\varphi_x(\mathbf{x}),\ \varphi_u(\mathbf{x})$	parts of the function $\varphi(\mathbf{x},\mathbf{u})$ [see (2.71)]
$\tilde{\varphi}_x(\mathbf{z}_1),\ \tilde{\varphi}_u(\mathbf{z}_1)$	functions $\varphi_x,\ \varphi_u$ in $\mathbf{z}_1$ coordinates
$\hat{\varphi}_x(\mathbf{z}_2),\ \hat{\varphi}_u(\mathbf{z}_2)$	functions $\varphi_x,\ \varphi_u$ in $\mathbf{z}_2$ coordinates
$\varphi_p(\mathbf{x}, y_d^{r_p})$	function $\varphi(\mathbf{x},u)$ with $u = u_{p,d}$ (Section 7.2)
$\tilde{\varphi}_p(\mathbf{z}_1, y_d^{r_p})$	function $\tilde{\varphi}(\mathbf{z}_1,u)$ with $u = \tilde{u}_{p,d}$ (Section 7.2)
$\hat{\varphi}_p(\mathbf{z}_2, y_d^{r_p})$	function $\hat{\varphi}(\mathbf{z}_2,u)$ with $u = \hat{u}_{p,d}$ (Section 7.2)
$\varphi_p^{(k)}(\cdot)$	kth derivative of φ along $\mathbf{f}_{p,d}$
$\tilde{\varphi}_p^{(k)}(\cdot)$	kth derivative of $\tilde{\varphi}$ along $\tilde{\mathbf{f}}_{p,d}$
$\hat{\varphi}_p^{(k)}(\cdot)$	kth derivative of $\hat{\varphi}$ along $\hat{\mathbf{f}}_{p,d}$
$\boldsymbol{\Phi}_p(\mathbf{x})$	coordinate transformation from $\mathbf{x}$ to $\mathbf{z}_p$ coordinates
$\boldsymbol{\Phi}_{p,\xi}(\mathbf{x})$	first r_p components of $\boldsymbol{\Phi}_p(\mathbf{x})$
$\boldsymbol{\Phi}_{p,\nu}(\mathbf{x})$	last $n - r_p$ components of $\boldsymbol{\Phi}_p(\mathbf{x})$
$\tilde{\boldsymbol{\Phi}}_p(\mathbf{z}_1)$	coordinate transformation from $\mathbf{z}_1$ to $\mathbf{z}_p$ coordinates
$\tilde{\boldsymbol{\Phi}}_{p,\xi}(\mathbf{z}_1)$	first r_p components of $\tilde{\boldsymbol{\Phi}}_p(\mathbf{z}_1)$
$\tilde{\boldsymbol{\Phi}}_{p,\nu}(\mathbf{z}_1)$	last $n - r_p$ components of $\tilde{\boldsymbol{\Phi}}_p(\mathbf{z}_1)$
$\tilde{\boldsymbol{\Phi}}_{2,\xi}^{-1}(\mathbf{z}_2)$	first r_1 components of $\tilde{\boldsymbol{\Phi}}_2^{-1}(\mathbf{z}_2)$
$\tilde{\boldsymbol{\Phi}}_{2,\nu}^{-1}(\mathbf{z}_2)$	last $n - r_1$ components of $\tilde{\boldsymbol{\Phi}}_2^{-1}(\mathbf{z}_2)$
χ_p	set within which the pth subsystem is active (see (2.69))
$\partial\chi$	switching surface
ψ	parameter characterizing an admissible eigenvalue region (Figure 4.3)
$\Psi(\mathbf{x})$	particular solution of a PDE (2.26), (6.16)
$\boldsymbol{\Psi}(\mathbf{x})$	transformation from spherical to Cartesian coordinates [see (3.7)]
Ω^R	neighborhood of $\mathbf{x}^*$ within which $\mathbf{R}(\mathbf{x}) \geq 0$ holds
$\Omega^{\dot{H}}$	neighborhood of $\mathbf{x}^*$ within which $\dot{H}(\mathbf{x}) \leq 0$ holds

$\Omega^{\dot{V}}$	neighborhood of $\mathbf{x}^*$ within which $\dot{V}(\mathbf{x}) \leq 0$ holds
Ω^{W}	neighborhood of $\mathbf{x}^*$ within which the W_i are positive definite
Ω^{W_3}	neighborhood of $\mathbf{x}^*$ within which W_3 is positive definite

Acronyms

AOT	asymptotic output tracking
DA	domain of attraction
EOT	exact output tracking
IDA	Interconnection and Damping Assignment
LLDA	local linear dynamics assignment
LMI	linear matrix inequality
PBC	passivity-based control
PDE	partial differential equation
pH	port Hamiltonian
spH	switched port Hamiltonian
SB	stability boundary
w.r.t.	with respect to
UEP	unstable equilibrium point

Chapter 1

Introduction

The objective of this thesis is to contribute to the development of constructive controller design methods for nonlinear systems. While the first part of the thesis is devoted to the control of smooth systems, the second part is dedicated to switched systems, which have received growing attention in the last two decades. We start this introduction by motivating our work in Section 1.1. Subsequently, we clarify the focus of the thesis and point out the main contributions in Section 1.2. To put our results in perspective, we review the state of the art in Section 1.3. In Section 1.4 we give an outline of the thesis, and finally we introduce some notation in Section 1.5.

1.1 Motivation

The ever increasing demand for dynamic performance and efficiency of control systems requires the use of sophisticated design methods which are based on precise models of the plant. Most physical systems are inherently nonlinear and often no satisfactory result can be achieved if only a linear approximation is considered for the controller design. For this reason, various nonlinear control design methods have emerged. In the last two decades, the notion of *passivity* has played a central role in this development (see e.g. the series of books [46], [104], [134], [151], [174]), one reason being that the resulting control laws tend to be more robust and energy efficient than those obtained by geometric design methods, such as feedback linearization, which have been popular since the 1980's (see e.g. [151]).

The passivity property essentially means that a system does not contain a source of energy or, in other words, that it cannot store more energy than supplied to it from the outside. The term *passivity-based control* (PBC) has been introduced in [136] to denote a control technique that achieves stabilization by rendering the closed loop system passive with respect to a desired energy function. However, the idea of shaping the energy of a system by feedback control dates back to the famous paper by Takegaki and Arimoto

[166] in 1981, where set point regulation of a robot manipulator is achieved by shaping its potential energy and injecting damping. While in "standard" PBC the desired energy function is specified a priori, at the beginning of the century, a second class of PBCs emerged with the methods of Controlled Lagrangians [14], [15] and *Interconnection and Damping Assignment (IDA)* [132], [140], where instead of the storage function the structure of the closed loop system is fixed to be Lagrangian or port Hamiltonian (pH), respectively. The set of assignable energy functions is then determined from the so-called matching equation. Throughout this thesis, we will make extensive use of the method IDA, which has already been successfully applied to a multitude of technical systems (see e.g. [4], [61], [67], [80], [84], [93], [131]).

A major difficulty in IDA is the tuning of the numerous controller parameters with respect to desired closed loop properties. Therefore, there is a need for tools and methods which enable the systematic and transparent tuning of IDA controllers, also in order to expedite the industrial application of the method. Besides the dynamic behavior of the closed loop system, an aspect that plays a central role in this context is the *domain of attraction* (DA) of the desired equilibrium point, which is the set of all initial states from which the system trajectory tends to that equilibrium. As a matter of fact, knowledge of the DA or at least a subset thereof is indispensable for the secure operation of the closed loop system. Clearly, the control law has to ensure that the DA is large enough to guarantee stability in the entire operating region. For example, when a set-point change is made, the actual system state must be contained in the DA of the new operating point. Moreover, the DA has to be large enough to provide robustness against disturbances, which is of particular importance for systems that must have high reliability, such as flight control or power systems. Let us briefly mention the Boeing F/A-18A/B/C/D Hornet aircraft as a motivating example. Many of these aircrafts have been lost due to an out-of-control flight departure phenomenon which is called "falling leaf" motion and can occur when the system state leaves the DA of the desired flight state e.g. due to a wind gust [77]. All these aspects have motivated us to come up with a systematic methodology to tune an IDA controller such that the DA is maximized, while simultaneously fulfilling the requirements regarding the dynamic performance. However, determining the DA of a general nonlinear system is a difficult task which remains unsolved up to now. Therefore, usually an inner estimate is determined using a Lyapunov function.

One central feature of IDA is that the assigned energy function qualifies as a Lyapunov function for the closed loop system and hence allows for estimating the DA of the desired equilibrium point. Since, in general, the energy function is *not radially unbounded*, this includes determining its largest bounded sublevel set. However, as noted in [61],

characterizing the largest bounded sublevel set of a general Lyapunov function is "*a very hard problem*". Moreover, if a suitable sublevel set is known, it consists, in general, of several different connected components, and an estimate of the DA is given by the component which contains the considered equilibrium point. Therefore, it is still difficult to decide whether a given initial state is contained in the estimated DA or in some other connected component of the sublevel set. In the case of time-varying systems, as they occur in the context of trajectory tracking control of nonlinear systems, estimating the DA is more complicated due to the explicit time-dependence of the energy function. Motivated by this, in this thesis we develop an approach that allows to estimate the closed loop DA with the help of the assigned energy function for both time-invariant and time-varying systems. Moreover, we obtain a representation of this estimate that enables us to easily decide whether a given state is contained therein.

Recently, the notions of dissipativity and passivity have been extended to the class of *switched systems* (see e.g. [191], [193], [194]), which has received a great deal of attention in the last decade, from both practitioners and researchers. One of the main reasons for the interest in this class of systems is the fact that, for a wide variety of technical systems, it is beneficial or even necessary to use a modeling framework which combines logic based switching with continuous differential equations, e.g. when the plant system contains switching elements, such as valves or electric switching devices, or when it has multiple modes of operation. Also, when modeling complex physical systems, some components are often approximated by switching elements in order to simplify the model and to avoid complex nonlinearities and stiffness [126]. Loosely speaking, switched systems are described by a state differential equation whose right-hand side is selected from a given family of vector fields (characterizing the dynamics of the so-called subsystems) by some switching rule. The latter is usually assumed to be either externally specified as a function of time (trajectory-independent switching) or to be state-dependent [113]. However, as can be seen e.g. in the application paper [94], switching rules that depend on the control input are of technical relevance as well. It is worth mentioning that piecewise affine (PWA) systems (sometimes also called piecewise-linear systems), that have been studied by Sontag already in the early 1980s (see [159], [160]), may be viewed as switched systems with state-dependent switching law and affine subsystem dynamics. Practical examples of switched systems can be found in various fields of application and include, for instance, hydraulic systems [94], chemical processes [123], automotive applications [157], the flying height regulation problem in hard disk drives [184], and even biological processes (see Example 1.3 in [155]).

While there is a large number of publications dealing with the stability analysis of

switched systems (see e.g. [7], [21], [38], [113], [114], [120], [192] and the references therein), much less effort has been made so far on the controller synthesis for this class of systems, despite its technical relevance. Therefore, as noted in [186], there is still a pressing need for constructive analytic methods that allow the transparent design of stabilizing controllers for switched systems. This control task is impeded by the fact that the stability properties of switched dynamical systems are radically different from those of smooth ones. In particular, systems of this class can exhibit unstable behavior, even if all subsystems taken by themselves are asymptotically stable. Therefore, it is not sufficient to stabilize each subsystem individually. In view of the successful application of passivity-based methods to smooth systems, it can be expected that they are also useful for switched systems [194]. This motivates the development of controller design techniques for switched systems that achieve stabilization by passivation. In particular, we present in this thesis an extension of the IDA approach to the class of switched systems. As in the smooth case, a major aspect we are concerned with is to put forth methods that enable the constructive design and the transparent tuning of stabilizing controllers.

Besides the pure stabilization of a desired equilibrium, in practice, it is often required that a specific quantity follows some predefined trajectory. Since that quantity is typically defined to be the output of the system, this problem is referred to as *output trajectory tracking problem*. This control task has been extensively studied for smooth systems (see e.g. [89], [110] and the references therein) and it is evident that it is highly relevant also for switched systems. It is desired that the reference trajectories can be freely chosen by the control engineer or operator of the system. The desired trajectories are commonly specified in terms of polynomials, trigonometric series or other smooth functions. Therefore, a fundamental question arising in this context is under what conditions we can find a control input such that a desired smooth output trajectory is tracked exactly [*exact output tracking (EOT) problem*]. Not surprisingly, this question is more involved than in the case of smooth systems, especially when the switching is trajectory-dependent, i.e., state- and/or input-dependent. For it is closely related to the existence of solutions of discontinuous differential equations and, as noted by Sussmann [163], this problem is more delicate than it is for smooth systems. As far as we are aware, no results are available that provide conditions under which the EOT problem is solvable for nonlinear switched systems. Therefore, we address this problem in the present thesis for bimodal[1] switched nonlinear systems with a single input and a single output.

Since, in a practical setup, disturbances and model uncertainties are present, in order to

[1] A switched system is called bimodal if it has two subsystems.

attain good tracking performance, normally a feedback controller needs to be designed which asymptotically drives the system output towards the prescribed reference trajectory. In the present thesis, we study this so-called *asymptotic output tracking (AOT) problem* for bimodal switched nonlinear single-input-single-output (SISO) systems. To the best of our knowledge, that problem has previously been considered only for one particular system [94], but no general results are available. As in the case of smooth nonlinear systems, the differential equations that govern the evolution of the tracking error are time-varying even if the plant dynamics are described by a time-invariant switched nonlinear system. This shows the need to develop also controller design methods for the stabilization of *time-varying switched systems*.

1.2 Focus and Contributions of this Thesis

In this thesis, we present methods for the *constructive* and *systematic* design of controllers for *smooth and switched nonlinear systems*. For both classes of systems we consider the *set-point* as well as the *trajectory tracking control* problem, and we are concerned with the systematic and transparent parametrization of the feedback laws regarding the size of the resulting DA and the closed loop dynamics. The presented methods are illustrated by means of several technical examples in order to demonstrate their practical applicability. With the exception of Chapter 7, the results in this thesis complement or extend the passivity-based controller design methodology IDA.

The main part of the thesis is divided into two parts. The first one is dedicated to the control of smooth dynamical systems and comprises the chapters 3–5. The two main problems addressed in this part are the estimation of the DA achieved by an IDA controller utilizing the assigned energy function and, based on that, the systematic tuning of such a controller to maximize the estimated DA and, at the same time, attain desired closed loop performance. Both issues are addressed not only for the time-invariant case but also in the context of time-varying systems as they arise when trajectory tracking is considered.

The second part of the thesis is devoted to the control of switched nonlinear systems and consists of the Chapters 6–8. We consider the case of arbitrary switching as well as the case of trajectory-dependent switching, where the switching law may depend on the state and/or the control input. The first main problem addressed in this part is the passivity-based stabilization of switched nonlinear systems, whose subsystems may, in general, be time-varying. The second issue under investigation is the output trajectory tracking problem, where we restrict our attention to bimodal switched SISO systems. We are interested in conditions under which the exact output tracking problem is solvable and

also study the asymptotic output tracking problem. The contributions of the individual chapters are summarized in the following:

Chapter 3: Estimating the Domain of Attraction We address the question of how to exploit the closed loop pH structure resulting from the application of IDA in order to obtain an estimate of the DA of the desired equilibrium point. More precisely, we are concerned with the problem of how to determine an as large as possible sublevel set of the assigned energy function which qualifies as an estimate of the DA in spite of the fact that this function is, in general, not radially unbounded. We develop an approach that allows to determine a suitable sublevel set without formulating any conditions on the energy function that go beyond those of the IDA method itself. For the effective computation of the corresponding level value, we present two numerical algorithms. The first one is based on a multidimensional grid and is relatively easy to implement, which is advantageous in terms of broad practical applicability. It is extended also to the case of time-varying closed loop systems. The second one uses numerically calculable bounds on real valued functions together with a generalized bisection algorithm. It is computationally more expensive, but bypasses the problem of choosing an appropriate grid. Both methods can also be applied to switched pH systems as they emerge in the context of the control scheme proposed in Chapter 6. The main contributions of this chapter are:

- an approach to estimate the DA achieved by an IDA controller based on the assigned energy function which is applicable for both time-invariant and time-varying systems, and
- two numerical algorithms for the effective computation of the estimated DA.

Chapter 4: Controller Design In this chapter we are concerned with the fundamental question of how to tune the large number of parameters that occur in IDA. To simplify the controller design process, we propose a specific parametrization which guarantees the positive semidefiniteness of the dissipation matrix without considering cumbersome inequality constraints, as they are obtained e.g. from Sylvester's criterion. Moreover, we outline a procedure to numerically approximate the boundary of the DA as estimated by the methods from Chapter 3. This allows, on the one hand, to determine whether a given initial state is contained in this set, and, on the other hand, to compute the volume of the estimated DA, which can be used to quantify its size. Based on this scalar measure we present an optimization approach to determine a controller parametrization which maximizes the estimated DA and simultaneously takes into account the desired dynamic

performance of the closed loop system. All methods presented in this chapter are applicable for time-varying systems as well. The main contributions of this chapter are:

- a specific parametrization of the design matrix that guarantees the positive semidefiniteness of the dissipation matrix, and
- an optimization procedure to determine a controller parametrization that maximizes the volume of the estimated DA while simultaneously taking account of desired closed loop performance.

Chapter 5: Examples We illustrate the application of the methods presented in the Chapters 3 and 4 and demonstrate their effectiveness for the set-point and trajectory tracking control of technical systems. We first consider a 2-dimensional numerical example for which the exact DA can be computed and an easy graphical visualization of the results is possible. As a technical example for the stabilization of time-invariant systems we take the excitation control of a synchronous generator, which is of major importance as it enhances the resilience of a power system to disturbances. The objective is to enlarge the DA and thereby to increase the so-called critical clearing time, which is an important security measure of a power system. We provide a comparison with another IDA controller from the literature [61] and show that considerably better results are achieved by employing the proposed techniques. As a third example, we study the trajectory tracking control of a magnetic levitation system – in particular the stabilization of the time-varying tracking error dynamics – in order to show the applicability of the proposed methods also in the time-varying case. In this context, experimental results obtained at a laboratory experiment are presented. The main contribution of this chapter is:

- the demonstration of the viability and effectiveness of the methods proposed in the Chapters 3 and 4 for the control of technical systems.

Chapter 6: Passivity-Based Control of Switched Nonlinear Systems An *analytic* and *constructive* controller design methodology for switched nonlinear control affine systems is presented. We introduce the class of switched port Hamiltonian (spH) systems and discuss their stability properties. Motivated by the latter, we propose an extension of the IDA approach to the class of switched systems that assigns an spH structure with a common energy function to the closed loop system and thereby achieves (asymptotic) stabilization. For a special class of switched systems, we derive a systematic procedure for the construction of suitable design matrices and the subsequent controller design. In this context, we derive conditions under which the matrix equation $\mathbf{A}\mathbf{X} + \mathbf{X}^T\mathbf{A}^T = \mathbf{Q}$ has a

solution whose symmetric portion is positive semidefinite. We also briefly consider the case where the switched system is already given in spH form, and we extend the method to incorporate integral as well as adaptive control. Moreover, we generalize the method to switched nonlinear systems with time-varying subsystems. The main contributions of this chapter are:

- a constructive and analytic passivity-based controller design methodology for switched nonlinear systems, and
- a systematic procedure for the construction of suitable design matrices and the subsequent controller design for a special class of switched systems.

Chapter 7: Output Trajectory Tracking of Bimodal Switched Systems Both the exact and the asymptotic output trajectory tracking problem are addressed for switched nonlinear SISO systems with two subsystems. We study trajectory-independent as well as trajectory-dependent switching, where in the latter case the switching law may also depend on the input. We derive necessary and sufficient conditions for the solvability of the exact output tracking (EOT) problem. Moreover, we explore the asymptotic output tracking (AOT) problem using the well known two-degree of freedom structure. In the case of trajectory-dependent switching, the stabilization of the tracking error dynamics is found to be quite involved. Therefore, we identify two special classes of switched systems for which the controller design simplifies considerably: a class of continuous bimodal switched nonlinear systems, and a class of bimodal switched linear systems. For the latter, we propose an LMI-based controller design approach. The main contributions of this chapter are:

- necessary as well as sufficient conditions for the solvability of the EOT problem for bimodal switched nonlinear SISO systems,
- the proof of a result that considerably simplifies the AOT problem for a class of continuous bimodal switched nonlinear systems, and
- an LMI-based approach to solve the AOT problem for a class of bimodal switched linear systems.

Chapter 8: Technical Applications We apply the results from the Chapters 6 and 7 to two technical systems in order to show their viability and effectiveness. First, we study the problem of tracking a desired speed trajectory with a DC motor, whose friction

characteristic is asymmetric in the angular velocity – a phenomenon that is well known for DC motors (see e.g. [6], [23], [55], [96]). The different friction behavior for positive and negative velocities leads to a plant model that exhibits state-dependent switching. As a second example, we consider a self-supplied variable displacement axial piston pump, where it is desired to make the load pressure track a prescribed trajectory. The model of this device exhibits input-dependent switching. Both systems are analyzed with respect to the solvability of the EOT problem and suitable feedforward controllers are designed. In order to attain asymptotic output tracking, the switched error dynamics are stabilized using the IDA-based controller design methodology from Chapter 6. To compute an estimate of the DA the approach proposed in Chapter 3 is utilized. Simulation results illustrate that a good dynamic performance is achieved by means of the proposed methods. The main contribution of this chapter is:

- the demonstration of the practical applicability and effectiveness of the results presented in the Chapters 6 and 7 using two technical application examples.

In summary, we present a variety of results on the constructive design of set-point as well as trajectory tracking controllers for both smooth and switched nonlinear systems.

1.3 Related Work

To put the material in this thesis in perspective, we give an overview of the state of the art in this section. In accordance with the main topics addressed in this thesis, the literature review is focused on the estimation and enlargement of the DA, the stabilization of switched systems, and the tracking control problem for switched systems. Each of the following subsections is dedicated to one of these topics.

1.3.1 Estimating and Enlarging the Domain of Attraction

As a result of the importance of the DA in the analysis and synthesis of nonlinear systems, its determination has been a topic of extensive research during the last 40 years. However, the computation of the exact DA for a general nonlinear system is a very hard problem and remains unsolved up to now despite intensive research efforts. A method which in principle allows the numerical computation of the exact DA – provided that it is applicable – has been proposed in [29]. It uses that, under some conditions, the boundary of the DA is formed by the stable manifolds of the equilibrium points on this boundary. Hence, it requires the identification of all relevant equilibrium points and the computation of their

stable manifolds, which makes it very involved for systems of dimension greater than 2. Moreover, the conditions for its applicability are restrictive as well as difficult to verify in general. Therefore, numerous methods have been developed to determine an inner approximation of the DA (see e.g. the survey paper [68]).

The vast majority of these methods is based on Lyapunov functions, i.e., the DA is approximated by a positively invariant sublevel set of a Lyapunov function. The most popular type of Lyapunov functions are definitely the quadratic ones [26], [37], [149], [170], whose sublevel sets are of course guaranteed to be bounded. While the authors of [37] and [26] aim to find the optimal quadratic Lyapunov function, i.e., the one which maximizes the volume of the estimate, in [149], [170] the Theorem of Ehlich and Zeller and its extensions are used to determine the largest sublevel set of a particular quadratic Lyapunov function which can be guaranteed to be contained in the DA. For polynomial systems, recently techniques which are based on sum-of-squares relaxations have become popular (see e.g. [167], [171]), where a polynomial Lyapunov function is computed by solving an optimization problem with LMI-constraints. In these approaches, boundedness of the sublevel sets is guaranteed by lower bounding the solution by a predefined radially unbounded function.

A method which utilizes Lyapunov functions that are not radially unbounded is the closest unstable equilibrium point (UEP) method, which is frequently employed for the transient stability analysis of electric power systems [27], [30] and has been formulated for general dynamical systems with hyperbolic equilibrium points in [31]. It yields an optimal estimate of the stability region in the sense that it is the largest one which can be obtained with the corresponding Lyapunov function. However, it requires that along any system trajectory the Lyapunov function is both strictly decreasing and a proper map. For network-reduction models, which are traditionally used for the transient stability analysis of power systems, such a function is known [27]. In general, however, these conditions are restrictive and particularly the second one is not easy to verify [27]. Specifically, in the context of IDA, usually none of the two conditions can be guaranteed. See also [61], in particular Remark 1, for a related discussion. Moreover, a key step of the method is the numerical computation of all equilibrium points of the system, which can be very involved and is a field of current research, see e.g. [107] for a discussion. For instance, it is shown in [107] that the dynamic gradient approaches, which have been proposed to overcome the drawbacks of the classic quasi-Newton methods (see e.g. [116]), may fail even for second order systems.

In [61], strong convexity of the energy function in a certain region is exploited to show boundedness of the sublevel sets. However, it can only be concluded that all sublevel sets contained in that region are bounded, but no particular sublevel set is obtained. Moreover,

strong convexity is only a sufficient condition and analytically verifying this property is very difficult for general energy functions. In [101], [177], the Ridge method [88], which is used in theoretical chemistry to find saddle points on potential energy surfaces, is employed to identify a suitable sublevel set of the energy function. However, this method is, in general, not suitable for determining a sublevel set that qualifies as an estimate of the DA. First, the algorithm requires one point on each side of the energy ridge on which the saddle point is located as input argument. Unlike when considering chemical reactions, in the context of estimating the DA there is usually no indication on how to choose these starting points. Moreover, even if a saddle point can be computed, there is no guarantee that it is the desired one, and, as can be seen from the discussion in Section 3.1, it is in general not true that the level value of interest is attained at a saddle point. In summary, there is no satisfactory method available to date which enables to estimate the DA of an IDA controller based on the assigned energy function. Therefore, we develop in Chapter 3 an approach to cope with this problem, which is *applicable to any IDA controlled system* even if it is *time-varying*.

As far as the systematic and transparent parametrization of IDA controllers is concerned, a useful contribution is the approach of *Local Linear Dynamics Assignment* (LLDA) proposed in [102], [103] (see Section 2.3). The basic idea is the assignment of desired eigenvalues to the closed loop linearization in order to specify (locally) the closed loop dynamics in a transparent manner. From this, a system of linear equations is derived for the design parameters. Moreover, a systematic procedure is outlined in these works, where the design and tuning of an IDA controller is divided into several steps. As motivated above, besides the transient behavior, another desirable objective is the enlargement of the DA of the desired equilibrium point. This goal is pursued in [61], where IDA is employed to enlarge the DA of the operating point of a synchronous generator. A comparison with our results is given in Section 5.2.4.

1.3.2 Stabilization of Switched Systems

Concerning the stabilization of switched systems, three different problems can be distinguished. One is to stabilize a switched system without continuous control input by identifying suitable switching signals or a suitable switching law. The paper [115] provides a good survey of approaches that have been proposed for switched linear systems in this regard. The design of switching laws and switching signals for switched nonlinear systems is addressed for example in [32], [112], [121], [189]. In a second case, both a continuous control input and the switching signal are available, i.e., the switched system can be

stabilized by designing a controller *and* a suitable switching law or switching signal. For this type of problem, several optimal control approaches have been proposed, e.g. in [11], [188]. In [48], an integrated synthesis of output feedback controllers together with switching laws has been proposed considering input constraints. In the third class of problems, the switching signal is not controllable and the task is to design a controller that stabilizes the switched system either for arbitrary (exogenous) switching signals or under some prescribed trajectory-dependent switching law. This is the stabilization task considered in this thesis. Therefore, our literature review is focused on this topic.

Numerous publications are available that deal with the controller synthesis for switched linear systems under arbitrary switching, where techniques based on linear matrix inequalities (LMI) are popular [34], [35], [125]. However, these methods are usually iterative in nature and not as transparent and interpretable as the classical analytic techniques, that are known from non-switched systems (such as pole-placement) [186]. An analytic controller design method for a very special class of continuous-time linear systems has been presented in [186] based on a stability result from [154] and has been transferred to the discrete-time case in [158]. There is also a number of publications dealing with the stabilization of PWA systems, i.e., state-dependent switching systems with affine subsystem dynamics. For example, Feng [50] studies the LMI-based design of piecewise linear controllers for uncertain PWA systems which achieve global stability or global stability with $\mathcal{H}_\infty$ performance. In [147], the Lyapunov-based design of both state and dynamic output feedback controllers has been cast as biconvex optimization problem and iterative algorithms for its suboptimal solution have been presented. In [146], the Lyapunov-based design of PWA control laws for PWA systems is formulated as optimization problem which is then relaxed to a finite set of convex optimization problems involving LMI constraints.

Less results are available for the stabilization of switched nonlinear systems and, to the best of our knowledge, there are no publications dealing with the control of time-varying switched systems (linear or nonlinear). In [180], an approach for the feedback stabilization of multi-input switched nonlinear system with two subsystems has been presented based on a common control Lyapunov function and an appropriate partitioning of the state space. However, there are no methods to systematically construct such a function for general switched systems, i.e., systems without a special structure. For switched nonlinear systems in strict feedback form, the *backstepping technique* has been applied in [181] and [118]. While the existence of a common stabilizing feedback function in every step of the iterative procedure is assumed in [181], Ma and Zhao [118] address the construction of such a function. Switched nonlinear feedforward systems are considered in [117] and the *integrator forwarding* technique is extended to obtain a control law that stabilizes

the system under arbitrary switching. In [25], another special class of switched nonlinear systems is studied, where all subsystems are in (generalized) Byrnes-Isidori canonical form. Under some further conditions, stabilization is achieved using the concept of Lyapunov functions with homogeneous derivatives. A model predictive control approach for switched systems has been presented in [123], which requires a control Lyapunov function for each individual subsystem. However, it is assumed that the switching signal is fixed a priori and thus the system is actually not a switched system, but a time-varying one (see Remark 2.4.1 and [78]).

In contrast to the LMI-based approaches mentioned above, the passivity-based controller design methodology presented in Chapter 6 is *completely analytic* and thus more in the spirit of classical techniques. Moreover, it is *constructive* in nature as opposed to the method in [180], which makes it necessary to guess a common control Lyapunov function, and, unlike the approaches in [25], [117], [118], [181], it is not restricted to a special class of switched systems. Furthermore, our approach is the first which is applicable also to time-varying switched systems.

1.3.3 Trajectory Tracking Control of Switched Systems

Even though output tracking in smooth systems has been widely studied (see e.g. [39], [71], [82], [83], [89], [110]) and is well understood by now, for switched systems, both the exact and the asymptotic output tracking problem pose different challenges due to the discontinuities in the dynamics. In spite of their practical relevance, few results are available on trajectory tracking control of switched systems. Some works deal with the trajectory tracking problem for switched systems with linear or affine subsystems. In [40], the EOT problem has been addressed for switched linear systems with predefined (finite) switching sequence (hence, the systems are not switched systems in the proper sense any more, see Remark 2.4.1). Li et al. [111] propose the design of a control law together with a class of average dwell time switching signals for switched linear time-varying delay systems such that the output tracks a reference signal. However, these reference signals are restricted to belong either to the class of square integrable ($\mathcal{L}_2$) signals or to a set of constants or step inputs. Moreover, the tracking error does not tend to zero, but instead the tracking performance is intended to be optimal with regard to some performance index.

While in the latter papers the switching is trajectory-independent, most of the publications that are concerned with the tracking problem for switched linear systems deal with the case of state-dependent switching. Sakurama and Sugie [148] consider bimodal PWA systems and address the problem of asymptotically tracking a desired output trajectory,

which is generated by another PWA system. However, the conditions for the existence of the proposed controller are, in general, very difficult to check. The authors also consider a special case, where the conditions become somewhat simpler, with one major restriction being, however, that the switching law may only depend on the tracking output. In [182] and [185], Wu and Ben Amara are concerned with the design of a regulator for switched bimodal linear systems which makes the system output asymptotically track a known sinusoidal reference trajectory while simultaneously being able to reject known sinusoidal disturbances. The approach makes use of the Q parametrization of regulators for the switched system and the proposed synthesis method is based on iteratively solving a set of LMIs. A decisive feature of the considered class of systems is, however, that switching from one mode to the other occurs when the regulation error exceeds or falls below a prescribed *nonzero* value, i.e., in the context of exact output tracking, systems of this type actually reduce to *non-switched* linear systems. Moreover, only sinusoidal reference trajectories are considered. In [183], the authors are concerned with the same class of systems, only in discrete time, and they adopt a similar approach in order to achieve adaptive output regulation against unknown sinusoidal exogenous inputs representing reference or disturbance signals. To this end, the Q-parameters are tuned online by an adaptation algorithm. In [184], this approach is applied to an experimental setup motivated by the flying height regulation problem in hard disk drives.

Galeani et. al [62] address the AOT problem for linear switched systems with state-dependent switching law whose state trajectories may be discontinuous at the switching times. The considered reference trajectories are periodic and parametrized as the output of an undriven exosystem. The approach is based on a discontinuous version of the classic internal model principle and the feedback gain design is done by iteratively solving a set of LMIs. In order to guarantee the existence of closed loop solution trajectories for an open set of initial conditions, the reference trajectories are assumed to be "admissible" meaning that the EOT problem is solvable for these trajectories. The authors note that "*guaranteeing the existence of admissible periodic references [...] for hybrid systems is, in general, rather complicated*". However, the problem of identifying such trajectories is not addressed in detail, but only some comments are provided.

While the aforementioned works deal with the output trajectory tracking problem, which is studied also in this thesis, in [173], the closely related problem of asymptotically tracking a desired state trajectory is addressed for multi-modal PWA systems. Both a state feedback and an observer-based output feedback control design are proposed instrumentalizing the results in [143] on convergence properties of PWA systems. In general, the presented approach requires the solution of a set of bilinear matrix inequalities, which is usually a

nontrivial task. To guarantee the solvability of the tracking problem, it is assumed that the desired state trajectory is an admissible solution of the system, i.e., that it can be tracked exactly.

Bernardo et al. [42] propose a model reference adaptive control scheme for bimodal PWA systems, where the objective is to track the states of a reference model either with a bounded error or asymptotically. However, both subsystems are assumed to be in controller canonical form, which means that the subsystems differ only in their actuated portions, and the overall system is assumed to be continuous at the switching surface. The approach utilizes the extension of passivity theory to switched systems presented in [194]. A preliminary experimental validation of the approach is presented in [41]. Recently, in [44] the authors have proposed a similar approach for multimodal PWA systems, where again all subsystems are assumed to be in controller canonical form.

To the best of our knowledge, there are no publications dealing with the exact or asymptotic output trajectory tracking problem for nonlinear switched systems in a general context. In [57], [94] the AOT problem is studied for a particular nonlinear system, namely a self-supplied variable displacement axial piston pump, which is considered as an example in Section 8.2. The mathematical model of this device is switching between two modes depending on the sign of the control input – a case which, apart from these two works, has not been addressed in the literature, yet, even for linear switched systems. In Chapter 7, we investigate for the first time the EOT and the AOT problem for *nonlinear* bimodal switched SISO systems and, in the case of trajectory-dependent switching, we allow the switching law to depend not only on the state but *also on the input*. The reference trajectories may be arbitrary smooth functions, i.e., we do not assume them to be periodic or to be generated by an exosystem as done in many of the works mentioned above. We obtain *easily checkable* conditions for the solvability of the EOT problem, and, for two classes of switched systems, we give results which considerably facilitate the design of a two-degree-of-freedom controller that solves the AOT problem.

1.4 Outline of the Thesis

The thesis starts with a review of some preliminaries in Chapter 2. The remainder of the thesis is divided into two parts labeled by I and II. The first part contains the Chapters 3–5 and is dedicated to smooth dynamical systems. Chapter 3 is devoted to the estimation of the DA based on the energy function assigned by the IDA method. The effective design of an IDA controller with an as large as possible estimated DA and desired closed loop performance is addressed in Chapter 4. The illustration and validation of the methods

presented in the preceding Chapters by means of examples is the subject of Chapter 5. The second part of the thesis comprises the Chapters 6–8 and is devoted to the control of switched nonlinear systems. In Chapter 6, the passivity-based stabilization of this class of systems is studied, while in Chapter 7 the exact and asymptotic output tracking problems are investigated. The proposed methods are validated using two technical examples in Chapter 8, and the thesis is concluded in Chapter 9. Appendix A reviews some mathematical background and Appendix B contains some technical proofs.

1.5 Notation

We denote by $\mathbb{R}$ the set of real numbers, by $\mathbb{R}^+$ the set of (strictly) positive real numbers, and by $\mathbb{R}_0^+$ the set of nonnegative real numbers. Furthermore, $\mathbb{N}$ is the set of positive integers and $\mathbb{N}_0$ the set of nonnegative integers. The n-dimensional real Euclidean space is denoted by $\mathbb{R}^n$, and $\mathbb{R}^{n\times m}$ is the set of real $n \times m$ dimensional matrices. The n-dimensional complex Euclidean space is referred to as $\mathbb{C}^n$, and the set of $n \times m$ dimensional complex matrices as $\mathbb{C}^{n\times m}$. A usual convention adopted in this thesis (though not exhaustively) is that scalars are denoted by lower case letters, vectors by bold lower case letters, and matrices by bold upper case letters. We refer to the ith component of a vector $\mathbf{x} \in \mathbb{R}^n$ as x_i, and to the (i, j)-entry of a matrix $\mathbf{M}$ as m_{ij}. We use the notation $\mathbf{M} = [m_{ij}]$, $i = 1, \ldots, n$, $j = 1, \ldots, m$ for an $n \times m$ dimensional matrix with the entries m_{ij}, and $\mathbf{M} = \operatorname{diag}\{m_{11}, \ldots, m_{nn}\}$ is an $n \times n$ dimensional diagonal matrix. The transpose of a matrix $\mathbf{M} \in \mathbb{C}^{n\times m}$ is $\mathbf{M}^T$, its conjugate complex is $\overline{\mathbf{M}}$, its conjugate transpose is $\mathbf{M}^* = \overline{\mathbf{M}}^T$, and its pseudoinverse is $\mathbf{M}^\dagger$. Furthermore, the inverse of an $n \times n$-dimensional matrix $\mathbf{M}$ is denoted by $\mathbf{M}^{-1}$, the transpose and the conjugate transpose of the inverse are denoted by $\mathbf{M}^{-T}$ and $\mathbf{M}^{-*}$, respectively. The range (column space) of a matrix $\mathbf{M}$ is denoted by $\mathcal{R}\{\mathbf{M}\}$ and the nullspace (kernel) by $\mathcal{N}\{\mathbf{M}\}$. We use $\mathbf{M} > 0$ ($\geq$, $<$, $\leq$) to denote a positive definite (positive semidefinite, negative definite, negative semidefinite) matrix $\mathbf{M}$. For $\mathbf{x} \in \mathbb{R}^n$, we denote by $\|\mathbf{x}\|$ the Euclidean vector norm, i.e., $\|\mathbf{x}\| = (\mathbf{x}^T\mathbf{x})^{1/2}$. Moreover, $\mathbf{I}_n$ is the n-dimensional unity matrix and $\mathbf{0}_{n\times m}$ the $n \times m$ dimensional zero matrix.

We denote by $\mathcal{C}^k$ the set of continuous functions that are at least k-times continuously differentiable. The gradient of a scalar $\mathcal{C}^1$ function $f : \mathbb{R}^n \to \mathbb{R}$ with respect to $\mathbf{x}$ is denoted by $\nabla_x f(\mathbf{x})$ and, by convention, is a column vector, whereas $\frac{\partial}{\partial \mathbf{x}} f(\mathbf{x})$ is a row vector, which is consistent with the usual definition of the Jacobian, i.e., $\nabla_x f(\mathbf{x}) = [\frac{\partial}{\partial \mathbf{x}} f(\mathbf{x})]^T$. The Hessian of a scalar $\mathcal{C}^2$ function $f : \mathbb{R}^n \to \mathbb{R}$ is denoted by $\nabla_x^2 f(\mathbf{x})$. The transpose of the gradient will oftentimes be denoted as $\nabla^T H(\mathbf{x}) = [\nabla H(\mathbf{x})]^T$. When clear from the context, the subindex of the operator ∇ as well as the arguments of functions will be omitted. For

a function $f(\cdot)$ with time-dependent arguments, e.g. $f(\mathbf{x}(t), \mathbf{y}(t))$, we will sometimes write $f(t)$ if we want to stress especially the time-dependency. Given a signal $\mathbf{z}$, we denote by $\mathbf{z}(t^-)$ the limit of $\mathbf{z}(\tau)$ as $\tau \to t$ from below, i.e., $\mathbf{z}(t^-) = \lim_{\tau \uparrow t} \mathbf{z}(\tau)$, and $\mathbf{z}(t^+)$ is defined accordingly. Moreover, we use the notation $\frac{d}{dt}(\cdot) = \dot{(\cdot)}$ for the total time derivative.

We denote the boundary of a set S by ∂S, its interior by intS, its closure by $\overline{\mathrm{S}}$ and its complement by S^c.

Chapter 2

Preliminaries

In this chapter, we introduce some further notation and recall some basic concepts and methods used throughout this thesis. First, we elaborate on the notion of the domain of attraction of asymptotically stable equilibria and its estimation by means of Lyapunov functions. We review the passivity-based control methodology *Interconnection and Damping Assignment (IDA)* [132], [140] and the recent approach of *Local Linear Dynamics Assignment (LLDA)* [102], [103], that enables the transparent tuning of IDA controllers. Further, we provide the basic mathematical framework within which we study switched systems in Part II of this thesis, and we review some results on the stability of this class of systems. Moreover, we outline an approach from [66] that is utilized in Section 3.4. It extends the Theorem of Ehlich and Zeller [47] in order to obtain numerically computable bounds for real valued functions.

2.1 Stability of Equilibria and the Domain of Attraction

One of our concerns in this thesis is the estimation and the maximization of the *domain of attraction*[1] *(DA)* of an equilibrium in the context of IDA. Therefore, this section briefly reviews the concept of the DA and its Lyapunov-based estimation for both time-invariant and time-varying systems. For a general introduction to nonlinear dynamical systems the reader is referred to the excellent books [95], [150], and [176].

2.1.1 Time-Invariant Systems

Consider the nonlinear time-invariant dynamical system

$$\dot{\mathbf{x}} = \mathbf{f}(\mathbf{x}) \ , \quad \mathbf{x}(t_0) = \mathbf{x}_0 \tag{2.1}$$

[1] Some authors use also use the terms “region of attraction”, “basin of attraction”, or “stability region” instead of “domain of attraction”.

where $\mathbf{x} \in \mathbb{R}^n$ and $\mathbf{f} : \mathbb{R}^n \to \mathbb{R}^n$ is locally Lipschitz. The solution of (2.1) starting from $\mathbf{x}_0$ at the initial time $t_0 \geq 0$ is denoted as $\mathbf{x}(t; \mathbf{x}_0, t_0)$, so that $\mathbf{x}(t_0; \mathbf{x}_0, t_0) = \mathbf{x}_0$. In the time-invariant case, it holds for any $T \in \mathbb{R}$ that $\mathbf{x}(t+T; \mathbf{x}_0, t_0+T) = \mathbf{x}(t; \mathbf{x}_0, t_0)$. Therefore, we assume, without loss of generality, that $t_0 = 0$ and write $\mathbf{x}(t; \mathbf{x}_0)$ instead of $\mathbf{x}(t; \mathbf{x}_0, 0)$. In the following, we are concerned with the stability and the DA of equilibrium points of (2.1). Recall that a vector $\mathbf{x}^*$ is an equilibrium of (2.1) if $\mathbf{f}(\mathbf{x}^*) = \mathbf{0}$.

Definition 2.1.1. An equilibrium point $\mathbf{x}^*$ of (2.1) is *stable* if, for each $\epsilon > 0$, there exists a $\delta = \delta(\epsilon) > 0$ such that

$$\|\mathbf{x}_0 - \mathbf{x}^*\| < \delta \quad \Rightarrow \quad \|\mathbf{x}(t, \mathbf{x}_0) - \mathbf{x}^*\| < \epsilon \tag{2.2}$$

holds for all $t \geq 0$. If, in addition, there is a $\zeta > 0$ such that $\|\mathbf{x}_0 - \mathbf{x}^*\| < \zeta$ implies that $\lim_{t\to\infty} \mathbf{x}(t, \mathbf{x}_0) = \mathbf{x}^*$, then $\mathbf{x}^*$ is said to be *asymptotically stable*.

If the considered equilibrium point $\mathbf{x}^*$ is clear from the context, we will sometimes say, with some abuse of terminology, that a system is stable, meaning that $\mathbf{x}^*$ is a stable equilibrium of the system. From a practical viewpoint, it is of great interest how far from an asymptotically stable equilibrium point the trajectory may be and still converge to this equilibrium. This leads us to the concept of the DA.

Definition 2.1.2. The *domain of attraction* (DA) of an asymptotically stable equilibrium $\mathbf{x}^*$ of (2.1) is the set of initial conditions

$$\mathrm{A}(\mathbf{x}^*) = \left\{ \mathbf{x}_0 \in \mathbb{R}^n \,\middle|\, \lim_{t\to+\infty} \mathbf{x}(t, \mathbf{x}_0) = \mathbf{x}^* \right\}. \tag{2.3}$$

The DA is an open, invariant, and connected set. Its boundary $\partial\mathrm{A}(\mathbf{x}^*)$ is called the *stability boundary* (SB) of $\mathbf{x}^*$ and is an $(n-1)$-dimensional closed, invariant set. As mentioned in Section 1.3, the problem of determining the exact DA for general nonlinear systems is unsolved up to now. However, an inner approximation can be obtained by instrumentalizing extensions of Lyapunov's theory due to Barbashin and Krasovskii [9] and La Salle [106].

To this end, let us first introduce some notation. We will call a function $V : \mathbb{R}^n \to \mathbb{R}$ *locally positive definite at* $\mathbf{x}^*$ if there is an open neighborhood $\Omega \subset \mathbb{R}^n$ of $\mathbf{x}^*$ such that $V(\mathbf{x}^*) = 0$ and $V(\mathbf{x}) > 0 \; \forall \, \mathbf{x} \in \Omega \backslash \{\mathbf{x}^*\}$. It is called *locally positive semidefinite at* $\mathbf{x}^*$ if $V(\mathbf{x}^*) = 0$ and the weaker condition $V(\mathbf{x}) \geq V(\mathbf{x}^*), \; \forall \, \mathbf{x} \in \Omega$ holds. A *sublevel set* of a $\mathcal{C}^r$, $r > 0$ function $V(\mathbf{x})$ is defined as

$$\mathrm{S}_c^V = \{ \mathbf{x} \in \mathbb{R}^n | \, V(\mathbf{x}) < c \} \tag{2.4}$$

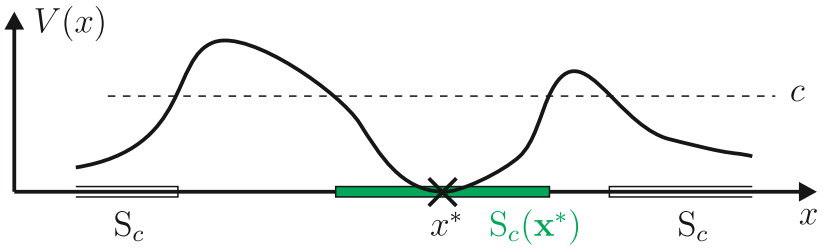

Figure 2.1: Connected components of a level set S_c.

with some constant $c \in \mathbb{R}$. When clear from the context, the superscript of S_c will be omitted. The closure of S_c is $\overline{\mathrm{S}}_c = \{\mathbf{x} \in \mathbb{R}^n | V(\mathbf{x}) \leq c\}$. Its boundary $\partial \mathrm{S}_c = \{\mathbf{x} \in \mathbb{R}^n | V(\mathbf{x}) = c\}$ is called *level set*. If c is a *regular value*[2] of $V(\mathbf{x})$, then, by the implicit function theorem, $\partial \mathrm{S}_c$ is an $(n-1)$-dimensional $\mathcal{C}^r$ submanifold of $\mathbb{R}^n$. In general, S_c consists of multiple *connected components* (see Figure 2.1). The connected component of S_c that contains $\mathbf{x}^*$ is denoted by $\mathrm{S}_c(\mathbf{x}^*)$ [if $c < V(\mathbf{x}^*)$, then $\mathrm{S}_c(\mathbf{x}^*) = \emptyset$]. We are ready to formulate the following theorem.

Theorem 2.1.1 (Krasovskii-LaSalle)**.** *Let $\mathbf{x}^*$ be an equilibrium of the system (2.1) and suppose there exists a $\mathcal{C}^1$ function $V : \mathbb{R}^n \to \mathbb{R}$ which is locally positive definite at $\mathbf{x}^*$ and a neighborhood $\Omega^{\dot{V}} \subset \mathbb{R}^n$ of $\mathbf{x}^*$ such that*

$$\dot{V}(\mathbf{x}) = \frac{d}{dt} V(\mathbf{x}) = \frac{\partial V(\mathbf{x})}{\partial \mathbf{x}} \mathbf{f}(\mathbf{x}) \leq 0 \tag{2.5}$$

holds for all $\mathbf{x} \in \Omega^{\dot{V}}$. If $c > 0$ is such that $\overline{\mathrm{S}}_c(\mathbf{x}^*) \subset \Omega^{\dot{V}}$, then $\overline{\mathrm{S}}_c(\mathbf{x}^*)$ is a positively invariant set. If in addition $\overline{\mathrm{S}}_c(\mathbf{x}^*)$ is bounded and the set

$$\mathrm{E} = \left\{ \mathbf{x} \in \overline{\mathrm{S}}_c(\mathbf{x}^*) \,\middle|\, \dot{V}(\mathbf{x}) = 0 \right\} \tag{2.6}$$

contains no trajectories of (2.1) except for $\mathbf{x}(t) \equiv \mathbf{x}^*$, then $\mathbf{x}^*$ is asymptotically stable and any solution starting in $\mathbf{x} \in \overline{\mathrm{S}}_c(\mathbf{x}^*)$ approaches $\mathbf{x}^*$ for $t \to \infty$.

Thus, a necessary condition is that $\overline{\mathrm{S}}_c(\mathbf{x}^*)$ contains no other equilibrium points than $\mathbf{x}^*$. A positive definite function $V(\mathbf{x})$ satisfying (2.5) is commonly referred to as *Lyapunov function*. It gets immediately clear that, under the conditions of the theorem, $\overline{\mathrm{S}}_c(\mathbf{x}^*)$ is contained in the DA of $\mathbf{x}^*$ and gives an inner approximation thereof.

[2]Recall that c is called a regular value of $V : \mathbb{R}^n \to \mathbb{R}$, if $\nabla V(\mathbf{x}) \neq \mathbf{0}$ holds for all $\mathbf{x} \in V^{-1}(c)$.

2.1.2 Time-Varying Systems

An unforced time-varying system is described for all $t \geq 0$ by a differential equation of the form

$$\dot{\mathbf{x}} = \mathbf{f}(\mathbf{x}, t) \ , \quad \mathbf{x}(t_0) = \mathbf{x}_0 \tag{2.7}$$

where $\mathbf{f} : \mathbb{R}^n \times [0, \infty) \to \mathbb{R}^n$ is locally Lipschitz and piecewise continuous in t. A vector $\mathbf{x}^*$ is an equilibrium of (2.7) if $\mathbf{f}(\mathbf{x}^*, t) = \mathbf{0}, \ \forall\, t \geq 0$. In contrast to the time-invariant case, the solutions of (2.7) are not invariant under a translation of t_0. As a consequence, it is not without loss of generality to assume that $t_0 = 0$ and hence we cannot omit the corresponding argument in $\mathbf{x}(t; \mathbf{x}_0, t_0)$. Moreover, the Definitions 2.1.1 and 2.1.2 need to be refined to account for the fact that the stability properties of a time-varying system may depend on t_0.

Definition 2.1.3. An equilibrium point $\mathbf{x}^*$ of (2.7) is

- *stable*, if, for each $\epsilon > 0$, there is a $\delta = \delta(\epsilon, t_0) > 0$ such that

$$\|\mathbf{x}_0 - \mathbf{x}^*\| < \delta \quad \Rightarrow \quad \|\mathbf{x}(t; \mathbf{x}_0, t_0) - \mathbf{x}^*\| < \epsilon \ , \quad \forall\, t \geq t_0 \geq 0 \ . \tag{2.8}$$

- *uniformly stable*, if δ can be chosen independently of t_0, i.e., $\delta = \delta(\epsilon)$.

- *asymptotically stable*, if it is stable and there is a $\zeta = \zeta(t_0) > 0$ such that $\|\mathbf{x}_0 - \mathbf{x}^*\| < \zeta$ implies that $\mathbf{x}(t; \mathbf{x}_0, t_0) \to \mathbf{x}^*$ as $t \to \infty$.

- *uniformly asymptotically stable*, if it is uniformly stable and there is a $\zeta > 0$ such that $\|\mathbf{x}_0 - \mathbf{x}^*\| < \zeta$ implies that $\mathbf{x}(t; \mathbf{x}_0, t_0)$ converges to $\mathbf{x}^*$ uniformly in t_0, i.e., for each ϵ there is $T = T(\epsilon)$ such that

$$\|\mathbf{x}_0 - \mathbf{x}^*\| < \zeta \quad \Rightarrow \quad \|\mathbf{x}(t; \mathbf{x}_0, t_0) - \mathbf{x}^*\| < \epsilon \ , \ \forall\, t \geq t_0 + T(\epsilon) \ . \tag{2.9}$$

Definition 2.1.4. The *domain of attraction* of a uniformly asymptotically stable equilibrium $\mathbf{x}^*$ of (2.7) is the set of initial conditions

$$\mathrm{A}(\mathbf{x}^*) = \left\{ \mathbf{x}_0 \in \mathbb{R}^n \middle| \lim_{t \to +\infty} \mathbf{x}(t; \mathbf{x}_0, t_0) = \mathbf{x}^* \ , \ \forall\, t_0 \in [0, \infty) \right\} . \tag{2.10}$$

Note that, according to this definition, a point $\mathbf{x}_0$ belongs to the DA only if for *any* initial time t_0 the trajectory starting from this point converges to the equilibrium $\mathbf{x}^*$. Hence, it is somewhat different from the definitions in [176] and [150], where the DA is defined for

a particular initial time t_0. Also in the time-varying case, an estimate of the DA can be obtained by means of a Lyapunov function, which may in general also depend explicitly on the time t. The following theorem is a direct consequence of the Theorems 3.8 and 4.4 in [95] and the proof of the latter[3].

Theorem 2.1.2. *Let $\mathbf{x}^*$ be an equilibrium of the system (2.1) and suppose there exists a $\mathcal{C}^1$ function $V : \mathbb{R}^n \times [0,\infty) \to \mathbb{R}$ and an open neighborhood $\Omega^W \subset \mathbb{R}^n$ of $\mathbf{x}^*$ such that*

$$W_1(\mathbf{x}) \leq V(\mathbf{x},t) \leq W_2(\mathbf{x}) \tag{2.11}$$

$$\dot{V}(\mathbf{x},t) = \frac{\partial V(\mathbf{x},t)}{\partial t} + \frac{\partial V(\mathbf{x},t)}{\partial \mathbf{x}}\mathbf{f}(\mathbf{x},t) \leq -W_3(\mathbf{x}) \tag{2.12}$$

$\forall\, t \in [0,\infty)$, $\forall\, \mathbf{x} \in \Omega^W$, where the $W_i : \mathbb{R}^n \to \mathbb{R}$, $i = 1,2,3$ satisfy

$$W_i(\mathbf{x}^*) = 0\ , \quad W_i(\mathbf{x}) > W_i(\mathbf{x}^*)\ ,\ \forall\, \mathbf{x} \in \Omega^W \backslash \{\mathbf{x}^*\}\ . \tag{2.13}$$

Then $\mathbf{x}^*$ is uniformly asymptotically stable. If $c > 0$ is such that $\overline{\mathrm{S}}_c^{W_1}(\mathbf{x}^*)$ is bounded and contained in Ω^W, then all solutions of (2.7) with $\mathbf{x}_0 \in \overline{\mathrm{S}}_c^{W_2}(\mathbf{x}^*)$ stay in $\overline{\mathrm{S}}_c^{W_1}(\mathbf{x}^*)$ and converge to $\mathbf{x}^*$ as $t \to \infty$.

If a time-varying function satisfies the left inequality in (2.11), it is said to be positive definite at $\mathbf{x}^*$, if it fulfills the right inequality, it is called *decrescent*. The above theorem makes clear that $\overline{\mathrm{S}}_c^{W_2}(\mathbf{x}^*)$ is contained in the DA and thus represents an inner approximation thereof. Note that we have presumed above that $W_3(\mathbf{x})$ is *strictly* positive in $\Omega^W \backslash \{\mathbf{x}^*\}$ implying that $\dot{V}(\mathbf{x},t)$ is strictly negative within this set. This is in contrast to the time-invariant case treated in the previous subsection, where we have required only $\dot{V}(\mathbf{x}) \leq 0$. The reason is that there is no extension of Theorem 2.1.1 to general time-varying systems, but only to special classes like periodic systems (see e.g. [176]) or asymptotically autonomous systems (see Section 4.3 in [95] for a short discussion on that topic).

2.2 Passivity-Based Control

This section provides the theoretical background of passivity-based control that will be needed in this thesis. For a more complete overview over the field, the reader is referred

[3] The theorem is stated somewhat different, but it is straightforward to adapt the proof to our formulation. In fact, the ball B_r in the proof of Theorem 4.4 in [95] is only utilized to ensure that the sublevel set of $W_1(\mathbf{x})$ is bounded.

to the books [46], [134], [174]. In the first subsection, we motivate the basic idea of passivity-based control by recalling some properties of passive systems. We then introduce the class of port-Hamiltonian systems, which are passive by nature. Based on that, we present the IDA method, which is the passivity-based control approach we will concentrate on in this thesis.

2.2.1 Dissipativity and Passivity

In this subsection, we briefly review the concepts of dissipativity and passivity as well as some related results that are relevant for the remainder. For a more general treatment the reader is referred to [174] or [179]. Originally, the notion of passivity was used in network theory to characterize rational transfer functions that can be realized solely with positive resistances, capacitances and inductances. But already in the 1960's it was studied in a control theoretic context due to its connection to stability (see e.g. [190]). While before passivity had been treated as pure input-output property, in the early 1970's Willems [179] studied passivity and the more general concept of dissipativity for nonlinear systems in state space representation and provided a system theoretic framework by introducing the notions of *storage function* and *supply rate*.

Consider a nonlinear system described by

$$\dot{\mathbf{x}} = \mathbf{f}(\mathbf{x}) + \mathbf{G}(\mathbf{x})\mathbf{u} \tag{2.14a}$$

$$\mathbf{y} = \mathbf{h}(\mathbf{x}) \tag{2.14b}$$

with the state $\mathbf{x} \in \mathbb{R}^n$, the control input $\mathbf{u} \in \mathbb{R}^m$, and the output $\mathbf{y} \in \mathbb{R}^m$, and let $\mathbf{f}(\mathbf{x})$, $\mathbf{G}(\mathbf{x})$, and $\mathbf{h}(\mathbf{x})$ be smooth functions. Further, suppose that $\mathbf{f}(\mathbf{x}^*) = \mathbf{0}$. For a particular $\mathbf{u}(t)$ the solution of (2.14a) is denoted as $\mathbf{x}(t; \mathbf{x}_0, \mathbf{u})$. We define the function $w : \mathbb{R}^m \times \mathbb{R}^m \to \mathbb{R}$, called the supply rate, and assume that for all $\mathbf{u} \in \mathbb{R}^m$ and all $\mathbf{x}_0 \in \mathbb{R}^n$ the output $\mathbf{y}(t) = \mathbf{h}(\mathbf{x}(t, \mathbf{x}_0, \mathbf{u}))$ of (2.14) is such that $\int_0^t |w(\mathbf{u}(\tau), \mathbf{y}(\tau))|\, d\tau < \infty$ holds for all $t \geq 0$.

Definition 2.2.1. The system (2.14) is said to be *dissipative* with supply rate w if there exists a $\mathcal{C}^0$ nonnegative function $H : \mathbb{R}^n \to \mathbb{R}$, called the *storage function*, such that for all $\mathbf{u} \in \mathbb{R}^m$, $\mathbf{x}_0 \in \mathbb{R}^n$, $t \geq 0$

$$H\left(\mathbf{x}(t)\right) - H\left(\mathbf{x}_0\right) \leq \int_0^t w\left(\mathbf{u}(\tau), \mathbf{y}(\tau)\right)\, d\tau\ . \tag{2.15}$$

Definition 2.2.2. The system (2.14) is said to be *passive*, if it is dissipative with the supply rate $w(\mathbf{u}, \mathbf{y}) = \mathbf{y}^T \mathbf{u}$.

The storage function can be interpreted as the energy of the system, the supply rate is the input power, and $\int_0^t w(\mathbf{u}(\tau), \mathbf{y}(\tau))\, d\tau$ is the energy supplied to the system from outside. Hence, what makes up a dissipative system is that the increase in its energy cannot be more than the energy supplied to it from outside. In other words, a dissipative system does not contain energy sources.

If the storage function is continuously differentiable, (2.15) is equivalent to $\dot{H}(\mathbf{x}) \leq w(\mathbf{u}, \mathbf{y})$ which is called the *differential dissipation inequality* and in case of passivity amounts to

$$\dot{H}(\mathbf{x}) \leq \mathbf{y}^T \mathbf{u} \,. \tag{2.16}$$

From (2.16), we see that for $\mathbf{u} \equiv \mathbf{0}$ the storage function satisfies $\dot{H}(\mathbf{x}) \leq 0$. Consequently, if $H(\mathbf{x})$ is positive definite at $\mathbf{x}^*$, it qualifies as a Lyapunov function and we can conclude that $\mathbf{x}^*$ is a stable equilibrium of the unforced system. Asymptotic stability can be established invoking the Krasovskii-LaSalle Theorem 2.1.1. To reinforce negativity of $\dot{H}(\mathbf{x})$, additionally a feedback of the form $\mathbf{u} = -\mathbf{K}_u \mathbf{y}$ with $\mathbf{K}_u > 0$ can be applied, which is known as *damping injection* or L_gV control[4]. If the system is zero-state detectable (see e.g. Definition 3.2.7 in [174]), by this means, asymptotic stability is achieved. This motivates the *passivity-based control* approach, which aims to render the closed loop system passive with respect to a desired storage function in order to achieve asymptotic stability of the desired equilibrium point.

2.2.2 Port-Hamiltonian Systems

In this subsection, we briefly describe the class of *port-Hamiltonian*[5] *(pH)* systems and review some of their properties. For further details we refer the reader to the important monograph [174] and the recent book [46]. Port-Hamiltonian systems can be regarded as a generalization of the well-known Hamiltonian systems, which are frequently used in mechanics. They naturally arise from network modeling of lumped-parameter physical systems and are inherently passive. In this thesis, we confine our attention to input-state-

[4]The name L_gV control stems from the fact that according to the *Hill-Moylan conditions* [81] the output must satisfy $\mathbf{y} = \mathbf{h}(\mathbf{x}) = L_gV(\mathbf{x})$, if the system is passive with storage function $V(\mathbf{x})$.

[5]We remark that systems of this type are also referred to as *port-controlled Hamiltonian systems with dissipation (PCHD systems)*, e.g. in [174], or as *port-controlled Hamiltonian (PCH systems)* systems, e.g. in [140].

output pH systems, which do not involve algebraic constraints, and are of the form

$$\dot{\mathbf{x}} = [\mathbf{J}(\mathbf{x}) - \mathbf{R}(\mathbf{x})] \nabla H(\mathbf{x}) + \mathbf{G}(\mathbf{x})\mathbf{u} \tag{2.17a}$$

$$\mathbf{y} = \mathbf{G}^T(\mathbf{x})\nabla H(\mathbf{x}) \tag{2.17b}$$

where $\mathbf{x} \in \mathbb{R}^n$ are the energy variables. The *port variables* $\mathbf{u}$ and $\mathbf{y}$ are conjugated variables, i.e., their product gives the power exchanged between the system and its environment (e.g. forces and velocities in a mechanical system). The $\mathcal{C}^1$ *Hamiltonian function* $H : \mathbb{R}^n \to \mathbb{R}$ represents the total energy stored in the system. The *interconnection matrix* $\mathbf{J} : \mathbb{R}^n \to \mathbb{R}^{n\times n}$ is skew symmetric $\mathbf{J}^T(\mathbf{x}) = -\mathbf{J}(\mathbf{x})$ and captures the internal interconnection structure of the system, while the full rank input matrix $\mathbf{G} : \mathbb{R}^n \to \mathbb{R}^{n\times m}$ represents the interconnection of the system with its environment. The *dissipation matrix* $\mathbf{R} : \mathbb{R}^n \to \mathbb{R}^{n\times n}$ is positive semidefinite $\mathbf{R}^T(\mathbf{x}) = \mathbf{R}(\mathbf{x}) \geq 0$ and specifies the resistive structure of the system.

Using the skew symmetry of $\mathbf{J}(\mathbf{x})$ we obtain

$$\dot{H}(\mathbf{x}) = -\nabla^T H(\mathbf{x})\mathbf{R}(\mathbf{x})\nabla H(\mathbf{x}) + \mathbf{y}^T\mathbf{u} \tag{2.18}$$

for the rate of change of the system's energy, where the first term on the right hand side describes the dissipation of energy in the resistive elements of the system. This term is nonpositive due to $\mathbf{R}(\mathbf{x}) \geq 0$ and hence we see that $\dot{H}(\mathbf{x}) \leq \mathbf{y}^T\mathbf{u}$. Consequently, if $H(\mathbf{x})$ is bounded from below[6], the pH system (2.17) is passive with storage function $H(\mathbf{x})$. This suggests that the passivation problem can be solved by assigning a pH structure to the closed-loop system, leading to the IDA methodology treated in the next subsection.

2.2.3 Interconnection and Damping Assignment

The IDA methodology was first proposed in [140] for the stabilization of physical systems described by pH models, and was then generalized in [132] to general affine systems of the form (2.14a). The central idea of IDA is to determine a static feedback law $\mathbf{u} = \mathbf{r}(\mathbf{x}) + \mathbf{v}$ that transforms (2.14a) into pH form, i.e.,

$$\mathbf{f}(\mathbf{x}) + \mathbf{G}(\mathbf{x})\left[\mathbf{r}(\mathbf{x}) + \mathbf{v}\right] \stackrel{!}{=} \left[\mathbf{J}(\mathbf{x}) - \mathbf{R}(\mathbf{x})\right]\nabla H(\mathbf{x}) + \mathbf{G}(\mathbf{x})\mathbf{v} \tag{2.19}$$

where $\mathbf{J}(\mathbf{x})$ and $\mathbf{R}(\mathbf{x})$ are the desired structure and dissipation matrix, respectively, and $H(\mathbf{x})$ is the desired energy function. The equation (2.19) is called *matching equation*. To

[6]With respect to the Definitions 2.2.1 and 2.2.2 note that, if $H(\mathbf{x})$ is bounded from below, it can be made nonnegative by simply adding a constant.

simplify the notation in the following, we introduce the matrix

$$\mathbf{F}(\mathbf{x}) = \mathbf{J}(\mathbf{x}) - \mathbf{R}(\mathbf{x}) \tag{2.20}$$

and refer to it as *design matrix* since it is selected by the control designer (the fact that the interconnection and dissipation structure of the closed loop system is specified by the designer actually led to the name IDA). Considering the symmetry properties of $\mathbf{J}(\mathbf{x})$ and $\mathbf{R}(\mathbf{x})$ it clearly holds that

$$\mathbf{R}(\mathbf{x}) = -\text{sym}\left\{\mathbf{F}(\mathbf{x})\right\} \ , \quad \text{where} \quad \text{sym}\left\{\mathbf{F}(\mathbf{x})\right\} = \frac{1}{2}\left[\mathbf{F}(\mathbf{x}) + \mathbf{F}^T(\mathbf{x})\right] \ . \tag{2.21}$$

The energy function is required to have an isolated minimum at the desired equilibrium $\mathbf{x}^*$, i.e., there must exist a neighborhood Ω of $\mathbf{x}^*$ such that

$$H(\mathbf{x}) > H(\mathbf{x}^*) \ , \quad \forall\, \mathbf{x} \in \Omega \backslash \{\mathbf{x}^*\} \ . \tag{2.22}$$

Since our primary goal is the (local) stabilization of $\mathbf{x}^*$ it is sufficient that, unlike in the previous section, the dissipation matrix $\mathbf{R}(\mathbf{x}) = -\text{sym}\{\mathbf{F}(\mathbf{x})\}$ is positive semidefinite only in an open neighborhood $\Omega^R \subset \mathbb{R}^n$ of $\mathbf{x}^*$. Then, there is an open neighborhood $\Omega^{\dot{H}}$ of $\mathbf{x}^*$ such that, with $\mathbf{v} = \mathbf{0}$, it holds for all $\mathbf{x} \in \Omega^{\dot{H}}$ that

$$\dot{H}(\mathbf{x}) = -\nabla^T H(\mathbf{x}) \mathbf{R}(\mathbf{x}) \nabla H(\mathbf{x}) \leq 0 \ . \tag{2.23}$$

Hence, the energy function qualifies as a Lyapunov function[7] for the closed loop system and can be used to establish (asymptotic) stability of $\mathbf{x}^*$.

Clearly, it holds that $\Omega^R \subset \Omega^{\dot{H}}$, but in general $\Omega^{\dot{H}}$ is larger than Ω^R. This is due to the fact that positive semidefiniteness of the dissipation matrix is necessary and sufficient for $\nabla^T H \mathbf{R} \nabla H \geq 0$ only if $\mathbf{R}$ is not a function of the states. Otherwise the expression cannot be looked upon as pure quadratic form and $\mathbf{R}(\mathbf{x}) \geq 0$ is only sufficient. In case that $\Omega^{\dot{H}} \neq \mathbb{R}^n$, the inequality (2.16) is also satisfied only locally and hence (with some abuse of notation) the closed loop system is "locally passive" with the new input $\mathbf{v}$ and the output $\mathbf{y} = \mathbf{G}^T \nabla H$.

It is immediately seen that there is a function $\mathbf{r}(\mathbf{x})$ such that (2.19) is satisfied only if $(\mathbf{f} - \mathbf{F}\nabla H) \in \mathcal{R}(\mathbf{G})$. Since normally $m < n$, this imposes a restriction on the choice of

[7] Since a Lyapunov function is usually required to be positive definite at $\mathbf{x}^*$ (see Theorem 2.1.1), but $H(\mathbf{x}^*)$ is not necessarily equal to zero, actually, we would have to use $V(\mathbf{x}) = H(\mathbf{x}) - H(\mathbf{x}^*)$ as Lyapunov function. Nevertheless, for simplicity, we say here and in the following that the energy function can be used as a Lyapunov function.

the design matrix $\mathbf{F}(\mathbf{x})$ and the energy function $H(\mathbf{x})$, respectively. Using the elementary result stated in Lemma 2 in [138] we deduce that (2.19) is fulfilled if and only if the control law is chosen as

$$\mathbf{r}(\mathbf{x}) = \left[\mathbf{G}^T(\mathbf{x})\mathbf{G}(\mathbf{x})\right]^{-1} \mathbf{G}^T(\mathbf{x}) \left[\mathbf{F}(\mathbf{x})\nabla H(\mathbf{x}) - \mathbf{f}(\mathbf{x})\right] \tag{2.24}$$

and $\mathbf{F}(\mathbf{x})$ and $H(\mathbf{x})$ satisfy the *projected matching equation*

$$\mathbf{G}^\perp(\mathbf{x})\mathbf{F}(\mathbf{x})\nabla H(\mathbf{x}) = \mathbf{G}^\perp(\mathbf{x})\mathbf{f}(\mathbf{x}) \tag{2.25}$$

where $\mathbf{G}^\perp$ is a full rank left annihilator of $\mathbf{G}$, i.e., $\mathbf{G}^\perp\mathbf{G} = \mathbf{0}$ and $\text{rank}\{\mathbf{G}^\perp\} = n - m$. The calculation of a solution to (2.25) is a crucial step in the design of an IDA controller and is therefore treated in the next subsection.

2.2.4 Solving the Projected Matching Equation

Three different ways have been proposed to solve the projected matching equation (2.25). In [132], the different procedures are illustrated by means of an example. In *algebraic IDA*, originally proposed in [59], the energy function is fixed making (2.25) an algebraic equation for the elements of $\mathbf{F}(\mathbf{x})$. In *parametrized IDA*, a certain structure is specified for the energy function. This approach has first been employed in [137] for the stabilization of underactuated mechanical systems requiring the energy function to be the sum of a kinetic energy term quadratic in the generalized momenta and a potential energy term that depends only on the generalized positions. In this thesis, we proceed as in the original paper [140], where the desired structure of the design matrix has been fixed. Then, (2.25) is a linear partial differential equation (PDE) from which the set of admissible energy functions has to be determined. This approach is known as *non-parametrized IDA* and is by far the most common one.

If we define $\mathbf{W}(\mathbf{x}) = \mathbf{G}^\perp(\mathbf{x})\mathbf{F}(\mathbf{x})$ and $\mathbf{s}(\mathbf{x}) = \mathbf{G}^\perp(\mathbf{x})\mathbf{f}(\mathbf{x})$, we can rewrite (2.25) as

$$\mathbf{W}(\mathbf{x})\nabla H(\mathbf{x}) = \mathbf{s}(\mathbf{x}) \ . \tag{2.26}$$

The solutions of this PDE – if they exist – are of the form $H(\mathbf{x}) = \Psi(\mathbf{x}) + \phi(\boldsymbol{\xi}(\mathbf{x}))$ with a *particular solution* $\Psi(\mathbf{x})$ and a *homogeneous* solution $\phi(\boldsymbol{\xi}(\mathbf{x}))$, which is an arbitrary function of $\boldsymbol{\xi} : \mathbb{R}^n \to \mathbb{R}^{n_\xi}$. The components of $\boldsymbol{\xi}(\mathbf{x})$ are solutions of the homogeneous PDE $\mathbf{W}(\mathbf{x})\nabla\xi_i(\mathbf{x}) = \mathbf{0}$ with independent differential at each point $\mathbf{x}$ (i.e., the gradient vectors are linearly independent) and are called *characteristic coordinates*. The homogeneous

solution $\phi(\boldsymbol{\xi}(\mathbf{x}))$ has to be chosen such that (2.22) holds. A sufficient condition for that is

$$\nabla H(\mathbf{x})|_{\mathbf{x}^*} = \mathbf{0} \,, \quad \nabla^2 H(\mathbf{x})\Big|_{\mathbf{x}^*} > 0 \,. \tag{2.27}$$

The remainder of this subsection is devoted to the solvability as well as the solution of the PDE (2.26). To this end, some differential geometric notions are required, which we introduce below. It is, however, not our intent to deliver an introduction to differential geometry or to PDEs in general. Rather, we aim to give an intuitive explanation of the concepts that will be used in the subsequent chapters. For good introductions to differential geometry in the context of control theory we refer the reader to [89] and [110] . For more comprehensive elaborations on that topic, for instance, the books [108] and [161] can be consulted. Since, for simplicity, no particular attention is paid to the domain of validity of the statements below, we indicate at this point that in general all results hold true only locally.

Let us recall the following differential geometric tools:

- *Lie derivative:* Given the $\mathcal{C}^1$ function $h : \mathbb{R}^n \to \mathbb{R}$ and the vector field $\mathbf{f} : \mathbb{R}^n \to \mathbb{R}^n$, the Lie derivative of h along $\mathbf{f}$ is defined as

$$L_f h(\mathbf{x}) = \frac{\partial h}{\partial \mathbf{x}} \mathbf{f}(\mathbf{x}) \,. \tag{2.28}$$

  Moreover, $L_f^k h(\mathbf{x}) = L_f(L_f^{k-1} h(\mathbf{x}))$ with $L_f^0 h = h$ and $L_f^1 = L_f h$. If $\mathbf{g} : \mathbb{R}^n \to \mathbb{R}^n$ is another vector field, then $L_g L_f h(\mathbf{x}) = L_g(L_f h(\mathbf{x}))$.

- *Lie bracket:* Consider the $\mathcal{C}^1$ vector fields $\mathbf{f} : \mathbb{R}^n \to \mathbb{R}^n$ and $\mathbf{g} : \mathbb{R}^n \to \mathbb{R}^n$. The Lie bracket is defined by

$$[\mathbf{f}, \mathbf{g}] = \frac{\partial \mathbf{g}}{\partial \mathbf{x}} \mathbf{f} - \frac{\partial \mathbf{f}}{\partial \mathbf{x}} \mathbf{g} \,. \tag{2.29}$$

- *Distribution:* Let $\mathbf{f}_1, \ldots, \mathbf{f}_k$ be vector fields. The mapping

$$\Delta(\mathbf{x}) = \operatorname{span} \{\mathbf{f}_1(\mathbf{x}), \ldots, \mathbf{f}_k(\mathbf{x})\} \tag{2.30}$$

  which assigns to any point $\mathbf{x}$ a linear subspace is called a distribution. If its dimension

$$\dim \Delta = \operatorname{rank} \left\{ \begin{bmatrix} \mathbf{f}_1(\mathbf{x}) & \ldots & \mathbf{f}_k(\mathbf{x}) \end{bmatrix} \right\} \tag{2.31}$$

  does not depend on $\mathbf{x}$, we say that Δ is *regular*.

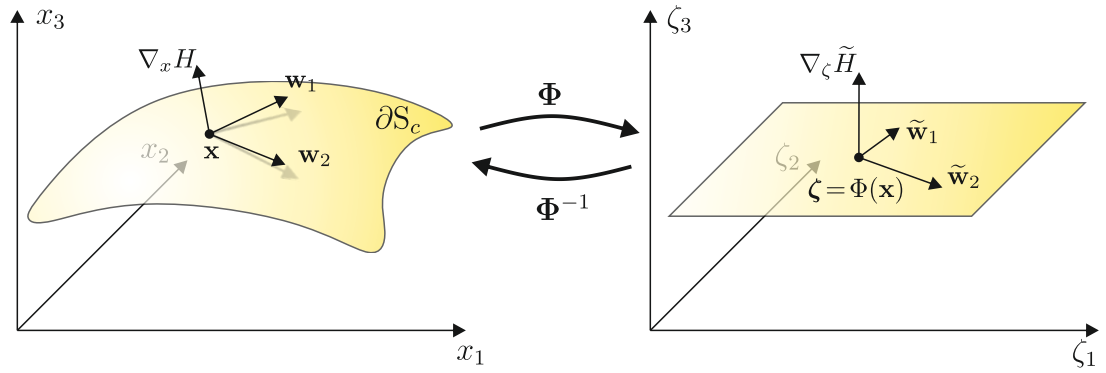

Figure 2.2: Solving the homogeneous PDE (2.33) by straightening out the distribution Δ_W.

- *Involutivity:* A regular distribution $\Delta = \operatorname{span}\{\mathbf{f}_1(\mathbf{x}), \ldots, \mathbf{f}_k(\mathbf{x})\}$ is involutive if for all $\mathbf{x}$ it holds that
$$[\mathbf{f}_i, \mathbf{f}_j] \in \Delta \ , \quad \forall\, i, j = 1, \ldots, k \ . \tag{2.32}$$

- *Involutive closure:* The involutive closure $\bar{\Delta}$ of a distribution Δ is the smallest involutive distribution containing Δ.

In order to determine the characteristic coordinates $\boldsymbol{\xi}(\mathbf{x})$ we have to consider the homogeneous PDE
$$\mathbf{W}(\mathbf{x}) \nabla H(\mathbf{x}) = \mathbf{0} \tag{2.33}$$
where we are looking for a function $H(\mathbf{x})$, whose gradient $\nabla H(\mathbf{x})$ is at any point $\mathbf{x}$ orthogonal to the rows $\mathbf{w}_i^T(\mathbf{x})$, $i = 1, \ldots, n-m$ of the matrix $\mathbf{W}(\mathbf{x})$. This is illustrated in Figure 2.2 (left) for the case $n = 3$, $m = 1$, where we assume that the rows of $\mathbf{W}(\mathbf{x})$ are linearly independent for all $\mathbf{x}$ implying that $\Delta_W(\mathbf{x}) = \operatorname{span}\{\mathbf{w}_1(\mathbf{x}), \mathbf{w}_2(\mathbf{x})\}$ is a regular distribution. If a solution $H(\mathbf{x})$ of (2.33) exists, then the gradient vector $\nabla H(\mathbf{x})$ is not only orthogonal to the rows of $\mathbf{W}(\mathbf{x})$ but also to the level sets $\partial \mathrm{S}_c$ of $H(\mathbf{x})$. Hence, the vector fields $\mathbf{w}_1(\mathbf{x})$ and $\mathbf{w}_2(\mathbf{x})$ are at any point $\mathbf{x}$ tangential to the manifold $\partial \mathrm{S}_c$ which contains that point. These manifolds are called *integral manifolds* and are, in a sense, the generalization of integral curves (solutions) of differential equations, which are everywhere tangential to a single vector field. If we start at $\mathbf{x}_0 \in \partial \mathrm{S}_{c_0}$ and follow the solutions curves of $\dot{\mathbf{x}} = \mathbf{w}_i(\mathbf{x})$, $i = 1, 2$ in alternating order and for arbitrary time intervals we always stay within the level set $\partial \mathrm{S}_{c_0}$.

Now suppose that we can find a coordinate transformation $\boldsymbol{\zeta} = \boldsymbol{\Phi}(\mathbf{x})$ such that the third component of the transformed vector fields $\widetilde{\mathbf{w}}_i(\boldsymbol{\zeta}) = \frac{\partial \boldsymbol{\Phi}}{\partial \mathbf{x}} \mathbf{w}_i \circ \boldsymbol{\Phi}^{-1}(\boldsymbol{\zeta})$ is zero [see Figure 2.2 (right)]. Then, the integral manifolds are parallel to the ζ_1-ζ_2-plane. This procedure is called *straightening out* of the distribution $\Delta_W(\mathbf{x})$. In the new coordinates, the homogeneous PDE can be easily solved: The gradient vector $\nabla_\zeta \widetilde{H}(\boldsymbol{\zeta})$ is orthogonal to the $\widetilde{\mathbf{w}}_i(\boldsymbol{\zeta})$, $i = 1, 2$

if and only if the function depends only on ζ_3, i.e., $\widetilde{H}(\boldsymbol{\zeta}) = \widetilde{H}(\zeta_3)$. Apart from that, it may be chosen arbitrary. Hence, clearly, $\xi(\mathbf{x}) = \Phi_3(\mathbf{x})$ is a characteristic coordinate of (2.33).

In general, this amounts to the following problem: Given the k-dimensional regular distribution $\Delta_W(\mathbf{x}) = \text{span}\{\mathbf{w}_1(\mathbf{x}), \ldots, \mathbf{w}_k(\mathbf{x})\}$ (where in our case $k = n - m$), find a diffeomorphism $\boldsymbol{\zeta} = \boldsymbol{\Phi}(\mathbf{x})$ such that in $\boldsymbol{\zeta}$ coordinates the image distribution satisfies

$$\tilde{\Delta}_W(\boldsymbol{\zeta}) = \text{span}\left\{\widetilde{\mathbf{w}}_1(\boldsymbol{\zeta}), \ldots, \widetilde{\mathbf{w}}_k(\boldsymbol{\zeta})\right\} = \text{span}\left\{\frac{\partial}{\partial\zeta_1}, \ldots, \frac{\partial}{\partial\zeta_k}\right\} \tag{2.34}$$

where the $\frac{\partial}{\partial\zeta_i}$, $i = 1, \ldots, k$ can be viewed as the first k basis vectors. We say that the diffeomorphism $\boldsymbol{\zeta} = \boldsymbol{\Phi}(\mathbf{x})$ *straightens out* the distribution Δ_W. The Frobenius Theorem gives an answer to the question under what condition such a diffeomorphism exists, see e.g. [110], [108].

Theorem 2.2.1 (Frobenius Theorem)**.** *Let Δ_W be a regular distribution with dimension k. A necessary and sufficient condition for the existence of a diffeomorphism that straightens out Δ_W is that Δ_W is involutive. In this case, each point $\mathbf{x}$ is contained in a k-dimensional integral manifold of Δ_W.*

Hence, if Δ_W is involutive, the PDE (2.33) is solvable with $n_\xi = m$ characteristic coordinates $\xi_i(\mathbf{x}) = \Phi_{k+i}(\mathbf{x})$, $i = 1, \ldots, m$. The $(n-m)$-dimensional integral manifolds can be represented as level sets $\{\mathbf{x} \in \mathbb{R}^n | \boldsymbol{\xi}(\mathbf{x}) = \mathbf{c}\}$ with $\mathbf{c} \in \mathbb{R}^m$. In the case where Δ_W is not involutive, we proceed along the same lines with its involutive closure $\bar{\Delta}_W$. Since $\dim \bar{\Delta}_W > \dim \Delta_W$, the number of characteristic coordinates n_ξ is then less than m.

Now we consider the inhomogeneous PDE (2.26). In [24], a condition for its solvability is given as follows.

Theorem 2.2.2. *Consider the PDE* (2.26) *and define*

$$\Delta_W = \text{span}\left\{\mathbf{W}^T(\mathbf{x})\right\}, \quad \Delta_{W,s} = \text{span}\left\{\begin{bmatrix}\mathbf{W}^T(\mathbf{x}) \\ \mathbf{s}^T(\mathbf{x})\end{bmatrix}\right\}. \tag{2.35}$$

Assume that the involutive closures $\bar{\Delta}_W$ and $\bar{\Delta}_{W,s}$ are regular. Then (2.26) *is solvable if and only if*

$$\dim \bar{\Delta}_W = \dim \bar{\Delta}_{W,s}. \tag{2.36}$$

Frequently, the design matrix $\mathbf{F}$ is chosen constant. If then a constant left annihilator $\mathbf{G}^\perp$ can be used, a constant matrix $\mathbf{W}$ is obtained. In this case, both assessing the solvability of the matching PDE (2.26) and determining its solutions simplify considerably. Therefore, this special case is discussed separately in the remainder of this subsection.

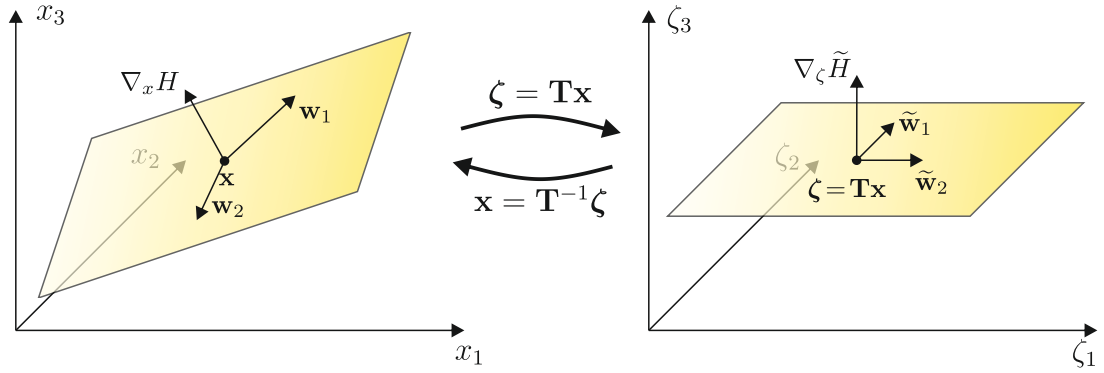

Figure 2.3: Solving the homogeneous PDE (2.33) with constant $\mathbf{W}$ by straightening out the distribution Δ_W.

First note that a distribution which is spanned by constant vector fields is of course involutive. Consequently, the homogeneous PDE (2.33) is solvable with m characteristic coordinates. In order to construct a coordinate transformation that straightens out Δ_W, obviously, we can choose the $n-m$ rows of $\mathbf{W}$ as new basis vectors (see Figure 2.3), i.e.,

$$\mathbf{x} = \underbrace{\begin{bmatrix}\mathbf{w}_1 & \dots & \mathbf{w}_{n-m} & \mathbf{t}_{n-m+1} & \dots & \mathbf{t}_n\end{bmatrix}}_{\mathbf{T}^{-1}} \boldsymbol{\zeta} \,. \tag{2.37}$$

The vectors $\mathbf{t}_i$, $i = n-m+1, \dots, n$ are chosen such that the columns of $\mathbf{T}$ form a basis of $\mathbb{R}^n$, i.e., $\operatorname{rank}\{\mathbf{T}\} = n$, but are otherwise arbitrary. Then, by construction, the vectors $\mathbf{w}_i$ transform to basis vectors, i.e., $\tilde{\mathbf{w}}_i = \mathbf{e}_i$, $i = 1, \dots, n-m$. Hence in $\boldsymbol{\zeta}$ coordinates the homogeneous PDE has the form

$$\begin{bmatrix}\mathbf{I}_{n-m} & \mathbf{0}_{(n-m)\times m}\end{bmatrix} \nabla_\zeta \tilde{H}(\boldsymbol{\zeta}) = \mathbf{0} \,. \tag{2.38}$$

and is solved by any function of the form $\tilde{H}(\boldsymbol{\zeta}) = \tilde{H}(\zeta_{n-m+1}, \dots\ \zeta_n)$.

Moreover, the solvability condition given in Theorem 2.2.2 simplifies considerably, if $\mathbf{W}$ is a constant matrix.

Proposition 2.2.1 ([103]). *The PDE* (2.26) *with a constant matrix* $\mathbf{W}$ *of full rank admits a solution if and only if for all* $i, j = 1, \dots, n-m$

$$L_{w_i} s_j(\mathbf{x}) - L_{w_j} s_i(\mathbf{x}) = 0 \,. \tag{2.39}$$

When it comes to computing the particular solution, the transformation (2.37) also is helpful as illustrated in the following example.

Example 2.2.1. Suppose the projected matching equation is given by

$$\begin{bmatrix} 1 & 0 & 2 \\ 0 & 2 & -1 \end{bmatrix} \nabla_x H(\mathbf{x}) = \begin{bmatrix} 2x_1^2 + x_2 \\ \sin(x_2) + x_3 \end{bmatrix} . \tag{2.40}$$

It is easily verified that this PDE is solvable according to Proposition 2.2.1. With the choice $\mathbf{t}_3 = [0\ 0\ 1]^T$ the matrix $\mathbf{T}^{-1}$ in (2.37) forms a basis of $\mathbb{R}^n$, and in $\boldsymbol{\zeta}$ coordinates (2.40) takes the form

$$\begin{bmatrix} \frac{\partial \tilde{H}(\boldsymbol{\zeta})}{\partial \zeta_1} \\ \frac{\partial \tilde{H}(\boldsymbol{\zeta})}{\partial \zeta_2} \end{bmatrix} = \begin{bmatrix} 2\zeta_1^2 + 2\zeta_2 \\ \sin(2\zeta_2) + 2\zeta_1 - \zeta_2 + \zeta_3 \end{bmatrix} . \tag{2.41}$$

By construction $\xi(\mathbf{x}) = \zeta_3 = -2x_1 + \frac{1}{2}x_2 + x_3$ is a characteristic coordinate, i.e., the homogeneous solution can be chosen as an arbitrary function of the form $\phi(-2x_1 + \frac{1}{2}x_2 + x_3)$. A particular solution is constructed from (2.41) as follows. From the first line we calculate

$$\tilde{\Psi}(\boldsymbol{\zeta}) = \int 2\zeta_1^2 + 2\zeta_2 \, d\zeta_1 + c(\zeta_2, \zeta_3) = \frac{2}{3}\zeta_1^3 + 2\zeta_2\zeta_1 + c(\zeta_2, \zeta_3) . \tag{2.42}$$

To determine $c(\zeta_2, \zeta_3)$, we substitute this expression into the second line of (2.41), with $\tilde{H}(\boldsymbol{\zeta}) = \tilde{\Psi}(\boldsymbol{\zeta})$, which yields

$$\frac{\partial}{\partial \zeta_2} c(\zeta_2, \zeta_3) = \sin(\zeta_2) - \zeta_2 + \zeta_3 . \tag{2.43}$$

By virtue of solvability of (2.40) the right hand side is independent of ζ_1. Hence, $c(\zeta_2, \zeta_3)$ can be determined by integration with respect to ζ_2 and we obtain

$$\tilde{\Psi}(\boldsymbol{\zeta}) = \frac{2}{3}\zeta_1^3 + 2\zeta_2\zeta_1 - \frac{1}{2}\cos(2\zeta_2) - \frac{1}{2}\zeta_2^2 + \zeta_3\zeta_2 . \tag{2.44}$$

Using the inverse coordinate transformation we finally get the general solution

$$H(\mathbf{x}) = \frac{2}{3}x_1^3 - \frac{1}{2}\cos(x_2) + \frac{1}{8}x_2^2 + \frac{1}{2}x_2x_3 + \phi(-2x_1 + \frac{1}{2}x_2 + x_3) . \tag{2.45}$$

2.2.5 IDA for Time-Varying Systems

It is straightforward to generalize the IDA approach to time-varying systems

$$\dot{\mathbf{x}} = \mathbf{f}(\mathbf{x}, t) + \mathbf{G}(\mathbf{x}, t)\mathbf{u} \tag{2.46}$$

if we allow the quantities in (2.17) to depend explicitly on the time t, yielding the class of *time-varying pH systems* (see also e.g. [58], where the closely related concept of generalized canonical transformations is applied for the stabilization of time-varying pH systems). The matching equation then takes the form

$$\mathbf{f}(\mathbf{x},t) + \mathbf{G}(\mathbf{x},t)\left(\mathbf{r}(\mathbf{x},t) + \mathbf{v}\right) \stackrel{!}{=} \mathbf{F}(\mathbf{x},t)\nabla H(\mathbf{x},t) + \mathbf{G}(\mathbf{x},t)\mathbf{v} \tag{2.47}$$

where $\mathbf{R}(\mathbf{x},t) = -\mathrm{sym}\{\mathbf{F}(\mathbf{x},t)\}$ must be positive semidefinite for all $(\mathbf{x},t) \in \Omega^R \times [0,\infty)$ with Ω^R an open neighborhood of the desired equilibrium $\mathbf{x}^*$. Furthermore, the Hamiltonian has to satisfy $H(\mathbf{x},t) > H(\mathbf{x}^*)$ for all $(\mathbf{x},t) \in \Omega \times [0,\infty)$, where Ω is some open set containing $\mathbf{x}^*$. The procedure for the design of the time-varying feedback function $\mathbf{r}(\mathbf{x},t)$ is completely analogue to the time-invariant case and hence is not described here.

In contrast to the time-invariant case, however, the time-varying pH structure on the right hand side of (2.47) does neither guarantee that the closed loop system is "locally passive" nor that $\mathbf{x}^*$ is a stable equilibrium. This is immediately seen by computing the rate of change of the time-varying energy function, which is given by

$$\dot{H}(\mathbf{x},t) = \frac{\partial}{\partial t}H(\mathbf{x},t) - \nabla_x^T H(\mathbf{x},t)\mathbf{R}(\mathbf{x},t)\nabla H(\mathbf{x},t) + \mathbf{y}^T\mathbf{v} \tag{2.48}$$

where $\mathbf{y} = \mathbf{G}^T(\mathbf{x},t)\nabla_x H(\mathbf{x},t)$. Since nothing can be said, in general, about the first summand $\nabla_t H(\mathbf{x},t)$, it is not possible to conclude from $\mathbf{R}(\mathbf{x},t) \geq 0$ that $\dot{H}(\mathbf{x},t) \leq \mathbf{y}^T\mathbf{v}$ holds. Moreover, $H(\mathbf{x},t) > H(\mathbf{x}^*)$, $\forall\,(\mathbf{x},t) \in \Omega \times [0,\infty)$ does neither ensure that $H(\mathbf{x},t)$ is positive definite at $\mathbf{x}^*$ nor that it is decrescent. As a consequence, the existence of functions $W_i(\mathbf{x})$, $i = 1,2,3$ satisfying (2.11), (2.12) has to be verified after the controller design. Nevertheless, the energy function is usually a good candidate for a Lyapunov function.

2.3 Local Linear Dynamics Assignment

Usually, the IDA methodology provides a large number of free parameters that can be utilized to achieve desired closed loop properties. Therefore, a key question is how to tune these parameters in order to meet the design specifications, one of them being the desired transient behavior. In [102], the approach *Local Linear Dynamics Assignment* (LLDA) has been proposed for a transparent and systematic parametrization of IDA controllers. This method has proven to be very useful and is frequently used throughout this thesis. In this section, it is first described for time-invariant systems and then generalized to the time-varying case in the second subsection.

2.3.1 Time-Invariant Systems

It is assumed that the plant model (2.14) can be represented in the form

$$\begin{bmatrix} \dot{\mathbf{x}}^\alpha \\ \dot{\mathbf{x}}^\nu \end{bmatrix} = \begin{bmatrix} \mathbf{f}^\alpha(\mathbf{x}) \\ \mathbf{f}^\nu(\mathbf{x}) \end{bmatrix} + \begin{bmatrix} \mathbf{G}^\alpha(\mathbf{x}) \\ \mathbf{0} \end{bmatrix} \mathbf{u} \tag{2.49}$$

where the state vector $\mathbf{x}$ is partitioned into *actuated* coordinates $\mathbf{x}^\alpha \in \mathbb{R}^m$ and *unactuated* coordinates $\mathbf{x}^\nu \in \mathbb{R}^{n-m}$. The design matrix $\mathbf{F}(\mathbf{x})$ is partitioned accordingly, turning the matching equation (2.19) into

$$\begin{bmatrix} \mathbf{f}^\alpha(\mathbf{x}) \\ \mathbf{f}^\nu(\mathbf{x}) \end{bmatrix} + \begin{bmatrix} \mathbf{G}^\alpha(\mathbf{x}) \\ \mathbf{0} \end{bmatrix} \mathbf{r}(\mathbf{x}) = \begin{bmatrix} \mathbf{F}^\alpha(\mathbf{x}) \\ \mathbf{F}^\nu(\mathbf{x}) \end{bmatrix} \nabla H(\mathbf{x}) \; . \tag{2.50}$$

The simplest left annihilator

$$\mathbf{G}^\perp = \begin{bmatrix} \mathbf{0}_{(n-m)\times m} & \mathbf{I}_{n-m} \end{bmatrix} \tag{2.51}$$

is used, yielding the projected matching equation

$$\mathbf{F}^\nu(\mathbf{x}) \nabla H(\mathbf{x}) = \mathbf{f}^\nu(\mathbf{x}) \; . \tag{2.52}$$

The basic idea of LLDA is to match the closed loop linearization with a predefined asymptotically stable linear system $\Delta\dot{\mathbf{x}} = \mathbf{A}_d \Delta\mathbf{x}$, where $\Delta\mathbf{x} = \mathbf{x} - \mathbf{x}^*$, i.e.,

$$\frac{\partial}{\partial \mathbf{x}} \left[\mathbf{F}(\mathbf{x}) \nabla H(\mathbf{x}) \right] \Big|_{\mathbf{x}^*} = \mathbf{A}_d \; . \tag{2.53}$$

The matrix $\mathbf{A}_d$ can be obtained by applying linear state feedback techniques to the linearization of the plant model (2.14) at $(\mathbf{x}^*, \mathbf{u}^*)$, where $\mathbf{u}^* = [\mathbf{G}^\alpha(\mathbf{x}^*)]^{-1} \mathbf{f}^\nu(\mathbf{x}^*)$ is the constant control input associated with $\mathbf{x}^*$. By this means, desired closed-loop dynamics, that can be quantitatively assessed via the eigenvalues of the state matrix $\mathbf{A}_d$, are achieved, at least in some neighborhood of $\mathbf{x}^*$. The matrix $\mathbf{A}_d$ is also partitioned into an actuated and an unactuated part

$$\mathbf{A}_d = \begin{bmatrix} \mathbf{A}^\alpha \\ \mathbf{A}^\nu \end{bmatrix} \; , \quad \text{where } \mathbf{A}^\nu = \frac{\partial \mathbf{f}^\nu(\mathbf{x})}{\partial \mathbf{x}} \; . \tag{2.54}$$

The following two assumptions are required for the applicability of LLDA.

Assumption 2.3.1. The plant model is of the form (2.49) and its linearization at $(\mathbf{x}^*, \mathbf{u}^*)$ is stabilizable.

Assumption 2.3.2. The projected matching equation (2.52) is solvable with a matrix $\mathbf{F}^\nu(\mathbf{x})$ which is such that the distribution $\Delta_{F,\nu} = \text{span}\{(\mathbf{F}^\nu(\mathbf{x}))^T\}$ spanned by its rows is regular with dimension $n - m$ and involutive in an open neighborhood of $\mathbf{x}^*$.

Concerning the first part of Assumption 2.3.1, note that any system of the form (2.14) can be transformed into the form (2.49) by a change of coordinates if the columns of $\mathbf{G}(\mathbf{x})$ span a regular involutive distribution (like e.g. in the case of a constant input matrix $\mathbf{G}$). The necessity of the second part of Assumption 2.3.1 is obvious since $\mathbf{A}_d$ is required to be Hurwitz. Assumption 2.3.2 assures, on the one hand, that a design matrix $\mathbf{F}(\mathbf{x})$ with full rank n can be chosen. This is required in order that (2.53) can be fulfilled with a Hurwitz (and hence regular) matrix $\mathbf{A}_d$. On the other hand, Assumption 2.3.2 ensures that the PDE (2.52) is solvable with the maximum number of m characteristic coordinates (see Theorem 2.2.1). The following theorem from [102], [103] summarizes the LLDA method.

Theorem 2.3.1. *Assume that the Assumptions 2.3.1 and 2.3.2 hold. Let* $H(\mathbf{x}) = \Psi(\mathbf{x}) + \phi(\boldsymbol{\xi}(\mathbf{x}))$ *be the solution of* (2.52) *and define*

$$\mathbf{Q}_\Psi^{\alpha\alpha} = \mathbf{F}^\alpha(\mathbf{x}^*) \left(\nabla^2 \Psi(\mathbf{x})\Big|_{\mathbf{x}^*} \right) [\mathbf{F}^\alpha(\mathbf{x}^*)]^T \ , \tag{2.55}$$

$$\mathbf{Q}_\phi^{\alpha\alpha} = \mathbf{F}^\alpha(\mathbf{x}^*) \left(\nabla^2 \phi(\mathbf{x})\Big|_{\mathbf{x}^*} \right) [\mathbf{F}^\alpha(\mathbf{x}^*)]^T \ . \tag{2.56}$$

If the parameters of $\phi(\boldsymbol{\xi}(\mathbf{x}))$ *and* $\mathbf{F}(\mathbf{x})$ *are chosen such that* $\nabla H_d(\mathbf{x})|_{\mathbf{x}^*} = \mathbf{0}$, $\mathbf{R}_d(\mathbf{x}^*) \geq 0$ *and*

$$\mathbf{Q}_\Psi^{\alpha\alpha} + \mathbf{Q}_\phi^{\alpha\alpha} = \mathbf{F}^\alpha(\mathbf{x}^*)(\mathbf{A}^\alpha)^T \ , \tag{2.57}$$

$$\mathbf{A}^\alpha[\mathbf{F}^\alpha(\mathbf{x}^*)]^T = \mathbf{F}^\alpha(\mathbf{x}^*)(\mathbf{A}^\alpha)^T \ , \tag{2.58}$$

$$\mathbf{A}^\alpha[\mathbf{F}^\nu(\mathbf{x}^*)]^T = \mathbf{F}^\alpha(\mathbf{x}^*)(\mathbf{A}^\nu)^T \ , \tag{2.59}$$

then (2.27) *and* (2.53) *hold.*

The equations (2.57)-(2.59) constitute a system of linear equations for the entries of $\mathbf{F}(\mathbf{x}^*)$ and $\mathbf{Q}_\phi^{\alpha\alpha}$. The latter matrix can be arbitrarily set by means of the homogeneous solution $\phi(\boldsymbol{\xi}(\mathbf{x}))$. Moreover, also the requirement $\nabla H_d(\mathbf{x})|_{\mathbf{x}^*} = \mathbf{0}$ can be fulfilled by an appropriate choice of $\phi(\boldsymbol{\xi}(\mathbf{x}))$ (see Propositions 4 and 11 in [103]). For instance, if we take $\phi(\boldsymbol{\xi}) = \boldsymbol{\mu}_1^T \boldsymbol{\xi} + \boldsymbol{\xi}^T \boldsymbol{\mu}_2 \boldsymbol{\xi}$ with $\boldsymbol{\mu}_1 \in \mathbb{R}^m$ and $\boldsymbol{\mu}_2 \in \mathbb{R}^{m \times m}$ constant, then $\nabla H_d(\mathbf{x})|_{\mathbf{x}^*} = \mathbf{0}$ can be ensured by $\boldsymbol{\mu}_1$, while $\boldsymbol{\mu}_2$ can be used to adjust the entries of $\mathbf{Q}_\phi^{\alpha\alpha}$. Normally, (2.57)-(2.59)

do not determine all design parameters, thus leaving free parameters in $\mathbf{F}(\mathbf{x})$ and $\phi(\boldsymbol{\xi}(\mathbf{x}))$, which can be used to enlarge the DA or to tune the (semi-) global behavior of the closed loop system.

In [102], [103], a systematic procedure is described for the application of LLDA with a constant design matrix $\mathbf{F}$.

Step 1: Specify the desired dynamics by choosing $\mathbf{A}_d$.

Step 2: Establish algebraic relations for the elements of $\mathbf{F}^\nu$ such that the solvability condition (2.39) is satisfied.

Step 3: Derive conditions for the elements of $\mathbf{F}$ to ensure $\mathbf{R} \geq 0$, e.g. by means of Sylvester's criterion (see [164]).

Step 4: Solve the PDE (2.52).

Step 5: Establish algebraic relations for the parameters in $\phi(\boldsymbol{\xi})$ such that $\nabla H_d(\mathbf{x})|_{\mathbf{x}^*} = \mathbf{0}$ holds.

Step 6: Solve the system of equations (2.57)-(2.59) and deduce from $\mathbf{Q}_\phi^{\alpha\alpha}$ suitable values for the parameters in $\phi(\boldsymbol{\xi})$.

Step 7: Fix the remaining free parameters.

2.3.2 LLDA for Trajectory Tracking Control

In [101], the LLDA approach has been extended to the time-varying case, in particular to the design of error controllers for trajectory tracking problems. Consider the system (2.14) and assume, for simplicity, that it has a single input and a single output, i.e., $m = 1$. Further, suppose that a desired output trajectory $y_d(t)$ is given for $t \in [0, \infty)$. In order to make the system output asymptotically track $y_d(t)$, frequently a two-degree-of-freedom structure [86] (see Figure 2.4) is employed. It consists of a feedforward part Σ_{FF} and a feedback part Σ_{FB}. The former provides a control input $u_d(t)$, which makes the system track the desired output trajectory in the open loop mode, and the corresponding state trajectory $\mathbf{x}_d(t)$. The purpose of the feedback part is to asymptotically stabilize the tracking error in the presence of model uncertainties and disturbances. The design and especially the tuning of a suitable feedback law by means of LLDA is the subject of this subsection. For the sake of simplicity, we assume that y is a flat output [52] of (2.14). Then, both the feedforward control $u_d(t)$ and the corresponding state trajectory $\mathbf{x}_d(t)$ can be given as functions of $y_d(t)$ and its time derivatives up to the order n, which we subsume in the vector $\mathbf{Y}_d$.

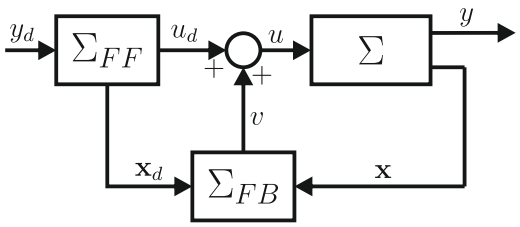

Figure 2.4: Two-degree-of-freedom control scheme with plant Σ, feedforward control Σ_{FF}, and feedback control Σ_{FB}.

The objective is to design a controller that achieves $\|\mathbf{e}(t)\| \to 0$ as $t \to \infty$, where $\mathbf{e} = \mathbf{x} - \mathbf{x}_d$. To this end, the dynamics of the tracking error are calculated as

$$\dot{\mathbf{e}} = \mathbf{f}(\mathbf{x}) + \mathbf{g}(\mathbf{x})(u_d + v) - \mathbf{f}(\mathbf{x}_d) - \mathbf{g}(\mathbf{x}_d)u_d \tag{2.60}$$

where we have used $u = u_d + v$ (see Figure 2.4). With $\mathbf{x} = \mathbf{e} + \mathbf{x}_d$ and the fact that both u_d and $\mathbf{x}_d$ can be expressed as functions of $\mathbf{Y}_d$ we obtain the time-varying *error system*

$$\dot{\mathbf{e}} = \mathbf{f}^e\left(\mathbf{e}, \mathbf{Y}_d(t)\right) + \mathbf{g}^e\left(\mathbf{e}, \mathbf{Y}_d(t)\right) v \ . \tag{2.61}$$

To render $\mathbf{e}^* = \mathbf{0}$ asymptotically stable, the IDA methodology is utilized so that the closed loop system can be represented in the form

$$\dot{\mathbf{e}} = \mathbf{F}(\mathbf{e}, t)\nabla_e H(\mathbf{e}, t) \ . \tag{2.62}$$

In order to apply the LLDA approach to the case at hand, effectively, we only have to add a time argument to all quantities in the previous subsection. Therefore, Theorem 2.3.1 is not explicitly reformulated for the time-varying case. As a result, it holds for all $t \geq 0$ that

$$\frac{\partial}{\partial \mathbf{e}}\left[\mathbf{F}(\mathbf{e}, t)\nabla H(\mathbf{e}, t)\right]\Big|_{\mathbf{e}^*} = \mathbf{A}_d(t) \quad \text{and} \quad \nabla_e^2 H(\mathbf{e}, t)|_{\mathbf{e}^*} > 0 \ . \tag{2.63}$$

It is important to note, however, that unlike in the time-invariant case, the time-varying eigenvalues of $\mathbf{A}_d(t)$ do, in general, not provide information about the dynamic behavior of the system $\dot{\mathbf{e}} = \mathbf{A}_d(t)\mathbf{e}$. The trajectories may even become unbounded, although the eigenvalues stay within the left halfplane (see e.g. [91], p. 607 for a simple example). There are, in fact, techniques that enable pole placement for linear time varying system (see e.g. [53], [172]) in the sense that the closed loop system is Lyapunov equivalent[8] to

[8]Two systems are called Lyapunov equivalent if they can be carried into another by a Lyapunov transformation. A transformation $\boldsymbol{\xi} = \mathbf{T}(t)\mathbf{x}$ is called Lyapunov transformation, if $\mathbf{T}(t)$, and $d\mathbf{T}(t)/dt$ are continuous and bounded and $\det\{\mathbf{T}(t)\} > c > 0$ holds for all $t \in [0, \infty)$.

a time-invariant system with prescribed poles. However, the resulting control laws tend to be rather complicated rendering also $\mathbf{A}^{\alpha}(t)$ quite complex. This makes the equations (2.57)-(2.59) as well as the resulting expressions for the controller parameters cumbersome.

Therefore, it is suggested in [101], [102] to choose the matrix $\mathbf{A}_d(t)$ such that, for all $t \geq 0$, its eigenvalues are located in the left half plane without considering the stability of $\dot{\mathbf{e}} = \mathbf{A}_d(t)\mathbf{e}$. For it is expected that the eigenvalue locations provide a good indication for the (local) dynamics of the closed loop error system if the desired trajectory $y_d(t)$ is sufficiently slow. Moreover, the stability analysis of the closed loop system (2.62) is done separately based on Theorem 2.1.2 using the energy function as Lyapunov function candidate. The procedure proposed in [101], [102] is described next.

First note that the time dependency of (2.61) and consequently of $\mathbf{A}^{\nu}(t)$ is only due to the time-variance of $\mathbf{Y}_d(t)$. With some abuse of notation, we will therefore use $\mathbf{A}^{\nu}(t)$ and $\mathbf{A}^{\nu}(\mathbf{Y}_d(t))$ interchangeably. In order to determine (constant) values for the entries of $\mathbf{A}^{\alpha}$, the matrix $\mathbf{A}^{\nu}$ is evaluated at an "average" value $\bar{\mathbf{Y}}$ yielding $\bar{\mathbf{A}}^{\nu} = \mathbf{A}^{\nu}(\bar{\mathbf{Y}}_d)$. Then $\mathbf{A}^{\alpha}$ is determined such that the eigenvalues of the matrix

$$\bar{\mathbf{A}}_d = \begin{bmatrix} \mathbf{A}^{\alpha} \\ \bar{\mathbf{A}}^{\nu} \end{bmatrix} \tag{2.64}$$

are located at desired positions in the left half plane. The vector $\bar{\mathbf{Y}}_d$ may be an average value along a particular trajectory $y_d(t)$ as in [101], [102] or an average point of an operating region specified by $\mathbf{Y}_{d,min} \leq \mathbf{Y}_d(t) \leq \mathbf{Y}_{d,max}$, where the inequality is to be interpreted component-wise (see Section 8.2). The latter is reasonable if the controller ought to be applicable not only for a particular $y_d(t)$, but for a whole set of reference trajectories. For LLDA, the matrix

$$\mathbf{A}_d(t) = \begin{bmatrix} \mathbf{A}^{\alpha} \\ \mathbf{A}^{\nu}(t) \end{bmatrix} \tag{2.65}$$

is used. Of course, its eigenvalues, and hence those of the closed loop linearization, vary along $y_d(t)$, being identical to the prescribed ones for $\mathbf{Y}_d(t) = \bar{\mathbf{Y}}_d$. Since $\mathbf{A}_d(t)$ depends continuously on $\mathbf{Y}_d(t)$, also the eigenvalues are continuous functions of $\mathbf{Y}_d$. In general, the described procedure leads to a design matrix $\mathbf{F}(\mathbf{e}, t)$ that explicitly depends on $\mathbf{Y}_d(t)$.

As an alternative, we suggest in this thesis to solve the system of equations (2.57)-(2.59) only for $\mathbf{Y}_d(t) = \bar{\mathbf{Y}}_d$. Also in this case the eigenvalues of the closed loop linearization are continuous functions of $\mathbf{Y}_d$ and coincide with the prescribed ones for $\mathbf{Y}_d(t) = \bar{\mathbf{Y}}_d$. It is not clear, in general, which approach gives better results in terms of the closed loop behavior. However, if LLDA is accomplished only for $\mathbf{Y}_d(t) = \bar{\mathbf{Y}}_d$, the corresponding set of equations

simplifies notably, and if a dependency of $\mathbf{F}$ on $\mathbf{Y}_d(t)$ is not necessary to ensure solvability of the projected matching equation, the resulting design matrix is independent of t (see Section 8.2 for an example).

2.4 Switched Systems

The objective of this section is to introduce the class of switched systems and to review some related results from the literature. As this topic has been and is still a field of extensive research, that has attracted a large number of scientists from different disciplines, it goes without saying that we cannot provide a comprehensive overview here but rather present merely the material that is needed in this thesis. In particular, we first describe the mathematical framework under which we study switched systems and define the solution concept that will be used. Subsequently, we review the concept of uniform stability and present some stability theorems including extensions of the Krasovskii-LaSalle Theorem to switched systems. For further informations on switched systems in general the reader is referred to the important book [113] and the survey paper [155] as well as the references therein. Concerning solvability and solution concepts, still the classic book by Fillipov [51] is an excellent reference, and the reader may also consult the tutorial account [33].

2.4.1 Notation and Solution Concept

Given the family of *subsystems*

$$\dot{\mathbf{x}} = \mathbf{f}_p(\mathbf{x}, t) + \mathbf{G}_p(\mathbf{x}, t)\mathbf{u} \,, \quad p \in \mathcal{P} \tag{2.66a}$$

$$y = \mathbf{h}_p(\mathbf{x}, t) \tag{2.66b}$$

with state $\mathbf{x} \in \mathbb{R}^n$, control input $\mathbf{u} \in \mathbb{R}^m$, output $\mathbf{y} \in \mathbb{R}^m$, and a finite index set $\mathcal{P} = \{1, \ldots, N\}$, we consider *switched systems* described by

$$\dot{\mathbf{x}} = \mathbf{f}_\sigma(\mathbf{x}, t) + \mathbf{G}_\sigma(\mathbf{x}, t)\mathbf{u} \,, \quad \sigma \in \mathcal{S} \,, \quad t \geq 0 \tag{2.67a}$$

$$y = \mathbf{h}_\sigma(\mathbf{x}, t) \,. \tag{2.67b}$$

For all $p \in \mathcal{P}$, the vector fields $\mathbf{f}_p : \mathbb{R}^n \times [0, \infty) \to \mathbb{R}^n$ and the columns of the matrices $\mathbf{G}_p : \mathbb{R}^n \times [0, \infty) \to \mathbb{R}^{n \times m}$ are locally Lipschitz in $\mathbf{x}$ and continuous in t, the maps $\mathbf{h}_p : \mathbb{R}^n \times [0, \infty) \to \mathbb{R}^m$ are continuous. The *switching signal* $\sigma : [t_0, \infty) \to \mathcal{P}$ specifies the *active subsystem* and is *piecewise constant*. By piecewise constant, we mean that the signal

has a finite number of discontinuities in every finite time interval and takes a constant value between its consecutive discontinuities. By convention, we take the switching signals to be continuous from the right, i.e., $\sigma(t) = \sigma(t^+)$ for all $t \geq t_0$. Its discontinuities $t_k,\ k \in \mathbb{N}_0$ are called *switching times* and it holds that $t_{k+1} > t_k$. Throughout this thesis, we assume the switching signal to be minimal, i.e., $\sigma(t_{k+1}) \neq \sigma(t_{k+1}^-)$. The set of all switching signals admissible in (2.67) is denoted by $\mathcal{S}$. Besides the set $\mathcal{S}_{pc}$ of all piecewise constant switching signals $\sigma(t)$, two different subsets of $\mathcal{S}_{pc}$ will be needed. Adopting the notation of [78], we denote by $\mathcal{S}_{average}[\tau_D, N_0]$ the set of all σ that possess an average dwell time $\tau_D > 0$ and a chatter bound $N_0 > 0$, i.e., the number of switching times in any open finite interval $(\tau_1, \tau_2) \subset [t_0, \infty)$ is bounded above by $N_0 + (\tau_2 - \tau_1)/\tau_D$. Moreover, we define the set $\mathcal{S}_{average} = \bigcup_{\tau_D>0, N_0>0} \mathcal{S}_{average}[\tau_D, N_0]$. Unless otherwise stated, we will assume that $\mathcal{S} = \mathcal{S}_{pc}$.

Throughout this thesis, the interpretation of the differential equation (2.67a) in terms of its solution is as described in the following definition. It corresponds to the standard solution concept usually applied in the switched systems literature, see e.g. [78], [120].

Definition 2.4.1. By a *solution* to (2.67a) we mean a triple $(\mathbf{x}, \mathbf{u}, t)$ consisting of a piecewise $\mathcal{C}^1$ curve $\mathbf{x} : \mathcal{I} \to \mathbb{R}^n$ with $\mathcal{I} = [t_0, T)$ or $\mathcal{I} = [t_0, T]$, where $t_0 < T \leq +\infty$, a piecewise constant switching signal $\sigma : \mathcal{I} \to \mathcal{P}$ and a piecewise continuous input $\mathbf{u} : \mathcal{I} \to \mathbb{R}^m$ for which

$$\dot{\mathbf{x}}(t) = \mathbf{f}_{\sigma(t)}(\mathbf{x}(t), t) + \mathbf{G}_{\sigma(t)}(\mathbf{x}(t))\mathbf{u}(t) \tag{2.68}$$

holds for all $(t_i, t_{i+1}) \cap \mathcal{I}$, $i = 0, 1, \ldots$. To indicate that the state trajectory starts from $\mathbf{x}_0$ at time t_0 we use the notation $\mathbf{x}(t; \mathbf{x}_0, t_0)$.

By a piecewise $\mathcal{C}^1$ curve, we mean a piecewise continuous signal whose derivative is also piecewise continuous. Since the notion of a *piecewise continuous function* is needed later on also in the context of multivariate functions, for convenience of the reader, we recall here the definition (see e.g. [51], [130]).

Definition 2.4.2. A function $\mathbf{f} : \mathbb{R}^r \to \mathbb{R}^s$ is called piecewise continuous in a finite domain $\mathrm{G} \subset \mathbb{R}^r$, if the domain G consists of a finite number of domains G_i, $i = 1, \ldots, l$ with disjoint interior and of a set $\mathrm{M} = \bigcup_{i=1}^{l} \partial\mathrm{G}_i$ of measure zero, which consists of boundary points of these domains, such that the function $f(\cdot)$ is continuous in each G_i and, when its argument approaches each point of the boundary, tends to a finite limit, possibly to different limits for different boundary points. If the domain G is infinite, then each finite part of the domain G must have common points only with a finite number of domains G_i.

Thus, a signal $\mathbf{s} : [t_0, \infty) \to \mathbb{R}^n$ is piecewise continuous, if it exhibits a finite number of discontinuities in any finite time interval and $\mathbf{s}(t_i^+)$ as well as $\mathbf{s}(t_i^-)$ are finite for all t_i. As in the case of the switching signal, we take piecewise continuous signals to be continuous from the right, i.e., $\mathbf{s}(t) = \mathbf{s}(t_i^+)$ for all $t \geq t_0$.

Remark 2.4.1. Frequently the question arises as to what is the difference between a switched system such as (2.67) and a time-varying system such as (2.7) or (2.68). As already pointed out by Hespanha in [78], the key distinction is that a time-varying system admits a family of solutions which is parametrized solely by the initial condition $\mathbf{x}(t_0)$, whereas the set of solutions to a switched system is parametrized by both the initial condition *and* the switching signal σ. Hence, when studying switched systems, one is typically interested in the properties of its solutions when the switching signal ranges over the set $\mathcal{S}$, and whether these properties are uniform over $\mathcal{S}$. For a particular switching signal (2.67) and (2.68) are of course identical.

If $\sigma(t)$ is an arbitrary function of time, we say that we have *trajectory-independent* switching. In many technical applications, however, we have to deal with *trajectory-depedent switching*, i.e., the value of the switching signal $\sigma(t) = \sigma(\mathbf{x}(t), \mathbf{u}(t))$ depends on the state $\mathbf{x}$ or on the input $\mathbf{u}$. Therefore, as done in [78], we define $\mathcal{S}$ to be a *relation* between the set of piecewise $\mathcal{C}^1$ signals $\mathbf{x}(t)$, the set of piecewise continuous input signals $\mathbf{u}(t)$, and the set of piecewise constant switching signals $\sigma(t)$. As a consequence, $\mathcal{S}$ is actually a set of admissible triples $(\mathbf{x}, \mathbf{u}, \sigma)$. Nevertheless, as in [78], we call $\mathcal{S}$, with some abuse of notation, the set of admissible switching signals. If the switching is trajectory-independent, $(\mathbf{x}, \mathbf{u}, \sigma) \in \mathcal{S}$ implies that also $(\bar{\mathbf{x}}, \bar{\mathbf{u}}, \sigma) \in \mathcal{S}$ for all other signals $\bar{\mathbf{x}}$ and $\bar{\mathbf{u}}$ such that the triple $(\bar{\mathbf{x}}, \bar{\mathbf{u}}, \sigma)$ is a solution to (2.67a). In this case, we simply write $\sigma \in \mathcal{S}$ with the understanding that $(\mathbf{x}, \mathbf{u}, \sigma) \in \mathcal{S}$ for any admissible combination of $\mathbf{x}$ and $\mathbf{u}$.

In this thesis, trajectory-dependent switching is addressed only in the context of two subsystems, i.e., $\mathcal{P} = \{1, 2\}$. Given the closed covering $\chi = \{\chi_p | p \in \mathcal{P}\}$ of $\mathbb{R}^n \times \mathbb{R}^m$ (i.e., the χ_p are closed sets $\chi_p \subset \mathbb{R}^n \times \mathbb{R}^m$ such that $\mathbb{R}^n \times \mathbb{R}^m = \chi_1 \cup \chi_2$), we consider the switching rule

$$\sigma(t) = i \quad \text{if} \quad (\mathbf{x}(t), \mathbf{u}(t)) \in \chi_i \, . \tag{2.69}$$

The corresponding set of triples $(\mathbf{x}, \mathbf{u}, \sigma) \in \mathcal{S}_{pc}$ satisfying $(\mathbf{x}(t), \mathbf{u}(t)) \in \chi_{\sigma(t)}$ is denoted by $\mathcal{S}[\chi]$. Throughout this thesis, the covering χ is disjoint and defined by

$$\begin{aligned} \chi_1 &= \{(\mathbf{x}, \mathbf{u}) \, | \varphi(\mathbf{x}, \mathbf{u}) \geq 0 \} \\ \chi_2 &= \{(\mathbf{x}, \mathbf{u}) \, | \varphi(\mathbf{x}, \mathbf{u}) \leq 0 \} \end{aligned} \tag{2.70}$$

where $\varphi(\mathbf{x}, \mathbf{u}) : \mathbb{R}^n \times \mathbb{R}^m \to \mathbb{R}$ is some smooth (i.e. $\mathcal{C}^\infty$) function affine in $\mathbf{u}$, i.e.,

$$\varphi(\mathbf{x}, \mathbf{u}) = \varphi_x(\mathbf{x}) + \boldsymbol{\varphi}_u^T(\mathbf{x})\mathbf{u} \ . \tag{2.71}$$

We assume that zero is a regular value of $\varphi(\mathbf{x}, \mathbf{u})$. Then, by the implicit function theorem, the boundary $\partial\chi = \partial\chi_1 = \partial\chi_2 = \{(\mathbf{x}, \mathbf{u}) | \varphi(\mathbf{x}, \mathbf{u}) = 0\}$ is an $(n + m - 1)$-dimensional submanifold of $\mathbb{R}^n \times \mathbb{R}^m$. Moreover, we assume that if there is an $\bar{\mathbf{x}}$ such that $\varphi_u(\bar{\mathbf{x}}) \neq 0$, then $\varphi_u(\mathbf{x}) \neq 0$ holds for all $\mathbf{x} \in \mathbb{R}^n$, i.e., if the switching is input-dependent, then this is the case for all $\mathbf{x}$. Note that (2.69) with (2.70) includes the cases, where the value of the switching signal depends only on the state or only on the input if $\varphi(\mathbf{x}, \mathbf{u})$ is chosen to be a function of the state or the input only.

Since $\partial\chi$ belongs to both sets χ_1 and χ_2, the switching law (2.69) is not well defined on $\partial\chi$ without making any further definition. Therefore, throughout this thesis, by convention, (2.69) is to be interpreted as follows. Let $\sigma(t_0) = 1$ if $(\mathbf{x}(t_0), \mathbf{u}(t_0)) \in \chi_1$ and $\sigma(t_0) = 2$ if $(\mathbf{x}(t_0), \mathbf{u}(t_0)) \in \chi_1^c$, where χ_1^c is the complement of χ_1. For all $t > t_0$, if $\sigma(t^-) = i$ and $(\mathbf{x}(t), \mathbf{u}(t)) \in \chi_i$, then we keep $\sigma(t) = i$. If for some t_i it holds that $\sigma(t_i^-) = 1$ but $(\mathbf{x}(t_i), \mathbf{u}(t_i)) \in \chi_1^c$, then switching to the second subsystem occurs, i.e., $\sigma(t_i) = 2$. Similarly, if $\sigma(t_i^-) = 2$ for some t_i but $(\mathbf{x}(t_i), \mathbf{u}(t_i)) \in \chi_2^c$, then we set $\sigma(t_i) = 1$.

If we consider the unforced (i.e., $\mathbf{u} \equiv 0$) system

$$\dot{\mathbf{x}} = \mathbf{f}_\sigma(\mathbf{x}, t) \ , \quad \sigma \in \mathcal{S} \ , \quad t \geq 0 \tag{2.72}$$

the set $\mathcal{S}$ consists of admissible pairs $(\mathbf{x}, \sigma)$ and χ is a covering of $\mathbb{R}^n$ with $\varphi(\cdot) : \mathbb{R}^n \to \mathbb{R}$ being a function of the state only. Accordingly, the switching law (2.69) simplifies to

$$\sigma(t) = i \quad \text{if } \mathbf{x}(t) \in \chi_i \ . \tag{2.73}$$

Remark 2.4.2. Any solution according to Definition 2.4.1 satisfies (2.68) in the sense of Carathéodory, but in the case of trajectory-dependent switching the converse is not true. If we apply the switching law (2.69) with the covering (2.70) and specify a particular piecewise continuous control input $\mathbf{u}(t)$, the switched system (2.67) is equivalent to a differential equation $\dot{\mathbf{x}} = \mathbf{f}(\mathbf{x}, t)$ with $\mathbf{f}(\mathbf{x}, t)$ piecewise continuous in $\mathbb{R}^n \times [0, \infty)$. A function $\mathbf{x}(t)$ defined on an open or closed interval $\mathcal{I}$ and absolutely continuous on each closed interval $[\alpha, \beta] \subset \mathcal{I}$ is a *Carathéodory solution* to this differential equation if it satisfies the integral equation $\mathbf{x}(t) = \mathbf{x}(t_0) + \int_{t_0}^t \mathbf{f}(\mathbf{x}(s), s)\, \mathrm{d}s$ for some $t_0 \in \mathcal{I}$ [51], [33]. This solution concept allows e.g. left- as well as right-accumulation points of event- or switching times[9]

[9] A point $\hat{t}$ is called a right (left)-accumulation point of event times if there is a sequence $\{t_i\}$ of event times with $t_i < (>)\, \hat{t}$ such that $\hat{t} = \lim_{i \to \infty} t_i = \hat{t} < \infty$ [76].

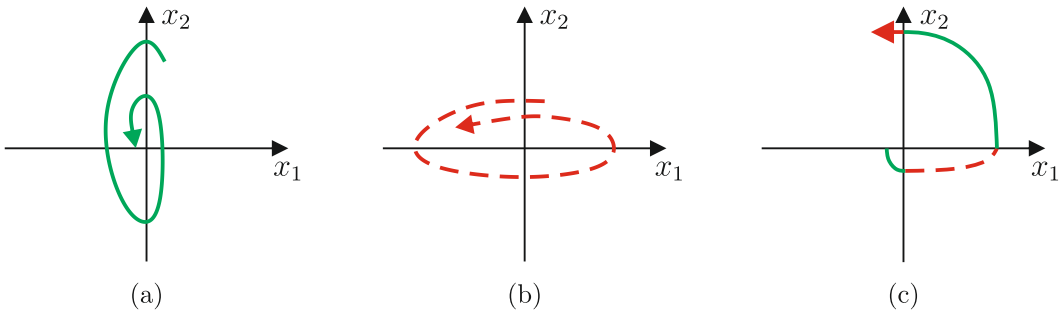

Figure 2.5: Switching between asymptotically stable systems.

[51], [76], where infinitely many switching events occur in finite time, which in contrast are ruled out by Definition 2.4.1.

Remark 2.4.3. If the switching law (2.69) is applied, there may be initial states for which a solution in the sense of Definition 2.4.1 and also in the sense of Carathéodory does not exist or only exists for finite T, even if it is bounded, i.e., does not exhibit finite escape time. In this case, Filippov's solution concept (see [51]) may be applied, which allows the existence of sliding modes. Although sliding modes are important from a theoretical as well as from a practical point of view, they may not be physically feasible, depending on how the switching is realized, and, moreover, the occurrence of sliding modes is often undesirable because of the *chattering* phenomenon, which causes excessive equipment wear, see e.g. [113], [87].

2.4.2 Stability

Stability is one of the most prevalent issues in the switched systems literature. To illustrate the basic problem, we consider the following situation. We have a planar (i.e., $n = 2$) linear switched system with two subsystems , i.e., $\mathcal{P} = \{1, 2\}$, which are asymptotically stable. Exemplary trajectories of both subsystem are shown in Figure 2.5(a) and Figure 2.5(b), respectively. If we choose the switching signal σ, for instance, such that in the 1st and 3rd quadrant the 1st subsystem is active and in the 2nd and 4th quadrant the 2nd subsystem, as shown in Figure 2.5(c), the trajectory of the switched system diverges. This simple example illustrates that switching can lead to instability even if all subsystems are asymptotically stable. Therefore, it is not sufficient to consider only the behavior of the individual subsystems, which makes the task of guaranteeing stability for a switched system more challenging than it is in the non-switched case.

Let us consider an unforced switched system of the form (2.72) and assume that all subsystems share a common equilibrium point denoted by $\mathbf{x}^*$, i.e., $\mathbf{f}_p(\mathbf{x}^*, t) = \mathbf{0}$ holds for all $t \geq 0$. Below we give the stability definitions used in the context of this class of systems.

Instead of just (asymptotic) stability, normally stability properties that are uniform over the set of admissible switching signals $\mathcal{S}$ are desired.

Definition 2.4.3. An equilibrium point $\mathbf{x}^*$ of (2.72) is said to be *uniformly stable*, if, for each $\epsilon > 0$, there is $\delta = \delta(\epsilon) > 0$, independent of t_0 and σ, such that

$$\|\mathbf{x}_0 - \mathbf{x}^*\| < \delta(\epsilon) \ , \ t_0 \geq 0 \ \Rightarrow \ \|\mathbf{x}(t) - \mathbf{x}^*\| < \epsilon \ , \ \forall\, t \geq t_0 \tag{2.74}$$

holds along all solutions $(\mathbf{x}, \sigma) \in \mathcal{S}$ of (2.72). If, in addition, there is a number $\zeta > 0$ such that for each ϵ there exists a $T = T(\epsilon)$ such that for all $(\mathbf{x}, \sigma) \in \mathcal{S}$

$$\|\mathbf{x}_0 - \mathbf{x}^*\| < \zeta \ , \ t_0 \geq 0 \ \Rightarrow \ \|\mathbf{x}(t) - \mathbf{x}^*\| < \epsilon \ , \ \forall\, t \geq T(\epsilon) \tag{2.75}$$

then we say that $\mathbf{x}^*$ is *uniformly asymptotically stable*.

In order to avoid confusion, some comments on the usage of the term "uniform" are in order. In Subsection 2.1.2, we have used this term to describe uniformity of the stability properties with respect to the initial time t_0 for time-varying systems. In the switched systems literature, "uniformity" refers to the multiple solutions of a switched system with *time-invariant* subsystems that one obtains as the switching signal ranges over $\mathcal{S}$. The stability definition above requires uniformity with respect to both the initial time t_0 and the switching signal $\sigma \in \mathcal{S}$ and includes the two definitions just mentioned as special cases. The *domain of attraction* $\mathrm{A}(\mathbf{x}^*)$ is defined as the set of initial conditions $\mathbf{x}_0$ such that for all $t_0 \in [0, \infty)$ and all $[\mathbf{x}(t; t_0, \mathbf{x}_0), \sigma] \in \mathcal{S}$ it holds that $\lim_{t \to +\infty} \mathbf{x}(t; t_0, \mathbf{x}_0) = \mathbf{x}^*$.

Lyapunov's direct method has a straightforward extension to switched systems, which can be used to establish uniform asymptotic stability. We first formulate the result for the general case, where the subsystems are time-varying, and then constrain our attention to time-invariant switched systems, for which much more results are available in the literature.

Theorem 2.4.1. *Let $\mathbf{x}^*$ be an equilibrium of the switched system (2.72). If there exists a $\mathcal{C}^1$ function $V : \mathbb{R}^n \times [0, \infty) \to \mathbb{R}$ and an open neighborhood $\Omega^W \subset \mathbb{R}^n$ of $\mathbf{x}^*$ such that*

$$W_1(\mathbf{x}) \leq V(\mathbf{x}, t) \leq W_2(\mathbf{x}) \tag{2.76}$$

$$\frac{\partial V(\mathbf{x}, t)}{\partial t} + \frac{\partial V(\mathbf{x}, t)}{\partial \mathbf{x}} \mathbf{f}_p(\mathbf{x}, t) \leq -W_3(\mathbf{x}) \tag{2.77}$$

$\forall\, p \in \mathcal{P}$, $\forall\, t \in [0, \infty)$, $\forall\, \mathbf{x} \in \Omega^W$, where the $W_i : \mathbb{R}^n \to \mathbb{R}$, $i = 1, 2, 3$ satisfy (2.13), then $\mathbf{x}^*$ is uniformly asymptotically stable. Moreover, if $c > 0$ is such that $\overline{\mathrm{S}}_c^{W_1}(\mathbf{x}^*)$ is bounded and contained in Ω^W, then $\overline{\mathrm{S}}_c^{W_2}(\mathbf{x}^*)$ is a subset of $\mathrm{A}(\mathbf{x}^*)$.

The function $V(\mathbf{x}, t)$ is referred to as *common Lyapunov function* for the family of systems $\dot{\mathbf{x}} = \mathbf{f}_p(\mathbf{x}, t)$, $p \in \mathcal{P}$. For time-invariant switched systems

$$\dot{\mathbf{x}} = \mathbf{f}_\sigma(\mathbf{x}) \tag{2.78}$$

the theorem simplifies as follows.

Theorem 2.4.2. *If there is a $\mathcal{C}^1$ function $V(\mathbf{x})$ that is positive definite at the equilibrium point $\mathbf{x}^*$ of (2.78), and an open neighborhood $\Omega^{\dot{V}} \subset \mathbb{R}^n$ of $\mathbf{x}^*$ such that*

$$\nabla^T V(\mathbf{x}) \mathbf{f}_p(\mathbf{x}) < 0 \ , \quad \forall\, \mathbf{x} \in \Omega^{\dot{V}} \setminus \{\mathbf{x}^*\} \ , \ \forall\, p \in \mathcal{P} \tag{2.79}$$

then $\mathbf{x}^*$ is uniformly asymptotically stable. If $c > 0$ is such that $\overline{\mathrm{S}}_c(\mathbf{x}^*)$ is bounded and contained in $\Omega^{\dot{V}}$, then $\overline{\mathrm{S}}_c(\mathbf{x}^*)$ is contained in $\mathrm{A}(\mathbf{x}^*)$.

Let us note that the condition (2.79) is sufficient only because $\mathcal{P}$ is a finite set. Otherwise the zero on the right hand side would have to be replaced by $-W(\mathbf{x})$ with $W(\mathbf{x})$ positive definite at $\mathbf{x}^*$. Moreover, it is interesting to know that, under some technical conditions, the existence of a common Lyapunov function can be shown to be not only sufficient but also necessary for the uniform asymptotic stability of a time-invariant system (2.78) with arbitrary switching. These conditions are satisfied under the assumptions made above, namely that $\mathcal{P}$ is finite and that all $\mathbf{f}_p$ are locally Lipschitz. This yields a justification for the common Lyapunov function approach, which also will be pursued in this thesis.

In case that a common Lyapunov function does not exist or is not known, *multiple Lyapunov functions* can be used to establish (asymptotic) stability for a particular class of switching signals $\mathcal{S} \subset \mathcal{S}_{pc}$. The approach has originally been proposed by Peleties [144] for switched linear systems and has been generalized to the nonlinear case by Branicky in the frequently cited paper [21]. Since then, a multitude of variants and extensions has been put forth, see e.g. [192], [38], [78], [109] and the references therein. In [109], multiple Lyapunov functions are employed for the stability analysis of time-varying switched systems, and Corollary 2 in this paper contains Theorem 2.4.1 as a special case. Let us mention that also the dissipativity and passivity concepts for switched systems that are based on multiple storage functions and the associated stability results (see e.g. [194], [191]) are closely related to the multiple Lyapunov function concept.

However, all these approaches have in common that further conditions have to be imposed to guarantee stability. In the simplest case, one Lyapunov function V_p is associated with each vector field $\mathbf{f}_p$ satisfying $\nabla^T V_p \mathbf{f}_p < 0$, which is analogue to (2.79), and *additionally* it is required that the condition $V_{\sigma(t_i)}(\mathbf{x}(t_i)) \leq V_{\sigma(t_i^-)}(\mathbf{x}(t_i^-))$ is fulfilled for every switching time

t_i (see [78]). For a time-dependent switching signal the latter condition is of course very difficult, if not impossible, to check a priori, i.e., without knowledge of the actual values of $\mathbf{x}(t_i)$ at the switching times. In the context of state-dependent switching the condition has to be satisfied only at the switching surfaces, but determining suitable Lyapunov functions for a given nonlinear switched system is in general a difficult task. In the linear case, however, this problem can be formulated as a linear matrix inequality (LMI) problem, for which efficient solvers are available [38]. Moreover, the multiple Lyapunov function approach is very useful for the construction of stabilizing state-dependent switching laws, see e.g. [113].

In the Theorems 2.4.1 and 2.4.2, the common Lyapunov function is required to be strictly decreasing along the subsystem trajectories (*strict common Lyapunov function*) in order to ensure asymptotic stability. In fact, the Krassovski-LaSalle Theorem, which allows us to establish asymptotic stability of non-switched time-invariant systems using non-strictly decreasing, so called *weak Lyapunov functions*, is not applicable to switched systems. In general, only the following much weaker result holds.

Theorem 2.4.3. *Let $\mathbf{x}^*$ be an equilibrium of the switched system* (2.72)*. Suppose there is a $\mathcal{C}^1$ function $V : \mathbb{R}^n \times [0,\infty) \to \mathbb{R}$ and an open neighborhood $\Omega^W \subset \mathbb{R}^n$ of $\mathbf{x}^*$ such that* (2.76) *and* (2.77) *hold for all $p \in \mathcal{P}$, all $t \in [0,\infty)$ and all $\mathbf{x} \in \Omega^W$, where $W_1(\mathbf{x})$ and $W_2(\mathbf{x})$ are continuous functions satisfying* (2.13) *and $W_3(\mathbf{x})$ is continuous and positive semidefinite, i.e., $W_3(\mathbf{x}^*) = 0$ and $W_3(\mathbf{x}) \geq 0,\ \forall\, \mathbf{x} \in \Omega^W$. Then, $\mathbf{x}^*$ is uniformly stable. Moreover, if $c > 0$ is such that $\bar{\mathrm{S}}_c^{W_1}(\mathbf{x}^*)$ is bounded and contained in Ω^W, then all trajectories starting in $\bar{\mathrm{S}}_c^{W_2}(\mathbf{x}^*)$ approach the set $\{\mathbf{x} \in \mathrm{S}_c^{W_1}(\mathbf{x}^*) | W_3(\mathbf{x}) = 0\}$ as $t \to \infty$.*

This follows directly from Theorem 4.4 in [95]. For time-invariant switched systems several extensions of the Krassovski-LaSalle theorem have been developed in the literature under some regularity assumptions regarding the distance between the consecutive switching times, see e.g. [7], [70], [78], [109], [120]. It has been illustrated by examples in [78] and [7] that some type of regularity in the switching signals is indeed needed to obtain Krassovski-LaSalle-like criteria for switched systems. The following theorem is contained in Theorem 2.3 in [120] as a special case, when only a single Lyapunov function is used instead of multiple ones.

Theorem 2.4.4. *Consider the switched system* (2.78) *and suppose that there is a function $V(\mathbf{x})$ that is positive definite at $\mathbf{x}^*$ and continuous functions $W_p(\mathbf{x})$, $p \in \mathcal{P}$ which are nonnegative in an open neighborhood $\Omega^W \subset \mathbb{R}^n$ of $\mathbf{x}^*$ such that*

$$\nabla^T V(\mathbf{x}) \mathbf{f}_p(\mathbf{x}) \leq -W_p(\mathbf{x}) , \quad \forall\, \mathbf{x} \in \Omega^W \ , \ \forall p \in \mathcal{P} \ . \tag{2.80}$$

Further, suppose that for any $\delta > 0$, any $p \in \mathcal{P}$ and any solution of $\dot{\mathbf{x}} = \mathbf{f}_p(\mathbf{x})$ satisfying $W(\mathbf{x}(t)) = 0,\ \forall\, t \in [0, \delta)$, we have $\mathbf{x}(0) = \mathbf{x}^*$. Then, if $\mathcal{S} \subset \mathcal{S}_{average}$, the equilibrium $\mathbf{x}^*$ is asymptotically stable. If $\mathcal{S} \subset \mathcal{S}_{average}[\tau_D, N_0]$ for some $\tau_D > 0$ and some $N_0 > 0$, then $\mathbf{x}^*$ is uniformly asymptotically stable. Moreover, if $c > 0$ is such that $\overline{\mathrm{S}}_c^V(\mathbf{x}^*)$ is bounded and contained in Ω^W, then $\overline{\mathrm{S}}_c^V(\mathbf{x}^*)$ is contained in $\mathrm{A}(\mathbf{x}^*)$.

In Section 2.2 we have addressed the passivity concept for non-switched systems and its application for feedback stabilization. The classic notion of passivity from Definition 2.2.2 obviously can be carried over to switched systems

$$\dot{\mathbf{x}} = \mathbf{f}_\sigma(\mathbf{x}) + \mathbf{G}_\sigma(\mathbf{x})\mathbf{u} \tag{2.81a}$$

$$\mathbf{y} = \mathbf{h}_\sigma(\mathbf{x})\ . \tag{2.81b}$$

We say that (2.81) is passive if there is a $\mathcal{C}^0$ storage function $H : \mathbb{R}^n \to \mathbb{R}$ such that for all $(\mathbf{x}, \mathbf{u}, \sigma) \in \mathcal{S}$ and all $t \geq 0$ it holds that

$$H(\mathbf{x}) - H(\mathbf{x}_0) \leq \int_0^t \mathbf{u}^T \mathbf{h}_{\sigma(\tau)}(\mathbf{x}(\tau))\, d\tau = \int_0^t \mathbf{u}^T \mathbf{y}\, d\tau\ . \tag{2.82}$$

2.5 Numerically Computable Bounds on Real-Valued Functions

In this section, we review parts of the theory developed in [66] as an extension of the Theorem of Ehlich and Zeller [47]. It will be used in Section 3.4 to compute guaranteed bounds for real-valued functions on a rectangular region in $\mathbb{R}^n$. Let $\mathrm{J}_i = [a_i, b_i]$, $i = 1, \ldots, n$ be subsets of the real line and $\mathrm{X}_i(N_i, \mathrm{J}_i)$, $N_i \in \mathbb{N}$ the set of Chebyshev points $x_j = \frac{a_i+b_i}{2} + \frac{b_i-a_i}{2}\cos(\frac{2j-1}{N_i}\frac{\pi}{2})$, $j = 1, \ldots, N_i$. Moreover, we define the hyperrectangle $\mathrm{J} \subset \mathbb{R}^n$ by $\mathrm{J} = \mathrm{J}_1 \times \ldots \times \mathrm{J}_n$ and the corresponding grid of Chebyshev points $\mathrm{X} = \mathrm{X}_1(N_1, \mathrm{N}_1) \times \ldots \times \mathrm{X}_n(N_n, \mathrm{J}_n)$. Suppose the function $F : \mathrm{J} \to \mathbb{R}$ can be approximated by a polynomial $P : \mathrm{J} \to \mathbb{R}^n$ of the form

$$P(\mathbf{x}) = \sum_{\alpha_1=0}^{\varrho_1} \ldots \sum_{\alpha_n=0}^{\varrho_n} a_{\alpha_1 \ldots \alpha_n} x_1^{\alpha_1} \ldots x_n^{\alpha_n} \tag{2.83}$$

such that $\max_{\mathbf{x}\in\mathrm{J}} |F(\mathbf{x}) - P(\mathbf{x})| \leq r$. Moreover, assume that $N_i > \varrho_i$, $i = 1, \ldots, n$ and define

$$K\left(\frac{\varrho}{N}\right) = C\left(\frac{\varrho_1}{N_1}\right) \ldots C\left(\frac{\varrho_n}{N_n}\right)\ , \quad \text{where } C(q) = \left[\cos\left(\frac{\pi}{2}q\right)\right]^{-1}\ . \tag{2.84}$$

Then, the inequalities

$$\|F\|^{\mathrm{J}} \leq B \;, \quad F^{\mathrm{J}}_{min} \geq \underline{B} \;, \quad F^{\mathrm{J}}_{max} \leq \overline{B} \tag{2.85}$$

hold with

$$B = K(\frac{\varrho}{N})\|F\|^{\mathrm{X}} + \left(K(\frac{\varrho}{N}) + 1\right) r \tag{2.86a}$$

$$\underline{B} = \frac{1}{2}\left\{\left(K(\frac{\varrho}{N}) + 1\right) F^{\mathrm{X}}_{min} - \left(K(\frac{\varrho}{N}) - 1\right) F^{\mathrm{X}}_{max}\right\} - \left(K(\frac{\varrho}{N}) + 1\right) r \tag{2.86b}$$

$$\overline{B} = \frac{1}{2}\left\{\left(K(\frac{\varrho}{N}) + 1\right) F^{\mathrm{X}}_{max} - \left(K(\frac{\varrho}{N}) - 1\right) F^{\mathrm{X}}_{min}\right\} + \left(K(\frac{\varrho}{N}) + 1\right) r \tag{2.86c}$$

where we have used the notations $\|F\|^{\mathrm{J}} = \sup_{\mathbf{x}\in\mathrm{J}} |F(\mathbf{x})|$ as well as $F^{J}_{min} = \min_{\mathbf{x}\in\mathrm{J}} F(\mathbf{x})$ and $F^{J}_{max} = \max_{\mathbf{x}\in\mathrm{J}} F(\mathbf{x})$.

Note that the polynomial $P(\mathbf{x})$ is not explicitly required but only the numbers ϱ_i and the approximation error r. In order to determine these quantities it is suggested in [66] to decompose $F(\mathbf{x})$ into simple terms. We assume here, for simplicity, that the function $F(\mathbf{x})$ can be represented as

$$F(\mathbf{x}) = Q_0(\mathbf{x}) + \sum_{k=0}^{l_1} Q_{1,k}(\mathbf{x})F_{1,k}(x_1) + \ldots + \sum_{k=0}^{l_n} Q_{n,k}(\mathbf{x})F_{n,k}(x_n) \tag{2.87}$$

where $Q_0 : \mathrm{J} \to \mathbb{R}$ and the $Q_{i,k} : \mathrm{J} \to \mathbb{R}$ are polynomials, and the $F_{i,k} : \mathrm{J}_i \to \mathbb{R}$ are smooth functions that depend only on *one* variable. For a more general treatment, the reader is referred to [66]. We use the notation $\varrho_i(Q_0)$ and $\varrho_i(Q_{i,k})$ for the maximum degree of x_i that appears in Q_0 and Q_{ik}, respectively.

It is well known (see e.g. [162]) that there are (univariate) polynomials $P_{i,k} : \mathrm{J}_i \to \mathbb{R}$ in x_i with prescribed degrees $\varrho_i(P_{i,k})$ such that

$$\|F_{i,k}(x_i) - P_{i,k}(x_i)\| \leq r_{i,k} = 2\left(\frac{b_i - a_i}{4}\right)^{\varrho_i(P_{i,k})+1} \frac{1}{(n+1)!} \left\|F^{(\varrho_i(P_{i,k})+1)}_{i,k}\right\|^{\mathrm{J}_i} \tag{2.88}$$

where $F^{(q)}_{i,k} = \frac{d^q}{dx_i^q} F_{i,k}(x_i)$. These polynomials can be obtained by polynomial interpolation using Chebyshev points as interpolation points. With Lemma 1.5 in [66] we get

$$r = \sum_{j=0}^{n} \sum_{k_j=0}^{l_j} \|Q_{j,k_j}\|^{\mathrm{J}} r_{j,k_j} \;, \tag{2.89a}$$

$$\varrho_i = \max\left\{\varrho_i(Q_0), \varrho_i(Q_{j,k_j}) + \varrho_i(P_{j,k_j}), j = 1, \ldots, n, k_j = 1, \ldots, l_j\right\} \tag{2.89b}$$

where $\varrho_i(P_{j,k_j}) = 0$ for $i \neq j$ and the r_{j,k_j} are calculated according to (2.88). In (2.89a), the values $\|Q_{j,k_j}\|^{\mathrm{J}}$ can also be substituted by upper bounds, which can be determined likewise by applying the inequalities (2.85), (2.86) with $r = 0$. The latter is due to the fact that the Q_{j,k_j} are polynomials.

Part I

Smooth Systems

Chapter 3

Estimating the Domain of Attraction

As we have seen in the previous chapter, the IDA methodology assigns a pH structure with a desired energy function to the closed loop system. In this chapter, we are concerned with the question how this pH structure can be exploited to determine an estimate of the DA of the desired equilibrium point. One central feature of IDA is that the energy function represents a natural Lyapunov function for the closed loop system and hence allows for estimating the DA. Since, in general, the energy function is not radially unbounded, this gives rise to the question how its largest bounded sublevel set can be determined. As outlined in Section 1.3.1, as yet there is no satisfactory method available to solve this problem. Recall that the conditions for the applicability of the closest UEP method [27], [31] can usually not be guaranteed in the context of IDA (see also Remark 1 in [61] and Section 3.1 below) and that exploiting strong convexity of the energy function, as done in [61], is only viable for simple energy functions and may lead to conservative estimates. Therefore, we develop in this chapter a numerical approach to estimate the DA of an IDA controller, which does not impose any requirements on the energy function that go beyond the conditions of IDA itself. The proposed method is able to deal with systems whose dissipation matrix is only locally positive semidefinite, and it can be extended also to the time-varying case. Parts of the results in this chapter have been published in [97].

The remainder of the chapter is organized as follows. After a formal problem statement in Section 3.1 we present the theoretical basis of the proposed method in Section 3.2. Based on that, we derive in Section 3.3 a numerical algorithm that allows to estimate the DA for both time-invariant and time-varying systems. In Section 3.4, an alternative algorithm is presented, which makes use of the numerically calculable bounds on real-valued functions reviewed in Section 2.5.

3.1 Problem Statement

The IDA method endows the closed loop system with a pH structure

$$\dot{\mathbf{x}} = \mathbf{F}(\mathbf{x})\nabla H(\mathbf{x}) \tag{3.1}$$

where the energy function $H(\mathbf{x})$ has a strict local minimum at the desired equilibrium $\mathbf{x}^*$ and $\mathbf{R}(\mathbf{x}) = -\text{sym}\{\mathbf{F}(\mathbf{x})\} \geq 0$ holds within an open neighborhood $\Omega^R \subset \mathbb{R}^n$ of $\mathbf{x}^*$. Without loss of generality, we assume throughout this first part of the thesis that $\mathbf{x}^* = \mathbf{0}$ and $H(\mathbf{0}) = 0$. By virtue of the pH structure, the energy function satisfies $\dot{H}(\mathbf{x}) \leq 0$ for all $\mathbf{x}$ within an open neighborhood $\Omega^{\dot{H}}$ of $\mathbf{x}^* = \mathbf{0}$ and thus is a Lyapunov function for the closed loop system.

In order to determine an estimate of the DA based on this Lyapunov function, we need to identify a level value $c > 0$ such that $\overline{\mathrm{S}}_c(\mathbf{0})$ is bounded and entirely contained in $\Omega^{\dot{H}}$. Then, we can invoke the Krassovski-LaSalle Theorem to verify that all trajectories starting within this set tend to the origin as $t \to \infty$. Since an as large as possible estimate of the DA is wanted, we are interested in the largest value c that satisfies these requirements. In the case of radially unbounded Lyapunov functions, that are typically used in this context, all sublevel sets are bounded and thus the only concern is negative (semi-) definiteness of their derivative along the system trajectories. However, the energy function $H(\mathbf{x})$ in (3.1), which is determined from a set of linear PDEs during the IDA controller design, is usually *not radially unbounded*. Moreover, the origin is usually not the only *critical point*[1] of the energy function. Since these points are equilibria of the closed loop system (3.1), a necessary condition for $\overline{\mathrm{S}}_c(\mathbf{x}^*)$ to be a subset of $\mathrm{A}(\mathbf{0})$ is that it contains no critical points of $H(\mathbf{x})$ other than the origin. In summary, all of this amounts to the following problem statement.

Problem 3.1.1. Find the largest level value $\hat{c}$ – henceforth called the *critical level value* – such that $\mathrm{S}_{\hat{c}}(\mathbf{0})$ is i) bounded, ii) a subset of $\Omega^{\dot{H}}$, and iii) does not contain critical points of the energy function other than the origin.

This is illustrated in Figure 3.1, where the sublevel set $\mathrm{S}_{\hat{c}}$ is depicted in green and its connected component containing the origin $\mathrm{S}_{\hat{c}}(\mathbf{0})$ is marked red. In the Figures 3.1(a) and 3.1(b), it is assumed that $\dot{H} \leq 0$ holds globally, i.e., the critical level value is solely determined by the requirements that $\mathrm{S}_{\hat{c}}(\mathbf{0})$ has to be bounded and may not contain critical points of $H(\mathbf{x})$ other than the origin. While in Figure 3.1(a) the level value can be increased

[1] Recall that $\mathbf{p}$ is called a critical point of a function $H : \mathbb{R}^n \to \mathbb{R}$, if $\nabla H|_{\mathbf{p}}$ vanishes.

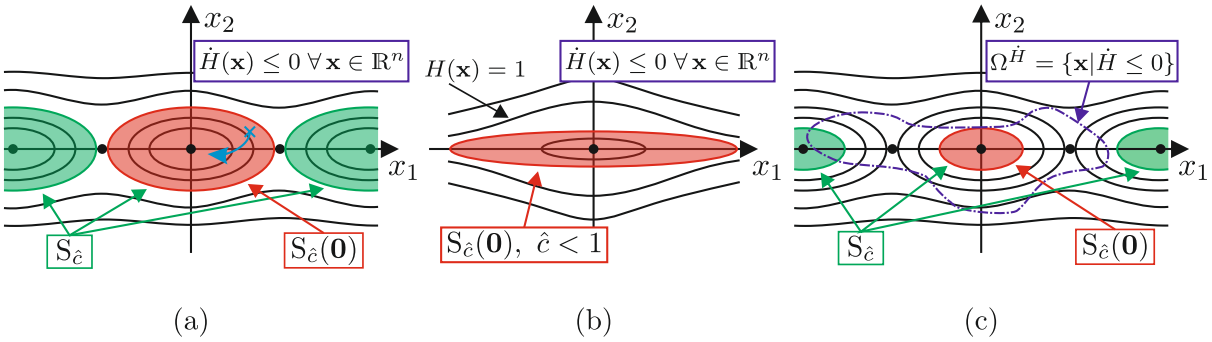

Figure 3.1: Estimating the DA by means of the energy function.

until $\partial \mathrm{S}(\mathbf{0})$ hits a critical point of $H(\mathbf{x})$, in Figure 3.1(b) the only critical point is the origin, but the sublevel sets become unbounded for level values $c \geq 1$. In Figure 3.1(c), the energy function is identical to the one in Figure 3.1(a), but $\dot{H} \leq 0$ is assumed to hold only within a neighborhood $\Omega^{\dot{H}}$ of the origin.

Considering the different situations illustrated in Figure 3.1, it becomes clear that in the context of IDA the energy function neither can be guaranteed to be (globally) strictly decreasing nor to be a proper map along any system trajectory. Hence, in general, none of the conditions for the applicability of the closest UEP method mentioned in Section 1.3.1 is fulfilled. This is of course even more so, if the closed loop system is a time-varying pH system

$$\dot{\mathbf{x}} = \mathbf{F}(\mathbf{x}, t) \nabla H(\mathbf{x}, t) \; , \quad \mathrm{sym}\{\mathbf{F}(\mathbf{x}, t)\} \leq 0 \; , \quad \forall \, \mathbf{x} \in \Omega^R \; , \; \forall \, t \geq 0 \tag{3.2}$$

as it is the case e.g. in tracking control problems (see Section 2.3.2 and the examples in the Sections 5.3 and 8.2), because there is no generalization of the closest UEP method to time-varying systems. As for time-invariant energy functions, we assume, without loss of generality, that $H(\mathbf{0}, t) = 0 \; \forall \, t \geq 0$. We have seen in Section 2.2.5, that in the time-varying case, the pH-structure does not guarantee stability any more. Hence, we use $H(\mathbf{x}, t)$ as a Lyapunov function candidate to verify that the IDA controller renders the origin uniformly asymptotically stable and to estimate the corresponding DA. According to Theorem 2.1.2 this amounts to the following Problem.

Problem 3.1.2. Find, if possible, positive definite functions $W_i(\mathbf{x})$, $i = 1, 2, 3$ satisfying (2.11), (2.12), and determine the largest level value $\hat{c}$ such that $\mathrm{S}_{\hat{c}}^{W_1}(\mathbf{0})$ is bounded and contained in Ω^{W_3}.

An estimate of the DA is then given by $\mathrm{S}_{\hat{c}}^{W_2}(\mathbf{0})$. Similar to the time-invariant case, $W_1(\mathbf{x})$ is in general not radially unbounded and hence boundedness of $\mathrm{S}_c^{W_1}(\mathbf{0})$ can usually be ensured only for sufficiently small level values c.

3.2 Theoretical Basis

In this section, we lay the theoretical foundation for the algorithms presented in the current chapter. In the course of that, the notion of (proper) star-shapedness with respect to (w.r.t) the origin will be needed. A set T is said to be (properly) star-shaped w.r.t. the origin, if for all $\mathbf{x} \in \bar{\mathrm{T}}$ the line segment between the origin and $\mathbf{x}$ is in $(\operatorname{int} \mathrm{T})\ \bar{\mathrm{T}}$, where $\operatorname{int} \mathrm{T}$ is the interior and $\bar{\mathrm{T}}$ the closure of T. The following definition is equivalent and more suitable for our needs.

Definition 3.2.1 ([54])**.** A simply connected set $\mathrm{T} \subset \mathbb{R}^n$ is called *star shaped w.r.t. the origin* if, for each $\mathbf{x} \in \partial\mathrm{T}$, the angle $\omega(\mathbf{x})$ between the outer normal to $\partial\mathrm{T}$ and the radial direction $\mathbf{x}$ satisfies $\omega(\mathbf{x}) \leq \pi/2$. It is called *properly star shaped w.r.t. the origin*, if $\omega(\mathbf{x}) < \pi/2$ holds.

The proofs of the following lemma and of Lemma 3.2.2 use some ideas from [28].

Lemma 3.2.1. *Let* $\mathrm{D} \subset \mathbb{R}^n$ *be a simply connected bounded set containing the origin. If* $\hat{c} = \min_{\mathbf{x}\in\partial D} H(\mathbf{x})$*, then* $\mathrm{S}_{\hat{c}}(\mathbf{0}) \subset \mathrm{D}$ *and hence is bounded.*

Proof. Let $\hat{\mathbf{x}} = \arg\min_{\mathbf{x}\in\partial D} H(\mathbf{x})$. Since $\hat{\mathbf{x}} \in \partial\mathrm{D}$, $\mathrm{S}_{\hat{c}}(\mathbf{0}) \cap \partial\mathrm{D} = \emptyset$. Hence, $\mathrm{S}_{\hat{c}}(\mathbf{0}) \cap \bar{\mathrm{D}}^c = \emptyset$, since otherwise $\mathrm{S}_{\hat{c}}(\mathbf{0})$ would not be connected. It follows that $\mathrm{S}_{\hat{c}}(\mathbf{0}) \subset \operatorname{int} \bar{\mathrm{D}}$, and since D is bounded, $\mathrm{S}_{\hat{c}}(\mathbf{0})$ is bounded. □

Based on this lemma, a bounded set $\mathrm{S}_{\hat{c}}(\mathbf{0})$ could be determined. However, it might be very small or even an empty set, if D is chosen such that $\hat{c} < 0$. Moreover, it is not guaranteed that $\mathrm{S}_{\hat{c}}(\mathbf{0})$ contains no other critical points of $H(\mathbf{x})$ than the origin.

Now we consider the restriction of $H(\mathbf{x})$ to a straight line $g_v(\lambda) = H(\lambda\mathbf{v})$ with $\lambda > 0$ and $\mathbf{v} \in \mathbb{S}^{n-1}$, where $\mathbb{S}^{n-1}$ denotes the $(n-1)$-dimensional unit sphere. We have the following lemma.

Lemma 3.2.2. *Let* $\mathrm{D} \subset \mathbb{R}^n$ *be an open simply connected bounded set which is star-shaped w.r.t. the origin. Assume that* $\frac{d}{d\lambda} g_v(\lambda) > 0$ *holds for all* $\mathbf{v} \in \mathbb{S}^{n-1}$ *and all* $\lambda > 0$ *such that* $\lambda\mathbf{v} \in \mathrm{D}$*. If* $\hat{c} = \min_{\mathbf{x}\in\partial D} H(\mathbf{x})$*, then*

1) $\mathrm{S}_{\hat{c}}(\mathbf{0}) \subset \mathrm{D}$ *and hence* $\mathrm{S}_{\hat{c}}(\mathbf{0})$ *is bounded.*

2) the only critical point of $H(\mathbf{x})$ *in* $\mathrm{S}_{\hat{c}}(\mathbf{0})$ *is* $\mathbf{x}^* = \mathbf{0}$.

3) the set $\{\mathrm{S}_b(\mathbf{0}) \cap \bar{D}^c\}$ *is nonempty for any* $b > \hat{c}$.

4) all sets $\mathrm{S}_a(\mathbf{0})$ *with* $a < \hat{c}$ *are properly star-shaped w.r.t. the origin.*

Proof. Part 1) follows readily from Lemma 3.2.1. Part 2) is obvious from the fact that $\frac{d}{d\lambda} g_v(\lambda) = (\nabla H(\mathbf{x})|_{\mathbf{x}=\lambda\mathbf{v}})^T \mathbf{v} > 0$ for all $\lambda\mathbf{v} \in \mathrm{D}\backslash\{\mathbf{0}\}$. Now consider any number $b > \hat{c}$. Then, there is a point $\mathbf{y} \in \partial\mathrm{D}$ with $\mathbf{y} \in \mathrm{S}_b(\mathbf{0})$. By the assumption made on $\frac{d}{d\lambda} g_v(\lambda)$, $\mathbf{y}$ belongs to the component $\mathrm{S}_b(\mathbf{0})$. Since $\mathbf{y} \in \partial\mathrm{D}$ for any neighborhood N of $\mathbf{y}$, it holds that $\mathrm{N} \cap \bar{\mathrm{D}}^c \neq \emptyset$. If N is chosen small enough, we have that $\mathrm{N} \cap \bar{\mathrm{D}}^c \neq \emptyset$ and $\mathrm{N} \subset \mathrm{S}_b(\mathbf{0})$, which proves Part 3) of the lemma. It follows from Part 1) that for $a < \hat{c}$ we have that $\bar{\mathrm{S}}_a(\mathbf{0}) \subset \operatorname{int} \mathrm{D}$ and therefore $\frac{d}{d\lambda} g_v(\lambda) = (\nabla H(\mathbf{x})|_{\mathbf{x}=\lambda\mathbf{v}})^T \mathbf{v} > 0$ holds for all $\mathbf{x} \in \partial\mathrm{S}_a(\mathbf{0})$. Since at any point $\mathbf{x} = \lambda\mathbf{v} \in \partial\mathrm{S}_a(\mathbf{0})$ the outer normal to $\partial\mathrm{S}_a(\mathbf{0})$ is given by $\nabla H(\mathbf{x})$ it follows that $\omega(\mathbf{x}) < \frac{\pi}{2}$. This proves Part 4) of the lemma. □

Given a function $H(\mathbf{x})$, the above results motivate the search for the largest set D which satisfies the conditions of Lemma 3.2.2 or, in particular, for the minimum value of $H(\mathbf{x})$ over its boundary $\partial\mathrm{D}$. To guarantee that the algorithm presented in Section 3.3 converges in a finite number of steps, the search is restricted to a ball $\mathrm{B}_R = \{\mathbf{x} \in \mathbb{R}^n : \|\mathbf{x}\| \leq R\}$, which is chosen considering the operating range of the system. Hence, it is desired to determine the maximum set $\mathrm{D} \subset \mathrm{B}_R$ which satisfies the conditions of Lemma 3.2.2. This is illustrated in Figure 3.2. The *radial function* $\rho_{\bar{D}} : \mathbb{S}^{n-1} \to \mathbb{R}_0^+$ of $\bar{D}$ associated with the origin

$$\begin{aligned} \rho_{\bar{D}}(\mathbf{v}) &= \sup\left\{a \geq 0 : a\mathbf{v} \in \bar{\mathrm{D}}\right\} \\ &= \sup\left\{0 < a < R : \left.\frac{d}{d\lambda} g_v(\lambda)\right|_{\lambda=a} > 0\right\} \end{aligned} \tag{3.3}$$

uniquely determines the set $\bar{\mathrm{D}}$ [8]. In general, the boundary of D is made up of parts of $\partial\mathrm{B}_R$, parts of the manifold M defined by $\nabla^T H(\mathbf{x})\mathbf{x} = 0$, and possibly $(n-1)$-dimensional objects T_i which are such that at all points $\mathbf{x} \in \mathrm{T}_i$ the radial direction $\mathbf{x}$ is tangential to T_i, see Figure 3.3. The following lemma is derived from (3.3) and Lemma 3.2.2.

Lemma 3.2.3. *Given a ball* B_R, *let* $\bar{\mathrm{D}}$ *be defined by* (3.3). *Then,* $\hat{c} = \min_{\mathbf{x}\in\partial D} H(\mathbf{x})$ *is the maximum level value such that i)* $\mathrm{S}_{\hat{c}}(\mathbf{0}) \subset \mathrm{B}_R$, *ii)* $\mathrm{S}_{\hat{c}}(\mathbf{0})$ *contains no critical points of* $H(\mathbf{x})$ *except the origin, and iii) for all* $0 < a < \hat{c}$, *the set* $\mathrm{S}_a(\mathbf{0})$ *is properly star-shaped w.r.t. to the origin.*

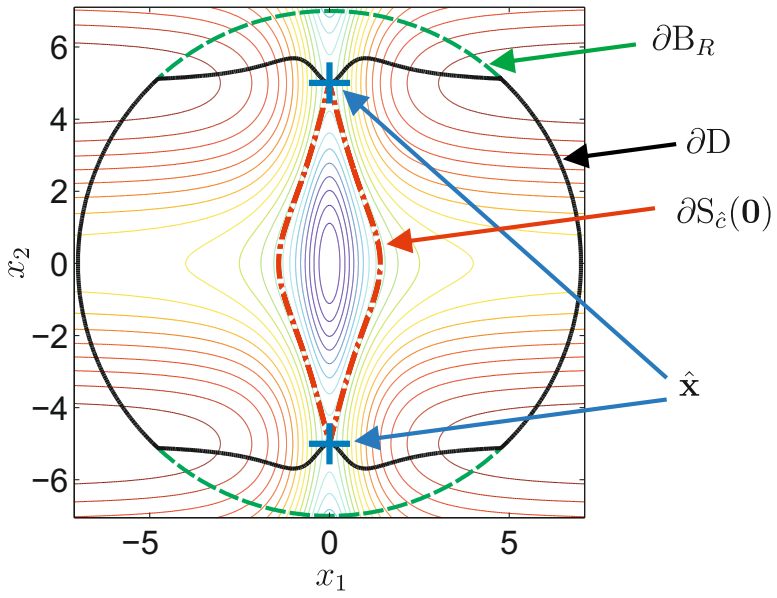

Figure 3.2: Contour plot of an exemplary energy function $H(\mathbf{x})$ with the largest set D (black solid) within B_R (green dashed) which satisfies the conditions of Lemma 3.2.2, points $\hat{\mathbf{x}}$ where $H(\mathbf{x})$ attains its minimum over $\partial \mathrm{D}$ (blue markers), and the corresponding level set $\partial \mathrm{S}_{\hat{c}}(\mathbf{0})$ (red dashed-dotted).

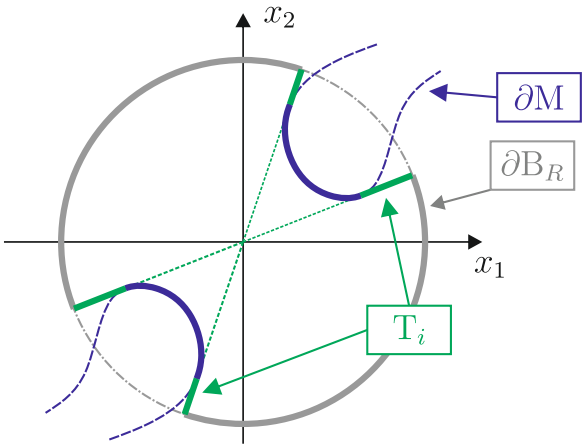

Figure 3.3: The boundary $\partial \mathrm{D}$ (thick lines) is, in general, composed of parts of M (blue), parts of $\partial \mathrm{B}_R$ (grey), and $(n-1)$-dimensional objects T_i (green).

In case that $\dot{H}(\mathbf{x}) \leq 0$ holds globally, this lemma provides a solution to Problem 3.1.1, however, with the restriction that the sublevel sets $\mathrm{S}_a(\mathbf{0})$, $0 < a < \hat{c}$ are properly star-shaped w.r.t. the origin. That means that there might be larger sublevel sets which meet all requirements of Problem 3.1.1 but are not star-shaped w.r.t. the origin. It should be

pointed out, however, that we have not imposed any conditions on the energy function except those of IDA itself. Also, it is remarked that, to our experience, most energy functions indeed have the property that the sublevel sets of interest are star-shaped w.r.t. the origin.

In case that $\dot{H}(\mathbf{x}) \leq 0$ is guaranteed only in a neighborhood $\Omega^{\dot{H}}$ of the origin, we additionally consider the restriction of $\dot{H}(\mathbf{x})$ to a straight line defined by $h_v(\lambda) = \dot{H}(\lambda \mathbf{v})$ with $\lambda > 0$ and $\mathbf{v} \in \mathbb{S}^{n-1}$. Similar to (3.3), we introduce the set $\bar{\mathrm{E}}$ characterized by its radial function $\rho_{\bar{E}}$ associated with the origin

$$\rho_{\bar{E}}(\mathbf{v}) = \sup \left\{ 0 < a < R : \left. \frac{d}{d\lambda} g_v(\lambda) \right|_{\lambda=a} > 0 \,,\ h_v(a\mathbf{v}) \leq 0 \right\} . \tag{3.4}$$

Then, the following lemma follows from Lemma 3.2.2 and (3.4).

Lemma 3.2.4. *Given a ball* B_R*, let* $\bar{\mathrm{E}}$ *be defined by* (3.4)*. Then,* $\hat{c} = \min_{\mathbf{x} \in \partial E} H(\mathbf{x})$ *is the maximum level value such that i)* $\mathrm{S}_{\hat{c}}(\mathbf{0}) \subset \mathrm{B}_R$*, ii)* $\mathrm{S}_{\hat{c}}(\mathbf{0})$ *contains no critical points of* $H(\mathbf{x})$ *except the origin, iii)* $\dot{H}(\mathbf{x}) \leq 0$ *holds for all* $\mathbf{x} \in \mathrm{S}_{\hat{c}}(\mathbf{0})$*, and iv) for all* $0 < a < \hat{c}$*, the set* $\mathrm{S}_a(\mathbf{0})$ *is properly star-shaped w.r.t. to the origin.*

The application of the Krassovski-LaSalle Theorem requires a *compact* positively invariant set, but $\mathrm{S}_{\hat{c}}(\mathbf{0})$ is not closed and $\bar{\mathrm{S}}_{\hat{c}}(\mathbf{0})$ might contain equilibrium points of the system other than the origin (see Figure 3.2). Therefore, in order to estimate the DA, we take a somewhat smaller level value $\hat{d} < \hat{c}$ and the corresponding compact sublevel set $\bar{\mathrm{S}}_{\hat{d}}(\mathbf{0})$.

Remark 3.2.1. The proposed approach can be easily adapted to control systems with constrained control inputs $|u_i| \leq \bar{u}_i$, $i = 1, \ldots, m$ by one of the two means outlined below. For simplicity of notation, we restrict ourselves to the case of a single input u with $|u| \leq \bar{u}$, but the generalization to the multi-input case is straightforward.

1) If the controller saturates, the derivative of the energy function, which is used for the definition of $\bar{\mathrm{E}}$ in (3.4), is given by

$$\dot{H}(\mathbf{x}) = \begin{cases} -\nabla^T H(\mathbf{x}) \mathbf{R}(\mathbf{x}) \nabla H(\mathbf{x}) & \text{if } |r(\mathbf{x})| \leq \bar{u} \\ \nabla^T H(\mathbf{x}) \left\{ \mathbf{f}(\mathbf{x}) + \mathbf{g}(\mathbf{x}) \mathrm{sgn}[r(\mathbf{x})] \bar{u} \right\} & \text{if } |r(\mathbf{x})| > \bar{u} \end{cases} . \tag{3.5}$$

A function $\dot{H}(\mathbf{x})$ of this form can be handled by the algorithm proposed in the subsequent section without any problems.

2) A somewhat simpler method, which, however, leads to more conservative estimates, is to determine the largest sublevel set of the energy function that, on the one hand, qualifies as an estimate of the DA for the unconstrained system and, on the other hand,

satisfies that $|r(\mathbf{x})| \leq \bar{u}$ holds for all $\mathbf{x}$ contained therein (see e.g. [73]). To guarantee the latter property, we define the function $r_v(\lambda) = (\lambda \mathbf{v})$ and add $|r_v(a\mathbf{v})| \leq \bar{u}$ in the definition (3.4). Although we will not elaborate on that, the algorithm presented in the next section can be adapted accordingly in an obvious manner.

The approach can also be extended to the time-varying case (Problem 3.1.2), if continuous functions $W_i(\mathbf{x})$, $i = 1, 2, 3$ are available that satisfy (2.11) and (2.12) and are locally positive definite at the origin. In addition, $W_1(\mathbf{x})$ has to be continuously differentiable. Note that, if the $W_i(\mathbf{x})$ are $\mathcal{C}^2$-functions, a sufficient condition for them being locally positive definite is that

$$\nabla W_i(\mathbf{x})|_{\mathbf{x}^*=\mathbf{0}} = \mathbf{0} \ , \quad \text{and} \quad \nabla^2 W(\mathbf{x})|_{\mathbf{x}^*=\mathbf{0}} > 0 \ , \ i = 1, 2, 3 \ . \tag{3.6}$$

If we identify $W_1(\mathbf{x})$ with $H(\mathbf{x})$ and $-W_3(\mathbf{x})$ with $\dot{H}(\mathbf{x})$, i.e., $g_v = W_1(\lambda \mathbf{v})$ and $h_v = -W_3(\lambda \mathbf{v})$, Lemma 3.2.4 can be used to determine a suitable level value $\hat{c}$. In order that $W_3(\mathbf{x})$ is positive definite on $\mathrm{S}_{\hat{c}}^{W_1}(\mathbf{0})$, we change the '$\leq$' in (3.4) to a strict '$<$'. Then $\mathrm{S}_{\hat{c}}^{W_2}(\mathbf{0})$ is the largest estimate of the DA within B_R that can be obtained with the functions $W_i(\mathbf{x})$, again with the restriction that $\mathrm{S}_a^{W_1}(\mathbf{0})$ is properly star-shaped w.r.t. the origin for all $0 < a < \hat{c}$.

3.3 Determining the Critical Level Value: Algorithm 1

In this section and the subsequent one, we present two numerical algorithms that allow to determine the critical level value $\hat{c}$. To this end, the method proposed in this section numerically approximates the radial functions (3.3) or (3.4). In the first subsection we focus our attention on the time-invariant case, the second subsection is devoted to time-varying pH systems.

3.3.1 Time-Invariant Systems

We divide the algorithm into five steps, each of which is illustrated in Figure 3.4. For ease of presentation, we assume for the moment that $\mathbf{R}(\mathbf{x}) \geq 0$ holds globally guaranteeing $\dot{H}(\mathbf{x}) \leq 0$ for all $\mathbf{x} \in \mathbb{R}^n$. Hence, our objective is to approximate $\rho_{\bar{D}}$ as defined in (3.3). Further, we assume that $\nabla^2 H(\mathbf{x})|_{\mathbf{x}=\mathbf{0}} > 0$. However, as will be outlined subsequent to the description of the algorithm, this assumption is actually not absolutely necessary.

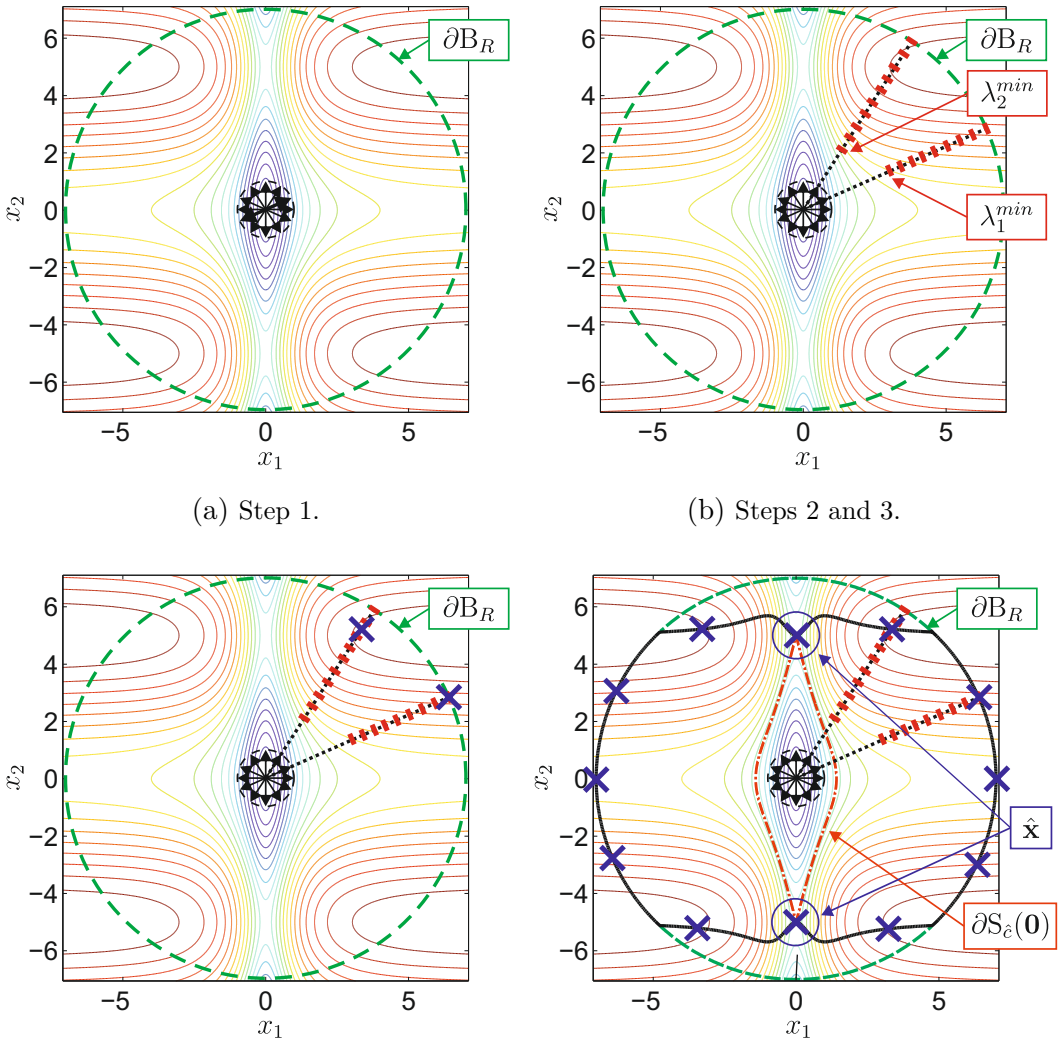

(a) Step 1.

(b) Steps 2 and 3.

(c) Step 4.

(d) Step 5.

Figure 3.4: Algorithm for the computation of $\hat{c}$ via discrete approximation of $\rho_{\bar{D}}$.

Step 1: Discretization of $\mathbb{S}^{n-1}$ In the first step of the algorithm, the unit sphere $\mathbb{S}^{n-1}$ is discretized using n-dimensional spherical coordinates $\mathbf{z} = [r, \theta_1, \ldots, \theta_{n-1}]^T$ introduced by

$$\begin{aligned} x_1 &= r\sin(\theta_{n-1})\ldots\sin(\theta_3)\sin(\theta_2)\sin(\theta_1) \\ x_2 &= r\sin(\theta_{n-1})\ldots\sin(\theta_3)\sin(\theta_2)\cos(\theta_1) \\ x_3 &= r\sin(\theta_{n-1})\ldots\sin(\theta_3)\cos(\theta_2) \\ &\vdots \\ x_{n-1} &= r\sin(\theta_{n-1})\cos(\theta_{n-2}) \\ x_n &= r\cos(\theta_{n-1}) \end{aligned} \tag{3.7}$$

with $r \in [0, \infty)$, $\theta_1 \in [0, 2\pi]$, and $\theta_2, \ldots, \theta_{n-1} \in [0, \pi]$ (see e.g. Appendix VII.2 in [127]). In the following, the mapping (3.7) is denoted by $\mathbf{x} = \mathbf{\Psi}(\mathbf{z})$. We obtain a uniform discretization $\mathcal{V} = \{\mathbf{v}_k | k = 1, \ldots, K\}$ of $\mathbb{S}^{n-1}$ using (3.7) with $\mathbf{v} = \mathbf{x}$, $r = 1$ and the sequences $\theta_{1,k_1} = k_1 \frac{2\pi}{K_1}$, $k_1 = 1, \ldots, K_1$, $\theta_{i,k_i} = k_i \frac{\pi}{K_i}$, $k_i = 0, \ldots, K_i$, $i = 2, \ldots, n-1$. The cardinality of the set $\mathcal{V}$ is $K = K_1 \prod_{j=2}^{n-1}(K_j + 1)$.

Next, the functions $g_{v,k}(\lambda) = H(\lambda \mathbf{v}_k)$, $0 < \lambda \leq R$, $k = 1, \ldots, K$ or, actually, their derivatives $g'_{v,k}(\lambda) = \frac{d}{d\lambda} g_{v,k}(\lambda)$ are analyzed in terms of the maximum λ such that $\lambda \mathbf{v}_k \in \bar{\mathrm{D}}$. This is done in the three steps described below, which are repeated for every direction $\mathbf{v}_k \in \mathcal{V}$.

Step 2: Initial estimate of $\rho_{\bar{D}}(\mathbf{v}_k)$ In this step, a value λ_k^{min} is computed such that $g'_{v,k}(\lambda)$ is guaranteed to be strictly positive within the interval $(0, \lambda_k^{min})$. We invoke Taylor's Theorem (see e.g Theorem 2.1 in [129]) to deduce that for some $\kappa \in (0, \lambda)$ we have that

$$g'_v(\lambda) = \underbrace{g'_{v,k}(0)}_{=0} + \underbrace{\frac{d}{d\lambda} g'_{v,k}(\lambda)\Big|_{\lambda=0}}_{>0} \lambda + \frac{1}{2} \frac{d^2}{d\lambda^2} g'_{v,k}(\lambda)\Big|_{\lambda=\kappa} \lambda^2 \,. \tag{3.8}$$

For the first term in this expression, we calculate $g'_{v,k}(0) = \nabla^T H(\mathbf{0}) \mathbf{v}_k = 0$. The second term in (3.8) is strictly positive because we have assumed that $\nabla^2 H(\mathbf{0}) > 0$ and

$$\frac{d}{d\lambda} g'_{v,k}(\lambda) = \mathbf{v}_k^T \, \nabla^2 H(\mathbf{x})\Big|_{\lambda \mathbf{v}_k} \mathbf{v}_k \quad \Rightarrow \quad \frac{d}{d\lambda} g'_{v,k}(\lambda)\Big|_{\lambda=0} = \mathbf{v}_k^T \nabla^2 H(\mathbf{0}) \mathbf{v}_k > 0 \,. \tag{3.9}$$

Using this, we deduce from (3.8) the lower bound

$$g'_{v,k}(\lambda) \geq \lambda \left[g''_{v,k}(0) - \frac{1}{2} \max_{\kappa \in [0,\lambda]} \left(\left| g'''_{v,k}(\kappa) \right| \right) \lambda \right] \,, \quad \lambda > 0 \tag{3.10}$$

where we have used the notation $g''_{v,k}(\lambda) = \frac{d}{d\lambda} g'_{v,k}(\lambda)$ and $g'''_{v,k}(\lambda) = \frac{d^2}{d\lambda^2} g'_{v,k}(\lambda)$. Since $\lambda > 0$, this bound is positive as long as the term in brackets is positive. As argued above, the first term in the bracket is a strictly positive constant, the second summand is zero for $\lambda = 0$ and monotonically decreasing with $\lambda > 0$. Thus, it is not difficult to see that the expression in brackets is positive for small λ and has a unique positive root λ_k^{min}, where it changes its sign from positive to negative. This root can be easily calculated using a simple one-dimensional root finding technique. The max-term in (3.10), or at least an upper bound for it, can be calculated quite easily in most cases, possibly supported by

computer algebra system like MAPLE or SAGE. This is illustrated by the following example (see also the example in Section 5.2).

Example 3.3.1. Let us consider the energy function

$$H(\mathbf{x}) = 5x_1^2 + 2x_1x_2 + 8x_2^2 - 7x_1^3 - x_2^4\cos(x_1x_2)\ , \tag{3.11}$$

which is positive definite at the origin, but not radially unbounded. We compute

$$\begin{aligned} g'''_{v,k}(\lambda) = -42v_{k,1}^3 + 96v_{k,1}v_{k,2}^5\lambda^3\sin(\lambda^2v_{k,1}v_{k,2}) + 60\lambda^5v_{k,1}^2v_{k,2}^6\cos(\lambda^2v_{k,1}v_{k,2}) \\ - 8\lambda^7v_{k,1}^3v_{k,2}^7\sin(\lambda^2v_{k,1}v_{k,2}) - 24\lambda v_{k,2}^4\cos(\lambda^2v_{k,1}v_{k,2})\ . \end{aligned} \tag{3.12}$$

In order to determine an upper bound for $\max_{\kappa\in[0,\lambda]}(|g'''_v(\kappa)|)$ we use

$$|a+b| \le |a| + |b|\ ,\quad \max_{a\in[0,b]}|\cos(a)| = 1\ ,\quad \max_{a\in[0,b]}|\sin(a)| = \begin{cases} \sin b & |b| < \frac{\pi}{2} \\ 1 & |b| \ge \frac{\pi}{2} \end{cases} \tag{3.13}$$

and obtain

$$\begin{aligned} \max_{\kappa\in[0,\lambda]}\left(\left|g'''_{v,k}(\kappa)\right|\right) \le 42\left|v_{k,1}^3\right| + 96\left|v_{k,1}v_{k,2}^5\lambda^3\sin(\lambda^2v_{k,1}v_{k,2})\right| + 60\left|\lambda^5v_{k,1}^2v_{k,2}^6\right| \\ + 8\left|\lambda^7v_{k,1}^3v_{k,2}^7\sin(\lambda^2v_{k,1}v_{k,2})\right| + 24\left|\lambda v_{k,2}^4\right| \end{aligned} \tag{3.14}$$

for $|\lambda^2v_{k,1}v_{k,2}| < \frac{\pi}{2}$ and

$$\max_{\kappa\in[0,\lambda]}\left(\left|g'''_{v,k}(\kappa)\right|\right) \le 42\left|v_{k,1}^3\right| + 96\left|v_{k,1}v_{k,2}^5\lambda^3\right| + 60\left|\lambda^5v_{k,1}^2v_{k,2}^6\right| + 8\left|\lambda^7v_{k,1}^3v_{k,2}^7\right| + 24\left|\lambda v_{k,2}^4\right| \tag{3.15}$$

for $|\lambda^2v_{k,1}v_{k,2}| \ge \frac{\pi}{2}$. Of course the bound (3.15) would also be valid for $|\lambda^2v_{k,1}v_{k,2}| < \frac{\pi}{2}$, but we use a piecewise defined function to obtain a tighter bound and thereby a better estimate for $\rho_{\bar{D}}(\mathbf{v}_k)$. Since (3.14) and (3.15) are identical for $|\lambda^2v_{k,1}v_{k,2}| = \frac{\pi}{2}$, the overall expression is continuous and the desired root λ_k^{min} can be computed numerically without any problems, for instance, by means of the *bisection method* (see e.g. [145]).

Step 3: Discretization of the interval $[\lambda_k^{min}, R]$ In the third step, the interval $[\lambda_k^{min}, R]$ is discretized into a sequence $\mathcal{L} = \{\lambda_{k,l} | l = 0, \ldots, L_k\}$, where $\lambda_{k,l} = \lambda_k^{min} + l\Delta\lambda_k$ and $\Delta\lambda_k = (R - \lambda_k^{min})/L_k$ for some positive integer L_k. The number λ_k^{min} can provide an indication on how fine the discretization should be, i.e., on how to choose the number of points L_k. We specify a priori a maximum and a minimum distance for the discrete points,

denoted by $\Delta\lambda^{max}$ and $\Delta\lambda^{min}$, respectively, which is valid for all k. Then, we set

$$L_k = \left\lceil \left(R - \lambda_k^{min}\right) \Big/ \max\left(\min\left(\lambda_k^{min}, \Delta\lambda^{max}\right), \Delta\lambda^{min}\right) \right\rceil \tag{3.16}$$

where $\lceil x \rceil$ denotes the *ceiling function*.

Step 4: Line Search In the fourth step, l is increased from 0 to $L_k - 1$ until the interval $[\lambda_{k,l}, \lambda_{k,l+1}]$ *brackets* a root of $g'_{v,k}(\lambda)$, in the sense that $g'_{v,k}(\lambda_{k,l+1}) < 0 < g'_{v,k}(\lambda_{k,l})$, or until $l = L_k - 1$ is reached. In the latter case, we set $\rho_{\bar{\mathrm{D}}}(\mathbf{v}_k) = R$. If a root of $g'_{v,k}(\lambda)$ is bracketed in an interval $[\lambda_{k,l}, \lambda_{k,l+1}]$, a one-dimensional zero-finding technique is applied to determine the root, say $\hat{\lambda}_k$, where a technique is preferable which maintains the bracketing, such as *regula falsi* or *Brent's method* [145]. Then, we set $\rho_{\bar{\mathrm{D}}}(\mathbf{v}_k) = \hat{\lambda}_k$.

Step 5: Determining the critical level value After the Steps 2–4 have been conducted for every $\mathbf{v}_k \in \mathcal{V}$, the pairs $[\mathbf{v}_k, \rho_{\bar{\mathrm{D}}}(\mathbf{v}_k)]$ constitute an approximation of the radial function $\rho_{\bar{\mathrm{D}}}(\mathbf{v})$ and thus a discrete representation of $\partial\mathrm{D}$. As $H(\mathbf{x}) \in \mathcal{C}^r$ holds with $r \geq 1$ the function $g'(\lambda, \mathbf{v}) = g'_v(\lambda)$ is uniformly continuous in $\bar{\mathrm{D}}$. Hence, if the grid size is sufficiently small, it can be concluded that $g'_{v,k}(\lambda_l) > 0$ for all $\mathbf{v}_k$ and $\lambda_{k,l} < \rho_{\bar{\mathrm{D}}}(\mathbf{v}_k)$ implies that the conditions of Lemma 3.2.2 are satisfied. To obtain $\hat{c} = \min_{\mathbf{x}\in\partial\mathrm{D}} H(\mathbf{x})$, first the value $\hat{a} = \min_{k\in\{1,\ldots,K\}} H(\rho_{\bar{\mathrm{D}}}(\mathbf{v}_k)\mathbf{v}_k)$ is determined. The associated index is denoted by $\hat{k}_a$ and the corresponding point is $\hat{\mathbf{x}}_a = \rho_{\bar{\mathrm{D}}}(\mathbf{v}_{\hat{k}_a})\mathbf{v}_{\hat{k}_a}$. Moreover, let $\hat{k}_i$, $i = 1, \ldots, n-1$ be defined by $\hat{\mathbf{x}}_a = \boldsymbol{\Psi}([\rho_{\bar{\mathrm{D}}}(\mathbf{v}_{\hat{k}_a}), \hat{k}_1 \frac{2\pi}{K_1}, \ldots, \hat{k}_{n-1} \frac{\pi}{K_{n-1}}])$.

Remark 3.3.1. Actually, the pairs $[\mathbf{v}_k, \rho_{\bar{\mathrm{D}}}(\mathbf{v}_k)]$ form a discrete representation only of those parts of $\partial\mathrm{D}$ that belong to $\partial\mathrm{B}_R$ and M, i.e., there are no points on the T_i (see also Figure 3.3). However, since at every point $\mathbf{x} \in \mathrm{T}_i$ the radial direction $\mathbf{x}/\|\mathbf{x}\|$ is tangential to T_i and $\nabla^T H(\mathbf{x})\mathbf{x}$ is positive everywhere on T_i, the function $H(\mathbf{x})$ cannot adopt its minimum there.

To take into account that $\hat{\mathbf{x}}$ might not be captured by the grid, optionally one of the following minimization problems can be solved with the initial point $\hat{\mathbf{x}}_a$. If $\rho_{\bar{\mathrm{D}}}(\mathbf{v}_{\hat{k}_a}) = R$, i.e. $\hat{\mathbf{x}}_a \in \partial\mathrm{B}_R$, the minimization problem is formulated in spherical coordinates

$$\min_{\boldsymbol{\theta}} \quad H(\boldsymbol{\Psi}([R, \theta_1, \ldots, \theta_{n-1}]^T)) \tag{3.17a}$$

$$\text{s.t.} \quad \theta_{i,\hat{k}_i - 1} \leq \theta_i \leq \theta_{i,\hat{k}_i + 1},\ i = 1, \ldots, n-1 \tag{3.17b}$$

where $\boldsymbol{\theta} = [\theta_1, \ldots, \theta_{n-1}]$. If $\rho_{\bar{\mathrm{D}}}(\mathbf{v}_{\hat{k}_a}) < R$ the problem

$$\min_{\mathbf{x}} \quad H(\mathbf{x}) \tag{3.18a}$$

$$\text{s.t.} \quad \nabla^T H(\mathbf{x})\mathbf{x} = 0,\ \mathbf{x}^T\mathbf{x} \leq R \tag{3.18b}$$

is solved. Assuming a sufficiently small grid, it can be expected that $\hat{\mathbf{x}}_a$ is close enough to the desired point such that a gradient based solver converges to that point. This finally yields $\hat{\mathbf{x}}$ and $\hat{c} = H(\hat{\mathbf{x}})$. If the optimization step is skipped for the sake of computational efficiency, then we have, of course, $\hat{\mathbf{x}} = \hat{\mathbf{x}}_a$ and $\hat{c} = \hat{a}$.

As mentioned in the previous section, the sublevel set $\bar{\mathrm{S}}_{\hat{c}}(\mathbf{0})$ is not suitable as an estimate of the DA since it might contain other critical points of the energy function than the origin. For this reason, and in order to compensate for numerical errors, we take the level value $\hat{d} = (1 - \epsilon_c)\hat{c}$, where $\epsilon_c > 0$ is small[2]. A point $\hat{\mathbf{x}}_d$ with $H(\hat{\mathbf{x}}_d) = \hat{d}$ is given by $\hat{\mathbf{x}}_d = \hat{\lambda}_d\hat{\mathbf{x}}$, where $\hat{\lambda}_d$ is the (unique) solution of

$$H(\lambda\hat{\mathbf{x}}) - \hat{d} = 0 \quad \lambda \in (0, 1) \tag{3.19}$$

which is determined by a one-dimensional root finding technique.

Note that we can of course skip Step 2 of the algorithm and instead choose $\lambda_k^{min} = 0$, which means that in Step 3 the complete interval $[0, R]$ is discretized with an a priori fixed step size $\Delta\lambda$. This obviates also the assumption $\nabla^2 H(0) > 0$ made at the beginning of this section as it is only required for the estimation of λ_k^{min}. However, Step 2 reduces the number of function evaluations, since it is not necessary to examine the interval $[0, \lambda_k^{min})$, and, as already utilized above, the size of λ_k^{min} gives an indication on how to choose the discretization of the remaining interval $[\lambda_k^{min}, R]$.

In case that $\dot{H}(\mathbf{x}) \leq 0$ can be guaranteed only locally, the algorithm proceeds in the same way, only that we do not merely examine $g'_{v_k}(\lambda)$ but simultaneously also $h_{v,k}(\lambda) = \dot{H}(\lambda\mathbf{v}_k)$ in terms of the largest λ_k such that $\lambda_k\mathbf{v}_k \in \bar{\mathrm{E}}$ (c.f. (3.4)). As a consequence, in Step 2 we determine two estimates $\lambda_{g,k}^{min}$ and $\lambda_{h,k}^{min}$ such that $g'_{v,k}(\lambda)$ is positive within $(0, \lambda_{g,k}^{min}]$ and $h_{v,k}(\lambda)$ is negative within $(0, \lambda_{h,k}^{min}]$. Then we take $\lambda_k^{min} = \min(\lambda_{g,k}^{min}, \lambda_{h,k}^{min})$ and determine in Step 3 a discretization of $[\lambda_k^{min}, R]$ as above. In Step 4, we then increase l until $[\lambda_{k,l}, \lambda_{k,l+1}]$ brackets a root of *either* $g'_{v,k}(\lambda)$ *or* $h_{v,k}(\lambda)$, or until we have reached $\partial\mathrm{B}_R$. In case that both $g'_{v,k}(\lambda)$ and $h_{v,k}(\lambda)$ change their sign in the same interval $[\lambda_{k,l}, \lambda_{k,l+1}]$, we determine

[2] If the optimization step is omitted, ϵ_c might be chosen somewhat larger to take into account that $\hat{\mathbf{x}}$ might not be captured by the grid.

both roots and take the smaller one as $\hat{\lambda}_k$. In this way, we obtain a discrete approximation of the radial function $\rho_{\bar{E}}(\mathbf{v})$ and hence of ∂E, based on which $\hat{c}$ can be computed. This is also done analogously to above with the only difference occurring, if a gradient based optimization is conducted after $\hat{a}$ and $\hat{\mathbf{x}}_a$ have been determined. Then, if $\rho_{\bar{\mathrm{D}}}(\mathbf{v}_{\hat{k}_a}) < R$, we have to distinguish whether $\hat{\mathbf{x}}_a$ corresponds to a zero of $g'_v(\lambda)$ or of $h_v(\lambda)$. In the former case, we solve the minimization problem (3.18a), (3.18b) with the additional constraint $\dot{H}(\mathbf{x}) \leq 0$. In the latter case, we set up the problem

$$\min_{\mathbf{x}} \quad H(\mathbf{x}) \tag{3.20}$$

$$\text{s.t.} \quad \dot{H}(\mathbf{x}) = 0,\ \nabla^T H(\mathbf{x})\mathbf{x} > 0,\ \mathbf{x}^T\mathbf{x} \leq R\,. \tag{3.21}$$

The procedure described above is exemplarily sketched in the Algorithm 3.1 for the 3 dimensional case, i.e., $n = 3$. The reason why we fix the dimension here is that we need to generate permutations of $n-1$ coordinates to build up the discretization $\mathcal{V}$ of the unit sphere. This is usually done by nesting $n-1$ `for` loops[3] as in the lines 4-10. Note further that, for brevity, we have omitted the optimization step in Algorithm 3.1 and thus $\hat{\mathbf{x}} = \hat{\mathbf{x}}_a$ and $\hat{c} = \hat{a}$.

Algorithm 3.1

Input: number of points K_1, K_2, max. and min. distance $\Delta\lambda^{max}$, $\Delta\lambda^{min}$, radius R
Output: level value $\hat{d}$

1: $K := K_1 K_2$;
2: $\mathcal{V} := \{\}$;
3: $k := 1$;
4: **for** $k_1 = 1 \ldots K_1$ **do** `# Discretization` $\mathcal{V}$ `of` $\mathbb{S}^{n-1}$
5: **for** $k_2 = 1 \ldots K_2$ **do**
6: $\mathbf{v}_k := [\sin(\theta_{2,k_2})\sin(\theta_{1,k_1}),\ \sin(\theta_{2,k_2})\cos(\theta_{1,k_1}),\ \cos(\theta_{2,k_2})]$;
7: $\mathcal{V} := \mathcal{V} \cup \{\mathbf{v}_k\}$;
8: $k := k + 1$;
9: **end for**
10: **end for**
11: $\hat{c} := \infty$;
12: $\hat{\mathbf{x}} := \mathbf{0}$;
13: **for** $k = 1 \ldots K$ **do** `# Loop over all` $\mathbf{v}_k \in \mathcal{V}$

[3] Another method that allows to do this in a generic way, i.e., without having different code for different dimensions, is described in Section 4.3.2 in [36].

14: determine $\lambda_{g,k}^{min}$; `# Estimate of` $\lambda_{g,k}^{min}$`, such that` $g'_{v,k}(\lambda) > 0$ `within` $(0, \lambda_{g,k}^{min})$
15: determine $\lambda_{h,k}^{min}$; `# Estimate of` $\lambda_{h,k}^{min}$`, such that` $h_{v,k}(\lambda) < 0$ `within` $(0, \lambda_{h,k}^{min})$
16: $\lambda_k^{min} := \min(\lambda_{g,k}^{min}, \lambda_{h,k}^{min})$;
17: $\Delta\lambda_k := (R - \lambda_k^{min})/L_k$ with L_k according to (3.16);
18: $\mathcal{L} := \{\lambda_{k,l} = \lambda_k^{min} + l\Delta\lambda_k | l = 0, \ldots, L_k\}$; `# Discretization` $\mathcal{L}$ `of` $[\lambda_k^{min}, R]$
19: flag:=0; `#` $flag = 1$ `indicates that a root has been found`
20: $\hat{\lambda}_{g,k} := R$;
21: $\hat{\lambda}_{h,k} := R$;
22: $l := 0$;
23: **while** $flag = 0 \ \wedge \ l < L_k$ **do** `# Line search until` $l = L_k - 1$ `or a root is found`
24: **if** $g'_{v_k}(\lambda_{k,l+1}) < 0$ **then** `#` $[\lambda_{k,l}, \lambda_{k,l+1}]$ `brackets a root of` $g'_{v_k}(\lambda)$
25: $\hat{\lambda}_{g,k}$:= determine root of $g'_{v_k}(\lambda)$ within $[\lambda_{k,l}, \lambda_{k,l+1}]$; `# e.g. Illinois algorithm`
26: $flag = 1$;
27: **end if**
28: **if** $h_{v,k}(\lambda_{k,l+1}) > 0$ **then** `#` $[\lambda_{k,l}, \lambda_{k,l+1}]$ `brackets a root of` $h_{v_k}(\lambda)$
29: $\hat{\lambda}_{h,k}$:= determine root of $h_{v_k}(\lambda)$ within $[\lambda_{k,l}, \lambda_{k,l+1}]$;
30: $flag = 1$;
31: **end if**
32: $l := l + 1$;
33: **end while**
34: $\hat{\lambda}_k := \min(\hat{\lambda}_{g,k}, \hat{\lambda}_{h,k})$;
35: **if** $H(\hat{\lambda}_k \mathbf{v}_k) < \hat{c}$ **then**
36: $\hat{c} := H(\hat{\lambda}_k \mathbf{v}_k)$;
37: $\hat{\mathbf{x}} := \hat{\lambda}_k \mathbf{v}_k$;
38: **end if**
39: **end for**
40: $\hat{d} := (1 - \epsilon_c)\hat{c}$;
41: $\hat{\lambda}_d$:= solve $H(\lambda\hat{\mathbf{x}}) - \hat{d} = 0$, $\lambda \in (0, 1)$;
42: $\hat{\mathbf{x}}_d := \hat{\lambda}_d \hat{\mathbf{x}}$;

Remark 3.3.2. Several modifications of this procedure are conceivable to increase the computational efficiency, e.g. the `while` loop in line 23 could be terminated as soon as $g_v(\lambda_{k,l+1}\mathbf{v}_k) > \hat{c}$. This, however, cannot be realized, if the execution of the loop ought to be parallelized. As an alternative, the search radius R could be gradually increased. That

means, the algorithm is first applied to a ball with radius R_1. If the resulting point $\hat{\mathbf{x}}$ is on the boundary of the ball, the region $\mathrm{B}_{R_2} \backslash \mathrm{B}_{R_1}$ with $R_2 > R_1$ is examined, and so on.

3.3.2 Time-Varying Systems

This section is devoted to the numerical solution of Problem 3.1.2, where the right hand side of the closed loop pH system is not only a function of the state but also exhibits an explicit dependence on the time t. In principle, the time-varying case differs from the time-invariant one only in that we have to determine time-invariant positive definite bounds $W_i(\mathbf{x})$, $i = 1, \ldots 3$ on the energy function $H(\mathbf{x}, t)$ and its derivative $\dot{H}(\mathbf{x}, t)$ satisfying (2.11), (2.12). Once such functions are available, clearly the algorithm from the previous section can be applied verbatim to find the largest level value $\hat{c}$ such that $\mathrm{S}_{\hat{c}}^{W_1}(\mathbf{0})$ is bounded and entirely contained in the region Ω^{W_3} within which $W_3(\mathbf{x})$ is positive definite. To this end, we redefine the functions $g_{v,k}$ and $h_{v,k}$ as $g_{v,k} = W_1(\lambda \mathbf{v}_k)$ and $h_{v,k} = -W_3(\lambda \mathbf{v}_k)$.

However, in many cases, the expressions $H(\mathbf{x}, t)$ and $\dot{H}(\mathbf{x}, t)$ are too cumbersome to derive suitable bounds $W_i(\mathbf{x})$, $i = 1, \ldots, 3$ analytically. Therefore, a numerical approach is pursued in the following. We assume that the behavior of the system (3.2) is of interest only on a finite time interval $[0, T]$ or that (3.2) is T-periodic in t, i.e., for all $(\mathbf{x}, t) \in \mathbb{R}^n \times [0, \infty)$ it holds that $H(\mathbf{x}, t + T) = H(\mathbf{x}, t)$ and $\mathbf{F}(\mathbf{x}, t + T) = \mathbf{F}(\mathbf{x}, t)$. In the context of output trajectory tracking, as treated in Section 2.3.2, this corresponds to the assumption that $y_d(t)$ is either defined only on a finite interval $[0, T]$ or T-periodic in t (see Remark 3.3.3 below for a relaxation of this assumption). Then, bounds $W_i(\mathbf{x})$ satisfying (2.11), (2.12) are given by

$$W_1(\mathbf{x}) = \min_{t \in [0,T]} H(\mathbf{x}, t) \ , \quad W_2(\mathbf{x}) = \max_{t \in [0,T]} H(\mathbf{x}, t) \ , \quad W_3(\mathbf{x}) = \min_{t \in [0,T]} -\dot{H}(\mathbf{x}, t) \ . \tag{3.22}$$

In order to numerically compute the expressions (3.22) for a particular point $\mathbf{x}$, different strategies can be applied. It has to be noted, however, that usually $H(\mathbf{x}, t)$ and $\dot{H}(\mathbf{x}, t)$ are not convex in t (or at least this cannot be easily proven) and hence the mere application of gradient based techniques might not yield the global minimum. The simplest strategy is to discretize $[0, T]$ into a sequence of N_T equidistant points $\mathcal{T} = \{t_j | j = 1 \ldots N_T\}$ and to approximate the extrema (3.22) by

$$W_1(\mathbf{x}) \approx \min_{t_j \in \mathcal{T}} H(\mathbf{x}, t_j) \ , \quad W_2(\mathbf{x}) \approx \max_{t_j \in \mathcal{T}} H(\mathbf{x}, t_j) \ , \quad W_3(\mathbf{x}) \approx \min_{t_j \in \mathcal{T}} -\dot{H}(\mathbf{x}, t_j) \ . \tag{3.23}$$

The error made in doing so is taken into account in the choice of the scaling factor $(1 - \epsilon_c)$.

Optionally, we can of course add some steps of a gradient based minimization technique to improve the accuracy of the result.

We remark that a very similar procedure has been applied in [101], [102] to determine the bounds $W_i(\mathbf{x})$. However, in this work the expressions (3.23) are a priori evaluated on a rectangular grid around the origin $\mathbf{x} = \mathbf{0}$ and then the required values $W_i(\mathbf{x})$ are gained by interpolation. In contrast, we compute the $W_i(\mathbf{x})$ exactly at those points at which they are requested by the algorithm. This seems to be more reasonable since it increases the accuracy, it avoids the interpolation operation, and it can reduce the number of points at which the expressions (3.23) must be evaluated. The latter is due to the fact that the line search in the direction $\mathbf{v}_k$ (Step 4 of the algorithm) stops as soon as it encounters a root of $g_{v,k}(\lambda)$ or $h_{v,k}(\lambda)$ implying that the functions $W_i(\mathbf{x})$ don't have to be evaluated at the remaining grid points in this direction.

Remark 3.3.3. In the context of trajectory tracking control, if y is a flat output, we have $H(\mathbf{e}, t) = H(\mathbf{e}, \mathbf{Y}_d(t))$ and $\dot{H}(\mathbf{e}, t) = \dot{H}(\mathbf{e}, \mathbf{Y}_d(t))$ (see Section 2.3.2). In this case, we can determine functions $W_i(\mathbf{e})$, $i = 1, 2, 3$ that are valid not only for a particular trajectory, but for all trajectories satisfying $\mathbf{Y}_d(t) \in \mathrm{D}_{\mathrm{op}},\ \forall\, t$, where D_{op} is an a priori specified operating region. To this end, we determine the extrema (3.23) over D_{op} instead of the time interval $[0, T]$. Then, any desired trajectory with $\mathbf{Y}_d(t) \in \mathrm{D}_{op},\ \forall\, t$ can be chosen (e.g. by the operator) without repeating the stability analysis and the computation of the DA for each $y_d(t)$ (see the Example in Section 8.2).

For the application of the algorithm described in the previous section, the derivatives $g'_{v,k}(\lambda) = \frac{d}{d\lambda} g_{v,k}(\lambda)$ of the functions $g_{v,k} = W_1(\lambda \mathbf{v}_k)$ are required. Since no symbolic expression is available for $W_1(\mathbf{x})$, they also have to be computed numerically, e.g. by means of finite differencing (see Chapter 8 in [129]). Using a *forward difference* approximation we obtain

$$g'_{v,k}(\lambda_{k,l}\mathbf{v}_k) \approx \frac{W_1(\lambda_{k,l}\mathbf{v}_k + \epsilon \mathbf{v}_k) - W_1(\lambda_{k,l}\mathbf{v}_k)}{\epsilon}\,. \tag{3.24}$$

The parameter ϵ is typically chosen as the square root of the *unit roundoff* (see [129] for a discussion).

To evaluate the expression (3.24), the value of $W_1(\mathbf{x})$ at the point $\lambda_{k,l}\mathbf{v}_k$ and at the point $\lambda_{k,l}\mathbf{v}_k + \epsilon \mathbf{v}_k$ is needed, which entails that the function $H(\mathbf{x}, t)$ has to be evaluated $2N_T$ times. Hence, calculating the derivative $g'_{v,k}(\lambda)$ is twice as expensive as computing $g_{v,k}(\lambda)$. In Step 4 of Algorithm 3.1, $g'_{v,k}(\lambda)$ is determined at every grid point, i.e., for every $\mathbf{v}_k$ and every $\lambda_{l,k}$. In order to reduce the computational effort, we can make the following modification.

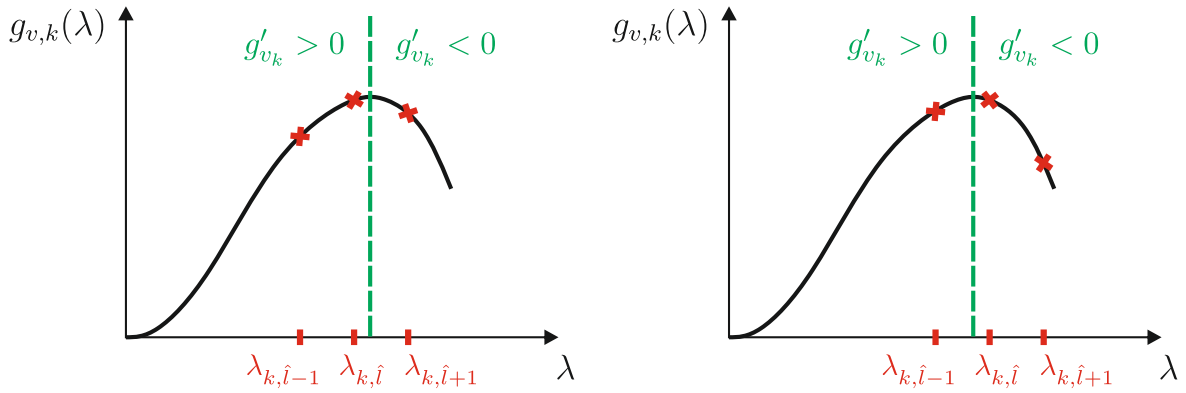

(a) Sign change of $g'_{v,k}(\lambda)$ in $[\lambda_{k,\hat{l}}, \lambda_{k,\hat{l}+1}]$.

(b) Sign change of $g'_{v,k}(\lambda)$ in $[\lambda_{k,\hat{l}-1}, \lambda_{k,\hat{l}}]$.

Figure 3.5: Line search in the time-varying case.

While increasing l, we do not check whether the interval $[\lambda_{k,l}, \lambda_{k,l+1}]$ brackets a root of $g'_{v,k}(\lambda)$ but whether $g_{v,k}(\lambda_{k,l+1}) < g_{v,k}(\lambda_{k,l})$, which requires only N_T evaluations of $H(\mathbf{x}, t)$. In case that for some $\hat{l}$ it holds that $g_{v,k}(\lambda_{k,\hat{l}+1}) < g_{v,k}(\lambda_{k,\hat{l}})$, it can be concluded, using the mean value theorem, that a sign change in $g'_{v,k}(\lambda)$ must have occurred within $[\lambda_{k,\hat{l}}, \lambda_{k,\hat{l}+1}]$ or in the previous interval (see also Figure 3.5). Thus, to identify the interval that brackets a root of $g'_{v,k}(\lambda)$, for each $\mathbf{v}_k$ the derivative $g'_{v,k}(\lambda)$ has to be evaluated at most at two points (see Algorithm 3.2 below).

If it happens that already in the first step of the line search it holds that $g_{v,k}(\lambda_{k,1}) < g_{v,k}(0) = 0$ or $h_{v,k}(\lambda_{k,1}) > h_{v,k}(0) = 0$, then either the grid has been chosen too coarse or at least one of the functions $W_1(\mathbf{x})$ or $W_3(\mathbf{x})$ is not locally positive definite. In this case, the grid size can be reduced, or we can check whether $\nabla W_1(\mathbf{0}) = \mathbf{0}$ and $\nabla W_3(\mathbf{0}) = \mathbf{0}$ as well as $\nabla^2 W_1(\mathbf{0}) > 0$ and $\nabla^2 W_3(\mathbf{0}) >$ are satisfied. Both the gradients and the Hessians can also be computed using a finite difference approximation (see [129], pp. 195-202).

Another modification of Algorithm 3.1, that we make in the time-varying case, is that Step 2 of Algorithm 3.1 is omitted since no symbolic expressions are available for the functions $W_1(\mathbf{x})$ and $W_3(\mathbf{x})$. As a consequence, we have $\lambda_k^{min} = 0$. The step size $\Delta\lambda_k = \Delta\lambda$ is chosen identical for all k and such that $R = L\Delta\lambda$ where $L \in \mathbb{N}$ is the number of discrete points in each direction $\mathbf{v}_k$. The resulting procedure is sketched below in Algorithm 3.2., again for the 3-dimensional case and without the optimization step. For ease of presentation, it is not checked in the pseudo code whether $g_{v,k}(\lambda_{k,1}) < 0$ or $h_{v,k}(\lambda_{k,1}) > 0$, i.e, whether a sign change occurs already in the first step of the line search.

Algorithm 3.2

Input: number of grid points K_1, K_2, step size $\Delta\lambda$, radius R

Output: level value $\hat{d}$

determine $\mathcal{V} := \{\mathbf{v}_k | k = 1, \ldots, K\}$; `# As in Algorithm 3.1, lines 1-10`
$\hat{c} := \infty$;
$\hat{\mathbf{x}} := \mathbf{0}$;
for $k = 1 \ldots K$ **do** `# Loop over all` $\mathbf{v}_k \in \mathcal{V}$
  $\mathcal{L} := \{\lambda_{k,l} = l\Delta\lambda_k | l = 0, \ldots, L\}$; `# Discretization` $\mathcal{L}$ `of` $[0, R]$
  $flag := 0$; `#` $flag = 1$ `indicates that a root has been found`
  $\hat{\lambda}_{g,k} := R$;
  $\hat{\lambda}_{h,k} := R$;
  $l := 0$;
  while $flag = 0 \ \wedge \ l \leq L$ **do** `# Line Search`
    if $g_{v_k}(\lambda_{k,l}) \geq g_{v_k}(\lambda_{k,l+1})$ **then**
      if $g'_{v_k}(\lambda_{k,l}) g'_{v_k}(\lambda_{k,l+1}) < 0$ **then**
        $\hat{\lambda}_{g,k} :=$ determine root of $g'_{v_k}(\lambda)$ within $[\lambda_{k,l}, \lambda_{k,l+1}]$;
      else
        $\hat{\lambda}_{g,k} :=$ determine root of $g'_{v_k}(\lambda)$ within $[\lambda_{k,l-1}, \lambda_{k,l}]$;
      end if
      $flag = 1$;
    end if
    if $h_{v,k}(\lambda_{k,l+1}) > 0$ **then** `#` $[\lambda_{k,l}, \lambda_{k,l+1}]$ `brackets a root of` $h_{v_k}(\lambda)$
      $\hat{\lambda}_{h,k} :=$ determine root of $h_{v_k}(\lambda)$ within $[\lambda_{k,l}, \lambda_{k,l+1}]$;
      $flag = 1$;
    end if
    $l := l + 1$;
  end while
  $\hat{\lambda}_k := \min(\hat{\lambda}_{g,k}, \hat{\lambda}_{h,k})$;
  if $W_1(\hat{\lambda}_k \mathbf{v}_k) < \hat{c}$ **then**
    $\hat{c} := W_1(\hat{\lambda}_k \mathbf{v}_k)$;
    $\hat{\mathbf{x}} := \hat{\lambda}_k \mathbf{v}_k$;
  end if
end for
$\hat{d} := (1 - \epsilon_c)\hat{c}$;
$\hat{\lambda}_d :=$ solve $W_1(\lambda\hat{\mathbf{x}}) - \hat{d} = 0$, $\lambda \in (0, 1)$;
$\hat{\mathbf{x}}_d := \hat{\lambda}_d \hat{\mathbf{x}}$;

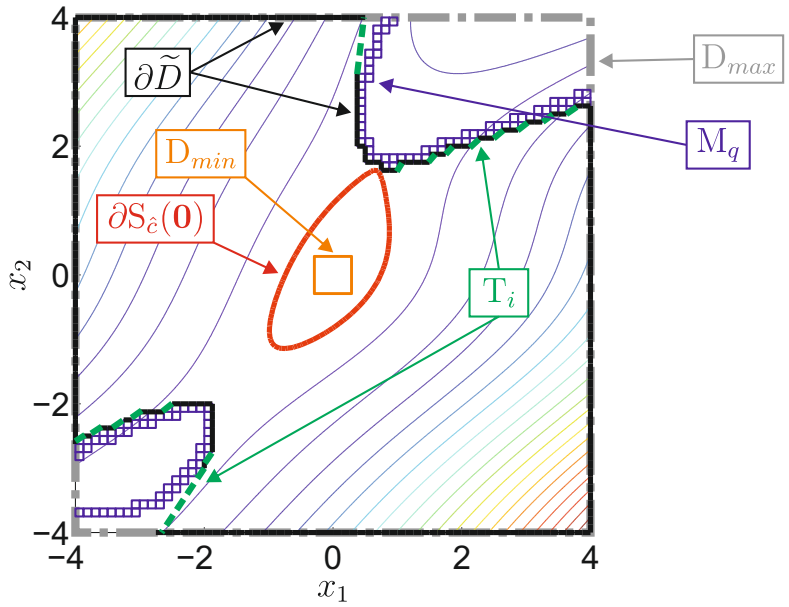

Figure 3.6: Algorithm for the computation of $\hat{c}$ using the bounds (2.86b) and (2.86c) on real valued functions.

3.4 Determining the Critical Level Value: Algorithm 2

In this section, an alternative to the algorithm proposed in the previous section is presented (see also [36]). While the success of the latter depends to some extent on the choice of the discretization, this problem is mostly mitigated here by applying the approach from Section 2.5, which enables the numerical computation of guaranteed bounds on real-valued functions, together with a generalized bisection algorithm. To this end, a symbolic expression for $H(\mathbf{x})$ is needed and consequently the method is restricted to the time-invariant case. Also, we require that the Hamiltonian $H(\mathbf{x})$ is smooth, i.e., $H(\mathbf{x}) \in \mathcal{C}^\infty$ and can be represented in the form (2.87). This implies that also the function

$$g(\mathbf{x}) = \nabla^T H(\mathbf{x})\mathbf{x} \tag{3.25}$$

can be expressed in this form. For simplicity, we assume that $\mathbf{R}(\mathbf{x}) \geq 0,\ \forall\, \mathbf{x} \in \mathbb{R}^n$ such that $\dot{H}(\mathbf{x}) \leq 0$ holds everywhere. The algorithm, which is illustrated in Figure 3.6, aims to determine the largest set D within a prescribed hyperrectangle D_{max} that is star-shaped w.r.t. the origin and has the property that $g(\mathbf{x}) = \nabla^T H(\mathbf{x})\mathbf{x} > 0$ holds for all $\mathbf{x} \in \mathrm{D} \setminus \{\mathbf{0}\}$. This set clearly satisfies the conditions of Lemma 3.2.2. For the computation of the minimum value $\hat{c}$ of $H(\mathbf{x})$ over the boundary of this set, also the theory from Section 2.5 is employed. The algorithm can be divided into the following four steps:

Step 1: Initial estimate D_{min} In the first step, an open set $\mathrm{D}_{min} \subset \mathbb{R}^n$ that contains the origin and within which $g(\mathbf{x})$ is positive definite is identified. To this end, we first determine a function $\gamma : \mathbb{R}_0^+ \to \mathbb{R}$ that satisfies $\gamma(r) \leq g(\mathbf{x})$ with $r = \|\mathbf{x}\|$. With $\nabla H(\mathbf{0}) = \mathbf{0}$ and $\nabla^2 H(\mathbf{0}) > 0$ it is not difficult to compute $g(\mathbf{0}) = 0$, $\nabla g(\mathbf{0}) = \mathbf{0}$ and $\nabla^2 g(\mathbf{0}) = 2\nabla^2 H(\mathbf{0}) > 0$. Then, we deduce from Taylor's Theorem that

$$g(\mathbf{x}) = \underbrace{g(\mathbf{0})}_{=0} + \underbrace{\nabla^T g(\mathbf{0})}_{=0}\mathbf{x} + \frac{1}{2}\mathbf{x}^T \underbrace{\nabla^2 g(\mathbf{0})}_{>0}\mathbf{x} + \mathcal{R}(\mathbf{x}) \quad \text{with } \mathcal{R}(\mathbf{x}) = \sum_{|\alpha|=3} \frac{D^\alpha g(\kappa\mathbf{x})}{\alpha!}\mathbf{x}^\alpha \tag{3.26}$$

holds for some $\kappa \in (0,1)$, where we have used multi-index notation (see Appendix A.1). Hence, it holds for $\|\mathbf{x}\| = r$ that

$$g(\mathbf{x}) \geq \frac{1}{2}r^2\lambda_{min}\left\{\nabla^2 g(\mathbf{0})\right\} + \mathcal{R}(\mathbf{x}) \geq \frac{1}{2}r^2\lambda_{min}\left\{\nabla^2 g(\mathbf{0})\right\} - \max_{\substack{\|\mathbf{x}\|=r \\ \kappa\in(0,1)}} |\mathcal{R}(\mathbf{x})| \,, \tag{3.27}$$

where $\lambda_{min}\{\nabla^2 g(\mathbf{0})\}$ is the minimum eigenvalue of $\nabla^2 g(\mathbf{0})$ and we have used that $\mathbf{x}^T\mathbf{P}\mathbf{x} \geq \lambda_{min}\|\mathbf{x}\|^2$ holds for any $\mathbf{P} > 0$. An upper bound for the maximum term in (3.27) is given by

$$\max_{\substack{\|\mathbf{x}\|=r \\ \kappa\in(0,1)}} |\mathcal{R}(\mathbf{x})| \leq \max_{\|\mathbf{x}\|\leq r} \left| \sum_{|\alpha|=3} D^\alpha g(\mathbf{x}) \, \frac{\mathbf{x}^\alpha}{\alpha!} \right| \leq \frac{1}{6}r^3 \sum_{|\alpha|=3} \max_{\|\mathbf{x}\|\leq r} |D^\alpha g(\mathbf{x})| \tag{3.28}$$

Using this in (3.27) we conclude that

$$\gamma(r) = \frac{1}{2}r^2\lambda_{min}\left\{\nabla^2 g(\mathbf{0})\right\} - \frac{1}{6}r^3 \sum_{|\alpha|=3} \max_{\|\mathbf{x}\|\leq r} |D^\alpha g(\mathbf{x})| \tag{3.29}$$

fulfills $\gamma(r) \leq g(\mathbf{x})$. The maximum terms can of course also be replaced by upper bounds. If we let r_{min} be the unique positive root of $\gamma(r)$, then $\gamma(r) > 0$ holds for all $r < r_{min}$ and thus $g(\mathbf{x}) > 0$ is satisfied for all $\mathbf{x}$ within the ball $\{\mathbf{x} : \|\mathbf{x}\| < r_{min}\}$. Since a rectangular D_{min} will be beneficial in the following, we take the largest square within that ball, i.e., $\mathrm{D}_{min} = \{\mathbf{x} : |x_i| < r_{min}/\sqrt{2}\}$.

Example 3.4.1. To illustrate how an upper bound on the maximum term in (3.29) can be obtained, we consider the Hamiltonian

$$H(\mathbf{x}) = 5x_1^2 + 2x_1x_2 + 8x_2^2 - x_2x_1^6 - x_2^3\cos(x_1) \,. \tag{3.30}$$

One of the derivatives $D^\alpha g(\mathbf{x})$, $|\alpha| = 3$ is

$$\frac{\partial^3 g(\mathbf{x})}{\partial x_1^3} = -840x_2x_1^3 - x_1x_2^3\cos(x_1) - 6x_2^3\sin(x_1) \,. \tag{3.31}$$

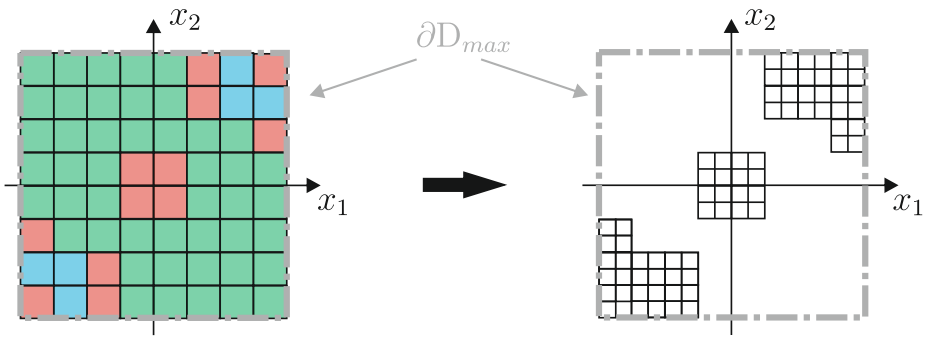

Figure 3.7: Illustration of the bisection.

For the maximum of its absolute value, we compute an upper bound as

$$\max_{\|\mathbf{x}\|\leq r} \left| \frac{\partial^3 g(\mathbf{x})}{\partial x_1^3} \right| \leq 840r^4 + r^4 + 6r^3 = 841r^4 - 6r^3 \tag{3.32}$$

where we have used (3.13) and $|\sin(x_1)| \leq 1$. Of course, we also could have determined a piecewise defined bound like in Example 3.3.1 taking into account that $\max_{\|\mathbf{x}\|\leq r} \sin(x_1) = \sin(r)$ for $r \leq \frac{\pi}{2}$. Upper bounds for the remaining derivatives can be calculated analogously and we finally obtain

$$\sum_{|\alpha|=3} \max_{\|\mathbf{x}\|\leq r} |D^\alpha g(\mathbf{x})| \leq 1051r^4 + 9r^3 + 21r^2 + 30r + 8 \,. \tag{3.33}$$

Step 2: Approximation of $\{\mathbf{x} \in \mathrm{D}_{max} | \nabla^T H(\mathbf{x})\mathbf{x} = 0\}$ In this step, the theory from Section 2.5 is combined with a bisection algorithm to determine an approximation of the set

$$\mathrm{M} = \{\mathbf{x} \in \mathrm{D}_{max} | \nabla^T H(\mathbf{x})\mathbf{x} = 0\} \,. \tag{3.34}$$

The procedure is inspired by the papers [149], [170]. The basic idea is illustrated in Figure 3.7. Suppose the rectangular region D_{max} has been subdivided into a number of equally sized hyperrectangles q_i, $i = 1, \ldots, N_q$ [Figure 3.7 (left)]. On each q_i we compute a lower bound and an upper bound for $g(\mathbf{x})$ using the inequalities (2.85), (2.86). The number of Chebyshev points in each dimension N_i is equal and denoted by N. Also, the degrees $\varrho_i(P_{i,k})$ of the polynomials $P_{i,k}$ that appear in (2.88) and (2.89b) are chosen identical, i.e, $\varrho_i(P_{i,k}) = d$ for all i, k. The grid of Chebyshev points on a hyperrectangle q_i is denoted by $\mathrm{X}(q_i)$, and we use the notation $g_{min}^{X(q_i)} = \min_{\mathbf{x}\in\mathrm{X}(q_i)} g(\mathbf{x})$ as well as $g_{max}^{X(q_i)} = \max_{\mathbf{x}\in\mathrm{X}(q_i)} g(\mathbf{x})$.

Three cases are distinguished: If the lower bound is positive or the upper bound is negative, then M does not intersect the rectangle and it is discarded. These rectangles

are flagged with $status(q_i) = 2$ and are marked green in Figure 3.7. If $g_{min}^{\mathrm{X}(N,q_i)} \leq 0$ and $g_{max}^{\mathrm{X}(N,q_i)} \geq 0$, the intersection of M and the rectangle is nonempty. In this case, the rectangle is further subdivided into 2^n rectangles, which means that every edge is bisected [Figure 3.7 (right)]. Rectangles of this type are flagged with $status(q_i) = 1$ and are illustrated in blue. If the value of $g(\mathbf{x})$ is negative at all points in $\mathrm{X}(N, q_i)$, but the computed upper bound is positive, it is not clear whether M has a nonempty intersection with the rectangle. In this case, either the polynomial degree d or the number of Chebyshev points N is incremented depending on which of the positive terms in (2.86c) is the larger one. As suggested in [149], we increase d if $(K+1)r > -\frac{1}{2}(K-1)g_{min}^{\mathrm{X}(N,q_i)}$, otherwise N is raised (Of course increasing d could make it necessary to increment also N in order to ensure that $N > \varrho_i$.). This is repeated until either $status(q_i) = 1$ or $status(q_i) = 2$ can be assigned to the rectangle, or until N or d reach the prescribed bounds N_{max} or d_{max}, respectively. In the latter case, $status(q_i) = 3$ is assigned. These rectangles are marked red in Figure 3.7. Like the rectangles with $status(q_i) = 1$, they are further subdivided into 2^n rectangles [Figure 3.7 (right)]. If $g(\mathbf{x}) > 0$ for all $\mathbf{x}$ in $\mathrm{X}(N, q_i)$, but the lower bound is negative, we proceed analogously. The whole procedure is repeated until the length of all edges of the q_i is smaller than a prescribed number δ_{min}. This amounts to Algorithm 3.3 which is given below.

Algorithm 3.3

Input: D_{max}, δ_{min}, N_{min}, d_{min}, N_{max}, d_{max}

Output: list M_q of q_i whose intersection with M is nonempty

```
1:  list := {D_max};                          # list of q_i that are to be analyzed
2:  status(D_max) := 0;
3:  while list ≠ ∅ do
4:    for ∀q_i ∈ list do
5:      N := N_min, d := d_min;
6:      loop
7:        determine g_min^X(q_i), g_max^X(q_i), K, r, B_, B¯ on q_i according to Section 2.5;
8:        if B¯ < 0 ∨ B_ > 0 then
9:          status(q_i) := 2;
10:         break;
11:       else if (B¯ > 0 ∧ g_max^X ≥ 0) ∧ (B_ < 0 ∧ g_min^X ≤ 0) then
12:         status(q_i) := 1;
13:         break;
```

14: **else if** $(\overline{B} > 0 \wedge g^{\mathrm{X}}_{max} < 0)$ **then**
15: **if** $-\frac{1}{2} \cdot (K-1) \cdot g^{\mathrm{X}}_{min} < (K+1) \cdot r$ **then**
16: increment d;
17: **else**
18: increment N;
19: **end if**
20: **else if** $(\underline{B} < 0 \wedge g^{\mathrm{X}}_{min} > 0)$ **then**
21: **if** $\frac{1}{2} \cdot (K-1) \cdot g^{\mathrm{X}}_{max} < (K+1) \cdot r$ **then**
22: increment d;
23: **else**
24: increment N;
25: **end if**
26: **end if**
27: **if** $N \geq N_{\max} \vee d \geq d_{\max}$ **then**
28: $status(q_i) := 3$;
29: **break**;
30: **end if**
31: **end loop**
32: **end for**
33: **for** $\forall q_i \in list$ **do**
34: $list := list \setminus \{q_i\}$;
35: **if** $status(q_i) = 2$ **then**
36: **next**;
37: **end if**
38: **if** $status(q_i) = 1 \vee status(q_i) = 3$ **then**
39: **if** $size(q_i) \leq \delta_{min}$ **then**
40: $\mathrm{M}_q := \mathrm{M}_q \cup \{q_i\}$;
41: **else**
42: $[q_{i,1}, q_{i,2}, \ldots, q_{i,2^n}] :=$ bisect every edge of q_i;
43: $list := list \cup \{q_{i,1}, q_{i,2}, \ldots, q_{i,2^n}\}$;
44: $status([q_{i,1}, q_{i,2}, \ldots, q_{i,2^n}]) := 0$;
45: **end if**
46: **end if**
47: **end for**
48: **end while**

Step 3: Computation of $\partial\widetilde{\mathrm{D}}$ In this step, an approximation $\partial\widetilde{\mathrm{D}}$ of the relevant part of the boundary $\partial\mathrm{D}$ is determined. Recall that for the computation of $\hat{c}$ only those parts $\partial\mathrm{D}$ are relevant which belong to M or $\partial\mathrm{D}_{max}$ (see Remark 3.3.1). Since D is star-shaped w.r.t. the origin, a point $\mathbf{x}$ of M or $\partial\mathrm{D}_{max}$ belongs to D if and only if the line segment between the origin and $\mathbf{x}$ does not intersect M, i.e., $k\mathbf{x} \notin \mathrm{M},\ \forall\, k \in (0,1)$. Loosely speaking, the point has to be "visible" from the origin (see Figure 3.3). Thus, we are interested in those hyperrectangles $q \in \mathrm{M}_q$ that "can be seen" from the origin, or, more precisely, in their faces that contain at least one visible point. Also, we subdivide $\partial\mathrm{D}_{max}$ into $n-1$-dimensional rectangles and determine the visible ones among them.

As $g(\mathbf{0}) = 0$, also the origin is contained in M. However, since $\mathbf{0} \notin \partial\mathrm{D}$, the corresponding 2^n rectangles in M_q can be discarded. To guarantee that they do not comprise other parts of M, only rectangles contained in D_{min} may be removed. Therefore, the minimum length δ_{min} in Algorithm 3.3 has to satisfy $\delta_{min} < r_{min}/\sqrt{2}$. In case that r_{min} is very small, of course one could choose a larger number δ_{min} and then analyze the region around the origin separately.

In order to determine $\partial\widetilde{\mathrm{D}}$, we proceed as outlined in Algorithm 3.4. First, we create a list $\mathcal{F}$ that contains the $n-1$ faces $\Diamond f$ of all $q \in \mathrm{M}_q$ except for those which are contained in D_{min} (lines 1-2). Each $\Diamond f \in \mathcal{F}$ is represented in the form

$$\Diamond f = \{\mathbf{x} \,|\mathbf{a}_{\Diamond f} \leq \mathbf{x} \leq \mathbf{b}_{\Diamond f}\} \tag{3.35}$$

where the inequalities are to be interpreted componentwise. By construction, one component of all $\mathbf{x} \in \Diamond f$ is identical, say the lth one. Hence, it holds that $\mathbf{b}_{\Diamond f} - \mathbf{a}_{\Diamond f} = \boldsymbol{\delta}_{\Diamond f}$ with $\delta_{\Diamond f,l} = 0$ and $\delta_{\Diamond f,j} = \delta_{f,j} > 0$ for $j \neq l$. We define $\boldsymbol{\delta}_f = [\delta_{f,1}, \ldots, \delta_{f,n}]^T$ and assign to every $\Diamond f \in \mathcal{F}$ a normal vector $\mathbf{n}_{\Diamond f}$ which is either $\mathbf{e}_l$ or $-\mathbf{e}_l$ with $\mathbf{e}_l$ the lth unit vector. The orientation is chosen such that it points outward from the corresponding rectangle q. Elements of $\mathcal{F}$ that exist twice, are removed since these are those faces, where two rectangles q adjoin each other (line 3). Moreover, faces $\Diamond f$ whose normal vector satisfies $\mathbf{n}_{\Diamond f}^T(\mathbf{a}_f + 0.5\boldsymbol{\delta}_{\Diamond f}) < 0$ can be discarded, where $(\mathbf{a}_f + 0.5\boldsymbol{\delta}_{\Diamond f})$ is the center of $\Diamond f$ (line 4). For they cannot be part of $\partial\widetilde{\mathrm{D}}$ according to Definition 3.2.1. In the next step, the boundary $\partial\mathrm{D}_{max}$ is subdivided into $n-1$-dimensional rectangles, whose size corresponds to $\boldsymbol{\delta}_f$, i.e., $\partial\mathrm{D}_{max}$ is discretized into rectangles that can be represented by (3.35) with $\delta_{\Diamond f,l} = 0$ for some integer $0 < l \leq n$ and $\delta_{\Diamond f,j} = \delta_{f,j}$ for $j \neq l$ (line 5).

Now it is checked for every element $\widehat{\Diamond f}$ of $\mathcal{F}$ that is not part of $\partial\mathrm{D}_{max}$ whether it hides vertices of the other elements $\Diamond f \in \mathcal{F}$ (lines 6-19). The vertices of $\Diamond f$ are denoted by $\mathbf{v}_m(\Diamond f) \in \mathbb{R}^n$, $m = 1, \ldots, 2^{n-1}$. A point $\mathbf{v}_m(\Diamond f)$ is hidden by $\widehat{\Diamond f}$ if and only if there is $0 < k < 1$ such that

$$\mathbf{0} \leq k\mathbf{v}_m(\Diamond f) - \mathbf{a}_{\widehat{\Diamond f}} \leq \boldsymbol{\delta}_{\widehat{\Diamond f}} \tag{3.36}$$

where $\mathbf{a}_{\widehat{\Diamond f}}$ and $\boldsymbol{\delta}_{\widehat{\Diamond f}}$ correspond to $\widehat{\Diamond f}$. Since $\delta_{\widehat{\Diamond f},\hat{l}} = 0$, it follows from the $\hat{l}$th line of this inequality that $k = a_{\widehat{\Diamond f},\hat{l}}/v_{m,\hat{l}}(\Diamond f)$. In case this k satisfies $0 < k < 1$, with this value the remaining $n-1$ inequalities are checked. To each vertex a status is assigned, where $status\{\mathbf{v}_m(\Diamond f)\} = 1$ means "hidden" and $status\{\mathbf{v}_m(\Diamond f)\} = 0$ "not hidden". If all vertices of a face $\Diamond f$ have status 1 it is regarded as hidden and removed from the list $\mathcal{F}$ (lines 15-17).

Algorithm 3.4

Input: D_{max}, D_{min}, M_q

Output: list $\partial\widetilde{\mathrm{D}}$ of $n-1$ faces that approximate the relevant part of $\partial\mathrm{D}$

1: $\mathcal{F} := \mathcal{F} \cup \{\Diamond f \,|q \in \mathrm{M}_q\}$; `# $n-1$-faces of all $q \in \mathrm{M}_q$`
2: $\mathcal{F} := \mathcal{F} \setminus \{\Diamond f | \Diamond f \in \mathrm{D}_{min}\}$; `# Remove faces contained in` D_{min}
3: $\mathcal{F} := \mathcal{F} \setminus \{\Diamond f \,|\exists \Diamond p \in \mathcal{F} \setminus \{\Diamond f\}$ s.t. $\Diamond f = \Diamond p\}$; `# Remove multiple elements`
4: $\mathcal{F} := \mathcal{F} \setminus \{\Diamond f \,\big|\mathbf{n}_{\Diamond f}^T(\mathbf{a}_f + 0.5\boldsymbol{\delta}_{\Diamond f}) < 0\}$;
5: $\mathcal{F} := \mathcal{F} \cup \{\Diamond f \,|\Diamond f \in \partial\mathrm{D}_{max}\}$; `# Add discretized boundary` $\partial\mathrm{D}_{max}$
6: **for** $\forall \widehat{\Diamond f} \in \mathcal{F} \setminus \{\Diamond f \,|\Diamond f \in \partial\mathrm{D}_{max}\}$ **do**
7: **for** $\forall \Diamond f \in \mathcal{F} \setminus \{\widehat{\Diamond f}\}$ **do**
8: **for** $m := 1, \ldots, 2^{n-1}$ **do** `# Loop over all vertices of` $\Diamond f$
9: **if** $\mathbf{v}_m(\Diamond f)$ is hidden by $\widehat{\Diamond f}$ **then**
10: $status\{\mathbf{v}_m(\Diamond f)\} = 1$;
11: **else**
12: $status\{\mathbf{v}_m(\Diamond f)\} = 0$;
13: **end if**
14: **end for**
15: **if** $status\{\mathbf{v}_m(\Diamond f)\} = 1\ , \forall\, m = 1, \ldots, 1^{n-1}$ **then** `#` $\Diamond f$ `hidden`
16: $\mathcal{F} := \mathcal{F} \setminus \{\Diamond f\}$; `# Remove` $\Diamond f$ `from` $\mathcal{F}$
17: **end if**
18: **end for**
19: **end for**
20: $\partial\widetilde{\mathrm{D}} := \mathcal{F}$;

Step 4: Estimate of $\hat{c}$ In the last step, the minimum value of $H(\mathbf{x})$ on $\partial\widetilde{\mathrm{D}}$ is determined using again the inequality (2.85) with (2.86b). For the first element $\Diamond f \in \partial\widetilde{\mathrm{D}}$, a lower bound of $H(\mathbf{x})$ is determined according to (2.85), (2.86b), with a maximum number N_{max} of Chebyshev points and a maximum polynomial degree d_{max}, and is assigned to $\hat{c}_{tmp}$.

Then on the next $\Diamond f \in \partial\widetilde{\mathrm{D}}$ a lower bound of $H(\mathbf{x})$ is calculated with N_{min} and d_{min}. If the obtained bound is larger then c_{tmp}, we move on to the next element. Otherwise, N and d are increased according to the same strategy as in Algorithm 3.3 until either N_{max} or d_{max} are reached or the obtained bound is larger than c_{tmp}. In the first case, the computed value is assigned to c_{tmp}, in the second case, we continue with the next element. After this procedure has been repeated for all elements in $\partial\widetilde{\mathrm{D}}$, an estimate $\tilde{c} \leq \hat{c}$ of the critical level value $\hat{c}$ is given by $\tilde{c} = c_{tmp}$. Since the lower bound (2.86b) is used to determine $\tilde{c}$, usually it holds that $\tilde{c} < \hat{c}$ and hence we do not scale $\tilde{c}$ like in (3.19), which entails that $\hat{d} = \tilde{c}$.

We would like to bring to the readers attention that the algorithm proposed in the present section does not require the choice of a discretization in the narrow sense. We merely have to choose δ_{min} which specifies the accuracy with which M is approximated. Since the algorithm is based on the bounds (2.85), (2.86b), (2.86c) it is, in principle, guaranteed, irrespective of the value δ_{min}, that the determined sublevel set $\overline{\mathrm{S}}_{\hat{d}}(\mathbf{0})$ is a subset of $\mathrm{A}(\mathbf{0})$. That means, it is not possible that the computed $\hat{d}$ is too large, but for great values δ_{min} we might obtain a quite conservative estimate. The only source of error is the procedure in Step 3. For it is not sure that a face is completely hidden if all its vertices are hidden. Although this case is very unlikely to cause problems, it cannot be ruled out theoretically. Of course the procedure could be modified accordingly, but only at the cost of increased numerical effort.

3.5 Concluding Remarks

In this chapter, we have addressed the question how the closed loop pH structure, which arises from the application of IDA, can be exploited to the full extent in the sense that one cannot only establish local stability of the desired equilibrium point by using the energy function as Lyapunov function, but also determine an as large as possible estimate of the corresponding DA. This is complicated by the fact the energy function, which is obtained by solving a system of linear PDEs, is in general not radially unbounded making it necessary to determine its largest bounded sublevel set. Additionally, the dissipation matrix might be positive semidefinite only in some neighborhood of the desired equilibrium entailing that the closed loop system is only “locally passive”. The main contribution of this chapter is a novel approach to estimate the DA of an equilibrium of a pH-system, which is applicable for both time-invariant and time-varying systems. We have established a theoretical result which allows to determine the largest bounded sublevel set of the energy function which is star shaped w.r.t. origin, positively invariant and does not contain

equilibrium points other than the origin. Based on that, we have developed two numerical algorithms. The first one uses a multidimensional grid, obtained from a discretization of the $(n-1)$-dimensional unit sphere, and is relatively easy to implement, which is desirable with regard to broad practical applicability. The second one combines the extension of the Theorem of Ehlich and Zeller reviewed in Section 2.5 with a generalized bisection algorithm. It is computationally more intense but circumvents the problem of choosing a suitable discretization.

Chapter 4

Controller Design

The previous chapter has been devoted to the problem how an estimate of the DA can be obtained by means of the closed loop energy function after an IDA controller has been designed and parametrized. In this chapter, we address the fundamental question of how to tune the large number of parameters, that typically occur in the IDA design process, such that the following requirements are met:

1) The most basic requirements are that the resulting dissipation matrix is positive semidefinite and that the energy function has a strict local minimum at the desired equilibrium, which guarantees stability of this point (at least in the time-invariant case).
2) Clearly, the dynamic behavior, specified in terms of the speed of the closed loop response, should be as desired.
3) As motivated already in Section 1.1, the DA of the desired equilibrium point should be as large as possible to assure stability in the operating region and robustness against disturbances.

A very useful tool that will be used in the following to achieve desired closed loop dynamics and to guarantee that the energy function has an isolated minimum at the desired equilibrium point is the LLDA approach [102], [103], which has been reviewed in Section 2.3. In order to guarantee positive (semi-) definiteness of the dissipation matrix, a specific parametrization of the design matrix is proposed in Section 4.1. To maximize the estimated DA, we first elaborate in Section 4.2 on the computation of its volume, which is used to quantify its size. Based on this measure, in Section 4.3 an optimization procedure is proposed to determine a controller parametrization which maximizes the estimated DA, while simultaneously taking account of desired closed loop performance. Parts of the results in this chapter have been presented in [97], [98].

4.1 Positive Semidefiniteness of the Dissipation Matrix

When designing an IDA controller, we have to ensure that the desired dissipation matrix $\mathbf{R}(\mathbf{x}) = -\text{sym}\{\mathbf{F}(\mathbf{x})\}$ is positive semidefinite, at least in some environment Ω^R of $\mathbf{x}^* = \mathbf{0}$. In order to identify admissible design matrices, we can invoke Sylvester's criterion[1] for positive semidefinite matrices (see [164] or [64], pp. 305-308) as done for instance in [102], [103]. This yields $\sum_{j=1}^{n} \binom{n}{j}$ inequalities for the (in general state-dependent) elements of $\mathbf{F}(\mathbf{x})$, e.g. 7 inequalities in the case $n = 3$. Even for problems of low dimension these inequalities can get very cumbersome making it quite difficult to determine a suitable controller parametrization, which in addition guarantees positive definiteness of the energy function and desired dynamic behavior. Therefore, we propose in this section a specific parametrization of the design matrix which assures positive semidefiniteness of the dissipation matrix by construction.

It is well known that a matrix $\mathbf{R}$ is positive semidefinite if and only if $\mathbf{R} = \mathbf{T}^T\mathbf{T}$ holds for some upper triangular matrix[2] $\mathbf{T}$ [12]. Now define the matrices $\mathbf{T}_{ij} \in \mathbb{R}^{n\times n}$ and $\mathbf{R}_{ij} \in \mathbb{R}^{n\times n}$ as

$$\mathbf{T}_{ij} = [t_{kl}]\,, \quad t_{kl} = \begin{cases} 1 & , k = i \wedge l = j \wedge k \leq l \\ 0 & , \text{otherwise} \end{cases} \tag{4.1}$$

$$\mathbf{R}_{ij} = \mathbf{T}_{ij} + \mathbf{T}_{ij}^T\,. \tag{4.2}$$

Then every upper triangular matrix $\mathbf{T}(\mathbf{x}) : \mathbb{R}^n \to \mathbb{R}^{n\times n}$ can be represented in the form

$$\mathbf{T}(\mathbf{x}) = \sum_{i=1}^{n}\sum_{j=i}^{n} k_{ij}(\mathbf{x})\mathbf{T}_{ij} \tag{4.3}$$

with functions $k_{ij}(\mathbf{x}) : \mathbb{R}^n \to \mathbb{R}$. Consequently,

$$\begin{aligned} \mathbf{R}(\mathbf{x}) &= \left(\sum_{i=1}^{n}\sum_{j=i}^{n} k_{ij}(\mathbf{x})\mathbf{T}_{ij}\right)^T \left(\sum_{i=1}^{n}\sum_{j=i}^{n} k_{ij}(\mathbf{x})\mathbf{T}_{ij}\right) \\ &= \sum_{i=1}^{n}\sum_{j=i}^{n}\sum_{k=1}^{i} k_{ki}(\mathbf{x})k_{kj}(\mathbf{x})\mathbf{R}_{ij} \end{aligned} \tag{4.4}$$

is a set of positive semidefinite matrices. If $k_{ii}(\mathbf{x}) \neq 0,\ \forall\, i$, then $\mathbf{R}(\mathbf{x}) > 0$. Hence, if the design matrix is chosen as $\mathbf{F}(\mathbf{x}) = \mathbf{J}(\mathbf{x}) - \mathbf{R}(\mathbf{x})$ with $\mathbf{J}(\mathbf{x}) = -\mathbf{J}^T(\mathbf{x})$ and $\mathbf{R}(\mathbf{x})$ as in

[1] Frequently, the term "Sylvester's criterion" is used only in the context of positive definite matrices. Following [164], we use it here also for its generalization to positive semidefinite matrices.

[2] For positive definite matrices $\mathbf{R} > 0$ this is the Cholesky factorization.

(4.4), then the entries of $\mathbf{J}(\mathbf{x})$ and the functions $k_{ij}(\mathbf{x})$ can be varied arbitrarily and it is guaranteed that $\mathbf{R}(\mathbf{x}) = -\mathrm{sym}\{\mathbf{F}(\mathbf{x})\} \geq 0$. In general, of course also functions $k_{ij}(\mathbf{x}, t)$, which explicitly depend on the time t, may be used in (4.4). This can be of interest, if an IDA controller is to be designed for a time-varying system. In this case, it might be desired that the design matrix is a function not only of the state but also of the time t.

Example 4.1.1. Consider the case $n = 2$. Then, the matrices $\mathbf{R}_{ij}$ are

$$\mathbf{R}_{11} = \begin{bmatrix} 1 & 0 \\ 0 & 0 \end{bmatrix} \quad , \quad \mathbf{R}_{12} = \begin{bmatrix} 0 & 1 \\ 1 & 0 \end{bmatrix} \quad , \quad \mathbf{R}_{22} = \begin{bmatrix} 0 & 0 \\ 0 & 1 \end{bmatrix} \tag{4.5}$$

and

$$\mathbf{R} = \begin{bmatrix} k_{11}^2 & k_{11}k_{12} \\ k_{11}k_{12} & k_{12}^2 + k_{22}^2 \end{bmatrix} \quad , \quad k_{ij} \in \mathbb{R} \tag{4.6}$$

is the set of all constant positive semidefinite matrices $\mathbf{R}$.

4.2 Quantifying the Domain of Attraction

In the previous chapter, we have presented two algorithms that allow to determine a level value $\hat{d}$ such that the connected component $\overline{\mathrm{S}}_{\hat{d}}(\mathbf{0})$ qualifies as an estimate of the DA of the desired equilibrium. Our objective in the sequel is to adjust the controller parameters so as to maximize the estimated DA, while simultaneously taking into account desired transient behavior. A quite natural measure to quantify the size of the estimated DA is the volume $V_{\hat{d}}$ of $\mathrm{S}_{\hat{d}}(\mathbf{0})$. For its computation an explicit representation of the manifold $\partial\mathrm{S}_{\hat{d}}(\mathbf{0})$, implicitly defined by $H(\mathbf{x}) - \hat{d} = 0$, is needed. This section describes an easy to implement procedure to numerically approximate $\partial\mathrm{S}_{\hat{d}}(\mathbf{0})$ and to calculate $V_{\hat{d}}$. While we explicitly consider only time-invariant systems here, the procedure applies verbatim also to the time-varying case, where an estimate of the DA is given by the sublevel set $\overline{\mathrm{S}}_{\hat{d}}^{W_2}(\mathbf{0})$ of $W_2(\mathbf{x})$. The only difference is that, in order to numerically approximate the latter, the gradient of $W_2(\mathbf{x})$ has to be determined numerically, e.g. by finite differencing as described in Section 8.1 of [129], since usually no symbolic expression is available.

It is desired to approximate the radial function $\rho_S(\mathbf{v})$ of the properly star shaped set $\mathrm{S}_{\hat{d}}(\mathbf{0})$ (c.f. (3.3)). Since any $\mathbf{v} \in \mathbb{S}^{n-1}$ has a unique description in spherical coordinates with $r = 1$, $\rho_S(\mathbf{v})$ can be considered as a function of $\boldsymbol{\theta} = [\theta_1, \ldots, \theta_{n-1}]$, i.e., $\rho_S(\mathbf{v}) = \rho_S(\boldsymbol{\theta})$ (with some abuse of notation). Hence, it is convenient to solve the problem in spherical coordinates $\mathbf{z} = \boldsymbol{\Psi}^{-1}(\mathbf{x})$. Let $\widetilde{H}(\mathbf{z}) = H \circ \boldsymbol{\Psi}(\mathbf{z})$, $\widetilde{\mathrm{S}}_{\hat{d}} = \boldsymbol{\Psi}^{-1}(\mathrm{S}_{\hat{d}}(\mathbf{0}))$ and $\widehat{\mathbf{z}} = [\hat{r}, \hat{\theta}_1, \ldots, \hat{\theta}_{n-1}] = \boldsymbol{\Psi}^{-1}(\hat{\mathbf{x}}_d)$. Moreover, we denote by $\widetilde{H}'(\mathbf{z})$ the Jacobian of $\widetilde{H}(\mathbf{z})$.

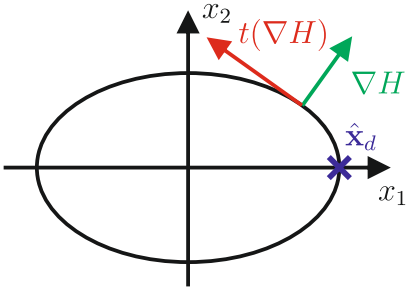

Figure 4.1: Numerical approximation of the level set $\partial \mathrm{S}_{\hat{d}}(\mathbf{0})$: the 2-dimensional case.

At first, the case $n = 2$ is discussed, in which $\partial \mathrm{S}_{\hat{d}}(\mathbf{0})$ has dimension 1 and its numerical approximation reduces to the well-known problem of tracing an implicitly defined curve $\mathbf{w}(s) \subset \widehat{H}^{-1}(0)$, where $\widehat{H}(\mathbf{z}) = \widetilde{H}(\mathbf{z}) - \hat{d}$ (see [1]). The curve is the local solution of the initial value problem

$$\frac{d}{ds}\mathbf{w} = \mathbf{t}\Big(\widehat{H}'(\mathbf{w})\Big) \,, \quad \mathbf{w}(0) = \hat{\mathbf{z}} \,. \tag{4.7}$$

Therein, $\mathbf{t}(\mathbf{A}) \in \mathbb{R}^n$ denotes the unique tangent vector induced by a matrix $\mathbf{A} \in \mathbb{R}^{(n-1)\times n}$ satisfying

$$\mathbf{A}\mathbf{t} = \mathbf{0} \tag{4.8}$$

$$\|\mathbf{t}\| = 1 \tag{4.9}$$

$$\det \begin{bmatrix} \mathbf{A}^T \\ \mathbf{t}^T \end{bmatrix} > 0 \,. \tag{4.10}$$

This is illustrated in Figure 4.1 (in $\mathbf{x}$-coordinates). With $\hat{\mathbf{x}}_d = \mathbf{\Psi}(\hat{\mathbf{z}})$ one point of the desired curve $\mathbf{w}(s)$ is already known. According to (4.8), the vector $\mathbf{t}(\widehat{H}')$ is at any point orthogonal to the gradient $\nabla H = (\widehat{H}')^T$ and thus tangential to the level curve. Hence, it is clear that we obtain $\partial \mathrm{S}_{\hat{d}}(\mathbf{0})$, if, starting from $\hat{\mathbf{z}}$, we always move in the direction given by $\mathbf{t}(\hat{H}')$. By the relation (4.9), the tangent vector is scaled to have unit length, and (4.10) specifies the direction in which the curve is traversed.

The problem (4.7) can be solved using solvers for initial value problems or, which is more efficient, by *Predictor-Corrector* methods described e.g. in [1], which exploit that the curve is a set of zero points of $\widehat{H}(\mathbf{z})$. In (4.7), it holds that $\widehat{H}'(\mathbf{z}) = (H' \circ \mathbf{\Psi}(\mathbf{z}))\frac{\partial}{\partial \mathbf{z}}\mathbf{\Psi}(\mathbf{z})$ and

$$\mathbf{t}\Big(\widehat{H}'(\mathbf{w})\Big) = \|\widetilde{H}'(\mathbf{w})\|^{-1} \left[-\left.\frac{\partial \widetilde{H}}{\partial \theta_1}\right|_{\mathbf{w}} \quad \left.\frac{\partial \widetilde{H}}{\partial r}\right|_{\mathbf{w}} \right]^T . \tag{4.11}$$

Now $\mathbf{w}(s)$ is traced via (4.7) until $w_2(s) - w_2(0) = 2\pi$. The interval $[0, 2\pi]$ is discretized

by $\theta_{1,k_1} = k_1 \frac{2\pi}{K_1}$, $k_1 = 0, \ldots, K_1$, where K_1 is not necessarily the same as in Section 3.3. By linear interpolation, pairs $[\theta_{1,k_1}, \rho_S(\theta_{1,k_1})]$ are obtained from the calculated path which approximate the function $\rho_S(\theta_1)$.

The volume of $\mathrm{S}_{\hat{d}}(\mathbf{0})$ is given by $V_{\hat{d}} = \int_{\mathrm{S}_{\hat{d}}(\mathbf{0})} \mathrm{d}V$. By one of the fundamental properties of multiple integrals it holds that [108]

$$V_{\hat{d}} = \int_{\widetilde{\mathrm{S}}_{\hat{d}}} |\det(\boldsymbol{\Psi}'(\mathbf{z}))| \, \mathrm{d}r \, \mathrm{d}\theta_1 \ldots \mathrm{d}\theta_{n-1} \tag{4.12}$$

i.e., for $n = 2$

$$V_{\hat{d}} = \int_{\widetilde{\mathrm{S}}_{\hat{d}}} r \, \mathrm{d}r \, \mathrm{d}\theta_1 \approx \frac{\pi}{K_1} \sum_{i=0}^{K_1} \rho_S^2(\theta_{1,i}) \tag{4.13}$$

where the discrete approximation of $\rho_S(\theta_1)$ and rectangular integration have been used.

This procedure readily generalizes to the higher-dimensional case. To this end, several curves $\mathbf{w}_i(s)$ are calculated on $\partial \mathrm{S}_{\hat{d}}(\mathbf{0})$ defined by $\widehat{\mathbf{H}}_i(\mathbf{z}) = \mathbf{0}$, where along $\mathbf{w}_i(s)$ all components of $\boldsymbol{\theta}$ are held constant except for θ_i. Consider e.g. $n = 3$. Then, $\widehat{\mathbf{H}}_1(\mathbf{z}) = [\widetilde{H}(\mathbf{z}) - \hat{d}, \theta_2 - \bar{\theta}_2]^T$ and $\widehat{\mathbf{H}}_2(\mathbf{z}) = [\widetilde{H}(\mathbf{z}) - \hat{d}, \theta_1 - \bar{\theta}_1]^T$ with $\bar{\theta}_1$ and $\bar{\theta}_2$ some fixed values. The curves $\mathbf{w}_i(s)$ are local solutions of

$$\frac{d}{ds}\mathbf{w} = \mathbf{t}\left(\widehat{\mathbf{H}}_i'(\mathbf{w})\right) \ , \ i = 1, 2 \ , \quad \mathbf{w}(0) = \mathbf{w}_0 \ . \tag{4.14}$$

As in the 2-dimensional case, our objective is to compute $\rho_S(\theta_{1,k_1}, \theta_{2,k_2})$ on a grid given by $\theta_{1,k_1} = k_1 \frac{2\pi}{K_1}$, $k_1 = 0, \ldots, K_1$ and $\theta_{2,k_2} = k_2 \frac{\pi}{K_2}$, $k_2 = 0, \ldots, K_2$. In a first step, we determine a sequence of values $\rho_S(\hat{\theta}_1, \theta_{2,k_2})$, $k_2 = 0, \ldots, K_2$. To this end, we follow the solution of (4.14) for $i = 2$ and $\mathbf{w}_0 = \hat{\mathbf{z}}$ (i.e., $\bar{\theta}_1 = \hat{\theta}_1$), forward and backward in s, and apply linear interpolation to obtain the desired values from the calculated path. In view of

$$\widehat{\mathbf{H}}_2' = \begin{bmatrix} \frac{\partial \widetilde{H}}{\partial r} & \frac{\partial \widetilde{H}}{\partial \theta_1} & \frac{\partial \widetilde{H}}{\partial \theta_2} \\ 0 & 1 & 0 \end{bmatrix} \tag{4.15}$$

it becomes clear that the vector $\mathbf{t}(\widehat{\mathbf{H}}_2'(\mathbf{w}))$ which satisfies (4.8)-(4.10) is given by

$$\mathbf{t}\left(\widehat{\mathbf{H}}_2'\right) = \left\| \begin{bmatrix} -\frac{\partial \widetilde{H}}{\partial \theta_2} & 0 & \frac{\partial \widetilde{H}}{\partial r} \end{bmatrix}^T \right\|^{-1} \begin{bmatrix} -\frac{\partial \widetilde{H}}{\partial \theta_2} & 0 & \frac{\partial \widetilde{H}}{\partial r} \end{bmatrix}^T \ . \tag{4.16}$$

In a second step, for each $\mathbf{w}_0 = [\rho_S(\hat{\theta}_1, \theta_{2,k_2}), \hat{\theta}_1, \theta_{2,k_2}]^T$ a curve $\mathbf{w}_1(s)$ is determined from (4.14), where $\mathbf{t}(\widehat{\mathbf{H}}_1'(\mathbf{w}))$ is given by

$$\mathbf{t}\left(\widehat{\mathbf{H}}_1'\right) = \left\| \begin{bmatrix} \frac{\partial \widetilde{H}}{\partial \theta_1} & -\frac{\partial \widetilde{H}}{\partial r} & 0 \end{bmatrix}^T \right\|^{-1} \begin{bmatrix} \frac{\partial \widetilde{H}}{\partial \theta_1} & -\frac{\partial \widetilde{H}}{\partial r} & 0 \end{bmatrix}^T \ . \tag{4.17}$$

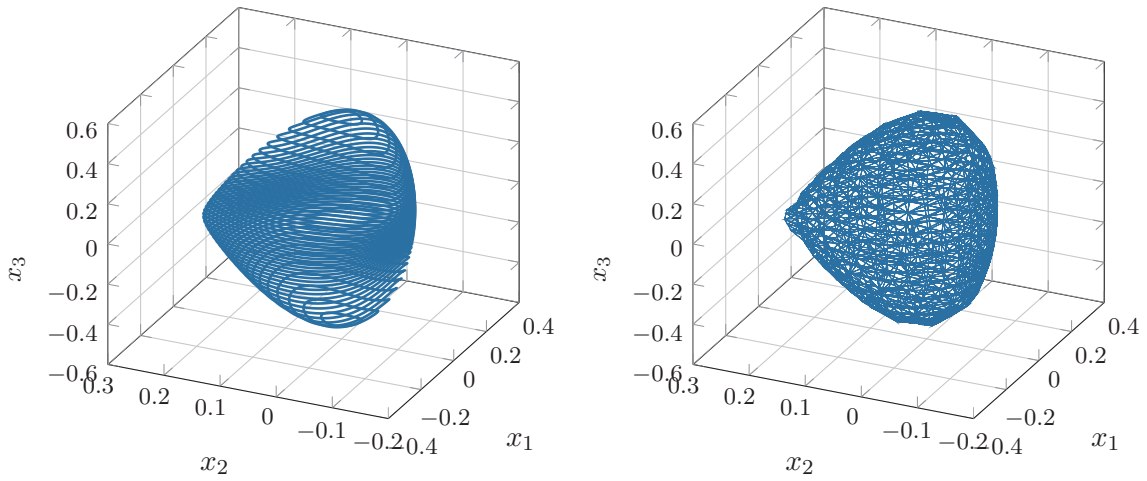

Figure 4.2: Numerical approximation of the level set $\mathrm{S}_{\hat{d}}(\mathbf{0})$ using the approach described in this section (left) and by means of the piecewise linear approximation method developed in [69] (right).

Applying again linear interpolation we finally obtain a discrete approximation of $\rho_S(\boldsymbol{\theta})$ by the $K = K_1 K_2$ values $\rho_S(\theta_{1,k_1}, \theta_{2,k_2})$.

This is illustrated in Figure 4.2 (left) for an exemplary level set of the energy function that results from the IDA design for a synchronous generator in Section 5.2. We remark that there are alternative techniques for approximating implicitly defined manifolds, for instance the piecewise linear approximation method developed in [69] (see also [1]). If the level set shown if Figure 4.2 (left) is approximated using this approach, the result depicted in Figure 4.2 (right) is obtained. For our purposes, the method described above has proven to be more suitable and, furthermore, the effort required for the implementation of the piecewise linear approximation methodology is considerably higher.

Also in the 3-dimensional case, we apply rectangular integration to (4.12) and obtain the formula

$$\begin{aligned} V_{\hat{d}} &= \int_0^{2\pi} \int_0^{\pi} \int_0^{\rho_S(\boldsymbol{\theta})} r^2 \sin(\theta_2)\, \mathrm{d}r\, \mathrm{d}\theta_2\, \mathrm{d}\theta_1 \\ &\approx \sum_{j=0}^{K_2} \sum_{i=0}^{K_1} \frac{2\pi}{3K_1} \rho_S^3(\theta_{1,i}, \theta_{2,j}) \left[\cos(\theta_{2,j}) - \cos(\theta_{2,j+1})\right] \ . \end{aligned} \tag{4.18}$$

for the volume.

Besides the computation of the volume, the numerical approximation of $\partial \mathrm{S}_{\hat{d}}(\mathbf{0})$ allows to validate the critical level value to some extent: Clearly, none of the curves $\mathbf{w}_i(s)$ may leave B_R. Another benefit is that, once $\rho_S(\boldsymbol{\theta})$ is available, it can be easily determined,

whether a given initial state $\mathbf{x}(0)$ is contained in the estimated DA by representing it in spherical coordinates, e.g. in the 3-dimensional case $[r(0)\ \theta_1(0)\ \theta_2(0)]^T = \boldsymbol{\Psi}^{-1}(\mathbf{x}(0))$. If $r(0) \leq \rho_S(\theta_1(0), \theta_2(0))$ then $\mathbf{x}(0) \in \overline{\mathrm{S}}_{\hat{d}}(\mathbf{0})$. The value $\rho_S(\theta_1(0), \theta_2(0))$ can be determined from the discrete approximation of $\rho_S(\boldsymbol{\theta})$ by interpolation.

4.3 Enlarging the Domain of Attraction

In this section, the maximization of the DA is formulated in terms of two slightly different optimization problems that can be solved using numerical methods. We first concentrate on the time-invariant case and briefly comment on the time-varying one at the end of the section. The objective function to be maximized is the volume $V_{\hat{d}}$ of $\mathrm{S}_{\hat{d}}(\mathbf{0})$. In order to take into account desired dynamic behavior, the eigenvalues of the closed loop linearization are considered. If fixed eigenvalues are specified and the Assumptions 2.3.1 and 2.3.2 are fulfilled, we make use of LLDA to establish dependencies between the controller parameters. The parameters that are not determined by the system of equations (2.57)-(2.59) are subsumed in the vector $\boldsymbol{\gamma}$, and we wish to determine a $\boldsymbol{\gamma}^*$ that maximizes $V_{\hat{d}}$. If the approach proposed in Section 4.1 is used to parametrize the design matrix, it is guaranteed that $\mathbf{R}(\mathbf{x}) \geq 0$ holds globally for all choices of $\boldsymbol{\gamma}$. Together with LLDA this ensures that $H(\mathbf{x})$ has a strict local minimum at the origin. Then, $\boldsymbol{\gamma}^*$ can be determined by solving the unconstrained optimization problem

$$\max_{\boldsymbol{\gamma}} \ V_{\hat{d}}(\boldsymbol{\gamma}) \ . \tag{4.19}$$

In case it is not guaranteed for all $\boldsymbol{\gamma}$ that $\mathbf{R}(\mathbf{x})$ is positive semidefinite, the solver might evaluate the objective function at points $\boldsymbol{\gamma}$ where $H(\mathbf{x})$ is not a suitable Lyapunov function. Then, actually it holds that $\hat{d} = H(\mathbf{0})$ and the algorithms presented in Chapter 3 cannot yield a meaningful result. Therefore, we check in advance whether the Hessians $\nabla^2 H(\mathbf{x})$ and $\nabla^2(-\dot{H}(\mathbf{x}))$ are positive definite. If not, the minimum eigenvalue of these matrices is returned to the solver instead of $V_{\hat{d}}$. Note that this does not ensure that $\mathbf{R}(\mathbf{x}) \geq 0$ is satisfied for the resulting controller parametrization, if this matrix is a function of the state. To enforce positive semidefiniteness of $\mathbf{R}(\mathbf{x})$ in this case, appropriate constraints need to be added to the optimization problem.

Instead of fixing the eigenvalues of the closed-loop linearization we can also merely specify an admissible region of the complex plane within which the eigenvalues may take any position (see Figure 4.3). This approach does of course not require the Assumptions 2.3.1

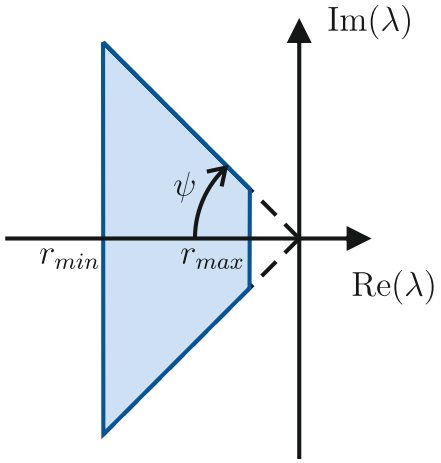

Figure 4.3: Admissible region for the eigenvalues.

and 2.3.2, and it provides more degrees of freedom that can be used for enlarging the DA. Rather than solving the system of equations (2.57)-(2.59), we formulate the constrained optimization problem

$$\max_{\boldsymbol{\gamma}} \quad V_{\hat{d}}(\boldsymbol{\gamma}) \tag{4.20a}$$

$$\text{s.t.} \quad r_{min} \leq \mathrm{Re}(\lambda_i) \leq r_{max} \tag{4.20b}$$

$$|\mathrm{Re}(\lambda_i)| \geq \tan(\psi)\,|\mathrm{Im}(\lambda_i)| \tag{4.20c}$$

where the parameters $r_{min} < 0$, $r_{max} < 0$ and $0 \leq \psi \leq \frac{\pi}{2}$ characterize the admissible region for the closed loop eigenvalues λ_i (see Figure 4.3). If $\mathbf{R}(\mathbf{0}) \geq 0$ holds (e.g. because of the parametrization proposed in Section 4.1) and the constraints (4.20b) and (4.20c) are satisfied, then the Hamiltonian $H(\mathbf{x})$ has an isolated minimum at the origin and is a suitable Lyapunov function (see Proposition 10 in [103]). However, it might happen during the optimization that the solver evaluates the objective function at a $\boldsymbol{\gamma}$ for which either $\mathbf{R}(\mathbf{0}) \geq 0$ is violated or the closed loop linearization has eigenvalues with nonnegative real part. Therefore, the objective function is appropriately modified as described subsequent to equation (4.19).

If the dissipation matrix is only positive semidefinite for the computed controller parameters, it has to be checked whether the trivial solution $\mathbf{x}^* = \mathbf{0}$ is indeed the only one which can stay identically in $\{\mathbf{x} \in \overline{\mathrm{S}}_{\hat{d}}(\mathbf{0}) | \dot{H}(\mathbf{x}) = 0\}$, as this cannot be accomplished during the optimization. It is noted that only the inner approximation $\overline{\mathrm{S}}_{\hat{d}}(\mathbf{0})$ of the DA can be maximized, which does not ensure that also the exact DA is enlarged. However, from a practical point of view, this estimate is of primary interest, since usually it is not possible to determine the exact DA.

Let us finally comment on the time-varying case. In Section 2.3.2, we have reviewed the application of LLDA for the stabilization of the time-varying error systems arising in trajectory tracking problems. In view of that, it is clear that with some obvious modifications the methods presented above can also be employed for this case of application, although we have explicitly treated only time-invariant control systems in the present section (see also the example in Section 5.3).

4.4 Concluding Remarks

In this chapter, we have been concerned with the problem of finding a suitable parametrization for an IDA controller, that satisfies the requirements regarding i) positive semidefiniteness of the dissipation matrix, ii) size of the DA, and iii) dynamic behavior of the resulting closed loop system. The main contributions can be summarized as follows: First, we have proposed a specific way of parameterizing the design matrix which guarantees positive semidefiniteness of the dissipation matrix irrespective of the chosen parameter values. To this end, we have exploited the fact that any positive semidefinite matrix can be represented as the product of a lower triangular matrix and its transpose. The approach makes it unnecessary to deal with the cumbersome inequalities resulting from Sylvester's criterion, which constitutes a clear practical advantage. Second, we have presented a method to determine a controller parametrization that maximizes the estimated DA and takes into account the desired speed of the closed loop response. To quantify the size of the estimated DA, a discrete approximation of its boundary is determined and, based on that, the enclosed volume is computed by numerical integration. An optimal controller parametrization is then obtained by maximizing this volume using a numerical optimization method. The desired dynamic behavior is specified in terms of the eigenvalues of the closed loop linearization. Either fixed eigenvalue locations are assigned prior to the optimization using the LLDA approach, or an admissible region is defined for the eigenvalues and considered as a constraint in the optimization.

Chapter 5

Examples

In this chapter, the methods developed in the preceding two chapters are applied to three example systems in order to demonstrate their practical applicability and effectiveness. We start in Section 5.1 with a numerical example, which is only 2-dimensional and allows the computation of the exact DA as well as an easy graphical visualization of the results. In this context, a comparison with a linear state feedback law is included since this type of controller is still frequently used in practice also for nonlinear systems. Subsequently, we address the excitation control of a synchronous generator, which is a problem of major technical relevance. The objective is to enlarge the DA in order to increase the so called *critical clearing time*, which is an important security measure of a power system. To show the capability of the proposed approach we compare the obtained controller to a benchmark controller, which has been designed in [61] using also the IDA methodology. As a third example, we consider the trajectory tracking control of a magnetic levitation system to demonstrate the effectiveness of the proposed methods also for time-varying systems. The controller that results from the optimization procedure is compared to the original one from [102] using a laboratory experiment.

5.1 Numerical Example

Consider the unstable nonlinear system [97]

$$\dot{\mathbf{x}} = \begin{bmatrix} x_2 + 2x_1 \\ x_1 + x_2^2 \end{bmatrix} + \begin{bmatrix} 1 \\ 0 \end{bmatrix} u \tag{5.1}$$

which is to be stabilized in $\mathbf{x}^* = \mathbf{0}$ by means of the IDA method. The design matrix $\mathbf{F}$ is chosen according to Section 4.1 resulting in a dissipation matrix of the form (4.6). With

$\mathbf{G}^{\perp} = [0,\ 1]$ the projected matching equation

$$\begin{bmatrix} -j_{12} - k_{11}k_{12} & -k_{12}^2 - c_{22}^2 \end{bmatrix} \nabla H(\mathbf{x}) = x_1 + x_2^2 \tag{5.2}$$

is obtained, which is solvable according to Proposition 2.2.1. A solution of (5.2) is

$$H(\mathbf{x}) = \frac{x_2^3}{3\nu_{12}} - \frac{x_2^2\nu_{11}}{2\nu_{12}^2} + \frac{x_1x_2}{\nu_{12}} + \mu_2\left(x_1 - \frac{x_2\nu_{11}}{\nu_{12}}\right)^2 \tag{5.3}$$

where $\nu_{11} = -j_{12} - k_{11}k_{12}$, $\nu_{12} = -k_{12}^2 - k_{22}^2$ and we have chosen $\phi(\xi) = \mu_2\xi^2$. As desired, it holds that $\nabla H(\mathbf{x})|_{\mathbf{x}=\mathbf{0}} = \mathbf{0}$. LLDA is employed with the prespecified system matrix $\mathbf{A}_d$ possessing two eigenvalues in -2. The equations (2.57)–(2.59) are solved for μ_2 and j_{12}. The parameters k_{11}, k_{12} and k_{22} remain as degrees of freedom for the enlargement of the DA. As an initial guess, the choice $k_{11}^{ini} = k_{22}^{ini} = 1$, $k_{12}^{ini} = 0$ is made resulting in $\mathbf{R}^{ini} = \mathbf{I}$.

We apply the algorithm presented in Section 3.3 to determine an estimate of the DA. We omit the second step of the algorithm and instead discretize the whole interval $[0, R]$. The Illinois algorithm, a variant of *regula falsi*, is employed as 1-dimensional root-finding technique. Moreover, the choices $R = 4$ and $\epsilon_c = 0.02$ are made. The level set $\partial\mathrm{S}_{\hat{d}}^{ini}(\mathbf{0})$, approximated as described in Section 4.2, is displayed in Figure 5.1 (left) together with a contour plot of the energy function $H^{ini}(\mathbf{x})$ and the exact stability boundary $\partial\mathrm{A}^{ini}(\mathbf{0})$, which has been identified by the method proposed in [29].

A genetic optimization algorithm provided by MATLAB (`ga`) is used (40 individuals, 15 generations) to solve the optimization problem (4.19) with $\boldsymbol{\gamma} = [k_{11},\ k_{12},\ k_{22}]^T$. For the initial population, the ranges $k_{11}, k_{22} \in [0, 100]$ and $k_{12} \in [-100, 100]$ are specified. The resulting controller configuration is $k_{11}^{opt} = 244.2$, $k_{12}^{opt} = -39.2$, $k_{22}^{opt} = -8.1$, $j_{12}^{opt} = -6936$, $\mu_2^{opt} = 3.63 \cdot 10^{-5}$. Figure 5.1 (right) shows a contour plot of $H^{opt}(\mathbf{x})$ together with $\partial\mathrm{S}_{\hat{d}}^{opt}(\mathbf{0})$ and $\partial\mathrm{A}^{opt}(\mathbf{0})$ (Observe the different scale of Figure 5.1 left and right). In Figure 5.2 (left) the estimated stability boundaries are compared, in Figure 5.2 (right) the exact ones. In both figures, the circular markers denote equilibrium points of the corresponding closed loop system. It can be seen that not only the estimated DA can be significantly enlarged by optimizing the controller parametrization, but also the exact one. It is remarked that $\hat{\mathbf{x}} \in \partial\mathrm{B}_R$, i.e. a larger estimate of the DA could be achieved for the optimized controller by choosing a larger R and possibly also a further enlargement of the DA via (4.19).

Since linear state feedback controllers are still frequently used in practice also for nonlinear systems, such a controller has been designed for comparison. To this end, (5.1) is linearized at $\mathbf{x}^* = \mathbf{0}$ and the control law $u = -\mathbf{r}^T\mathbf{x} = -[6,\ 5]\mathbf{x}$ is determined, which

assigns two eigenvalues in -2 to the linearization, and thus the same eigenvalues which have been used for LLDA above. To determine an estimate of the DA which is achieved by this controller, a standard procedure is applied. First, the Lyapunov equation

$$\mathbf{A}_d^T\mathbf{P} + \mathbf{P}\mathbf{A}_d = -\mathbf{I} \tag{5.4}$$

with $\mathbf{A}_d$ the state matrix of the closed-loop linearization is solved to obtain a local quadratic Lyapunov function $V(\mathbf{x}) = \mathbf{x}^T\mathbf{P}\mathbf{x}$. Then the largest sublevel set is determined within which it holds that $\dot{V}(\mathbf{x}) < 0$ except at $\mathbf{x}^* = \mathbf{0}$, where $\dot{V}(\mathbf{x})$ is the derivative of $V(\mathbf{x})$ along the trajectories of (5.1) with $u = -\mathbf{r}^T\mathbf{x}$. Figure 5.2 shows the estimated (left) and the exact SB (right) for the linear controller as orange dotted line. As can be seen, both the estimated and the exact DA corresponding to the initial IDA controller are smaller than those of the linear one. However, after the optimization significantly larger DAs – estimated as well as exact – are achieved by the IDA controller. For a comparison of the time response curves of the different closed loop sytems the reader is referred to [97].

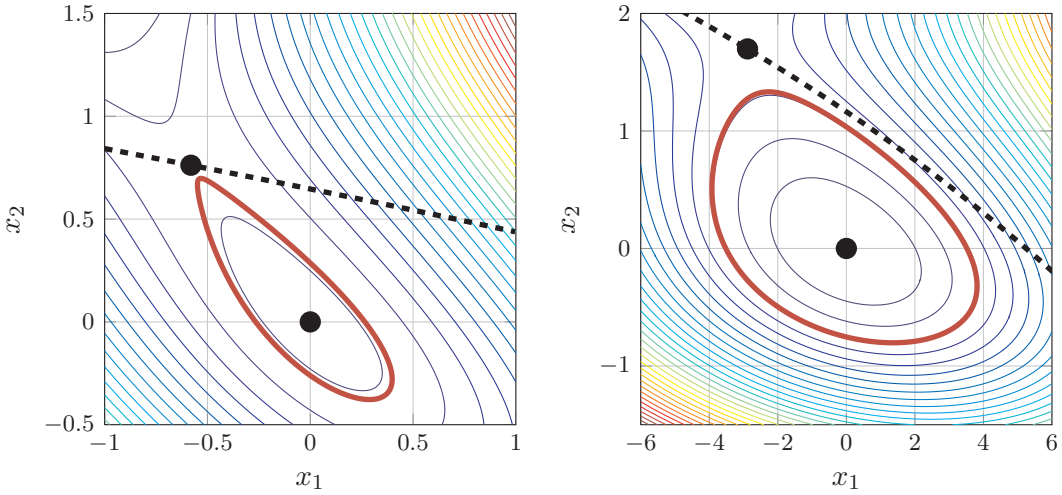

Figure 5.1: Contour plot of the energy function together with $\partial \mathrm{S}_{\hat{d}}(\mathbf{0})$ (red solid) and $\partial \mathrm{A}(\mathbf{0})$ (black dashed) for the initial (left) and the optimized (right) IDA controller.

5.2 Excitation Control of a Synchronous Generator

The problem of transient stability is of fundamental importance for the secure operation of power systems and has become a major operating constraint especially in regions that rely on long distance transfers of bulk power [27]. It is associated with the question whether a power system reaches an acceptable steady-sate operating condition after a large

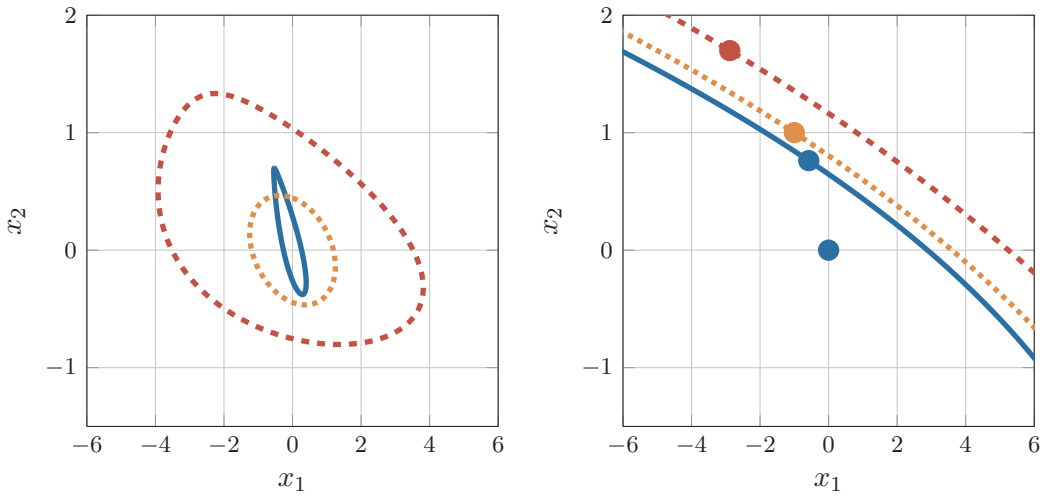

Figure 5.2: Comparison of the estimated (left) and exact stability boundaries (right): initial IDA controller (blue solid), optimized IDA controller (red dashed), and linear controller (orange dotted).

disturbance or fault (e.g. a short circuit) has occurred. The fault changes the network topology whereby the system is driven away from its stable steady state. After some time, called the *clearing time*, the fault is cleared by the protective system operation. The key issue is, whether at this point the system state belongs to the DA of the post-fault equilibrium. For a particular fault, the maximum clearing time for which this is the case is called the *critical clearing time*.

Numerous control strategies have been proposed to improve the transient stability of power systems, including feedback linearization (see e.g. [124]) and more recently also passivity-based techniques (see e.g. [10], [61]). To reduce the complexity, often each generator is considered separately, while the other machines and components are regarded as infinite bus. A frequently used model for this single machine infinite bus system (SMIB) is the classical third-order flux-decay model [142] given by

$$\begin{bmatrix} \dot{x}_1 \\ \dot{x}_2 \\ \dot{x}_3 \end{bmatrix} = \begin{bmatrix} b_3 \cos(x_2) - b_4 x_1 + E \\ x_3 \\ -b_1 x_1 \sin(x_2) - b_2 x_2 + P \end{bmatrix} + \begin{bmatrix} 1 \\ 0 \\ 0 \end{bmatrix} u \tag{5.5}$$

where x_1 is the internal voltage, x_2 the load angle and x_3 the shaft speed deviation from the synchronous speed. The mechanic input power P and the field voltage E are held constant and the control input u is added to the field voltage. The values of the parameters b_i, $i = 1, \ldots, 4$ as well as of P and E are taken from [60], [61] and are given in Table 5.1. The parameter b_2 is assumed to be zero, which is a typical assumption for machines with round

Table 5.1: Parameters of the SMIB model.

Parameter	Value (pu)
b_1	34.29
b_2	0
b_3	0.149
b_4	0.3341
E	0.2593
P	28.22

rotor [60]. Therefore, the corresponding term in (5.5) is omitted in the following. The open loop system has an asymptotically stable equilibrium point at $\mathbf{x}^* = [1.055\ 0.8945\ 0]$, which is to be stabilized. The adjacent equilibrium at $\mathbf{x}_u^* = [0.8287\ 1.452\ 0]$ is unstable [61], [142]. The control objective is to enlarge the DA of $\mathbf{x}^*$ in order to increase the critical clearing time. Another aspect which is of major importance is the transient performance of the machine following a fault.

5.2.1 IDA Controller Design

Our objective in the following is to perform a systematic IDA design and to optimize the controller parameters regarding the size of the DA by means of the tools presented in the Chapters 3 and 4. Note that the system (5.5) is of the form (2.49) enabling the application of LLDA. The design matrix $\mathbf{F} = \mathbf{J} - \mathbf{R}$ is chosen constant and is parametrized as suggested in Section 4.1 yielding

$$\mathbf{J} = \begin{bmatrix} 0 & j_{12} & j_{13} \\ -j_{12} & 0 & j_{23} \\ -j_{13} & -j_{23} & 0 \end{bmatrix}, \quad \mathbf{R} = \begin{bmatrix} k_{11}^2 & k_{11}k_{12} & k_{11}k_{13} \\ k_{11}k_{12} & k_{12}^2 + k_{22}^2 & k_{12}k_{13} + k_{22}k_{23} \\ k_{11}k_{13} & k_{12}k_{13} + k_{22}k_{23} & k_{13}^2 + k_{23}^2 + k_{33}^2 \end{bmatrix}. \tag{5.6}$$

In the notation of Section 2.3, the first row of $\mathbf{F}$ is $\mathbf{F}^\alpha$, the remaining two rows form $\mathbf{F}^\nu$.

Using the left annihilator $\mathbf{G}^\perp = [\mathbf{0},\ \mathbf{I}_2]$ the projected matching equation $\mathbf{F}^\nu \nabla H(\mathbf{x}) = \mathbf{f}^\nu(\mathbf{x})$ is obtained. Since $\mathbf{F}^\nu$ is constant, the Proposition 2.2.1 can be used to assess its solvability yielding the condition

$$\nu_{23} + b_1 \sin x_2 \nu_{11} + b_1 x_1 \cos(x_2)\nu_{12} = 0\,, \quad \forall\, \mathbf{x} \in \mathbb{R}^n \tag{5.7}$$

where, for compactness, the elements of $\mathbf{F}^\nu$ have been abbreviated by ν_{ij}. Thus, we have

to choose the parameters in (5.6) such that

$$0 = \nu_{11} = k_{11}k_{12} - j_{12} \tag{5.8a}$$
$$0 = \nu_{12} = k_{12}^2 + k_{22}^2 \tag{5.8b}$$
$$0 = \nu_{23} = k_{13}^2 + k_{23}^2 + k_{33}^2 \ . \tag{5.8c}$$

It is easily seen that this requires $k_{12} = k_{22} = k_{13} = k_{23} = k_{33} = 0$ and $j_{12} = 0$ resulting in[1]

$$\mathbf{J} = \begin{bmatrix} 0 & 0 & j_{13} \\ 0 & 0 & j_{23} \\ -j_{13} & -j_{23} & 0 \end{bmatrix} , \quad \mathbf{R} = \begin{bmatrix} k_{11}^2 & 0 & 0 \\ 0 & 0 & 0 \\ 0 & 0 & 0 \end{bmatrix} . \tag{5.9}$$

Consequently, it is not possible to solve the matching PDE with a strictly positive definite dissipation matrix.

To determine the set of admissible energy functions from the projected matching equation, we straighten out the distribution $\Delta_{F,\nu}$ by means of the coordinate transformation (2.37) with $\mathbf{t}_3 = [1\ 0\ 0]^T$. The particular solution thus obtained is

$$\Psi(\mathbf{x}) = \frac{1}{2j_{23}}x_3^2 - \frac{b_1}{j_{2,3}}\cos(x_2)x_1 + \frac{b_1 j_{13}}{j_{23}^2}\sin(x_2) - \frac{P}{j_{23}}x_2 \ . \tag{5.10}$$

The homogeneous solution is selected as

$$\phi(\xi) = \mu_1\xi + \mu_2\xi^2 \tag{5.11}$$

with the characteristic coordinate

$$\xi = \zeta_1 = x_1 - \frac{j_{13}}{j_{23}}x_2 \ . \tag{5.12}$$

Taking into account that, being an equilibrium of the SMIB model (5.5), the point $\mathbf{x}^*$ satisfies $P - b_1 x_1^* \sin(x_2^*) = 0$, the necessary condition $\nabla H(\mathbf{x})|_{\mathbf{x}^*} = \mathbf{0}$ is met with the choice

$$\mu_1 = \frac{b_1}{j_{23}}\cos(x_2^*) + 2\mu_2\left(\frac{j_{13}}{j_{23}}x_2^* - x_1^*\right) \ . \tag{5.13}$$

The remaining parameters j_{13}, j_{23}, c_{11} and μ_2 have to be selected such that $\nabla^2 H(\mathbf{x})|_{\mathbf{x}^*} > 0$

[1] For another – as far as the definiteness of the dissipation matrix is concerned, considerably more complex – example the reader is referred to [98], where the proposed parametrization has been used to guarantee the positive definiteness of a 4×4 dimensional dissipation matrix.

and such that the requirements regarding transient behavior and size of the DA are satisfied.

5.2.2 Application of LLDA

At first, we apply LLDA in order to specify desired closed loop dynamics and to guarantee a strict local minimum of the energy function at $\mathbf{x}^*$. The eigenvalues of the matrix $\mathbf{A}_d$ in (2.53) are located in -7 by an appropriate choice of $\mathbf{A}^\alpha$. From the system of equations (2.57)–(2.59) we deduce $j_{13} = 1.2119k_{11}^2$, $j_{23} = 0.2606k_{11}^2$, and $\mu_2 = 10.5/k_{11}^2$ leaving k_{11} as free parameter. It turns out, however, that the value of k_{11} can be set arbitrarily as it has no influence on the resulting control law or the estimate of the DA. If we set $k_{11} = 2$, we obtain $j_{13}^{ini} = 4.8475$, $j_{23}^{ini} = 1.0425$ and $\mu_2^{ini} = 2.6250$, i.e., for this particular system no degrees of freedom remain for the optimization of the DA if we assign fixed eigenvalues.

We apply the algorithm from Section 3.3 to determine the critical level value and therewith an estimate of the DA. First, we observe that $H(\mathbf{x})$ can be represented as

$$H(\mathbf{x}) = \frac{1}{2j_{23}}x_3^2 + H_{12}(x_1, x_2) \tag{5.14}$$

i.e., the coordinate x_3 enters the energy function only in the purely quadratic term $\frac{1}{2j_{23}}x_3^2$, where $j_{23} > 0$. Consequently, it suffices to merely consider $H_{12}(x_1, x_2)$ for the computation of the critical level value. Furthermore, we don't have to examine $\dot{H}(\mathbf{x})$ since $\mathbf{R} \geq 0$ is guaranteed by the parametrization of the design matrix (5.6). In order that the equilibrium point is the origin, we introduce the coordinate system $\mathbf{z} = \mathbf{x} - \mathbf{x}^*$.

For the calculation of λ_k^{min} in the second step of the algorithm, the terms $g''_{v,k}(0)$ and $\max_{\xi\in[0,\lambda]}(|g'''_{v,k}(\xi)|)$ are required (c.f. (3.10)). The calculation of the former is straightforward. An upper bound for the max-term can be determined similar to Example 3.3.1. After the coordinate shift the energy function contains sine and cosine terms which depend on the argument $z_2 + x_2^*$, where $x_2^* = 0.8945$. Thus we apply the addition theorems for trigonometric functions to express the function $g'''_{v,k}(\lambda)$ as

$$\begin{aligned} g'''_{v,k}(\lambda) = {} & \frac{v_{k,2}^2 v_{k,1}}{j_{23}}\left(64.4\cos(\lambda v_{k,2}) - 80.2\sin(\lambda v_{k,2})\right) \\ & - \frac{v_{k,2}^3}{j_{23}}\left(22.6\sin(\lambda v_{k,2}) + 28.2\cos(\lambda v_{k,2})\right) + \frac{v_{k,2}^3 v_{k,1}\lambda}{j_{23}}\left(26.7\cos(\lambda v_{k,2}) - 21.5\sin(\lambda v_{k,2})\right) \\ & + \frac{j_{13}v_{2,k}^3}{j_{23}^2}\left(26.7\sin(\lambda v_{k,2}) - 21.5\cos(\lambda v_{k,2})\right). \end{aligned}$$

Then, as in Example 3.3.1, we use the relations in (3.13) to derive the upper bound

$$\begin{aligned}\max_{\xi\in[0,\lambda]}\left(\left|g'''_{v,k}(\xi)\right|\right) \leq\ & 64.4\left|\frac{{v_{k,2}}^2 v_{k,1}}{j_{23}}\right| + 80.2\left|\frac{{v_{k,2}}^2 v_{k,1}\sin(\lambda v_{k,2})}{j_{23}}\right| + 21.5\left|\frac{{v_{k,2}}^3\lambda v_{k,1}\sin(\lambda v_{k,2})}{j_{23}}\right| \\ & + 22.6\left|\frac{{v_{k,2}}^3\sin(\lambda v_{k,2})}{j_{23}}\right| + 26.7\left|\frac{{v_{k,2}}^3\lambda v_{k,1}}{j_{23}}\right| + 28.2\left|\frac{{v_{k,2}}^3}{j_{23}}\right| \\ & + 21.5\left|\frac{j_{13}{v_{k,2}}^3}{{j_{23}}^2}\right| + 26.7\left|\frac{j_{13}{v_{k,2}}^3\sin(\lambda v_{k,2})}{{j_{23}}^2}\right|\end{aligned}$$

for $|\lambda v_{k,2}| < \frac{\pi}{2}$ and

$$\max_{\xi\in[0,\lambda]}\left(\left|g'''_{v,k}(\xi)\right|\right) \leq 144.6\left|\frac{{v_{k,2}}^2 v_{k,1}}{j_{23}}\right| + 48.2\left|\frac{{v_{k,2}}^3\lambda v_{k,1}}{j_{23}}\right| + 50.9\left|\frac{{v_{k,2}}^3}{j_{23}}\right| + 48.2\left|\frac{j_{13}{v_{k,2}}^3}{{j_{23}}^2}\right|$$

for $|\lambda v_{k,2}| \geq \frac{\pi}{2}$.

As one-dimensional root-finding technique, again the Illinois algorithm is employed. Moreover, we choose $R = 2$, $\epsilon_c = 0.01$, $\Delta\lambda^{max} = 0.02$, and $\Delta\lambda^{min} = \frac{1}{5}\Delta\lambda^{max} = 4\cdot 10^{-3}$. The number of grid points K_1 is set to 200. We apply the interior-point algorithm provided by the MATLAB function `fmincon` to solve the optimization problems (3.17), (3.18) and provide the solver with analytic expressions for the gradients. The level value $\hat{d}$ is 0.0142, the corresponding level set, which is the estimated stability boundary, is depicted in Figure 5.3(a). The volume of the estimated DA is calculated as described in Section 4.2 and amounts to $V_{\hat{d}}^{ini} = 0.0669$. We remark that the chosen grid is so fine that the optimization at the end is actually unnecessary. It changes the result only from the 7th decimal place on.

Since the dissipation matrix is only positive semidefinite, we invoke the Krasovskii-LaSalle Theorem to establish asymptotic stability of $\mathbf{x}^*$. This has already been done in [60]. However, in this analysis it is assumed that b_2 is a positive parameter, although it is later set to zero. If we take into account that $b_2 = 0$, it becomes more elaborate to show that no trajectory can stay identically in $\{\mathbf{x} \in \overline{\mathrm{S}}_{\hat{d}}(\mathbf{x}^*) | \dot{H}(\mathbf{x}) = 0\}$ except for $\mathbf{x}^*$. For convenience, the analysis in the following is conducted in $\mathbf{x}$ coordinates, and we assume for obvious reasons that $k_{11} \neq 0$.

It follows from

$$0 = \dot{H}(\mathbf{x}) = \left(\frac{\partial H}{\partial \mathbf{x}}\right)^T \mathbf{R}\frac{\partial H}{\partial \mathbf{x}} = k_{11}^2\left(\frac{\partial H}{\partial x_1}\right)^2 \tag{5.15}$$

that along any trajectory $\mathbf{x}(t)$ that belongs identically to the set $\{\mathbf{x} \in \overline{\mathrm{S}}_{\hat{d}}(\mathbf{x}^*) | \dot{H}(\mathbf{x}) = 0\}$ it

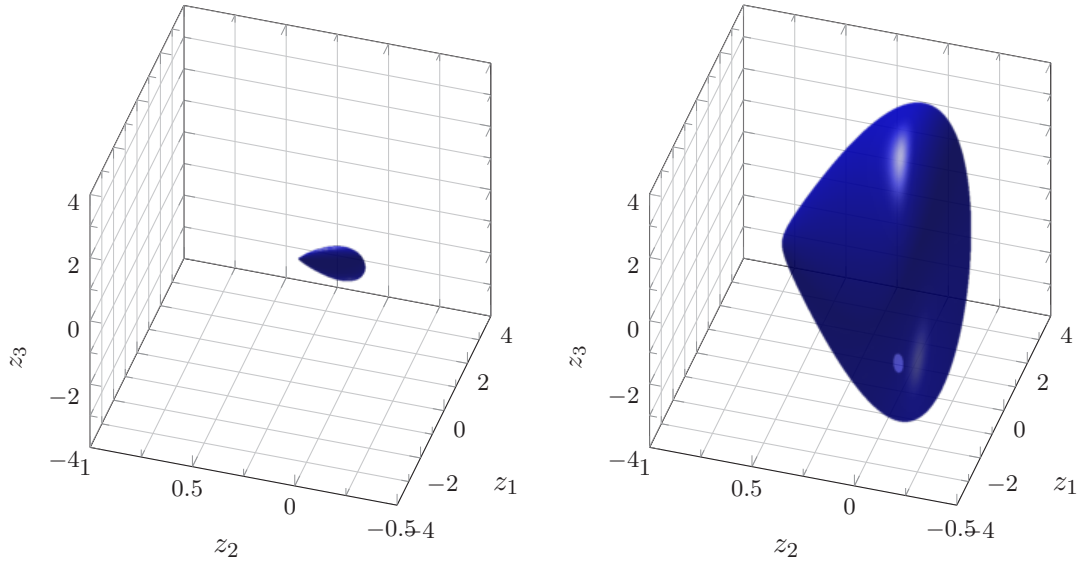

(a) Initial controller with LLDA. (b) Optimized controller.

Figure 5.3: Estimated stability boundary for (a) the initial IDA controller parametrized by LLDA and (b) the controller resulting from the optimization.

must hold that $a(\mathbf{x}) = \frac{\partial H}{\partial x_1} \equiv 0$. Substituting this into the closed loop dynamics yields

$$\dot{x}_1 = j_{13}\frac{\partial H}{x_3} = \frac{j_{13}}{j_{23}}x_3 \tag{5.16a}$$

$$\dot{x}_2 = j_{23}\frac{\partial H}{\partial x_3} = x_3 \tag{5.16b}$$

$$\dot{x}_3 = -\,j_{23}\frac{\partial H}{\partial x_2}\,. \tag{5.16c}$$

It follows from $a(\mathbf{x}) \equiv 0$ that also

$$\dot{a}(\mathbf{x}) = \frac{b_1}{j_{23}}\sin(x_2)x_3 \equiv 0 \tag{5.17}$$

$$\ddot{a}(\mathbf{x}) = \frac{b_1}{j_{23}}\cos(x_2)x_3^2 - b_1\sin(x_2)\frac{\partial H}{\partial x_2} \equiv 0\,. \tag{5.18}$$

At first, our objective is to show that $x_3 \equiv 0$ has to be satisfied along any trajectory $\mathbf{x}(t)$ that satisfies $a(\mathbf{x}(t)) \equiv 0$. It can be seen from (5.17) that for any point of such a trajectory either $\sin(x_2) = 0$ or $x_3 = 0$ must be fulfilled. Now assume that $x_3 \neq 0$ at some point. Then, $\sin(x_2) = 0$ must hold. Substituting this into (5.18) it follows immediately that this implies also $x_3 = 0$. Hence, we conclude that $x_3(t) \equiv 0$. Since $\frac{\partial H}{\partial x_3} = \frac{1}{j_{23}}x_3$ this implies that $\frac{\partial H}{x_3} \equiv 0$.

Another implication is that $\dot{x}_3 \equiv 0$ and thus it follows from (5.16c) that $\frac{\partial H}{\partial x_2} \equiv 0$. Summarizing, we have shown that any trajectory that stays identically in $\{\mathbf{x} \in \overline{\mathrm{S}}_{\hat{d}}(\mathbf{x}^*) | \dot{H}(\mathbf{x}) = 0\}$ satisfies $\nabla H(\mathbf{x}(t)) = 0$. Since $\mathbf{x}^*$ is the only critical point contained in the positively invariant sublevel set $\overline{\mathrm{S}}_{\hat{d}}(\mathbf{x}^*)$ any trajectory starting within this set converges to $\mathbf{x}^*$.

5.2.3 Maximization of the DA

Now the proposed optimization is conducted. Since all controller parameters are set, if the eigenvalues of the closed loop linearization are fixed, the constrained optimization problem (4.20) is solved. It holds for any $c \in \mathbb{R}$ that $H(\mathbf{x}, cj_{13}, cj_{23}, \mu_2/c) = 1/c\, H(\mathbf{x}, j_{13}, j_{23}, \mu_2)$ and $\mathbf{F}(cj_{13}, cj_{23}, \sqrt{c}\, k_{11}) = c\, \mathbf{F}(j_{13}, j_{23}, k_{11})$ (with obvious abuse of notation) and hence, without loss of generality, we can fix j_{23} as $j_{23} = 10$. Consequently, the vector of design variables is $\boldsymbol{\gamma} = [j_{13}, \mu_2, k_{11}]^T$. The admissible region for the eigenvalues is specified by $r_{max} = -1$, $r_{min} = -20$ and $\psi = \frac{\pi}{4}$ (see Figure 4.3). To determine the critical level value, we again employ the algorithm from Section 3.3 with all parameters as given above except for the radius R, which is increased to $R = 4$.

First, we apply a genetic optimization algorithm provided by MATLAB (`ga`) with 350 individuals and the maximum number of generations set to 25. After the genetic algorithm terminates, the optimization is continued using `fmincon`. By this means, we obtain the controller parameters $j_{13}^{opt} = 262$, $\mu_2^{opt} = 5.95 \cdot 10^{-2}$, and $k_{11}^{opt} = 18.7$. The corresponding estimate of the DA is shown in Figure 5.3(b). Its volume is $V_{\hat{d}}^{opt} = 22.92$ and hence 342 times the volume $V_{\hat{d}}^{ini}$ before the optimization. The corresponding closed loop linearizion has one real eigenvalue in -16.4 and a conjugate complex eigenvalue pair in $-12.6 \pm 12.2i$. In Figure 5.4, the transient response curves of the states z_1 and z_2 (the deviations of the internal voltage and the load angle from their stationary values) are shown for both controller parametrizations – the initial one determined by means of LLDA and the one obtained from the optimization. The initial value is $\mathbf{z}(0) = [-0.1, 0.1, -0.2]^T$ and has been chosen such that it is contained in the estimated DA of both closed loop systems. It can be seen that the optimized controller achieves a faster and still sufficiently damped system response. We remark that, not surprisingly, the control effort of the optimized controller is higher than that of the initial one.

5.2.4 Comparison with a Benchmark Controller

Galaz *et al.* [60], [61] also have designed an IDA controller for the synchronous generator (5.5) with the objective to enlarge the DA and to increase by this means the critical clearing time. To this end, they first transform the SMIB model into pH form and, based

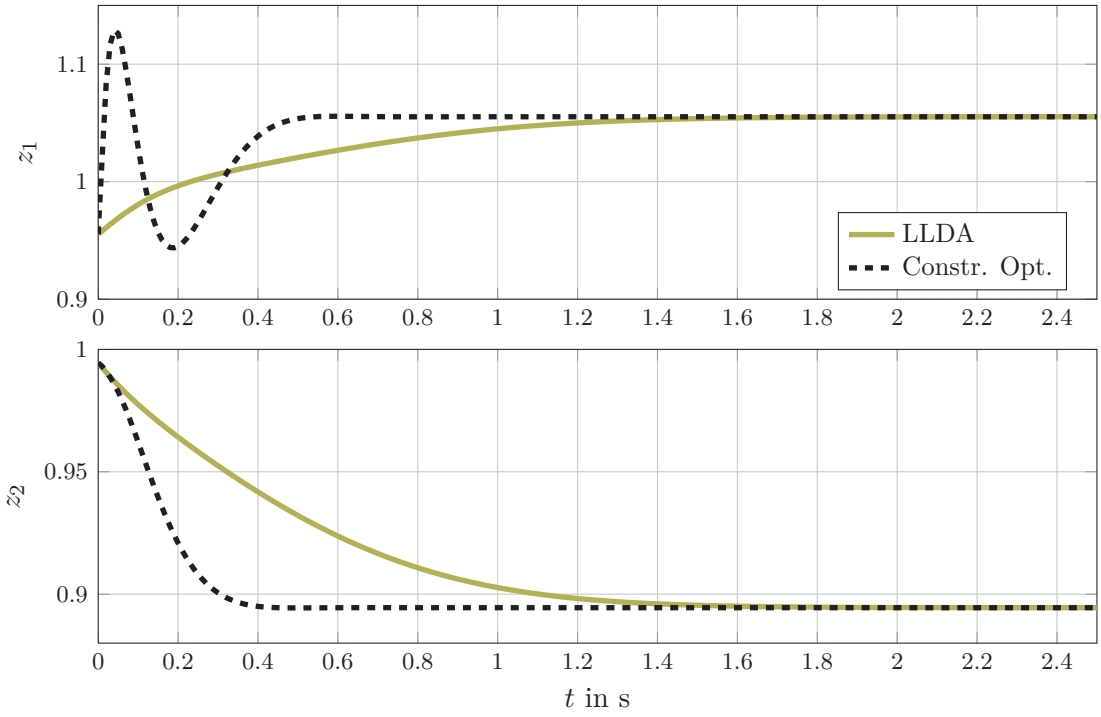

Figure 5.4: Transient responses for the initial controller (LLDA) and the controller obtained from the constrained optimization problem.

on that, deduce a physically motivated IDA controller. As mentioned in Section 1.3.1, the authors exploit that the sublevel sets of a strongly convex function are bounded, i.e., they determine a controller parametrization such that $\nabla^2 H(\mathbf{x}) > \epsilon \mathbf{I}$ holds for some $\epsilon > 0$ and all $\mathbf{x}$ within a certain region around $\mathbf{x}^*$. Then the largest sublevel set which is entirely contained in this region is an estimate of the DA. However, neither is the corresponding level value explicitly known nor is it possible to conclude that the DA of the closed loop system contains the DA of the open loop system (see Remark 3 in [61]).

In order to demonstrate the effectiveness of the methods proposed in this thesis, we compare our results with those achieved in [60], [61]. In these works, three differently tuned IDA controllers are applied to the SMIB model under consideration. The estimated DA is, however, for all three parameterizations identical since they only differ in the damping injection term, that is denoted by k_v and does not influence the energy function. From the three controllers we have taken the one[2] with $k_v = 0.07$ as it achieves the best transient behavior. If we choose $j_{13}^{bm} = 10.761$, $j_{23}^{bm} = 13.451$, $\mu_2^{bm} = 2.858$ and $k_{11}^{bm} = 1$, the control law derived above is identical to this controller. The volume of the corresponding estimate of the DA is $V_{\hat{d}}^{bm} = 26.14$ and is thus slightly larger than the value $V_{\hat{d}}^{opt}$ achieved in the

[2]The values of the two remaining parameters are $\alpha_1 = -0.8$ and $\alpha_2 = 76.88$. They are given here because they cannot be found in the paper [61] but only in the thesis [60].

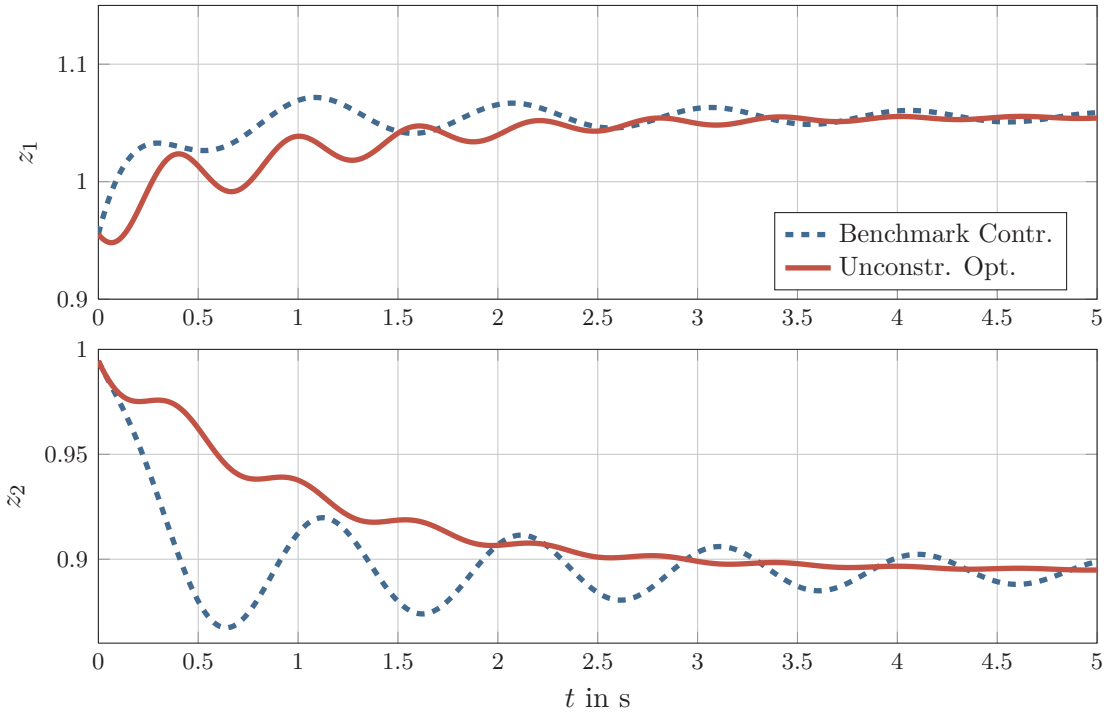

Figure 5.5: Comparison of the controller from [61] and the controller obtained from the unconstrained optimization in terms of the transient behavior.

previous subsection. If we have a look at the eigenvalues of the linearization, however, we find that aside a real eigenvalue at -4.94 there is a complex eigenvalue pair located at $-0.39 \pm 6.33i$. Obviously, the oscillation that corresponds to this pair is very weakly damped, which also becomes apparent in the time response curves shown in Figure 5.5.

Therefore, we repeat the optimization of the DA without the constraints (4.20b), (4.20c), i.e., without specifying desired dynamic behavior. In this case, the vector of design variables $\boldsymbol{\gamma}$ consists only of j_{13} and μ_2 because the energy function is not affected by k_{11} and hence neither is the estimated DA. To solve the optimization problem, we again employ the genetic algorithm provided by the MATLAB function `ga` with 250 individuals and a maximum number of 30 generations. This yields the parameter values $j_{13}^{opt,2} = 32.55$ and $\mu_2^{opt,2} = 0.5564$. The estimated DA is depicted in Figure 5.6(a) and has a volume of $V_{\hat{d}}^{opt,2} = 73.27$. It is thus almost 3 times as big as the estimated DA that corresponds to the controller parametrization from [60], [61]. A comparison of both estimates in the z_1-z_2-plane is shown in Figure 5.6(b). The value of $k_{11}^{opt,2}$ is set to 1.5. The eigenvalues of the closed loop linearization are then located in -14.09 and $-1.86 \pm 7.35i$. In Figure 5.5, the time response curves of z_1 and z_2 are depicted for both closed loop systems and $\mathbf{z}(0) = [-0.1, 0.1, -0.2]^T$. It can be seen that the controller which results from the

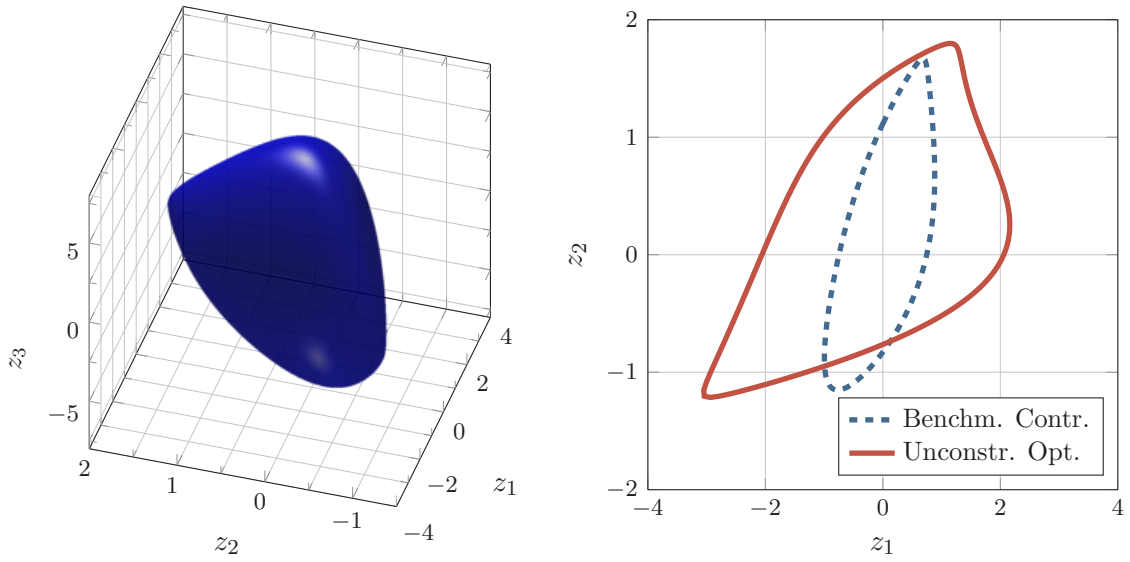

(a) Estimated stability boundary.

(b) Comparison in the z_1-z_2-plane.

Figure 5.6: Estimated DA for the controller that results from the unconstrained optimization (a) and comparison with the estimated DA achieved with the controller from [61] (b).

optimization achieves a much less oscillating system response. The control effort of the two controllers is very similar.

Recall that, in the context of power systems, the primary objective, which motivated the maximization of the DA, was to increase the critical clearing time. Therefore, we compare the controller obtained from the latest optimization with that from [60], [61] also in terms of this security measure. Like in Section 6.1 of [61], we consider a short circuit that results from connecting the machine's terminal to ground via a small impedance. After the clearing time the short circuit is removed. As in [61] and [10], the critical clearing time is determined by simulating short circuits with increasing clearing time. For the controller from [61], the critical clearing time is found to be 220ms, which matches the value given in the paper, whereas for the optimized controller determined above the critical clearing time is 310 ms.

5.2.5 Application of Algorithm 2

For the purpose of illustration, we finally apply the algorithm from Section 3.4 to determine an estimate of the DA. The controller parameters are set to $j_{13}^{bm} = 10.761$, $j_{23}^{bm} = 13.451$, $\mu_2^{bm} = 2.858$ and $k_{11}^{bm} = 1$, which corresponds to the controller from [61]. The function $\gamma(r)$ is determined similar to Example 3.4.1. Its positive root is $r_{min} = 0.41$, which yields $\mathrm{D}_{min} = \{\mathbf{x} : |x_i| < 0.29,\ i = 1, 2\}$. The rectangle D_{max} is chosen as $\mathrm{D}_{max} = \{\mathbf{x} : |x_i| \leq$

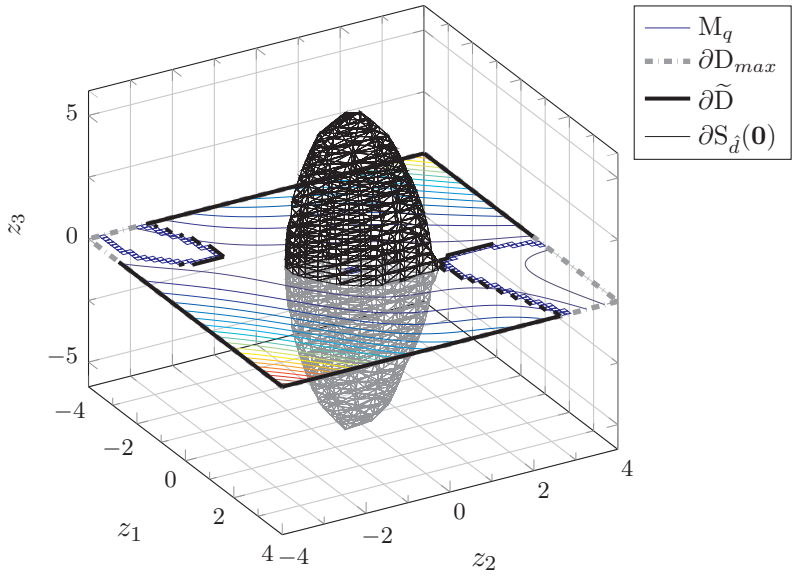

Figure 5.7: Estimating the DA with Algorithm 2.

4, $i = 1, 2\}$ and δ_{min} is set to $0.2 < r_{min}/\sqrt{2} = 0.29$. The result is depicted in Figure 5.7, where the piecewise linear approach from [69] has been used to approximate $\partial\mathrm{S}_{\hat{d}}(\mathbf{0})$. The obtained level value is $\hat{d} = \tilde{c} = 0.0438$. It is slightly smaller than the value computed above with Algorithm 1, which has been 0.0443. One reason for this is that the minimum of $H(\mathbf{x})$ on $\partial\widetilde{\mathrm{D}}$ is calculated by means of the inequality (2.85) (2.86b) and thus is actually a lower bound.

5.3 Trajectory Tracking Control of a Magnetic Levitation System

This section deals with the trajectory tracking control of a levitated ball, in particular with the estimation and the maximization of the DA of the time-varying error system. The lab setup is depicted in Figure 5.8 (left), a schematic diagram is shown in Figure 5.8 (right). The system essentially consists of an iron object in the magnetic field generated by an electromagnet and a laser sensor, that allows to determine the distance s. The mathematical model of the plant is given by [102]

$$\begin{bmatrix} \dot{x}_1 \\ \dot{x}_2 \\ \dot{x}_3 \end{bmatrix} = \begin{bmatrix} -\frac{R}{L(x_2)} x_1 \\ \frac{x_3}{m} \\ \frac{1}{2} \frac{L'(x_2)}{L^2(x_2) x_1^2 + mg} \end{bmatrix} + \begin{bmatrix} 1 \\ 0 \\ 0 \end{bmatrix} u \tag{5.19}$$

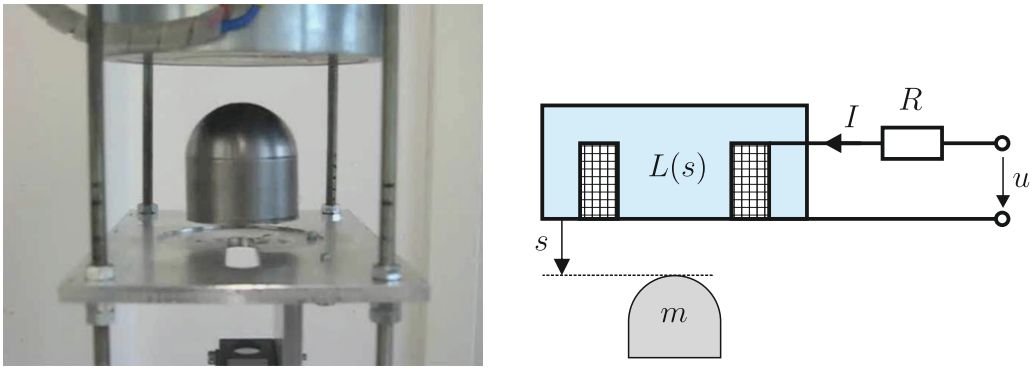

Figure 5.8: Magnetic levitation system: lab setup (left) and schematic diagram (right).

Table 5.2: Parameters of the magnetic levitation system [102].

Model parameter	Symbol	Value	Unit
Mass of the ball	m	$91.8 \cdot 10^{-3}$	kg
Inductance of the magnet	L_{inf}	$62.8 \cdot 10^{-3}$	H
Parameter of the inductance model	a	$9.89 \cdot 10^{-5}$	H
Parameter of the inductance model	b	$4.97 \cdot 10^{-3}$	H
Resistance of the magnet	R	2.19	Ω

where x_1 is the magnetic flux, $x_2 = s$ the distance of the ball from the magnet, $x_3 = m\dot{s}$ the momentum of the ball, and the control input u is the voltage at the coil. The inductance is approximated by

$$L(x_2) = L_\infty + \frac{a}{b + x_2} = \frac{a}{c}\frac{b + c + x_2}{b + x_2}\,, \quad c = \frac{a}{L_\infty} \tag{5.20}$$

and we have used the abbreviation $L'(x_2) = \frac{\partial L(x_2)}{\partial x_2}$ in (5.19). The model parameters are given in Table 5.2.

The control objective is to levitate the ball such that its position $x_2 = s$, that we define as output of the system $y = x_2$, (asymptotically) tracks a desired periodic trajectory given by

$$y_d(t) = C_1 + C_2 \sin(\omega t) \tag{5.21}$$

with $C_1 = 10\,\text{mm}$, $C_2 = 5\,\text{mm}$ and $\omega = 6\,\frac{1}{\text{s}}$. In order to solve this problem, in [101], [102] a two-degree-of-freedom control scheme is applied (see Section 2.3.2). Using that $y = x_2$ is a

flat output it is straightforward to derive a suitable feedforward control

$$u_d(t) = \sqrt{2am(g-\ddot{y}(t))}\left(\frac{\dot{y}_d(t)}{c} + \frac{R}{a}(b+y_d(t))\right) - \frac{am(b+c+y_d(t))\dddot{y}_d(t)}{c\sqrt{2am(g-\ddot{y}_d(t))}} \tag{5.22}$$

and corresponding trajectories of the state variables

$$\begin{aligned} x_{d,1}(t) &= \frac{1}{c}\sqrt{2am(g-\ddot{y}_d(t))}(b+c+y_d(t)) \\ x_{d,2}(t) &= y_d(t) \\ x_{d,3}(t) &= m\dot{y}_d(t)\ . \end{aligned} \tag{5.23}$$

After the input transformation $u = u_d(t)+v$ the dynamics of the tracking error $\mathbf{e} = \mathbf{x}-\mathbf{x}_d(t)$ are given by

$$\dot{\mathbf{e}} = \begin{bmatrix} -R\frac{c}{a}\left(\frac{\beta(e_2,t)}{\gamma(e_2,t)}(x_{d,1}(t)+e_1) - \frac{\beta(0,t}{\gamma(0,t)}x_{d,1}(t)\right) \\ \frac{e_3}{m} \\ -\frac{c^2}{2a}\left(\frac{(x_{d,1}(t)+e_1)^2}{\gamma^2(e_2,t)} - \frac{x_{d,1}^2(t)}{\gamma^2(0,t)}\right) \end{bmatrix} + \begin{bmatrix} 1 \\ 0 \\ 0 \end{bmatrix} v \tag{5.24}$$

with the abbreviations

$$\begin{aligned} \beta(e_2,t) &= b + x_{d,2}(t) + e_2 \\ \gamma(e_2,t) &= \beta(e_2,t) + c\ . \end{aligned} \tag{5.25}$$

In order to asymptotically stabilize $\mathbf{e}^* = \mathbf{0}$ and achieve desired closed loop dynamics, in [101], [102] an IDA controller has been designed and parametrized by means of LLDA (see Section 2.3.2). The derivation is briefly summarized below. A subtle choice of $\mathbf{F}(\mathbf{e},t)$ makes it possible to achieve both solvability of the matching PDE and (local) positive definiteness of the dissipation matrix. The design matrix can be represented as

$$\mathbf{F}(\mathbf{e},t) = \begin{bmatrix} 1 & 0 & 0 \\ 0 & \frac{\hat{\nu}_{23}\gamma^2(0,t)}{2m\hat{\nu}_{12}x_{d,1}(t)(\gamma(0,t)+e_2)} & 0 \\ 0 & 0 & \frac{c^2}{2a\gamma^2(e_2,t)} \end{bmatrix} \underbrace{\begin{bmatrix} \hat{\alpha}_{11} & \hat{\alpha}_{12} & \hat{\alpha}_{13} \\ 0 & \hat{\nu}_{12} & \hat{\nu}_{13} \\ \hat{\nu}_{21} & 0 & \hat{\nu}_{23} \end{bmatrix}}_{\hat{\mathbf{F}}(t)} \tag{5.26}$$

where the time argument has been omitted for the elements of $\hat{\mathbf{F}}(t)$. The corresponding energy function $H(\mathbf{e},t) = \Psi(\mathbf{e},t) + \phi(\xi)$ consists of the particular solution

$$\Psi(\mathbf{e},t) = \frac{1}{2}\mathbf{e}^T\mathbf{Q}^\Psi(t)\mathbf{e} - \frac{1}{3\hat{\nu}_{21}}e_1^3 + \frac{x_{d,1}^2(t)}{\hat{\nu}_{23}\gamma^2(0,t)}\left(e_2^2e_3 - \frac{\hat{\nu}_{13}}{3\hat{\nu}_{12}}e_2^3\right) \tag{5.27}$$

where

$$\mathbf{Q}^{\Psi}(t) = 2\begin{bmatrix} -\frac{x_{d,1}(t)}{\hat{\nu}_{21}} & 0 & \\ 0 & -\frac{\hat{\nu}_{13}x_{d,1}^2(t)}{\hat{\nu}_{12}\hat{\nu}_{23}\gamma(0,t)} & \frac{x_{d,1}^2(t)}{\hat{\nu}_{23}\gamma(0,t)} \\ 0 & \frac{x_{d,1}^2(t)}{\hat{\nu}_{23}\gamma(0,t)} & 0 \end{bmatrix} \tag{5.28}$$

and the homogeneous solution $\phi(\xi) = \frac{1}{2}\mu_2\xi^2$, where the characteristic coordinate is given by

$$\xi = \begin{bmatrix} 1 & 0 & 0 \end{bmatrix} \hat{\mathbf{F}}^{-T}(t)\mathbf{e} \, . \tag{5.29}$$

In order to simplify the dissipation matrix, the choices

$$\hat{\alpha}_{12} = 0 \, , \quad \hat{\nu}_{21} = -\frac{2a}{c^2}\gamma^2(0,t)\hat{\alpha}_{13} \tag{5.30}$$

are made. Moreover, the application of LLDA yields

$$\hat{\alpha}_{13} = \frac{c^2}{2a}\frac{a_{\alpha,13}\hat{\nu}_{23} + 2\hat{\alpha}_{11}x_{d,1}(t)}{a_{\alpha,11}\gamma^2(0,t)} \, , \quad \hat{\nu}_{13} = \frac{-a_{\alpha,12}\hat{\nu}_{12}}{a_{\alpha,13}} + \frac{2\hat{\nu}_{12}}{a_{\alpha,13}\hat{\nu}_{23}}\frac{\hat{\alpha}_{13}x_{d,1}^2(t)}{\gamma(0,t)} \tag{5.31}$$

$$\mu_2 = a_{\alpha,11}\hat{\alpha}_{11} + a_{\alpha,13}\hat{\alpha}_{13} - \frac{c^2}{a}\frac{\hat{\alpha}_{11}^2 x_{d,1}(t)}{\hat{\alpha}_{13}\gamma^2(0,t)} \, . \tag{5.32}$$

The entries $a_{\alpha,1i}$, $i = 1,2,3$ of $\mathbf{A}^{\alpha}$ are determined such that the eigenvalues of $\bar{\mathbf{A}}_d = [(\mathbf{A}^{\alpha})^T \ (\bar{\mathbf{A}}^{\nu})^T]^T$ are located in -50, where $\bar{\mathbf{A}}^{\nu}$ is obtained by evaluating the unactuated part of the linearization of (5.24) at an average point $\bar{\mathbf{x}}_d$ of the desired state trajectory $\mathbf{x}_d(t)$, which corresponds to the steady component C_1 of $y_d(t)$. The resulting values are $a_{\alpha,11} = 150$, $a_{\alpha,12} = 2164.55$, and $a_{\alpha,12} = 676.19$.

With the choices made for the parameters above, $\hat{\nu}_{12}$ disappears from both the design matrix and the energy function. Thus, $\hat{\alpha}_{11}$ and $\hat{\nu}_{23}$ remain as free parameters, which are to be chosen such that $H(\mathbf{e},t)$ qualifies as a Lyapunov function and, what is more, the estimated DA of $\mathbf{e}^* = \mathbf{0}$ is as large as possible. In [101], the values of these two parameters have been determined by a heuristic approach (see [177] for details): First, a genetic optimization algorithm is used to maximize the smallest eigenvalue of $\mathbf{R}(\mathbf{0},t)$ in the (discretized) interval $[0,T]$, where $T = \frac{\pi}{3}$ is the period of $y_d(t)$, in order to achieve $\mathbf{R}(\mathbf{0},t) > 0$, $\forall\, t$. It turns out, however, that the resulting dissipation matrix becomes indefinite already for very small values of e_2. Therefore, the optimization is repeated with the eigenvalues of $\mathbf{R}(\mathbf{e},t)$ not only evaluated at the origin but also at 4 other points of the form $[0 \ \bar{e}_2 \ 0]^T$. In this way, a notable enlargement of the estimated DA is achieved. The obtained parameter values are $\hat{\alpha}_{11}^{ini} = -1\cdot 10^6$ and $\hat{\nu}_{23}^{ini} = -500$. As mentioned already in Section 3.3.2, the computation of the functions $W_i(\mathbf{x})$, $i = 1,2,3$ is done in a way very similar to that used in this thesis. In

order to determine the largest suitable sublevel set of $W_1(\mathbf{e})$ in [101], [177] the Ridge method is applied, which, as discussed in Section 1.3.1, is in general not applicable for this task.

We apply the algorithm presented in Section 3.3 to estimate the DA of $\mathbf{e}^* = \mathbf{0}$ for $\hat{\alpha}_{11} = \hat{\alpha}_{11}^{ini}$ and $\hat{\nu}_{23} = \hat{\nu}_{23}^{ini}$. For convenience, we convert the components e_2 and e_3 in mm and $\frac{\text{mm}}{\text{s}}$, respectively. Furthermore, considering the values of x_1 that are necessary to levitate the ball at a position x_2, we scale e_1 for the computation by a factor 100 in order that it is approximately in the same magnitude as e_2 and e_3. The parameters of Algorithm 3.2 are chosen as follows: $R = 25$, $\epsilon_c = 0.05$, $\Delta\lambda = 0.5$, $K_1 = 100$ and $K_2 = 50$.

A closer examination reveals that the energy function $H(\mathbf{e}, t)$ only depends on $x_{d,1}(t)$ and $x_{d,2}(t)$ but not on $x_{d,3}(t)$. From (5.23) we observe that $x_{d,2}(t) = y_d(t)$ and that $x_{d,1}(t)$ is a function of $y_d(t)$ and $\ddot{y}_d(t) = -C_2 \sin(\omega t)\omega^2$ only. Hence, the time t enters into $H(\mathbf{e}, t)$ only via the function $\sin(\omega t)$ and, consequently, for the computation of $W_1(\mathbf{e})$ and $W_2(\mathbf{e})$ according to (3.23) only two subintervals of $[0, T]$ need to be discretized, e.g. $[0, \frac{T}{4}]$ and $[\frac{T}{2}, \frac{3T}{4}]$. The derivative of the energy function $\dot{H}(\mathbf{e}, t)$ contains both sine and cosine terms, and thus the whole interval $[0, T]$ must be considered to determine $W_3(\mathbf{e})$. The number of points N_T in $\mathcal{T}$ is set to 60, and accordingly the two subintervals $[0, \frac{T}{4}]$ and $[\frac{T}{2}, \frac{3T}{4}]$ are each discretized with 15 points.

As a consequence, computing $W_3(\mathbf{e})$ is twice as expensive as computing $W_1(\mathbf{e})$. Therefore, some adjustments are made to the algorithm described in Section 3.3. Instead of computing directly the discrete approximation of $\rho_{\bar{E}}(\mathbf{v})$, we determine in a first step $\rho_{\bar{D}}(\mathbf{v})$ and the minimum value of $W_1(\mathbf{e})$ over $\partial\mathrm{D}$, say $\tilde{d}$. To this end, we don't have to evaluate $W_3(\mathbf{e})$. Then a discrete representation of the level set $\partial\mathrm{S}_{\tilde{d}}^{W_1}(\mathbf{0})$ is computed as described in Section 4.2, which means that its radial function $\rho_{S,\tilde{d}}(\mathbf{v})$ is numerically approximated. In a second step, we determine the radial function of the set $\bar{\mathrm{E}} \cap \bar{\mathrm{S}}_{\tilde{d}}^{W_1}(\mathbf{0})$ and the minimum value of $W_1(\mathbf{e})$ over its boundary, which clearly is equal to the critical level value. To do so, we proceed in the same way as described in Algorithm 3.2 only that we do not consider $g_v(\lambda)$ and that we restrict the search to $\mathrm{S}_{\tilde{d}}^{W_1}(\mathbf{0})$ instead to the ball B_R. For the line search the intervals $[0, \rho_{S,\tilde{d}}(\mathbf{v}_k)]$ are discretized with

$$L_k = \left\lceil \rho_{S,\tilde{d}}(\mathbf{v}_k)/\Delta\lambda \right\rceil \tag{5.33}$$

points. This procedure yields of course the same critical level value as Algorithm 3.2, but has proven to be somewhat faster for this particular case, because $W_3(\mathbf{e})$ has to be evaluated only within $\mathrm{S}_{\tilde{d}}^{W_1}(\mathbf{0})$. For $\hat{\alpha}_{11} = \hat{\alpha}_{11}^{ini}$, and $\hat{\nu}_{23} = \hat{\nu}_{23}^{ini}$, the computed level value $\hat{d} = 0.6327$ and the corresponding volume of $\mathrm{S}_{\hat{d}}^{W_2}(\mathbf{0})$ is $V_{\hat{d}}^{ini} = 4.42\,\mathrm{Vmm}^2$. The gradients of $W_1(\mathbf{e})$ and $W_3(\mathbf{e})$, which are needed for the numerical approximation of $\partial\mathrm{S}_{\tilde{d}}^{W_1}(\mathbf{0})$ and $\partial\mathrm{S}_{\hat{d}}^{W_3}(\mathbf{0})$, have been computed using a forward difference approximation [129].

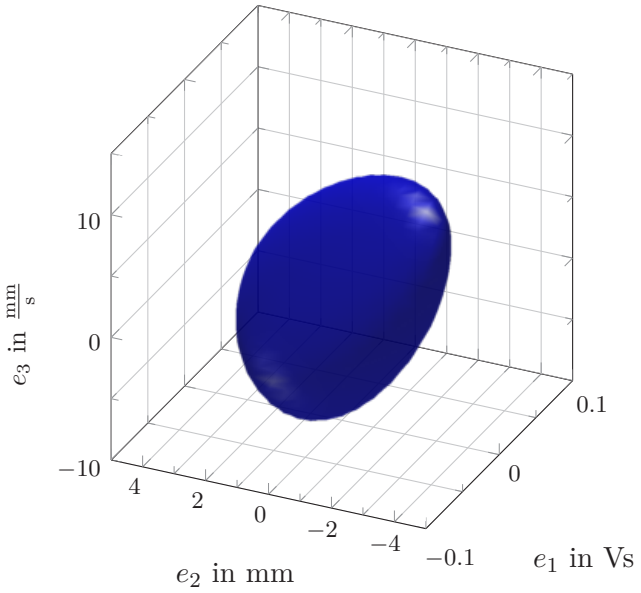

Figure 5.9: DA of $\mathbf{e}^* = \mathbf{0}$ with the optimized error controller.

In order to enlarge the estimated DA, we apply the optimization approach proposed in Section 4.3. Since LLDA has already been accomplished, we solve the unconstrained maximization problem (4.19) with $\boldsymbol{\gamma} = [\hat{\alpha}_{11}\ \hat{\nu}_{23}]^T$. We apply the simplex search method `fminsearch`, which is provided by MATLAB, and use $\hat{\alpha}_{11}^{ini}$ and $\hat{\nu}_{23}^{ini}$ as initial values. The result is $\hat{\alpha}_{11}^{opt} = -1.13 \cdot 10^6$ and $\hat{\nu}_{23}^{opt} = -443$. The estimated DA is depicted in Figure 5.9 and has a volume of $V_{\hat{d}}^{opt} = 5.59\,\text{Vmm}^2$, which is an improvement of 26.5% as compared to the initial parametrization. We remark that also by means of the genetic algorithm `ga` no better results could be obtained. Recall, however, that the initial parametrization was already the result of a heuristic optimization conducted in [101], [177].

The control law resulting from the choice $\hat{\alpha}_{11} = \hat{\alpha}_{11}^{opt}$ and $\hat{\nu}_{23} = \hat{\nu}_{23}^{opt}$ has been implemented at the lab setup and compared to the initial controller. In Figure 5.10, the measurement results are shown for both controllers. Repeated disturbances, realized by short voltage pulses, drive the ball away from the desired reference trajectory. While the optimized controller achieves a larger (estimated) DA than the initial one, it can be seen that the dynamic behavior of the two controller is very similar and that both of them are able to compensate errors in a fast way.

5.4 Concluding Remarks

In this chapter, we have demonstrated by means of three examples how the methods presented in the Chapters 3 and 4 can be applied to systematically design IDA controllers for nonlinear systems and to effectively estimate and enlarge the DA of the closed loop

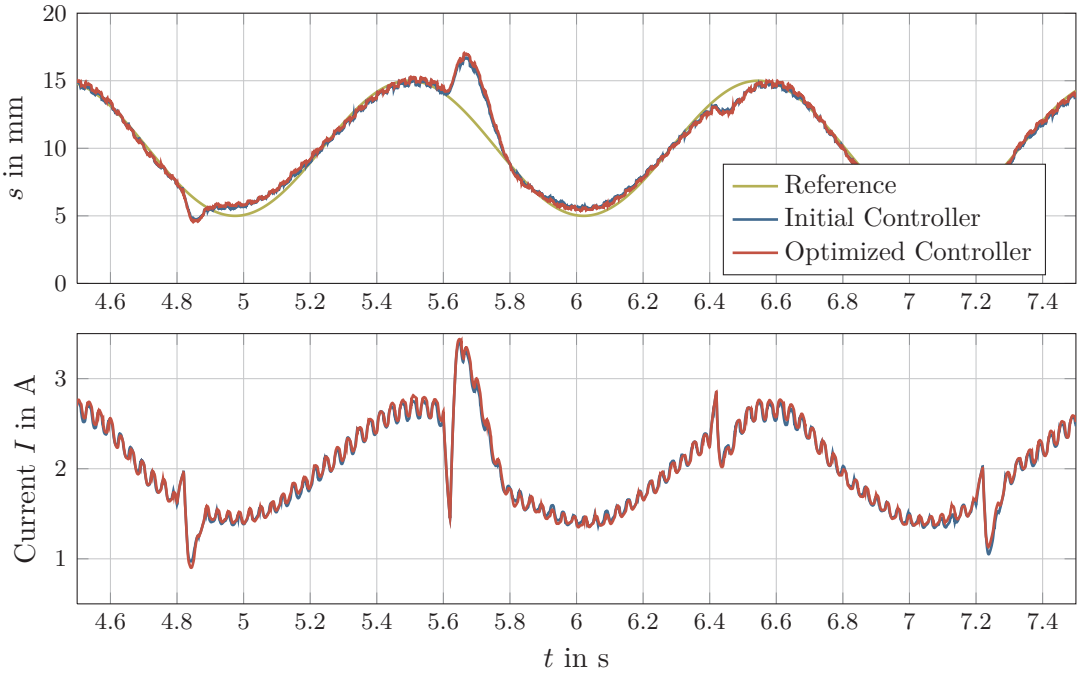

Figure 5.10: Comparison of the initial controller from [101] and the controller obtained from the optimization: While the optimized controller achieves a larger (estimated) DA, the dynamic behavior of the two controllers is very similar.

system. In the first two examples we have illustrated how the parametrization of the design matrix proposed in Section 4.1 simplifies the systematic IDA design procedure by guaranteeing positive semidefiniteness of the dissipation matrix without cumbersome inequality constraints. With the aid of the optimization procedure from Chapter 4, together with the algorithms from Chapter 3 in all three examples a considerable enlargement of the DA has been achieved as compared to the initial controller parametrizations, that have been obtained by sole application of LLDA. Simultaneously, it has still been possible to transparently specify desired transient behavior in terms of eigenvalue locations. In the first example, the resulting controller has been found to give better results than a linear controller. In the example of the synchronous generator, our controller has outperformed an IDA controller designed in [60], [61] with respect to both size of the DA and the closely related critical clearing time as well as transient performance. In the example of the magnetic levitation system, the proposed methods have proven to be successfully applicable also to the most general case, in which the energy function is time-varying and the dissipation matrix is only positive definite in some neighborhood of the desired equilibrium point.

Part II

Switched Systems

Chapter 6

Passivity-Based Control of Switched Nonlinear Systems

With this chapter we start the second part of the thesis which is devoted to the control of switched systems and consists of three chapters. The present Chapter 6 addresses the problem of stabilizing a switched system at a desired equilibrium point. Subsequently, in Chapter 7, both the exact and the asymptotic tracking of a desired output trajectory are treated. In Chapter 8, the theoretical results are applied for the tracking control of two technical systems.

The aim of this chapter is to develop an *analytic* and *constructive* controller design method for the asymptotic stabilization of switched nonlinear and in general time-varying systems which undergo arbitrary switching. To this end, we introduce the class of *switched port-Hamiltonian (spH) systems* and discuss their stability properties. Motivated by that, we extend the IDA methodology, which has proven to be a powerful tool for the control of smooth nonlinear systems in the first part of this thesis, to the class of switched systems. We propose to assign an spH structure with common energy function to the closed loop system in order to solve the asymptotic stabilization problem. Like in the non-switched case, the set of energy functions which can be assigned to the closed loop system is obtained from the solution of a system of linear PDEs, which are parametrized by the chosen design matrices. However, it is often not easy to find admissible design matrices for all subsystems such that these PDEs are solvable and, additionally, there remain enough degrees of freedom for the shaping of the energy function. Therefore, a systematic procedure for the choice of these matrices and the subsequent controller design is proposed for a special class of switched systems. In this context, we present a new result on the matrix equation $\mathbf{A}\mathbf{X} + \mathbf{X}^T\mathbf{A}^T = \mathbf{Q}$. A preliminary version of the results in this chapter has been presented in [99].

This chapter is organized as follows: In Section 6.1, we give a formal statement of the considered controller synthesis problem. Subsequently, we introduce in Section 6.2 the class of spH systems. In Section 6.3, the proposed design methodology is presented in its general form. In Section 6.4, we develop for a special class of systems a systematic procedure for the controller design. In Section 6.5, we briefly elaborate on the case that the plant is already in spH-form, and in Section 6.6 the proposed method is extended to include integral and adaptive control. The stabilization of switched nonlinear systems with time-varying subsystems is addressed in Section 6.7. In Section 6.8, we comment on the tuning of the controllers, and in Section 6.9, the proposed procedure is illustrated by means of two numerical examples.

6.1 Problem Statement

In this chapter, we consider switched nonlinear and in general time-varying systems of the form

$$\dot{\mathbf{x}} = \mathbf{f}_\sigma(\mathbf{x}, t) + \mathbf{G}_\sigma(\mathbf{x}, t)\mathbf{u}_\sigma \ , \quad \sigma \in \mathcal{S} \tag{6.1}$$

with the state $\mathbf{x} \in \mathbb{R}^n$, the input vectors $\mathbf{u}_p \in \mathbb{R}^{m_p}$ and $\operatorname{rank}\{\mathbf{G}_p(\mathbf{x}, t)\} = m_p$ for all $p \in \mathcal{P}$ and all $t \in [0, \infty)$. The vector fields $\mathbf{f}_p : \mathbb{R}^n \times [0, \infty) \to \mathbb{R}^n$ and the m_p columns of the matrices $\mathbf{G}_p : \mathbb{R}^n \times [0, \infty) \to \mathbb{R}^{n \times m_p}$ are continuous in t and locally Lipschitz in $\mathbf{x}$ on $[0, \infty) \times \mathrm{D}$, where the domain $\mathrm{D} \subset \mathbb{R}^n$ contains the equilibrium $\mathbf{x}^*$ which is to be stabilized. The switching can be either trajectory-independent or trajectory-dependent according to the switching rules (2.69) or (2.73). For the basic definitions on switched systems as well as for a differentiation of this class of from the class of (non-switched) time-varying systems, the reader is referred to Section 2.4. We assume throughout this chapter that the switching signal is piecewise constant, which, together with the regularity assumptions imposed on the drift vector fields and the input matrices, ensures the existence of a solution in the sense of Definition 2.4.1 for piecewise continuous input signals. If the switching is trajectory-dependent, this is of course not guaranteed in general and has to be checked for the closed loop system in each particular case.

The assignable equilibria of the pth subsystem are the elements of the set

$$\mathcal{E}_p = \left\{ \mathbf{x} \in \mathbb{R}^n \,\middle|\, \mathbf{G}_p^\perp(\mathbf{x}, t)\mathbf{f}_p(\mathbf{x}, t) = \mathbf{0}, \ \forall\, t \in \mathbb{R}_0^+ \right\} \tag{6.2}$$

with $\mathbf{G}_p^\perp(\mathbf{x}, t)$ a full rank left annihilator of $\mathbf{G}_p(\mathbf{x}, t)$. We assume that the intersection $\mathcal{E} = \bigcap_{p=1}^N \mathcal{E}_p$ is nonempty and $\mathbf{x}^* \in \mathcal{E}$ holds for the desired equilibrium point $\mathbf{x}^*$. The latter

is necessary for the stabilizability of $\mathbf{x}^*$ for all $\sigma \in \mathcal{S}_{pc}$. The controller synthesis problem considered in this chapter can be formally stated as follows.

Problem 6.1.1. Given (6.1) and a desired equilibrium $\mathbf{x}^* \in \mathcal{E}$, find functions $\mathbf{r}_p : \mathbb{R}^n \times [0, \infty) \to \mathbb{R}^{m_p}$ such that $\mathbf{x}^*$ is a uniformly asymptotically stable equilibrium of the closed-loop system

$$\dot{\mathbf{x}} = \mathbf{f}_\sigma(\mathbf{x}, t) + \mathbf{G}_\sigma(\mathbf{x}, t)\mathbf{r}_\sigma(\mathbf{x}, t) \ , \quad \sigma \in \mathcal{S} \tag{6.3}$$

in the sense of Definition 2.4.3.

We make the following assumption.

Assumption 6.1.1. The switching signal is not known a priori, but its instantaneous value is detectable in real time.

As a matter of fact, this will be satisfied in many applications, see e.g. [157]. If the switching is trajectory-dependent according to (2.69) or (2.73), the assumption is without loss of generality since in the context of state feedback $\mathbf{u} = \mathbf{r}_\sigma(\mathbf{x}, t)$ both the state and the control input are known. Also, if the switching is orchestrated by a supervisory controller, the switching signal is normally available. Moreover, it will be possible in some cases to design a common control law for all subsystems, i.e., $\mathbf{r}_p(\mathbf{x}, t) = \mathbf{r}(\mathbf{x}, t), \ \forall\, p \in \mathcal{P}$, which obviates Assumption 6.1.1.

6.2 Switched Port-Hamiltonian Systems

In this section, we introduce the class of switched port-Hamiltonian (spH) systems, which are a generalization of the pH models reviewed in Section 2.2.2, and discuss some of its stability properties. An spH-system is described by

$$\dot{\mathbf{x}} = \left[\mathbf{J}_\sigma(\mathbf{x}) - \mathbf{R}_\sigma(\mathbf{x})\right] \nabla H_\sigma(\mathbf{x}) + \mathbf{G}_\sigma(\mathbf{x})\mathbf{u}_\sigma \tag{6.4a}$$

$$\mathbf{y} = \mathbf{G}_\sigma^T(\mathbf{x}) \nabla H_\sigma(\mathbf{x}) \tag{6.4b}$$

with the state $\mathbf{x} \in \mathbb{R}^n$, the input vectors $\mathbf{u}_p \in \mathbb{R}^{m_p}$, the collocated outputs given by $\mathbf{G}_\sigma^T \nabla H_\sigma$, and the switching signal $\sigma : [0, \infty) \to \mathcal{P}$. The structure matrices $\mathbf{J}_p : \mathbb{R}^n \to \mathbb{R}^{n \times n}$ are skew symmetric $\mathbf{J}_p^T = -\mathbf{J}_p$, the dissipation matrices $\mathbf{R}_p : \mathbb{R}^n \to \mathbb{R}^{n \times n}$ are positive semidefinite $\mathbf{R}_p = \mathbf{R}_p^T \geq 0$, and the input matrices $\mathbf{G}_p : \mathbb{R}^n \to \mathbb{R}^{n \times m_p}$ satisfy $\operatorname{rank}\{\mathbf{G}_p\} = m_p$. The energy functions have a strict local minimum at the common equilibrium point $\mathbf{x}^*$, i.e., there is an open neighborhood $\Omega \subset \mathbb{R}^n$ of $\mathbf{x}^*$ such that

$$H_p(\mathbf{x}) > H_p(\mathbf{x}^*) \ , \quad \forall\, \mathbf{x} \in \Omega \backslash \{\mathbf{x}^*\} \tag{6.5}$$

holds for all $p \in \mathcal{P}$. By virtue of the pH-structure, the rate of change of energy in each individual subsystem is

$$\dot{H}_p(\mathbf{x}) = -\nabla^T H_p(\mathbf{x}) \mathbf{R}_p(\mathbf{x}) \nabla H_p(\mathbf{x}) + \mathbf{y}^T \mathbf{u}_p \leq \mathbf{y}^T \mathbf{u}_p \tag{6.6}$$

which shows that every subsystem taken by itself is passive, and if we take into account (6.5), also stable. But, as illustrated at the beginning of Section 2.4.2, this does not imply stability of $\mathbf{x}^*$ for arbitrary switching signals. In order to identify an admissible subset of $\mathcal{S}_{pc}$ for which $\mathbf{x}^*$ is a stable equilibrium of (6.4), the multiple Lyapunov function approach mentioned in Section 2.4.2 could be used.

However, if we confine ourselves to spH systems with a *common energy function* $H(\mathbf{x})$, i.e., $H_p(\mathbf{x}) = H(\mathbf{x}),\ \forall\, p \in \mathcal{P}$, the overall system (6.4) is passive with respect to the storage function $H(\mathbf{x})$. In view of (6.5) and (6.6), the function $H(\mathbf{x})$ qualifies as a common Lyapunov function and hence the following stability result is a direct consequence of Theorem 2.4.2.

Theorem 6.2.1. *Consider an spH system* (6.4) *with common energy function* $H(\mathbf{x})$*, i.e.,* $H_p(\mathbf{x}) = H(\mathbf{x}),\ \forall\, p \in \mathcal{P}$*, satisfying* (6.5) *and* $\mathbf{u}_\sigma \equiv \mathbf{0}$*. The following properties hold: (i) The equilibrium* $\mathbf{x}^*$ *is uniformly stable. (ii) If, additionally,* $\mathbf{R}_p(\mathbf{x}) > 0,\ \forall\, \mathbf{x} \in \Omega$ *is fulfilled for all* $p \in \mathcal{P}$*, then* $\mathbf{x}^*$ *is uniformly asymptotically stable.*

If $\mathbf{R}_p(\mathbf{x}) > 0,\ \forall\, \mathbf{x} \in \Omega,\ \forall\, p \in \mathcal{P}$, uniform asymptotic stability directly follows from Theorem 2.4.2, because $H(\mathbf{x})$ is guaranteed to be a strict common Lyapunov function. If, for one or more $p \in \mathcal{P}$, the dissipation matrix is only positive semidefinite, $H(\mathbf{x})$ might be merely a weak common Lyapunov function, in which case Krassovski-LaSalle-like criteria, like Theorem 2.4.4, have to be invoked to establish asymptotic stability of $\mathbf{x}^*$. An estimate of the DA can be obtained by means of $H(\mathbf{x})$ as described in Section 2.4.2.

6.3 Controller Design

In this section, we present an *analytic* and *constructive*[1] controller design methodology which solves Problem 6.1.1. For now, we confine ourselves to the case where the $\mathbf{f}_p(\mathbf{x})$ and $\mathbf{G}_p(\mathbf{x})$ are time-invariant, i.e.,

$$\dot{\mathbf{x}} = \mathbf{f}_\sigma(\mathbf{x}) + \mathbf{G}_\sigma(\mathbf{x}) \mathbf{u}_\sigma\ , \quad \sigma \in \mathcal{S}\ . \tag{6.7}$$

[1] The method is constructive in the sense that the solution of the stabilization problem is characterized by a set of linear PDEs and a set of inequalities (see the example in Section 8.1).

The general time-varying case will be treated in Section 6.7. Motivated by the stability properties of spH systems with common energy function (see Theorem 6.2.1), we intend to design a switched static feedback controller $\mathbf{u}_\sigma = \mathbf{r}_\sigma(\mathbf{x})$ which transforms (6.7) into spH form

$$\dot{\mathbf{x}} = [\mathbf{J}_\sigma(\mathbf{x}) - \mathbf{R}_\sigma(\mathbf{x})]\,\nabla H(\mathbf{x}) \tag{6.8}$$

where $\mathbf{J}_p(\mathbf{x}) = -\mathbf{J}_p^T(\mathbf{x})$ and $\mathbf{R}_p(\mathbf{x}) = \mathbf{R}_p^T(\mathbf{x}) \geq 0$, $p \in \mathcal{P}$ are some desired interconnection and dissipation matrices, and the common energy function $H(\mathbf{x})$ has a strict local minimum at the desired equilibrium point $\mathbf{x}^*$.

The following theorem presents the method in its general form. A systematic procedure for the controller design is proposed in the subsequent Section 6.4 for a special class of switched systems.

Theorem 6.3.1. *Assume there are matrices $\mathbf{G}_p^\perp(\mathbf{x})$, $\mathbf{J}_p(\mathbf{x}) = -\mathbf{J}_p^T(\mathbf{x})$, $\mathbf{R}_p(\mathbf{x}) = \mathbf{R}_p^T(\mathbf{x}) \geq 0$ and a function $H(\mathbf{x})$ satisfying the system of linear partial differential equations*

$$\mathbf{G}_p^\perp(\mathbf{x})\,[\mathbf{J}_p(\mathbf{x}) - \mathbf{R}_p(\mathbf{x})]\,\nabla H(\mathbf{x}) = \mathbf{G}_p^\perp(\mathbf{x})\mathbf{f}_p(\mathbf{x}) \tag{6.9}$$

for all $p \in \mathcal{P}$, where $\mathbf{G}_p^\perp(\mathbf{x}) : \mathbb{R}^n \to \mathbb{R}^{(n-m_p)\times n}$ is a full rank left annihilator of $\mathbf{G}_p(\mathbf{x})$ (i.e., $\mathbf{G}_p^\perp(\mathbf{x})\mathbf{G}_p(\mathbf{x}) = \mathbf{0}$). Further, suppose that there is an open neighborhood $\Omega \subset \mathrm{D}$ of the desired equilibrium $\mathbf{x}^*$ such that

$$H(\mathbf{x}) > H(\mathbf{x}^*)\,, \quad \forall\, \mathbf{x} \in \Omega \backslash \{\mathbf{x}^*\}\,. \tag{6.10}$$

Then, the switching controller

$$\mathbf{u}_\sigma = \left[\mathbf{G}_\sigma^T(\mathbf{x})\mathbf{G}_\sigma(\mathbf{x})\right]^{-1}\mathbf{G}_\sigma^T(\mathbf{x})\Big\{[\mathbf{J}_\sigma(\mathbf{x}) - \mathbf{R}_\sigma(\mathbf{x})]\,\nabla H(\mathbf{x}) - \mathbf{f}_\sigma(\mathbf{x})\Big\} \tag{6.11}$$

transforms (6.1) *into spH-form*

$$\dot{\mathbf{x}} = [\mathbf{J}_\sigma(\mathbf{x}) - \mathbf{R}_\sigma(\mathbf{x})]\,\nabla H(\mathbf{x}) \tag{6.12}$$

and $\mathbf{x}^*$ is a uniformly stable equilibrium.

Proof. Similar to the proof of Proposition 1 in [132] (see also Section 2.2.3), we set the right hand side of (6.1), with $\mathbf{u} = \mathbf{r}_\sigma(\mathbf{x})$, equal to the right hand side of (6.12) to obtain the set of matching equations

$$\mathbf{f}_p(\mathbf{x}) + \mathbf{G}_p(\mathbf{x})\mathbf{r}_p(\mathbf{x}) = \left[\mathbf{J}_p(\mathbf{x}) - \mathbf{R}_p(\mathbf{x})\right] \nabla H(\mathbf{x}) \;, \quad p \in \mathcal{P} \;. \tag{6.13}$$

Multiplying (6.13) with $\mathbf{G}_p^\perp(\mathbf{x})$ for all $p \in \mathcal{P}$ yields the set of *projected matching equations* (6.9). The control law (6.11) is obtained by solving (6.13) for $\mathbf{r}_p(\mathbf{x})$ for all $p \in \mathcal{P}$ by means of the pseudo inverse. Uniform stability of $\mathbf{x}^*$ directly follows from Theorem 6.2.1. □

To simplify the notation, as in the first part of this thesis, we define the design matrices

$$\mathbf{F}_p(\mathbf{x}) = \mathbf{J}_p(\mathbf{x}) - \mathbf{R}_p(\mathbf{x}) \tag{6.14}$$

which satisfy

$$\mathbf{R}_p(\mathbf{x}) = -\mathrm{sym}\left\{\mathbf{F}_p(\mathbf{x})\right\} = -\frac{1}{2}\left[\mathbf{F}_p(\mathbf{x}) + \mathbf{F}_p^T(\mathbf{x})\right] \geq 0 \;. \tag{6.15}$$

If the structure of these matrices is fixed, the equations (6.9) constitute a system of $N_{pde} = \sum_{p=1}^{N}(n - m_p)$ linear PDEs

$$\underbrace{\begin{bmatrix} \mathbf{G}_1^\perp(\mathbf{x})\mathbf{F}_1(\mathbf{x}) \\ \vdots \\ \mathbf{G}_N^\perp(\mathbf{x})\mathbf{F}_N(\mathbf{x}) \end{bmatrix}}_{\mathbf{W}:\mathbb{R}^n \to \mathbb{R}^{N_{pde} \times n}} \nabla H(\mathbf{x}) = \underbrace{\begin{bmatrix} \mathbf{G}_1^\perp(\mathbf{x})\mathbf{f}_1(\mathbf{x}) \\ \vdots \\ \mathbf{G}_N^\perp(\mathbf{x})\mathbf{f}_N(\mathbf{x}) \end{bmatrix}}_{\mathbf{s}:\mathbb{R}^n \to \mathbb{R}^{N_{pde}}} \tag{6.16}$$

from which the set of admissible energy functions has to be determined. This is similar to the non-switched case, with the difference that the total number of PDEs N_{pde} is, in general, greater than n. Nevertheless, the solvability can be assessed using Theorem[2] 2.2.2. Hence, if the involutive closures $\bar{\Delta}_W$, $\bar{\Delta}_{W,s}$ of the distributions

$$\Delta_W = \mathrm{span}\{\mathbf{W}^T(\mathbf{x})\}, \;\; \Delta_{W,s} = \mathrm{span}\left\{\begin{bmatrix} \mathbf{W}^T(\mathbf{x}) \\ \mathbf{s}^T(\mathbf{x}) \end{bmatrix}\right\} \tag{6.17}$$

are regular, there exists a function $H(\mathbf{x})$ satisfying (6.16) if and only if

$$\dim \bar{\Delta}_W = \dim \bar{\Delta}_{W,s} \;. \tag{6.18}$$

[2]Let us remark that in [24] this solvability condition has indeed been formulated only for the case $N_{pde} < n$. This assumption is, however, not necessary (see also [165]).

Obviously, it is necessary for the solvability of (6.16) that $\mathbf{s}(\mathbf{x}) \in \mathcal{R}\{\mathbf{W}(\mathbf{x})\}$, or equivalently dim Δ_W = dim $\Delta_{W,s} = r \leq n$. Since we assume Δ_W and $\Delta_{W,s}$ to be regular, this implies that there are indices k_i, $i \in \{1, \ldots, r\}$, such that $H(\mathbf{x})$ is a solution of (6.16) if and only if it satisfies

$$\underbrace{\begin{bmatrix} \mathbf{w}_{k_1}^T(\mathbf{x}) \\ \vdots \\ \mathbf{w}_{k_r}^T(\mathbf{x}) \end{bmatrix}}_{\widetilde{\mathbf{W}}:\mathbb{R}\to\mathbb{R}^{r\times n}} \nabla H(\mathbf{x}) = \underbrace{\begin{bmatrix} s_{k_1}(\mathbf{x}) \\ \vdots \\ s_{k_r}(\mathbf{x}) \end{bmatrix}}_{\tilde{\mathbf{s}}:\mathbb{R}\to\mathbb{R}^{r}} \tag{6.19}$$

where we denote by $\mathbf{w}_i^T(\mathbf{x})$ the rows of $\mathbf{W}(\mathbf{x})$ and by $s_i(\mathbf{x})$ the components of $\mathbf{s}(\mathbf{x})$.

If the solvability condition (6.18), or equivalently dim $\bar{\Delta}_{\widetilde{W}}$ = dim $\bar{\Delta}_{\widetilde{W},\tilde{s}}$, is fulfilled, as in the non-switched case, the admissible energy functions are of the form

$$H(\mathbf{x}) = \Psi(\mathbf{x}) + \phi\left(\boldsymbol{\xi}(\mathbf{x})\right) \tag{6.20}$$

i.e., they are composed of a particular solution $\Psi(\mathbf{x})$ of (6.16) and a homogeneous solution $\phi\left(\boldsymbol{\xi}(\mathbf{x})\right)$, which is an arbitrary function of the characteristic coordinates $\boldsymbol{\xi} : \mathbb{R}^n \to \mathbb{R}^{n_\xi}$ (see Section 2.2.4). According to the Frobenius Theorem 2.2.1, the number of characteristic coordinates that are available for the energy shaping is $n_\xi = n - \dim\ \bar{\Delta}_W = n - \dim\ \bar{\Delta}_{\widetilde{W}}$. The function $\phi(\cdot)$ is chosen such that(6.10) holds, which is usually done using the sufficient condition (2.27).

In [140], it is shown that the IDA methodology is"universally stabilizing". This also holds true for the proposed generalization to switched systems, in the sense that the approach generates all control laws of the form $\mathbf{u}_\sigma = \mathbf{r}_\sigma(\mathbf{x})$ which uniformly asymptotically stabilize (6.7) under arbitrary switching, i.e., for $\mathcal{S} = \mathcal{S}_{pc}$.

Lemma 6.3.1. *Consider the finite family of $\mathcal{C}^1$ vector fields $\{\mathbf{f}_p(\mathbf{x}), p \in \mathcal{P}\}$. If the switched system $\dot{\mathbf{x}} = \mathbf{f}_\sigma(\mathbf{x})$ possesses an equilibrium $\mathbf{x}^*$ which is uniformly asymptotically stable for arbitrary switching signals $\sigma \in \mathcal{S}_{pc}$, then there is a $\mathcal{C}^\infty$ function $H(\mathbf{x})$ satisfying* (6.10) *and matrix-valued $\mathcal{C}^0$ functions $\mathbf{J}_p(\mathbf{x}) = -\mathbf{J}_p^T(\mathbf{x})$ and $\mathbf{R}_p(\mathbf{x}) = \mathbf{R}_p^T(\mathbf{x}) \geq 0$ such that for all $p \in \mathcal{P}$*

$$\mathbf{f}_p(\mathbf{x}) = \left[\mathbf{J}_p(\mathbf{x}) - \mathbf{R}_p(\mathbf{x})\right] \nabla H(\mathbf{x}) \ . \tag{6.21}$$

Proof. From the converse Lyapunov theorem in [119] it is known that there is a neighborhood Ω of $\mathbf{x}^*$ such that all subsystems share a common $\mathcal{C}^\infty$ Lyapunov function $H(\mathbf{x})$ with a strict local minimum at $\mathbf{x}^*$ and $\nabla^T H(\mathbf{x})\mathbf{f}_p(\mathbf{x}) < 0$ for all $\mathbf{x} \in \Omega \backslash \{\mathbf{x}^*\}$ and all $p \in \mathcal{P}$. Then the desired result follows by applying the proof of Lemma 1 in [140] to every subsystem. □

An immediate consequence of this Lemma is the following Proposition.

Proposition 6.3.1. *Consider the switched system* (6.1) *and let* $\mathbf{f}_p(\mathbf{x})$ *and the columns of* $\mathbf{G}_p(\mathbf{x})$ *be* $\mathcal{C}^1$ *vector fields. If there are* $\mathcal{C}^1$ *functions* $\mathbf{r}_p(\mathbf{x}) : \mathbb{R}^n \to \mathbb{R}^{m_p}$, $p \in \mathcal{P}$ *such that the closed loop system* $\dot{\mathbf{x}} = \mathbf{f}_\sigma(\mathbf{x}) + \mathbf{G}_\sigma(\mathbf{x})\mathbf{r}_\sigma(\mathbf{x})$ *possesses a uniformly stable equilibrium point* $\mathbf{x}^*$ *for arbitrary switching signals* $\sigma \in \mathcal{S}_{pc}$, *then there are matrices* $\mathbf{G}_p^\perp(\mathbf{x})$, $\mathbf{J}_p(\mathbf{x}) = -\mathbf{J}_p^T(\mathbf{x})$, $\mathbf{R}_p(\mathbf{x}) = \mathbf{R}_p^T(\mathbf{x}) \geq 0$ *and a function* $H(\mathbf{x})$ *satisfying the conditions of Theorem 6.3.1.*

Remark 6.3.1. If a system with state-dependent switching law (2.70), (2.73) is to be stabilized, it would be sufficient to assign an spH structure (6.4) with *different energy functions* to the closed loop system, if we additionally require that these functions coincide on the switching surface[3], i.e.,

$$H_1(\mathbf{x}) = H_2(\mathbf{x}) \ , \quad \forall\, \mathbf{x} \in \partial\chi \ . \tag{6.22}$$

For (6.22) implies that $H_{\sigma(t_i)}(\mathbf{x}(t_i)) = H_{\sigma(t_i^-)}(\mathbf{x}(t_i^-))$ holds for all switching times, and hence, taking into account (6.5) and (6.6), uniform stability of $\mathbf{x}^*$ can be established employing the multiple Lyapunov function approach (see Section 2.4.2). If we aim to endow the closed loop system with a structure like that, we obtain two separate matching PDEs – one for each energy function – which have to be solved under the additional constraint (6.22). It turns out, however, that this poses a very difficult problem even for simple numerical examples. Therefore, this approach is not pursued further in this thesis.

Remark 6.3.2. In some cases a switching controller can be beneficial for non-switched systems as well, for instance when conflicting performance requirements are present. Then, appropriately switching (or scheduling) between differently tuned controllers can often considerably enhance the performance compared to a single control law, see e.g. [100] where we have applied a control strategy of this kind for the driving state adaptive control of an active vehicle suspension. In order to ensure uniform asymptotic stability of the desired equilibrium for any switching sequence, a common Lyapunov function for all subsystems of the resulting closed loop switched system is needed. However, to the best of our knowledge, no methods are available for nonlinear systems that allow to guarantee the existence of such a function in a constructive manner except for the one we have presented in [98]. The approach is contained in Theorem 6.3.1 as a special case, if all $\mathbf{f}_p(\mathbf{x})$ and $\mathbf{G}_p(\mathbf{x})$ are identical, but different $\mathbf{J}_p(\mathbf{x})$ and $\mathbf{R}_p(\mathbf{x})$ are chosen. In [98], we have proposed a systematic procedure for the design of a suitable family of controllers and have applied it to an active vehicle suspension. For details the reader is referred to this paper.

[3]Recall that, throughout this thesis, we consider, in the context of trajectory-dependent switching, only bimodal switched systems.

6.4 Systematic Controller Design for a Special Class of Systems

In many cases, it is not an easy task to find suitable design matrices $\mathbf{F}_p(\mathbf{x})$, $p \in \mathcal{P}$ with $\mathrm{sym}\{\mathbf{F}_p(\mathbf{x})\} \leq 0$ such that the matching PDE (6.16) has a solution which attains a strict local minimum at the desired operating point. That's why, in this section, we present for a special class of bimodal switched nonlinear systems a systematic procedure for the construction of these matrices and the ensuing controller design.

6.4.1 The Considered Class of Systems

We consider switched nonlinear systems of the form

$$\begin{bmatrix} \dot{\mathbf{x}}^\alpha \\ \dot{\mathbf{x}}^\nu \end{bmatrix} = \begin{bmatrix} \mathbf{f}_\sigma^\alpha(\mathbf{x}) \\ \mathbf{f}_\sigma^\nu(\mathbf{x}) \end{bmatrix} + \begin{bmatrix} \mathbf{G}_\sigma^\alpha(\mathbf{x}) \\ \mathbf{0} \end{bmatrix} \mathbf{u} \tag{6.23}$$

with $\mathbf{x}^\alpha \in \mathbb{R}^m$, $\mathbf{x}^\nu \in \mathbb{R}^{n-m}$, $\mathbf{u} \in \mathbb{R}^m$ consisting of only two subsystems, i.e., $\mathcal{P} = \{1, 2\}$. This type of systems may be viewed as the switched version of the class of systems (2.49) considered in the context of LLDA. Note that, as opposed to the previous section, both subsystems have the same number of control inputs m. It is not difficult to show that a general switched system (6.7) with $\mathcal{P} = \{1, 2\}$ and $m_1 = m_2 = m$ can be transformed into the form (6.23) by a change of coordinates if and only if (i) the columns of the input matrices span regular involutive distributions of dimension m, and (ii) it holds that $\mathrm{span}\{\mathbf{G}_1(\mathbf{x})\} = \mathrm{span}\{\mathbf{G}_2(\mathbf{x})\}$. Otherwise, the form (6.23) with $\mathbf{G}_p^\alpha = \mathbf{I}_m$ can be achieved by a dynamical extension of both subsystems with $x_{n+1} = u_1, \ldots, x_{n+m} = u_m$ and $\dot{x}_{n+1} = v_1, \ldots, \dot{x}_{n+m} = v_m$, where the v_i, $i = 1, \ldots, m$ are the new control inputs.

In accordance with (6.23), the design matrices are partitioned into submatrices $\mathbf{F}_p^\alpha : \mathbb{R}^n \to \mathbb{R}^{m \times n}$ and $\mathbf{F}_p^\nu : \mathbb{R}^n \to \mathbb{R}^{(n-m) \times n}$ yielding the matching equations

$$\begin{bmatrix} \mathbf{F}_p^\alpha(\mathbf{x}) \\ \mathbf{F}_p^\nu(\mathbf{x}) \end{bmatrix} \nabla H(\mathbf{x}) = \begin{bmatrix} \mathbf{f}_p^\alpha(\mathbf{x}) \\ \mathbf{f}_p^\nu(\mathbf{x}) \end{bmatrix} + \begin{bmatrix} \mathbf{G}_p^\alpha(\mathbf{x}) \\ \mathbf{0} \end{bmatrix} \mathbf{r}_p(\mathbf{x}) \,, \quad p \in \{1, 2\} \,. \tag{6.24}$$

With the simplest left annihilators $\mathbf{G}_p^\perp = [\mathbf{0},\ \mathbf{I}]$ the projected matching equation (6.16) is

$$\underbrace{\begin{bmatrix} \mathbf{F}_1^\nu(\mathbf{x}) \\ \mathbf{F}_2^\nu(\mathbf{x}) \end{bmatrix}}_{\mathbf{W}(\mathbf{x})} \nabla H(\mathbf{x}) = \underbrace{\begin{bmatrix} \mathbf{f}_1^\nu(\mathbf{x}) \\ \mathbf{f}_2^\nu(\mathbf{x}) \end{bmatrix}}_{\mathbf{s}(\mathbf{x})} \,. \tag{6.25}$$

The matrices $\mathbf{F}_p^\nu(\mathbf{x})$ are chosen such that the distributions $\Delta_{F,p} = \text{span}\{(\mathbf{F}_p^\nu(\mathbf{x}))^T\}$ spanned by their rows have constant dimension $n-m$ in a neighborhood of the desired equilibrium $\mathbf{x}^*$. This is necessary in order that the design matrices $\mathbf{F}_p(\mathbf{x})$ can have full rank in a neighborhood of $\mathbf{x}^*$. If the latter is not the case, the closed loop system might have equilibria that are not extrema of the energy function.

From $\dim \Delta_{F,p} = n-m$ it follows that $\dim \bar{\Delta}_W \geq \dim \Delta_W \geq \dim \Delta_{F,p} = n-m$, where we have used that $\Delta_{F,p} \subseteq \Delta_W$. Thus, regarding the number of available characteristic coordinates, we conclude that $n_\xi = n - \dim \bar{\Delta}_W \leq m$. From an energy shaping perspective, it is of course desirable that the projected matching equation is solvable with a maximum number of $n_\xi = m$ characteristic coordinates in order that the design freedom is as large as possible. We remark that solvability of (6.25) with m characteristic coordinates is also necessary in order that LLDA (see Section 2.3) can be applied for a systematic controller parametrization. According to the Frobenius Theorem 2.2.1 and Theorem 2.2.2, this is the case if and only if $\dim \bar{\Delta}_{W,s} = \dim \bar{\Delta}_W = n-m$. Together with $\dim \Delta_{F,p} = n-m$ we deduce the requirement $\bar{\Delta}_{W,s} = \Delta_{W,s} = \text{span}\{[\mathbf{F}_1^\nu(\mathbf{x}),\ \mathbf{f}_1^\nu(\mathbf{x})]^T\} = \text{span}\{[\mathbf{F}_2^\nu(\mathbf{x}),\ \mathbf{f}_2^\nu(\mathbf{x})]^T\}$. Hence, there must exist a regular matrix $\mathbf{C}(\mathbf{x})$ such that $[\mathbf{F}_2^\nu(\mathbf{x}),\ \mathbf{f}_2^\nu(\mathbf{x})] = \mathbf{C}(\mathbf{x})[\mathbf{F}_1^\nu(\mathbf{x}),\ \mathbf{f}_1^\nu(\mathbf{x})]$ holds. While $\mathbf{F}_2^\nu(\mathbf{x}) = \mathbf{C}(\mathbf{x})\mathbf{F}_1^\nu(\mathbf{x})$ can be achieved by a suitable choice of the design parameters, the $\mathbf{f}_p^\nu(\mathbf{x})$ are determined by the system dynamics (6.23). Therefore, the following assumption is imposed on the considered class of systems.

Assumption 6.4.1. There is a function $\mathbf{C} : \mathbb{R}^n \to \mathbb{R}^{(n-m)\times(n-m)}$ with $\text{rank}\{\mathbf{C}(\mathbf{x})\} = n-m$ such that $\mathbf{f}_2^\nu(\mathbf{x}) = \mathbf{C}(\mathbf{x})\mathbf{f}_1^\nu(\mathbf{x})$ holds in a neighborhood of $\mathbf{x}^*$. Moreover, in this neighborhood, the algebraic and geometric multiplicity of all eigenvalues of $\mathbf{C}(\mathbf{x})$ with non-positive real part is equal.

The first part of this assumption implies that the system of PDEs (6.25) is equivalent to

$$\mathbf{F}_p^\nu(\mathbf{x})\nabla H(\mathbf{x}) = \mathbf{f}_p^\nu(\mathbf{x}) \tag{6.26}$$

with $p = 1$ *or* $p = 2$, if the matrices $\mathbf{F}_p^\nu(\mathbf{x})$ are chosen as suggested above, i.e., $\mathbf{F}_2^\nu(\mathbf{x}) = \mathbf{C}(\mathbf{x})\mathbf{F}_1^\nu(\mathbf{x})$. The second part of the assumption is of technical nature. It is used to simplify the proof of Theorem 6.4.3 later on.

6.4.2 Positive Semidefiniteness of the Dissipation Matrices

In order that the feedback law transforms the system (6.23) into spH form it is necessary that both dissipation matrices are positive semi-definite

$$\mathbf{R}_p(\mathbf{x}) = -\text{sym}\{\mathbf{F}_p(\mathbf{x})\} \geq 0\ , \quad p \in \{1,2\}\ . \tag{6.27}$$

In fact, it would be beneficial if both dissipation matrices are positive definite, which means that each of them has n strictly positive eigenvalues. Because in this case, uniform asymptotic stability for arbitrary switching signals $\sigma \in \mathcal{S}_{pc}$ directly follows from Theorem 6.2.1, and there is no need to apply Krasovskii-LaSalle-like stability criteria, which impose some restrictions on the admissible switching signals regarding the distance between the consecutive discontinuities (c.f. Theorem 2.4.4).

Therefore, in the following, we analyze how many positive eigenvalues can at the maximum be assigned to the dissipation matrices in case that we choose the design matrices such that $\mathbf{F}_2^\nu(\mathbf{x}) = \mathbf{C}(\mathbf{x})\mathbf{F}_1^\nu(\mathbf{x})$, as it is suggested by the discussion at the end of the previous subsection. To begin with, we partition the design matrices according to

$$\mathbf{F}_p(\mathbf{x}) = \begin{bmatrix} \mathbf{F}_p^A(\mathbf{x}) & \mathbf{F}_p^B(\mathbf{x}) \\ \mathbf{F}_p^C(\mathbf{x}) & \mathbf{F}_p^D(\mathbf{x}) \end{bmatrix}, \quad p \in \{1, 2\} \tag{6.28}$$

with $\mathbf{F}_p^A(\mathbf{x}) : \mathbb{R}^n \to \mathbb{R}^{m \times m}$ and appropriate dimensions of the remaining submatrices. Comparing this with (6.24), we see that $\mathbf{F}_p^\alpha(\mathbf{x}) = [\mathbf{F}_p^A(\mathbf{x}),\ \mathbf{F}_p^B(\mathbf{x})]$ and $\mathbf{F}_p^\nu(\mathbf{x}) = [\mathbf{F}_p^C(\mathbf{x}),\ \mathbf{F}_p^D(\mathbf{x})]$. We have the following Lemma.

Lemma 6.4.1. *Given* $\mathbf{C}(\mathbf{x})$ *and* $\mathbf{F}_1^\nu(\mathbf{x})$*, let* $\mathbf{F}_2^\nu(\mathbf{x}) = \mathbf{C}(\mathbf{x})\mathbf{F}_1^\nu(\mathbf{x})$*. The dissipation matrices* $\mathbf{R}_1(\mathbf{x})$ *and* $\mathbf{R}_2(\mathbf{x})$ *can be rendered positive semidefinite (definite) simultaneously if and only if*

$$\mathbf{F}_1^D(\mathbf{x}) + \left(\mathbf{F}_1^D(\mathbf{x})\right)^T \leq 0 \ (< 0) \tag{6.29}$$

$$\mathbf{C}(\mathbf{x})\mathbf{F}_1^D(\mathbf{x}) + \left(\mathbf{F}_1^D(\mathbf{x})\right)^T \mathbf{C}^T(\mathbf{x}) \leq 0 \ (< 0)\ . \tag{6.30}$$

Proof. With the partitioning defined in (6.28) and $\mathbf{F}_2^C(\mathbf{x}) = \mathbf{C}(\mathbf{x})\mathbf{F}_1^C(\mathbf{x})$ as well as $\mathbf{F}_2^D(\mathbf{x}) = \mathbf{C}(\mathbf{x})\mathbf{F}_1^D(\mathbf{x})$ we obtain

$$\mathbf{R}_1 = -\frac{1}{2}\begin{bmatrix} \mathbf{F}_1^A + \left(\mathbf{F}_1^A\right)^T & \mathbf{F}_1^B + \left(\mathbf{F}_1^C\right)^T \\ \mathbf{F}_1^C + \left(\mathbf{F}_1^B\right)^T & \mathbf{F}_1^D + \left(\mathbf{F}_1^D\right)^T \end{bmatrix} \tag{6.31}$$

$$\mathbf{R}_2 = -\frac{1}{2}\begin{bmatrix} \mathbf{F}_2^A + \left(\mathbf{F}_2^A\right)^T & \mathbf{F}_2^B + \left(\mathbf{F}_1^C\right)^T \mathbf{C}^T \\ \mathbf{C}\mathbf{F}_1^C + \left(\mathbf{F}_2^B\right)^T & \mathbf{C}\mathbf{F}_1^D + \left(\mathbf{F}_1^D\right)^T \mathbf{C}^T \end{bmatrix}\ . \tag{6.32}$$

Now suppose that $\mathbf{R}_1(\mathbf{x}) \geq\ (> 0)$ and $\mathbf{R}_2(\mathbf{x}) \geq\ (> 0)$. Then, (6.29) and (6.30) directly follow from Theorem A.2.1 and Proposition A.2.1 in Appendix A.2, which proves necessity.

To prove sufficiency, let us first point out that the matrices $\mathbf{F}_p^\alpha = [\mathbf{F}_p^A,\ \mathbf{F}_p^B]$, $p \in \{1, 2\}$ can be chosen independently of each other. If we take e.g. $\mathbf{F}_p^A = \operatorname{diag}\{\alpha_{p,ii}\}$, $i \in \{1, \ldots, m\}$,

$p \in \{1,2\}$ with $\alpha_{p,ii} < 0$ and $\mathbf{F}_1^B(\mathbf{x}) = -[\mathbf{F}_1^C(\mathbf{x})]^T$ as well as $\mathbf{F}_2^B(\mathbf{x}) = -[\mathbf{F}_1^C(\mathbf{x})]^T\mathbf{C}^T(\mathbf{x})$, we get

$$\mathbf{R}_1 = \operatorname{diag}\left[\mathbf{R}_1^A,\ -\operatorname{sym}\left\{\mathbf{F}_1^D\right\}\right] \tag{6.33}$$

$$\mathbf{R}_2 = \operatorname{diag}\left[\mathbf{R}_2^A,\ -\operatorname{sym}\left\{\mathbf{C}\mathbf{F}_1^D\right\}\right] \tag{6.34}$$

with $\mathbf{R}_p^A = -\operatorname{diag}\{\alpha_{p,ii}\}$. If (6.29) and (6.30) are satisfied, then obviously it holds that $\mathbf{R}_1(\mathbf{x}) \geq 0$ (> 0) and $\mathbf{R}_2(\mathbf{x}) \geq 0$ (> 0). □

In the sequel, let, for a square matrix $\mathbf{A} \in \mathbb{R}^{n\times n}$, the number of eigenvalues in the right half plane, in the left half plane, and on the imaginary axis be denoted by $i_+(\mathbf{A})$, $i_-(\mathbf{A})$ and $i_0(\mathbf{A})$, respectively. Moreover, let $i_+^r(\mathbf{A})$, $i_-^r(\mathbf{A})$, and $i_0^r(\mathbf{A})$ be defined analogously for real valued eigenvalues.

Lemma 6.4.2. *Let* $\mathbf{R}^A \in \mathbb{R}^{m\times m}$, $\mathbf{R}^B \in \mathbb{R}^{m\times(n-m)}$, $\mathbf{R}^D \in \mathbb{R}^{(n-m)\times(n-m)}$, *and*

$$\mathbf{R} = \begin{bmatrix} \mathbf{R}^A & \mathbf{R}^B \\ \left(\mathbf{R}^B\right)^T & \mathbf{R}^D \end{bmatrix}. \tag{6.35}$$

If $\mathbf{R} \geq 0$ *and* $\mathbf{R}^D \geq 0$, *then*

$$\max_{\mathbf{R}^A,\ \mathbf{R}^B} i_+(\mathbf{R}) = m + i_+(\mathbf{R}^D)\ . \tag{6.36}$$

Proof. see Appendix B.1. □

In order that both dissipation matrices are positive semidefinite, according to Lemma 6.4.1, the matrix inequalities (6.29) and (6.30) have to be fulfilled. The latter can be formulated equivalently as equation

$$\mathbf{C}(\mathbf{x})\mathbf{X}(\mathbf{x}) + \mathbf{X}^T(\mathbf{x})\mathbf{C}^T(\mathbf{x}) = \mathbf{Q}(\mathbf{x}) \tag{6.37}$$

with $\mathbf{X}(\mathbf{x}) = -\mathbf{F}_1^D(\mathbf{x})$ and some (arbitrary) positive semidefinite matrix $\mathbf{Q}^T(\mathbf{x}) = \mathbf{Q}(\mathbf{x}) \geq 0$. For this reason, this type of matrix equation is analyzed in the next subsection with respect to the question under what conditions it has a solution satisfying $\operatorname{sym}\{\mathbf{X}\} \geq 0$.

6.4.3 The Equation $\mathbf{A}\mathbf{X} + \mathbf{X}^T\mathbf{A}^T = \mathbf{Q}$

The matrix equation

$$\mathbf{A}\mathbf{X} + \mathbf{X}^T\mathbf{A}^T = \mathbf{Q} \tag{6.38}$$

with $\mathbf{A}, \mathbf{Q} \in \mathbb{R}^{n\times n}$, $\mathbf{Q} = \mathbf{Q}^T$ and the unknown $\mathbf{X} \in \mathbb{R}^{n\times n}$, has been investigated in several publications including e.g. [18], [85], [105], [169]. The following result from [169] characterizes the solvability of (6.38) and the structure of its solution.

Theorem 6.4.1 ([169])**.** *(a) The matrix equation* (6.38) *is solvable if and only if* $\mathbf{E}_A\mathbf{Q}\mathbf{E}_A = \mathbf{0}$*, where* $\mathbf{E}_A = \mathbf{I} - \mathbf{A}\mathbf{A}^\dagger$ *is the orthogonal projector onto the nullspace of* $\mathbf{A}$*. The solution* $\mathbf{X} = \mathbf{X}^p + \mathbf{X}^h$ *is composed of a particular part* $\mathbf{X}^p$ *and the solution* $\mathbf{X}^h$ *of the corresponding homogeneous matrix equation (i.e., with* $\mathbf{Q} = \mathbf{0}$*).*

(b) In case that $\mathbf{Q} \geq 0$*, the equation* (6.38) *is solvable if and only if* $\mathcal{R}(\mathbf{Q}) \subseteq \mathcal{R}(\mathbf{A})$*.*

(c) If $\mathbf{A}$ *is regular, then* $\mathbf{X}^h = \mathbf{U}\mathbf{A}^T$ *with an arbitrary matrix* $\mathbf{U} = -\mathbf{U}^T$*.*

However, to the best of our knowledge, to date there are no results on the definiteness of the symmetric part $\mathrm{sym}\{\mathbf{X}\}$ of the solution of (6.38). Our results on this topic are summarized in the theorem stated next.

Theorem 6.4.2. *Consider the matrix equation* (6.38) *with* $\mathbf{Q} = \mathbf{Q}^T \geq 0$*. Let the algebraic and geometric multiplicity of all eigenvalues of* $\mathbf{A}$ *with non-positive real part be equal. There are solutions* $\mathbf{X}$ *with* $\mathrm{sym}\{\mathbf{X}\} \geq 0$ *if and only if all left eigenvectors of* $\mathbf{A}$ *corresponding to real non-positive eigenvalues are in* $\mathcal{N}\{\mathbf{Q}\}$*. Then, it holds that*

$$\max_{\mathbf{X}^h,\mathbf{Q}} \; i_+\Big(\mathrm{sym}\{\mathbf{X}\}\Big) = n - i_-^r(\mathbf{A}) \; . \tag{6.39}$$

In particular, for all $\mathbf{Q}$ *whose nullspace is spanned exactly by these left eigenvectors it holds that*

$$\max_{\mathbf{X}^h} \; i_+\Big(\mathrm{sym}\{\mathbf{X}\}\Big) = n - i_-^r(\mathbf{A}) \; . \tag{6.40}$$

Proof. see Appendix B.2. □

Remark 6.4.1. The assumption in Theorem 6.4.2 that the algebraic and geometric multiplicity of all eigenvalues of $\mathbf{A}$ with nonpositive real parts is equal is of technical nature and made to simplify the proof.

For the choice of the design matrices we deduce the following result.

Theorem 6.4.3. *Given* $\mathbf{C}(\mathbf{x})$ *satisfying Assumption 6.4.1, there exist matrices* $\mathbf{F}_1(\mathbf{x})$ *and* $\mathbf{F}_2(\mathbf{x})$ *with* $\mathbf{F}_2^\nu(\mathbf{x}) = \mathbf{C}(\mathbf{x})\mathbf{F}_1^\nu(\mathbf{x})$ *such that both* $\mathbf{R}_1(\mathbf{x})$ *and* $\mathbf{R}_2(\mathbf{x})$ *are positive semidefinite and it holds that*

$$\max \; i_+\Big(\mathbf{R}_p(\mathbf{x})\Big) = n - i_-^r\Big(\mathbf{C}(\mathbf{x})\Big) \; , \quad p \in \{1, 2\} \; . \tag{6.41}$$

Proof. In the sequel, let $\mathbf{X}(\mathbf{x}) = -\mathbf{F}_1^D(\mathbf{x})$. From Lemma 6.4.1 we known that $\mathbf{R}_p(\mathbf{x}) \geq 0$, $p \in \{1, 2\}$ is possible if and only if $\mathbf{X}(\mathbf{x}) + \mathbf{X}^T(\mathbf{x}) \geq 0$ and

$$\mathbf{C}(\mathbf{x})\mathbf{X}(\mathbf{x}) + \mathbf{X}^T(\mathbf{x})\mathbf{C}^T(\mathbf{x}) = \mathbf{Q}(\mathbf{x}) \tag{6.42}$$

are satisfied for a $\mathbf{Q}(\mathbf{x}) \geq 0$. It is trivial to establish that such matrices always exist, take e.g. $\mathbf{X} = \mathbf{0}$, $\mathbf{Q} = \mathbf{0}$. With $\mathbf{X} = -\mathbf{F}_1^D$ and (6.32), (6.42), we find that $\mathbf{R}_2^D = \frac{1}{2}[\mathbf{C}\mathbf{X} + \mathbf{X}^T\mathbf{C}^T] = \frac{1}{2}\mathbf{Q}$. Hence, we conclude from Theorem 6.4.2 that a solution $\mathbf{X}$ with $\mathbf{X}+\mathbf{X}^T \geq 0$ exists if and only if all left eigenvectors of $\mathbf{C}$ corresponding to real non-positive eigenvalues are contained in $\mathcal{N}\{\mathbf{R}_2^D\}$. By Assumption 6.4.1, the matrix $\mathbf{C}$ has full rank and thus no zero eigenvalues. For this reason, it holds that $\max i_+(\mathbf{R}_2^D) = (n-m) - i_-^r(\mathbf{C})$. Furthermore, it follows from Theorem 6.4.2 that the maximum number of positive eigenvalues of $\mathbf{R}_1^D = \frac{1}{2}(\mathbf{X} + \mathbf{X}^T)$ is also given by $\max i_+(\mathbf{R}_1^D) = (n-m) - i_-^r(\mathbf{C})$. Since $\mathbf{R}_p^A$ and $\mathbf{R}_p^B$, $p \in \{1, 2\}$ can be chosen freely via $\mathbf{F}_p^\alpha$ (c.f. (6.31), (6.32)), the assertion follows with Lemma 6.4.2. □

The following corollary is an immediate consequence of Theorem 6.4.3.

Corollary 6.4.1. *Given* $\mathbf{C}(\mathbf{x})$ *satisfying Assumption 6.4.1, there exist matrices* $\mathbf{F}_1(\mathbf{x})$ *and* $\mathbf{F}_2(\mathbf{x})$ *with* $\mathbf{F}_2^\nu(\mathbf{x}) = \mathbf{C}(\mathbf{x})\mathbf{F}_1^\nu(\mathbf{x})$ *such that both* $\mathbf{R}_1(\mathbf{x})$ *and* $\mathbf{R}_2(\mathbf{x})$ *are positive definite, if and only if* $i_-^r(\mathbf{C}(\mathbf{x})) = 0$.

6.4.4 Construction of the Design Matrices

In order to obtain suitable design matrices $\mathbf{F}_p(\mathbf{x})$, $p \in \{1, 2\}$ with $\mathbf{R}_p(\mathbf{x}) \geq 0$, $p \in \{1, 2\}$ we need to determine a matrix $\mathbf{X}(\mathbf{x}) = -\mathbf{F}_1^D(\mathbf{x})$ which satisfies $\mathrm{sym}\{\mathbf{X}(\mathbf{x})\} \geq 0$ and (6.37) for a positive semidefinite matrix $\mathbf{Q}(\mathbf{x})$. As the matrix $\mathbf{F}_1^\nu(\mathbf{x})$ has to be chosen such that the projected matching equations are solvable, and it is desired to tune the controller by varying the parameters in the design matrices, our objective is to construct not only one such matrix but a whole set of admissible matrices.

Since, by assumption, $\mathbf{C}(\mathbf{x})$ is a regular matrix, the equation (6.37) has an infinite number of solutions of the form $\mathbf{X}(\mathbf{x}) = \mathbf{X}^p(\mathbf{x}) + \mathbf{X}^h(\mathbf{x})$ with a particular solution $\mathbf{X}^p(\mathbf{x})$ and the solution

$$\mathbf{X}^h(\mathbf{x}) = \mathbf{U}(\mathbf{x})\mathbf{C}^T(\mathbf{x}) \tag{6.43}$$

of the corresponding homogeneous matrix equation $\mathbf{C}\mathbf{X} + \mathbf{X}^T\mathbf{C}^T = \mathbf{0}$, where $\mathbf{U}(\mathbf{x}) = -\mathbf{U}^T(\mathbf{x})$ can be chosen arbitrary (see Theorem 6.4.1). Moreover, there is of course an infinite number of positive semidefinite matrices $\mathbf{Q}(\mathbf{x})$.

As we have already seen in Section 4.1, we can obtain a set of positive semidefinite matrices utilizing that, given an upper triangular matrix $\mathbf{T}(\mathbf{x})$, it holds that $\mathbf{Q}(\mathbf{x}) = \mathbf{T}^T(\mathbf{x})\mathbf{T}(\mathbf{x}) \geq 0$. Similar to the $\mathbf{R}_{ij}$ in Section 4.1, let us define matrices $\mathbf{Q}_{ij} \in \mathbb{R}^{(n-m)\times(n-m)}$, $i = 1, \ldots, n-m$, $j = i, \ldots, n-m$ with all entries equal to zero except for the ith entry in the jth row and the jth entry in the ith row, which are both equal to one. Then, all matrices given by

$$\mathbf{Q}(\mathbf{x}) = \sum_{i=1}^{n-m} \sum_{j=i}^{n-m} \sum_{k=1}^{i} k_{ki}(\mathbf{x}) k_{kj}(\mathbf{x}) \mathbf{Q}_{ij} \tag{6.44}$$

with arbitrary functions $k_{ij} : \mathbb{R}^n \to \mathbb{R}$ are positive semidefinite. For a more detailed derivation the reader is referred to Section 4.1.

Now let $\mathbf{X}_{ij}^p(\mathbf{x}) : \mathbb{R}^n \to \mathbb{R}^{(n-m)\times(n-m)}$ be a particular solution of (6.37) for $\mathbf{Q}(\mathbf{x}) = \mathbf{Q}_{ij}$. Since $\mathbf{C}(\mathbf{x})$ has been assumed to be a regular matrix, solvability is guaranteed by Theorem 6.4.1. Then, due to linearity of the matrix equation (6.37)

$$\mathbf{X}^p(\mathbf{x}) = \sum_{i=1}^{n-m} \sum_{j=i}^{n-m} \sum_{k=1}^{i} k_{ki}(\mathbf{x}) k_{kj}(\mathbf{x}) \mathbf{X}_{ij}^p(\mathbf{x}) \tag{6.45}$$

represents a set of particular solutions to (6.37) for all $\mathbf{Q}(\mathbf{x})$ in (6.44). By adding the homogeneous solution (6.43), we finally obtain a set of matrices satisfying $\operatorname{sym}\{\mathbf{C}(\mathbf{x})\mathbf{X}(\mathbf{x})\} \geq 0$ as

$$\mathbf{X}(\mathbf{x}) = \underbrace{\sum_{i=1}^{n-m} \sum_{j=i}^{n-m} \sum_{k=1}^{i} k_{ki}(\mathbf{x}) k_{kj}(\mathbf{x}) \mathbf{X}_{ij}^p(\mathbf{x})}_{\mathbf{X}^p(\mathbf{x})} + \underbrace{\mathbf{U}(\mathbf{x})\mathbf{C}^T(\mathbf{x})}_{\mathbf{X}^h(\mathbf{x})} . \tag{6.46}$$

Unfortunately, in general, nothing can be said about the definiteness of the symmetric part of the solutions (6.45) and (6.46). In order to ensure that $\operatorname{sym}\{\mathbf{X}(\mathbf{x})\} \geq 0$, we have to formulate conditions for the functions $k_{ij}(\mathbf{x})$ and $\mathbf{U}(\mathbf{x})$ or, in particular, for their parameters, e.g. by means of Sylvester's criterion. Note that, if we have $i_-^r(\mathbf{C}(\mathbf{x})) = 0$, according to the last part of Theorem 6.4.2, positive semidefiniteness of $\operatorname{sym}\{\mathbf{X}(\mathbf{x})\}$ can always be achieved independently of the $k_{ij}(\mathbf{x})$ in (6.44) and (6.46) by a suitable choice of the homogeneous solution (6.43). In the following, two special cases concerning the location of the eigenvalues of $\mathbf{C}(\mathbf{x})$ are discussed.

If the eigenvalues of $\mathbf{C}(\mathbf{x})$ satisfy $\lambda_i + \lambda_j^* \neq 0, \ \forall\, i, j$, then the Lyapunov equation

$$\mathbf{C}(\mathbf{x})\mathbf{X}_{ij}^p(\mathbf{x}) + \mathbf{X}_{ij}^p(\mathbf{x})\mathbf{C}^T(\mathbf{x}) = \mathbf{Q}_{ij} \tag{6.47}$$

has a unique symmetric solution $\mathbf{X}_{ij}^p(\mathbf{x}) = (\mathbf{X}_{ij}^p(\mathbf{x}))^T$ [3]. This means that we can choose

symmetric matrices $\mathbf{X}_{ij}^p(\mathbf{x})$, which implies that all particular solutions in (6.45) are symmetric and satisfy a Lyapunov equation

$$\mathbf{C}(\mathbf{x})\mathbf{X}^p(\mathbf{x}) + \mathbf{X}^p(\mathbf{x})\mathbf{C}^T(\mathbf{x}) = \mathbf{Q}(\mathbf{x}) \geq 0\,. \tag{6.48}$$

In case that the pair $[\mathbf{C}(\mathbf{x}), \mathbf{Q}(\mathbf{x})]$ is point-wise controllable in the linear sense, it follows from Theorem 6.19 in [3] that $i_\pm(\mathbf{X}^p(\mathbf{x})) = i_\pm(\mathbf{C}(\mathbf{x}))$.

Hence, if all eigenvalues of $\mathbf{C}(\mathbf{x})$ are located in the right half plane, we conclude that $\mathbf{X}^p(\mathbf{x}) = (\mathbf{X}^p(\mathbf{x}))^T > 0$. The controllability condition is trivially satisfied if the functions $k_{ij}(\mathbf{x})$ are chosen such that $\mathbf{Q}(\mathbf{x})$ in (6.44) is positive definite, i.e., $k_{ii} \neq 0,\ \forall\, i$. Nevertheless, for the solutions $\mathbf{X}(\mathbf{x})$ in (6.46), in general, we only can say that $\mathrm{sym}\{\mathbf{X}(\mathbf{x})\} \geq 0$ holds for sufficiently small $\mathbf{U}(\mathbf{x})$, unless the latter matrix can be chosen such that $\mathrm{sym}\{\mathbf{X}^h(\mathbf{x})\} \geq 0$.

Example 6.4.1. Consider the matrix

$$\mathbf{C} = \begin{bmatrix} 1 & 0 \\ 3 & 1 \end{bmatrix} \tag{6.49}$$

with both eigenvalues equal to 1 and thus located in the right halfplane. By solving (6.37) with $\mathbf{X}_{ij}^p(\mathbf{x}) = (\mathbf{X}_{ij}^p(\mathbf{x}))^T$, or equivalently (6.47), for the right hand sides $\mathbf{Q}_{11}$, $\mathbf{Q}_{12}$, $\mathbf{Q}_{22}$ we obtain the matrices

$$\mathbf{X}_{11}^p = \begin{bmatrix} \frac{1}{2} & -\frac{3}{4} \\ -\frac{3}{4} & \frac{9}{4} \end{bmatrix},\ \mathbf{X}_{22}^p = \begin{bmatrix} 0 & 0 \\ 0 & \frac{1}{2} \end{bmatrix},\ \mathbf{X}_{12}^p = \begin{bmatrix} 0 & \frac{1}{2} \\ \frac{1}{2} & -\frac{3}{2} \end{bmatrix}. \tag{6.50}$$

The homogeneous solution (6.43) is given by

$$\mathbf{X}^h = \begin{bmatrix} 0 & \rho \\ -\rho & 0 \end{bmatrix} \mathbf{C}^T = \begin{bmatrix} 0 & \rho \\ -\rho & -3\rho \end{bmatrix}. \tag{6.51}$$

Then, according to (6.46), the general solution of (6.37) can be formulated as

$$\begin{aligned} \mathbf{X} &= k_{11}^2 \mathbf{X}_{11}^p + \left(k_{22}^2 + k_{12}^2\right) \mathbf{X}_{22}^p + k_{12}k_{11}\mathbf{X}_{12}^p + \mathbf{X}^h \\ &= \begin{bmatrix} -\frac{1}{2}k_{11}^2 & \frac{3}{4}k_{11}^2 - \frac{1}{2}k_{12}k_{11} - \rho \\ \frac{3}{4}k_{11}^2 - \frac{1}{2}k_{12}k_{11} + \rho & -\frac{9}{4}k_{11}^2 - \frac{1}{2}k_{22}^2 - \frac{1}{2}k_{12}^2 + \frac{3}{2}k_{12}k_{11} + 3\rho \end{bmatrix}. \end{aligned} \tag{6.52}$$

Obviously, the symmetric portion of the homogeneous solution

$$\mathrm{sym}\{\mathbf{X}^h\} = \mathrm{diag}\,\{[0\ \ -3\rho]\} \tag{6.53}$$

is negative semidefinite for $\rho > 0$ and hence ρ has to be sufficiently small in order to guarantee $\mathbf{X} + \mathbf{X}^T \geq 0$. Using Sylvester's criterion we derive the condition

$$24\rho < 9k_{11}^2 + 4k_{22}^2 \,. \tag{6.54}$$

For positive definiteness, additionally k_{11} has to be different from zero.

Next, we consider the case that $\mathbf{C}(\mathbf{x})$ has only *complex-valued* eigenvalues in the *left* half plane. We know from Theorem 6.4.2 that positive semidefiniteness of $\mathrm{sym}\{\mathbf{X}(\mathbf{x})\}$ is possible. However, using the same arguments as in the previous case, we conclude that $\mathbf{X}^p(\mathbf{x})$ is negative definite, if the controllability condition is fulfilled. Consequently, $\mathrm{sym}\{\mathbf{X}(\mathbf{x})\} \geq 0$ can only be achieved by a suitable choice of $\mathbf{U}(\mathbf{x})$ which guarantees that $\mathrm{sym}\{\mathbf{X}^h(\mathbf{x})\}$ is positive definite and sufficiently large.

Example 6.4.2. Consider the matrix

$$\mathbf{C} = \begin{bmatrix} -1 & 1 \\ -1 & 0 \end{bmatrix} \tag{6.55}$$

with the eigenvalues $\lambda_{1,2} = -\frac{1}{2} \pm i\frac{1}{2}\sqrt{3}$. Similar to Example 6.4.1 above we determine the set of particular solutions (6.45) as

$$\mathbf{X}^p = (\mathbf{X}^p)^T = \begin{bmatrix} -\frac{1}{2}(k_{11}^2 + k_{22}^2 + k_{12}^2) & -\frac{1}{2}(k_{22}^2 + k_{12}^2) \\ -\frac{1}{2}(k_{22}^2 + k_{12}^2) & -\frac{1}{2}k_{11}^2 - k_{22}^2 - k_{12}^2 + k_{12}k_{11} \end{bmatrix} \tag{6.56}$$

and we assume that $k_{11}, k_{22} \neq 0$ to ensure $\mathbf{Q} > 0$. The homogeneous solution and its symmetric portion are given by

$$\mathbf{X}^h = \begin{bmatrix} \rho & 0 \\ \rho & \rho \end{bmatrix} \,, \quad \mathrm{sym}\{\mathbf{X}^h\} = \begin{bmatrix} \rho & \frac{1}{2}\rho \\ \frac{1}{2}\rho & \rho \end{bmatrix} . \tag{6.57}$$

It can be seen that $\mathbf{X}^p$ is indeed a negative definite matrix as both diagonal entries are negative and their absolute value is greater than that of the off-diagonal entries. However, the symmetric portion of $\mathbf{X}^h$ is positive definite for all $\rho > 0$. As a consequence, we can achieve positive definiteness of $\mathrm{sym}\{\mathbf{X}\} = \mathbf{X}^p + \mathrm{sym}\{\mathbf{X}^h\}$ for all k_{ij} by choosing $\rho > 0$ sufficiently large.

6.4.5 Systematic Procedure

After we have determined a set of suitable matrices $\mathbf{X}(\mathbf{x})$, the matrix $\mathbf{F}_1^\nu(\mathbf{x})$ is chosen as $\mathbf{F}_1^\nu(\mathbf{x}) = [\mathbf{F}_1^C(\mathbf{x}),\ -\mathbf{X}(\mathbf{x})]$. Then, with some modifications, the systematic procedure, that

has been proposed in [102], [103] for the design of (non-switched) IDA controllers (see Section 2.3.1), can be applied to determine the feedback functions $\mathbf{r}_1(\mathbf{x})$ and $\mathbf{r}_2(\mathbf{x})$. This is outlined in the following.

Step 1: Solvability of the matching equation The structure of the functions $\mathbf{F}_1^C(\mathbf{x})$, $k_{ij}(\mathbf{x})$ and $\mathbf{U}(\mathbf{x})$ has to be chosen such that the projected matching equation (6.26) is solvable according to Theorem 2.2.2. This is especially simple if the structure of the functions can be chosen such that (at least) one of the two matrices $\mathbf{F}_1^\nu(\mathbf{x})$, $\mathbf{F}_2^\nu(\mathbf{x})$ is constant. In this case, according to Proposition 2.2.1, checking the solvability of the projected matching equation (6.25) reduces to verifying that

$$\frac{\partial}{\partial \mathbf{x}} f_{k,i}^\nu(\mathbf{x}) \boldsymbol{\nu}_{k,j} - \frac{\partial}{\partial \mathbf{x}} f_{k,j}^\nu(\mathbf{x}) \boldsymbol{\nu}_{k,i} = 0 \tag{6.58}$$

for all $i, j = 1, \ldots, n-m$, where k is the index of the constant design matrix $\mathbf{F}_k^\nu$ and $\boldsymbol{\nu}_{k,i}$ is the ith column of $(\mathbf{F}_k^\nu)^T$. From this condition, constraints for the (constant) entries of $\mathbf{F}_k^\nu$ can be easily derived.

Step 2: Positive Semidefiniteness of $\mathbf{R}_p(\mathbf{x})$ In this step, conditions are formulated for $\mathbf{F}_1(\mathbf{x})$, $\mathbf{F}_2(\mathbf{x})$ in order to guarantee $\mathbf{R}_p(\mathbf{x}) \geq 0$, $p \in \{1, 2\}$. To this end, we first derive conditions to ensure that $\mathbf{R}_1^D(\mathbf{x}) = \operatorname{sym}\{\mathbf{X}(\mathbf{x})\} \geq 0$ (see the discussion in the previous subsection). Positive semidefiniteness of $\mathbf{R}_2^D(\mathbf{x}) = \frac{1}{2}\mathbf{Q}(\mathbf{x})$ is guaranteed by construction. Subsequently, we formulate conditions for $\mathbf{F}_1^C(\mathbf{x})$, $\mathbf{F}_1^\alpha(\mathbf{x})$ and $\mathbf{F}_2^\alpha(\mathbf{x})$ in order to ensure that the dissipation matrices are positive semidefinite. For this task, the following result can be used, which is an immediate consequence of Proposition A.2.1 and Theorem A.2.1 in Appendix A.2.

Proposition 6.4.1. *If $\mathbf{R}_p^D > 0$, then $\mathbf{R}_p > 0$ if and only if*

$$\mathbf{R}_p^A - \mathbf{R}_p^B \left(\mathbf{R}_p^D\right)^{-1} \left(\mathbf{R}_p^B\right)^T > 0 \,. \tag{6.59}$$

If $\mathbf{R}_p^D \geq 0$, then $\mathbf{R}_p \geq 0$ if and only if

$$\left(\mathbf{I} - \mathbf{R}_p^D \left(\mathbf{R}_p^D\right)^\dagger\right) \left(\mathbf{R}_p^B\right)^T = \mathbf{0} \,, \tag{6.60a}$$

$$\mathbf{R}_p^A - \mathbf{R}_p^B \left(\mathbf{R}_p^D\right)^\dagger \left(\mathbf{R}_p^B\right)^T \geq 0 \,. \tag{6.60b}$$

The condition (6.59) allows to verify the positive definiteness of the $n \times n$ matrix $\mathbf{R}_p$ by checking the positive definiteness of a smaller $m \times m$-dimensional matrix. In the case of

positive semidefiniteness, the additional condition (6.60a) appears. But this is an equality constraint, which is much easier to handle than inequality constraints as they arise from the application of Sylvester's criterion. Note that the conditions of Proposition 6.4.1 can be satisfied by choosing the matrices $\mathbf{F}_p^\alpha(\mathbf{x})$ as in the proof of Lemma 6.4.1.

Step 3: Solving the matching PDE In this step, the projected matching equation (6.26) is solved, where we can choose either $p = 1$ or $p = 2$ depending on which PDE is easier to handle. This yields the set of common energy functions $H(\mathbf{x}) = \Psi(\mathbf{x}) + \phi(\boldsymbol{\xi}(\mathbf{x}))$ which can be assigned to the closed-loop system.

Step 4: Controller tuning The parameters in $\mathbf{F}_1^\nu(\mathbf{x})$ and the function $\phi(\boldsymbol{\xi}(\mathbf{x}))$ are chosen such that (2.27) holds, guaranteeing a strict local minimum of $H(\mathbf{x})$ at $\mathbf{x}^*$. The parameters in $\mathbf{F}_1^\alpha(\mathbf{x})$ and $\mathbf{F}_2^\alpha(\mathbf{x})$ as well as the remaining degrees of freedom in $\mathbf{F}_1^\nu(\mathbf{x})$ are used to optimize the controller performance or to enlarge the estimated DA. For estimating and enlarging the DA, the algorithms presented in Part I of the thesis can be applied verbatim.

6.4.6 The case $m_1 \neq m_2$

The procedure described above can be readily transferred to systems of the form (6.23) with $m_1 \neq m_2$, where we assume without loss of generality that $m_1 < m_2$. Analogously to Assumption 6.4.1, we assume that there is a full rank matrix $\mathbf{C} : \mathbb{R}^n \to \mathbb{R}^{(n-m_2)\times(n-m_1)}$ such that $\mathbf{f}_2^\nu(\mathbf{x}) = \mathbf{C}(\mathbf{x})\mathbf{f}_1^\nu(\mathbf{x})$ holds in some neighborhood of the desired equilibrium $\mathbf{x}^*$. As in the previous case, we choose $\mathbf{F}_2^\nu(\mathbf{x}) = \mathbf{C}(\mathbf{x})\mathbf{F}_1^\nu(\mathbf{x})$. The set of admissible energy functions has to be determined from (6.26) with $p = 1$. For what follows, we introduce a partitioning of the submatrix $\mathbf{F}_1^D(\mathbf{x})$ according to

$$\mathbf{F}_1^D(\mathbf{x}) = \begin{bmatrix} \mathbf{F}_1^{DA}(\mathbf{x}) & \mathbf{F}_1^{DB}(\mathbf{x}) \\ \mathbf{F}_1^{DC}(\mathbf{x}) & \mathbf{F}_1^{DD}(\mathbf{x}) \end{bmatrix} \tag{6.61}$$

with $\mathbf{F}_1^{DD} : \mathbb{R}^n \to \mathbb{R}^{(n-m_2)\times(n-m_2)}$. Using similar arguments as in the proof of Lemma 6.4.1, it follows that positive semi-definiteness of both dissipation matrices is possible if and only if $\operatorname{sym}\{\mathbf{F}_1^D\} \leq 0$ and

$$\mathbf{C}(\mathbf{x}) \begin{bmatrix} \mathbf{F}_1^{DB}(\mathbf{x}) \\ \mathbf{F}_1^{DD}(\mathbf{x}) \end{bmatrix} + \begin{bmatrix} \left(\mathbf{F}_1^{DB}(\mathbf{x})\right)^T & \left(\mathbf{F}_1^{DD}(\mathbf{x})\right)^T \end{bmatrix} \mathbf{C}^T(\mathbf{x}) = \mathbf{Q}(\mathbf{x}) \tag{6.62}$$

hold for some $\mathbf{Q}(\mathbf{x}) \geq 0$. Hence, in order to construct a set of suitable matrices $\mathbf{F}_1^D$, we need to determine a general solution to the matrix equation (6.37), where, in contrast to the case before, $\mathbf{C}$ and $\mathbf{X} = -[(\mathbf{F}_1^{DB})^T\ (\mathbf{F}_1^{DD})^T]^T$ are not quadratic. This can be done following the same procedure as described in Subsection 6.4.4. According to Corollary 3.2 in [169], the solutions $\mathbf{X}_{ij}^p(\mathbf{x})$ for the right hand sides $\mathbf{Q}_{ij}$, $i = 1, \ldots, n-m_2$, $j = i, \ldots, n-m_2$ exist. The homogeneous solution $\mathbf{X}^h$ is also given in [169]. The general solution is then

$$\mathbf{X}(\mathbf{x}) = \underbrace{\sum_{i=1}^{n-m} \sum_{j=i}^{n-m_2} \sum_{k=1}^{i} k_{ki}(\mathbf{x}) k_{kj}(\mathbf{x}) \mathbf{X}_{ij}^p(\mathbf{x})}_{\mathbf{X}^p(\mathbf{x})} + \underbrace{\mathbf{U}(\mathbf{x})\mathbf{C}^T(\mathbf{x}) + \left(\mathbf{I} - \mathbf{C}^\dagger(\mathbf{x})\mathbf{C}(\mathbf{x})\right)\mathbf{V}(\mathbf{x})}_{\mathbf{X}^h(\mathbf{x})} \tag{6.63}$$

with both $\mathbf{U}(\mathbf{x}) = -\mathbf{U}^T(\mathbf{x})$ and $\mathbf{V}(\mathbf{x})$ arbitrary. In comparison to (6.46), the only difference occurs in the homogeneous solution. In order to guarantee that $\mathrm{sym}\{\mathbf{F}_1^D\} \leq 0$, Sylvester's criterion is used.

6.5 Controller Design for SPH-Systems

The controller design can simplify considerably, if the plant model (6.7) is already given in spH form with a common energy function, i.e., if the drift vector fields have the special form

$$\mathbf{f}_p(\mathbf{x}) = \mathbf{F}_p(\mathbf{x})\nabla H(\mathbf{x}) , \quad p \in \mathcal{P} \tag{6.64}$$

with $\mathrm{sym}\{\mathbf{F}_p(\mathbf{x})\} \leq 0$ and $\mathrm{rank}\{\mathbf{F}_p(\mathbf{x})\} = n$. This is the case, when energy-based techniques have been applied to build the model (see e.g. [90], [46]) and the switching is due to changes in the interconnection and damping structure. Since the minimum of the open loop energy function is usually not the desired equilibrium point, control action is added to stabilize the switched system at the operating point of interest. Moreover, it is desired to improve the transient behavior and hence the performance of the system. For the controller design, we again utilize Theorem 6.3.1. We leave the interconnection and dissipation matrices unchanged and only intend to shape the energy in order to achieve the control objectives. This obviates the nontrivial step of constructing suitable design matrices and leads to a generalization of the so called basic IDA approach (see e.g. [139]) to the class of spH systems, which is stated in the following corollary of Theorem 6.3.1.

Corollary 6.5.1. *Assume that the switched system* (6.7) *is given in spH form, i.e., the drift vector fields are of the form* (6.64)*, and that there is a function* $H_a : \mathbb{R}^n \to \mathbb{R}$ *such*

that

$$\begin{bmatrix} \mathbf{G}_1^{\perp}(\mathbf{x})\mathbf{F}_1(\mathbf{x}) \\ \vdots \\ \mathbf{G}_N^{\perp}(\mathbf{x})\mathbf{F}_N(\mathbf{x}) \end{bmatrix} \nabla H_a(\mathbf{x}) = \mathbf{0} \tag{6.65}$$

and $H_d(\mathbf{x}) = H(\mathbf{x}) + H_a(\mathbf{x})$ *has a strict local minimum at the desired equilibrium* $\mathbf{x}^*$*. Then the control* $u = \mathbf{G}_\sigma^\dagger(\mathbf{x})\mathbf{F}_\sigma(\mathbf{x})\nabla H_a(\mathbf{x})$ *transforms* (6.7), (6.64) *into* $\dot{\mathbf{x}} = \mathbf{F}_\sigma(\mathbf{x})\nabla H_d(\mathbf{x})$ *and* $\mathbf{x}^*$ *is a uniformly stable equilibrium.*

We assume, without loss of generality, that $m_1 \leq m_p$, $p \in \mathcal{P}$. Since the matrices $\mathbf{F}_p(\mathbf{x})$ are regular, it follows from the Frobenius Theorem 2.2.1 that the maximum number of independent solutions of (6.65) is m_1. In order that the number of characteristic coordinates is indeed equal to m_1, which yields maximum freedom for the energy shaping, it is necessary that there are full rank matrices $\mathbf{K}_p : \mathbb{R}^n \to \mathbb{R}^{(n-m_p)\times(n-m_1)}$ such that

$$\mathbf{G}_p^{\perp}(\mathbf{x})\mathbf{F}_p(\mathbf{x}) = \mathbf{K}_p(\mathbf{x})\mathbf{G}_1^{\perp}(\mathbf{x})\mathbf{F}_1(\mathbf{x}) \;, \quad p \in \mathcal{P} \;. \tag{6.66}$$

In order that $\mathbf{x}^*$ is an equilibrium of the closed loop system, the function $H_a(\mathbf{x})$ has to be chosen such that $\nabla H_d(\mathbf{x}^*) = \mathbf{0}$. For the case that (6.65) is solvable with the maximum number of characteristic coordinates, i.e., $\boldsymbol{\xi} : \mathbb{R}^n \to \mathbb{R}^{m_1}$, we have the following result.

Proposition 6.5.1. *Given a desired equilibrium point* $\mathbf{x}^* \in \mathcal{E}$*, assume that* (6.65) *possesses* m_1 *independent solutions subsumed in the vector-valued function* $\boldsymbol{\xi}(\mathbf{x})$ *and let*

$$H_a(\mathbf{x}) = \frac{1}{2}\left[\boldsymbol{\xi}(\mathbf{x}) - \mathbf{c}\right]^T \mathbf{K}_a \left[\boldsymbol{\xi}(\mathbf{x}) - \mathbf{c}\right] \tag{6.67}$$

with $\mathbf{K}_a > 0$ *and* $\mathbf{c} = \boldsymbol{\xi}(\mathbf{x}^*) + \mathbf{K}_a^{-1}(\nabla\boldsymbol{\xi}(\mathbf{x}^*))^\dagger \nabla H(\mathbf{x}^*)$*. Then,* $\mathbf{x}^*$ *is an equilibrium of the closed loop system* $\dot{\mathbf{x}} = \mathbf{F}_\sigma(\mathbf{x})\nabla H_d(\mathbf{x})$*.*

Proof. First, we observe that $\nabla H(\mathbf{x}^*) \in \mathcal{R}\{\nabla\boldsymbol{\xi}(\mathbf{x}^*)\}$, which can be seen as follows. It holds that $\mathbf{G}_1^{\perp}\mathbf{F}_1\nabla\boldsymbol{\xi} = \mathbf{0}$. Since $\mathbf{G}_1^{\perp}$ and $\mathbf{F}_1$ are both full rank matrices, also $\mathbf{G}_1^{\perp}\mathbf{F}_1 \in \mathbb{R}^{(n-m_1)\times n}$ has full rank and thus an m_1-dimensional nullspace. Since the m_1 columns of $\nabla\boldsymbol{\xi}$ are linearly independent, they clearly span the nullspace of $\mathbf{G}_1^{\perp}\mathbf{F}_1$. Moreover, as $\mathbf{x}^* \in \mathcal{E}$ it holds that $\mathbf{G}_1^{\perp}\mathbf{F}_1\nabla H(\mathbf{x}^*) = \mathbf{0}$ and thus $\nabla H(\mathbf{x}^*) \in \mathcal{N}\{\mathbf{G}_1^{\perp}(\mathbf{x}^*)\mathbf{F}_1(\mathbf{x}^*)\} = \mathcal{R}\{\nabla\boldsymbol{\xi}(\mathbf{x}^*)\}$.

With the choice (6.67) we calculate

$$\nabla H_d(\mathbf{x}^*) = \nabla H(\mathbf{x}^*) + \nabla H_a(\mathbf{x}^*) = \nabla H(\mathbf{x}^*) - \nabla\boldsymbol{\xi}(\mathbf{x}^*)(\nabla\boldsymbol{\xi}(\mathbf{x}^*))^\dagger \nabla H(\mathbf{x}^*) \;. \tag{6.68}$$

Since $\nabla\boldsymbol{\xi}(\nabla\boldsymbol{\xi})^\dagger$ is the orthogonal projector onto $\mathcal{R}\{\nabla\boldsymbol{\xi}\}$ and $\nabla H(\mathbf{x}^*) \in \mathcal{R}\{\nabla\boldsymbol{\xi}(\mathbf{x}^*)\}$, it readily follows that $\nabla H_d(\mathbf{x}^*) = \mathbf{0}$. □

Additionally, it has to be verified, of course, that the choice (6.67) renders $\mathbf{x}^*$ a strict local minimum of $H_d(\mathbf{x})$, i.e., that, for instance, $\nabla^2 H_d(\mathbf{x}^*) > 0$.

6.6 Some Extensions

In practical engineering, one usually has to deal with modeling errors and unknown disturbances acting on the system, which can cause the closed loop system to behave in an undesirable way, e.g. they may result in a steady state deviation from the desired equilibrium point. An advantage of the control scheme proposed in this chapter is that it can be extended in a quite straightforward manner to include *integral* and *adaptive control* while preserving the closed loop spH structure. By these means, we are able to compensate for model uncertainties and/or disturbances and, in this way, to increase the robustness of the control system.

6.6.1 Integral Control

It is well known for (non-switched) pH systems that regulation of the passive output and rejection of constant input disturbances can be achieved by adding integral control of the passive output [135]. In [45], this concept is transferred to the closely related class of Brayton-Moser models. Based on these ideas, we extend Theorem 6.3.1 in order to allow for integral control of the switched system (6.7).

Proposition 6.6.1. *Consider the switched nonlinear system* (6.7) *with* $m_p = m$, $p \in \mathcal{P}$ *and a constant input disturbance* $\mathbf{d} \in \mathbb{R}^m$

$$\dot{\mathbf{x}} = \mathbf{f}_\sigma(\mathbf{x}) + \mathbf{G}_\sigma(\mathbf{x})(\mathbf{u} + \mathbf{d}) \,, \quad \sigma \in \mathcal{S} \,. \tag{6.69}$$

Assume that there are matrices $\mathbf{F}_p(\mathbf{x}) = \mathbf{J}_p(\mathbf{x}) - \mathbf{R}_p(\mathbf{x})$, $p \in \mathcal{P}$ *and a function* $H(\mathbf{x})$ *satisfying the conditions of Theorem 6.3.1 for the desired equilibrium* $\mathbf{x}^* \in \mathcal{E}$. *Moreover, suppose the control law*

$$\begin{aligned} \dot{\boldsymbol{\eta}} &= \mathbf{K}_I \mathbf{G}_\sigma^T(\mathbf{x}) \nabla H(\mathbf{x}) \\ \mathbf{u} &= \mathbf{r}_\sigma(\mathbf{x}) = \left[\mathbf{G}_\sigma^T(\mathbf{x})\mathbf{G}_\sigma(\mathbf{x})\right]^{-1} \mathbf{G}_\sigma^T(\mathbf{x}) \left[\mathbf{F}_\sigma(\mathbf{x})\nabla H(\mathbf{x}) - \mathbf{f}_\sigma(\mathbf{x})\right] - \boldsymbol{\eta} \end{aligned} \tag{6.70a}$$

with $\mathbf{K}_I$ *some constant positive definite matrix is applied to* (6.69). *Then the following holds.*

(i) The equilibrium $(\mathbf{x}^*, \mathbf{d})$ *is stable.*

(ii) If in a neighborhood $\Omega^R \subset \mathbb{R}^n$ *of* $\mathbf{x}^*$ *it holds that* $\mathbf{R}_p(\mathbf{x}) > 0$ *for all* $p \in \mathcal{P}$*, then there is a constant* $c > 0$ *such that*

$$\lim_{t\to\infty} \mathbf{x}(t) \to \mathbf{x}^* \tag{6.71}$$

for all $(\mathbf{x}(0), \boldsymbol{\eta}(0))$ *with* $\|(\mathbf{x}(0), \boldsymbol{\eta}(0)) - (\mathbf{x}^*, \mathbf{d})\| < c$.

Proof. If we define the new energy function

$$W(\mathbf{x}, \boldsymbol{\eta}) = H(\mathbf{x}) + \frac{1}{2} (\boldsymbol{\eta} - \mathbf{d})^T \mathbf{K}_I^{-1} (\boldsymbol{\eta} - \mathbf{d}) \tag{6.72}$$

the closed loop system (6.69), (6.70) can be represented in spH form

$$\begin{bmatrix} \dot{\mathbf{x}} \\ \dot{\boldsymbol{\eta}} \end{bmatrix} = \underbrace{\begin{bmatrix} \mathbf{F}_\sigma(\mathbf{x}) & -\mathbf{G}_\sigma(\mathbf{x})\mathbf{K}_I \\ \mathbf{K}_I \mathbf{G}_\sigma^T(\mathbf{x}) & \mathbf{0} \end{bmatrix}}_{\mathbf{F}_{I,\sigma}(\mathbf{x})} \nabla W(\mathbf{x}, \boldsymbol{\eta}) \; . \tag{6.73}$$

Since, by assumption, $H(\mathbf{x})$ possesses a strict local minimum at $\mathbf{x}^*$, clearly $(\mathbf{x}^*, \mathbf{d})$ is a strict local minimum of $W(\mathbf{x}, \boldsymbol{\eta})$. Moreover, it holds that $\mathbf{R}_{I,p} = -\mathrm{sym}\{\mathbf{F}_{I,p}\} \geq 0$, where $\mathbf{F}_{I,p}$ is defined in (6.73). Hence, (i) follows from Theorem 6.2.1.

In case that, for all $p \in \mathcal{P}$, the matrix $\mathbf{R}_p(\mathbf{x})$ is positive definite in some neighborhood $\Omega^R \subset \mathbb{R}^n$ of $\mathbf{x}^*$, there is $c > 0$ such that $\mathrm{S}_c^W(\mathbf{x}^*, \mathbf{d})$ is bounded and contained in $\Omega^R \times \mathbb{R}^m$, and it holds that

$$\begin{aligned} &\bigcup_{p\in\mathcal{P}} \left\{ (\mathbf{x}, \boldsymbol{\eta}) \in \mathrm{S}_c^W (\mathbf{x}^*, \mathbf{d}) \,\middle|\, \nabla^T W \mathbf{R}_{I,p} \nabla W = 0 \right\} = \\ &\bigcup_{p\in\mathcal{P}} \left\{ (\mathbf{x}, \boldsymbol{\eta}) \in \mathrm{S}_c^W (\mathbf{x}^*, \mathbf{d}) \,\middle|\, \nabla^T H \mathbf{R}_p \nabla H = 0 \right\} = \left\{ (\mathbf{x}, \boldsymbol{\eta}) \in \mathrm{S}_c^W (\mathbf{x}^*, \mathbf{d}) \,|\mathbf{x} = \mathbf{x}^* \right\} \; . \end{aligned} \tag{6.74}$$

Thus (ii) follows from Theorem 2.4.3 with $W_3(\mathbf{x}, \boldsymbol{\eta}) = \min_{\mathbf{x}} \nabla^T H \mathbf{R}_p \nabla H$. □

Of course, the results hold globally, if $H(\mathbf{x})$ is radially unbounded and all dissipation matrices $\mathbf{R}_p(\mathbf{x})$ are positive (semi-)definite for all $\mathbf{x} \in \mathbb{R}^n$. Moreover, note that Proposition 6.6.1 (ii) says nothing about the limit of $\boldsymbol{\eta}$ as $t \to \infty$. If we assume that $\sigma \in \mathcal{S}_{average}$, then the equilibrium $(\mathbf{x}^*, \mathbf{d})$ is asymptotically stable, which includes that $\boldsymbol{\eta} \to \mathbf{d}$ for $t \to \infty$. In case that $\sigma \in \mathcal{S}_{average}[\tau_D, N_0]$, the equilibrium $(\mathbf{x}^*, \mathbf{d})$ is uniformly asymptotically stable. This follows from Theorem 2.4.4 as every closed loop subsystem is zero-state small-time observable with the output $\mathbf{y} = -\nabla^T W \mathbf{R}_{I,p} \nabla W$. The latter is immediately seen by substituting $\mathbf{x} = \mathbf{x}^*$ into (6.73).

6.6.2 Adaptive Control

In case that there are parametric uncertainties in the model of the plant, adaptive control can be applied to compensate for the errors induced by the uncertain terms in the feedback functions. An adaptive controller for pH systems whose Hamiltonian depends linearly on some uncertain parameters is presented in [187]. A similar idea is used in [72] in combination with a Casimir function based energy shaping method for time-varying pH systems. The adaptive control scheme proposed in [152] allows both the interconnection and damping matrix as well as the Hamiltonian to depend on the perturbed parameters as long as a certain matching condition is satisfied. A very similar approach is also used in [178]. In [45], the power-based control method for Brayton-Moser equations, originally proposed in [133] and [65], is extended to include adaptive control. Inspired by the ideas in these papers, we expand in the following the result of Theorem 6.3.1 to obtain an adaptive control scheme for nonlinear switched systems (6.7).

We suppose that only the drift vector fields of (6.7) involve parametric uncertainties and that $m_p = m$, $p \in \mathcal{P}$, which means that the model is of the form

$$\dot{\mathbf{x}} = \mathbf{f}_\sigma(\mathbf{x}, \boldsymbol{\theta}) + \mathbf{G}_\sigma(\mathbf{x})\mathbf{u} \tag{6.75}$$

where $\boldsymbol{\theta} \in \Lambda \subset \mathbb{R}^s$ is an unknown constant vector denoting the parametric uncertainty, and the set Λ is such that it contains the origin. In case that $\boldsymbol{\theta} = \mathbf{0}$, the model (6.75) is equal to the nominal one.

Proposition 6.6.2. *Consider the system* (6.75)*. Assume that there are matrices* $\mathbf{F}_p(\mathbf{x}, \boldsymbol{\theta})$, $p \in \mathcal{P}$ *and a function* $H(\mathbf{x}, \boldsymbol{\theta})$ *satisfying the conditions of Theorem 6.3.1 for all* $\boldsymbol{\theta} \in \Lambda$*. Further, assume that the control law* (6.11) *can be represented in the form*

$$\mathbf{u} = \boldsymbol{\gamma}_\sigma(\mathbf{x}) + \boldsymbol{\Upsilon}_\sigma(\mathbf{x})\mathbf{z} \tag{6.76}$$

where $\boldsymbol{\gamma}_p : \mathbb{R}^n \to \mathbb{R}^m$ *and* $\boldsymbol{\Upsilon}_p : \mathbb{R}^n \to \mathbb{R}^{m \times l}$*,* $p \in \mathcal{P}$ *are known functions and* $\mathbf{z} \in \mathbb{R}^l$ *is an unknown constant vector related to* $\boldsymbol{\theta}$*. Now suppose the control law*

$$\dot{\hat{\mathbf{z}}} = -\mathbf{K}_z \boldsymbol{\Upsilon}_\sigma^T(\mathbf{x}) \mathbf{G}_\sigma^T(\mathbf{x}) \nabla H(\mathbf{x}, \boldsymbol{\theta}) \tag{6.77a}$$

$$u = \boldsymbol{\gamma}_\sigma(\mathbf{x}) + \boldsymbol{\Upsilon}_\sigma(\mathbf{x})\hat{\mathbf{z}} \tag{6.77b}$$

with $\hat{\mathbf{z}}$ *the estimate of* $\mathbf{z}$ *and* $\mathbf{K}_z$ *some constant positive definite matrix is applied to* (6.69)*. Then the following holds.*

(i) The equilibrium $(\mathbf{x}^*, \mathbf{z})$ *is stable.*

(ii) If in a neighborhood $\Omega^R \subset \mathbb{R}^n$ *of* $\mathbf{x}^*$ *it holds that* $\mathbf{R}_p(\mathbf{x}) > 0$ *for all* $p \in \mathcal{P}$*, then there is a constant* $c > 0$ *such that*

$$\lim_{t\to\infty} \mathbf{x}(t) \to \mathbf{x}^* \tag{6.78}$$

for all $(\mathbf{x}(0), \hat{\mathbf{z}}(0))$ *with* $\|(\mathbf{x}(0), \boldsymbol{\eta}(0)) - (\mathbf{x}^*, \mathbf{z})\| < c$.

Proof. The proof follows the same lines as the proof of Proposition 6.6.1. With the function

$$W = H(\mathbf{x}, \boldsymbol{\theta}) + \frac{1}{2} (\hat{\mathbf{z}} - \mathbf{z})^T \mathbf{K}_z^{-1} (\hat{\mathbf{z}} - \mathbf{z}) \tag{6.79}$$

we can express the closed loop system (6.75), (6.77) in spH form

$$\begin{bmatrix} \dot{\mathbf{x}} \\ \dot{\hat{\mathbf{z}}} \end{bmatrix} = \begin{bmatrix} \mathbf{F}_\sigma(\mathbf{x}, \boldsymbol{\theta}) & \mathbf{G}_\sigma(\mathbf{x}) \boldsymbol{\Upsilon}_p(\mathbf{x}) \mathbf{K}_z \\ -\mathbf{K}_z \boldsymbol{\Upsilon}_p^T(\mathbf{x}) \mathbf{G}_\sigma^T(\mathbf{x}) & \mathbf{0} \end{bmatrix} \nabla W(\mathbf{x}, \hat{\mathbf{z}}, \boldsymbol{\theta}) \; . \tag{6.80}$$

The rest of the proof is completely analogous to the proof of Proposition 6.6.1 and is therefore omitted. □

Requiring that the conditions of Theorem 6.3.1 are satisfied for all $\boldsymbol{\theta} \in \Lambda$ means that $\mathbf{R}_p(\mathbf{x}, \boldsymbol{\theta}) = -\text{sym}\{\mathbf{F}_p(\mathbf{x}, \boldsymbol{\theta})\} \geq 0$ holds for all $\boldsymbol{\theta} \in \Lambda$ and all $p \in \mathcal{P}$ and that $H(\mathbf{x}, \boldsymbol{\theta})$ has a strict local minimum in $\mathbf{x}^*$ for all $\boldsymbol{\theta} \in \Lambda$. Moreover, the information to evaluate the update law (6.77a) has to be available, i.e., either the expression has to be independent of $\boldsymbol{\theta}$ or the terms containing $\boldsymbol{\theta}$ must be known from the measurements. A case in which these requirements are satisfied is e.g. the one in which the parameter uncertainties are matched, i.e., there exist matrix valued functions $\boldsymbol{\Upsilon}_p : \mathbb{R}^n \to \mathbb{R}^{m\times l}$ such that for all $p \in \mathcal{P}$

$$\mathbf{f}_p(\mathbf{x}, \boldsymbol{\theta}) - \mathbf{f}_p(\mathbf{x}, \mathbf{0}) = \mathbf{G}_p(\mathbf{x}) \boldsymbol{\Upsilon}_p(\mathbf{x}) \mathbf{z} \; . \tag{6.81}$$

Then, the projected matching equations (6.9) are independent of $\boldsymbol{\theta}$. Hence, the design matrices and the energy function are independent of $\boldsymbol{\theta}$ which implies that also the update law (6.77a) does not depend on the uncertainty. Moreover, the control law can be represented in the desired form (6.76)

$$\mathbf{u} = \underbrace{\mathbf{G}_\sigma^\dagger(\mathbf{x}) \left[\mathbf{F}_\sigma(\mathbf{x}) \nabla H(\mathbf{x}) - \mathbf{f}_\sigma(\mathbf{x}, \mathbf{0})\right]}_{\boldsymbol{\gamma}_\sigma(\mathbf{x})} + \boldsymbol{\Upsilon}_\sigma(\mathbf{x}) \mathbf{z} \; . \tag{6.82}$$

Here we have used that $\mathbf{G}_p^\dagger(\mathbf{x}) \mathbf{f}(\mathbf{x}, \boldsymbol{\theta}) = \mathbf{G}_p^\dagger(\mathbf{x}) \mathbf{f}(\mathbf{x}, \mathbf{0}) + \boldsymbol{\Upsilon}_p(\mathbf{x}) \mathbf{z}$ which follows from (6.81). It is interesting to note that the control law (6.11) is not required to depend linearly on the unknown parameters $\boldsymbol{\theta}$ but only a linear reparametrization in terms of $\mathbf{z}$ is necessary.

The adaptive control approach does not require persistent excitation. However, it is in general not guaranteed that $\hat{\mathbf{z}}$ converges to its true value $\mathbf{z}$. In order to show convergence of the estimate $\hat{\mathbf{z}}$ we again have to invoke Krasovskii-LaSalle-like criteria like Theorem 2.4.4. Therefore, it is worthwhile mentioning that, in case that $\mathbf{R}_p(\mathbf{x}) > 0$ holds for all $p \in \mathcal{P}$ and all $\mathbf{x} \in \Omega^R$, all subsystems of (6.80) are zero-state small-time observable with the output $\mathbf{y} = -\nabla^T H \mathbf{R}_p \nabla H$ if and only if $l < n$ and $\operatorname{rank}\{\mathbf{G}_p(\mathbf{x}^*)\boldsymbol{\Upsilon}_p(\mathbf{x}^*)\} = l$.

6.7 Controller Design for Time-Varying Switched Systems

In this section, we deal with the stabilization of time-varying switched systems (6.1). In principle, the ideas of the previous sections can be readily applied to this problem. We aim at designing a time-varying state feedback law of the form $\mathbf{u}_\sigma = \mathbf{r}_\sigma(\mathbf{x}, t)$ such that the closed loop system can be represented as *time-varying spH system* with common energy function

$$\dot{\mathbf{x}} = \mathbf{F}_\sigma(\mathbf{x}, t)\nabla H(\mathbf{x}, t) \tag{6.83}$$

where, for all $t \in \mathbb{R}_0^+$ and all $\mathbf{x}$ in some neighborhood $\Omega^R \subset \mathbb{R}^n$ of the desired equilibrium point $\mathbf{x}^*$, the design matrices $\mathbf{F}_p : \mathbb{R}^n \times \mathbb{R}_0^+ \to \mathbb{R}^{n\times n}$ satisfy $\operatorname{sym}\{\mathbf{F}_p(\mathbf{x}, t)\} \leq 0$, and the Hamiltonian $H : \mathbb{R}^n \times \mathbb{R}_0^+ \to \mathbb{R}$ has a strict local minimum at $\mathbf{x}^*$, i.e. there exists an open neighborhood $\Omega \subset \mathbb{R}^n$ of $\mathbf{x}^*$ such that

$$H(\mathbf{x}, t) > H(\mathbf{x}^*, t), \quad \forall\, \mathbf{x} \in \Omega \backslash \{\mathbf{x}^*\}\ ,\ \forall\, t \in \mathbb{R}_0^+\ . \tag{6.84}$$

We assume, without loss of generality, that $\mathbf{x}^* = \mathbf{0}$. As in the non-switched case, the major restriction is that, in contrast to time-invariant spH systems with common energy function, the origin is not guaranteed to be stable, if the Hamiltonian explicitly depends on the time t. In this case, the derivative of the energy function along the trajectories of the pth subsystem is given by

$$\frac{\partial H(\mathbf{x}, t)}{\partial t} + \left(\frac{\partial H(\mathbf{x}, t)}{\partial \mathbf{x}}\right)^T \mathbf{R}_p(\mathbf{x}, t)\frac{\partial H(\mathbf{x}, t)}{\partial \mathbf{x}}\ . \tag{6.85}$$

Since nothing can be said, in general, about the sign of the first term in this expression, the value of the energy function might also increase along the trajectories of the subsystem. Nevertheless, $H(\mathbf{x}, t)$ is a good candidate for a common Lyapunov function, and, if we

succeed in showing that (6.85) is (locally) non-positive for all $p \in \mathcal{P}$, the following stability properties can be deduced invoking the Theorems 2.4.1 and 2.4.3 in Section 2.4.2.

Theorem 6.7.1. *Consider the system* (6.83) *and suppose that there is an open neighborhood* $\Omega^W \subset \mathbb{R}^n$ *of* $\mathbf{x}^* = \mathbf{0}$ *such that*

$$W_1(\mathbf{x}) \leq H(\mathbf{x}, t) \leq W_2(\mathbf{x}) \tag{6.86}$$

$$\frac{\partial H(\mathbf{x}, t)}{\partial t} + \left(\frac{\partial H(\mathbf{x}, t)}{\partial \mathbf{x}}\right)^T \mathbf{R}_p(\mathbf{x}, t) \frac{\partial H(\mathbf{x}, t)}{\partial \mathbf{x}} \leq W_3(\mathbf{x}) \tag{6.87}$$

holds for all $p \in \mathcal{P}$, *all* $t \geq 0$ *and all* $\mathbf{x} \in \Omega^W$, *where* $W_1(\mathbf{x})$, $W_2(\mathbf{x})$ *are continuous positive definite functions and* $W_3(\mathbf{x})$ *is a continuous positive semidefinite function on* Ω^W. *Moreover, let* $c > 0$ *be such that* $\overline{\mathrm{S}}_c^{W_1}(\mathbf{0})$ *is bounded and contained in* Ω^W.

(i) The origin is uniformly stable. Moreover, all trajectories starting in $\overline{\mathrm{S}}_c^{W_2}(\mathbf{x}^*)$ *approach the set* $\{\mathbf{x} \in \mathrm{S}_c^{W_1}(\mathbf{0}) | W_3(\mathbf{x}) = 0\}$ *as* $t \to \infty$.

(ii) If W_3 *is positive definite on* Ω^W, *then the origin is uniformly asymptotically stable and all trajectories starting in* $\overline{\mathrm{S}}_c^{W_2}(\mathbf{x}^*)$ *tend to the origin as* $t \to \infty$.

In case that the functions $W_i(\mathbf{x})$, $i = 1, 2, 3$ cannot be determined analytically due to the complexity of the appearing expressions, with a minor adaptation, the procedure described in Section 3.3.2 for non-switched systems can be applied in order to check the conditions (6.86) and (6.87) and to obtain an estimate of the DA (see the example in Section 8.2).

The design of the control law $\mathbf{u}_\sigma = \mathbf{r}_\sigma(\mathbf{x}, t)$ such that for all $p \in \mathcal{P}$ it holds that

$$\mathbf{f}_p(\mathbf{x}, t) + \mathbf{G}_p(\mathbf{x}, t)\mathbf{r}_p(\mathbf{x}, t) = \mathbf{F}_p(\mathbf{x}, t)\nabla H(\mathbf{x}, t) \tag{6.88}$$

follows exactly the same steps as in the time-invariant case, with the only difference that the design matrices, the left annihilators and the energy function are, in general, time dependent. Of course, also the systematic procedure described in Section 6.4 can be applied verbatim. The matrix $\mathbf{C}(\mathbf{x}, t)$ as well as the functions $k_{ij}(\mathbf{x}, t)$ in (6.46) are then allowed to be time-varying and Assumption 6.4.1 has to be valid for all $t \in [0, \infty)$.

6.8 Tuning of the Controller

As in the non-switched case in Part I of this thesis, a central question is how to choose the large number of parameters in the switching control laws obtained by the methodology

proposed in the preceding sections. In order to assess the dynamics of the individual subsystems of the closed loop system, we can of course consider the eigenvalues of their linearizations, and it is indeed common practice in the control of switched linear systems to assign suitable eigenvalues to the closed loop subsystems, see e.g. [125], [186]. Moreover, the methods from Chapter 3 clearly can be applied to determine an estimate of the DA of the closed loop spH systems. Hence, the methods that have been used for the tuning of non-switched IDA controllers in Part I, can also be applied to the case of switched systems, one major benefit being that, in this way, it can also be ensured easily that $\nabla^2 H(\mathbf{x}^*) > 0$ and thus that the energy function has a strict local minimum at $\mathbf{x}^*$.

If the plant model allows the application of the systematic procedure proposed in Section 6.4, the LLDA methodology (see Section 2.3) can be utilized, at least for the parametrization of one feedback function, i.e., either for $\mathbf{r}_1(\mathbf{x})$ or for $\mathbf{r}_2(\mathbf{x})$. Of course, also for the parametrization of the second feedback function, the linearization of the closed loop subsystem can be considered in order to get an idea of its dynamic behavior. However, it will, in general, not be possible to assign arbitrary eigenvalues to this linearization.

If the procedure from Section 6.4 is not applicable, this implies that also the conditions for the use of LLDA are not satisfied. However, we can prescribe an admissible region for the closed loop eigenvalues of the linearized subsystems as in Figure 4.3 by specifying suitable values for r_{min}, r_{max} and ψ. Then we solve the optimization problem (4.20), where the constraints (4.20b), (4.20c) have to be fulfilled for the eigenvalues of all subsystems. Moreover, we have to add constraints that guarantee the positive semidefiniteness of the dissipation matrices.

Since, from a practical point of view, the issue of transient response is very important, at this point the natural question arises whether it can be guaranteed that the closed loop switched system exhibits good dynamic behavior, if the dynamics of the individual subsystems are well-behaved. This will be briefly discussed in the following in terms of the shape of the transient response and the rate at which the state trajectories converge to the desired equilibrium point. We consider the switched linear system

$$\dot{\mathbf{x}} = \mathbf{A}_\sigma \mathbf{x}, \quad \sigma(t) : [0, \infty) \to \{1, 2\} \tag{6.89}$$

which can be regarded as the linearization of the nonlinear closed loop system above. The transient response of such a system is determined by the eigenvalues *and* by the eigenvectors of the matrices $\mathbf{A}_p$. Especially the overshoot in the transient phases after the switching events depends to a large extent on the orientation of the eigenvectors, which normally cannot be influenced by state feedback in a transparent way. It is due to these

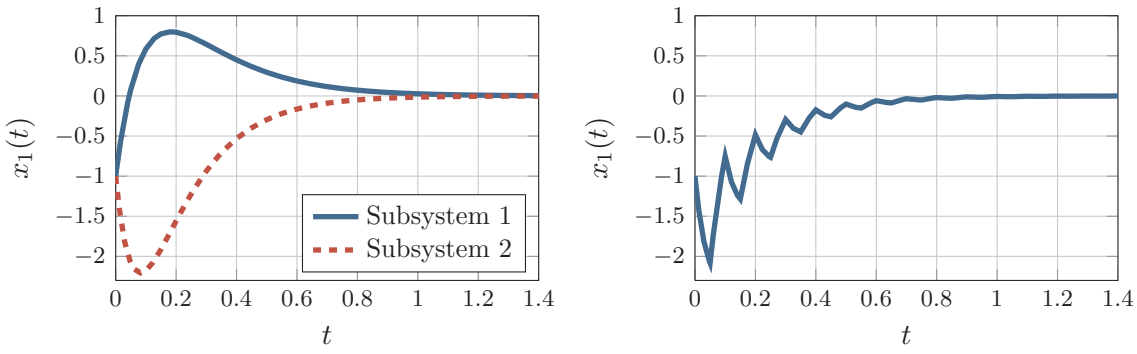

(a) Individual Subsystems.

(b) Switched System.

Figure 6.1: Transient response curves of the subsystems in comparison with those of the switched system.

overshoots that the switched system (6.89) can exhibit a rather ugly transient response, as illustrated in the following example. We remark that these overshoots are also the reason why switching between asymptotically stable subsystems may lead to unbounded state trajectories.

Example 6.8.1. Consider the switched linear system (6.89) with

$$\mathbf{A}_1 = \begin{bmatrix} -10 & -20 \\ 0 & -5 \end{bmatrix}, \quad \mathbf{A}_2 = \begin{bmatrix} -15 & 54 \\ 0 & -6 \end{bmatrix}. \tag{6.90}$$

Due to the upper triangular structure of both matrices the subsystems are guaranteed to have a common quadratic Lyapunov function [113]. The transient response curves of x_1 for the individual subsystems are shown in Figure 6.1(a). The transient response of x_1 for the switched system is depicted in Figure 6.1(b). The switching signal has been chosen such that switching occurs every 0.05 s starting with $\sigma(0) = 2$. The initial state is $\mathbf{x}(0) = [-1, -1]^T$. While the transient responses of the individual subsystems are fairly well-behaved, that of the switched system exhibits a quite ugly shape since, in practical applications, we are typically interested in smooth system responses.

A general discussion on the relationship between the eigenstructure (eigenvalues and eigenvectors) of the matrices $\mathbf{A}_p$ and the shape of the transient response for systems, whose subsystem matrices solely have real eigenvectors, is given by Shorten and Narendra in [156]. The conclusion can be summarized as follows: In order to obtain a smooth transient response, the matrices $\mathbf{A}_1$ and $\mathbf{A}_2$ should share as many eigenvectors and associated eigenvalues as possible, and especially the eigenvectors corresponding to slow eigenvalues should be common to both matrices. It is clear, however, that this requirement can be

fulfilled by means of state feedback only in very special (academic) cases. Hence, we can conclude that, in general, it is difficult to achieve a smoothly shaped transient response of a switched system by means of state feedback in a constructive manner.

In contrast, in our experience, the rate at which the system states decay to zero can normally be influenced quite transparently by specifying suitable eigenvalue locations. However, since also the orientation of the eigenvectors changes, if the controller assigns a different set of eigenvalues to the subsystem matrices, it is worthwhile pointing out that also the rate of decay is not only determined by the eigenvalues but also by the eigenvectors.

Example 6.8.2 (Example 6.8.1 cont'd). Obviously, the matrices $\mathbf{A}_1$ and $\mathbf{A}_2$ in the previous example have the eigenvalues $\lambda_{1,1} = -10$, $\lambda_{1,2} = -5$ and $\lambda_{2,1} = -15$, $\lambda_{2,2} = -6$, respectively. The eigenvectors are $\mathbf{v}_{1,1} = [2, 0]^T$, $\mathbf{v}_{1,2} = [4, -1]^T$ and $\mathbf{v}_{2,1} = [3, 0]^T$, $\mathbf{v}_{2,2} = [6, 1]^T$. While leaving the eigenvalues and the second eigenvector of both subsystem matrices as they are, we change the eigenvectors $\mathbf{v}_{1,1}$, $\mathbf{v}_{2,1}$ to $\tilde{\mathbf{v}}_{1,1} = [2, -0.3]^T$, $\tilde{\mathbf{v}}_{2,1} = [3, 0.1]^T$ yielding the new switched system $\dot{\mathbf{x}} = \tilde{\mathbf{A}}_\sigma \mathbf{x}$ with

$$\tilde{\mathbf{A}}_1 = \begin{bmatrix} -17.5 & -50 \\ 1.875 & 2.5 \end{bmatrix}, \quad \tilde{\mathbf{A}}_2 = \begin{bmatrix} -17.5 & -50 \\ -0.375 & -3.75 \end{bmatrix}. \tag{6.91}$$

It can be verified that the function $V = \mathbf{x}^T \mathbf{P} \mathbf{x}$ with

$$\mathbf{P} = \begin{bmatrix} 3.13 & 7.46 \\ 7.46 & 141.65 \end{bmatrix} \tag{6.92}$$

is a common quadratic Lyapunov function. In Figure 6.2(a), the evolution of the 2-norm $\|\mathbf{x}(t)\|$ is depicted for the 1st subsystem of both the original switched system (with $\mathbf{A}_1$ and $\mathbf{A}_2$) and the modified one (with $\tilde{\mathbf{A}}_1$ and $\tilde{\mathbf{A}}_2$). We observe that the curve which corresponds to the subsystem with $\tilde{\mathbf{A}}_1$ shows a considerably higher overshoot than the one of the original subsystem with $\mathbf{A}_1$. However, after the overshoot has been absorbed, both trajectories decay to zero similarly fast. This is in contrast to the switched systems, whose transient responses are depicted in Figure 6.2(b). Here, we observe a significantly slower convergence of $\|\mathbf{x}(t)\|$ to zero for the modified switched system as compared to the original one, although the eigenvalue locations are identical. The switching signal is the same as in the previous example 6.8.1.

6.9 Illustrative Examples

The purpose of this section is to illustrate the use of the methods proposed in this chapter. Both systems considered below allow the application of the design procedure described in

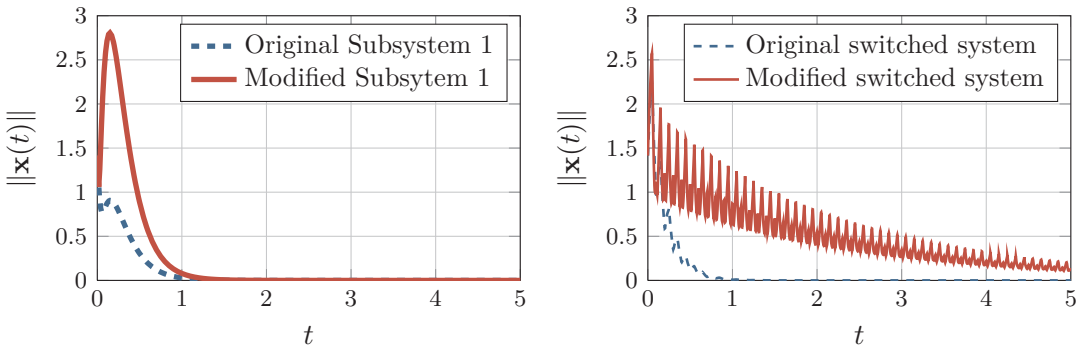

(a) 1st Subsystem. (b) Switched System.

Figure 6.2: Influence of the eigenvectors on the decay rate of a switched linear system.

Section 6.4. While in the first example the matrix $\mathbf{C}$ is constant, the second one illustrates the case of a state-dependent matrix $\mathbf{C}(\mathbf{x})$. An example, where the controller design has to be accomplished without the procedure from Section 6.4 is given in Section 8.1.

6.9.1 Constant Matrix C

Consider the system

$$\dot{\mathbf{x}} = \mathbf{f}_\sigma(\mathbf{x}) + \mathbf{g}_\sigma(\mathbf{x})u\,, \quad \sigma \in \mathcal{S}_{pc} \tag{6.93}$$

with

$$\mathbf{f}_1(\mathbf{x}) = \begin{bmatrix} -x_1x_3^2 + 4x_2 \\ 3x_1 \\ 5x_2 - 7x_3^3 \end{bmatrix},\ \mathbf{g}_1(\mathbf{x}) = \begin{bmatrix} 1 + x_1^2 \\ 0 \\ 0 \end{bmatrix},\ \mathbf{f}_2(\mathbf{x}) = \begin{bmatrix} -x_2x_3 - x_1 \\ 3x_1 \\ 9x_1 + 5x_2 - 7x_3^3 \end{bmatrix},\ \mathbf{g}_2(\mathbf{x}) = \begin{bmatrix} 3 + x_3 \\ 0 \\ 0 \end{bmatrix}$$

and the desired equilibrium $\mathbf{x}^* = \mathbf{0}$. The system is of the form (6.23) and it holds that $\mathbf{f}_2^\nu(\mathbf{x}) = \mathbf{C}\mathbf{f}_1^\nu(\mathbf{x})$ with the matrix $\mathbf{C}$ given in (6.49). For this matrix, the set of solutions to (6.37) has been constructed in Example 6.4.1 and is given in (6.52). Suitable matrices $\mathbf{F}_1^\nu$ are then obtained by setting $\mathbf{F}_1^\nu = [\mathbf{F}_1^C,\ -\mathbf{X}]$ with a constant matrix $\mathbf{F}_1^C = [\nu_{1,11},\, \nu_{1,21}]^T$.

Step 1: Solvability of the matching equation Since $\mathbf{F}_1^\nu$ is constant, we can employ (6.58) in order to check the solvability of (6.25). We obtain the condition

$$3\nu_{1,21} + \frac{5}{2}k_{11}^2 + 21x_3^2\left(\frac{3}{4}k_{11}^2 - \frac{1}{2}k_{12}k_{11} - \rho\right) \stackrel{!}{=} 0 \tag{6.94}$$

which is satisfied, if we choose $\nu_{1,21} = -\frac{5}{6}k_{1,1}^2$ and $\rho = \frac{3}{4}k_{11}^2 - \frac{1}{2}k_{12}k_{11}$.

Step 2: Positive Definiteness of $\mathbf{R}_p$ In order to guarantee $\mathbf{R}_p > 0$, $p \in \{1, 2\}$, as in the proof of Lemma 6.4.1, we choose $\mathbf{F}_p^B = -(\mathbf{F}_p^C)^T$, $p \in \{1, 2\}$ such that the dissipation matrices take the form (6.33), (6.34). Then, $\mathbf{R}_1 > 0$ holds, if $F_1^A = \alpha_{1,11} < 0$ and $\mathrm{sym}\{\mathbf{X}\} > 0$. With the choice made for ρ above, it follows from (6.54) that $\mathrm{sym}\{\mathbf{X}\} > 0$ if

$$-4k_{22}^2 + 9k_{11}^2 - 12k_{12}k_{11} < 0\ . \tag{6.95}$$

Similarly, for $\mathbf{R}_2 > 0$ it must hold that $F_2^A = \alpha_{2,11} < 0$ and $\mathrm{sym}\{\mathbf{CX}\} = \mathbf{Q} > 0$, where the latter is guaranteed by construction if $k_{11},\ k_{22} \neq 0$.

Step 3: Solving the matching PDE As $\boldsymbol{\nu}_{j,1}$ in $\mathbf{F}_1^\nu$ is constant, the solution of the projected matching equations (6.26) is easily calculated as described in Section 2.2.4. The matrix $\mathbf{T}^{-1}$ in (2.37) is $\mathbf{T}^{-1} = [\mathbf{t}_1\ \ (\mathbf{F}_1^\nu)^T]$, where we set $\mathbf{t}_1 = [\frac{1}{k_{11}^2(k_{22}^2+k_{12}^2)},\ 0,\ 0]^T$. Then, z_1 is a characteristic coordinate and we choose $\phi(z_1) = \mu_2 z_1^2$.

Step 4: Controller tuning In order to obtain suitable parameters, LLDA is applied to the first subsystem, where $\mathbf{A}_{d,1}$ has three eigenvalues in -3. From the corresponding system of equations (2.57)-(2.59), dependencies of the form $\alpha_{1,11} = \alpha_{1,11}(k_{11}, k_{12}, k_{22})$, $\nu_{1,11} = \nu_{1,11}(k_{11}, k_{12}, k_{22})$, $\mu_2 = \mu_2(k_{11}, k_{12}, k_{22})$ are obtained. For simplicity, k_{12} is fixed at -1. The remaining free parameters $\alpha_{2,11}$, k_{11}, and k_{22} are chosen such that the closed loop linearization of the second subsystem has the eigenvalues $\lambda_{1,2} = -0.91$, $\lambda_{2,2} = -7.9$, and $\lambda_{3,2} = -12.9$ yielding $k_{11} = -407$, $k_{22} = -800$, and $\alpha_{2,11} = -100$. The corresponding energy function $H(\mathbf{x})$ is strongly convex on $\mathbb{R}^3$ and hence radially unbounded. This together with the fact that both dissipation matrices are constant and positive definite establishes global uniform asymptotic stability of $\mathbf{x}^* = \mathbf{0}$. Figure 6.3 shows the transient response of the closed loop system and the corresponding control input u for an initial state $\mathbf{x}(0) = [2,\ 1,\ -1]^T$ and a random switching signal.

Now suppose that a constant input disturbance $d = 5$ is acting on the system (c.f. (6.69)). Figure 6.4(a) shows the corresponding transient response curves of the closed loop system for the initial state $\mathbf{x}(0) = [2,\ 1,\ -1]^T$ and a random switching signal. Apparently, the disturbance keeps the state from converging to the origin. If we add integral action according to Proposition 6.6.1 with $K_I = 2 \cdot 10^5$, the result depicted in 6.4(b) is obtained. We observe that, as expected, the integral controller drives the state to the origin despite the disturbance.

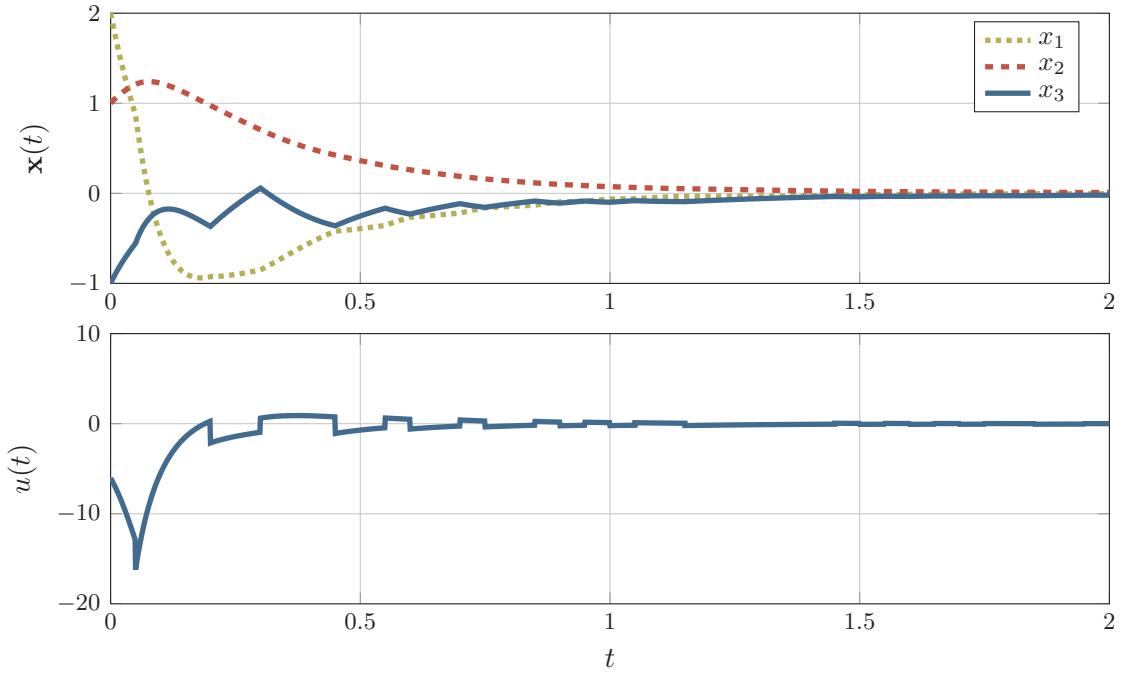

Figure 6.3: Transient response curves of the closed loop switched system with $\mathbf{x}(0) = [2,\ 1,\ -1]^T$ and a random switching signal (upper), and the corresponding control input (lower).

6.9.2 State-dependent Matrix $\mathbf{C}(\mathbf{x})$

To illustrate the case of a state-dependent matrix $\mathbf{C}(\mathbf{x})$ we consider the system (6.93) with

$$\mathbf{f}_1(\mathbf{x}) = \begin{bmatrix} -2x_2^2 + x_1x_2 \\ 3x_1 \\ -3x_1^2 + 5x_2 - 7x_3^3 \end{bmatrix},\ \mathbf{g}_1(\mathbf{x}) = \begin{bmatrix} 3 + x_3 \\ 0 \\ 0 \end{bmatrix},\ \mathbf{f}_2(\mathbf{x}) = \begin{bmatrix} -x_1x_3^2 + 4x_2 \\ 3x_1 \\ 5x_2 - 7x_3^3 \end{bmatrix},\ \mathbf{g}_2 = \begin{bmatrix} 1 \\ 0 \\ 0 \end{bmatrix}$$

and $\mathbf{x}^* = \mathbf{0}$. The system is again of the form (6.23) and it is not difficult to see that $\mathbf{f}_2^\nu(\mathbf{x}) = \mathbf{C}(\mathbf{x})\mathbf{f}_1^\nu(\mathbf{x})$ holds with the state-dependent matrix

$$\mathbf{C}(\mathbf{x}) = \begin{bmatrix} 1 & 0 \\ x_1 & 1 \end{bmatrix}. \tag{6.96}$$

After a set of suitable matrices $\mathbf{F}_1^\nu(\mathbf{x})$ has been constructed as in the example above, the matrix $\mathbf{F}_2^\nu(\mathbf{x}) = \mathbf{C}(\mathbf{x})\mathbf{F}_1^\nu(\mathbf{x})$ is

$$\mathbf{F}_2^\nu(\mathbf{x}) = \begin{bmatrix} \nu_{1,11}(\mathbf{x}) & -\frac{1}{2}k_{11}^2 & \nu_{2,13}(\mathbf{x}) \\ \nu_{1,11}(\mathbf{x})x_1 + \nu_{1,21}(\mathbf{x}) & \nu_{2,22}(\mathbf{x}) & -\frac{1}{2}k_{22}^2 - \frac{1}{2}k_{12}^2 \end{bmatrix}. \tag{6.97}$$

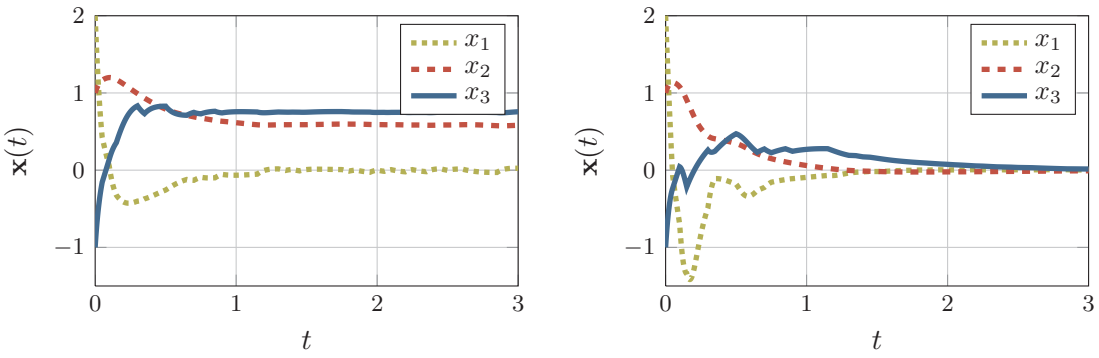

(a) Without integral control.

(b) With integral control.

Figure 6.4: Transient response of the closed loop system with a constant input disturbance.

with $\nu_{2,13}(\mathbf{x}) = \frac{1}{4}k_{11}^2 x_1 - \frac{1}{2}k_{12}k_{11} - \rho(\mathbf{x})$, $\nu_{2,22}(\mathbf{x}) = -\frac{1}{4}k_{11}^2 x_1 - \frac{1}{2}k_{12}k_{11} + \rho(\mathbf{x})$. It can be rendered constant by the choices $\rho(\mathbf{x}) = \frac{1}{4}k_{11}^2 x_1 + \kappa_1$ and $\nu_{1,21}(\mathbf{x}) = -x_1\nu_{1,11} + \kappa_2$ with constants $\nu_{1,11}$, κ_1 and κ_2. Now the simplified solvability condition (6.58) can be applied with $k = 2$ to deduce that the projected matching equations are solvable, if we choose $\kappa_1 = -\frac{1}{2}k_{12}k_{11}$ and $\kappa_2 = -\frac{5}{6}k_{11}^2$. The rest of the controller design is analogous to the previous example and is therefore omitted.

6.10 Concluding Remarks

In this chapter, we have presented a passivity-based controller design method for the uniform asymptotic stabilization of switched nonlinear systems, whose subsystems may, in general, be time-varying. Instrumental for our developments were the stability properties of spH systems discussed in Section 6.2, which suggested that the stabilization problem can be solved by assigning an spH structure with common energy function to the closed loop system. Our approach is thus a natural extension of the IDA method, which has been successfully applied to various types of technical systems (see also Part I of this thesis). The main features of the proposed control scheme can be summarized as follows: (i) It is completely analytic and more in the spirit of classical techniques, like e.g. pole placement, as opposed to LMI-based design methods which, although widely used for the stabilization of switched linear systems, lack transparency and interpretability. (ii) It is constructive in nature, i.e., there is, for instance, no need to guess a common control Lyapunov function. (iii) It is not restricted to a special class of switched systems. In fact, it has been shown for the case of time-invariant subsystems that the method generates all static feedback laws for which the closed loop system is uniformly asymptotically stable. (iv) The special closed

loop structure allows the straightforward incorporation of integral and adaptive control. (v) The procedure is amenable for computer algebra systems like e.g. MAPLE or SAGE.

Although the approach is constructive, the involved mathematical expressions can get cumbersome making it often nontrivial to determine design matrices that satisfy all conditions. For this reason, we have provided for a class of bimodal switched systems a systematic procedure for the choice of suitable design matrices as well as for the subsequent controller design. Extending this procedure to other classes of switched systems, possibly supported by numerical tools, is a matter of future research. In this chapter, the proposed control approach has been illustrated by means of numerical examples. In Chapter 8, its effectiveness will be shown also for technical systems.

Chapter 7

Output Trajectory Tracking of Bimodal Switched Systems

In the previous chapter, we have proposed a control scheme for the set-point regulation of switched nonlinear systems. Another typical control problem that frequently arises in practical engineering is to make a certain (scalar) quantity track a predefined trajectory. As this quantity is usually defined to be the output of the system, this problem is referred to as *output trajectory tracking*. It has been extensively studied for smooth dynamical systems, but, surprisingly, has not received much attention in the context of switched systems. To the best of our knowledge, this problem has not been addressed for nonlinear switched systems, yet (see also Section 1.3.3).

In this chapter, we consider both the *exact and the asymptotic output tracking problem* for switched nonlinear single-input-single-output (SISO) systems with two subsystems. We are concerned with trajectory-independent as well as trajectory-dependent switching. In the latter case, we also study the situation where the switching law depends on the control input. This situation, although of technical relevance (see e.g. [57], [94]), is usually not treated in the hybrid and switched systems literature. The desired output trajectory can, in principle, be freely chosen by the designer, i.e., we do not assume that the trajectories are periodic or that they are generated by an exosystem like in the output regulation framework (c.f. Section 1.3.3). Since the reference trajectories are commonly specified in terms of polynomials, trigonometric series or other smooth functions, we focus our attention on the class of smooth reference trajectories.

The main contribution of this chapter is twofold. First, we give necessary and sufficient conditions for the solvability of the exact output tracking (EOT) problem. This issue is, especially in the case of trajectory-dependent switching, considerably more delicate than it is for smooth systems. In the latter case it is sufficient for the solvability of the EOT

problem that the relative degree is well-defined and the internal dynamics are input-to-state stable. In the case of switched systems, however, it could happen, for instance, that an output trajectory is infeasible because at some point the corresponding state trajectory enters the switching surface and cannot be continued on either side of it such that the system output keeps tracking the reference. The result is an infinitely fast chattering. Furthermore, we explore the asymptotic output tracking (AOT) problem for switched nonlinear systems, which also turns out to be more involved than in the case of smooth systems as soon as the switching law is trajectory-dependent. Therefore, we identify two special classes of switched systems for which the controller design simplifies considerably. This constitutes the second main contribution of this chapter.

The remainder is organized as follows. In Section 7.1, we give a formal statement of the problems considered in this chapter, and we establish some notation needed in the sequel. Section 7.2 is devoted to the solvability of the EOT problem for systems with both trajectory-independent and trajectory-dependent switching. The asymptotic tracking of a desired output trajectory is addressed in Section 7.3, and we wrap up the chapter with some concluding remarks in Section 7.4.

7.1 Problem statement

Throughout this chapter we consider switched nonlinear SISO systems described by

$$\dot{\mathbf{x}} = \mathbf{f}_\sigma(\mathbf{x}) + \mathbf{g}_\sigma(\mathbf{x})u\ , \quad \sigma \in \mathcal{S} \tag{7.1a}$$

$$y = h(\mathbf{x}) \tag{7.1b}$$

with state $\mathbf{x} \in \mathbb{R}^n$, control input $u \in \mathbb{R}$, and output $y \in \mathbb{R}$, which consist of two subsytems, i.e, $\mathcal{P} = \{1, 2\}$. The vector fields $\mathbf{f}_p : \mathbb{R}^n \to \mathbb{R}^n$, $\mathbf{g}_p : \mathbb{R}^n \to \mathbb{R}^n$, $p \in \mathcal{P}$ and the map $h : \mathbb{R}^n \to \mathbb{R}$ are assumed to be sufficiently smooth[1]. Moreover, we can assume without loss of generality that $h(\mathbf{0}) = 0$. Note that the output function $h(\mathbf{x})$ is identical for both subsystems.

The problem we consider is the design of a control such that the output $y(t)$ of (7.1) tracks a desired output trajectory $y_d(t)$ either exactly or asymptotically. We assume that the reference signals $y_d(t)$ satisfy $y_d \in \mathcal{C}^k$ with k sufficiently large, and that all derivatives up to the order k are bounded. The EOT problem for the case of trajectory-independent and the case of trajectory-dependent switching can be formally stated as follows:

[1]By "sufficiently smooth" we mean that all partial derivatives that are needed in the following are defined and continuous.

Problem 7.1.1 (EOT problem for trajectory-independent switching)**.** Given (7.1) together with a switching signal $\sigma \in \mathcal{S}$ and a desired output trajectory $y_d(t) \in \mathcal{C}^k$ with k sufficiently large, find, if any, pairs consisting of an initial state $\mathbf{x}_d(0) = \mathbf{x}_0$ and a piecewise continuous, bounded control $u_d(t)$ such that the corresponding solution $\mathbf{x}_d(t)$ with $\mathbf{x}_d(0) = \mathbf{x}_0$ is bounded and satisfies $y_d(t) = h(\mathbf{x}_d(t))$ for all $t \geq 0$.

Problem 7.1.2 (EOT problem for trajectory-dependent switching)**.** Given (7.1) together with the switching law (2.69) and a desired output trajectory $y_d(t) \in \mathcal{C}^k$ with k sufficiently large, find, if any, pairs consisting of an initial state $\mathbf{x}_d(0) = \mathbf{x}_0$ and a piecewise continuous, bounded control $u_d(t)$ such that the corresponding solution $\mathbf{x}_d(t)$ with $\mathbf{x}_d(0) = \mathbf{x}_0$ exists, is bounded and satisfies $y_d(t) = h(\mathbf{x}_d(t))$ for all $t \in [0, T)$ with $T > 0$.

Note that Problem 7.1.2 requires a solution only to exist locally, i.e., on a time interval of positive length. A comment on this will be included in due course. If the EOT problem is solvable, we can determine a pair or, in general, a set of pairs $(\mathbf{x}_d(0), u_d(t))$ for which the output $y(t)$ of the switched system (7.1) exactly follows the desired reference trajectory $y_d(t)$. However, we usually cannot expect that the actual initial state $\mathbf{x}(0)$ exactly coincides with one of these suitable initial states $\mathbf{x}_d(0)$. Moreover, in a practical setup, disturbances and model uncertainties will cause a deviation of the output trajectory from the desired one. Therefore, we need to introduce feedback action in order to appropriately stabilize and robustify the system. It is desired to design a controller such that, for all initial states $\mathbf{x}(0)$ sufficiently close to the desired one $\mathbf{x}_d(0)$, asymptotic output tracking is achieved, i.e. $e_y(t) = y(t) - y_d(t) \to 0$ as $t \to \infty$. Moreover, we demand that for every $\epsilon > 0$ there is $\delta > 0$ such that $e_y(0) < \delta$ implies $e_y(t) < \epsilon$ for all $t \geq 0$, which entails that, if $e_y(0) = 0$, then $e_y(t) = 0$ for all $t > 0$. This is a quite natural and common requirement, but not necessary in general to achieve asymptotic output tracking (c.f. Remark 4.5.2 in [89]). Note that it implies that solvability of the EOT problem is a necessary prerequisite for the solvability of the AOT problem. Therefore, in what follows, we can always assume in the context of AOT that a state trajectory $\mathbf{x}_d(t)$ with $y_d(t) = h(\mathbf{x}_d(t))$ and a corresponding input trajectory $u_d(t)$ are available. Formally, all of this can be summarized for trajectory-independent (trajectory-dependent) switching in the following problem.

Problem 7.1.3 (AOT problem)**.** Given (7.1) together with a switching signal $\sigma \in \mathcal{S}$ (the switching law (2.69)) and a desired output trajectory $y_d(t) \in \mathcal{C}^k$ with k sufficiently large and a corresponding trajectory $\mathbf{x}_d(t)$, find a piecewise continuous function $\zeta : \mathcal{O}_1 \times [0, \infty) \to \mathbb{R}$, defined on an open neighborhood $\mathcal{O}_1$ of $(\mathbf{x}_d(0), \mathbf{x}_d(0))$ in $\mathbb{R}^n \times \mathbb{R}^n$, such that for all $\mathbf{x}(0)$

within an open neighborhood $\mathcal{O}_2$ of $\mathbf{x}_d(0)$ in $\mathbb{R}^n$ the solution of

$$\dot{\mathbf{x}} = \mathbf{f}_\sigma(\mathbf{x}) + \mathbf{g}_\sigma(\mathbf{x})\zeta(\mathbf{x}, \mathbf{x}_d, t) \tag{7.2a}$$

$$y = h(\mathbf{x}) \tag{7.2b}$$

satisfies:

1) for every $\epsilon > 0$ there is $\delta > 0$ such that $e_y(0) < \delta \Rightarrow e_y(t) < \epsilon$ for all $t \geq 0$.

2) $e_y(t) \to 0$ as $t \to \infty$.

3) both the input $u(t)$ and the state trajectory $\mathbf{x}(t)$ are bounded.

Assumption 7.1.1. Both subsystems $\dot{\mathbf{x}} = \mathbf{f}_p(\mathbf{x}) + \mathbf{g}_p(\mathbf{x})u\ ,\ y = h(\mathbf{x})$, $p \in \{1, 2\}$ have well defined relative degree r_p in $\mathbb{R}^n$, i.e., for all $\mathbf{x}$ in $\mathbb{R}^n$ it holds that

$$L_{g_p} L_{f_p}^k h(\mathbf{x}) = 0 \quad \text{for } k = 0, \ldots, r_p - 2 \tag{7.3}$$

$$L_{g_p} L_{f_p}^{r_p - 1} h(\mathbf{x}) \neq 0 \tag{7.4}$$

We emphasize that the assumption that the relative degree is *globally* well defined is not necessary and only made for simplicity of exposition (see Remark 7.2.2 for a short discussion). Without loss of generality, we assume that $r_1 \geq r_2$.

Using a notation similar to that in [83], we define the derivatives $y^{(k)}(t) = \frac{d^k}{dt^k} y(t)$ as well as $\mathbf{Y}^k = [y, y^{(1)}, \ldots, y^{(k-1)}]^T$. Moreover, we set $\mathbf{U}^k = [u, u^{(1)}, \ldots, u^{(k-1)}]^T$. The kth derivative of $h(\mathbf{x})$ along the trajectories of the pth subsystem is denoted by $h_p^{(k)}$. Assumption 7.1.1 implies that

$$h_p^{(k)}(\mathbf{x}) = L_{f_p}^k h(\mathbf{x})\ ,\ k = 1, \ldots, r_p - 1\ , \qquad h_p^{(r_p)}(\mathbf{x}) = L_{f_p}^{r_p} h(\mathbf{x}) + L_{g_p} L_{f_p}^{r_p - 1} h(\mathbf{x}) u\ . \tag{7.5}$$

For $k > r_p$ it holds that

$$h_p^{(k)}\left(\mathbf{x}, u, \ldots, u^{(k-r_p)}\right) = \frac{\partial h_p^{(k-1)}}{\partial \mathbf{x}} \left[\mathbf{f}_p(\mathbf{x}) + \mathbf{g}_p(\mathbf{x})u\right] + \frac{\partial h_p^{(k-1)}}{\partial \mathbf{U}^{k-r_p}} \frac{d}{dt} \mathbf{U}^{k-r_p}\ . \tag{7.6}$$

Similar to $\mathbf{Y}^{r_p}$, let the maps $\mathbf{h}_p^{r_p} : \mathbb{R}^n \to \mathbb{R}^{r_p}$ be defined by

$$\mathbf{h}_p^{r_p}(\mathbf{x}) = \begin{bmatrix} h(\mathbf{x}) & h_p^{(1)}(\mathbf{x}) & \ldots & h_p^{(r_p - 1)}(\mathbf{x}) \end{bmatrix}^T \tag{7.7}$$

i.e., $\mathbf{h}_p^{r_p}(\mathbf{x})$ contains the time derivatives of $h(\mathbf{x})$ along the trajectories of the p-th subsystem up to the order $r_p - 1$. Correspondingly, we define for the case where r_1 is strictly larger than r_2 the map $\mathbf{h}_2^{r_1} : \mathbb{R}^n \times \mathbb{R}^{r_1 - r_2}$, which subsumes the time derivatives of $h(\mathbf{x})$ along the

trajectories of the 2nd subsystem up to the order $r_1 - 1$, i.e.,

$$\mathbf{h}_2^{r_1}(\mathbf{x}, \mathbf{U}^{r_1-r_2}) = \begin{bmatrix} h(\mathbf{x}) & h_2^{(1)}(\mathbf{x}) & \dots & h_2^{(r_1-1)}(\mathbf{x}, \mathbf{U}^{r_1-r_2}) \end{bmatrix}^T . \tag{7.8}$$

7.2 The Exact Output Tracking Problem

In this section, conditions for the solvability of the EOT problem for the switched system (7.1) are presented. We begin performing the change of coordinates

$$\mathbf{z}_1 = \begin{bmatrix} \boldsymbol{\xi}_1^T & \boldsymbol{\eta}_1^T \end{bmatrix}^T = \boldsymbol{\Phi}_1(\mathbf{x}) \tag{7.9}$$

with

$$\boldsymbol{\xi}_1 = \boldsymbol{\Phi}_{1,\xi}(\mathbf{x}) = \mathbf{h}_1^{r_1}(\mathbf{x}) , \quad \boldsymbol{\eta}_1 = \boldsymbol{\Phi}_{1,\eta}(\mathbf{x}) \tag{7.10}$$

where $\boldsymbol{\Phi}_{1,\eta}(\mathbf{x})$ is chosen such that $\boldsymbol{\Phi}(\mathbf{x})$ is a diffeomorphism, at least in a neighborhood of some point $\mathbf{x}_0$. The existence of a suitable function $\boldsymbol{\Phi}_{1,\eta}(\mathbf{x})$ is guaranteed by virtue of Assumption 7.1.1, see [89]. Throughout this chapter, we use a tilde to denote quantities associated with these new coordinates, i.e. the subsystems of (7.1) are represented by

$$\dot{\mathbf{z}}_1 = \tilde{\mathbf{f}}_p(\mathbf{z}_1) + \tilde{\mathbf{g}}_p(\mathbf{z}_1)u \tag{7.11a}$$

$$y = \tilde{h}(\mathbf{z}_1) = \xi_{1,1} \tag{7.11b}$$

where $p \in \{1, 2\}$ and

$$\tilde{\mathbf{f}}_p(\mathbf{z}_1) = \frac{\partial \boldsymbol{\Phi}_1}{\partial \mathbf{x}} \mathbf{f}_p \circ \boldsymbol{\Phi}_1^{-1}(\mathbf{z}_1) , \quad \tilde{\mathbf{g}}_p(\mathbf{z}_1) = \frac{\partial \boldsymbol{\Phi}_1}{\partial \mathbf{x}} \mathbf{g}_p \circ \boldsymbol{\Phi}_1^{-1}(\mathbf{z}_1) . \tag{7.12}$$

The change of coordinates (7.9), (7.10) puts the 1st subsystem in *input-output normal form*[2]

$$\begin{aligned} \dot{\xi}_{1,1} &= \xi_{1,2} \\ &\dots \\ \dot{\xi}_{1,r_1-1} &= \xi_{1,r_1} \\ \dot{\xi}_{1,r_1} &= \tilde{\alpha}_1(\boldsymbol{\xi}_1, \boldsymbol{\eta}_1) + \tilde{\beta}_1(\boldsymbol{\xi}_1, \boldsymbol{\eta}_1)u \end{aligned} \tag{7.13a}$$

$$\dot{\boldsymbol{\eta}} = \tilde{\mathbf{p}}_1(\boldsymbol{\xi}_1, \boldsymbol{\eta}_1) + \tilde{\mathbf{q}}_1(\boldsymbol{\xi}_1, \boldsymbol{\eta}_1)u \tag{7.13b}$$

$$y = \tilde{h}(\mathbf{z}_1) = \xi_{1,1} \tag{7.13c}$$

[2]We remark that some authors refer to (7.13) as *normal form* only when $\tilde{\mathbf{q}}_1 = \mathbf{0}$ (see e.g. [89]).

where $\tilde{\alpha}_1(\mathbf{z}_1) = L_{f_1}^{r_1} h \circ \mathbf{\Phi}_1^{-1}(\mathbf{z}_1)$, $\tilde{\beta}_1(\mathbf{z}_1) = L_{g_1} L_{f_1}^{r_1-1} h \circ \mathbf{\Phi}_1^{-1}(\mathbf{z}_1)$, $\tilde{\mathbf{p}}_1(\mathbf{z}_1) = L_{f_1} \mathbf{\Phi}_{1,\eta} \circ \mathbf{\Phi}_1^{-1}(\mathbf{z}_1)$ and $\tilde{\mathbf{q}}_1(\mathbf{z}_1) = L_{g_1} \mathbf{\Phi}_{1,\eta} \circ \mathbf{\Phi}_1^{-1}(\mathbf{z}_1)$. The function[3] $\tilde{\mathbf{h}}_1^{r_1}(\mathbf{z}_1) = \mathbf{h}_1^{r_1}(\mathbf{x}) \circ \mathbf{\Phi}^{-1}(\mathbf{z}_1)$ is the identity map, but will often be used for notational convenience.

Similar to (7.9), (7.10), we define the set of coordinates

$$\mathbf{z}_2 = \begin{bmatrix} \boldsymbol{\xi}_2^T & \boldsymbol{\eta}_2^T \end{bmatrix}^T = \tilde{\mathbf{\Phi}}_2(\mathbf{z}_1) \tag{7.14}$$

with

$$\boldsymbol{\xi}_2 = \tilde{\mathbf{\Phi}}_{2,\xi}(\mathbf{z}_1) = \tilde{\mathbf{h}}_2^{r_2}(\mathbf{z}_1) \ , \quad \boldsymbol{\eta}_2 = \tilde{\mathbf{\Phi}}_{2,\eta}(\mathbf{z}_1) \tag{7.15}$$

where $\tilde{\mathbf{h}}_2^{r_2}(\mathbf{z}_1) = \mathbf{h}_2^{r_2}(\mathbf{x}) \circ \mathbf{\Phi}_1^{-1}(\mathbf{z}_1)$ and $\tilde{\mathbf{\Phi}}_{2,\eta}(\mathbf{z}_1)$ again is chosen such that $\tilde{\mathbf{\Phi}}_2(\mathbf{z}_1)$ is a diffeomorphism in a neighborhood of $\mathbf{x}_0$. Obviously, the transformation from $\mathbf{x}$ to $\mathbf{z}_2$ coordinates is given by $\mathbf{z}_2 = \mathbf{\Phi}_2(\mathbf{x}) = \tilde{\mathbf{\Phi}}_2 \circ \mathbf{\Phi}_1(\mathbf{x})$. To indicate that a quantity is given in $\mathbf{z}_2$ coordinates, in the sequel, the hat symbol will be used. In $\mathbf{z}_2$ coordinates, the 2nd subsystem has input-output normal form, i.e.,

$$\begin{aligned}
\dot{\xi}_{2,1} &= \xi_{2,2} \\
&\dots \\
\dot{\xi}_{2,r_2-1} &= \xi_{2,r_2} \\
\dot{\xi}_{2,r_2} &= \hat{\alpha}_2(\boldsymbol{\xi}_2, \boldsymbol{\eta}_2) + \hat{\beta}_2(\boldsymbol{\xi}_2, \boldsymbol{\eta}_2) u
\end{aligned} \tag{7.16a}$$

$$\dot{\boldsymbol{\eta}}_2 = \hat{\mathbf{p}}_2(\boldsymbol{\xi}_2, \boldsymbol{\eta}_2) + \hat{\mathbf{q}}_2(\boldsymbol{\xi}_2, \boldsymbol{\eta}_2) u \tag{7.16b}$$

$$y = \xi_{2,1} \tag{7.16c}$$

with $\hat{\alpha}_2(\mathbf{z}_2)$, $\hat{\beta}_2(\mathbf{z}_2)$, $\hat{\mathbf{p}}_2(\mathbf{z}_2)$ and $\hat{\mathbf{q}}_2(\mathbf{z}_2)$ defined analogously to (7.13). Note that $\tilde{\Phi}_{2,1}(\mathbf{z}_1) = \xi_{1,1}$ and hence $\xi_{2,1} = \xi_{1,1}$. The inverse of $\tilde{\mathbf{\Phi}}_2(\mathbf{z}_1)$ is partitioned as

$$\mathbf{z}_1 = \begin{bmatrix} \boldsymbol{\xi}_1 \\ \boldsymbol{\eta}_1 \end{bmatrix} = \tilde{\mathbf{\Phi}}_2^{-1}(\mathbf{z}_2) = \begin{bmatrix} \tilde{\mathbf{\Phi}}_{2,\xi}^{-1}(\mathbf{z}_2) \\ \tilde{\mathbf{\Phi}}_{2,\eta}^{-1}(\mathbf{z}_2) \end{bmatrix} \tag{7.17}$$

with[4] $\tilde{\mathbf{\Phi}}_{2,\xi}^{-1} : \mathbb{R}^n \to \mathbb{R}^{r_1}$ and $\tilde{\mathbf{\Phi}}_{2,\eta}^{-1} : \mathbb{R}^n \to \mathbb{R}^{n-r_1}$. For notational convenience, we also introduce the function $\tilde{\mathbf{\Phi}}_1(\mathbf{z}_1) = \mathbf{z}_1$.

As Assumption 7.1.1 above, the following assumption is also made only for simplicity of exposition and the presented results can be transferred to the general case in a straightforward manner (see Remark 7.2.2).

Assumption 7.2.1. The mappings $\Phi_1(\mathbf{x})$, $\Phi_2(\mathbf{x})$ are global coordinate transformations.

[3] Recall that the Lie derivative is not affected by changes of coordinates [110].

[4] Note that, with some abuse of notation, the superscript "-1" of $\tilde{\mathbf{\Phi}}_{2,\xi}^{-1}(\mathbf{z}_2)$ and $\tilde{\mathbf{\Phi}}_{2,\eta}^{-1}(\mathbf{z}_2)$ is only used to indicate that these functions are parts of $\tilde{\mathbf{\Phi}}_2^{-1}(\mathbf{z}_2)$.

As is well known from the theory on smooth systems (see e.g. [89]), in order to achieve exact output tracking on intervals $[t_i, t_{i+1})$ within which the 1st subsystem is active, i.e., $\sigma(t_i) = 1$, the state $\mathbf{z}_{1,d}(t_i)$ at time t_i has to satisfy

$$\tilde{\mathbf{h}}_1^{r_1}(\mathbf{z}_{1,d}(t_i)) = \boldsymbol{\xi}_{1,d}(t_i) = \mathbf{Y}_d^{r_1}(t_i) \; . \tag{7.18}$$

Moreover, for all $t \in [t_i, t_{i+1})$, the control input necessarily has to be chosen as

$$u_d(t) = \tilde{u}_{1,d}\left(\boldsymbol{\xi}_1, \boldsymbol{\eta}_1, y_d^{(r_1)}\right) = \tilde{\beta}_1^{-1}(\boldsymbol{\xi}_1, \boldsymbol{\eta}_1)\left(y_d^{(r_1)} - \tilde{\alpha}_1(\boldsymbol{\xi}_1, \boldsymbol{\eta}_1)\right) \; . \tag{7.19}$$

Using this in (7.13) we obtain

$$\begin{aligned} \dot{\xi}_{1,1} &= \xi_{1,2} \\ &\dots \\ \dot{\xi}_{1,r} &= y_d^{(r_1)}(t) \\ \dot{\boldsymbol{\eta}}_1 &= \tilde{\mathbf{p}}_1(\boldsymbol{\xi}_1, \boldsymbol{\eta}_1) + \tilde{\mathbf{q}}_1(\boldsymbol{\xi}_1, \boldsymbol{\eta}_1) u \; . \end{aligned} \tag{7.20}$$

Since by construction $\boldsymbol{\xi}_1 = \boldsymbol{\xi}_{1,d} = \mathbf{Y}_d^{r_1}$, it can be seen from (7.19) that on $[t_i, t_{i+1})$ the input trajectory $u_d(t)$ is given by $u_d = \tilde{u}_{1,d}(\mathbf{Y}_d^{r_1}, \boldsymbol{\eta}_{1,d}, y_d^{(r_1)})$, where

$$\dot{\boldsymbol{\eta}}_{1,d} = \tilde{\mathbf{p}}_1\left(\mathbf{Y}_d^{r_1}, \boldsymbol{\eta}_{1,d}\right) + \tilde{\mathbf{q}}_1\left(\mathbf{Y}_d^{r_1}, \boldsymbol{\eta}_{1,d}\right) \tilde{u}_{1,d}\left(\mathbf{Y}_d^{r_1}, \boldsymbol{\eta}_{1,d}, y_d^{(r_1)}\right) \; . \tag{7.21}$$

Similarly, for exact output tracking on intervals $[t_i, t_{i+1})$ with $\sigma(t_i) = 2$

$$\tilde{\mathbf{h}}_2^{r_2}(\mathbf{z}_{1,d}(t_i)) = \mathbf{Y}_d^{r_2}(t_i) \tag{7.22}$$

must be fulfilled and the control is

$$u_d = \hat{u}_{2,d}(\boldsymbol{\xi}_2, \boldsymbol{\eta}_2, y_d^{(r_2)}) = \hat{\beta}_2^{-1}(\boldsymbol{\xi}_2, \boldsymbol{\eta}_2)\left(y_d^{(r_2)} - \hat{\alpha}_2(\boldsymbol{\xi}_2, \boldsymbol{\eta}_2)\right) \; . \tag{7.23}$$

The input trajectory that achieves exact output tracking on $[t_i, t_{i+1})$ is then given by $u_d = \hat{u}_{2,d}(\mathbf{Y}_d^{r_2}, \boldsymbol{\eta}_{2,d}, y_d^{(r_2)})$ with

$$\dot{\boldsymbol{\eta}}_{2,d} = \hat{\mathbf{p}}_2\left(\mathbf{Y}_d^{r_2}, \boldsymbol{\eta}_{2,d}\right) + \hat{\mathbf{q}}_2\left(\mathbf{Y}_d^{r_2}, \boldsymbol{\eta}_{2,d}\right) \hat{u}_{2,d}\left(\mathbf{Y}_d^{r_2}, \boldsymbol{\eta}_{2,d}, y_d^{(r_2)}\right) \; . \tag{7.24}$$

7.2.1 Trajectory-Independent Switching

Now we are ready to state the first proposition which gives necessary and sufficient conditions for the solvability of the EOT problem for switched systems with a trajectory-independent switching signal $\sigma(t) \in \mathcal{S}_{pc}$.

Proposition 7.2.1. *Suppose that the Assumptions 7.1.1 and 7.2.1 hold. Then Problem 7.1.1 is solvable if and only if there is* $\mathbf{z}_{1,d}(0)$ *such that*

1) at time $t = 0$ *it holds that*

$$\tilde{\mathbf{h}}_{\sigma(0)}^{r_{\sigma(0)}}\left(\mathbf{z}_{1,d}(0)\right) = \mathbf{Y}_d^{r_{\sigma(0)}}(0)\ . \tag{7.25}$$

2) for every switching time t_i *with* $\sigma(t_i^-) = 1$, $\sigma(t_i) = 2$ *it holds that*

$$\tilde{\mathbf{\Phi}}_{2,\xi}\left(\mathbf{Y}_d^{r_1}(t_i), \boldsymbol{\eta}_{1,d}(t_i)\right) - \mathbf{Y}_d^{r_2}(t_i) = \mathbf{0} \tag{7.26}$$

3) for all switching times t_i *with* $\sigma(t_i^-) = 2$, $\sigma(t_i) = 1$ *it is satisfied that*

$$\mathbf{Y}_d^{r_1}(t_i) - \tilde{\mathbf{\Phi}}_{2,\xi}^{-1}\left(\mathbf{Y}_d^{r_2}(t_i), \boldsymbol{\eta}_{2,d}(t_i)\right) = \mathbf{0} \tag{7.27}$$

4) the trajectories $\boldsymbol{\eta}_{p,d}(t)$, $p \in \mathcal{P}$, *which satisfy* (7.21) *for all* t *in intervals* (t_i, t_{i+1}) *with* $\sigma(t_i) = 1$, (7.24) *for all* t *in* (t_i, t_{i+1}) *with* $\sigma(t_i) = 2$ *and* $\boldsymbol{\eta}_{\sigma(0),d}(0) = \tilde{\mathbf{\Phi}}_{\sigma(0),\eta}(\mathbf{z}_{1,d}(0))$ *as well as*

$$\boldsymbol{\eta}_{1,d}(t_i) = \tilde{\mathbf{\Phi}}_{2,\eta}^{-1}\left(\mathbf{Y}_d^{r_2}(t_i), \boldsymbol{\eta}_{2,d}(t_i^-)\right)\ , \quad \text{for } t_i \text{ with } \sigma(t_i^-) = 2,\ \sigma(t_i) = 1 \tag{7.28a}$$

$$\boldsymbol{\eta}_{2,d}(t_i) = \tilde{\mathbf{\Phi}}_{2,\eta}\left(\mathbf{Y}_d^{r_1}(t_i), \boldsymbol{\eta}_{1,d}(t_i^-)\right)\ , \quad \text{for } t_i \text{ with } \sigma(t_i^-) = 1,\ \sigma(t_i) = 2 \tag{7.28b}$$

are bounded.

Proof. To prove necessity, suppose that there is a piecewise continuous control input $u_d(t)$ such that the corresponding solution $\mathbf{z}_{1,d}(t)$ satisfies $\tilde{h}_1(\mathbf{z}_{1,d}(t)) = y_d(t)$ for all $t \geq 0$. Then for all t in intervals $[t_i, t_{i+1})$ with $\sigma(t_i) = 1$ we have

$$\mathbf{Y}^{r_1}(t) = \tilde{\mathbf{h}}_1^{r_1}\left(\mathbf{z}_{1,d}\left(t\right)\right) = \boldsymbol{\xi}_{1,d}(t) = \mathbf{Y}_d^{r_1}(t)\ . \tag{7.29}$$

Accordingly, for all t in intervals $[t_i, t_{i+1})$ with $\sigma(t_i) = 2$ it holds that

$$\mathbf{Y}^{r_2}(t) = \tilde{\mathbf{h}}_2^{r_2}\left(\mathbf{z}_{1,d}(t)\right) = \boldsymbol{\xi}_{2,d}(t) = \mathbf{Y}_d^{r_2}(t) \tag{7.30}$$

From this, it gets immediately clear that (7.25) holds.

Being a solution of (7.11), the state trajectory $\mathbf{z}_{1,d}(t)$ is continuous and therefore $\mathbf{z}_{1,d}(t_i^-) = \mathbf{z}_{1,d}(t_i)$ must be satisfied for any t_i, which obviously implies $\mathbf{z}_{2,d}(t_i^-) = \mathbf{z}_{2,d}(t_i)$.

Thus, for any switching time t_i with $\sigma(t_i^-) = 1$, $\sigma(t_i) = 2$, the relation

$$\tilde{\boldsymbol{\Phi}}_2 \left(\begin{bmatrix} \boldsymbol{\xi}_{1,d}(t_i^-) \\ \boldsymbol{\eta}_{1,d}(t_i^-) \end{bmatrix} \right) = \begin{bmatrix} \boldsymbol{\xi}_{2,d}(t_i) \\ \boldsymbol{\eta}_{2,d}(t_i) \end{bmatrix} \tag{7.31}$$

holds, where we have used that $\mathbf{z}_{2,d}(t_i^-) = \tilde{\boldsymbol{\Phi}}_2(\mathbf{z}_{1,d}(t_i^-))$. Moreover, we observe from (7.29) and (7.30) that $\boldsymbol{\xi}_{1,d}(t_i^-) = \mathbf{Y}_d^{r_1}(t_i)$ and $\boldsymbol{\xi}_{2,d}(t_i) = \mathbf{Y}_d^{r_2}(t_i)$. Substituting this into (7.31) yields

$$\tilde{\boldsymbol{\Phi}}_2 \left(\begin{bmatrix} \mathbf{Y}_d^{r_1}(t_i) \\ \boldsymbol{\eta}_{1,d}(t_i^-) \end{bmatrix} \right) = \begin{bmatrix} \mathbf{Y}_d^{r_2}(t_i) \\ \boldsymbol{\eta}_{2,d}(t_i) \end{bmatrix} . \tag{7.32}$$

Note that, clearly, $\mathbf{Y}_d^{r_1}(t_i^-) = \mathbf{Y}_d^{r_1}(t_i)$ holds for all t_i due to the differentiability assumption imposed on y_d. From the first r_2 rows of this equation, it can be seen that (7.26) holds.

In a similar manner, we obtain

$$\tilde{\boldsymbol{\Phi}}_2^{-1} \left(\begin{bmatrix} \mathbf{Y}_d^{r_2}(t_i) \\ \boldsymbol{\eta}_{2,d}(t_i^-) \end{bmatrix} \right) = \begin{bmatrix} \mathbf{Y}_d^{r_1}(t_i) \\ \boldsymbol{\eta}_{1,d}(t_i) \end{bmatrix} . \tag{7.33}$$

for switching times t_i with $\sigma(t_i^-) = 2$, $\sigma(t_i) = 1$, where we have used $\mathbf{z}_{1,d}(t_i^-) = \mathbf{z}_{1,d}(t_i)$ and $\mathbf{z}_{1,d}(t_i^-) = \tilde{\boldsymbol{\Phi}}_2^{-1}(\mathbf{z}_{2,d}(t_i^-))$ together with $\boldsymbol{\xi}_{2,d}(t_i^-) = \mathbf{Y}_d^{r_2}(t_i)$ and $\boldsymbol{\xi}_{1,d}(t_i) = \mathbf{Y}_d^{r_1}(t_i)$. The first r_1 rows of this equation establish the condition (7.27).

As far as the evolution of $\boldsymbol{\eta}_{p,d}$ is concerned, it is clear that in intervals (t_i, t_{i+1}) with $\sigma(t_i) = 1$ the evolution of $\boldsymbol{\eta}_{1,d}$ is governed by (7.21), and similarly in intervals (t_i, t_{i+1}) with $\sigma(t_i) = 2$ the behavior of $\boldsymbol{\eta}_{2,d}$ is described by the differential equation (7.24). Moreover, the initial condition clearly is determined by $\boldsymbol{\eta}_{\sigma(0),d}(0) = \tilde{\boldsymbol{\Phi}}_{\sigma(0),\eta}(\mathbf{z}_{1,d}(0))$. The relations (7.28a), (7.28b) are obtained from the last $n - r_1$ rows of (7.33) and the last $n - r_2$ rows of (7.32), respectively. Furthermore, $\boldsymbol{\eta}_{\sigma(t),d}$ has to be bounded in order that $\mathbf{z}_{1,d}(t)$ is bounded.

In order to prove sufficiency, we only need to show that under the conditions of the proposition $\boldsymbol{\xi}_{1,d}(t_i) = \mathbf{Y}_d^{r_1}(t_i)$ holds for every t_i with $\sigma(t_i) = 1$ and $\boldsymbol{\xi}_{2,d}(t_i) = \mathbf{Y}_d^{r_2}(t_i)$ is satisfied for every t_i with $\sigma(t_i) = 2$ (c.f. (7.18) and (7.22)). This easily follows by induction. For $t_0 = 0$ it holds true due to (7.25). Now assume that $\boldsymbol{\xi}_{1,d}(t_i) = \mathbf{Y}_d^{r_1}(t_i)$ holds for t_i with $\sigma(t_i) = 1$. Then $\sigma(t_{i+1}) = 2$ and $\boldsymbol{\xi}_{2,d}(t_{i+1}) = \mathbf{Y}_d^{r_2}(t_{i+1})$. Because, if $\boldsymbol{\xi}_{1,d}(t_i) = \mathbf{Y}_d^{r_1}(t_i)$ holds, then $u_d(t) = \tilde{u}_{d,1}$ yields exact tracking within $[t_i, t_{i+1})$ and hence $\boldsymbol{\xi}_{1,d}(t_{i+1}^-) = \mathbf{Y}_d^{r_1}(t_{i+1}^-)$. Using (7.26) we conclude that

$$\boldsymbol{\xi}_{2,d}(t_{i+1}) = \tilde{\boldsymbol{\Phi}}_{2,\xi} \left(\begin{bmatrix} \boldsymbol{\xi}_{1,d}(t_{i+1}^-) \\ \boldsymbol{\eta}_{1,d}(t_{i+1}^-) \end{bmatrix} \right) = \tilde{\boldsymbol{\Phi}}_{2,\xi} \left(\begin{bmatrix} \mathbf{Y}_d^{r_1}(t_{i+1}) \\ \boldsymbol{\eta}_{1,d}(t_{i+1}^-) \end{bmatrix} \right) = \mathbf{Y}_d^{r_2}(t_{i+1}) . \tag{7.34}$$

In the same manner, it can be derived that $\boldsymbol{\xi}_{1,d}(t_{i+1}) = \mathbf{Y}_d^{r_1}(t_{i+1})$ holds in case that $\boldsymbol{\xi}_{2,d}(t_i) = \mathbf{Y}_d^{r_2}(t_i)$ is satisfied for $\sigma(t_i) = 2$ using condition (7.27). Boundedness of the state and input trajectory follows immediately from boundedness of $\boldsymbol{\eta}_{\sigma(t),d}(t)$ and $\mathbf{Y}_d^{r_1}(t)$. This completes the proof. □

The first row of both (7.26) and (7.27) is of course trivially satisfied. The conditions involve the switched differential equation determining the evolution of the internal states $\boldsymbol{\eta}_{p,d}$ (see part 4) of the proposition), which makes them difficult to verify in general. If we are given a finite time interval $[0, t_f]$ and a particular output trajectory $y_d : [0, t_f] \to \mathbb{R}$ together with a switching signal $\sigma : [0, t_f] \to \mathcal{P}$ with $\sigma \in \mathcal{S}$, a solution can be obtained by numerical integration. However, it is, in general, not possible to identify a set of output trajectories for which exact tracking is possible *a priori*. In some cases, one can predefine the structure of $y_d(t)$, e.g. by a polynomial of a certain order, and calculate an analytic expression for $\boldsymbol{\eta}_{p,d}(t)$ depending on the polynomial coefficients. Then, a set of polynomial output trajectories $y_d(t)$ can be identified which can be exactly tracked by the system output.

If $y = z_{1,1}$ is a flat output [52] for both subsystems, i.e., $r_1 = r_2 = n$, then there is no internal dynamics and the conditions in the proposition become purely algebraic. Moreover, (7.26) and (7.27) are equivalent, as can be easily verified. In this case, a set of output trajectories for which the conditions are fulfilled can be immediately identified.

Example 7.2.1. Consider the linear switched system given in $\mathbf{z}_1$-coordinates

$$\dot{\mathbf{z}}_1 = \widetilde{\mathbf{A}}_\sigma \mathbf{z}_1 + \tilde{\mathbf{g}}_\sigma u \,, \quad \widetilde{\mathbf{A}}_1 = \begin{bmatrix} 0 & 1 \\ -2 & -4 \end{bmatrix} \,, \quad \widetilde{\mathbf{A}}_2 = \begin{bmatrix} -1 & 2 \\ -2 & -4 \end{bmatrix} \,, \quad \tilde{\mathbf{g}}_1 = \tilde{\mathbf{g}}_2 = \begin{bmatrix} 0 \\ 1 \end{bmatrix} \tag{7.35a}$$

$$y = z_{1,1} \,. \tag{7.35b}$$

Obviously, y is a flat output for both subsystems, i.e., $r_1 = r_2 = 2$. We determine

$$\tilde{\boldsymbol{\Phi}}_2(\mathbf{z}_1) = \begin{bmatrix} z_{1,1} & -z_{1,1} + 2z_{1,2} \end{bmatrix}^T \tag{7.36}$$

and from (7.26) (recall that (7.26) and (7.27) are equivalent when y is a flat output) we get

$$\begin{bmatrix} y_d(t_i) \\ -y_d(t_i) + 2\dot{y}_d(t_i) \end{bmatrix} - \begin{bmatrix} y_d(t_i) \\ \dot{y}_d(t_i) \end{bmatrix} = 0 \,. \tag{7.37}$$

We conclude that the EOT problem is solvable if and only if the desired trajectory satisfies $y_d(t_i) = \dot{y}_d(t_i)$ for all t_i.

We remark that in the special case where both subsystems are linear, like in the example above, also the conditions given in [40] could be used. However, the conditions in Proposition 7.2.1 provide more insight and their application is much easier, especially in the case where y is a flat output.

7.2.2 Trajectory-Dependent Switching: The Case $r_1 = r_2$

In the remainder of this section, we investigate the EOT problem for systems (7.1) with state- and/or input-dependent switching according to (2.69), (2.70). In many applications, it is desired that the control designer or even the operator can freely specify a trajectory for the output quantity. Therefore, it is of interest whether a switched system is capable of exactly tracking *arbitrary* trajectories $y_d(t)$. As we have seen in the previous subsection, this is not possible for trajectory-independent switching as in this case exact output tracking can only be achieved for suitable combinations of switching signal and desired trajectory. If the switching is trajectory-dependent, exact tracking of arbitrary output trajectories $y_d(t)$ is possible under some conditions. It is the main objective of this subsection and the subsequent one to derive these conditions.

In this subsection, we consider the case that $r_1 = r_2 = r$. The next subsection will then be devoted to systems with $r_2 < r_1$. First, we establish necessary conditions for the general situation, in which $r < n$. Afterwards, sufficient conditions are deduced assuming that y is a flat output for both subsystems, i.e., $r = n$.

7.2.2.1 Necessary Conditions

Let us define $\tilde{\mathbf{f}}_{1,d}(\mathbf{z}_1, y_d^{(r)}(t)) = \tilde{\mathbf{f}}_1(\mathbf{z}_1) + \tilde{\mathbf{g}}(\mathbf{z}_1)\tilde{u}_{1,d}(\mathbf{z}_1, y_d^{(r)}(t))$. We recall that $\mathbf{\Phi}_{1,\eta}(\mathbf{x})$ can always be chosen such that $L_g\Phi_{1,i} = 0$ for all $r+1 \leq i \leq n$ [89], which entails $\tilde{\mathbf{q}}_1(\mathbf{z}_1) = \mathbf{0}$. Hence we can assume that $\dot{\mathbf{z}}_1 = \tilde{\mathbf{f}}_{1,d}(\mathbf{z}_1, y_d^{(r)}(t))$ can be represented component-wise as

$$\begin{aligned} \dot{\xi}_{1,1} &= \xi_{1,2} \\ &\dots \\ \dot{\xi}_{1,r} &= y_d^{(r)}(t) \\ \dot{\boldsymbol{\eta}}_1 &= \tilde{\mathbf{p}}_1(\boldsymbol{\xi}_1, \boldsymbol{\eta}_1)\,. \end{aligned} \tag{7.38}$$

In the same manner, we define $\hat{\mathbf{f}}_{2,d}(\mathbf{z}_2, y_d^{(r)}(t)) = \hat{\mathbf{f}}_2(\mathbf{z}_2) + \hat{\mathbf{g}}(\mathbf{z}_2)\hat{u}_{2,d}(\mathbf{z}_2, y_d^{(r)}(t))$, and we also assume in the following that $\tilde{\mathbf{\Phi}}_{2,\eta}(\mathbf{z}_1)$ has been chosen such that $\hat{\mathbf{q}}_2(\mathbf{z}_2) = \mathbf{0}$.

We first identify points on the switching surface $\partial\chi$ at which switching can take place for some $y_d(t)$. In $\mathbf{z}_1$ coordinates, the manifold $\partial\chi$ is described by $\tilde{\varphi}(\mathbf{z}_1, u) = 0$ where

$\tilde{\varphi}(\mathbf{z}_1, u) = \varphi(\mathbf{\Phi}_1^{-1}(\mathbf{z}_1), u) = \tilde{\varphi}_x(\mathbf{z}_1) + \tilde{\varphi}_u(\mathbf{z}_1)u$. Similarly, in $\mathbf{z}_2$ coordinates we have $\hat{\varphi}(\mathbf{z}_2, u) = \tilde{\varphi}(\tilde{\mathbf{\Phi}}_2^{-1}(\mathbf{z}_2), u) = \hat{\varphi}_x(\mathbf{z}_2) + \hat{\varphi}_u(\mathbf{z}_2)u$. Let $\tilde{\varphi}_1(\mathbf{z}_1, y_d^{(r)}) = \tilde{\varphi}(\mathbf{z}_1, \tilde{u}_{1,d})$ and

$$\dot{\tilde{\varphi}}_1(\mathbf{z}_1, y_d^{(r)}, y_d^{(r+1)}) = \frac{\partial \tilde{\varphi}(\mathbf{z}_1)}{\partial \mathbf{z}_1} \tilde{\mathbf{f}}_{1,d}(\mathbf{z}_1, y^{(r)}) + \tilde{\varphi}_u(\mathbf{z}_1)\dot{\tilde{u}}_{1,d}(\mathbf{z}_1, y_d^{(r)}, y_d^{(r+1)}) \tag{7.39}$$

be the rate of change of $\tilde{\varphi}(\mathbf{z}_1, u)$ along the trajectories of the 1st subsystem with the control $u = \tilde{u}_{1,d}$. The higher derivatives are denoted by $\tilde{\varphi}_1^{(j)}(\mathbf{z}_1, y_d^{(r)}, \ldots, y_d^{(r+j)})$, $j = 2, 3, \ldots$. Accordingly, we define $\tilde{\varphi}_2(\mathbf{z}_1, y_d^{(r)}) = \tilde{\varphi}(\mathbf{z}_1, \tilde{u}_{2,d})$, and we refer to the time derivatives of $\tilde{\varphi}(\mathbf{z}_1, u)$ along the trajectories of the 2nd subsystem with the input $u = \tilde{u}_{2,d}$ as $\tilde{\varphi}_2^{(j)}(\mathbf{z}_1, y_d^{(r)}, \ldots, y_d^{(r+j)})$, $j = 1, 2, \ldots$. For compactness of notation, we will often write $\tilde{\varphi}_p(t)$ and $\tilde{\varphi}_p^{(j)}(t)$, $p \in \mathcal{P}$ if we want to stress especially the time-dependency.

Let S_1 be the set of $\mathbf{z}_1 \in \mathbb{R}^n$ for which there is $(y_d^{(r)}, y_d^{(r+1)}, \ldots)$ such that $\tilde{\varphi}_1(\mathbf{z}_1, y_d^{(r)}) = 0$ and for some $j \in \mathbb{N}_0$ it holds that $\tilde{\varphi}_1^{(i)} = 0$ for $i \leq 2j$ and $\tilde{\varphi}_1^{(2j+1)} < 0$. Analogously, the set S_2 contains all $\mathbf{z}_1 \in \mathbb{R}^n$ for which there is $(y_d^{(r)}, y_d^{(r+1)}, \ldots)$ such that $\tilde{\varphi}_2(\mathbf{z}_1, y_d^{(r)}) = 0$ and for some $j \in \mathbb{N}_0$ it holds that $\tilde{\varphi}_2^{(i)} = 0$ for $i \leq 2j$ and $\tilde{\varphi}_2^{(2j+1)} > 0$. Moreover, we define $\mathrm{S} = \mathrm{S}_1 \cup \mathrm{S}_2$. If $\tilde{\varphi}(\mathbf{z}_1, u)$ depends on the control input, by assumption (see Section 2.4.1), it holds that $\tilde{\varphi}_u(\mathbf{z}_1) \neq 0$ for all $\mathbf{z}_1$. It is easily verified that in this case $\mathrm{S}_1 = \mathrm{S}_2 = \mathbb{R}^n$.

The set S_1 contains all points $\mathbf{z}_1$ with the property that we can find $(y_d^{(r)}, y_d^{(r+1)}, \ldots)$ such that $\tilde{\varphi}_1(\mathbf{z}_1, y_d^{(r)}) = 0$ and the first nonzero derivative $\tilde{\varphi}_1^{(j)}$ is of odd order and negative. At these points switching from the 1st to the 2nd subsystem can occur, as is easily seen by a Taylor expansion of $\tilde{\varphi}_1(t)$ in t. Assume that $\tilde{\varphi}_1(\tau) = 0$ for some τ and $\tilde{\varphi}_1^{(k)}(\tau) < 0$ with k an odd integer and $\tilde{\varphi}_1^{(i)}(\tau) = 0$ for all $0 < i < k$. Since $\tilde{\varphi}_1^{(k)}(\mathbf{z}_1(t), y_d^{(r)}(t), \ldots, y_d^{(r+k)}(t))$ is continuous in t there is an $\epsilon > 0$ such that it remains negative within the interval $(\tau - \epsilon, \tau + \epsilon)$. Then, it follows from Taylor's Theorem (see e.g. Theorem 2.1 in [129]) that for any $\bar{t} \in (-\epsilon, \epsilon)$ it holds that

$$\begin{aligned} \tilde{\varphi}_1(\tau + \bar{t}) &= \tilde{\varphi}_1(\tau) + \dot{\tilde{\varphi}}(\tau)\bar{t} + \ldots + \tilde{\varphi}_1^{(k-1)}(\tau)\frac{\bar{t}^{k-1}}{(k-1)!} + \tilde{\varphi}_1^{(k)}(\tau + \delta\bar{t})\frac{\bar{t}^k}{k!} = \\ &= \tilde{\varphi}_1^{(k)}(\tau + \delta\bar{t})\frac{\bar{t}^k}{k!} \end{aligned} \tag{7.40}$$

where $\delta \in (0, 1)$. Since $\tau + \delta\bar{t} \in (\tau - \epsilon, \tau + \epsilon)$, we have $\tilde{\varphi}_1^{(k)}(\tau + \delta\bar{t}) < 0$. Therefore, $\tilde{\varphi}_1(t) > 0$ for $t \in (\tau - \epsilon, \tau)$ and $\tilde{\varphi}_1(t) < 0$ for $t \in (\tau, \tau + \epsilon)$, which shows that the trajectory crosses the switching surface. In the same manner, it can be derived that at all $\mathbf{z}_1 \in \mathrm{S}_2$ switching from the 2nd to the 1st subsystem is possible.

In order that a particular trajectory $y_d(t)$ can be tracked exactly, as in the case of trajectory-independent switching, the initial state $\mathbf{z}_{1,d}(0)$ has to satisfy $\mathbf{Y}_d^r(0) = \tilde{\mathbf{h}}_{\sigma(0)}^r(\mathbf{z}_{1,d}(0))$. In

the present case of trajectory-dependent switching, the switching law depends, in general, on the state and the input. Consequently, a necessary prerequisite for Problem 7.1.2 to be solvable for all desired output trajectories $y_d(t)$ is that for all $\mathbf{Y}_d^r \in \mathbb{R}^r$ and all $y_d^{(r+1)}$ there is at least one pair consisting of $\mathbf{z}_1 \in \mathbb{R}^n$ and $p \in \mathcal{P}$ such that

$$\tilde{\mathbf{h}}_p^r(\mathbf{z}_1) = \mathbf{Y}_d^r \quad \text{and} \quad \left[\mathbf{z}_1^T \ \tilde{u}_{p,d}(\mathbf{z}_1, y_d^{(r)})\right]^T \in \chi_p \ . \tag{7.41}$$

If there is more than one such pair, it is desirable that exact tracking is possible for all of them – analogously to the non-switched case, where the initial value of $\boldsymbol{\eta}$ can be chosen arbitrary.

Theorem 7.2.1. *Consider the system* (7.1) *with the switching law* (2.69) *and suppose that the Assumptions 7.1.1 and 7.2.1 are satisfied and that* $r_1 = r_2 = r$*. A necessary condition for the solvability of Problem 7.1.2 for all* $y_d(t)$ *and all pairs satisfying* (7.41) *is that for all* $\mathbf{z}_1 \in \mathrm{S}$ *and all* $i \in \{2, \dots, r\}$ *it holds that*

$$L_{\tilde{f}_2}^{i-1} \tilde{h}(\mathbf{z}_1) - z_{1,i} = 0 \ . \tag{7.42}$$

Proof. We have already seen above that for every $\bar{\mathbf{z}}_1 \in \mathrm{S}_1$ there is a trajectory $\mathbf{z}_{1,d}(t)$ of (7.38) satisfying $\mathbf{z}_{1,d}(\tau) = \bar{\mathbf{z}}_1$ for some time τ and $\mathbf{z}_{1,d}(t) \in \operatorname{int} \chi_1$, $t \in (\tau - \epsilon, \tau)$ for some $\epsilon > 0$ as well as $\mathbf{z}_{1,d}(t) \in \operatorname{int} \chi_2$, $t \in (\tau, \tau + \epsilon)$. An analogous result holds true for all $\bar{\mathbf{z}}_1 \in \mathrm{S}_2$. Hence, if we vary over all $y_d(t)$ and all pairs $(\mathbf{z}_{1,d}(0), p)$ satisfying (7.41), exact tracking requires that the switching surface is traversed at any point $\mathbf{z}_1 \in \mathrm{S}$. Now suppose that, for a particular $y_d(t)$, there is a solution $\mathbf{z}_{1,d}(t)$ of

$$\dot{\mathbf{z}}_{1,d}(t) = \tilde{\mathbf{f}}_{\sigma(t),d}\left(\mathbf{z}_{1,d}(t), y_d^{(r)}(t)\right) \tag{7.43}$$

in the sense of Definition 2.4.1 such that $\tilde{h}(\mathbf{z}_{1,d}(t)) = y_d(t)$. Then, for all t in intervals $[t_i, t_{i+1})$ with $\sigma(t_i) = 1$, we have

$$\mathbf{Y}^r(t) = \tilde{\mathbf{h}}_1^r(\mathbf{z}_{1,d}(t)) = \boldsymbol{\xi}_{1,d}(t) = \mathbf{Y}_d^r(t) \tag{7.44}$$

and, for all t in intervals $[t_i, t_{i+1})$ with $\sigma(t_i) = 2$, it holds that

$$\mathbf{Y}^r(t) = \tilde{\mathbf{h}}_2^r(\mathbf{z}_{1,d}(t)) = \boldsymbol{\xi}_{2,d}(t) = \mathbf{Y}_d^r(t) \ . \tag{7.45}$$

From (7.45), it can be seen that for switching times t_i with $\sigma(t_i^-) = 1$, $\sigma(t_i) = 2$ we have that $\tilde{\mathbf{h}}_2^r(\mathbf{z}_{1,d}(t_i)) = \mathbf{Y}_d^r(t_i)$ and it follows from (7.44) that $\mathbf{Y}_d^r(t_i) = \boldsymbol{\xi}_1(t_i^-)$. Using this and

continuity of $\mathbf{z}_{1,d}(t)$, i.e., $\mathbf{z}_{1,d}(t_i^-) = \mathbf{z}_{1,d}(t_i)$, we conclude that

$$\boldsymbol{\xi}_{1,d}(t_i) = \tilde{\mathbf{h}}_2^r \left(\boldsymbol{\xi}_{1,d}(t_i), \boldsymbol{\eta}_{1,d}(t_i) \right) \ . \tag{7.46}$$

Obviously, the same relation must be satisfied for switching times t_i with $\sigma(t_i^-) = 2$ and $\sigma(t_i) = 1$. Thus, we conclude that

$$\boldsymbol{\xi}_1 = \tilde{\mathbf{h}}_2^r \left(\boldsymbol{\xi}_1, \boldsymbol{\eta} \right) \tag{7.47}$$

must hold for any point $\mathbf{z}_1$ at which switching can occur and hence for all $\mathbf{z}_1 \in \mathrm{S}$. The first row of this equation is trivially satisfied since $\tilde{h}(\mathbf{z}_1) = \xi_{1,1}$, and thus (7.42) follows. □

Since $\mathrm{S} = \mathbb{R}^n$ if $\tilde{\varphi}_u(\mathbf{z}_1) \neq 0$, in this case, the conditions (7.42) have to be satisfied for all $\mathbf{z}_1 \in \mathbb{R}^n$. This leads to the following corollary.

Corollary 7.2.1. *Assume that the Assumptions 7.1.1 and 7.2.1 are satisfied and that $r_1 = r_2 = r$. Moreover, suppose that $\tilde{\varphi}_u(\mathbf{z}_1) \neq 0$. Then it is necessary for the solvability of Problem 7.1.2 for all $y_d(t)$ and all pairs satisfying* (7.41) *that for all $i \in \{1, \ldots, r-1\}$*

$$\tilde{f}_{2,i}(\mathbf{z}_1) = \xi_{1,i+1} \quad \text{and} \quad \tilde{g}_{2,i} = 0 \ . \tag{7.48}$$

Note that the conditions (7.48) imply that, with the control $u = \tilde{u}_{\sigma,d}$, the input-output dynamics of both subsystems are identical, i.e., only the internal dynamics are allowed to switch. In the remainder of this subsection, we will therefore assume that $\tilde{\varphi}(\mathbf{z}_1)$ is independent of u, i.e., $\tilde{\varphi}_u(\mathbf{z}_1) = 0$. In this case, verifying the conditions of Theorem 7.2.1 requires us to identify the set S, which sometimes may not be an easy task. The following Lemma[5] states that, if $\mathrm{S} \neq \emptyset$ and we suppose that all functions in (7.1), i.e, $\mathbf{f}_p(\mathbf{x})$, $\mathbf{g}_p(\mathbf{x})$, $p \in \mathcal{P}$ and $h(\mathbf{x})$, and $\varphi(\mathbf{x})$ are analytic in $\mathbb{R}^n$, then we can just as well check whether (7.42) holds for all $\mathbf{z}_1 \in \partial\chi$.

Lemma 7.2.1. *Assume that the Assumptions 7.1.1 and 7.2.1 are satisfied and that $r_1 = r_2 = r$. Further, assume that $\mathbf{f}_p(\mathbf{x})$, $\mathbf{g}_p(\mathbf{x})$, $p \in \mathcal{P}$ and $h(\mathbf{x})$ as well as $\varphi(\mathbf{x})$ are analytic in $\mathbb{R}^n$. If $\mathrm{S} \neq \emptyset$, a necessary condition for the solvability of Problem 7.1.2 for all $y_d(t)$ and all pairs satisfying* (7.41) *is that* (7.42) *holds for all $i \in \{2, \ldots, r\}$ and all $\mathbf{z}_1 \in \partial\chi$.*

Proof. see Appendix B.3. □

[5]The author thanks Prof. Ravi Banavar for help with the proof of this lemma.

Now consider the special case of a *linear* switched system

$$\dot{\mathbf{z}}_1 = \widetilde{\mathbf{A}}_\sigma \mathbf{z}_1 + \tilde{\mathbf{g}}_\sigma u \ , \quad y = \tilde{\mathbf{c}}^T \mathbf{z}_1 \tag{7.49}$$

with $r_1 = r_2 = r$, and let $\tilde{\varphi}(\mathbf{z}_1) = \tilde{\mathbf{n}}^T \mathbf{z}_1 + \tilde{m}$ be an affine function. Furthermore, let $\tilde{\mathbf{a}}_{p,i}^T$, $i = 1, \ldots, n$ denote the rows of the matrices $\widetilde{\mathbf{A}}_p$. For this class of systems, the coordinate transformation $\tilde{\mathbf{\Phi}}_2(\cdot)$ is linear and can be represented as $\tilde{\mathbf{\Phi}}_2(\mathbf{z}_1) = \widetilde{\mathbf{T}}_2 \mathbf{z}_1$. According to the partitioning of $\tilde{\mathbf{\Phi}}_2(\mathbf{z}_1)$ and $\tilde{\mathbf{\Phi}}_2^{-1}(\mathbf{z}_1)$, we introduce the partitioning

$$\widetilde{\mathbf{T}}_2 = \begin{bmatrix} \widetilde{\mathbf{T}}_{2,\xi} \\ \widetilde{\mathbf{T}}_{2,\eta} \end{bmatrix} \ , \quad \widetilde{\mathbf{T}}_2^{-1} = \begin{bmatrix} \widetilde{\mathbf{T}}_{2,\xi}^{-1} \\ \widetilde{\mathbf{T}}_{2,\eta}^{-1} \end{bmatrix} \ . \tag{7.50}$$

The following result can be deduced from Theorem 7.2.1.

Lemma 7.2.2. *Consider the system* (7.49) *with the switching law defined by* (2.70), (2.73) *with* $\tilde{\varphi}(\mathbf{z}_1) = \tilde{\mathbf{n}}^T \mathbf{z}_1 + \tilde{m}$, *and suppose that* S *is nonempty. If* $\tilde{m} \neq 0$, *the conditions* (7.42) *are satisfied if and only if for all* $i \in \{1, \ldots, r-1\}$ *it holds that* $\tilde{\mathbf{a}}_{2,i} = \tilde{\mathbf{a}}_{1,i}$ *and* $\tilde{g}_{2,i} = 0$. *In the case where* $\tilde{m} = 0$, *the conditions* (7.42) *are met if and only if*

$$\operatorname{rank} \left\{ \begin{bmatrix} \tilde{\mathbf{n}}^T \\ \widetilde{\mathbf{T}}_{2,\xi} - \mathbf{I}_{r \times n} \end{bmatrix} \right\} = 1 \tag{7.51}$$

where $\mathbf{I}_{r \times n} = [\mathbf{I}_{r \times r}, \ \mathbf{0}_{r \times (n-r)}]$.

Proof. For the considered class of systems, the conditions (7.42) are equivalent to $\mathbf{z}_1 = \widetilde{\mathbf{T}}_{2,\xi} \mathbf{z}_1$ or $(\widetilde{\mathbf{T}}_{2,\xi} - \mathbf{I}_{r \times n}) \mathbf{z}_1 = \mathbf{0}$ being satisfied for all $\mathbf{z}_1$ with $\tilde{\mathbf{n}} \mathbf{z}_1 + \tilde{m} = 0$, where we have used Lemma 7.2.1 and the fact that linear functions clearly are analytic. First, consider the case, where $\tilde{m} \neq 0$. The set of $\mathbf{z}_1$ satisfying $\tilde{\mathbf{n}} \mathbf{z}_1 = -\tilde{m}$ can be represented in the form $\mathbf{z}_1 = \mathbf{z}_1^p + \mathbf{z}_1^h$ with $\mathbf{z}_1^p$ a fixed vector satisfying $\tilde{\mathbf{n}} \mathbf{z}_1^p = -\tilde{m}$ and $\mathbf{z}_1^h$ an arbitrary element of $\mathcal{N}\{\tilde{\mathbf{n}}^T\}$. Note that, since $\tilde{m} \neq 0$, it must hold that $\mathbf{z}_1^p \notin \mathcal{N}\{\tilde{\mathbf{n}}^T\}$. Now, observe that $(\widetilde{\mathbf{T}}_{2,\xi} - \mathbf{I}_{r \times n}) \mathbf{z}_1 = \mathbf{0}$ can only be fulfilled for all $\mathbf{z}_1 = \mathbf{z}_1^p + \mathbf{z}_1^h$, if $\mathbf{z}_1^p \in \mathcal{N}\{(\widetilde{\mathbf{T}}_{2,\xi} - \mathbf{I}_{r \times n})\}$ and $\mathcal{N}\{\tilde{\mathbf{n}}^T\} \subset \mathcal{N}\{(\widetilde{\mathbf{T}}_{2,\xi} - \mathbf{I}_{r \times n})\}$. Since the dimension of $\mathcal{N}\{\tilde{\mathbf{n}}^T\}$ is $n-1$ and $\mathbf{z}_1^p \notin \mathcal{N}\{\tilde{\mathbf{n}}^T\}$, this entails that the nullspace of $(\widetilde{\mathbf{T}}_{2,\xi} - \mathbf{I}_{r \times n})$ has to be n-dimensional, which is equivalent to $\widetilde{\mathbf{T}}_{2,\xi} = \mathbf{I}_{r \times n}$. It is easily verified that this holds if and only if $\tilde{\mathbf{a}}_{2,i} = \tilde{\mathbf{a}}_{1,i}$ and $\tilde{g}_{2,i} = 0$ are fulfilled for all $i \in \{1, \ldots, r-1\}$. In the case where $\tilde{m} = 0$, it holds that $\mathbf{z}_1^p = \mathbf{0}$ and hence $\mathcal{N}\{\tilde{\mathbf{n}}^T\} = \mathcal{N}\{(\widetilde{\mathbf{T}}_{2,\xi} - \mathbf{I}_{r \times n})\}$ has to be satisfied. From this the condition (7.51) follows. □

Note that, like (7.48), the conditions $\tilde{\mathbf{a}}_{2,i}^T = \tilde{\mathbf{a}}_{1,i}^T$ and $\tilde{g}_{2,i} = \tilde{g}_{1,i} = 0$, $i \in \{1, \ldots, r-1\}$ imply that, after substituting the control $u = \tilde{u}_{d,\sigma}(\mathbf{z}_1, y_d^{(r)})$ into (7.49), the input-output

dynamics of both subsystems are identical and only the internal dynamics are allowed to switch. Moreover, it is worthwhile noting that (7.51) is equivalent to the existence of a vector[6] $\mathbf{k} \in \mathbb{R}^r$ such that $\widetilde{\mathbf{T}}_{2,\xi} = \mathbf{I}_{r\times n} + \mathbf{k}\tilde{\mathbf{n}}^T$, as this will be used in the proof of Theorem 7.2.3 later on in this subsection.

The following example illustrates some of the aspects treated above and shows that the conditions in Theorem 7.2.1 are indeed only necessary.

Example 7.2.2. Consider the simple switched linear system

$$\dot{\mathbf{z}}_1 = \widetilde{\mathbf{A}}_\sigma \mathbf{z}_1 + \tilde{\mathbf{g}}u\ , \quad \widetilde{\mathbf{A}}_1 = \begin{bmatrix} 0 & 0 \\ -1 & -1 \end{bmatrix} \quad \widetilde{\mathbf{A}}_2 \begin{bmatrix} 0 & 0 \\ 1 & -2 \end{bmatrix}\ , \quad \tilde{\mathbf{g}} = \begin{bmatrix} 1 \\ 0 \end{bmatrix} \tag{7.52}$$

given in $\mathbf{z}_1$ coordinates and let $y = z_{1,1}$ and $\tilde{\varphi}(\mathbf{z}_1) = z_{1,2}$. Obviously, it holds that $r_1 = r_2 = r = 1$, and we can choose $\mathbf{z}_2 = \mathbf{z}_1$, i.e., $\tilde{\mathbf{\Phi}}_2(\cdot)$ is the identity map. Moreover, it is easily seen that $\tilde{u}_{d,1} = \dot{y}_d$ and also $\tilde{u}_{d,2} = \dot{y}_d$. The systems $\dot{\mathbf{z}}_1 = \tilde{\mathbf{f}}_{d,p}(\mathbf{z}_1, \dot{y}_d(t))$ are obtained simply by replacing u in (7.52) by $\dot{y}_d$. Although the conditions of Theorem 7.2.1 are of course satisfied due to the fact that $r = 1$, we determine the set S_1 for the purpose of illustration. With $\tilde{\varphi}_1(\mathbf{z}_1) = z_{1,2}$ we calculate

$$\dot{\tilde{\varphi}}_1(\mathbf{z}_1) = \dot{z}_{1,2} = -z_{1,1} - z_{1,2}\ . \tag{7.53}$$

On the switching surface $\partial\chi$ we have $z_{1,2} = 0$ and therefore $\dot{\tilde{\varphi}}_1|_{\partial\chi} = -z_{1,1}$. Thus, all states $\mathbf{z}_1 = [z_{1,1}, 0]^T$ with $z_{1,1} > 0$ are elements of S_1, while all $\mathbf{z}_1 = [z_{1,1}, 0]$ with $z_{1,1} < 0$ do not belong to this set. If $\mathbf{z}_1 = \mathbf{0}$ we obtain $\dot{\tilde{\varphi}}_1 = 0$. It is not difficult to see that we can also achieve $\ddot{\tilde{\varphi}}_1 = 0$ for $\mathbf{z}_1 = \mathbf{0}$ by choosing $\dot{y}_d = 0$. Now, we consider

$$\tilde{\varphi}_1^{(3)} = -z_{1,2} - z_{1,1} + \dot{y}_d - \ddot{y}_d \tag{7.54}$$

for $\mathbf{z}_1 = \mathbf{0}$ and $\dot{y}_d = 0$. By choosing $\ddot{y}_d > 0$, we get $\tilde{\varphi}_1^{(3)} < 0$, which shows that also $\mathbf{z}_1 = \mathbf{0}$ belongs to S_1. In an analogous manner S_2 can be determined.

As remarked above, the system at hand clearly satisfies the conditions of Theorem 7.2.1. Nevertheless, the EOT problem is not solvable for all $y_d(t)$, as can be seen by looking at the vector fields $\tilde{\mathbf{f}}_{d,p}(\mathbf{z}_1, \dot{y}_d(t))$ at the switching surface. This is illustrated in Figure 7.1. The components in $z_{1,1}$-direction are equal to $\dot{y}_d$ and can be chosen arbitrary. The crucial observation is that, for $z_{1,1} > 0$, the projections $\tilde{\mathbf{f}}_{d,p}^N$ of the vector fields $\tilde{\mathbf{f}}_{d,p}$ onto the normal to $\partial\chi$, i.e., their components in $z_{1,2}$-direction, both point towards the switching surface,

[6] We remark that the first component of $\mathbf{k}$ is zero because the first row of $\widetilde{\mathbf{T}}_{2,\xi}$ is $[1,\ \mathbf{0}_{1\times(n-1)}]$.

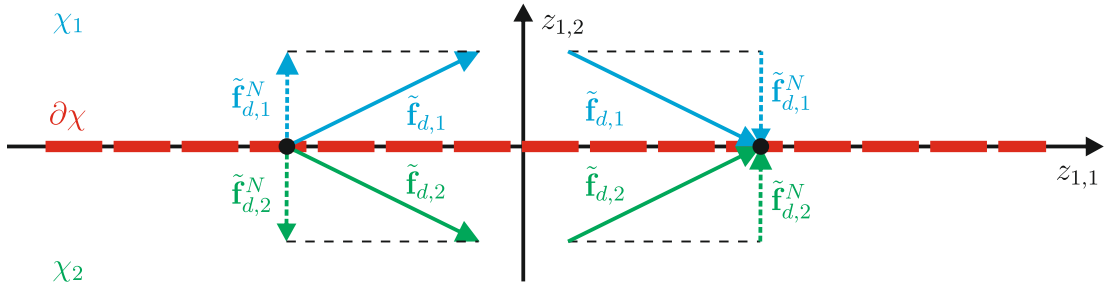

Figure 7.1: The vector fields $\tilde{\mathbf{f}}_{d,1}$ (blue) and $\tilde{\mathbf{f}}_{d,2}$ (green) at two exemplary points of the switching surface $\partial\chi$ (red dashed).

which shows that the state trajectory cannot cross $\partial\chi$. Hence, if $\mathbf{z}_1$ reaches $\partial\chi$ at some time τ, no solution in the sense of Definition 2.4.1 exists[7] for $t > \tau$. Further, note that there are y_d for which the state trajectory necessarily reaches $\partial\chi$ irrespective of the choice of $z_{1,2}(0)$, e.g. $y_d(t) = c$ with c a positive constant.

7.2.2.2 Sufficient Conditions

Of course it is desirable to have not only necessary but also *sufficient* conditions for the solvability of the EOT problem. To derive such conditions, in the sequel, we consider the special case where $r = n$, i.e., y is a flat output of both subsystems. We have the following theorem.

Theorem 7.2.2. *Consider the system* (7.1) *with the switching law* (2.73) *and suppose that the Assumptions 7.1.1 and 7.2.1 are satisfied and that* $r_1 = r_2 = n$. *Then the EOT problem 7.1.2 is solvable for all* $y_d(t)$ *if*

1) it holds that

$$\chi_1 \cup \tilde{\mathbf{\Phi}}_2(\chi_2) = \mathbb{R}^n \tag{7.55}$$

2) for all $\mathbf{z}_1 \in \partial\chi$ *and all* $i \in \{2, \dots, n\}$ *it holds that*

$$L^{i-1}_{\tilde{f}_2}\tilde{h}(\mathbf{z}_1) - z_{1,i} = 0\ . \tag{7.56}$$

Proof. It follows from (7.55) that for all $\mathbf{Y}^n_d(0)$ there is either $\mathbf{z}_{1,d}(0) \in \chi_1$ such that $\mathbf{Y}^n_d(0) = \tilde{\mathbf{\Phi}}_1(\mathbf{z}_{1,d}(0)) = \mathbf{z}_{1,d}(0)$ or $\mathbf{z}_{1,d}(0) \in \chi_2$ such that $\mathbf{Y}^n_d(0) = \tilde{\mathbf{\Phi}}_2(\mathbf{z}_{1,d}(0))$. First assume

[7] For this example, a solution in the sense of Filippov exists and the motion of the system along the sliding surface $\partial\chi$ would be determined by $\dot{\mathbf{z}}_1 = [\dot{y}_d, 0]^T$. Thus, exact output tracking would be achieved. It is, however, not difficult to find examples, where also with this solution concept exact output tracking is impossible.

that $\mathbf{z}_{1,d}(0) \in \chi_1$. Then the control $\tilde{u}_{1,d}(\mathbf{Y}_d^n(t), y_d^{(n)}(t))$ achieves exact output tracking as long as $\mathbf{z}_{1,d}(t) = \tilde{\mathbf{\Phi}}_1^{-1}(\mathbf{Y}_d^n(t)) \in \chi_1$. Now suppose that, for some time t_1 and for some $\epsilon > 0$, it holds that $\mathbf{z}_{1,d}(t_1) = \tilde{\mathbf{\Phi}}_1^{-1}(\mathbf{Y}_d^n(t_1)) \in \partial\chi$ and $\tilde{\mathbf{\Phi}}_1^{-1}(\mathbf{Y}_d^n(t)) \notin \chi_1$ for all $t \in (t_1, t_1 + \epsilon)$ (If $\mathbf{z}_1(t_1) \in \partial\chi_1$ and there is no such ϵ, then $\mathbf{Y}_d^n(t)$ is such that the trajectory $\mathbf{z}_1(t)$ either only "touches" the switching surface or remains within this surface. In both cases no switching occurs.). Then, in order to track the desired output trajectory, we have to switch from the 1st to the 2nd subsystem. To show that, in spite of this switching, exact output tracking is possible, we prove that $\mathbf{z}_{1,d}(t)$ can be continued in χ_2 such that $\mathbf{Y}_d^n(t) = \tilde{\mathbf{\Phi}}_2(\mathbf{z}_{1,d}(t))$ for all $t \in [t_1, t_1 + \epsilon)$. It follows from (7.56) that $\tilde{\mathbf{\Phi}}_2(\mathbf{z}_{1,d}(t_1)) = \tilde{\mathbf{\Phi}}_1(\mathbf{z}_{1,d}(t_1)) = \mathbf{Y}_d^n(t_1)$. Moreover, since $\mathbf{z}_{1,d}(t) = \tilde{\mathbf{\Phi}}_1^{-1}(\mathbf{Y}_d^n(t)) \notin \chi_1,\ \forall\, t \in (t_1, t_1 + \epsilon)$ and (7.55) hold, we see that for any $\bar{t}_1 \in [t_1, t_1 + \epsilon)$ there must be a $\bar{\mathbf{z}}_1 \in \chi_2$ such that $\mathbf{Y}_d^n(\bar{t}_1) = \tilde{\mathbf{\Phi}}_2(\bar{\mathbf{z}}_1)$. Hence, using continuity of $\tilde{\mathbf{\Phi}}_2(\mathbf{z}_1)$ we conclude that there is $\mathbf{z}_{1,d}(t) \in \chi_2$ such that $\mathbf{Y}_d^n(t) = \tilde{\mathbf{\Phi}}_2(\mathbf{z}_{1,d}(t))$ holds for all $t \in [t_1, t_1 + \epsilon)$. Consequently, exact output tracking can be achieved using the control $\hat{u}_{2,d}(\mathbf{Y}_d^n(t), y_d^{(n)}(t))$ on $[t_1, t_2)$, i.e., until the state trajectory hits the switching surface at the second switching time $t_2 > t_1$ and switching from the 2nd to the 1st subsystem becomes necessary. For this situation, the proof is completely analogous and is therefore omitted. By repeating these arguments for all switching times, we obtain the desired result. □

Recall that solvability of the EOT problem 7.1.2 means that exact tracking of $y_d(t)$ can be achieved on a time interval $[0, T)$ of positive length $T > 0$. However, the only reason that a global solution might not exist, i.e., $T < \infty$, is that the intervals (t_i, t_{i+1}), on which existence of a solution has been shown above, are getting smaller and smaller such that a right accumulation point of switching times occurs. Since $\mathbf{z}_1 = \tilde{\mathbf{\Phi}}_1(\mathbf{z}_1) = \tilde{\mathbf{h}}_1^n(\mathbf{z}_1)$ and for all $\mathbf{z}_1 \in \partial\chi$ it holds that $\tilde{\mathbf{h}}_2^n(\mathbf{z}_1) = \tilde{\mathbf{h}}_1^n(\mathbf{z}_1) = \mathbf{z}_1$, this would imply that $\tilde{\varphi}(\mathbf{Y}_d^n(t))$ has an accumulation point of zeros in $[0, \infty)$, which can be ruled out for any reasonable reference trajectory $y_d(t)$.

Note that in the case where $\mathbf{f}_p(\mathbf{x})$, $\mathbf{g}_p(\mathbf{x})$, $p \in \mathcal{P}$ and $h(\mathbf{x})$ as well as $\varphi(\mathbf{x})$ are analytic functions, the conditions of Theorem 7.2.2 are also necessary. Necessity of (7.55) follows from the fact that, if the EOT problem is solvable for all trajectories $y_d(t)$, then for every $\mathbf{Y}_d^n(0)$ there has to be either $\mathbf{z}_{1,d}(0) \in \chi_1$ such that $\mathbf{Y}_d^n(0) = \tilde{\mathbf{\Phi}}_1(\mathbf{z}_{1,d}(0)) = \mathbf{z}_{1,d}(0)$ or $\mathbf{z}_{1,d}(0) \in \chi_2$ such that $\mathbf{Y}_d^n(0) = \tilde{\mathbf{\Phi}}_2(\mathbf{z}_{1,d}(0))$. Necessity of (7.56) can be deduced from Theorem 7.2.1 and Lemma 7.2.1, since S is clearly non-empty in the case $r = n$. This can be seen from the fact that we can always choose a trajectory such that for some $\tau_1,\ \tau_2$ it holds that $\tilde{\mathbf{\Phi}}_1^{-1}(\mathbf{Y}_d^n(\tau_1)) \in \chi_1$ and $\tilde{\mathbf{\Phi}}_1^{-1}(\mathbf{Y}_d^n(\tau_2)) \notin \chi_1$.

It is interesting to note that, under the conditions (7.55) and (7.56), the initial state satisfying $\mathbf{Y}_d^n(0) = \tilde{\mathbf{\Phi}}_1(\mathbf{z}_{1,d}(0)) = \mathbf{z}_{1,d}(0)$ with $\mathbf{z}_{1,d}(0) \in \chi_1$ or $\mathbf{Y}_d^n(0) = \tilde{\mathbf{\Phi}}_2(\mathbf{z}_{1,d}(0))$ with $\mathbf{z}_{1,d}(0) \in \chi_2$ is unique, which can be concluded from the following Lemma.

Lemma 7.2.3. *Under the conditions* (7.55) *and* (7.56) *the map* $\tilde{\mathbf{\Phi}} : \mathbb{R}^n \to \mathbb{R}^n$ *defined by*

$$\tilde{\mathbf{\Phi}}(\mathbf{z}_1) = \begin{cases} \tilde{\mathbf{\Phi}}_1(\mathbf{z}_1) & \text{if } \mathbf{z}_1 \in \operatorname{int} \chi_1 \\ \tilde{\mathbf{\Phi}}_2(\mathbf{z}_1) & \text{if } \mathbf{z}_1 \in \chi_2 \end{cases} \tag{7.57}$$

is bijective.

Proof. see Appendix B.4. □

Finally, consider again the special case of a switched *linear* system (7.49) with $r = n$ and $\tilde{\varphi}(\mathbf{z}_1) = \tilde{\mathbf{n}}^T \mathbf{z}_1$. We have chosen $\tilde{m} = 0$ since otherwise, according to Lemma 7.2.2, the vector fields $\tilde{\mathbf{f}}_{1,d}$ and $\tilde{\mathbf{f}}_{2,d}$ have to be identical and consequently the solvability of the EOT problem is obvious. In the proof of the following proposition, we will use the matrix $\widetilde{\mathbf{T}}_1$, which is such that $\tilde{\mathbf{\Phi}}_1(\mathbf{z}_1) = \widetilde{\mathbf{T}}_1 \mathbf{z}_1$, i.e., $\widetilde{\mathbf{T}}_1 = \mathbf{I}$.

Theorem 7.2.3. *Consider the linear switched system* (7.49) *with the switching law* (2.73) *and* $\tilde{\varphi}(\mathbf{z}_1) = \tilde{\mathbf{n}}^T \mathbf{z}_1$. *Assume, without loss of generality, that* $\|\tilde{\mathbf{n}}\| = 1$. *Then the EOT problem 7.1.2 is solvable for all trajectories* $y_d(t)$ *if and only if there is a vector* $\mathbf{k} \in \mathbb{R}^n$ *such that*

$$\widetilde{\mathbf{T}}_2 = \mathbf{I} + \mathbf{k}\tilde{\mathbf{n}}^T \tag{7.58}$$

and it holds that

$$\mathbf{k}^T \tilde{\mathbf{n}} > -1 \, . \tag{7.59}$$

Proof. Necessity of (7.58) follows immediately from Lemma 7.2.2. Now let $\mathrm{Q}_1 \subset \mathbb{R}^n$ be the set of vectors which can be represented in the form $\widetilde{\mathbf{T}}_1 \mathbf{z}_1$ with $\mathbf{z}_1 \in \chi_1$, i.e., satisfying $\tilde{\mathbf{n}}^T \mathbf{z}_1 \geq 0$. Analogously define Q_2 to be the set of of vectors which can be expressed as $\widetilde{\mathbf{T}}_2 \mathbf{z}_1$ with $\mathbf{z}_1 \in \chi_2$. Since it is a necessary condition for the exact tracking of all $y_d(t)$ that, for every $\mathbf{Y}_d^n(0)$, there is $p \in \{1, 2\}$ and $\mathbf{z}_{1,d}(0) \in \chi_p$ such that $\mathbf{Y}_d^n(0) = \tilde{\mathbf{\Phi}}_p(\mathbf{z}_{1,d}(0))$, it clearly must hold that $\tilde{\mathbf{\Phi}}_1(\chi_1) \cup \tilde{\mathbf{\Phi}}_2(\chi_2) = \mathbb{R}^n$ and hence, in the linear case, $\mathrm{Q}_1 \cup \mathrm{Q}_2 = \mathbb{R}^n$. Now we introduce another coordinate system defined by $\mathbf{z}_3 = \widetilde{\mathbf{T}}_3 \mathbf{z}_1$ with the matrix $\widetilde{\mathbf{T}}_3$ given by

$$\tilde{\mathbf{T}}_3^{-1} = \begin{bmatrix} \tilde{\mathbf{n}} & \tilde{\mathbf{t}}_{3,2} & \dots & \tilde{\mathbf{t}}_{3,n} \end{bmatrix} \tag{7.60}$$

where the vectors $\tilde{\mathbf{t}}_{3,2}, \dots, \tilde{\mathbf{t}}_{3,n}$ are chosen linearly independent and such that $\tilde{\mathbf{t}}_{3,i}^T \tilde{\mathbf{n}} = 0$ for $i \in \{2, \dots, n\}$. In these coordinates, clearly $\breve{\varphi}(\mathbf{z}_3) = \tilde{\mathbf{n}}^T \tilde{\mathbf{T}}_3^{-1} \mathbf{z}_3 = z_{3,1}$, i.e., switching depends on the sign of $z_{3,1}$. Moreover, the vectors $\mathbf{Y}^n$ in Q_1 can be represented by

$$\mathbf{Y}^n = \widetilde{\mathbf{T}}_1 \widetilde{\mathbf{T}}_3^{-1} \mathbf{z}_3 = \widetilde{\mathbf{T}}_3^{-1} \mathbf{z}_3 \tag{7.61}$$

with $z_{3,1} \in \mathbb{R}_0^+$ and $z_{3,i} \in \mathbb{R}$, $i \in \{2, \ldots, n\}$. Similarly, the elements $\mathbf{Y}^n$ of Q_2 are given by

$$\mathbf{Y}^n = \tilde{\mathbf{T}}_2 \tilde{\mathbf{T}}_3^{-1} \mathbf{z}_3 = (\mathbf{I} + \mathbf{k}\tilde{\mathbf{n}}^T)\tilde{\mathbf{T}}_3^{-1}\mathbf{z}_3 = \left(\tilde{\mathbf{T}}_3^{-1} + \mathbf{k}[1\ \mathbf{0}_{1\times(n-1)}]\right)\mathbf{z}_3 \tag{7.62}$$

with $z_{3,1} \leq 0$ and $z_{3,i} \in \mathbb{R}$, $i \in \{2, \ldots, n\}$. We conclude that Q_1 is the set of all vectors of the form $\gamma\tilde{\mathbf{n}} + \mathbf{w}$ with $\gamma \geq 0$ and $\mathbf{w} \in \Lambda$ where Λ denotes the $n-1$-dimensional linear subspace $\Lambda = \mathrm{span}\{\mathbf{t}_{3,2}, \ldots, \mathbf{t}_{3,n}\}$. Similarly, it follows from (7.62) that the elements of Q_2 can be expressed by $\gamma(\tilde{\mathbf{n}} + \mathbf{k}) + \mathbf{w}$ with $\gamma \leq 0$ and $\mathbf{w} \in \Lambda$. Using that $\tilde{\mathbf{n}}$ is orthogonal to Λ, we conclude that $\mathrm{Q}_1 \cup \mathrm{Q}_2 = \mathbb{R}^n$ holds true if and only if

$$\{\mathbf{m}\,|\mathbf{m} = \gamma\tilde{\mathbf{n}}, \gamma \geq 0\} \cup \left\{\mathbf{m}\,\middle|\mathbf{m} = \gamma\left[(\tilde{\mathbf{n}} + \mathbf{k})^T\tilde{\mathbf{n}}\right]\tilde{\mathbf{n}}, \gamma \leq 0\right\} = \{\mathbf{m}\,|\mathbf{m} = \gamma\tilde{\mathbf{n}}, \gamma \in \mathbb{R}\} \tag{7.63}$$

where $[(\tilde{\mathbf{n}} + \mathbf{k})^T\tilde{\mathbf{n}}]\tilde{\mathbf{n}}$ is the orthogonal projection of $(\tilde{\mathbf{n}} + \mathbf{k})$ onto $\tilde{\mathbf{n}}$. This is fulfilled if and only if $[(\tilde{\mathbf{n}} + \mathbf{k})^T\tilde{\mathbf{n}}] > 0$, from which (7.59) is obtained using $\tilde{\mathbf{n}}^T\tilde{\mathbf{n}} = \|\tilde{\mathbf{n}}\|^2 = 1$.

Sufficiency now immediately follows noting that with $\mathrm{Q}_1 \cup \mathrm{Q}_2 = \mathbb{R}^n$ and (7.58) the conditions of Theorem 7.2.2 are satisfied. □

7.2.3 Trajectory-Dependent Switching: The Case $r_1 > r_2$

In this subsection, we consider the case where the relative degrees of the two subsystems are different, and, without loss of generality, we assume that $r_1 > r_2$. In this case, $\dot{\mathbf{z}}_2 = \hat{\mathbf{f}}_{2,d}(\mathbf{z}_2, y_d^{(r_2)})$ can be represented in the form

$$\begin{aligned} \dot{\xi}_{2,1} &= \xi_{2,2} \\ &\cdots \\ \dot{\xi}_{2,r_2} &= y^{(r_2)}(t) \\ \dot{\boldsymbol{\eta}}_2 &= \hat{\mathbf{p}}_2(\boldsymbol{\xi}_2, \boldsymbol{\eta}_2) \end{aligned} \tag{7.64}$$

where we have used that $\tilde{\boldsymbol{\Phi}}_{2,\eta}(\mathbf{z}_1)$ can always be chosen such that $\hat{\mathbf{q}}_2(\mathbf{z}_2) = \mathbf{0}$. For exact output tracking, the initial state has to satisfy

$$\tilde{\mathbf{h}}_p^{r_p}(\mathbf{z}_1(0)) = \mathbf{Y}_d^{r_p} \quad \text{and} \quad \left[\mathbf{z}_1^T(0)\ \ \tilde{u}_{p,d}(\mathbf{z}_1(0), y_d^{(r_p)}(0))\right]^T \in \chi_p \tag{7.65}$$

for a $p \in \mathcal{P}$. Note that, for simplicity of notation, we omit throughout this section the index "d" of $\mathbf{z}_{1,d}$ with the understanding that $\mathbf{z}_1(t) = \mathbf{z}_{1,d}(t)$.

7.2.3.1 Necessary Conditions

As in the previous subsection, we first derive necessary conditions for the solvability of the EOT problem. Subsequently, we will establish also sufficient conditions assuming that y is a flat output of the 1st subsystem. We have the following result.

Theorem 7.2.4. *Consider the system* (7.1) *with the switching law* (2.69)*, and suppose that the Assumptions 7.1.1 and 7.2.1 are satisfied and that* $r_1 > r_2$*. Suppose further that there is a* $\bar{\mathbf{z}}_1$ *for which there exists* $(\bar{y}_d^{(r_2)}, \bar{y}_d^{(r_2+1)})$ *such that* $\tilde{\varphi}_2(\bar{\mathbf{z}}_1, \bar{y}_d^{(r_2)}) = 0$ *and* $\dot{\tilde{\varphi}}_2(\bar{\mathbf{z}}_1, \bar{y}_d^{(r_2)}, \bar{y}_d^{(r_2+1)}) > 0$*. Then, it is necessary for the solvability of Problem 7.1.2 for all* $y_d(t)$ *and all pairs satisfying* (7.65) *that*

i) $r_1 - r_2 = 1$

ii) it holds for all $i \in \{1, \dots, r_1 - 2\}$ *that*

$$\tilde{f}_{2,i}(\mathbf{z}_1) = \xi_{1,i+1} \tag{7.66}$$

$$\tilde{g}_{2,i}(\mathbf{z}_1) = 0 \tag{7.67}$$

iii) the switching surface $\partial\chi$ *is identical to the manifold*

$$\mathrm{N} = \left\{ [\mathbf{z}_1^T, u]^T \,\middle|\, \tilde{f}_{2,r_1-1}(\mathbf{z}_1) + \tilde{g}_{2,r_1-1}(\mathbf{z}_1)u - z_{1,r_1} = 0 \right\} . \tag{7.68}$$

Proof. Suppose that exact output tracking is achieved for all $y_d(t)$ and all pairs satisfying (7.65). Then the control necessarily has to be $\tilde{u}_{d,1}(\mathbf{z}_1, y_d^{(r_1)})$ for intervals $[t_i, t_{i+1})$ with $\sigma(t_i) = 1$ and $\tilde{u}_{d,2}(\mathbf{z}_1, y_d^{(r_2)})$ for intervals $[t_i, t_{i+1})$ with $\sigma(t_i) = 2$. After substituting this into (7.1), the switched system is of the form $\dot{\mathbf{z}}_1 = \tilde{\mathbf{f}}_{\sigma,d}(\mathbf{z}_1, y^{(r_\sigma)})$. By assumption, there is a point $\bar{\mathbf{z}}_1 = [\bar{\boldsymbol{\xi}}_1^T, \bar{\boldsymbol{\eta}}_1^T]^T$ and a corresponding $(\bar{y}_d^{(r_2)}, \bar{y}_d^{(r_2+1)})$ such that $\tilde{\varphi}_2(\bar{\mathbf{z}}_1, \bar{y}_d^{(r_2)}) = 0$ and $\dot{\tilde{\varphi}}_2(\bar{\mathbf{z}}_1, \bar{y}_d^{(r_2)}, \bar{y}_d^{(r_2+1)}) > 0$. Consequently, there is a trajectory $\mathbf{z}_1(t)$ of (7.64) and a corresponding $\tilde{u}_{2,d}(t)$ satisfying $[\mathbf{z}_1(\tau), \tilde{u}_{2,d}(\tau)] = [\bar{\mathbf{z}}_1, \tilde{u}_{2,d}(\bar{\mathbf{z}}_1, \bar{y}_d^{(r_2)})] \in \partial\chi$ for some time τ and $[\mathbf{z}_1(t), \tilde{u}_{2,d}(t)] \in \operatorname{int}\chi_2$, $t \in (\tau - \epsilon, \tau)$ for some $\epsilon > 0$ as well as $[\mathbf{z}_1(t), \tilde{u}_{2,d}(t)] \in \operatorname{int}\chi_1$, $t \in (\tau, \tau + \epsilon)$. Since $y(t) = y_d(t)$ is fulfilled for all $t \in (\tau - \epsilon, \tau + \epsilon)$, it holds for this trajectory that

$$\mathbf{Y}^{r_1}(t) = \tilde{\mathbf{h}}_1^{r_1}(\mathbf{z}_1(t)) = \boldsymbol{\xi}_1(t) = \mathbf{Y}_d^{r_1}(t) \tag{7.69}$$

for all $t \in [\tau, \tau + \epsilon)$ and

$$\mathbf{Y}^{r_1}(t) = \tilde{\mathbf{h}}_2^{r_1}(\mathbf{z}_1(t), \mathbf{U}^{r_1 - r_2}) = \mathbf{Y}_d^{r_1}(t) \tag{7.70}$$

for all $t \in (\tau - \epsilon, \tau]$. It follows from (7.69) that $\mathbf{Y}_d^{r_1}(\tau) = \boldsymbol{\xi}_1(\tau)$ and from (7.70) that $\mathbf{Y}_d^{r_1}(\tau) = \mathbf{h}_2^{r_1}[\boldsymbol{\xi}_1(\tau^-), \boldsymbol{\eta}_1(\tau^-), \mathbf{U}^{r_1-r_2}(\tau^-)]$. Since $\mathbf{z}_1(\tau^-) = \mathbf{z}_1(\tau) = \bar{\mathbf{z}}_1$, we conclude that

$$\bar{\boldsymbol{\xi}}_1 = \tilde{\mathbf{h}}_2^{r_1}\left(\bar{\boldsymbol{\xi}}_1, \bar{\boldsymbol{\eta}}_1, \mathbf{U}_{d,2}^{r_1-r_2}\left(\bar{\mathbf{z}}_1, \bar{y}_d^{r_2}, \ldots, \bar{y}_d^{(r_1-1)}\right)\right) \tag{7.71}$$

where $\mathbf{U}_{d,2}^{r_1-r_2}$ contains $\tilde{u}_{2,d}$ and its derivatives up to the order $r_1 - r_2 - 1$. This relation can be expressed component-wise as

$$\bar{\xi}_{1,2} - \tilde{h}_2^{(1)}(\bar{\boldsymbol{\xi}}_1, \bar{\boldsymbol{\eta}}_1) = 0 \tag{7.72a}$$

$$\vdots$$

$$\bar{\xi}_{1,r_2} - \tilde{h}_2^{(r_2-1)}(\bar{\boldsymbol{\xi}}_1, \bar{\boldsymbol{\eta}}_1) = 0 \tag{7.72b}$$

$$\bar{\xi}_{1,r_2+1} - \bar{y}_d^{(r_2)} = 0 \tag{7.72c}$$

$$\bar{\xi}_{1,r_2+2} - \bar{y}_d^{(r_2+1)} = 0 \tag{7.72d}$$

$$\vdots$$

$$\bar{\xi}_{1,r_1} - \bar{y}_d^{(r_1-1)} = 0 \tag{7.72e}$$

where we have used that $\tilde{h}_2^{(r_2)}[\boldsymbol{\xi}_1, \boldsymbol{\eta}_1, \tilde{u}_{d,2}(\mathbf{z}_1, y_d^{(r_2)})] = y_d^{(r_2)}$ by construction of $\tilde{u}_{d,2}$ and hence $\tilde{h}_2^{(r_2+1)}(\boldsymbol{\xi}_1, \boldsymbol{\eta}_1, \tilde{u}_{d,2}, \dot{\tilde{u}}_{d,2}) = y_d^{(r_2+1)}$ for all $t \in (\tau - \epsilon, \tau)$.

In order to see that $r_1 - r_2 = 1$ must hold true, assume that this is not the case, i.e., $r_1 - r_2 > 1$. Then the relation (7.72d) must be satisfied. Since $\dot{\tilde{\varphi}}_2(\bar{\mathbf{z}}_1, \bar{y}_d^{(r_2)}, \bar{y}_d^{(r_2+1)}) > 0$ is fulfilled with strict inequality sign, there is an interval $\mathrm{I}_{r_2+1} = (\bar{y}_d^{(r_2+1)} - \delta, \bar{y}_d^{(r_2+1)} + \delta)$ with $\delta > 0$ such that $\dot{\tilde{\varphi}}_2(\bar{\mathbf{z}}_1, \bar{y}_d^{(r_2)}, y_d^{(r_2+1)}) > 0$ is also satisfied for all $y_d^{(r_2+1)} \in \mathrm{I}_{r_2+1}$. This means that (7.72d) has to be valid also for all $y_d^{(r_2+1)} \in \mathrm{I}_{r_2+1}$ (Note that $\tilde{\varphi}(\bar{\mathbf{z}}_1, \bar{y}_d^{(r_2)}) = 0$ holds independently of the value of $y_d^{(r_2+1)}$), which clearly leads to a contradiction. Hence, we conclude that $r_1 - r_2 = 1$ (Recall that $r_1 > r_2$, by assumption).

Next, we prove that the switching surface $\partial\chi$ has to be identical to the manifold N characterized in (7.68). To this end, we first show that $\tilde{\varphi}_u(\mathbf{z}_1) \neq 0$. As can be seen from (7.72c), it holds that[8]

$$\bar{\xi}_{1,r_1} - y_d^{(r_2)} = 0 \tag{7.73}$$

with $y_d^{(r_2)} = \bar{y}_d^{(r_2)}$. In the case where $\tilde{\varphi}_u(\mathbf{z}_1) \neq 0$, there is a unique $\bar{y}_d^{(r_2)}$ such that

$$\tilde{\varphi}(\bar{\mathbf{z}}_1) = \tilde{\varphi}_x(\bar{\mathbf{z}}_1) + \tilde{\varphi}_u(\bar{\mathbf{z}}_1)\tilde{u}_{d,2}(\bar{\mathbf{z}}_1, \bar{y}_d^{(r_2)}) = 0\,. \tag{7.74}$$

If, however, $\tilde{\varphi}_u(\mathbf{z}_1) = 0$, then $\tilde{\varphi}(\mathbf{z}_1) = \tilde{\varphi}_x(\bar{\mathbf{z}}_1) = 0$ is valid independently of the value of $y_d^{(r_2)}$. Moreover, using the same argument as above, there is a $\delta > 0$ such that, for all $y_d^{(r_2)}$

[8] In the index of $\bar{\xi}_{1,r_1}$ we use that, as shown above, $r_2 + 1 = r_1$.

in $\mathrm{I}_{r_2} = (\bar{y}_d^{(r_2)} - \delta, \bar{y}_d^{(r_2)} + \delta)$, it holds that $\dot{\tilde{\varphi}}_2(\bar{\mathbf{z}}_1, \bar{y}_d^{(r_2)}) > 0$. Consequently, if $\tilde{\varphi}_u(\bar{\mathbf{z}}_1) = 0$, the relation (7.73) has to be fulfilled for any $y_d^{(r_2)} \in \mathrm{I}_{r_2}$, which is a contradiction. Hence, we conclude that $\tilde{\varphi}_u(\bar{\mathbf{z}}_1) \neq 0$ must be satisfied. This, by assumption (see Section 2.4.1), entails that $\tilde{\varphi}_u(\mathbf{z}_1) \neq 0$ holds for all $\mathbf{z}_1 \in \mathbb{R}^n$.

Then, for any $\mathbf{z}_1$, there is a unique control input, given by $u_\chi(\mathbf{z}_1) = -\tilde{\varphi}_u^{-1}(\mathbf{z}_1)\tilde{\varphi}_x(\mathbf{z}_1)$, such that $(\mathbf{z}_1, u_\chi) \in \partial\chi$. Considering the expression for $\hat{u}_{d,2}$ in (7.23), we see that we can always choose a $y_d^{(r_2)}$ such that $\hat{u}_{2,d} = u_\chi(\mathbf{z}_1)$. Moreover, it is easily checked that the value of $\dot{\tilde{\varphi}}_2$ can be freely chosen via $y_d^{(r_2+1)}$ and hence such that $\dot{\tilde{\varphi}}_2 > 0$. Thus, at any point $(\mathbf{z}_1, u_\chi(\mathbf{z}_1))$, $\mathbf{z}_1 \in \mathbb{R}^n$ switching from the 2nd to the 1st subsystem can occur. As a consequence, the relation (7.71) must hold for any point $(\mathbf{z}_1, u)$ of the switching surface, which implies that

$$\xi_{1,r_1} - \tilde{h}_2^{(r_2)}(\mathbf{z}_1, u) = \xi_{1,r_1} - L_{\tilde{f}_2}^{r_2}\tilde{h}(\mathbf{z}_1) - L_{\tilde{g}_2}L_{\tilde{f}_2}^{r_2-1}\tilde{h}(\mathbf{z}_1)u = 0 \tag{7.75}$$

must be satisfied for every $(\mathbf{z}_1, u) \in \partial\chi$. Due to the relative degree assumption, this equation can be globally solved for

$$u = \frac{\xi_{1,r_1} - L_{\tilde{f}_2}^{r_2}\tilde{h}(\mathbf{z}_1)}{L_{\tilde{g}_2}L_{\tilde{f}_2}^{r_2-1}\tilde{h}(\mathbf{z}_1)} \tag{7.76}$$

determining for every $\mathbf{z}_1$ the *unique* u for which (7.75) holds. Consequently, the set of pairs $(\mathbf{z}_1, u)$ satisfying $\tilde{\varphi}(\mathbf{z}_1, u) = 0$ has to be identical to the set of $(\mathbf{z}_1, u)$ for which (7.75) is fulfilled.

Since, for every $\mathbf{z}_1 \in \mathbb{R}^n$, there is a corresponding u_χ such that $(\mathbf{z}_1, u_\chi) \in \partial\chi$, the first $r_1 - 2$ equations in (7.72), which do not depend on u, must be fulfilled for every $\mathbf{z}_1 \in \mathbb{R}^n$. From the first one we obtain

$$\xi_{1,2} = \tilde{h}_2^{(1)}(\boldsymbol{\xi}_1, \boldsymbol{\eta}_1) = L_{\tilde{f}_2}\tilde{h}(\mathbf{z}_1) + L_{\tilde{g}_2}\tilde{h}(\mathbf{z}_1)u = \tilde{f}_{2,1}(\mathbf{z}_1) \tag{7.77}$$

where, for obvious reasons, we have assumed that $r_1 > 2$, which entails that $r_2 > 1$ and hence $L_{\tilde{g}_2}\tilde{h}(\mathbf{z}_1) = \tilde{g}_{2,1}(\mathbf{z}_1) = 0$ (If $r_1 = 2$, then (7.72) consists only of one equation, namely (7.72c)).

If $r_1 > 3$, we use (7.77) in the second equation of (7.72) and obtain

$$\xi_{1,3} = \tilde{h}_2^{(2)}(\boldsymbol{\xi}_1, \boldsymbol{\eta}_1) = L_{\tilde{f}_2}^2\tilde{h}(\mathbf{z}_1) + L_{\tilde{f}_2}L_{\tilde{g}_2}\tilde{h}(\mathbf{z}_1)u = \tilde{f}_{2,2}(\mathbf{z}_1) + \tilde{g}_{2,2}(\mathbf{z}_1)u = \tilde{f}_{2,2}(\mathbf{z}_1) \tag{7.78}$$

where $L_{\tilde{f}_2}L_{\tilde{g}_2}\tilde{h}(\mathbf{z}_1) = \tilde{g}_{2,2}(\mathbf{z}_1) = 0$ follows from the fact that $r_1 > 3$ implies $r_2 > 2$. Continuing in this way, we get the conditions (7.66) and (7.67), and by substituting these into (7.75), we obtain (7.68). This completes the proof. □

Note that the assumption in Theorem 7.2.4 that there is a $\bar{\mathbf{z}}_1$ and a corresponding pair $(\bar{y}_d^{(r_2)}, \bar{y}_d^{(r_2+1)})$ such that $\tilde{\varphi}(\bar{\mathbf{z}}_1, \bar{y}_d^{(r_2)}) = 0$ and $\dot{\tilde{\varphi}}_2(\bar{\mathbf{z}}_1, \bar{y}_d^{(r_2)}, \bar{y}_d^{(r_2+1)}) > 0$ is not very restrictive. It is clearly satisfied if $\tilde{\varphi}_u(\mathbf{z}_1) \neq 0$ holds. In case that $\tilde{\varphi}_u(\mathbf{z}_1) = 0$, it simply means that there is at least one point of the switching surface at which, for some $y_d^{(r_2)}$, the vector field $\tilde{\mathbf{f}}_{2,d}(\mathbf{z}_1, y^{(r_2)})$ points towards this surface.

In order that the necessary conditions in Theorem 7.2.4 are satisfied, the 2nd subsystem $\dot{\mathbf{z}}_1 = \tilde{f}_2(\mathbf{z}_1) + \tilde{g}_2(\mathbf{z}_1)u$ must be of the form

$$\begin{aligned} \dot{z}_{1,1} &= \xi_{1,2} \\ &\vdots \\ \dot{z}_{1,r_1-1} &= \xi_{1,r_1} + [\tilde{\varrho}_x(\mathbf{z}_1) + \tilde{\varrho}_u(\mathbf{z}_1)u] \\ \dot{z}_{1,r_1} &= \tilde{f}_{2,r_1}(\mathbf{z}_1) + \tilde{g}_{2,r_1}(\mathbf{z}_1)u \\ &\vdots \\ \dot{z}_{1,n} &= \tilde{f}_{2,n}(\mathbf{z}_1) + \tilde{g}_{2,n}(\mathbf{z}_1)u \end{aligned} \tag{7.79}$$

where $\tilde{\varrho}(\mathbf{z}_1, u) = \tilde{\varrho}_x(\mathbf{z}_1) + \tilde{\varrho}_u(\mathbf{z}_1)u$ is such that

$$\{\, (\mathbf{z}_1, u) \in \mathbb{R}^n \times \mathbb{R} |\, \tilde{\varrho}_x(\mathbf{z}_1) + \tilde{\varrho}_u(\mathbf{z}_1)u = 0\} = \{\, (\mathbf{z}_1, u) \in \mathbb{R}^n \times \mathbb{R} |\, \tilde{\varphi}_x(\mathbf{z}_1) + \tilde{\varphi}_u(\mathbf{z}_1)u = 0\} \ . \tag{7.80}$$

Furthermore, it holds that $\tilde{\varrho}_u(\mathbf{z}_1) \neq 0, \ \forall\, \mathbf{z}_1$. The functions $\tilde{\varrho}_p$ and $\tilde{\varrho}_p^{(i)}$, $p = 1, 2$, $i \in \mathbb{N}$ are defined analogously to $\tilde{\varphi}_p$ and $\tilde{\varphi}_p^{(i)}$. In view of (7.79), the control $\tilde{u}_{2,d}$ is given by

$$\tilde{u}_{2,d} = \tilde{\varrho}_u^{-1}(\mathbf{z}_1) \left(y^{(r_1-1)} - z_{1,r_1} - \tilde{\varrho}_x(\mathbf{z}_1) \right) \ . \tag{7.81}$$

By substituting this into $\tilde{\varrho}(\mathbf{z}_1, u)$, we obtain

$$\tilde{\varrho}_2(\mathbf{z}_1, y^{(r_1-1)}) = y_d^{(r_1-1)} - z_{1,r_1} \ . \tag{7.82}$$

Moreover, $\tilde{\mathbf{h}}_2^{r_2}(\mathbf{z}_1)$ is the identity map and hence $\tilde{\mathbf{\Phi}}_2(\mathbf{z}_1)$ can be chosen to be the identity map.

As far as condition (7.65) is concerned, there is always an initial state $\mathbf{z}_1(0)$ such that

$$\tilde{\mathbf{h}}_2^{r_2}(\mathbf{z}_1(0)) = \mathbf{Y}_d^{r_2} \quad \text{and} \quad \left[\mathbf{z}_1^T(0) \ \tilde{u}_{2,d}(\mathbf{z}_1, y_d^{(r_2)}) \right]^T \in \chi_2 \ . \tag{7.83}$$

Because the first condition can be satisfied by choosing $[z_{1,1}, \ldots, z_{1,r_1-1}]^T = \mathbf{Y}_d^{n-1}$ and the second one can be fulfilled by choosing $\eta_{2,1} = z_{1,r_1} > y_d^{(r_1-1)}$ (see (7.82)).

Remark 7.2.1. No additional conditions are obtained if we consider a point of $\partial\chi$, at which switching from the 1st to the 2nd subsystem occurs. In this case, the analogue to (7.71) is $[\bar{\xi}_{1,1}, \ldots, \bar{\xi}_{1,r_2}]^T = \tilde{\mathbf{h}}_2^{r_2}(\bar{\mathbf{z}}_1)$, which is included in (7.71).

7.2.3.2 Sufficient Conditions

We observe from (7.79) that in $\mathbf{z}_1$ coordinates the first $r_1 - 2$ components of the switched system must be identical and the $(r_1 - 1)$-th component has to be continuous (but not differentiable!) at the switching surface. In order to derive not only necessary but sufficient conditions, we will assume in the remainder of this subsection that $r_1 = n$, i.e., y is a flat output of the 1st subsystem, and that also the nth component of the switched system is continuous at the switching surface. The 2nd subsystem is then of the form

$$\begin{aligned} \dot{z}_{1,1} &= \xi_{1,2} \\ &\vdots \\ \dot{z}_{1,n-1} &= \xi_{1,n} + [\tilde{\varrho}_x(\mathbf{z}_1) + \tilde{\varrho}_u(\mathbf{z}_1)u] \\ \dot{z}_{1,n} &= \tilde{\alpha}_1(\mathbf{z}_1) + \tilde{\beta}_1(\mathbf{z}_1)u + b_n(\mathbf{z}_1)\,[\tilde{\varrho}_x(\mathbf{z}_1) + \tilde{\varrho}_u(\mathbf{z}_1)u] \end{aligned} \tag{7.84}$$

with some function $b_n : \mathbb{R}^n \to \mathbb{R}$ and $\tilde{\varrho}(\mathbf{z}_1, u)$ satisfying (7.80). This class of systems belongs to the family of continuous switching system, which have been investigated in a different context e.g. by Branicky [19], [20] (see also e.g. [41], [43]), and includes technical examples like the self-supplied variable displacement axial piston pump treated in [57], [94] (see also Section 8.2). Note that the question whether for that class of systems exact tracking of all y_d is possible is not trivial at all, as the following simple example illustrates.

Example 7.2.3. Consider the linear switched system given in $\mathbf{z}_1$ coordinates

$$\dot{\mathbf{z}}_1 = \tilde{\mathbf{A}}\mathbf{z}_1 + \tilde{\mathbf{g}}_\sigma u\,, \quad \tilde{\mathbf{A}} = \begin{bmatrix} 0 & 1 \\ 1 & -4 \end{bmatrix}\,, \quad \tilde{\mathbf{g}}_1 = \begin{bmatrix} 0 \\ 1 \end{bmatrix}\,, \quad \tilde{\mathbf{g}}_2 = \begin{bmatrix} \tilde{\varrho}_u \\ k\tilde{\varrho}_u \end{bmatrix} \tag{7.85}$$

with $\tilde{\varrho}_u$ and k some constants, and let the switching surface be characterized by $\tilde{\varphi} = u$. It is easily determined that

$$\tilde{u}_{1,d} = \ddot{y}_d + 4\dot{y}_d - y_d \quad \text{and} \quad \tilde{u}_{2,d} = \tilde{\varrho}_u^{-1}(\dot{y}_d - z_{1,2}) \tag{7.86}$$

where the evolution of $z_{1,2}$ in the second relation is governed by

$$\dot{z}_{1,2} = y_d - (4 + k)z_{1,2} + k\dot{y}_d\,. \tag{7.87}$$

We observe that the value of $\tilde{u}_{d,1}$ is determined by y_d, $\dot{y}_d$ and $\ddot{y}_d$, whereas $\tilde{u}_{d,2}$ only depends on $\dot{y}_d$ and the solution of (7.87), which is also not affected by $\ddot{y}_d$ but only by y_d and $\dot{y}_d$. Note that, contrary to the state, the input is allowed to jump at the switching instants. Already in this simple example, it is far from being obvious whether the EOT problem is solvable for all y_d. If we consider, for example, the situation where the 2nd subsystem is active, then it is not evident whether $\tilde{u}_{1,d}$ is nonnegative in case that $\tilde{u}_{2,d}$ becomes positive. In the case where the 1st subsystem is active and $\tilde{u}_{d,1}$ becomes negative at some switching time t_i, it holds that $u_{2,d}(t_i) = 0$. This is because exact output tracking with the 1st subsystem implies $z_{1,2,d}(t_i) = \dot{y}_d(t_i)$. However, it is not easy to decide if from there $u_{2,d}$ will evolve towards $u_{2,d} < 0$.

Before we present the sufficient conditions for the solvability of the EOT problem, we first state the following lemma, which will be needed in the proof of the theorem below.

Lemma 7.2.4. *Consider the system* (7.1) *with* $r_1 = n$ *and assume that in* $\mathbf{z}_1$*-coordinates the second subsystem is of the form* (7.84)*. Further, let* $\kappa(\mathbf{z}_1, \boldsymbol{\gamma}) : \mathbb{R}^n \times \mathbb{R}^k \to \mathbb{R}$ *and* $\boldsymbol{\gamma} : \mathbb{R}_0^+ \to \mathbb{R}^k$ *be sufficiently smooth functions. If* $\dot{\kappa}_1(\mathbf{z}_1, \boldsymbol{\gamma}, \dot{\boldsymbol{\gamma}})$ *is the derivative of* $\kappa(\mathbf{z}_1, \boldsymbol{\gamma})$ *along the trajectories of* $\dot{\mathbf{z}}_1 = \tilde{\mathbf{f}}_{d,1}(\mathbf{z}_1, y_d^{(n)})$*, i.e.,*

$$\dot{\kappa}_1 = \frac{\partial \kappa}{\partial \mathbf{z}_1} \tilde{f}_{1,d} + \frac{\partial \kappa}{\partial \boldsymbol{\gamma}} \dot{\boldsymbol{\gamma}} \tag{7.88}$$

then the derivative of κ *along the trajectories of* $\dot{\mathbf{z}}_1 = \tilde{\mathbf{f}}_{d,2}(\mathbf{z}_1, y_d^{(n-1)})$*, i.e.,*

$$\dot{\kappa}_2 = \frac{\partial \kappa}{\partial \mathbf{z}_1} \tilde{f}_{2,d} + \frac{\partial \kappa}{\partial \boldsymbol{\gamma}} \dot{\boldsymbol{\gamma}} \tag{7.89}$$

can be represented in the form

$$\dot{\kappa}_2 = \dot{\kappa}_1 + \left[\frac{\partial \kappa}{\partial z_{1,n-1}} + \frac{\partial \kappa}{\partial z_{1,n}} \left(\frac{\tilde{\beta}_1}{\tilde{\varrho}_u} + b_n \right) \right] \tilde{\varrho}_2 - \frac{\tilde{\beta}_1}{\tilde{\varrho}_u} \frac{\partial \kappa}{\partial z_{1,n}} \tilde{\varrho}_1 \, . \tag{7.90}$$

Proof. See Appendix B.5. □

Theorem 7.2.5. *Consider the system* (7.1) *with the switching law* (2.69), (2.70) *and suppose that the Assumptions 7.1.1 and 7.2.1 are satisfied. Moreover, assume that* $r_1 = n$*. Let the 2nd subsystem be of the form* (7.84) *with* (7.80) *satisfied, and assume that* $\mathbf{f}_p(\mathbf{x})$*,* $\mathbf{g}_p(\mathbf{x})$*,* $h(\mathbf{x})$*, and* $\varrho(\mathbf{x}, u)$ *are analytic functions. Further suppose that the scalar system*

$$\dot{z}_{1,n} = \tilde{\alpha}_1(\mathbf{Y}_d^{n-1}, z_{1,n}) - \frac{\tilde{\beta}_1(\mathbf{Y}_d^{n-1}, z_{1,n})}{\tilde{\varrho}_u(\mathbf{Y}_d^{n-1}, z_{1,n})} \tilde{\varrho}_x(\mathbf{Y}_d^{n-1}, z_{1,n}) + \rho(\mathbf{Y}_d^{n-1}, z_{1,n}) \left(y_d^{(n-1)} - z_{1,n} \right) \tag{7.91}$$

with

$$\rho(\mathbf{Y}_d^{n-1}, z_{1,n}) = \left(\frac{\tilde{\beta}_1(\mathbf{Y}_d^{n-1}, z_{1,n})}{\tilde{\varrho}_u(\mathbf{Y}_d^{n-1}, z_{1,n})} + b_n(\mathbf{Y}_d^{n-1}, z_{1,n}) \right) \tag{7.92}$$

is input-to-state stable with respect to the inputs $\mathbf{Y}_d^{n-1}$, $y_d^{(n-1)}$. *Then, the EOT problem 7.1.2 is solvable for all* $y_d(t)$, *analytic on* $[0, \infty)$, *if it holds that* $\frac{\tilde{\beta}_1(\mathbf{z}_1)}{\tilde{\varrho}_u(\mathbf{z}_1)} > 0$.

Proof. The result can be proven by induction. It follows from the discussion above that there is always a $\mathbf{z}_1(0)$ and a $p \in \mathcal{P}$ such that (7.65) holds. Hence, exact output tracking is achieved either by $\tilde{u}_{1,d}(t)$ or $\tilde{u}_{2,d}(t)$ until the trajectory traverses the switching surface $\partial\chi$ at some time t_1. We show in the following that exact tracking is attained in any interval $[t_i, t_{i+1})$, if the desired output trajectory has been exactly tracked in $[t_{i-1}, t_i)$. We will make use of the fact that, since (7.80) holds, the switching surface is equivalently described by the function $\varrho(\cdot)$. In the remainder of this proof we assume that $(\mathbf{z}_1, u) \in \chi_1$ if $\tilde{\varrho}(\mathbf{z}_1, u) \geq 0$ and $(\mathbf{z}_1, u) \in \chi_2$ if $\tilde{\varrho}(\mathbf{z}_1, u) \leq 0$. For the other case that $(\mathbf{z}_1, u) \in \chi_1$ if $\tilde{\varrho}(\mathbf{z}_1, u) \leq 0$ and $(\mathbf{z}_1, u) \in \chi_2$ if $\tilde{\varrho}(\mathbf{z}_1, u) \geq 0$ the proof follows exactly along the same lines. At first, we consider the situation where $[\mathbf{z}_1(t), \tilde{u}_{\sigma,d}(t)]$ traverses the switching surface from χ_1 to χ_2, i.e., where $\sigma(t_i^-) = 1$ and $\sigma(t_i) = 2$. We have that

$$\tilde{\varrho}_1\left(\mathbf{z}_1(t_i), y^{(n)}(t_i)\right) = \tilde{\varrho}_x\left(\mathbf{z}_1(t_i)\right) + \tilde{\varrho}_u\left(\mathbf{z}_1(t_i)\right) \underbrace{\tilde{\beta}_1^{-1}\left(\mathbf{z}_1(t_i)\right)\left(y_d^{(n)}(t_i) - \tilde{\alpha}_1(\mathbf{z}_1(t_i))\right)}_{\tilde{u}_{d,1}(t_i)} = 0\,. \tag{7.93}$$

Using that the composition of analytic functions is again analytic and the fact that the solution $\mathbf{z}_1(t)$ of $\dot{\mathbf{z}}_1 = \mathbf{f}_{1,d}(\mathbf{z}_1, y_d^n(t))$ is analytic if the right hand side is an analytic function (see e.g. [75]), we conclude that $\tilde{\varrho}_1(t)$ is an analytic function of t. Consequently, if it changes its sign at t_i from positive to negative, then there is an odd integer $i' > 0$ such that $\tilde{\varrho}_1^{(i')}(t_i) < 0$ and $\tilde{\varrho}_1^{(j)}(t_i) = 0$ hold for all $0 \leq j < i'$.

Since $\tilde{\mathbf{h}}_2^{r_2}(\mathbf{z}_1)$ is the identity map, it holds that $\boldsymbol{\xi}_2(t_i) = [\mathbf{I}_{n-1}, 0]\boldsymbol{\xi}_1(t_i^-) = \mathbf{Y}_d^{n-1}(t_i)$ and, consequently, the control $\tilde{u}_{d,2}(\mathbf{z}_1, y_d^{(n-1)})$ makes the system output exactly track the desired trajectory, provided that, for this control and the corresponding $\mathbf{z}_1(t)$ satisfying $\dot{\mathbf{z}}_1(t) = \tilde{\mathbf{f}}_{2,d}(\mathbf{z}_1(t), y_d^{(n-1)}(t))$, there is $\epsilon > 0$ such that $[\mathbf{z}_1^T(t), \tilde{u}_{2,d}(t)] \in \chi_2$ holds for all $t \in [t_i, t_i + \epsilon)$. To show that this is satisfied, we consider $\tilde{\varrho}_2(\mathbf{z}_1, y_d^{(n-1)})$ and its derivatives along the trajectories of $\dot{\mathbf{z}}_1 = \tilde{\mathbf{f}}_{2,d}(\mathbf{z}_1, y_d^{(n-1)})$ at t_i. According to (7.82), we have that

$$\tilde{\varrho}_2(\mathbf{z}_1, y_d^{(n-1)}) = y_d^{(n-1)} - z_{1,n}\,. \tag{7.94}$$

Since $y_d(t)$ is exactly tracked for $t \in [t_{i-1}, t_i)$, it holds that $z_{1,n}(t_i) = y_d^{(n-1)}(t_i)$ and hence

$\tilde{\varrho}_2(\mathbf{z}_1(t_i), y_d^{(n-1)}(t_i)) = 0$. The rate of change of $\tilde{\varrho}_2(\mathbf{z}_1, y_d^{(n-1)})$ calculates to

$$\dot{\tilde{\varrho}}_2\left(\mathbf{z}_1, y_d^{(n-1)}, y_d^{(n)}\right) = y_d^{(n)} \underbrace{-\tilde{\alpha}_1(\mathbf{z}_1) + \frac{\tilde{\beta}_1(\mathbf{z}_1)}{\tilde{\varrho}_u(\mathbf{z}_1)}\tilde{\varrho}_x(\mathbf{z}_1) - \left(\frac{\tilde{\beta}_1(\mathbf{z}_1)}{\tilde{\varrho}_u(\mathbf{z}_1)} + b_n(\mathbf{z}_1)\right)(y_d^{(n-1)} - z_{1,n})}_{-\dot{z}_{1,n}} .$$

From this and (7.93), it is not hard to see that

$$\dot{\tilde{\varrho}}_2\left(\mathbf{z}_1, y_d^{(n-1)}, y_d^{(n)}\right) = \frac{\tilde{\beta}_1(\mathbf{z}_1)}{\tilde{\varrho}_u(\mathbf{z}_1)}\tilde{\varrho}_1(\mathbf{z}_1, y_d^{(n)}) - \underbrace{\left(\frac{\tilde{\beta}_1(\mathbf{z}_1)}{\tilde{\varrho}_u(\mathbf{z}_1)} + b_n(\mathbf{z}_1)\right)}_{\rho(\mathbf{z}_1)}\tilde{\varrho}_2(\mathbf{z}_1, y_d^{(n-1)}) . \tag{7.95}$$

Hence, with (7.93) and $\tilde{\varrho}_2(\mathbf{z}_1(t_i), y_d^{(n-1)}(t_i)) = 0$, it follows that $\dot{\tilde{\varrho}}_2(t_i) = 0$. Now we use Lemma 7.2.4 to calculate the derivative of $\tilde{\varrho}_1(\mathbf{z}_1, y_d^{(n)})$ along the trajectories of $\dot{\mathbf{z}}_1 = \tilde{\mathbf{f}}_{2,d}(\mathbf{z}_1, y_d^{(n-1)})$ and therewith obtain

$$\begin{aligned}\ddot{\tilde{\varrho}}_2 &= \frac{\partial(\tilde{\beta}_1/\tilde{\varrho}_u)}{\partial \mathbf{z}_1}\tilde{f}_{2,d}\tilde{\varrho}_1 + \frac{\tilde{\beta}_1}{\tilde{\varrho}_u}\left[\frac{\partial\tilde{\varrho}_1}{\partial\mathbf{z}_1}\tilde{f}_{2,d} + \frac{\partial\tilde{\varrho}_1}{\partial y_d^{(n)}}y_d^{(n+1)}\right] - \frac{\partial\rho}{\partial\mathbf{z}_1}\tilde{f}_{2,d}\tilde{\varrho}_2 - \rho\dot{\tilde{\varrho}}_2 \\ &= \frac{\tilde{\beta}_1}{\tilde{\varrho}_u}\dot{\tilde{\varrho}}_1 + \frac{\partial(\tilde{\beta}_1/\tilde{\varrho}_u)}{\partial\mathbf{z}_1}\tilde{f}_{2,d}\tilde{\varrho}_1 - \frac{\tilde{\beta}_1^2}{\tilde{\varrho}_u^2}\frac{\partial\tilde{\varrho}_1}{\partial z_{1,n}}\tilde{\varrho}_1 + \frac{\tilde{\beta}_1}{\tilde{\varrho}_u}\left(\frac{\partial\tilde{\varrho}_1}{\partial z_{1,n-1}} + \frac{\partial\tilde{\varrho}_1}{\partial z_{1,n}}\rho\right)\tilde{\varrho}_2 - \frac{\partial\rho}{\partial\mathbf{z}_1}\tilde{f}_{2,d}\tilde{\varrho}_2 - \rho\dot{\tilde{\varrho}}_2 .\end{aligned} \tag{7.96}$$

It is important to note here that $\dot{\tilde{\varrho}}_1$ denotes the derivative of ϱ along the trajectories of the *first* subsystem $\dot{\mathbf{z}}_1 = \tilde{\mathbf{f}}_{1,d}(\mathbf{z}_1, y_d^{(n)})$ (see Lemma 7.2.4 and the definition of $\dot{\tilde{\varrho}}_1$ in (7.39)). With $\tilde{\varrho}_1(t_i) = 0$, $\tilde{\varrho}_2(t_i) = 0$ and $\dot{\tilde{\varrho}}_2(t_i) = 0$ as well as $\frac{\tilde{\beta}_1(\mathbf{z}_1)}{\tilde{\varrho}_u(\mathbf{z}_1)} > 0$ we obtain

$$\ddot{\tilde{\varrho}}_2(t_i) = \frac{\tilde{\beta}_1(\mathbf{z}_1(t_i))}{\tilde{\varrho}_u(\mathbf{z}_1(t_i))}\dot{\tilde{\varrho}}_1(t_i) \leq 0 . \tag{7.97}$$

If $\dot{\tilde{\varrho}}_1(t_i) = 0$, we use again Lemma 7.2.4 to calculate $\tilde{\varrho}_2^{(3)}(t_i)$, and with $\tilde{\varrho}_1(t_i) = 0$, $\tilde{\varrho}_2(t_i) = 0$, $\dot{\tilde{\varrho}}_1(t_i) = 0$, $\dot{\tilde{\varrho}}_2(t_i) = 0$, and $\ddot{\tilde{\varrho}}_2(t_i) = 0$ we can conclude that $\tilde{\varrho}_2^{(3)}(t_i) = \frac{\tilde{\beta}_1(\mathbf{z}_1(t_i))}{\tilde{\varrho}_u(\mathbf{z}_1(t_i))}\ddot{\tilde{\varrho}}_1(t_i) = 0$. Continuing in this way we finally get

$$\tilde{\varrho}_2^{(i'+1)}(t_i) = \frac{\tilde{\beta}_1(\mathbf{z}_1)}{\tilde{\varrho}_u(\mathbf{z}_1)}\tilde{\varrho}_1^{(i')}(t_i) < 0 . \tag{7.98}$$

From this we conclude that there is $\epsilon > 0$ such that $[\mathbf{z}_1(t), \tilde{u}_{2,d}(t)] \in \chi_2$ for all $t \in [t_i, t_i + \epsilon)$ using a Taylor argument.

Next, we examine a switching time t_i at which $[\mathbf{z}_1(t), \tilde{u}_{\sigma,d}(t)]$ traverses the switching surface from χ_2 to χ_1. At t_i it holds that

$$\tilde{\varrho}_2(t_i) = y_d^{(n-1)}(t_i) - z_{1,n}(t_i) = 0 \,. \tag{7.99}$$

Moreover, using the same arguments as before, $\tilde{\varrho}_2(t)$ is analytic, and hence, if its sign changes at t_i from negative to positive, there is an odd integer $i'' > 0$ such that $\tilde{\varrho}_2^{(i'')}(t_i) > 0$ and $\tilde{\varrho}_1^{(j)}(t_i) = 0$ for all $0 < j < i''$. Since $y(t) = y_d(t)$ for all $t \in [t_{i-1}, t_i)$ we have $[z_{1,1}(t_i), \dots, z_{1,n-1}(t_i)]^T = \boldsymbol{\xi}_2(t_i^-) = \mathbf{Y}_d^{n-1}(t_i)$ (recall that $\tilde{\boldsymbol{\Phi}}_2(\cdot)$ is the identity map). Moreover, we observe from (7.99) that $z_{1,n}(t_i) = y_d^{(n-1)}(t_i)$ and hence $\boldsymbol{\xi}_1(t_i) = \mathbf{z}_1(t_i) = \mathbf{Y}_d^n(t_i)$. Consequently, the control $\tilde{u}_{d,1}(\mathbf{z}_1(t), y_d^{(n)}(t))$ achieves exact output tracking, provided that there is an $\epsilon > 0$ such that $[\mathbf{z}_1^T(t), \tilde{u}_{1,d}(t)] \in \chi_1$ holds true for all $t \in [t_i, t_i + \epsilon)$ where $\mathbf{z}_1(t)$ fulfills $\dot{\mathbf{z}}_1(t) = \tilde{\mathbf{f}}_{1,d}(\mathbf{z}_1(t), y_d^{(n-1)}(t))$. In order to show that such an ϵ exists, similar to above, we consider $\tilde{\varrho}_1(\mathbf{z}_1, y_d^{(n)})$ and its derivatives along the trajectories of $\dot{\mathbf{z}}_1 = \tilde{\mathbf{f}}_{1,d}(\mathbf{z}_1, y_d^{(n)})$ at t_i. Making use of (7.95) and (7.99) as well as $\frac{\tilde{\beta}_1(\mathbf{z}_1)}{\tilde{\varrho}_u(\mathbf{z}_1)} > 0$ we infer that

$$\tilde{\varrho}_1(\mathbf{z}_1, y_d^{(n)}) = \frac{\tilde{\varrho}_u(\mathbf{z}_1)}{\tilde{\beta}_1(\mathbf{z}_1)} \dot{\tilde{\varrho}}_2(\mathbf{z}_1, y_d^{(n-1)}, y_d^{(n)}) \geq 0 \,. \tag{7.100}$$

If $\tilde{\varrho}_1(\mathbf{z}_1, y_d^{(n)}) > 0$, then $[\mathbf{z}_1(t_i), \tilde{u}_{1,d}(t_i)] \in \operatorname{int} \chi_1$, and thus clearly there is an $\epsilon > 0$ such that $[\mathbf{z}_1(t), \tilde{u}_{1,d}(t)] \in \chi_1$ for all $t \in [t_i, t_i + \epsilon)$. Now assume that $\tilde{\varrho}_1(t_i) = 0$, which implies that $\dot{\tilde{\varrho}}_2(t_i) = 0$. By substituting this together with $\tilde{\varrho}_1(t_i) = 0$ and $\tilde{\varrho}_2(t_i) = 0$ into (7.96) we deduce that

$$\dot{\tilde{\varrho}}_1(t_i) = \frac{\tilde{\varrho}_u(\mathbf{z}_1(t_i))}{\tilde{\beta}_1(\mathbf{z}_1(t_i))} \ddot{\tilde{\varrho}}_2(t_i) = 0 \,. \tag{7.101}$$

Then we further differentiate (7.96) along the vector field $\tilde{\mathbf{f}}_{2,d}$ applying again Lemma 7.2.4. Utilizing $\tilde{\varrho}_1(t_i) = 0$, $\tilde{\varrho}_2(t_i) = 0$, $\dot{\tilde{\varrho}}_1(t_i) = 0$, $\dot{\tilde{\varrho}}_2(t_i) = 0$ as well as $\ddot{\tilde{\varrho}}_2(t_i) = 0$ in the obtained expression, we deduce that

$$\ddot{\tilde{\varrho}}_1(t_i) = \frac{\tilde{\varrho}_u(\mathbf{z}_1(t_i))}{\tilde{\beta}_1(\mathbf{z}_1(t_i))} \tilde{\varrho}_2^{(3)}(t_i) \geq 0 \,. \tag{7.102}$$

This argument can be repeated until we arrive at

$$\tilde{\varrho}_1^{(i''-1)}(t_i) = \frac{\tilde{\varrho}_u(\mathbf{z}_1(t_i))}{\tilde{\beta}_1(\mathbf{z}_1(t_i))} \tilde{\varrho}_2^{(i'')}(t_i) > 0 \,. \tag{7.103}$$

From this we conclude that there is $\epsilon > 0$ such that $[\mathbf{z}_1^T(t), \tilde{u}_{1,d}(t)] \in \chi_1$.

As far as boundedness of $\mathbf{z}_1(t)$ is concerned, we only have to consider the state $\eta_{2,1} = z_{1,n}$ since boundedness of all other components of $\mathbf{z}_1$ is guaranteed by virtue of $z_{1,j}(t) = y_d^{(j-1)}(t)$, $\forall\, j = 1, \ldots, n-1$, where $y_d^{(0)} = y_d$. In intervals $[t_i, t_{i+1})$ with $\sigma(t_i) = 1$ it also holds that $z_{1,n}(t) = y_d^{(n-1)}(t)$. However, one may wonder whether it could happen that beyond some finite switching time the system remains in the 2nd mode and $z_{1,n}$ diverges. But this is prevented by the input-to-state stability of (7.91), which guarantees that $z_{1,n}$ remains bounded while $\sigma(t) = 2$. □

Remark 7.2.2. All results in this section can be easily transferred to the case where the Assumptions 7.1.1 and 7.2.1 do not hold, i.e., where the relative degrees and the coordinate transformation $\mathbf{\Phi}_1$ and $\mathbf{\Phi}_2$ are only locally well defined. Then we consider some open set $\mathcal{O} \subset \mathbb{R}^n$ within which both the relative degrees and the coordinate transformations are well defined. The trajectories y_d and the initial values of $\boldsymbol{\eta}_1$ and $\boldsymbol{\eta}_2$ then have to be such that the state trajectory remains within $\mathcal{O}$. Obviously, this set has to be chosen such that $\partial\chi \cap \mathcal{O} \neq \emptyset$ since otherwise no switching can occur.

7.3 The Asymptotic Output Tracking Problem

In this section, the AOT Problem 7.1.3 is considered. To solve it, we apply the well known two-degree-of-freedom control scheme [86] consisting of a feedforward and a feedback part (see Figure 7.2). The feedforward controller essentially solves the EOT problem, i.e., it provides an input trajectory $u_d(t)$ and the corresponding signal $\mathbf{x}_d(t)$ such that $h(\mathbf{x}_d(t)) = y_d(t)$. In the case of trajectory-dependent switching, the switching signal that corresponds to the trajectories $u_d(t)$ and $\mathbf{x}_d(t)$ is denoted by $\sigma_d(t)$, and we also use the index "d" to distinguish the discontinuities $t_{i,d}$ of $\sigma_d(t)$ from those of $\sigma(t)$. In the case of trajectory-independent switching, the switching signal is externally specified and we have $\sigma_d(t) = \sigma(t)$.

We can assume that suitable $u_d(t)$, $\mathbf{x}_d(t)$ exist since solvability of the EOT problem is necessary for solvability of the AOT problem, as outlined in Section 7.1. The feedback controller is provided with $\mathbf{x}_d(t)$ and $\sigma_d(t)$ and is designed such that the system is stabilized and robustified against disturbances. The overall control law is of the form

$$u = \zeta(\mathbf{x}, \mathbf{x}_d, t) = u_d(t) + v(t) = u_d(t) + r(\mathbf{x}, \mathbf{x}_d, t) \tag{7.104}$$

with $r : \mathcal{O}_1 \times [0, \infty) \to \mathbb{R}$ a piecewise continuous function constituting the feedback part Σ_{FB} and $\mathcal{O}_1$ an environment of $(\mathbf{x}_d(0), \mathbf{x}_d(0))$ in $\mathbb{R}^n \times \mathbb{R}^n$.

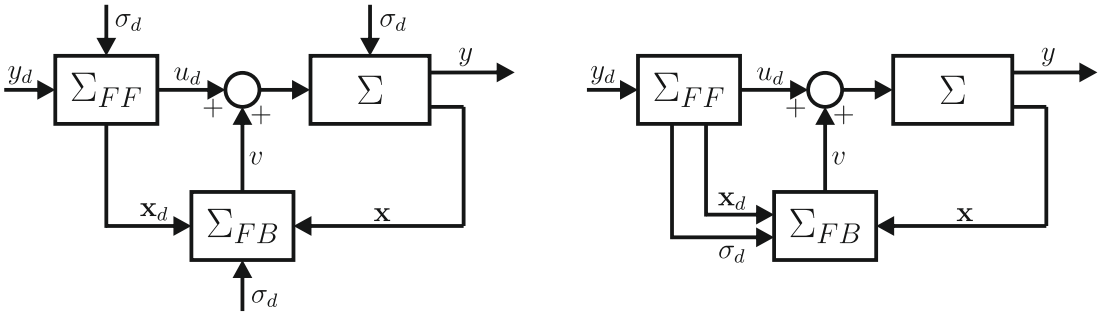

Figure 7.2: Two-degree-of-freedom control scheme with the switched system Σ, the feedforward control Σ_{FF}, and the feedback control Σ_{FB} for trajectory-independent switching (left) and trajetory-dependent switching (right).

7.3.1 Trajectory-Independent Switching

We begin with the AOT problem for systems with trajectory-independent switching. We first calculate the dynamics of the state tracking error $\mathbf{e} = \mathbf{x} - \mathbf{x}_d$ as

$$\dot{\mathbf{e}} = \dot{\mathbf{x}} - \dot{\mathbf{x}}_d = \mathbf{f}_\sigma(\mathbf{x}) - \mathbf{g}_\sigma(\mathbf{x})(u_d + v) - \mathbf{f}_{\sigma_d}(\mathbf{x}_d) - \mathbf{g}_{\sigma_d}(\mathbf{x}_d)u_d \tag{7.105a}$$

$$= \underbrace{\mathbf{f}_{\sigma_d}(\mathbf{e}+\mathbf{x}_d) - \mathbf{f}_{\sigma_d}(\mathbf{x}_d) + \mathbf{g}_{\sigma_d}(\mathbf{e}+\mathbf{x}_d)u_d - \mathbf{g}_{\sigma_d}(\mathbf{x}_d)u_d}_{\mathbf{f}^e_{\sigma_d}(\mathbf{e},t)} + \underbrace{\mathbf{g}_{\sigma_d}(\mathbf{e}+\mathbf{x}_d)}_{\mathbf{g}^e_{\sigma_d}(\mathbf{e},t)} v \ . \tag{7.105b}$$

To obtain the last equality, we have used $\mathbf{x} = \mathbf{e} + \mathbf{x}_d$ and the fact that, in the case of trajectory-independent switching, it holds that $\sigma(t) = \sigma_d(t)$. The objective is to design the feedback part Σ_{FB} in Figure (7.2) such that the equilibrium $\mathbf{e}^* = \mathbf{0}$ of this *error system* is (uniformly) asymptotically stable. If we succeed in doing so, clearly, the AOT problem is solved.

The error system is a switched nonlinear system with two time-varying subsystems

$$\dot{\mathbf{e}} = \mathbf{f}^e_{\sigma_d(t)}(\mathbf{e},t) + \mathbf{g}^e_{\sigma_d(t)}(\mathbf{e},t)v \ . \tag{7.106}$$

In order to determine a stabilizing feedback

$$v = r(\mathbf{x}, \mathbf{x}_d, t) = r_{\sigma_d(t)}(\mathbf{e},t) \tag{7.107}$$

with continuous functions $r_p(\mathbf{e},t)$ the passivity-based controller design methodology proposed in Chapter 6 can be applied. To the best of our knowledge, so far there are no other approaches for the stabilization of time-varying switched nonlinear systems.

7.3.2 Trajectory-Dependent Switching

The situation is more involved, if we consider the AOT problem for systems with state- and/or input-dependent switching. This is due to the fact that, in the case where $\mathbf{e} \neq \mathbf{0}$, or equivalently $\mathbf{x} \neq \mathbf{x}_d$, there is no reason why $[\mathbf{x}_d(t_{i,d}), u_d(t_{i,d})] \in \partial\chi$ should imply $[\mathbf{x}(t_{i,d}), u(t_{i,d})] \in \partial\chi$. Thus, in general the discontinuities t_i of the switching signal $\sigma(t)$ do not coincide with the discontinuities $t_{i,d}$ of $\sigma_d(t)$, which means that $\sigma_d(t) \neq \sigma(t)$. As a consequence, the error system

$$\dot{\mathbf{e}} = \dot{\mathbf{x}} - \dot{\mathbf{x}}_d = \mathbf{f}_\sigma(\mathbf{e} + \mathbf{x}_d) - \mathbf{g}_\sigma(\mathbf{e} + \mathbf{x}_d)(u_d + v) - \mathbf{f}_{\sigma_d}(\mathbf{x}_d) - \mathbf{g}_{\sigma_d}(\mathbf{x}_d)u_d \tag{7.108}$$

is a switched system with *four* subsystems

$$\dot{\mathbf{e}} = \mathbf{f}^e_{\sigma^e}(\mathbf{e}, t) + \mathbf{g}^e_{\sigma^e}(\mathbf{e}, t)v \tag{7.109}$$

where the switching signal $\sigma^e : [0, \infty) \to \Gamma$, $\Gamma = \{1, \ldots, 4\}$ is defined as

$$\sigma^e(t) = \begin{cases} 1 & \text{if } \sigma(t) = 1,\ \sigma_d(t) = 1 \\ 2 & \text{if } \sigma(t) = 2,\ \sigma_d(t) = 2 \\ 3 & \text{if } \sigma(t) = 1,\ \sigma_d(t) = 2 \\ 4 & \text{if } \sigma(t) = 2,\ \sigma_d(t) = 1 \end{cases} . \tag{7.110}$$

The subsystems

$$\dot{\mathbf{e}} = \mathbf{f}^e_\gamma(\mathbf{e}, t) + \mathbf{g}^e_\gamma(\mathbf{e}, t)v\ , \quad \gamma \in \Gamma \tag{7.111}$$

are defined accordingly. In order to solve the AOT problem, our objective is to determine a controller

$$v = r(\mathbf{x}, \mathbf{x}_d, t) = r_{\sigma^e(t)}(\mathbf{e}, t) \tag{7.112}$$

which makes $\mathbf{e}^* = \mathbf{0}$ a uniformly asymptotically stable equilibrium of (7.109).

The design of a stabilizing feedback for a switched nonlinear system with four time-varying subsystems is of course not an easy task at all. In addition, note that $\mathbf{e}^* = \mathbf{0}$ is *not* an admissible equilibrium of the 3rd and the 4th subsystem. Nevertheless, $\mathbf{e}^* = \mathbf{0}$ is of course an equilibrium of the overall error system (7.109) for $v = 0$ since the 3rd and the 4th subsystem do not become active, if the deviation between $\mathbf{x}(t)$ and $\mathbf{x}_d(t)$ vanishes, and for $\gamma \in \{1, 2\}$ it holds that $\mathbf{f}^e_\gamma(\mathbf{e}^*, t) = \mathbf{0}$. However, the fact that the equilibrium which is to be stabilized is not an admissible equilibrium of all subsystems further impedes the design of a stabilizing controller. Since in this case, it is obviously not possible to determine a

feedback law such that the closed loop subsystems have a common Lyapunov function. In fact, it will be necessary to exploit the fact that the 3rd and the 4th subsystem can only be active in certain situations, namely when the signs of $\varphi(\mathbf{x}, u)$ and $\varphi(\mathbf{x}_d, u_d)$ are different.

Another aspect that needs to be taken into account in the controller design is the existence of solutions. While the existence of the trajectories $\mathbf{x}_d(t)$ and $u_d(t)$ is ensured by the assumption that the EOT problem is solvable, this is not necessarily true for the trajectories $\mathbf{x}(t)$, $u(t)$ of the system (7.1) with $u(t) = u_d(t) + r_{\sigma^e(t)}(\mathbf{e}, t)$. Suppose, for instance, that $\varphi(u) = u$, and consider the situation where $u_d > 0$ and $u = u_d + r_1(\mathbf{e}, t)$ crosses the switching surface from $u > 0$ to $u < 0$ because $r_1(\mathbf{e}, t)$ becomes smaller than $-u_d$. This causes the signal σ to change its value from 1 to 2 and thus σ^e switches from 1 to 3. If it happens that $u = u_d + r_3(\mathbf{e}, t)$ is positive, the closed loop trajectory fails to exist. Similar situations can also occur in the case of state-dependent switching.

In summary, we can conclude that the design of a suitable feedback controller for the error system (7.109) is a difficult task. Therefore, we consider in the next two subsections two special classes of switched systems for which the stabilization of the tracking error simplifies considerably as compared to the general case discussed above.

7.3.3 A Special Class of Switched Nonlinear Systems

In this subsection, we study a class of switched nonlinear systems for which it suffices to consider only the 1st and the 2nd subsystem of (7.109) for the controller design. The developments below are inspired by the interesting paper [94], where the AOT problem has been addressed for the particular case of an axial piston pump. For this system switching occurs, when the control input changes its sign, and the model derived in [57], [94] is included a as special case in the class of systems treated below.

We consider switched nonlinear systems (7.1) with switching law (2.69) and

$$\mathbf{f}_2(\mathbf{x}) = \mathbf{f}_1(\mathbf{x}) + \mathbf{b}\varrho_x(\mathbf{x}) \;, \quad \mathbf{g}_2(\mathbf{x}) = \mathbf{g}_1(\mathbf{x}) + \mathbf{b}\varrho_u(\mathbf{x}) \;, \tag{7.113}$$

where $\mathbf{b} \in \mathbb{R}^n$ and $\varrho_x(\mathbf{x})$ and $\varrho_u(\mathbf{x})$ are such that (7.80) holds. With (7.113) the 2nd subsystem can be rewritten as

$$\begin{aligned} \dot{\mathbf{x}} &= \mathbf{f}_2(\mathbf{x}) + \mathbf{g}_2(\mathbf{x})u \\ &= \mathbf{f}_1(\mathbf{x}) + \mathbf{g}_1(\mathbf{x})u + \mathbf{b}\left\{\varrho_x(\mathbf{x}) + \varrho_u(\mathbf{x})u\right\} \;. \end{aligned} \tag{7.114}$$

Obviously, the overall switched system is continuous (but, in general, not continuously differentiable) at the switching surface $\partial\chi$, and hence belongs to the class of continuous

switching systems (c.f. [19], [20]). Since solvability of the EOT problem is necessary for solvability of the AOT problem, we assume that the system fulfills the necessary conditions in the Theorems 7.2.1 or 7.2.4, respectively. Note that the class of systems for which Theorem 7.2.5 gives a sufficient condition for the solvability of the EOT problem satisfies (7.113) (in $\mathbf{z}_1$ coordinates), if b_n in (7.84) is a constant. We also remark that the class of systems considered in this subsection includes as special cases the class of continuous piecewise linear systems and the class of continuous bimodal piecewise affine systems treated in [41], [43], respectively.

If (7.113) is satisfied, only with $\mathbf{b} = \mathbf{b}(\mathbf{x})$ a $\mathcal{C}^1$ function of the state, then around points $\mathbf{x}^\circ$ where $\mathbf{b}(\mathbf{x}^\circ) \neq 0$ there is a local change of coordinates $\boldsymbol{\vartheta} = \boldsymbol{\Psi}(\mathbf{x})$ such that in the new coordinates the 2nd subsystem has the form (7.114), i.e., such that $\frac{\partial \boldsymbol{\Psi}(\mathbf{x})}{\mathbf{x}} \mathbf{b}(\mathbf{x})$ is constant. This follows from the *Flow-Box Theorem* (see e.g. [128], Theorem 2.26). Moreover, all developments in this subsection can be readily transferred to the case where $\mathbf{b}(\mathbf{x}) = \bar{\mathbf{b}} c(\mathbf{x})$, where $\bar{\mathbf{b}} \in \mathbb{R}^n$ is constant and $c : \mathbb{R}^n \to \mathbb{R}$ satisfies either $c(\mathbf{x}) \geq 0, \ \forall \mathbf{x}$ or $c(\mathbf{x}) \leq 0, \ \forall \mathbf{x}$.

Remark 7.3.1. If $\varphi_u(\mathbf{x}) = 0$, in some cases we can use a switched input transformation $u = \varsigma_\sigma(\mathbf{x}, v)$ to achieve the form (7.114). Such a transformation exists, if and only if $\mathbf{g}_1(\mathbf{x}) \in \mathcal{R}(\mathbf{g}_2(\mathbf{x}))$ and there exists a vector $\mathbf{b}$ and a function $\varrho_x(\mathbf{x})$ such that

$$[\mathbf{f}_2(\mathbf{x}) - \mathbf{f}_1(\mathbf{x}) - \mathbf{b}\varrho_x(\mathbf{x})] \in \mathcal{R}\left(\mathbf{g}_2(\mathbf{x})\right) \tag{7.115}$$

holds. Not surprisingly this implies that $\mathbf{g}_2^\perp(\mathbf{x})[\mathbf{f}_2(\mathbf{x}) - \mathbf{f}_1(\mathbf{x})]$ is continuous at $\partial\chi$, where $\mathbf{g}_2^\perp(\mathbf{x})$ is a full rank left annihilator of $\mathbf{g}_2(\mathbf{x})$. Suppose for example that $r_1 = n = 2$ and that the $2nd$ subsystem is

$$\begin{aligned} \dot{x}_1 &= f_{1,1}(\mathbf{x}) + \varphi_x(\mathbf{x}) \\ \dot{x}_2 &= f_{2,2}(\mathbf{x}) + g_{2,2}(\mathbf{x})u \ . \end{aligned} \tag{7.116}$$

Then, the input transformation $u = \varsigma_\sigma(\mathbf{x}, v)$ with $\varsigma_2 = g_{2,2}^{-1}(\mathbf{x})[f_{1,2}(\mathbf{x}) + g_{1,2}(\mathbf{x})v - f_{2,2}(\mathbf{x})]$ and $\varsigma_1 = v$ achieves the form (7.114) with $\mathbf{b} = [1 \ 0]^T$, $\varrho_x = \varphi_x$, and the new input v.

We have the following result for the class of switched nonlinear systems (7.1) that satisfy (7.113).

Theorem 7.3.1. *Assume that the 2nd subsystem of* (7.1) *is of the form* (7.114)*. Moreover, suppose that there is an open neighborhood* $\mathcal{O} \subset \mathbb{R}^n$ *of* $\mathbf{e} = \mathbf{0}$ *and functions* $r : \mathcal{O} \times [0, \infty) \to \mathbb{R}$ *and* $V : \mathcal{O} \times [0, \infty) \to \mathbb{R}$ *such that*

$$W_1(\mathbf{e}) \leq V(\mathbf{e}, t) \leq W_2(\mathbf{e}) \tag{7.117}$$

$$\frac{\partial V(\mathbf{e},t)}{\partial t}+\frac{\partial V(\mathbf{e},t)}{\partial \mathbf{e}}\left[\mathbf{f}_{\gamma}^{e}(\mathbf{e},t)+\mathbf{g}_{\gamma}^{e}(\mathbf{e},t)r(\mathbf{e},t)\right]\leq -W_3(\mathbf{e}) \tag{7.118}$$

holds for $\gamma\in\{1,2\}$*, all* $t\geq 0$ *and all* $\mathbf{e}\in\mathcal{O}$*, where* $W_1(\mathbf{e})$*,* $W_2(\mathbf{e})$*, and* $W_3(\mathbf{e})$ *are continuous positive definite functions on* $\mathcal{O}$*. Then the controller* $v=r(\mathbf{e},t)$ *renders the equilibrium* $\mathbf{e}=\mathbf{0}$ *of* (7.109) *uniformly asymptotically stable.*

Proof. Let the error system (7.109) in closed loop with the controller $v=r(\mathbf{e},t)$ be denoted as

$$\dot{\mathbf{e}}=\mathbf{f}_{cl,\sigma^e}^{e}(\mathbf{e},t)=\mathbf{f}_{\sigma^e}^{e}(\mathbf{e},t)+\mathbf{g}_{\sigma^e}^{e}(\mathbf{e},t)r(\mathbf{e},t)\ . \tag{7.119}$$

Since the 2nd subsystem of (7.1) is of the form (7.114), the 3rd subsystem of the error system (7.109) can be rewritten as

$$\begin{aligned}\dot{\mathbf{e}}&=\mathbf{f}_3^e(\mathbf{e},t)+\mathbf{g}_3^e(\mathbf{e},t)v\\&=\mathbf{f}_1(\mathbf{x})+\mathbf{g}_1(\mathbf{x})(u_d+v)-[\mathbf{f}_2(\mathbf{x}_d)+\mathbf{g}_2(\mathbf{x}_d)u_d]\\&=\mathbf{f}_1(\mathbf{x})+\mathbf{g}_1(\mathbf{x})(u_d+v)-[\mathbf{f}_1(\mathbf{x}_d)+\mathbf{g}_1(\mathbf{x}_d)u_d+\mathbf{b}\left\{\varrho_x(\mathbf{x}_d)+\varrho_u(\mathbf{x}_d)u_d\right\}]\\&=\mathbf{f}_1^e(\mathbf{e},t)+\mathbf{g}_1^e(\mathbf{e},t)v-\mathbf{b}\left\{\varrho_x(\mathbf{x}_d)+\varrho_u(\mathbf{x}_d)u_d\right\}.\end{aligned} \tag{7.120}$$

But it also holds true for this subsystem that

$$\begin{aligned}\dot{\mathbf{e}}&=\mathbf{f}_3^e(\mathbf{e},t)+\mathbf{g}_3^e(\mathbf{e},t)v\\&=\mathbf{f}_2(\mathbf{x})+\mathbf{g}_2(\mathbf{x})(u_d+v)-\mathbf{b}\left\{\varrho_x(\mathbf{x})+\varrho_u(\mathbf{x})u\right\}-[\mathbf{f}_2(\mathbf{x}_d)+\mathbf{g}_2(\mathbf{x}_d)u_d]\\&=\mathbf{f}_2^e(\mathbf{e},t)+\mathbf{g}_2^e(\mathbf{e},t)v-\mathbf{b}\left\{\varrho_x(\mathbf{x})+\varrho_u(\mathbf{x})u\right\}\ .\end{aligned} \tag{7.121}$$

Hence, we get for the closed loop subsystem

$$\begin{aligned}\dot{\mathbf{e}}=\mathbf{f}_{cl,3}^{e}(\mathbf{e},t)&=\mathbf{f}_{cl,1}^{e}(\mathbf{e},t)-\mathbf{b}\left\{\varrho_x(\mathbf{x}_d)+\varrho_u(\mathbf{x}_d)u_d\right\}\\&=\mathbf{f}_{cl,2}^{e}(\mathbf{e},t)-\mathbf{b}\left\{\varrho_x(\mathbf{x})+\varrho_u(\mathbf{x})u\right\}\ .\end{aligned} \tag{7.122}$$

In the same manner, we deduce that

$$\begin{aligned}\dot{\mathbf{e}}=\mathbf{f}_{cl,4}^{e}(\mathbf{e},t)&=\mathbf{f}_{cl,1}^{e}(\mathbf{e},t)+\mathbf{b}\left\{\varrho_x(\mathbf{x})+\varrho_u(\mathbf{x})u\right\}\\&=\mathbf{f}_{cl,2}^{e}(\mathbf{e},t)+\mathbf{b}\left\{\varrho_x(\mathbf{x}_d)+\varrho_u(\mathbf{x}_d)u_d\right\}\ .\end{aligned} \tag{7.123}$$

By virtue of (7.118),

$$\frac{\partial V(\mathbf{e},t)}{\partial t}+\frac{\partial V(\mathbf{e},t)}{\partial \mathbf{e}}\mathbf{f}_{cl,\gamma}^{e}(\mathbf{e},t)\leq -W_3(\mathbf{e}) \tag{7.124}$$

holds for $\gamma\in\{1,2\}$. For the derivative of $V(\mathbf{e},t)$ along the trajectories of the 3rd subsystem,

we obtain

$$\frac{\partial V}{\partial t} + \frac{\partial V}{\partial \mathbf{e}}\mathbf{f}^e_{cl,3}(\mathbf{e},t) \tag{7.125a}$$

$$= \underbrace{\frac{\partial V}{\partial t} + \frac{\partial V}{\partial \mathbf{e}}\mathbf{f}^e_{cl,1}(\mathbf{e},t)}_{\leq -W_3(\mathbf{e})} - \frac{\partial V}{\partial \mathbf{e}}\mathbf{b}\left\{\varrho_x(\mathbf{x}_d) + \varrho_u(\mathbf{x}_d)u_d\right\} \tag{7.125b}$$

$$= \underbrace{\frac{\partial V}{\partial t} + \frac{\partial V}{\partial \mathbf{e}}\mathbf{f}^e_{cl,2}(\mathbf{e},t)}_{\leq -W_3(\mathbf{e})} - \frac{\partial V}{\partial \mathbf{e}}\mathbf{b}\left\{\varrho_x(\mathbf{x}) + \varrho_u(\mathbf{x})u\right\} \tag{7.125c}$$

where we have used (7.122). We know that, if $\sigma^e = 3$, then $\varrho(\mathbf{x}_d, u_d) = \varrho_x(\mathbf{x}_d) + \varrho_u(\mathbf{x}_d)u_d \leq 0$ and $\varrho(\mathbf{x}, u) = \varrho_x(\mathbf{x}) + \varrho_u(\mathbf{x})u \geq 0$. From (7.124), it can be seen that the first two terms in both (7.125b) and (7.125c) are smaller or equal to $-W_3(\mathbf{e})$. Now assume that $\frac{\partial V}{\partial \mathbf{e}}\mathbf{b} \geq 0$. Then, we can use $\varrho(\mathbf{x}, u) = \varrho_x(\mathbf{x}) + \varrho_u(\mathbf{x})u \geq 0$ in (7.125c) to conclude that $\frac{\partial V}{\partial t} + \frac{\partial V}{\partial \mathbf{e}}\mathbf{f}^e_{cl,3}(\mathbf{e},t) \leq -W_3(e)$. In case that $\frac{\partial V}{\partial \mathbf{e}}\mathbf{b} \leq 0$, the same can be deduced from (7.125b) with $\varrho_x(\mathbf{x}_d) + \varrho_u(\mathbf{x}_d)u_d \leq 0$. This shows that, whenever $\sigma^e = 3$, the derivative of $V(\mathbf{e},t)$ along the trajectories of the $3rd$ subsystem (7.125a) is bounded from above by $-W_3(\mathbf{e})$.

Utilizing (7.123), it can be derived in the same manner that

$$\frac{\partial V(\mathbf{e},t)}{\partial t} + \frac{\partial V(\mathbf{e},t)}{\partial \mathbf{e}}\mathbf{f}^e_{cl,4}(\mathbf{e},t) < -W_3(\mathbf{e}) \tag{7.126}$$

holds every time that $\sigma^e = 4$. Hence, we have shown that the derivative of the function $V(\mathbf{e},t)$ along all trajectories of the closed loop error system (7.119) is bounded above by $-W_3(\mathbf{e})$. Thus, uniform asymptotic stability of $\mathbf{e} = \mathbf{0}$ follows from Theorem 2.4.1. □

The theorem essentially states that for the considered class of systems it suffices to consider only the first two subsystems of (7.109) for the design of an error controller, provided that we are able to find a *common* feedback law and a corresponding *common* Lyapunov function for the two closed loop subsystems. This substantially simplifies the design task as compared to the general situation, where we need to stabilize a time-varying switched system with *four* subsystems. Recall also that $\mathbf{e}^* = \mathbf{0}$ is an admissible equilibrium of the first two subsystems, whereas this is not true for the 3rd and the 4th one.

7.3.4 Switched Linear Systems with $r_1 = r_2$

In this subsection, we consider the class of switched linear systems (7.49) which satisfy $r_1 = r_2 = r$. We assume that the switching law is of the form $\varphi(\mathbf{x}) = \mathbf{n}^T\mathbf{x}$ as otherwise the unactuated portions of the input-output dynamics of both subsystems have to be identical

in order that the EOT problem can be solvable (see Subsection 7.2.2). Without loss of generality, all results are given in the $\mathbf{z}_1$ coordinate frame. The state tracking error in these coordinates is defined as $\mathbf{e}_1(t) = \mathbf{z}_1(t) - \mathbf{z}_{1,d}(t)$, and, accordingly, in $\mathbf{z}_2$ coordinates we let $\mathbf{e}_2(t) = \mathbf{z}_2(t) - \mathbf{z}_{2,d}(t)$.

First note that, unlike with non-switched systems, also in the case where both subsystems of (7.1) are linear, a time-varying error system (7.109) is obtained. In particular, the 3rd and the 4th subsystem are time-varying (see also the example in Section 8.1). If the plant model belongs to the class of systems treated in the previous subsection, we, nevertheless, have to design a controller only for a time-invariant switched linear system consisting of the 1st and the 2nd subsystem of (7.109). In the general case, however, the time-variance renders the controller design task more complicated and also hampers the application of LMI-based methodologies, which are often used for the stabilization of switched linear systems.

For the class of systems treated in this subsection, a time-invariant representation of the error system can be obtained, enabling the use of LMI-based controller design techniques. To this end, we switch the feedforward part Σ_{FF} together with the plant, i.e., we use $u_d(t) = \tilde{u}_{\sigma,d}(t)$ instead of $u_d(t) = \tilde{u}_{\sigma_d,d}(t)$ as feedforward control, which entails that the evolution of the desired state trajectory $\mathbf{z}_{1,d}(t)$ is governed by the same differential equation as the motion of the plant. In this way, we enforce that $\sigma_d(t) = \sigma(t)$, and thereby obtain an error system whose continuous dynamics is described by

$$\begin{aligned} \dot{\mathbf{e}}_1 = \dot{\mathbf{z}}_1 - \dot{\mathbf{z}}_{1,d} &= \widetilde{\mathbf{A}}_\sigma \mathbf{z}_1 + \tilde{\mathbf{g}}_\sigma (u_d + v) - \widetilde{\mathbf{A}}_\sigma \mathbf{z}_{1,d} - \tilde{\mathbf{g}}_\sigma u_d \\ &= \widetilde{\mathbf{A}}_\sigma \mathbf{e}_1 + \tilde{\mathbf{g}}_\sigma v \end{aligned} \tag{7.127}$$

which is a switched linear system with two time-invariant subsystems. This strategy, however, leads to jumps in the desired state trajectory $\mathbf{z}_{1,d}(t)$ at the switching times t_i since $\mathbf{z}_{1,d}^T(t_i) \notin \partial\chi$. This, in turn, entails instantaneous jumps of the error $\mathbf{e}_1(t)$, such that the dynamics of the tracking error are described by a switched system with impulse effects. In the case where $r_1 = r_2$, the jumps in $\mathbf{e}_1(t)$ can be characterized in the form

$$\mathbf{e}_1(t_i) = \widetilde{\mathcal{R}}\left(\sigma(t_i), \sigma(t_i^-)\right) \mathbf{e}_1(t_i^-) \; . \tag{7.128}$$

In the sequel, explicit expressions are derived for the matrices $\widetilde{\mathcal{R}}(2,1)$ and $\widetilde{\mathcal{R}}(1,2)$. To this end, let us define the quantities $\mathbf{e}_{\eta,p} = \boldsymbol{\eta}_p - \boldsymbol{\eta}_{p,d}$ and $\mathbf{e}_{\xi,p} = \boldsymbol{\xi}_p - \boldsymbol{\xi}_{p,d}$, $p \in \{1,2\}$. We first consider switching times t_i with $\sigma(t_i^-) = 2$, $\sigma(t_i) = 1$. Using continuity of $\mathbf{z}_1(t)$, the

jump in the error $\Delta\mathbf{e}_1(t_i) = \mathbf{e}_1(t_i) - \mathbf{e}_1(t_i^-)$ is

$$\Delta\mathbf{e}_1(t_i) = \mathbf{z}_{1,d}(t_i^-) - \mathbf{z}_{1,d}(t_i) \; . \tag{7.129}$$

With $\boldsymbol{\xi}_{1,d}(t_i) = \mathbf{Y}_d^r(t_i) = \boldsymbol{\xi}_{2,d}(t_i^-) = \widetilde{\mathbf{T}}_{2,\xi}\mathbf{z}_{1,d}(t_i^-)$ we get

$$\Delta\mathbf{e}_1(t_i) = \begin{bmatrix} \boldsymbol{\xi}_{1,d}(t_i^-) \\ \boldsymbol{\eta}_{1,d}(t_i^-) \end{bmatrix} - \begin{bmatrix} \widetilde{\mathbf{T}}_{2,\xi}\mathbf{z}_{1,d}(t_i^-) \\ \boldsymbol{\eta}_{1,d}(t_i) \end{bmatrix} \; . \tag{7.130}$$

Similar to (7.28a), we choose $\boldsymbol{\eta}_{1,d}(t_i) = \boldsymbol{\eta}_{1,d}(t_i^-) = \widetilde{\mathbf{T}}_{2,\eta}^{-1}\mathbf{z}_{2,d}(t_i^-)$, such that the last $n-r$ components of $\Delta\mathbf{e}_1(t_i)$ vanish. By substituting $\mathbf{z}_{1,d}(t_i^-) = \mathbf{z}_1(t_i^-) - \mathbf{e}_1(t_i^-)$ into (7.130) we then obtain

$$\Delta\mathbf{e}_1(t_i) = \begin{bmatrix} \boldsymbol{\xi}_1(t_i^-) - \mathbf{e}_{\xi,1}(t_i^-) - \widetilde{\mathbf{T}}_{2,\xi}\left(\mathbf{z}_1(t_i^-) - \mathbf{e}_1(t_i^-)\right) \\ \mathbf{0} \end{bmatrix} \; . \tag{7.131}$$

Since we assume that the necessary conditions for EOT derived in Subsection 7.2.2 are satisfied, in particular (7.42), and $\mathbf{z}_1(t_i) \in \partial\chi$, it holds that $\boldsymbol{\xi}_1(t_i) - \widetilde{\mathbf{T}}_{2,\xi}\mathbf{z}_1(t_i) = 0$. Hence, we have

$$\mathbf{e}_1(t_i) = \mathbf{e}_1(t_i^-) + \Delta\mathbf{e}(t_i) = \underbrace{\begin{bmatrix} \widetilde{\mathbf{T}}_{2,\xi} \\ \begin{bmatrix}\mathbf{0} & \mathbf{I}_{n-r}\end{bmatrix} \end{bmatrix}}_{\widetilde{\mathcal{R}}(1,2)} \mathbf{e}_1(t_i^-) \; . \tag{7.132}$$

Similarly, it can be derived for switching times t_i with $\sigma(t_i^-) = 1$, $\sigma(t_i) = 2$ that

$$\mathbf{e}_2(t_i) = \begin{bmatrix} \widetilde{\mathbf{T}}_{2,\xi}^{-1} \\ \begin{bmatrix}\mathbf{0} & \mathbf{I}_{n-r}\end{bmatrix} \end{bmatrix} \mathbf{e}_2(t_i^-) \; . \tag{7.133}$$

Therefore,

$$\mathbf{e}_1(t_i) = \underbrace{\widetilde{\mathbf{T}}_2^{-1}\begin{bmatrix} \widetilde{\mathbf{T}}_{2,\xi}^{-1} \\ \begin{bmatrix}\mathbf{0} & \mathbf{I}_{n-r}\end{bmatrix} \end{bmatrix}\widetilde{\mathbf{T}}_2}_{\widetilde{\mathcal{R}}(2,1)} \mathbf{e}_1(t_i^-) \; . \tag{7.134}$$

In order to find a stabilizing control law $v = \tilde{\mathbf{k}}_\sigma^T\mathbf{e}_1$ for the error system defined by (7.127), (7.132), and (7.134), we can use the following result from [79].

Lemma 7.3.1. *Consider the switched linear system with impulse effects*

$$\dot{\mathbf{x}} = \mathbf{A}_\sigma\mathbf{x} \tag{7.135}$$

$$\mathbf{x}(t_i) = \mathcal{R}\left(\sigma(t_i), \sigma(t_i^-)\right)\mathbf{x}(t_i^-) \; . \tag{7.136}$$

If there are positive definite matrices $\mathbf{Q}_p,\ p \in \mathcal{P}$ *satisfying*

$$\mathbf{Q}_p\mathbf{A}_p + \mathbf{A}_p^T\mathbf{Q}_p < 0, \quad p \in \mathcal{P} \tag{7.137}$$

$$\mathcal{R}^T(p,q)\mathbf{Q}_p\mathcal{R}(p,q) \leq \mathbf{Q}_q\ , \quad p,q \in \mathcal{P} \tag{7.138}$$

then the system (7.135), (7.136) *is exponentially stable.*

The proof uses the multiple Lyapunov function approach (see Section 2.4.2) with the Lyapunov-like functions $V_p(\mathbf{x}) = \mathbf{x}^T\mathbf{Q}_p\mathbf{x}$, $p \in \mathcal{P}$. In particular, the condition (7.138) guarantees that for any switching instant

$$V_{\sigma(t_i)}\left(\mathbf{x}(t_i)\right) \leq V_{\sigma(t_i^-)}(\mathbf{x}(t_i^-))\ . \tag{7.139}$$

In view of Lemma 7.3.1, we seek to determine vectors $\tilde{\mathbf{k}}_p^T \in \mathbb{R}^{1\times n}$ and matrices $\widetilde{\mathbf{Q}}_p > 0$, $p \in \mathcal{P}$ such that the conditions (7.137) and (7.138) are satisfied with the dynamic matrices of the closed loop subsytems $\widetilde{\mathbf{A}}_{cl,p} = \widetilde{\mathbf{A}}_p - \tilde{\mathbf{g}}_p\tilde{\mathbf{k}}_p$ and the matrices $\tilde{\mathcal{R}}(p,q)$ derived above. From (7.137) we obtain

$$\left(\widetilde{\mathbf{A}}_p - \tilde{\mathbf{g}}_p\tilde{\mathbf{k}}_p\right)\widetilde{\mathbf{Q}}_p^{-1} + \widetilde{\mathbf{Q}}_p^{-1}\left(\widetilde{\mathbf{A}}_p - \tilde{\mathbf{g}}_p\tilde{\mathbf{k}}_p\right)^T < 0\ . \tag{7.140}$$

With the standard change of variables $\tilde{\mathbf{P}}_p = \widetilde{\mathbf{Q}}_p^{-1}$, $\tilde{\mathbf{l}}_p = \tilde{\mathbf{k}}_p\tilde{\mathbf{P}}_p$ [16], these conditions can be rewritten as LMI in the unknowns $\tilde{\mathbf{P}}_p$ and $\tilde{\mathbf{l}}_p$

$$\widetilde{\mathbf{A}}_p\tilde{\mathbf{P}}_p + \tilde{\mathbf{P}}_p\widetilde{\mathbf{A}}_p^T - \tilde{\mathbf{g}}_p\tilde{\mathbf{l}}_p - \tilde{\mathbf{l}}_p^T\tilde{\mathbf{g}}_p^T < 0\ . \tag{7.141}$$

Hence, we have to determine matrices $\widetilde{\mathbf{Q}}_p$, $\tilde{\mathbf{P}}_p$ and $\tilde{\mathbf{l}}_p$ which satisfy (7.141) and

$$\widetilde{\mathcal{R}}^T(p,q)\widetilde{\mathbf{Q}}_p\widetilde{\mathcal{R}}(p,q) \leq \widetilde{\mathbf{Q}}_q\ , \quad p,q \in \mathcal{P} \tag{7.142}$$

$$\tilde{\mathbf{P}}_p\widetilde{\mathbf{Q}}_p = \mathbf{I}\ , \quad p \in \mathcal{P}\ . \tag{7.143}$$

Unfortunately, the unknowns $\tilde{\mathbf{P}}_p$, $\tilde{\mathbf{Q}}_p$ appear nonlinearly in the equality condition (7.143), which hampers the application of an LMI solver. In the case where the matrices $\widetilde{\mathcal{R}}(p,q)$ are nonsingular, this problem can be circumvented as explained below. If one of the matrices $\widetilde{\mathcal{R}}(p,q)$ is singular, for instance, the approach proposed in [49] could be used to deal with the bilinear constraint (7.143).

In the case where $\widetilde{\mathcal{R}}(1,2)$ is nonsingular, we clearly can choose $\widetilde{\mathbf{T}}_{2,\eta} = [\mathbf{0},\ \mathbf{I}_{n-r}]$. This yields $\widetilde{\mathcal{R}}(1,2) = \widetilde{\mathbf{T}}_2$ and $\widetilde{\mathcal{R}}(2,1) = \widetilde{\mathbf{T}}_2^{-1}$. The latter is easily verified using the formulas for the inverse of a block matrix, see e.g. Appendix A.5.5 in [17]. If y is a flat output for both

subsystems, i.e. $r_1 = r_2 = n$, of course the relations $\widetilde{\mathcal{R}}(1,2) = \widetilde{\mathbf{T}}_2$ and $\widetilde{\mathcal{R}}(2,1) = \widetilde{\mathbf{T}}_2^{-1}$ are trivially fulfilled. Then the controller design can be done based on the following proposition employing an LMI solver as provided e.g. by MATLAB.

Proposition 7.3.1. *If $\widetilde{\mathbf{T}}_{2,\eta} = [\mathbf{0}, \mathbf{I}_{n-r}]$, then there are matrices $\widetilde{\mathbf{Q}}_p$, $\tilde{\mathbf{k}}_p$ satisfying the conditions* (7.140), (7.142) *if and only if there exist $\widetilde{\mathbf{P}}_1 > 0$ and $\tilde{\mathbf{l}}_p$, $p \in \mathcal{P}$ such that*

$$\widetilde{\mathbf{A}}_1\widetilde{\mathbf{P}}_1 + \widetilde{\mathbf{P}}_1\widetilde{\mathbf{A}}_1^T - \tilde{\mathbf{g}}_1\tilde{\mathbf{l}}_1 - \tilde{\mathbf{l}}_1^T\tilde{\mathbf{g}}_1^T < 0 \tag{7.144}$$

$$\widehat{\mathbf{A}}_2\widetilde{\mathbf{P}}_1 + \widetilde{\mathbf{P}}_1\widehat{\mathbf{A}}_2^T - \hat{\mathbf{g}}_2\tilde{\mathbf{l}}_2 - \tilde{\mathbf{l}}_2^T\hat{\mathbf{g}}_2^T < 0 \tag{7.145}$$

where $\widehat{\mathbf{A}}_2 = \widetilde{\mathbf{T}}_2\widetilde{\mathbf{A}}_2\widetilde{\mathbf{T}}_2^{-1}$ and $\hat{\mathbf{g}}_2 = \widetilde{\mathbf{T}}_2\tilde{\mathbf{g}}_2$. Then it holds that

$$\widetilde{\mathbf{Q}}_1 = \widetilde{\mathbf{P}}_1^{-1}\,, \quad \widetilde{\mathbf{Q}}_2 = \widetilde{\mathbf{T}}_2^T\widetilde{\mathbf{P}}_1^{-1}\widetilde{\mathbf{T}}_2 \quad \tilde{\mathbf{k}}_1 = \tilde{\mathbf{l}}_1\widetilde{\mathbf{P}}_1^{-1}\,, \quad \tilde{\mathbf{k}}_2 = \tilde{\mathbf{l}}_2\widetilde{\mathbf{P}}_1^{-1}\widetilde{\mathbf{T}}_2\,. \tag{7.146}$$

Proof. The condition (7.144) is identical to (7.141) for $p = 1$, which has been obtained with the change of variables $\widetilde{\mathbf{P}}_p = \widetilde{\mathbf{Q}}_p^{-1}$, $\tilde{\mathbf{l}}_p = \tilde{\mathbf{k}}_p\widetilde{\mathbf{P}}_p$. Moreover, as argued above, if $\widetilde{\mathbf{T}}_{2,\eta} = [\mathbf{0}, \mathbf{I}_{n-r}]$, then $\widetilde{\mathcal{R}}(1,2) = \widetilde{\mathbf{T}}_2$ and $\widetilde{\mathcal{R}}(2,1) = \widetilde{\mathbf{T}}_2^{-1}$. Thus, the inequalities (7.142) take the form

$$\widetilde{\mathbf{T}}_2^T\widetilde{\mathbf{Q}}_1\widetilde{\mathbf{T}}_2 - \widetilde{\mathbf{Q}}_2 \leq 0 \tag{7.147}$$

$$\widetilde{\mathbf{T}}_2^{-T}\widetilde{\mathbf{Q}}_2\widetilde{\mathbf{T}}_2^{-1} - \widetilde{\mathbf{Q}}_1 \leq 0\,. \tag{7.148}$$

These two conditions are satisfied if and only if $\widetilde{\mathbf{Q}}_2 = \widetilde{\mathbf{T}}_2^T\widetilde{\mathbf{Q}}_1\widetilde{\mathbf{T}}_2$ and hence $\widetilde{\mathbf{Q}}_2^{-1} = \widetilde{\mathbf{T}}_2^{-1}\widetilde{\mathbf{Q}}_1^{-1}\widetilde{\mathbf{T}}_2^{-T}$. By substituting this into (7.140), and by multiplication with $\widetilde{\mathbf{T}}_2$ on the left and $\widetilde{\mathbf{T}}_2^T$ on the right, we obtain

$$\underbrace{\widetilde{\mathbf{T}}_2\widetilde{\mathbf{A}}_2\widetilde{\mathbf{T}}_2^{-1}}_{\widehat{\mathbf{A}}_2}\widetilde{\mathbf{Q}}_1^{-1} + \widetilde{\mathbf{Q}}_1^{-1}\underbrace{\widetilde{\mathbf{T}}_2^{-T}\widetilde{\mathbf{A}}_2^T\widetilde{\mathbf{T}}_2^T}_{\widehat{\mathbf{A}}_2^T} - \underbrace{\widetilde{\mathbf{T}}_2\tilde{\mathbf{g}}_2}_{\hat{\mathbf{g}}_2}\tilde{\mathbf{k}}_2\widetilde{\mathbf{T}}_2^{-1}\widetilde{\mathbf{Q}}_1^{-1} - \widetilde{\mathbf{Q}}_1^{-1}\widetilde{\mathbf{T}}_2^{-T}\tilde{\mathbf{k}}_2^T\underbrace{\tilde{\mathbf{g}}_2^T\widetilde{\mathbf{T}}_2^T}_{\hat{\mathbf{g}}_2^T} < 0\,. \tag{7.149}$$

With the change of variables $\widetilde{\mathbf{P}}_1 = \widetilde{\mathbf{Q}}_1^{-1}$ and $\tilde{\mathbf{l}}_2 = \tilde{\mathbf{k}}_2\widetilde{\mathbf{T}}_2^{-1}\widetilde{\mathbf{Q}}_1^{-1}$ we finally get (7.145) and (7.146). □

Note that $\widetilde{\mathbf{Q}}_2 = \widetilde{\mathbf{T}}_2^T\widetilde{\mathbf{Q}}_1\widetilde{\mathbf{T}}_2$ implies that both conditions (7.147), (7.148) are fulfilled with equality. As a consequence, (7.139) also holds with equality, i.e., we have $\widetilde{V}_{\sigma(t_i)}(\mathbf{z}_1(t_i)) = \widetilde{V}_{\sigma(t_i^-)}(\mathbf{z}_1(t_i^-))$ for all switching times t_i.

7.4 Concluding Remarks

In this chapter, we have studied the output trajectory tracking problem for bimodal switched nonlinear SISO systems. First, we have provided necessary and sufficient conditions to

answer the question when there exists a piecewise continuous input for a system with trajectory-independent switching such that its output exactly tracks a desired trajectory. It has been shown that this is only possible for special pairs of switching signal and desired output trajectory. In case that the output of interest is a flat output for both subsystems, suitable pairs can be identified quite easily based on the derived conditions without solving any differential equations. Although in this chapter we have constrained ourselves to the case of two subsystems, this result can be extended to general switched systems in a straightforward manner.

Moreover, we have examined the EOT problem for systems with state- and/or input-dependent switching. We have established necessary conditions under which this problem is solvable for all bounded output trajectories with bounded derivatives. Under some additional hypotheses, involving that the output is a flat output for one of the subsystems, also sufficient conditions have been obtained. The derived conditions are not only of theoretical interest, but are also important from a practical point of view. The sufficient conditions guarantee the safe operation of the system for arbitrary reference trajectories. The necessary conditions specify precise situations where, to achieve exact output tracking, it is inevitable to either restrict the desired trajectories to a special class or to appropriately modify the model of the technical system, e.g. in cases where the switching arises from an approximation made during the modeling process. Instrumental for our developments have been, as in the case of smooth systems, the concept of relative degree and the input-output normal form, as generalized to nonlinear control affine SISO systems by Isidori.

A further topic which has been addressed in this chapter is the solution of the AOT problem by means of a two-degree-of-freedom control scheme. While this is straightforward in the case of trajectory-independent switching, it turns out to be more delicate for systems with state- and/or input-dependent switching law, since in this case the error system is, in general, a time-varying switched nonlinear system with four subsystems instead of two. The stabilization problem is further complicated by the fact that the desired equilibrium point $\mathbf{e}^* = \mathbf{0}$ is not an admissible equilibrium for two of these subsystems. Motivated by that, we have shown that for two special classes of switched systems the design of a stabilizing error controller can be simplified considerably.

Chapter 8

Technical Applications

In this chapter, two technical systems are considered in order to further illustrate the results developed in the Chapters 6 and 7, and to underscore their practical relevance and applicability. First we are concerned with the problem of tracking a desired speed trajectory with a DC motor having an asymmetric friction characteristic. It is well known that the friction behavior of DC motors may change with the direction of rotation [6], [23], [55]. In [23], "*it was found to be essential to have a* [friction] *model which is asymmetric in the angular velocity*". This asymmetry leads to different models for positive and negative values of the angular velocity and thus to a switched system with state-dependent switching law. The second application we are dealing with in this chapter is the pressure control of a self-supplied variable displacement axial piston pump as it is used, for instance, in injection molding machines [94]. The mathematical model of this system exhibits switching depending on the sign of the control input, which is due to the fact that the pump is self-supplied.

Both systems are examined with regard to the solvability of the EOT problem, and suitable feedforward controllers are designed. In order to solve the AOT problem, the error systems are stabilized by means of the IDA technique for switched systems presented in Chapter 6. While in the case of the axial piston pump the systematic procedure proposed in Section 6.4 can be employed, the error controller for the DC motor is designed using the general approach from Section 6.3. In addition, using the results from Section 7.3.4, an LMI-based controller is determined to solve the AOT problem for the DC motor.

8.1 DC Motor with Asymmetric Friction Characteristic

This section is devoted to the trajectory tracking control of a DC motor with asymmetric friction characteristic. The friction torque is modeled solely by viscous damping in the following. Other friction effects can be taken into account by adding a LuGre-model-based

Table 8.1: Parameters of the DC motor.

Model parameter	Symbol	Value	Unit
Damping coefficient for $\omega \geq 0$	d_1	3×10^{-3}	Nms/rad
Damping coefficient for $\omega \leq 0$	d_2	4×10^{-3}	Nms/rad
Inductance	L	3.6×10^{-3}	H
Resistance	R	1.71	Ω
Rotor inertia	J	6×10^{-5}	Nms^2/rad
Torque constant	k	0.1	Nm/A

friction compensation scheme similar to that in [55] and [153]. Since, in contrast to these contributions, for the system at hand the friction does not occur in the actuated coordinate, some modifications are necessary, which are, however, beyond the scope of this thesis. If we define the state vector by $\mathbf{x} = [I, \omega]^T$ with I the current through the motor and ω the angular speed of the rotor, the model of the DC motor is given by

$$\dot{\mathbf{x}} = \mathbf{A}_\sigma \mathbf{x} + \mathbf{g}u \,, \quad \mathbf{A}_1 = \begin{bmatrix} -\frac{R}{L} & -\frac{k}{L} \\ \frac{k}{J} & -\frac{d_1}{J} \end{bmatrix}, \quad \mathbf{A}_2 = \begin{bmatrix} -\frac{R}{L} & -\frac{k}{L} \\ \frac{k}{J} & -\frac{d_2}{J} \end{bmatrix}, \quad \mathbf{g} = \begin{bmatrix} \frac{1}{L} \\ 0 \end{bmatrix} \tag{8.1}$$

where R denotes the resistance, L the inductance, k the torque constant and J the inertia of the rotor. The control input u is the input voltage. In order to incorporate the asymmetric behavior, the coefficient of viscous friction d_p, $p \in \{1, 2\}$ is switched according to the sign of $x_2 = \omega$, i.e., the switching law is given by (2.69) and (2.70) with $\varphi(\mathbf{x}) = x_2$. The parameter values are given in Table 8.1.

8.1.1 Feedforward Design

It is intended to design a controller such that the output

$$y = x_2 = \omega \tag{8.2}$$

asymptotically tracks a desired trajectory $y_d(t)$. Since solvability of the AOT problem requires solvability of the EOT problem, the latter is examined first. It is easy to check that (8.2) is a flat output for both subsystems of (8.1), and, consequently, it holds that

$r_1 = r_2 = n = 2$. We determine the coordinate transformation

$$\mathbf{z}_1 = \begin{bmatrix} \xi_{1,1} \\ \xi_{1,2} \end{bmatrix} = \mathbf{\Phi}_1(\mathbf{x}) = \mathbf{h}_1^2(\mathbf{x}) = \underbrace{\begin{bmatrix} 0 & 1 \\ \frac{k}{J} & -\frac{d_1}{J} \end{bmatrix}}_{\mathbf{T}_1} \mathbf{x} \; . \tag{8.3}$$

In these coordinates, the 1st subsystem of (8.1) is given by

$$\begin{aligned} \dot{\xi}_{1,1} &= \xi_{1,2} \\ \dot{\xi}_{1,2} &= -\frac{Rd_1 + k^2}{JL}\xi_{1,1} - \frac{RJ + d_1 L}{JL}\xi_{1,2} + \frac{k}{JL}u \\ y &= \xi_{1,1} \end{aligned} \tag{8.4}$$

and we get $\tilde{\varphi}(\mathbf{z}_1) = \tilde{\varphi}_x(\mathbf{z}_1) = \xi_{1,1}$, i.e., $\tilde{\varphi}_u(\mathbf{z}_1) = 0$ and $\tilde{\mathbf{n}}^T = [1 \; 0]$ with $\|\tilde{\mathbf{n}}\| = 1$ (c.f. Theorem 7.2.3). The 2nd subsystem possesses the form

$$\begin{aligned} \dot{\xi}_{1,1} &= \xi_{1,2} + (d_1 - d_2)\xi_{1,1} \\ \dot{\xi}_{1,2} &= -\frac{Rd_1 + k^2}{JL}\xi_{1,1} - \frac{RJ + d_1 L}{JL}\xi_{1,2} + \frac{k}{JL}u + \frac{d_1 d_2 - d_1^2}{J^2}\xi_{1,1} \\ y &= \xi_{1,1} \; . \end{aligned} \tag{8.5}$$

Hence, the coordinate transformation $\tilde{\mathbf{\Phi}}_2(\mathbf{z}_1)$ is given by

$$\mathbf{z}_2 = \underbrace{\begin{bmatrix} 1 & 0 \\ d_1 - d_2 & 1 \end{bmatrix}}_{\widetilde{\mathbf{T}}_2} \mathbf{z}_1 \; . \tag{8.6}$$

It is not difficult to see that $\widetilde{\mathbf{T}}_2 = \mathbf{I}_2 + \mathbf{k}\tilde{\mathbf{n}}^T$ with $\mathbf{k}^T = [0 \; d_1 - d_2]$. Since $\mathbf{k}^T\tilde{\mathbf{n}} = 0 > -1$ the conditions of Theorem 7.2.3 for the solvability of the EOT problem are satisfied. The trajectories $u_d(t)$ and $\mathbf{x}_d(t)$ corresponding to a desired speed trajectory $y_d(t)$ are given by

$$x_{d,1}(t) = \frac{J}{k}\dot{y}_d(t) + \frac{d_{\sigma_d}}{k}y_d(t) \tag{8.7}$$

$$x_{d,2}(t) = y_d(t) \tag{8.8}$$

$$u_d(t) = \frac{1}{k}\left[JL\ddot{y}_d(t) + (RJ + d_{\sigma_d}L)\,\dot{y}_d + \left(k^2 + Rd_{\sigma_d}\right)y_d\right] \; . \tag{8.9}$$

Note that σ_d is used in (8.9), which is equal to 1, if the *desired* angular velocity is positive, and equal to 2, if the desired angular velocity is negative.

8.1.2 IDA Controller Design

In order to solve the AOT problem, the feedforward controller from the previous subsection needs to be augmented by a suitable feedback controller that stabilizes the tracking error (see Section 7.3). In this subsection, the passivity-based control scheme proposed in Chapter 6 is applied to determine a suitable feedback law. As an alternative, in the subsequent subsection, an LMI-based controller is designed using the results from Subsection 7.3.4.

The 1st and the 2nd subsystem of the error system (7.109) are given by

$$\dot{\mathbf{e}} = \mathbf{A}_p\mathbf{e} + \mathbf{g}v \ , \quad p \in \{1, 2\} \ . \tag{8.10}$$

For the 3rd subsystem, we get

$$\dot{\mathbf{e}} = \mathbf{A}_1\mathbf{e} + \mathbf{g}v + \begin{bmatrix} 0 & 1 \end{bmatrix}^T \frac{d_2 - d_1}{J} x_{d,2}(t) \tag{8.11}$$

and the 4th subsystem is

$$\dot{\mathbf{e}} = \mathbf{A}_2\mathbf{e} + \mathbf{g}v + \begin{bmatrix} 0 & 1 \end{bmatrix}^T \frac{d_1 - d_2}{J} x_{d,2}(t) \ . \tag{8.12}$$

It has been mentioned in Subsection 7.3.4 that, in contrast to non-switched systems, in the case of trajectory-dependent switching, we obtain a time-varying error system even if all subsystems of the plant model are linear and time-invariant. This can be seen in (8.11) and (8.12). Note also that $\mathbf{e}^* = \mathbf{0}$ is indeed not an admissible equilibrium for these two subsystems except for the trivial case that $x_{d,2}(t) \equiv 0$.

In order to simplify the controller design, we observe that in $\mathbf{x}$-coordinates the plant model can be rewritten as in (7.114) with

$$\mathbf{b} = \begin{bmatrix} 0 \\ \frac{d_1 - d_2}{J} \end{bmatrix} \tag{8.13}$$

and thus belongs to the special class of systems treated in Subsection 7.3.3. Therefore, according to Theorem 7.3.1, it suffices to find a common control law together with a common Lyapunov function such that the switched system consisting only of the first two subsystems of the error system (8.10) is asymptotically stabilized. This is a switched linear system with time-invariant subsystems. It does, however, not belong to the special class treated in Section 6.4, and thus the proposed systematic procedure cannot be applied.

Solving the projected matching equations

With the simple left annihilators $\mathbf{G}_p^{\perp} = [0,\ 1]$, $p = 1, 2$ the projected matching equations (6.9) are obtained as

$$\begin{bmatrix} f_{1,21} & f_{1,22} \\ f_{2,21} & f_{2,22} \end{bmatrix} \nabla H(\mathbf{e}) = \begin{bmatrix} \frac{k}{J} e_1 - \frac{d_1}{J} e_2 \\ \frac{k}{J} e_1 - \frac{d_2}{J} e_2 \end{bmatrix} \tag{8.14}$$

where $f_{p,ij}$ denotes the (i,j)-element of the design matrix $\mathbf{F}_p$, $p \in \{1, 2\}$. From the solvability condition (2.39), we get

$$k f_{2,21} - d_1 f_{2,22} - k f_{1,21} + d_2 f_{1,22} = 0 \tag{8.15}$$

which can be fulfilled by choosing

$$f_{1,22} = \frac{1}{d_2} \left(k f_{1,21} - k f_{2,12} + d_1 f_{2,22} \right) \ . \tag{8.16}$$

The solution of (8.14) is given by

$$H(\mathbf{e}) = c \mathbf{e}^T \mathbf{Q} \mathbf{e} \tag{8.17}$$

with

$$c = \left[2J \left(-f_{1,21} f_{2,22} d_2 + f_{2,21} f_{1,21} k - f_{2,21}^2 k + f_{2,21} f_{2,22} d_1 \right) \right]^{-1} \tag{8.18}$$

and

$$\mathbf{Q} = \begin{bmatrix} k^2 (f_{1,21} - f_{2,21}) - k f_{2,22} (d_2 - d_1) & -k d_2 (f_{1,21} - f_{2,21}) \\ -k d_2 (f_{1,21} - f_{2,21}) & f_{1,21} d_2^2 - f_{2,21} d_1 d_2 \end{bmatrix} \ . \tag{8.19}$$

Note that the homogeneous PDE corresponding to (8.14) has only the trivial solution, and hence $H(\mathbf{e})$ is the unique solution of (8.14).

Conditions for a strict local minimum of $H(\mathbf{e})$

As desired, the gradient of $H(\mathbf{e})$ vanishes at the desired equilibrium $\mathbf{e}^* = \mathbf{0}$. In order to guarantee a strict local minimum at this point, we render the Hessian of the energy function $\nabla^2 H(\mathbf{e}) = 2c\mathbf{Q}$ positive definite. By Sylvester's criterion, it must hold that

$$\det \left(\nabla^2 H(\mathbf{e}^*) \right) = \det \left(2c\mathbf{Q} \right) = \frac{2}{J} \left(d_2 - d_1 \right) k d_2 c > 0 \tag{8.20}$$

which is satisfied if $c > 0$ because $d_2 > d_1$ (see Table 8.1). If we choose $f_{2,21}$ and $f_{2,22}$ such that

$$k f_{2,21} - d_2 f_{2,22} > 0 \quad \Leftrightarrow \quad f_{2,21} > \frac{d_2}{k} f_{2,22} \tag{8.21}$$

then $c > 0$ holds if and only if

$$f_{1,21} > f_{2,21} \frac{k f_{2,21} - d_1 f_{2,22}}{k f_{2,21} - d_2 f_{2,22}} \,. \tag{8.22}$$

In addition, we require the second diagonal entry of $\mathbf{Q}$ to be positive

$$f_{1,21} d_2^2 - f_{2,21} d_1 d_2 > 0 \quad \Leftrightarrow \quad f_{1,21} > \frac{d_1 d_2}{d_2^2} f_{2,21} \,. \tag{8.23}$$

Together with (8.20) this implies that also the first diagonal entry of $\nabla^2 H(\mathbf{e})$ is positive and thus $\nabla^2 H(\mathbf{e}) > 0$ is guaranteed by Sylvester's criterion.

Conditions for positive definiteness of the dissipation matrices

In order to satisfy the conditions of Theorem 7.3.1, we need to design a common control law for both subsystems. As the actuated component of both subsystems is identical, this is achieved by choosing $f_{2,11} = f_{1,11}$ and $f_{2,12} = f_{1,12}$. Moreover, we simplify $\mathbf{R}_1$ by setting $f_{1,12} = -f_{1,21}$. Then, we obtain the dissipation matrices

$$\mathbf{R}_1 = \begin{bmatrix} -f_{1,11} & 0 \\ 0 & -\frac{1}{d_2}\left(k f_{1,21} - k f_{2,21} + d_1 f_{2,22}\right) \end{bmatrix} \tag{8.24}$$

$$\mathbf{R}_2 = \begin{bmatrix} -f_{1,11} & \frac{1}{2}\left(f_{1,21} - f_{2,21}\right) \\ \frac{1}{2}\left(f_{1,21} - f_{2,21}\right) & -f_{2,22} \end{bmatrix} . \tag{8.25}$$

To guarantee that they are both positive definite, we again invoke Sylvester's criterion to derive the conditions

$$f_{1,11} < 0 \tag{8.26}$$

$$f_{1,21} < -\frac{d_1}{k} f_{2,22} + f_{2,21} \tag{8.27}$$

$$f_{1,11} f_{2,22} - \frac{1}{4}\left(f_{1,21} - f_{2,21}\right)^2 > 0 \,. \tag{8.28}$$

Obviously, (8.26) and (8.28) imply that $f_{2,22} < 0$.

Controller Tuning

In order to determine admissible values for the controller parameters, we can proceed as follows: First we choose $f_{2,22} < 0$ and $f_{2,21}$ such that (8.21) holds. Subsequently, we determine a value for $f_{1,21}$ which satisfies the inequalities (8.27), (8.22) and (8.23), whose

right hand sides only depend on $f_{2,22}$ and $f_{2,21}$. The right hand side of (8.27) is greater than $f_{2,21}$ because $f_{2,22} < 0$. The fractions in (8.22) and (8.23) are each smaller than 1 due to $d_2 > d_1$, and thus the right hand sides of both conditions are smaller than $f_{2,21}$ Therefore, there is always an admissible value for $f_{1,21}$. Finally, $f_{1,11} < 0$ is used to satisfy (8.28). It is worthwhile noting that all conditions are satisfied, if $f_{1,11}$ and $f_{2,22}$ are negative and we choose $f_{2,21} = f_{1,21}$ such that (8.21) holds true. This choice makes $\mathbf{R}_2$ a diagonal matrix.

Aside from compliance with the conditions derived above, another important aspect that needs to be taken into account for the choice of the controller parameters is the dynamic behavior of the closed loop system. Since the application of LLDA requires the existence of m characteristic coordinates, this technique cannot be employed in the case at hand. Therefore, we use numerical optimization to determine controller parameters that achieve good dynamic behavior. The vector of design variables is $\boldsymbol{\gamma} = [f_{1,11}, f_{1,21}, f_{2,21}, f_{2,22}]$. In Section 6.8, we have suggested to solve the optimization problem (4.20a)-(4.20c), i.e., to maximize the volume of the DA, while the eigenvalues of the (linearized) closed loop subsystems are constrained to some admissible region in the left half plane (Figure 4.3). However, the considered closed loop system is globally uniformly asymptotically stable for any admissible controller parametrization, and thus the volume of the DA is not a meaningful objective function. Therefore, we set up the minimization problem

$$\min_{\boldsymbol{\gamma}} \ \max_{i,p} \left\{ \mathrm{Re}\Big[\lambda_i\Big(\mathbf{A}^e_{cl,p}(\boldsymbol{\gamma})\Big)\Big]\right\} \tag{8.29}$$

subject to

$$r_{min} \leq \min_{i,p} \left\{ \mathrm{Re}\Big[\lambda_i\Big(\mathbf{A}_{cl,p}(\boldsymbol{\gamma})\Big)\Big]\right\} \leq r_{max} \ , \quad \forall\ i,p \tag{8.30}$$

$$\Big|\mathrm{Re}\Big[\lambda_i\Big(\mathbf{A}_{cl,p}(\boldsymbol{\gamma})\Big)\Big]\Big| \geq \tan(\psi) \Big|\mathrm{Im}\Big[\lambda_i\Big(\mathbf{A}_{cl,p}(\boldsymbol{\gamma})\Big)\Big]\Big| \geq 0 \ , \quad \forall\ i,p \tag{8.31}$$

and the constraints (8.26), (8.27), (8.28), where $\mathbf{A}_{cl,p}$, $p = 1, 2$ denotes the closed-loop dynamic matrices. That means, we try to move the eigenvalues of the closed loop subsystems as far to the left as possible within the region illustrated in Figure 8.1, where we have chosen $r_{max} = 0$, $r_{min} = -550$, and $\psi = \frac{\pi}{4}$. Recall that the Hessian of the energy function is guaranteed to be positive definite at $\mathbf{e}^*$ if the closed loop eigenvalues are located in the left half plane and the dissipation matrices are positive definite. For this reason, the constraints (8.21)-(8.23) don't have to be included in the minimization problem.

We use `fmincon`, which is provided by MATLAB, to solve the problem. The initial value is chosen as $\boldsymbol{\gamma}_0 = [-5, 1, 1, -5]$, which satisfies all conditions derived above. We obtain

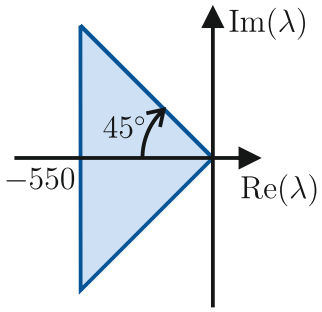

Figure 8.1: Admissible region for the eigenvalues of the closed-loop subsystems.

$f_{1,11} = -1.5 \cdot 10^3$, $f_{1,21} = f_{2,21} = 2.9 \cdot 10^3$, $f_{2,22} = -1.7 \cdot 10^3$ (rounded to multiples of 10^2). The resulting eigenvalues of $\mathbf{A}_{cl,1}$ are $-456 \pm 157i$, the eigenvalues of $\mathbf{A}_{cl,2}$ are $-464 \pm 177i$. The corresponding control law is given by

$$v = \begin{bmatrix} -1.39 & -0.31 \end{bmatrix} \mathbf{e} \,. \tag{8.32}$$

Simulation results are shown in Figure 8.2. The desired trajectory is a sine wave with frequency 10 Hz and an amplitude of 30 $[\frac{\text{rad}}{\text{s}}]$. The initial value of $\mathbf{x}$ has been set to $\mathbf{x}(0) = [10, \ -30]^T$ which results in $\mathbf{e}(0) = [8.87, \ -30]^T$. At 0.11 s a disturbance torque of 0.5 Nm is acting on the motor for 7.5 ms. As expected, the rotor speed tracks the desired trajectory, and, moreover, the controller is able to compensate tracking errors in a fast manner.

8.1.3 LMI-Based Controller Design

Since the motor model (8.1) is linear and it holds that $r_1 = r_2$, we can also apply the method proposed in Subsection 7.3.4 to solve the AOT problem. To this end, we switch the feedforward control together with the plant, i.e., we use σ instead of σ_d in (8.9), and design a stabilizing error controller using Proposition 7.3.1. The matrices $\widetilde{\mathbf{A}}_1$ and $\widetilde{\mathbf{A}}_2$ as well as $\tilde{\mathbf{g}}_1$ and $\tilde{\mathbf{g}}_2$ immediately come out of (8.4) and (8.5), the matrix $\widetilde{\mathbf{T}}_2$ is given in (8.6). We use the command `feasp` provided by MATLAB to solve the LMIs

$$\widetilde{\mathbf{A}}_1\widetilde{\mathbf{P}}_1 + \widetilde{\mathbf{P}}_1\widetilde{\mathbf{A}}_1^T - \tilde{\mathbf{g}}_1\tilde{\mathbf{l}}_1 - \tilde{\mathbf{l}}_1^T\tilde{\mathbf{g}}_1^T < -\alpha\widetilde{\mathbf{P}}_1 \tag{8.33}$$

$$\widehat{\mathbf{A}}_2\widetilde{\mathbf{P}}_1 + \widetilde{\mathbf{P}}_1\widehat{\mathbf{A}}_2^T - \hat{\mathbf{g}}_2\tilde{\mathbf{l}}_2 - \tilde{\mathbf{l}}_2^T\hat{\mathbf{g}}_2^T < -\alpha\widetilde{\mathbf{P}}_1 \tag{8.34}$$

for the unknowns $\widetilde{\mathbf{P}}_1 = \widetilde{\mathbf{P}}_1^T > 0$ and $\tilde{\mathbf{l}}_p$, $p \in \mathcal{P}$, where $\alpha > 0$ is some positive scalar. The LMIs are identical to (7.144) and (7.145) in Proposition 7.3.1 except that we have

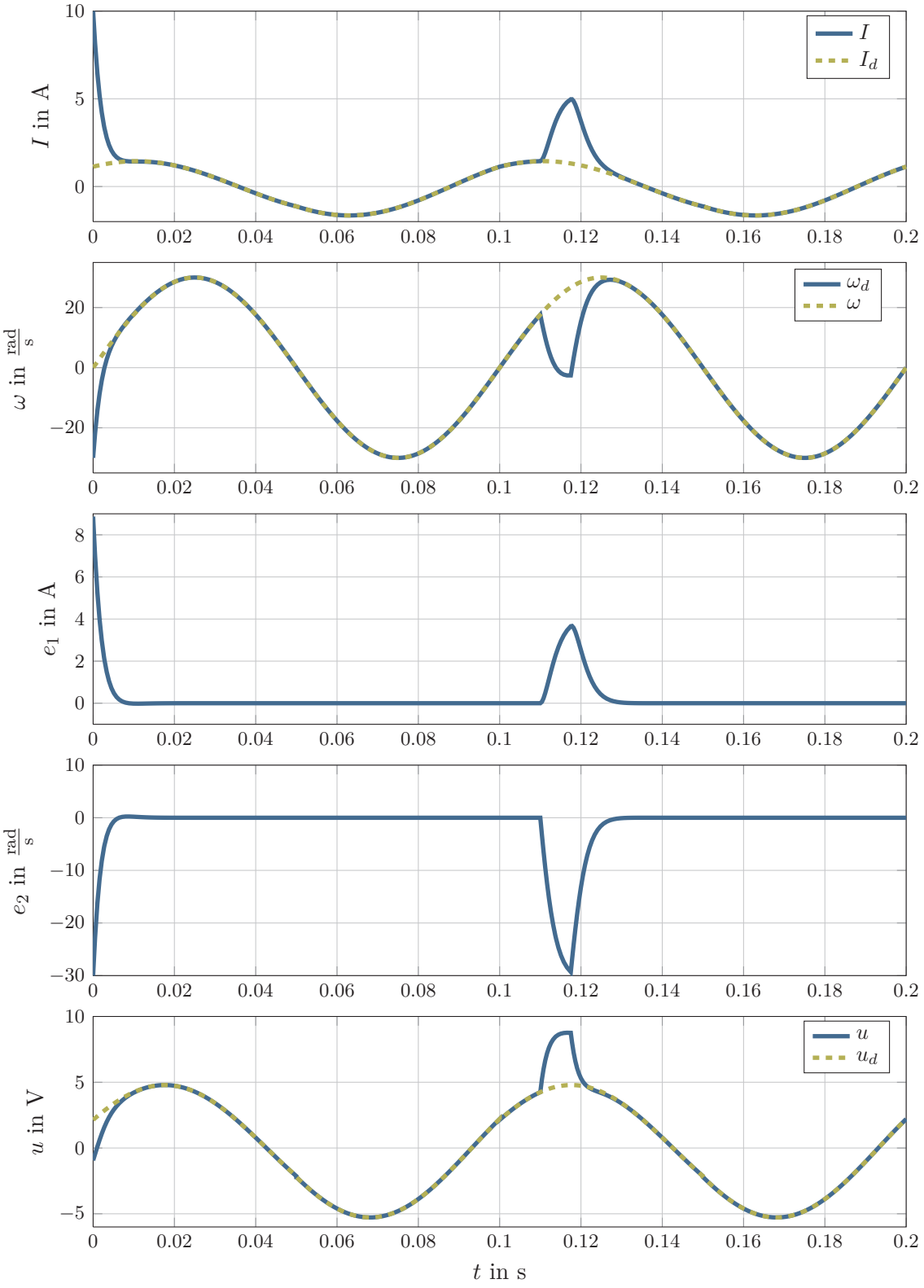

Figure 8.2: Simulation results for the DC motor with IDA-based error controller, initial value $\mathbf{x}(0) = [10,\ -30]^T$, and a disturbance torque acting on the motor at time $t = 0.11\,\mathrm{s}$.

replaced the zeros on the right hand sides by the term $-\alpha\widetilde{\mathbf{P}}_1$. Of course any set of matrices $\widetilde{\mathbf{P}}_1 = \widetilde{\mathbf{P}}_1^T > 0$, $\tilde{\mathbf{l}}_p$, $p \in \mathcal{P}$ that solves (8.33) and (8.34) also satisfies (7.144) and (7.145). However, the expression $-\alpha\widetilde{\mathbf{P}}_1$ on the right hand side guarantees that in any time interval (t_i, t_{i+1}) within which the pth subsystem is active, it holds that $\dot{\widetilde{V}}_p(t) < -\alpha\widetilde{V}_p(t)$ and therefore $\widetilde{V}_p(t) \leq e^{-\alpha t}\widetilde{V}_p(t_i)$. Consequently, we can specify by α an exponential decay rate for the Lyapunov functions and thereby influence the dynamic behavior of the closed loop system.

With $\alpha = 50$, we obtain the solution

$$\widetilde{\mathbf{P}}_1 = \begin{bmatrix} 4.20 \cdot 10^{-3} & -1.58 \cdot 10^{-1} \\ -1.58 \cdot 10^{-1} & 7.91 \end{bmatrix}, \quad \tilde{\mathbf{l}}_1^T = \begin{bmatrix} 4.51 \cdot 10^{-4} \\ 1.54 \cdot 10^{-2} \end{bmatrix}, \quad \tilde{\mathbf{l}}_2^T = \begin{bmatrix} 5.17 \cdot 10^{-4} \\ 1.78 \cdot 10^{-2} \end{bmatrix}. \tag{8.35}$$

In $\mathbf{x}$ coordinates, the control law is then given by $v = -\mathbf{k}_\sigma^T\mathbf{x}$ with

$$\mathbf{k}_1 = \tilde{\mathbf{l}}_1\widetilde{\mathbf{P}}_1^{-1}\mathbf{T}_1 = \begin{bmatrix} -1.51 & -9.74 \cdot 10^{-2} \end{bmatrix}, \quad \mathbf{k}_2 = \tilde{\mathbf{l}}_2\widetilde{\mathbf{P}}_1^{-1}\widetilde{\mathbf{T}}_2\mathbf{T}_1 = \begin{bmatrix} -1.57 & -9.70 \cdot 10^{-2} \end{bmatrix}$$

where $\mathbf{T}_1$ and $\widetilde{\mathbf{T}}_2$ are given in (8.3) and (8.6), respectively.

Simulation results are shown in Figure 8.3. The desired trajectory $\omega_d(t)$ is the same sine wave as in the previous subsection, the initial state is $\mathbf{x}(0) = [-1 \ -5]^T$ resulting in $\mathbf{e}(0) = [-2.13 \ -5]$. As above, at time $t = 0.11$s a disturbance torque of 0.5 Nm is acting on the motor for 7.5 ms. Both the error e_1 in the motor current and the error e_2 in the motor speed tend to zero asymptotically. Moreover, it can be clearly seen that switching the feedforward control together with the plant leads to jumps in the trajectory of the desired current I_d causing jumps in the error state e_1. In Figure 8.4 the time curves of the Lyapunov functions $V_1 = \mathbf{e}^T\mathbf{Q}_1\mathbf{e}$ and $V_2 = \mathbf{e}^T\mathbf{Q}_2\mathbf{e}$ are depicted. The jumps in the error e_1 lead to instantaneous changes of the value of both Lyapunov functions. As intended it holds, for any switching time, that $V_{\sigma(t_i)}(\mathbf{e}(t_i)) = V_{\sigma(t_i^-)}(\mathbf{e}(t_i^-))$.

8.2 Self Supplied Variable Displacement Axial Piston Pump

In this section, we study the tracking controller design for a self supplied variable displacement axial piston pump as considered in [57], [94]. This type of pumps allows to adjust the volume flow at constant input speed by varying the displacement of the pump. This is done by tilting a swash plate by means of a hydraulic actuator. The volume flow into this actuator q_a thus represents the control input. A schematic diagram of the hydraulic circuit

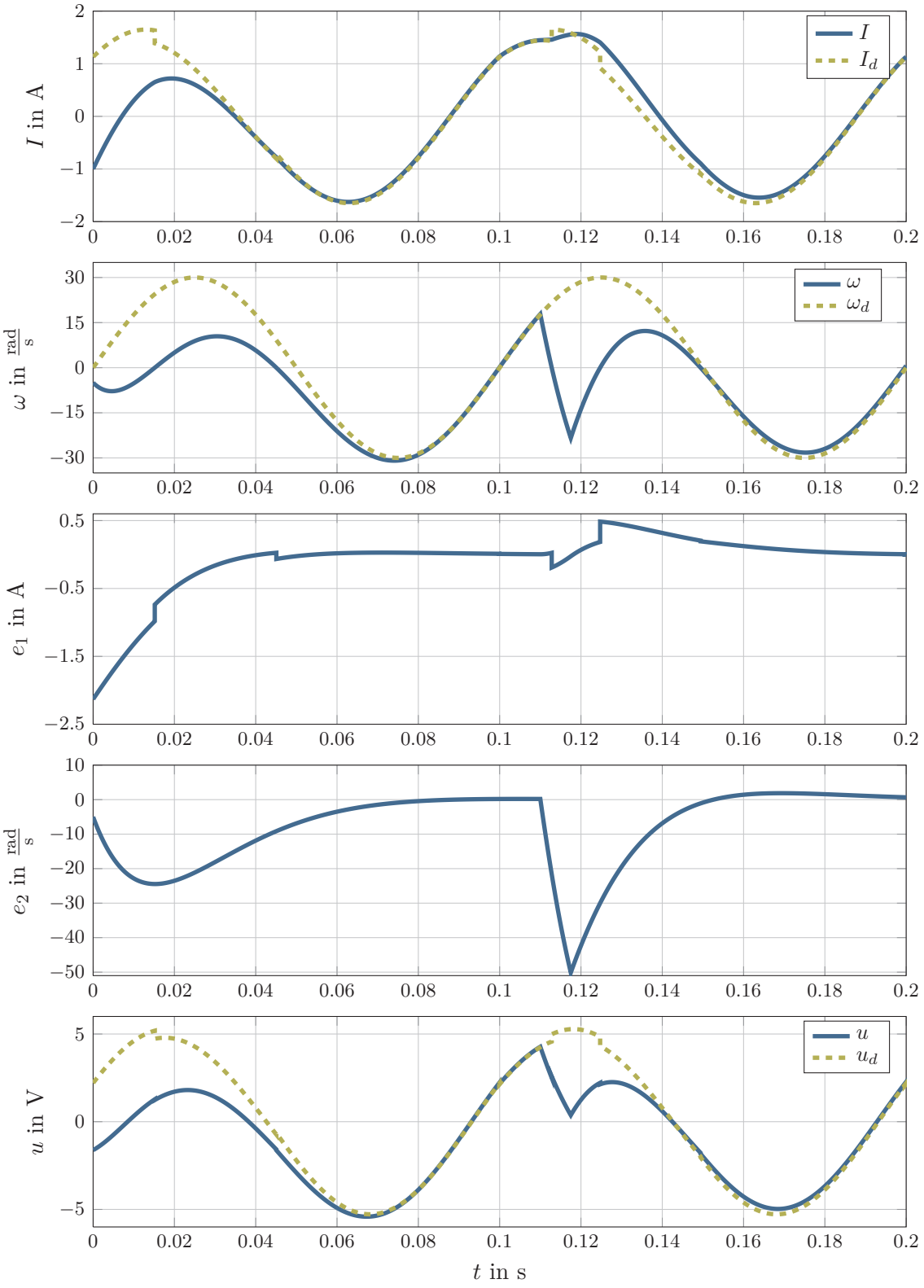

Figure 8.3: Simulation results for the DC motor with LMI-based error controller, initial value $\mathbf{x}(0) = [-1,\ -5]^T$, and a disturbance torque acting on the motor at $t = 0.11\,\mathrm{s}$.

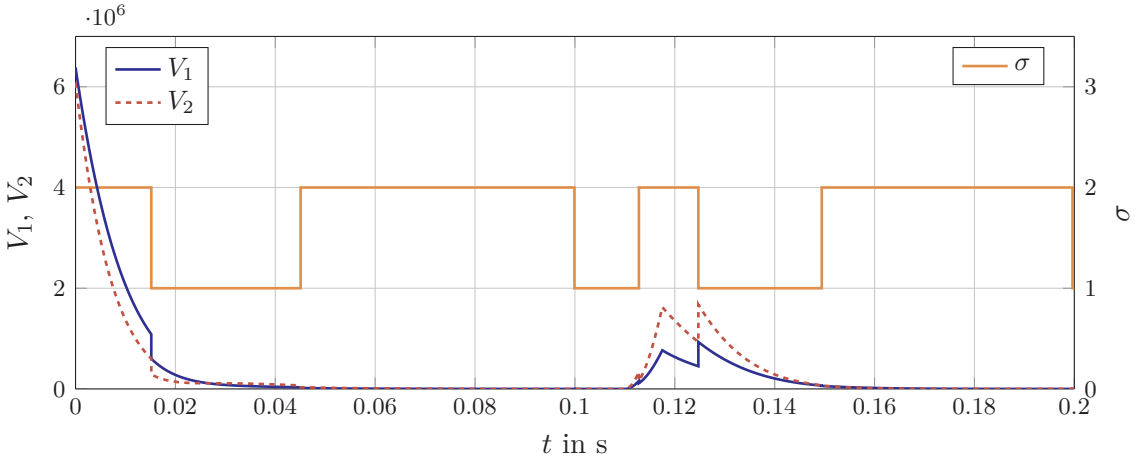

Figure 8.4: Lyapunov functions V_1 and V_2 together with the switching signal σ for the LMI-based error controller with $\mathbf{x}(0) = [-1,\ -5]^T$ and a disturbance torque acting on the motor at $t = 0.11\,\mathrm{s}$.

is depicted in Figure 8.5. The pump under consideration is self-supplied, which means that the volume flow that is necessary to adjust the swash plate angle is taken from the output volume flow q_p of the pump. The hydraulic actuator is single acting, and the restoring force is provided by a spring. Positive volume flows q_a, which cause a decrease of the swash plate angle, are taken from the output of the pump, while negative volume flows, which occur when the swash plate angle is increased by the spring force, are carried to the tank. This yields a switching mathematical model because in the former case the volume flow through the load q_l is given by $q_l = q_p - q_a$, while in the latter case we have $q_l = q_p$. For a more detailed description of the system, the interested reader is referred to [57], [94].

The simplified model of the pump used in the following has been derived in [57] from a more detailed higher dimensional one based on a singular perturbation analysis. We define the state vector $\mathbf{x} = [\psi_p\ p_l]^T$, where ψ_p is the swash plate angle and p_l is the load pressure. Then the model is given by

$$\dot{\mathbf{x}} = \mathbf{f}(\mathbf{x}) + \mathbf{g}_\sigma u\ , \quad \mathbf{f}(\mathbf{x}) = \begin{bmatrix} 0 \\ \frac{\beta}{V_l}\left(k_p x_1 - k_l\sqrt{x_2}\right) \end{bmatrix}\ , \quad \mathbf{g}_1 = \begin{bmatrix} -\frac{1}{A_a r_a} \\ 0 \end{bmatrix}\ , \quad \mathbf{g}_2 = \begin{bmatrix} -\frac{1}{A_a r_a} \\ -\frac{\beta}{V_l} \end{bmatrix} \tag{8.36}$$

where A_a is the effective area of the hydraulic actuator, r_a is its effective radius, V_l is the load volume, β is the bulk modulus of the oil, k_p the pump coefficient, and k_l denotes the coefficient of the load orifice. The control input is the actuator volume flow $u = q_a$ and the switching law is given by (2.69), (2.70), where $\varphi(u) = -u$, i.e., for $u \leq 0$ the 1st subsystem is active, for $u \geq 0$ the 2nd one. The values of the model parameters have been taken from [94] and are given in Table 8.2.

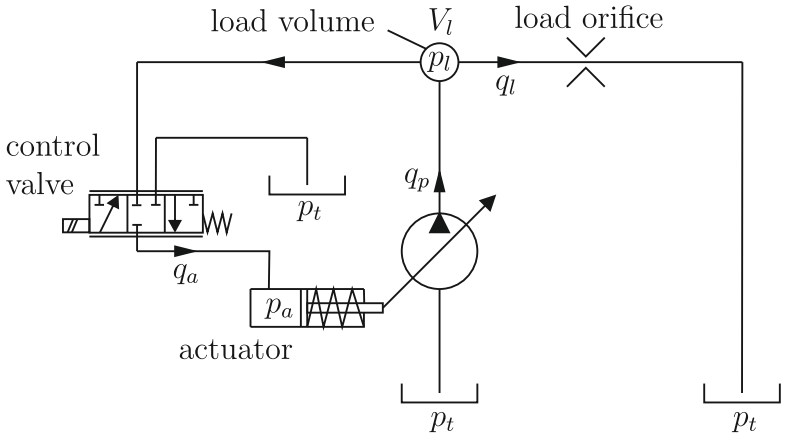

Figure 8.5: Schematic diagram of the axial piston pump [94].

Table 8.2: Parameters of the pump.

Model parameter	Symbol	Value	Unit
Bulk modulus	β	1.6×10^9	Pa
Effective area of the actuator	A_a	300	mm^2
Effective radius of the actuator	r_a	50	mm
Load coefficient	k_l	50×10^{-9}	$\text{m}^3/\text{s}\sqrt{\text{Pa}}$
Load volume	V_l	1.5	l
Pump coefficient	k_p	2.23×10^{-3}	m^3/s

8.2.1 Feedforward Design

We intend to design a controller which makes the load pressure

$$y = h(\mathbf{x}) = x_2 = p_l \tag{8.37}$$

asymptotically track a desired trajectory $y_d(t)$. Note that, in view of the model equations (8.36), $y_d(t)$ obviously has to satisfy $y_d(t) \geq 0$. Again, we first analyze the system with regard to the solvability of the EOT problem, which is necessary for the solvability of the AOT problem. Since $L_{g_1}h(\mathbf{x}) = 0$, $L_{g_1}L_{f_1}h(\mathbf{x}) = -\frac{\beta k_p}{A_a r_a V_l}$ the 1st subsystem has a well defined relative degree $r_1 = 2 = n$, and from $L_{g_2}h(\mathbf{x}) = -\frac{\beta}{V_l}$ we conclude that $r_2 = 1$. Consequently, it holds that $r_1 > r_2$.

The $\mathbf{z}_1$ coordinate system is given by

$$\mathbf{z}_1 = \begin{bmatrix} \xi_{1,1} \\ \xi_{1,2} \end{bmatrix} = \mathbf{\Phi}_1(\mathbf{x}) = \mathbf{h}_1^2(\mathbf{x}) = \begin{bmatrix} x_2 \\ \frac{\beta}{V_l}\left(k_p x_1 - k_l\sqrt{x_2}\right) \end{bmatrix}. \tag{8.38}$$

The change of coordinates $\mathbf{z}_1 = \mathbf{\Phi}_1(\mathbf{x})$ puts the 1st subsystem into the form

$$\dot{\xi}_{1,1} = \xi_{1,2} \tag{8.39}$$

$$\dot{\xi}_{1,2} = -\frac{\beta k_l}{2V_l}\frac{\xi_{1,2}}{\sqrt{\xi_{1,1}}} - \frac{\beta k_p}{V_l A_a r_a}u\,. \tag{8.40}$$

In the same coordinates, the 2nd subsystem is given by

$$\dot{\xi}_{1,1} = \xi_{1,2} - \frac{\beta}{V_l}u \tag{8.41}$$

$$\dot{\xi}_{1,2} = -\frac{\beta k_l}{2V_l}\frac{\xi_{1,2}}{\sqrt{\xi_{1,1}}} - \frac{\beta k_p}{V_l A_a r_a}u + \frac{\beta^2 k_l}{2V_l^2\sqrt{\xi_{1,1}}}u\,. \tag{8.42}$$

Thus, it takes the form (7.84) and we identify

$$\tilde{\alpha}_1(\mathbf{z}_1) = -\frac{\beta k_l}{2V_l}\frac{\xi_{1,2}}{\sqrt{\xi_{1,1}}}\,, \quad \tilde{\beta}_1 = -\frac{\beta k_p}{V_l A_a r_a}\,, \quad b_n(\mathbf{z}_1) = -\frac{\beta k_l}{2V_l\sqrt{\xi_{1,1}}}\,, \quad \tilde{\varrho}_x = 0\,, \quad \tilde{\varrho}_u = -\frac{\beta}{V_l}\,.$$

Moreover, (7.80) is satisfied.

In Theorem 7.2.5, the requirement that the differential equation (7.91) is input-to-state stable has been imposed to guarantee that the internal state of the 2nd subsystem remains bounded for all reference trajectories. For the considered system this is verified more easily in $\mathbf{x}$ coordinates (see below) and has already been noted in [94]. Since all physical parameters are positive it holds further that $\frac{\tilde{\beta}_1(\mathbf{z}_1)}{\tilde{\varrho}_u(\mathbf{z}_1)} > 0$ and hence the EOT problem is solvable according to Theorem 7.2.5.

As long as $u_d(t) \leq 0$ (i.e., $\varphi(u_d) \geq 0$ and hence $\sigma_d = 1$), the trajectory $\mathbf{x}_d(t)$ corresponding to a desired trajectory $y_d(t)$ is

$$\begin{bmatrix} x_{d,1}(t) \\ x_{d,2}(t) \end{bmatrix} = \begin{bmatrix} \psi_{p,d}(t) \\ p_{l,d}(t) \end{bmatrix} = \begin{bmatrix} \frac{V_l}{\beta k_p}\dot{y}_d(t) + \frac{k_l}{k_p}\sqrt{y_d(t)} \\ y_d(t) \end{bmatrix} \tag{8.43}$$

and the feedforward control is given by

$$u_d(t) = -\frac{A_a r_a}{k_p}\left(\frac{V_l}{\beta}\ddot{y}_d(t) + \frac{k_l}{2}\frac{\dot{y}_d(t)}{\sqrt{y_d(t)}}\right)\,. \tag{8.44}$$

In intervals $[t_i, t_{i+1})$ with $u_d(t) \geq 0$ (i.e., $\varphi(u_d) \leq 0$ and thus $\sigma_d = 2$), we have

$$x_{d,2}(t) = p_{l,d}(t) = y_d(t) \tag{8.45}$$

and $x_{d,1}(t) = \psi_{p,d}(t)$ is the solution of the initial value problem

$$\dot{x}_{d,1} = -\frac{k_p}{A_a r_a} x_{d,1} + \frac{1}{A_a r_a}\left(k_l\sqrt{y_d(t)} + \frac{V_l}{\beta}\dot{y}_d(t)\right), \quad x_{d,1}(t_i) = \frac{V_l}{\beta k_p}\dot{y}_d(t_i) + \frac{k_l}{k_p}\sqrt{y_d(t_i)}\,. \tag{8.46}$$

The corresponding feedforward control is given by

$$u_d(t) = -\frac{V_l}{\beta}\dot{y}_d(t) + k_p x_{d,1}(t) - k_l\sqrt{y_d(t)}\,. \tag{8.47}$$

Now, note that the 2nd subsystem is in input-output normal form already in $\mathbf{x}$ coordinates. The internal dynamics are described by the differential equation (8.46), and it is clear that $x_{d,1}$ remains bounded for all bounded $\mathbf{Y}_d^2(t)$.

8.2.2 IDA Controller Design

In this subsection, we use the controller design methodology presented in Chapter 6 to determine an error controller that asymptotically stabilizes the tracking error. We observe that in $\mathbf{x}$ coordinates the 2nd subsystem can be rewritten as

$$\dot{\mathbf{x}} = \mathbf{f}(\mathbf{x}) + \underbrace{\left[\mathbf{g}_1 + [0,\ 1]^T \varrho_u\right]}_{\mathbf{g}_2} u \tag{8.48}$$

and hence the model of the pump (8.36) belongs to the special class of systems considered in Subsection 7.3.3. Therefore, we can again invoke Theorem 7.3.1 to conclude that it suffices to consider only the 1st and the 2nd subsystem of the error system (7.109) given by

$$\begin{bmatrix}\dot{e}_1\\ \dot{e}_2\end{bmatrix} = \underbrace{\begin{bmatrix}0\\ \frac{\beta}{V_l}\left(k_p e_1 - k_l\sqrt{e_2 + x_{d,2}(t)} + k_l\sqrt{x_{d,2}(t)}\right)\end{bmatrix}}_{\mathbf{f}_1^e(\mathbf{e},t)} + \underbrace{\begin{bmatrix}-\frac{1}{A_a r_1}\\ 0\end{bmatrix}}_{\mathbf{g}_1^e} v \tag{8.49}$$

and

$$\begin{bmatrix}\dot{e}_1\\ \dot{e}_2\end{bmatrix} = \underbrace{\begin{bmatrix}0\\ \frac{\beta}{V_l}\left(k_p e_1 - k_l\sqrt{e_2 + x_{d,2}(t)} + k_l\sqrt{x_{d,2}(t)}\right)\end{bmatrix}}_{\mathbf{f}_2^e(\mathbf{e},t)} + \underbrace{\begin{bmatrix}-\frac{1}{A_a r_1}\\ -\frac{\beta}{V_l}\end{bmatrix}}_{\mathbf{g}_2^e} v \tag{8.50}$$

for the controller design, provided that we are able to find a common feedback law together with a corresponding common Lyapunov function.

It is our intention to apply the systematic procedure described in Section 6.4 for the controller design. Since the switched system made up of (8.49) and (8.50) does not have the desired form (6.23), we introduce with

$$e_3 = v \ , \quad \dot{e}_3 = \bar{v} \tag{8.51}$$

the new state variable e_3 and the new input $\bar{v}$. In order that the first component of $\mathbf{e}$ is the actuated one as in (6.23), we *renumber the error states* such that $e_1 = v$, $e_2 = \psi_p - \psi_{p,d}$, and $e_3 = p_l - p_{l,d}$. By this means, we obtain a switched system with the 1st subsystem given by

$$\begin{bmatrix} \dot{e}_1 \\ \dot{e}_2 \\ \dot{e}_3 \end{bmatrix} = \begin{bmatrix} 0 \\ -\frac{1}{A_a r_1} e_1 \\ \frac{\beta}{V_l}\left(k_p e_2 - k_l\sqrt{e_3 + p_{l,d}(t)} + k_l\sqrt{p_{l,d}(t)}\right) \end{bmatrix} + \begin{bmatrix} 1 \\ 0 \\ 0 \end{bmatrix} \bar{v} \tag{8.52}$$

and the 2nd subsystem by

$$\begin{bmatrix} \dot{e}_1 \\ \dot{e}_2 \\ \dot{e}_3 \end{bmatrix} = \begin{bmatrix} 0 \\ -\frac{1}{A_a r_1} e_1 \\ \frac{\beta}{V_l}\left(k_p e_2 - k_l\sqrt{e_3 + p_{l,d}(t)} + k_l\sqrt{p_{l,d}(t)} - e_1\right) \end{bmatrix} + \begin{bmatrix} 1 \\ 0 \\ 0 \end{bmatrix} \bar{v} \ . \tag{8.53}$$

Obviously, this system has the desired form (6.23), and it is not difficult to see that it satisfies Assumption 6.4.1 with

$$\mathbf{C} = \begin{bmatrix} 1 & 0 \\ \kappa & 1 \end{bmatrix} \ , \quad \text{where } \kappa = \frac{r_a A_a \beta}{V_l} \ . \tag{8.54}$$

The eigenvalues of this matrix are $\lambda_1 = \lambda_2 = 1$. Thus, it follows from Theorem 6.4.3 that there are design matrices $\mathbf{F}_1$, $\mathbf{F}_2$ with $\mathbf{F}_1^\nu = \mathbf{C}\mathbf{F}_2^\nu$ such that both dissipation matrices are positive definite.

Construction of the design matrices

In order to construct a set of suitable design matrices, as in the example in Section 6.9.1, we follow the procedure described in Section 6.4.4. We determine the set of solutions of

$$\mathbf{C}\mathbf{X} + \mathbf{X}^T\mathbf{C}^T = \mathbf{Q} \tag{8.55}$$

for all $\mathbf{Q} \geq 0$ according to (6.46), where $\mathbf{C}$ is given by (8.54). Setting $\mathbf{F}_1^\nu = [\mathbf{F}_1^C,\ -\mathbf{X}]$ with $\mathbf{F}_1^C = [\nu_{1,11},\ \nu_{1,21}]^T$ we obtain

$$\mathbf{F}_1^\nu = \begin{bmatrix} \nu_{1,11} & -\frac{1}{2}k_{11}^2 & \frac{1}{4}k_{11}^2\kappa - \frac{1}{2}k_{12}k_{11} + \rho \\ \nu_{1,21} & \frac{1}{4}k_{11}^2\kappa - \frac{1}{2}k_{12}k_{11} + \rho & -\frac{1}{2}\left(\frac{1}{2}k_{11}^2\kappa^2 + k_{22}^2 + k_{12}^2 - k_{12}k_{11}\kappa\right) - \kappa\rho \end{bmatrix} \tag{8.56}$$

and

$$\mathbf{F}_2^\nu = \mathbf{C}\mathbf{F}_1^\nu = \begin{bmatrix} \nu_{1,11} & -\frac{1}{2}k_{11}^2 & \frac{1}{4}k_{11}^2\kappa - \frac{1}{2}k_{12}k_{11} + \rho \\ \kappa\nu_{1,11} + \nu_{1,21} & -\frac{1}{4}k_{11}^2\kappa - \frac{1}{2}k_{12}k_{11} - \rho & -\frac{1}{2}k_{22}^2 - \frac{1}{2}k_{12}^2 \end{bmatrix} . \tag{8.57}$$

Invoking Sylvester's criterion, we deduce the conditions

$$k_{11} \neq 0\ , \qquad \frac{1}{4}k_{11}^4\kappa^2 + k_{11}^2k_{22}^2 + 2k_{11}^2\kappa\rho > 0 \tag{8.58}$$

for $\mathrm{sym}\{\mathbf{X}\} > 0$.

Solvability of the projected matching equation

We consider the projected matching equation (6.26) for $p = 1$. Since we have chosen the design matrices independent of $\mathbf{x}$, we can utilize the condition (2.39) to assess its solvability. We obtain

$$-\frac{\nu_{1,21}}{A_a r_a} + \frac{\beta k_p k_{11}^2}{2V_l} + \frac{\beta k_l\left(\frac{1}{4}k_{11}^2\kappa - \frac{1}{2}k_{12}k_{11} + \rho\right)}{2V_l\sqrt{e_3 + p_{l,d}(t)}} = 0 \tag{8.59}$$

which can be satisfied by setting

$$\rho = \frac{1}{2}k_{12}k_{11} - \frac{1}{4}k_{11}^2\kappa\ , \quad \nu_{1,21} = \frac{A_a r_a \beta k_p k_{11}^2}{2V_l}\ . \tag{8.60}$$

Positive Definiteness of the dissipation matrices

To achieve positive definiteness of $\mathbf{R}_1 = -\mathrm{sym}\{\mathbf{F}_1\}$, we choose $\mathbf{F}_1^B = -(\mathbf{F}_1^C)^T$, i.e.,

$$\alpha_{1,12} = -\nu_{1,11}\ , \quad \alpha_{1,13} = -\nu_{1,21} = -\frac{A_a r_a \beta k_p k_{11}^2}{2Vl}\ . \tag{8.61}$$

Then, $\mathbf{R}_1$ is of the form (6.33) and thus positive definite, if $\mathbf{F}_1^A = \alpha_{11,1} < 0$ and $\mathrm{sym}\{\mathbf{X}\} > 0$. The latter holds true, if $c_{11} \neq 0$ and

$$k_{11}^2k_{22}^2 - \frac{1}{4}k_{11}^4\kappa^2 + k_{11}^3k_{12}\kappa > 0 \tag{8.62}$$

which is obtained by substituting the expression assigned to ρ in (8.60) into (8.58). Positive definiteness of $\mathbf{R}_2$ will be ensured after the feedback function $\mathbf{r}_1(\mathbf{e},t)$ has been designed.

Solving the projected matching equation

A solution of the the projected matching equation can be obtained as outlined in Section 2.2.4. The matrix $\mathbf{T}^{-1}$ in (2.37) is $\mathbf{T}^{-1} = [\mathbf{t}_1\ (\mathbf{F}_1^\nu)^T]$ with $\mathbf{t}_1 = [1\ 0\ 0]^T$. In these coordinates, a particular solution is given by

$$\begin{aligned}\Psi^\zeta(\boldsymbol{\zeta},t) = -\frac{1}{A_a r_a}\zeta_1\zeta_2 - \frac{\nu_{1,11}}{2A_a r_a}\zeta_2^2 - \frac{\beta k_p k_{11}^2}{2V_l}\zeta_2\zeta_3 + \frac{\beta k_p k_{11}}{2V_l}\left(\frac{k_{11}\kappa}{2} - k_{12}\right)\zeta_3^2 \\ + \frac{\beta k_l\left[4p_{l,d}(t) - 2(k_{22}^2+k_{12}^2)\zeta_3\right]^{3/2}}{6V_l(k_{22}^2+k_{12}^2)} + \frac{\beta k_l\sqrt{p_{l,d}(t)}}{V_l}\zeta_3\ .\end{aligned} \tag{8.63}$$

Moreover, ζ_1 is a characteristic coordinate. The homogeneous solution is chosen as $\phi^\zeta(\zeta_1) = \mu_2\zeta_1^2$, whereby, as desired, $\nabla H(\mathbf{e},t)|_{\mathbf{e}=\mathbf{0}} = \mathbf{0}$ is achieved for

$$H(\mathbf{e},t) = \left[\Psi^\zeta(\boldsymbol{\zeta},t) + \Phi^\zeta(\zeta_1)\right]_{\boldsymbol{\zeta}=\mathbf{T}\mathbf{e}}\ . \tag{8.64}$$

Controller tuning

In order to obtain suitable values for the design parameters, as suggested in Section 6.8, we apply LLDA to the 1st subsystem. Since the closed loop error system is time-varying, we proceed as described in Section 2.3.2. Assuming that the operating region of the pump is between $p_{l,d,min} = 40\,\text{bar}$ and $p_{l,d,max} = 100\,\text{bar}$, we evaluate the unactuated part of the linearization of the first subsystem (8.52)

$$\mathbf{A}_1^\nu = \begin{bmatrix} -\frac{1}{A_a r_a} & 0 & 0 \\ 0 & \frac{\beta k_p}{V_l} & -\frac{\beta k_l}{2V_l\sqrt{p_{l,d}}} \end{bmatrix} \tag{8.65}$$

at an average pressure of $\bar{p}_{l,d} = 70\,\text{bar}$ to obtain $\bar{\mathbf{A}}_1^\nu$. The submatrix $\bar{\mathbf{A}}_1^\alpha$ is chosen such that $\bar{\mathbf{A}}_{1,d}$ has three eigenvalues in -100. As we have suggested at the end of Section 2.3.2, we solve the equations (2.57)-(2.59) only for $p_{l,d}(t) = \bar{p}_{l,d}$ in order to obtain constant design matrices. This yields expressions of the form $\alpha_{1,11} = \alpha_{1,11}(k_{11},k_{12},k_{22})$, $\nu_{1,11} = \nu_{1,11}(k_{11},k_{12},k_{22})$, $\mu_2 = \mu_2(k_{11},k_{12},k_{22})$. The remaining free parameters k_{11},k_{12},k_{22} are chosen such that $\alpha_{11} > 0$ and (8.62) hold. Suitable values are $k_{11} = 2$, $k_{12} = -2$ and $k_{22} = \frac{3}{2}$.

The entries of $\mathbf{F}_2^\alpha$ remain as free parameters. They have to be chosen such that a common controller is obtained, i.e., $r_1(\mathbf{e},t) = r_2(\mathbf{e},t)$, where the feedback functions r_p, $p \in \{1,2\}$ are given by (6.11). Since the actuated components of both subsystems (8.52),

(8.53) are identical, this is fulfilled, if we choose $\mathbf{F}_2^\alpha = \mathbf{F}_1^\alpha$. It is easily checked that this choice also leads to a positive definite dissipation matrix $\mathbf{R}_2$. The eigenvalues of the closed loop linearization of the 2nd subsystem are located in $-129.3 \pm 86.4i$ and -41.3.

Now we need to verify that the conditions of Theorem 7.3.1 are satisfied. To this end, we derive time invariant bounds $W_i(\mathbf{e})$, $i = 1, 2, 3$ satisfying (6.86), (6.87) and show that they are positive definite. The bounds $W_1(\mathbf{e})$ and $W_2(\mathbf{e})$ for the Hamiltonian $H(\mathbf{e}, t)$ are obtained as follows. The function $H(\mathbf{e}, t)$ can be written as

$$H(\mathbf{e},t) = \mathbf{e}^T\mathbf{Q}\mathbf{e} \underbrace{-17.07\sqrt{p_{l,d}(t)}e_3 + 11.38\Big(-p_{l,d}^{\frac{3}{2}}(t) + \sqrt{e_3 + p_{l,d}(t)}p_{l,d}(t) + \sqrt{e_3 + p_{l,d}(t)}e_3\Big)}_{\vartheta(e_3, p_{l,d}(t))} \tag{8.66}$$

with a constant matrix $\mathbf{Q} > 0$. Note that the energy function is only well-defined, if the argument of the square root is nonnegative. Since we have assumed that the operating range of the pump is $p_{l,d} \in [40\,\text{bar}, 100\,\text{bar}]$ this means that the error in the pressure must not be smaller than $-40\,\text{bar}$. From (8.66), we observe that only the part of the energy function which is denoted by $\vartheta(e_3, t)$ is time dependent. This function satisfies for all $p_{l,d} > 0$ that

$$\vartheta(0, p_{l,d}) = 0\,, \quad \frac{\partial}{\partial e_3}\vartheta(e_3, p_{l,d})\bigg|_{e_3=0} = 0 \tag{8.67}$$

and

$$\frac{\partial^2}{\partial e_3^2}\vartheta(e_3, p_{l,d}) > 0\,, \quad \forall\, e_3 > -40\,\text{bar}\,. \tag{8.68}$$

Hence, $\vartheta(e_3, p_{l,d})$ is strictly convex in e_3 for all $p_{l,d}$ and attains its minimum in $e_3 = 0$. Consequently, the energy function is strictly convex in $\mathbf{e}$ for all $p_{l,d}$. Moreover, it holds that

$$\frac{\partial}{\partial p_{l,d}}\vartheta(e_3, p_{l,d})|_{e_3=0} = 0\,, \quad \forall\, p_{l,d} \tag{8.69}$$

and

$$\frac{\partial^2}{\partial p_{l,d}\partial e_3}\vartheta(e_3, p_{l,d}) = -\frac{8.53\left(\sqrt{e_3 + p_{l,d}} - \sqrt{p_{l,d}}\right)}{\sqrt{p_{l,d}}\sqrt{e_3 + p_{l,d}}}\,. \tag{8.70}$$

The latter is, for all admissible $p_{l,d}$, equal to zero if $e_3 = 0$, positive if $e_3 < 0$ and negative if $e_3 > 0$. Hence, we conclude that $\frac{\partial}{\partial p_{l,d}}\vartheta(e_3, p_{l,d}) \leq 0$ for all admissible $p_{l,d}$ and e_3. As a consequence, a time-invariant lower bound for $H(\mathbf{e}, t)$ is $W_1(\mathbf{e}) = H(\mathbf{e}, 100\,\text{bar})$, and a time-invariant upper bound is given by $W_2(\mathbf{e}) = H(\mathbf{e}, 40\,\text{bar})$. According to the above considerations, both functions attain their minimum at $\mathbf{e} = \mathbf{0}$ and are strictly convex over $\mathbb{R}^2 \times [40, \infty)$. Thus, they are positive definite.

In order to determine a function $W_3(\mathbf{e})$ satisfying (6.87), we consider the term

$$\begin{aligned}\frac{\partial}{\partial t}H(\mathbf{e},p_{l,d}(t)) &= \frac{\partial}{\partial p_{l,d}}H(\mathbf{e},p_{l,d})\dot{p}_{l,d}\\ &= -\frac{8.53}{\sqrt{p_{l,d}}\sqrt{e_3+p_{l,d}}}\left[e_3\sqrt{e_3+p_{l,d}}-2e_3\sqrt{p_{l,d}}-2p_{l,d}^{\frac{3}{2}}+2p_{l,d}\sqrt{e_3+p_{l,d}}\right]\dot{p}_{l,d}\ .\end{aligned} \tag{8.71}$$

It holds, for all $p_{l,d}$, that $\frac{\partial}{\partial p_{l,d}}H(\mathbf{e},p_{l,d})|_{e_3=0}=0$ and

$$\frac{\partial^2}{\partial p_{l,d}\partial e_3}H(\mathbf{e},p_{l,d}) = -\frac{8.53\left(\sqrt{e_3+p_{l,d}}-\sqrt{p_{l,d}}\right)}{\sqrt{p_{l,d}}\sqrt{e_3+p_{l,d}}} \tag{8.72}$$

which is zero for $e_3=0$, negative for $e_3>0$ and positive for $e_3<0$. Hence, we conclude that $\frac{\partial}{\partial p_{l,d}}H(\mathbf{e},p_{l,d})<0$ for all $e_3\neq 0$. Now we assume that in the operating region of the system it holds that $|\dot{p}_{l,d}|\leq \dot{p}_{l,d,max}=1000\frac{\text{bar}}{\text{s}}$. Then the function $W_3(\mathbf{e})=\min\{W_{3,1},W_{3,2}\}$ satisfies (6.87) for all $p_{l,d}(t)\in[40,100]$ and $|\dot{p}_{l,d}(t)|\leq 1000$, where

$$W_{3,p}=\min_{p_{l,d}\in[40,100]}\left(\frac{\partial H(\mathbf{e},p_{l,d})}{\partial \mathbf{e}}\right)^T\mathbf{R}_p\frac{\partial H(\mathbf{e},p_{l,d})}{\partial \mathbf{e}}+\frac{\partial}{\partial p_{l,d}}H(\mathbf{e},p_{l,d})\dot{p}_{l,d,max}\ ,\ p\in\{1,2\}\ . \tag{8.73}$$

Based on these results, we determine in the following the DA of the equilibrium $\mathbf{e}^*=\mathbf{0}$ of the closed loop error system. To this end, we have to determine the largest bounded sublevel set of $W_1(\mathbf{e})$ within which $W_3(\mathbf{e})$ is positive definite *and* $e_3\geq -p_{l,d,min}=-40\,\text{bar}$. The latter requirement ensures that $p_l=e_3(t)+p_{d,min}\geq$ holds along all trajectories starting within the estimated DA, and thus that the argument of the square root in (8.36) is nonnegative. In principle, we could use the algorithm presented in Section 3.3.2 to obtain a suitable level value. However, the largest bounded sublevel set of $W_1(\mathbf{e})$ within which $e_3\geq -p_{l,d,min}$ holds, say $\mathrm{S}_{\tilde{d}}^{W_1}(\mathbf{0})$, can be calculated analytically. Therefore, we proceed similar to the example in Section 5.3. That means, we determine, in a first step, a discrete representation of $\partial\mathrm{S}_{\tilde{d}}^{W_1}(\mathbf{0})$, and, in a second step, the largest sublevel set $\mathrm{S}_{\hat{c}}^{W_1}(\mathbf{0})$ within $\mathrm{S}_{\tilde{d}}^{W_1}(\mathbf{0})$ that satisfies $W_3(\mathbf{e})>0$, $\forall\,\mathbf{e}\in\mathrm{S}_{\hat{c}}^{W_1}(\mathbf{0})\setminus\{\mathbf{0}\}$.

Since $W_1(\mathbf{e})$ is a strictly convex function, we can determine the level value $\tilde{d}$ by solving the minimization problem $\min_{\mathbf{e}}W_1(\mathbf{e})$ under the constraint $e_3=-p_{l,d,min}$. To do so, we substitute $e_3=-p_{l,d,min}$ into $W_1(\mathbf{e})$ and solve the linear system of equations $\frac{\partial}{\partial e_i}W_1(e_1,e_2,-p_{l,d,min})=0$, $i=1,2$. This yields the point $\tilde{\mathbf{e}}_{\tilde{d}}=[0,\ 1.15p_{l,d,min},\ -p_{l,d,min}]^T$. With $p_{l,d,min}=40\,\text{bar}$, the corresponding level value is $\tilde{d}=93.32$.

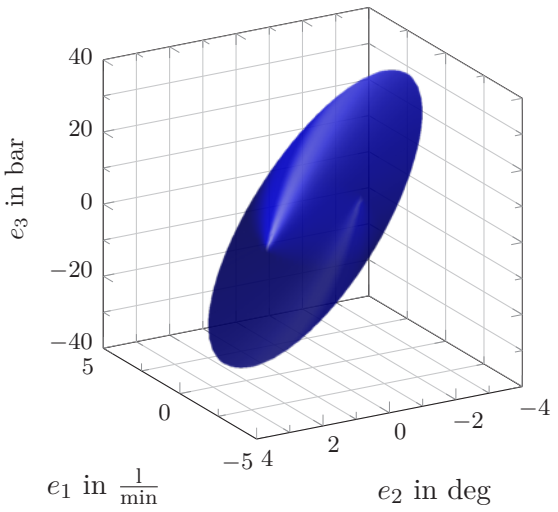

Figure 8.6: Estimated stability boundary for the closed loop axial piston pump.

In order to determine the level value $\hat{c}$, we proceed similar to Algorithm 3.2 in Section 3.3.2, only that we do not consider $g_v(\lambda)$ and that we restrict the search to $\mathrm{S}_{\tilde{d}}^{W_1}(\mathbf{0})$ instead to the ball B_R. Like the minimum over all times t in Section 3.3.2, the minimum (8.73) over all $p_{l,d}$ in the operating region is determined by discretizing the interval $[p_{l,d,min}, p_{l,d,max}]$ into a sequence of points $p_{l,d,1}, \ldots, p_{l,d,N}$ with $N = 30$. It turns out that $\hat{c} = \tilde{d}$, i.e., the estimate of the DA is determined by the requirement that $e_3(t) \geq -p_{l,d,min}$, $\forall\, t$ must hold true for all trajectories starting therein. The estimated stability boundary is depicted in Figure 8.6. It is worth pointing out that the utilized functions $W_i(\mathbf{e})$, $i = 1, 2, 3$ meet the requirements of Theorem 6.7.1 not only for a particular trajectory $p_{l,d}(t)$, but for all desired trajectories of the load pressure in the operating region, i.e., $p_{l,d}(t) \in [p_{,ld,max}, p_{l,d,min}]$ and $|\dot{p}_{l,d}(t)| \leq \dot{p}_{l,d,max}$. As a consequence, the stability result and the estimated DA are valid for all these trajectories (see also Remark 3.3.3). Simulation results are shown in Figure 8.7. The desired trajectory of the load pressure is specified (in bar) by the following piecewise defined polynomial

$$p_{l,d}(t) = \begin{cases} 1.5 \cdot 10^4 t^3 - 4.5 \cdot 10^3 t^2 + 100 & \text{for } 0 \leq t \leq 0.2 \\ 40 & \text{for } 0.2 < t \leq 0.4 \\ -1.5 \cdot 10^4 t^3 + 2.25 \cdot 10^4 t^2 - 1.08 \cdot 10^4 t + 1720 & \text{for } 0.4 < t \leq 0.6 \end{cases} . \tag{8.74}$$

The initial values have been set to $\psi(0) = 4.1°$, $p_l(0) = 90\,\text{bar}$, and $v(0) = 0$ resulting in the initial error state $\mathbf{e}(0) = [0\ 0\ -10\,\text{bar}]$ (recall the dynamic extension (8.51)). At $t = 0.25\,\text{s}$ a disturbance $\mathbf{d} = [0, 3000\,\frac{\text{bar}}{\text{s}}]^T$ is acting on the right hand side of the model

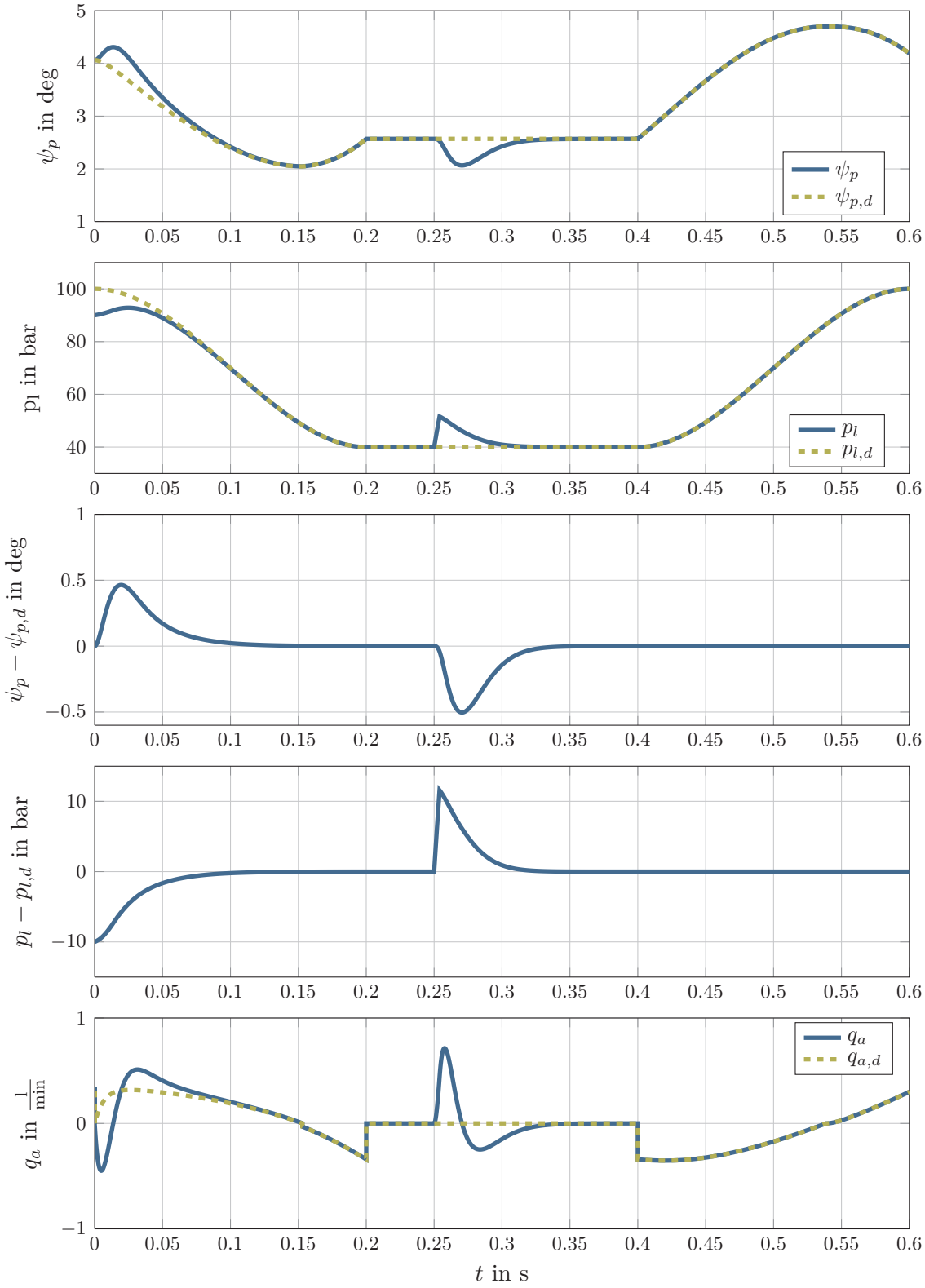

Figure 8.7: Simulation results for the self-supplied variable displacement axial piston pump with an IDA-based error controller, initial values $\psi(0) = 4.1°$, $p_l(0) = 90\,\text{bar}$, and a disturbance acting on the system at $t = 0.25\,\text{s}$.

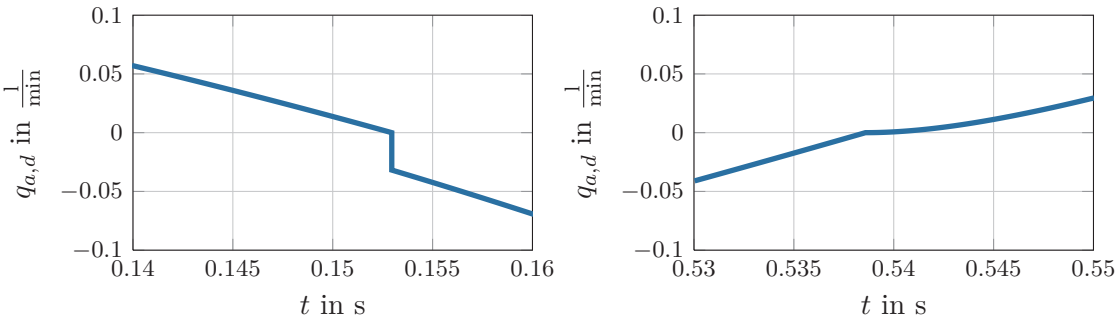

Figure 8.8: Feedforward control $u_d = q_{a,d}$ at the switching times $t_{1,d}$ (left) and $t_{2,d}$ (right).

(8.36) for 4 ms causing a deviation from the reference trajectory. As desired, the tracking error tends to zero and the load pressure asymptotically tracks the desired trajectory.

In Figure 8.8, the feedforward control $u_d(t) = q_{a,d}(t)$ is shown at the switching times $t_{1,d}$ and $t_{2,d}$. It can bee seen that $q_{a,d}$ exhibits a jump when switching from the 2nd to the 1st subsystem occurs at $t_{1,d}$ [see Figure 8.8 (right)], while it is continuous, when the system switches from the 1st to the 2nd subsystem at $t_{2,d}$. Moreover, it can be seen that, after $t_{2,d}$, the control $q_{a,d}$ has slope zero, i.e., $\dot{q}_{a,d}(t_{2,d}) = 0$. Considering that $\tilde{\varrho} = -\frac{\beta}{V_l} q_a$, these observations are consistent with the results in the proof of Theorem 7.2.5. The jumps in the control input at 0.2 s and 0.4 s (see Figure 8.7) are due to the fact that the second derivative of the piecewise defined reference trajectory (8.74) is not continuous at these time instants.

8.3 Concluding Remarks

In this chapter, two technical systems have been used to demonstrate the applicability of the results presented in the Chapters 6 and 7: a DC motor with asymmetric friction characteristic and a self supplied variable displacement axial piston pump. In the motor model *state-dependent switching* occurs due to the different friction behavior for positive and negative values of the angular velocity, while the mathematical model of the axial piston pump exhibits *input-dependent switching* because of the fact that the pump is self supplied.

Using the conditions derived in Section 7.2, we have been able to show that for both systems the EOT problem is solvable. In order to solve the AOT problem, we have used a two-degree-of-freedom structure comprising a feedforward part and an error controller. It has been found that the design of the latter can be considerably simplified by means of the result proven in Subsection 7.3.3. In order to effectively construct a feedback law

that asymptotically stabilizes $\mathbf{e}^* = \mathbf{0}$, we have applied the IDA-based controller design methodology for switched systems proposed in Chapter 6. This approach has enabled us to determine controllers for the switched time-varying error systems in a systematic manner, which is a crucial aspect regarding practical applicability. Moreover, it has been found that the controllers achieve good dynamic performance in terms of speed and shape of the transient response. In the case of the axial piston pump, a further advantage of the method has been exploited, namely that the common energy function, that constructively comes out of the controller design process, can be utilized to estimate the DA. Besides the IDA based control schemes, also the LMI-based design methodology proposed in Section 7.3.4 has been successfully verified using the example of the DC motor.

Chapter 9

Conclusion

The design of high performance control systems generally relies on model-based control methods, and, in most cases, nonlinear models are necessary to achieve the required accuracy. Moreover, in the last two decades, switched systems have proven to provide a powerful framework for the modeling of a wide range of technical systems. Therefore, the development of constructive techniques for the control of both smooth and switched nonlinear systems is an important issue. Furthermore, from a practical point of view, methods that allow the systematic and transparent tuning of the controllers are of great interest.

This thesis is primarily devoted to the development of new methods for the constructive design and the systematic tuning of passivity-based controllers for smooth and switched nonlinear systems. The main problems that have been addressed are: (1) the estimation and enlargement of the DA of IDA controllers; (2) passivity-based stabilization of switched nonlinear systems; and (3) the output trajectory tracking problem for bimodal switched nonlinear SISO systems. In the following, we highlight the main results that have been presented on each of these topics.

The first main contribution is the development of methods for estimating and enlarging the DA of IDA controllers. We have proposed an approach to determine the largest bounded sublevel set of the assigned energy function which qualifies as an estimate of the DA and, additionally, is star-shaped w.r.t. the considered equilibrium point. It is viable for any IDA controlled system and can also be applied in the time-varying case. Based on this result, two numerical algorithms have been presented for the computation of the corresponding level value. The first one is based on a multidimensional grid obtained from discretizing the $(n-1)$-dimensional unit sphere. The second one exploits numerically calculable bounds on real valued functions. The tuning of the IDA controller to attain a maximum estimated DA and good dynamic performance has been posed as an optimization

problem, where the size of the estimated DA is quantified by its volume. To enable the computation of this quantity, an explicit representation of the boundary of the estimated DA is determined by numerical approximation. The desired transient behavior is taken into account utilizing the LLDA approach. In order to guarantee the positive semidefiniteness of the dissipation matrix without adding constraints to the optimization problem, a specific parametrization of the design matrix has been proposed, which is also of interest on its own.

The proposed methods allow us to estimate the DA of an IDA controller based on the assigned energy function and thus to fully exploit the closed loop pH structure, that is a fundamental feature of IDA. Moreover, the presented optimization approach enables the systematic and transparent tuning of IDA controllers so as to achieve both a large DA and high dynamic performance. This has been shown by several examples, where the obtained IDA feedback laws also have outperformed two benchmark controllers in terms of both size of the DA and dynamic performance. Moreover, the procedure is relatively easy to implement, which is desirable in the interest of broad practical applicability. The proposed parametrization of the design matrix allows us to guarantee the positive semidefiniteness of the dissipation matrix without considering complex inequalities, which constitutes a clear practical advantage.

Furthermore, we have presented in Chapter 6 a constructive passivity-based controller design methodology for switched nonlinear systems, which assigns an spH structure to the closed loop system and in this sense represents a natural extension of the conventional IDA method. The key observation which motivated our development has been that spH systems are uniformly (asymptotically) stable. The methodology is constructive in nature and its application is not restricted to switched systems of a special class. In fact, the method has been shown to generate all static feedback laws that render the closed loop system uniformly asymptotically stable. Moreover, it is applicable also for the stabilization of time-varying switched systems. For a special class of bimodal switched systems, we have put forth a systematic procedure that enables the straightforward construction of suitable design matrices and simplifies the ensuing controller design considerably. The tuning of the controller parameters is accomplished with the help of LLDA. An estimate of the DA can be determined by employing the methods presented in Chapter 3. It has been demonstrated by examples that the proposed strategy is a viable tool for the control of technical systems. Simulation results have shown that the resulting control laws achieve good dynamic performance.

The third main contribution of this thesis is to investigate the output trajectory tracking problem for bimodal switched nonlinear SISO systems. We have derived necessary and

sufficient conditions for the solvability of the EOT problem under trajectory-independent switching. It has been found that these conditions can be satisfied only for special pairs of switching signal and reference trajectory. Moreover, we have investigated the EOT problem for systems with state- and/or input-dependent switching law, which constitutes one of the main results of Chapter 7. We have proven necessary conditions under which this problem is solvable for all bounded reference trajectories with bounded derivatives. Under some additional hypothesis, including that the tracking output is a flat output for at least one of the two subsystems, we have also established sufficient conditions. Besides the EOT problem, we have also explored the solution of the AOT problem using a two-degree-of-freedom structure. Since it has been found that in the case of trajectory-dependent switching the stabilization of the tracking error dynamics is, in general, quite involved, we have identified two classes of switched systems for which the design of an error controller can be facilitated considerably.

The conditions for the solvability of the EOT problem are not only theoretically interesting, but also of significant practical importance. The necessary conditions enable to identify situations where, in order to realize exact output tracking, it is inevitable to either restrict the reference trajectories to a special class, or to appropriately modify the model, especially when the switching behavior is due to approximations made to reduce the model complexity. The sufficient conditions can be used to guarantee the reliable operation of a technical system for arbitrary reference trajectories. The practical relevance of the results that we have presented on the AOT problem is quite apparent. As illustrated by two technical examples, they considerably simplify the design of an output tracking controller for two classes of switched systems.

Interesting areas of future research are:

i) In Section 6.4 we have presented a systematic method for the passivity-based stabilization of a class of switched nonlinear systems. It would be very useful to extend this procedure to other classes of switched systems, possibly supported by numerical tools.

ii) When studying the output trajectory tracking problem in Chapter 7, we have restricted our attention to bimodal switched SISO systems. It is interesting to investigate this issue for more general classes of switched systems, which have multiple inputs and outputs and/or more than two subsystems. A closely related problem that occurs if the considered switched system is not able to track arbitrary output trajectories is to identify admissible reference trajectories that satisfy the requirements dictated by the technical problem at hand.

iii) The methods in this thesis enable the constructive design and the systematic tuning of IDA controllers for smooth and switched systems. Hence, they could be used to implement a toolbox that allows the largely automated design and tuning of IDA controllers in interaction with the user. This can be accomplished by combining computer algebra systems with numerical tools.

iv) It would be very interesting to further extend the IDA method in order to handle switched and non-switched systems with impulse effects like, for instance, mechanical systems with unilateral constraints [22]. A concrete example, that recently has received a great deal of attention, is a bipedal walking robot (see e.g. [2]). Methods are to be developed that allow the constructive design and transparent tuning of IDA controllers also for these types of systems. In [74], the IDA method has been adapted for the stabilization of (non-switched) pH systems with impulses. However, the given conditions are very complicated, and the authors do not address the question of how to obtain a solution.

v) Another passivity-based controller design method that uses the pH framework is *Control by Interconnection* (see e.g. [138] for an excellent survey), which, in some cases, leads to dynamic *output feedback controllers*. The basic idea is to interconnect the plant, which has to be given in pH form, with another pH system, that represents the controller. In order to shape the overall energy of the closed loop system, a relation between the states of the controller and the plant is established using so-called *Casimir functions*. It would be interesting to generalize the Control by Interconnection method to the class of spH systems. This implies the computation of Casimir functions which are common to all subsystems of the closed loop spH system.

vi) In many applications it is not possible to measure the whole state vector making the application of an observer inevitable for the implementation of state feedback laws. Thus, from a practical point of view, the design of observers for switched nonlinear systems is a highly relevant problem. In [13], [147], [173], the design of observer-based controllers is addressed for linear switched systems, but we are not aware of any publication that is dealing with this problem in a nonlinear context. For non-switched nonlinear systems, an observer design framework, that is inspired by the Immersion and Invariance approach [5], has been proposed in [92] and applied in combination with an IDA controller in [175]. It would be interesting to investigate the use of this observer design technique also for switched nonlinear systems.

Appendix A

Mathematical Background

A.1 Multi-Index Notation

A *multi-index* $\alpha = (\alpha_1, \ldots, \alpha_n)$ is an n-tuple of nonnegative integers. Given $\mathbf{x} \in \mathbb{R}^n$ and a multi-index α, we use the notation

$$\mathbf{x}^\alpha = x_1^{\alpha_1} \cdot x_2^{\alpha_2} \cdots x_n^{\alpha_n} \tag{A.1}$$

for a *monomial* in the n variables $x_1, \ldots, x_n$. For example, if $\alpha = (2, 3)$, then $\mathbf{x}^\alpha = x_1^2 x_2^3$. Further, we denote by $|\alpha| = \alpha_1 + \ldots + \alpha_n$ the *total degree* of the monomial $\mathbf{x}^\alpha$ and we define the factorial as

$$\alpha! = \alpha_1! \cdots \alpha_n! \, . \tag{A.2}$$

A polynomial with total degree N is then written as

$$P = \sum_{|\alpha|=N} a_\alpha \mathbf{x}^\alpha \, . \tag{A.3}$$

Moreover, given a function $f : \mathbb{R}^n \to \mathbb{R}$ and a multi-index α, the notation

$$D^\alpha f(\mathbf{x}) = \frac{\partial^{|\alpha|} f(\mathbf{x})}{\partial x_1^{\alpha_1} \ldots \partial x_n^{\alpha_n}} \tag{A.4}$$

is used for the partial derivatives. For example, if $f : \mathbb{R}^2 \to \mathbb{R}$ and $\alpha = (1, 2)$, then

$$D^\alpha f(\mathbf{x}) = \frac{\partial^3}{\partial x_1 \partial x_2^2} f(\mathbf{x}) \, . \tag{A.5}$$

A.2 Schur Complements and Positive Semidefinite Matrices

Consider a symmetric matrix $\mathbf{M} \in \mathbb{R}^n$ partitioned as

$$\mathbf{M} = \begin{bmatrix} \mathbf{A} & \mathbf{B} \\ \mathbf{B}^T & \mathbf{C} \end{bmatrix} . \tag{A.6}$$

The *Schur complement* of $\mathbf{A}$ is defined as

$$\mathbf{S}_M^A = \mathbf{C} - \mathbf{B}^T \mathbf{A}^\dagger \mathbf{B} \tag{A.7}$$

with $\mathbf{A}^\dagger$ the pseudo-inverse of $\mathbf{A}$. The Schur complement of $\mathbf{C}$ is

$$\mathbf{S}_M^C = \mathbf{A} - \mathbf{B}\mathbf{C}^\dagger \mathbf{B}^T . \tag{A.8}$$

In the following, we summarize some results on the relation between the Schur complements and the positive (semi-) definiteness of a matrix $\mathbf{M}$, which can be found e.g. in [63] (see also Appendix A.5.5 in [17]).

Proposition A.2.1 (Propositions 16.1 in [63])**.** *For any symmetric matrix* (A.6)*, if* $\mathbf{C}$ *is invertible, the following properties hold:*

(1) $\mathbf{M} > 0$ *if and only if* $\mathbf{C} > 0$ *and* $\mathbf{A} - \mathbf{B}\mathbf{C}^{-1}\mathbf{B}^T > 0$*.*

(2) If $\mathbf{C} > 0$*, then* $\mathbf{M} \geq 0$ *if and only if* $\mathbf{A} - \mathbf{B}\mathbf{C}^{-1}\mathbf{B}^T \geq 0$*.*

Proposition A.2.2 (Propositions 16.2 in [63])**.** *For any symmetric matrix* (A.6)*, if* $\mathbf{A}$ *is invertible, the following properties hold:*

(1) $\mathbf{M} > 0$ *if and only if* $\mathbf{A} > 0$ *and* $\mathbf{C} - \mathbf{B}^T\mathbf{A}^{-1}\mathbf{B} > 0$*.*

(2) If $\mathbf{A} > 0$*, then* $\mathbf{M} \geq 0$ *if and only if* $\mathbf{C} - \mathbf{B}^T\mathbf{A}^{-1}\mathbf{B} \geq 0$*.*

Theorem A.2.1 (Theorem 16.1. in [63])**.** *Given a symmetric matrix* (A.6)*, the following conditions are equivalent:*

(1) $\mathbf{M} \geq 0$*.*

(2) $\mathbf{A} \geq 0\ , \quad (\mathbf{I} - \mathbf{A}\mathbf{A}^\dagger)\mathbf{B} = \mathbf{0}\ , \quad \mathbf{C} - \mathbf{B}^T\mathbf{A}^\dagger\mathbf{B} \geq 0.$

(3) $\mathbf{C} \geq 0\ , \quad (\mathbf{I} - \mathbf{C}\mathbf{C}^\dagger)\mathbf{B}^T = \mathbf{0}\ , \quad \mathbf{A} - \mathbf{B}\mathbf{C}^\dagger\mathbf{B}^T \geq 0.$

Appendix B

Technical Proofs

B.1 Proof of Lemma 6.4.2

From Theorem 2.3 in [168] it is known that

$$i_{\pm}(\mathbf{R}) = i_{\pm}(\mathbf{R}^A) + i_{\pm}\begin{bmatrix} \mathbf{0} & \mathbf{E}_{\mathbf{R}}^A \mathbf{R}^B \\ \left(\mathbf{R}^B\right)^T \mathbf{E}_{\mathbf{R}}^A & \mathbf{S}_{\mathbf{R}}^A \end{bmatrix} \tag{B.1}$$

where $\mathbf{S}_{\mathbf{R}}^A = \mathbf{R}^D - (\mathbf{R}^B)^T (\mathbf{R}^A)^\dagger \mathbf{R}^B$ is the Schur complement of $\mathbf{R}^A$ and $\mathbf{E}_{\mathbf{R}}^A = \mathbf{I} - \mathbf{R}^A (\mathbf{R}^A)^\dagger$ is the orthogonal projector onto $\mathcal{R}\{\mathbf{R}^A\}$. With Theorem A.2.1 above we conclude from $\mathbf{R} \geq 0$ that $\mathbf{R}^A \geq 0$, $\mathbf{E}_{\mathbf{R}}^A \mathbf{R}^B = \mathbf{0}$, and $\mathbf{S}_{\mathbf{R}}^A \geq 0$. Hence, it holds that $i_+(\mathbf{R}) = i_+(\mathbf{R}^A) + i_+(\mathbf{S}_{\mathbf{R}}^A) \leq i_+(\mathbf{R}^A) + i_+(\mathbf{R}^D)$. That the latter relation can be satisfied with equality sign follows from (B.1) with $\mathbf{R}^B = \mathbf{0}$.

B.2 Proof of Theorem 6.4.2

In order to prove necessity, suppose that there is a matrix $\mathbf{X}_0$ with $\mathrm{sym}\{\mathbf{X}_0\} \geq 0$, i.e., $\mathbf{X}_0 + \mathbf{X}_0^T \geq 0$, satisfying

$$\mathbf{A}\mathbf{X}_0 + \mathbf{X}_0^T \mathbf{A}^T = \mathbf{Q} \geq 0 \, . \tag{B.2}$$

Let $\mathbf{v}_i$ denote the left eigenvectors of $\mathbf{A}$, i.e. $\mathbf{v}^* \mathbf{A} = \lambda_i \mathbf{v}_i^*$, $1 \leq i \leq n$. Multiplication of (B.2) by $\mathbf{v}_i^*$ on the left and $\mathbf{v}_i$ on the right yields

$$\lambda_i \mathbf{v}_i^* \mathbf{X}_0 \mathbf{v}_i + \lambda_i^* \mathbf{v}_i^* \mathbf{X}_0^T \mathbf{v}_i = \mathbf{v}_i^* \mathbf{Q} \mathbf{v}_i \geq 0 \, , \quad 0 \leq i \leq n \tag{B.3}$$

and for real eigenvalues, i.e., $\lambda_i = \lambda_i^*$,

$$\lambda_i \mathbf{v}_i^* \left(\mathbf{X}_0 + \mathbf{X}_0^T\right) \mathbf{v}_i = \mathbf{v}_i^* \mathbf{Q} \mathbf{v}_i \geq 0 \, . \tag{B.4}$$

Since $\mathbf{v}_i^* \left(\mathbf{X}_0 + \mathbf{X}_0^T\right) \mathbf{v}_i \geq 0$ and $\mathbf{v}_i^* \mathbf{Q} \mathbf{v}_i \geq 0$, for left eigenvectors $\mathbf{v}_i$ corresponding to real negative eigenvalues $\lambda_i < 0$, it has to be fulfilled that $\mathbf{v}_i \in \mathcal{N}\{\mathbf{X}_0 + \mathbf{X}_0^T\}$, and for left eigenvectors corresponding to real non-positive eigenvalues $\lambda_i \leq 0$, it must hold that $\mathbf{v}_i \in \mathcal{N}\{\mathbf{Q}\}$. Hence, $i_0(\mathrm{sym}\{\mathbf{X}_0\}) \geq i_-^r(\mathbf{A})$ and it follows immediately that $\mathrm{sym}\{\mathbf{X}_0\}$ cannot have more than $n - i_-^r(\mathbf{A})$ positive eigenvalues.

To prove sufficiency, we show in the following that, for every $\mathbf{Q}$ which satisfies $\mathbf{v}_i \in \mathcal{N}\{\mathbf{Q}\}$ for all left eigenvectors $\mathbf{v}_i$ of $\mathbf{A}$ corresponding to non-positive eigenvalues, there exists in fact a solution $\mathbf{X}$ which satisfies (6.40). Note that, under the formulated condition for $\mathbf{Q}$, it holds that $\mathcal{R}(\mathbf{Q}) \subseteq \mathcal{R}(\mathbf{A})$, and hence equation (6.38) is solvable according to Theorem 6.4.1.

It is well known that there is a nonsingular matrix $\mathbf{V}$ such that $\mathbf{A}^T = \mathbf{V}\mathbf{D}\mathbf{V}^{-1}$, where $\mathbf{D}$ is a Jordan matrix and $\mathbf{V}$ contains the eigenvectors and generalized eigenvectors of $\mathbf{A}^T$, which are the *left* eigenvectors and generalized *left* eigenvectors of $\mathbf{A}$ [122]. Using this, (6.38) can be transformed into

$$\mathbf{D}^* \widehat{\mathbf{X}} + \widehat{\mathbf{X}}^* \mathbf{D} = \widehat{\mathbf{Q}} \tag{B.5}$$

with $\widehat{\mathbf{X}} = \mathbf{V}^* \mathbf{X} \mathbf{V}$ and $\widehat{\mathbf{Q}} = \mathbf{V}^* \mathbf{Q} \mathbf{V}$. The matrix $\mathbf{D}$ is partitioned into blocks according to $\mathbf{D} = \mathrm{diag}\{\mathbf{D}_{11}, \mathbf{D}_{22}, \mathbf{D}_{33}, \mathbf{D}_{44}\}$, where $\mathbf{D}_{11} \in \mathbb{C}^{n_1 \times n_1}$ contains all eigenvalues in the right half plane, $\mathbf{D}_{22} \in \mathbb{C}^{n_2 \times n_2}$ the complex eigenvalues with non-positive real part, $\mathbf{D}_{33} \in \mathbb{R}^{n_3 \times n_3}$ the zero eigenvalues, and $\mathbf{D}_{44} \in \mathbb{R}^{n_4 \times n_4}$ the negative real eigenvalues. The matrix $\mathbf{D}_{22}$ is such that every eigenvalue λ_j is followed by its conjugate complex $\bar{\lambda}_j$, i.e., $\mathbf{D}_{22} = \mathrm{diag}\{\ldots, \lambda_j, \bar{\lambda}_j, \ldots\}$. This form can always be achieved by ordering the eigenvectors and generalized eigenvectors in $\mathbf{V}$ appropriately. After partitioning $\widehat{\mathbf{X}}$ and $\widehat{\mathbf{Q}}$ into blocks accordingly

$$\widehat{\mathbf{X}} = \left[\widehat{\mathbf{X}}_{ik}\right] \ , \ i,k \in \{1,\ldots,4\} \ , \ \widehat{\mathbf{X}}_{ik} \in \mathbb{C}^{n_i \times n_k} \tag{B.6}$$

$$\widehat{\mathbf{Q}} = \left[\widehat{\mathbf{Q}}_{ik}\right] \ , \ i,k \in \{1,\ldots,4\} \ , \ \widehat{\mathbf{Q}}_{ik} \in \mathbb{C}^{n_i \times n_k} \tag{B.7}$$

and taking into account that both sides of (B.5) are Hermitian, the equation breaks up into 10 matrix equations

$$\mathbf{D}_{ii}^* \widehat{\mathbf{X}}_{ik} + \widehat{\mathbf{X}}_{ki}^* \mathbf{D}_{kk} = \widehat{\mathbf{Q}}_{ik} \ , \ i \in \{1,\ldots,4\}, \ k \in \{i,\ldots,4\}. \tag{B.8}$$

In the following, we let $\widehat{\mathbf{X}}_{[1,l]} = [\widehat{\mathbf{X}}_{ik}]$, $i,k \in \{1,\ldots,l\}$, and analogously we define $\widehat{\mathbf{Q}}_{[1,l]}$.

For $i = k = 1$, if we choose $\widehat{\mathbf{X}}_{11}$ to be Hermitian, i.e., $\widehat{\mathbf{X}}_{11} = \widehat{\mathbf{X}}_{11}^*$, the matrix equation (B.8) turns into a Lyapunov equation, which by virtue of $i_+(\mathbf{D}_{11}) = n_1$ and $\widehat{\mathbf{Q}}_{11} > 0$ has a unique positive definite solution $\widehat{\mathbf{X}}_{11} = \widehat{\mathbf{X}}_{11}^* > 0$ [141].

Next, we consider (B.8) for $i = k = 2$, i.e.,

$$\mathbf{D}_{22}^{*}\widehat{\mathbf{X}}_{22} + \widehat{\mathbf{X}}_{22}^{*}\mathbf{D}_{22} = \widehat{\mathbf{Q}}_{22} \tag{B.9}$$

where $\mathbf{D}_{22} = \mathrm{diag}\{\lambda_1, \ldots, \lambda_{n_2}\}$ with $\lambda_{2i} = \bar{\lambda}_{2i-1}$, $i \in \{1, \ldots, \frac{n_2}{2}\}$. For simplicity of notation, we have numbered the eigenvalues in $\mathbf{D}_{22}$ starting from 1. The matrix $\widehat{\mathbf{X}}_{22} \in \mathbb{C}^{n_2 \times n_2}$ possesses the following structure. If we partition it into 2×2 blocks $\Theta_{jl} = \|\theta_{rs}\|$, $j, l \in \{1, \ldots, \frac{n_2}{2}\}$, $r, s \in \{1, 2\}$, then $\theta_{22} = \bar{\theta}_{11}$ and $\theta_{21} = \bar{\theta}_{12}$. This follows from the fact that $\mathbf{X}$ is a real matrix, and thus complex eigenvalues as well as the corresponding eigenvectors occur as conjugate pairs. Hence, we see that

$$\Theta_{jl} = \begin{bmatrix} \theta_{11} & \theta_{12} \\ \theta_{21} & \theta_{22} \end{bmatrix} = \begin{bmatrix} \mathbf{v}_j^{*} \\ \bar{\mathbf{v}}_j^{*} \end{bmatrix} \mathbf{X} \begin{bmatrix} \mathbf{v}_l & \bar{\mathbf{v}}_l \end{bmatrix} = \begin{bmatrix} \mathbf{v}_j^{*}\mathbf{X}\mathbf{v}_l & \mathbf{v}_j^{*}\mathbf{X}\bar{\mathbf{v}}_l \\ \bar{\mathbf{v}}_j^{*}\mathbf{X}\mathbf{v}_l & \bar{\mathbf{v}}_j^{*}\mathbf{X}\bar{\mathbf{v}}_l \end{bmatrix} = \begin{bmatrix} \mathbf{v}_j^{*}\mathbf{X}\mathbf{v}_l & \mathbf{v}_j^{*}\mathbf{X}\bar{\mathbf{v}}_l \\ \overline{\mathbf{v}_j^{*}\mathbf{X}\bar{\mathbf{v}}_l} & \overline{\mathbf{v}_j^{*}\mathbf{X}\mathbf{v}_l} \end{bmatrix} \tag{B.10}$$

where $\mathbf{v}_j, \bar{\mathbf{v}}_j$ and $\mathbf{v}_l, \bar{\mathbf{v}}_l$ are the complex conjugate pairs of eigenvectors corresponding to the conjugate pairs of eigenvalues $\lambda_j, \bar{\lambda}_j$ and $\lambda_l, \bar{\lambda}_l$. The same considerations apply to the structure of $\widehat{\mathbf{Q}}_{22} = \mathbf{V}_2^{*}\mathbf{Q}\mathbf{V}_2$. The matrix equation (B.9) can be replaced by a system of scalar equations, which, due to this special structure of $\widehat{\mathbf{X}}_{22}$ and $\widehat{\mathbf{Q}}_{22}$, appear in complex conjugate pairs. Considering this together with the Hermitian structure of (B.9), we obtain $\frac{1}{4}(n_2^2 + 2n_2)$ scalar equations

$$\bar{\lambda}_\alpha x_{\alpha\beta} + \bar{x}_{\beta\alpha}\lambda_\beta = q_{\alpha\beta}\ , \quad \alpha = 1, 3, \ldots, \frac{n_2}{2} - 1\ ,\ \beta = \alpha, \ldots, n_2 \tag{B.11}$$

with $x_{\alpha\beta}$ the entries[1] of $\widehat{\mathbf{X}}_{22}$. After substituting $\lambda_\alpha = \lambda_\alpha^r + i\lambda_\alpha^i$, $\lambda_\beta = \lambda_\beta^r + i\lambda_\beta^i$, $q_{\alpha\beta} = q_{\alpha\beta}^r + iq_{\alpha\beta}^i$ and $x_{\alpha\beta} = x_{\alpha\beta}^r + ix_{\alpha\beta}^i$ into (B.11) and separating the equations into real and imaginary terms we get

$$\lambda_\alpha^r x_{\alpha\beta}^r + \lambda_\alpha^i x_{\alpha\beta}^i + \lambda_\beta^r x_{\beta\alpha}^r + \lambda_\beta^i x_{\beta\alpha}^i = q_{\alpha\beta}^r \tag{B.12}$$

$$\lambda_\alpha^r x_{\alpha\beta}^i - \lambda_\alpha^i x_{\alpha\beta}^r - \lambda_\beta^r x_{\beta\alpha}^i + \lambda_\beta^i x_{\beta\alpha}^r = q_{\alpha\beta}^i\ . \tag{B.13}$$

For $\beta = \alpha$, the relation (B.13) is trivially satisfied as $q_{\alpha\alpha}^i = 0$ holds for all α, and (B.12) turns into $2\lambda_\alpha^r x_{\alpha\alpha}^r + 2\lambda_\alpha^i x_{\alpha\alpha}^i = q_{\alpha\alpha}$. We observe that the real part $x_{\alpha\alpha}^r$ can be chosen arbitrarily positive since the latter equation can be satisfied with $x_{\alpha\alpha}^i$. Since the αth entry of the main diagonal of $\widehat{\mathbf{X}}_{22} + \widehat{\mathbf{X}}_{22}^{*}$ is precisely $2x_{\alpha\alpha}^r$, we conclude that this matrix can be rendered positive definite by choosing the $x_{\alpha\alpha}^r$ sufficiently large. Since all other blocks of

[1] For the sake of notational simplicity, the index '22' is not written in $x_{\alpha\beta}$.

$\widehat{\mathbf{X}}_{[1,2]} + \widehat{\mathbf{X}}^*_{[1,2]}$ are independent of the $x^r_{\alpha\alpha}$ and $\widehat{\mathbf{X}}_{11} + \widehat{\mathbf{X}}^*_{11}$ is positive definite, we can use Theorem A.2.1 to conclude that $\widehat{\mathbf{X}}_{[1,2]} + \widehat{\mathbf{X}}^*_{[1,2]}$ can always be made positive definite by making the $x^r_{\alpha\alpha}$ sufficiently large.

For $i = k = 3$, we obtain from (B.8) the matrix equation

$$\mathbf{D}^*_{33}\widehat{\mathbf{X}}_{33} + \widehat{\mathbf{X}}^*_{33}\mathbf{D}_{33} = \widehat{\mathbf{Q}}_{33} \tag{B.14}$$

where $\widehat{\mathbf{Q}}_{33} = \mathbf{V}^*_3\mathbf{Q}\mathbf{V}_3$ and the columns of $\mathbf{V}_3$ are the left eigenvectors that correspond to the zero eigenvalues of $\mathbf{A}$. In view of the conditions of the theorem, these are contained in the nullspace of $\mathbf{Q}$ and consequently $\widehat{\mathbf{Q}}_{33} = \mathbf{0}$. Moreover, since the algebraic and geometric multiplicity of eigenvalues with non-positive real part is equal, it holds that $\mathbf{D}_{33} = \mathbf{0}$. Hence, (B.14) is trivially satisfied independently of $\widehat{\mathbf{X}}_{33}$. As a consequence, this matrix can be chosen such that $\widehat{\mathbf{X}}_{33} + \widehat{\mathbf{X}}^*_{33} > 0$.

Next, we consider (B.8) for $k = 3$, $i \in \{1, 2\}$, i.e.,

$$\mathbf{D}^*_{ii}\widehat{\mathbf{X}}_{i3} + \widehat{\mathbf{X}}^*_{3i}\mathbf{D}_{33} = \widehat{\mathbf{Q}}_{i3},\ i \in \{1, 2\}\ . \tag{B.15}$$

Since $\widehat{\mathbf{Q}}_{i3} = \mathbf{V}^*_i\mathbf{Q}\mathbf{V}_3$ and the columns of $\mathbf{V}_3$ are elements of $\mathcal{N}\{\mathbf{Q}\}$ it holds that $\widehat{\mathbf{Q}}_{i3} = \mathbf{0}$ for all i. Using this together with $\mathbf{D}_{33} = \mathbf{0}$ we conclude that (B.15) turns into $\mathbf{D}^*_{ii}\widehat{\mathbf{X}}_{i3} = \mathbf{0}$, $i \in \{1, 2\}$. Since $\mathbf{D}_{ii}$ is a regular matrix for $i \in \{1, 2\}$, it is necessary that $\widehat{\mathbf{X}}_{i3} = \mathbf{0}$, while $\widehat{\mathbf{X}}_{3i}$ can be chosen arbitrary (e.g. $\widehat{\mathbf{X}}_{3i} = \mathbf{0}$). This shows that $\widehat{\mathbf{X}}_{[1,3]} + \widehat{\mathbf{X}}^*_{[1,3]} > 0$ is always possible, if $\widehat{\mathbf{X}}_{[1,2]} + \widehat{\mathbf{X}}^*_{[1,2]} > 0$.

Now we choose $\widehat{\mathbf{X}}_{i4} = \widehat{\mathbf{X}}^*_{4i} = \mathbf{0}$, $i = 1, \ldots, 4$. Since, by assumption, all left eigenvectors of $\mathbf{A}$ corresponding to real negative eigenvalues are contained in the nullspace of $\mathbf{Q}$, it holds that $\widehat{\mathbf{Q}}_{i4} = \widehat{\mathbf{Q}}^*_{4i} = \mathbf{0}$ for all $i \in \{1, \ldots, 4\}$. As a consequence, the remaining equations $\mathbf{D}^*_{ii}\widehat{\mathbf{X}}_{i4} + \widehat{\mathbf{X}}^*_{4i}\mathbf{D}_{44} = \widehat{\mathbf{Q}}_{i4}$, $i \in \{1, \ldots, 4\}$ are trivially fulfilled.

With that said, $\widehat{\mathbf{X}}+\widehat{\mathbf{X}}^*$ is a positive semi-definite matrix with $n_4 = i^r_-(\mathbf{A})$ zero eigenvalues and $n - n_4 = n - i^r_-(\mathbf{A})$ positive eigenvalues. Consequently, $\mathbf{X} = \mathbf{V}^{-*}\widehat{\mathbf{X}}\mathbf{V}^{-1}$ is a real solution of (6.38) and $\mathbf{X} + \mathbf{X}^T \geq 0$ possesses $i^r_-(\mathbf{A})$ zero eigenvalues and $n - i^r_-(\mathbf{A})$ positive eigenvalues. We remark that, in order that $\mathbf{X} = \mathbf{V}^{-*}\widehat{\mathbf{X}}\mathbf{V}^{-1}$ is a real matrix, we also have to take into account the special structure of $\widehat{\mathbf{X}}_{12}$ and $\widehat{\mathbf{X}}_{21}$ which arises from the fact that the left eigenvectors corresponding to complex eigenvalues occur in conjugate pairs (see the discussion on the structure of $\widehat{\mathbf{X}}_{22}$ above).

B.3 Proof of Lemma 7.2.1

By assumption, $\mathrm{S} \neq \emptyset$ and hence we can choose some $\bar{\mathbf{z}}_{1,1} \in \mathrm{S} \subseteq \partial\chi$. Since $\bar{\mathbf{z}}_{1,1} \in \partial\chi$, it holds that $\tilde{\varphi}(\bar{\mathbf{z}}_{1,1}) = 0$ and, by assumption, we have that $\nabla\tilde{\varphi}(\bar{\mathbf{z}}_{1,1}) \neq 0$ and that $\tilde{\varphi}(\mathbf{z}_1)$ is analytic. Therefore, from the analytic inverse function theorem [56], we conclude that there exists an open neighborhood $\mathrm{U}_1 = \mathrm{U}_1' \times \mathrm{U}_1''$ of $\bar{\mathbf{z}}_{1,1}$ with $\mathrm{U}_1' \subset \mathbb{R}^{n-1}$, $\mathrm{U}_1'' \subset \mathbb{R}^1$ and an analytic function $w_1 : \mathrm{U}_1' \to \mathrm{U}_1''$ such that for some j_1

$$\{\mathbf{z}_1 \in \mathrm{U}_1' \times \mathrm{U}_1'' \,|\tilde{\varphi}_x(\mathbf{z}_1) = 0\} = \left\{(\mathbf{z}_1^{j_1}, z_{1,j_1}) \in \mathrm{U}_1' \times \mathrm{U}_1'' \,\middle|\, z_{1,j_1} = w_1(\mathbf{z}_1^{j_1})\right\} \tag{B.16}$$

where $\mathbf{z}_1^{j_1}$ denotes the vector $\mathbf{z}_1$ with the j_1-th component omitted. Since $\bar{\mathbf{z}}_{1,1} \in \mathrm{S}$, by continuity of $\tilde{\varphi}_p^{(i)}(\mathbf{z}_1)$, $i = 0, 1, 2, \ldots$, $p \in \mathcal{P}$, there is a neighborhood $\mathcal{O} \subset \mathrm{U}'$ of $\bar{\mathbf{z}}_1^{j_1}$ such that $\{\mathbf{z}_1 | z_{1,j_1} = w_1(\mathbf{z}_1^{j_1}),\ \mathbf{z}_1^{j_1} \in \mathcal{O}\} \in \mathrm{S}$. Now let $\zeta_{1,i}(\mathbf{z}_1^{j_1})$ be the restriction of $\tilde{h}_2^{(i-1)}(\mathbf{z}_1) - z_{1,i}$ to the set $\{\mathbf{z}_1 \in \mathrm{U}_1' \times \mathrm{U}_1'' | z_{1,j_1} = w_1(\mathbf{z}_1^{j_1})\} \subset \partial\chi$, i.e.,

$$\zeta_{1,i}(\mathbf{z}_1^{j_1}) = \tilde{h}_2^{(i-1)}(\mathbf{z}_1) - z_{1,i}\Big|_{z_{1,j_1} = w_1(\mathbf{z}_1^{j_1})}\ , \quad i \in \{2, \ldots, r\}\ . \tag{B.17}$$

According to (7.42), it must be satisfied that $\zeta_{1,i}(\mathbf{z}_1^{j_1}) = 0$ for all $i \in \{2, \ldots, r\}$ and all $\mathbf{z}_1^{j_1} \in \mathcal{O}$. As $\zeta_{1,i}(\mathbf{z}_1^{j_1})$ is the composition of two analytic functions, it is itself an analytic function. Since an analytic function which is zero on an open set is zero everywhere (see e.g. [161]), we conclude that $\zeta_{1,i}(\mathbf{z}_1^{j}) = 0$ for all $\mathbf{z}_1^{j_1} \in \mathrm{U}_1'$ and all $i \in \{2, \ldots, r\}$. In case that $\mathrm{U}_1' \times \mathrm{U}_1'' = \mathbb{R}^n$, this finishes the proof. Otherwise, we take another point $\bar{\mathbf{z}}_{1,2} \notin \mathrm{U}_1$ with $\tilde{\varphi}_x(\bar{\mathbf{z}}_{1,2}) = 0$ such that the open neighborhood $\mathrm{U}_2 = \mathrm{U}_2' \times \mathrm{U}_2''$ of $\bar{\mathbf{z}}_{1,2}$, on which a function $w_2(\mathbf{z}_1^{j_2})$ like in (B.16) exists, satisfies $U_2 \cap U_1 \neq \emptyset$. Since $\zeta_{i,2}(\mathbf{z}_1^{j}) = h_2^{(i-1)}(\mathbf{z}_1) - z_{1,i}|_{z_{1,j_2} = w_2(\mathbf{z}_1^{j})} = 0$ holds on the intersection $\{\mathbf{z}_1 | \mathbf{z}_1^{j} \in \mathrm{U}_1',\ z_{1,j_2} = w_2(\mathbf{z}_1^{j_2})\} \cap \{\mathbf{z}_1 | \mathbf{z}_1^{j} \in \mathrm{U}_1',\ z_{1,j_1} = w_1(\mathbf{z}_1^{j_1})\}$, as above we deduce that $\boldsymbol{\zeta}_{2,i}(\mathbf{z}_1^{j_2}) = 0$ holds for all $\mathbf{z}_1^{j_2} \in \mathrm{U}_2'$ and all $i \in \{2, \ldots, r\}$. Repeating this argument, we conclude that $h_2^{(i-1)}(\mathbf{z}_1) - z_{1,i} = 0$ must hold for all $\mathbf{z}_1 \in \partial\chi$ and all $i \in \{2, \ldots, r\}$, which completes the proof.

B.4 Proof of Lemma 7.2.3

Since both $\tilde{\boldsymbol{\Phi}}_1(\mathbf{z}_1) = \mathbf{I}(\cdot)$ and $\tilde{\boldsymbol{\Phi}}_2(\mathbf{z}_1)$ are diffeomorphisms and (7.55) holds by assumption, we only have to prove that $\chi_1 \cap \tilde{\boldsymbol{\Phi}}_2(\operatorname{int}\chi_2) = \emptyset$. Note that (7.56) implies that $\tilde{\boldsymbol{\Phi}}_1(\partial\chi) = \tilde{\boldsymbol{\Phi}}_2(\partial\chi) = \partial\chi$. By virtue of (7.55), it holds that $\chi_2 \subseteq \tilde{\boldsymbol{\Phi}}_2(\chi_2)$. Moreover, since $\tilde{\boldsymbol{\Phi}}_1(\mathbf{z}_1)$ is the identity map, the image of χ_1 under $\tilde{\boldsymbol{\Phi}}_1(\mathbf{z}_1)$ is χ_1. Now assume that $\chi_1 \cap \tilde{\boldsymbol{\Phi}}_2(\operatorname{int}\chi_2) = \emptyset$

is not satisfied. Then we can find two points $\bar{\mathbf{z}}_{1,1} \in \operatorname{int}\chi_2$ and $\bar{\mathbf{z}}_{1,2} \in \operatorname{int}\chi_2$ such that $\tilde{\mathbf{\Phi}}_2(\bar{\mathbf{z}}_{1,1}) \in \chi_1$ and $\tilde{\mathbf{\Phi}}_2(\bar{\mathbf{z}}_{1,2}) \in \chi_2$. Connect these two points by a path which completely lies in the interior of χ_2. The image of this path under $\tilde{\mathbf{\Phi}}_2(\cdot)$ necessarily has to traverse $\partial\chi$ (in the image space). This is, however, a contradiction to the fact that $\tilde{\mathbf{\Phi}}_2(\cdot)$ is a diffeomorphism. Since $\tilde{\mathbf{\Phi}}_2(\partial\chi) = \partial\chi$, there cannot be a point in the interior of χ_2 which is mapped to a point of $\partial\chi$.

B.5 Proof of Lemma 7.2.4

The derivative of κ along the trajectories of $\dot{\mathbf{z}}_1 = \tilde{\mathbf{f}}_{d,1}(\mathbf{z}_1, y_d^{(n)})$ can be written as

$$\dot{\kappa}_1 = \frac{\partial \kappa}{\partial z_{1,1}} z_{1,2} + \ldots + \frac{\partial \kappa}{\partial z_{1,n-1}} z_{1,n} + \frac{\partial \kappa}{\partial z_{1,n}} y_d^{(n)} + \frac{\partial \kappa}{\partial \boldsymbol{\gamma}} \dot{\boldsymbol{\gamma}} \,. \tag{B.18}$$

The derivative of the function along the trajectories of $\dot{\mathbf{z}}_1 = \tilde{\mathbf{f}}_{d,2}(\mathbf{z}_1, y_d^{(n-1)})$ is

$$\dot{\kappa}_2 = \frac{\partial \kappa}{\partial z_{1,1}} z_{1,2} + \ldots + \frac{\partial \kappa}{\partial z_{1,n-1}} y_d^{(n-1)} + \frac{\partial \kappa}{\partial z_{1,n}} \left[\tilde{\alpha}_1 - \frac{\tilde{\beta}_1}{\tilde{\varrho}_u} \tilde{\varrho}_x + \left(\frac{\tilde{\beta}_1}{\tilde{\varrho}_u} + b_n \right) (y_d^{(n-1)} - \mathbf{z}_{1,n}) \right] + \frac{\partial \kappa}{\partial \boldsymbol{\gamma}} \dot{\boldsymbol{\gamma}} \,. \tag{B.19}$$

Now we rewrite $y_d^{(n-1)}$ as

$$y_d^{(n-1)} = z_{1,n} + (y_d^{(n-1)} - z_{1,n}) = z_{1,n} + \tilde{\varrho}_2(\mathbf{z}_1, y_d^{(n-1)}) \tag{B.20}$$

and the term $\tilde{\alpha}_1 - \frac{\tilde{\beta}_1}{\tilde{\varrho}_u} \tilde{\varrho}_x$ as

$$\tilde{\alpha}_1 - \frac{\tilde{\beta}_1}{\tilde{\varrho}_u} \tilde{\varrho}_x = y_d^{(n)} - \frac{\tilde{\beta}_1}{\tilde{\varrho}_u} \tilde{\varrho}_x - y_d^{(n)} + \tilde{\alpha}_1 = y_d^{(n)} - \frac{\tilde{\beta}_1}{\tilde{\varrho}_u} \underbrace{\left(\tilde{\varrho}_x + \frac{\tilde{\varrho}_u}{\tilde{\beta}_1} (y_d^{(n)} - \tilde{\alpha}_1) \right)}_{\tilde{\varrho}_1(\mathbf{z}_1, y_d^{(n)})} \,. \tag{B.21}$$

By substituting these two expressions into (B.19) and comparing it to (B.18), the desired result is obtained.

Bibliography

[1] E.L. Allgower and K. Georg. *Introduction to Numerical Continuation Methods*. SIAM, 2003.

[2] A. Ames, K. Galloway, J. W. Grizzle, and K. Sreenath. Rapidly exponentially stabilizing control Lyapunov functions and hybrid zero dynamics. *IEEE Trans. Autom. Contr.,* to appear.

[3] A. C. Antoulas. *Approximation of Large-Scale Dynamical Systems*. SIAM, 2005.

[4] A. Astolfi and R. Ortega. Energy based stabilization of the angular velocity of a rigid body operating in failure configuration. *J Guidance Control Dynam*, 25(1):184–187, 2002.

[5] A. Astolfi and R. Ortega. Immersion and invariance: A new tool for stabilization and adaptive control of nonlinear systems. *IEEE Trans. Automat. Contr.*, 48(4):590–606, 2003.

[6] K. J. Aström and C. Canudas-de Wit. Revisiting the LuGre friction model. *IEEE Control Syst. Mag.*, 28(6):101–114, 2008.

[7] A. Bacciotti and L. Mazzi. An invariance principle for nonlinear switched systems. *Syst. Control Lett.*, 54(11):1109 – 1119, 2005.

[8] A. Baillo and A. Cuevas. On the estimation of a star-shaped set. *Adv. Appl. Prob.*, 33(4):717–726, 2001.

[9] E. A. Barbashin and N. N. Krasovskii. On the stability of motion in the large. *Dok. Akad. Nauk.*, 86:453–456, 1952. (in Russian).

[10] A. S. Bazanella, P. V. Kokotović, and A. S. e Silva. A dynamic extension for L_gV controllers. *IEEE Trans. Automat. Contr.*, 44(3):588–592, 1999.

[11] S. C. Bengea and R. A. DeCarlo. Optimal control of switching systems. *Automatica*, 41(1):11 – 27, 2005.

[12] R. Bhatia. *Positive Definite Matrices*. Princeton University Press, 2007.

[13] F. Blanchini, S. Miani, and F. Mesquine. A separation principle for linear switching systems and parametrization of all stabilizing controllers. *IEEE Trans. Automat. Contr.*, 54(2):279–292, 2009.

[14] A. M. Bloch, D. E. Chang, N. E. Leonard, and J. E. Marsden. Controlled Lagrangians and the stabilization of mechanical systems. II. Potential shaping. *IEEE Trans. Automat. Contr.*, 46(10):1556–1571, 2001.

[15] A. M. Bloch, N. E. Leonard, and J. E. Marsden. Controlled Lagrangians and the stabilization of mechanical systems. I. The first matching theorem. *IEEE Trans. Automat. Contr.*, 45(12):2253–2270, 2000.

[16] S. Boyd, L. El Ghaoui, E. Feron, and V. Balakrishnan. *Linear Matrix Inequalities in System and Control Theory*. SIAM, Philadelphia, 1994.

[17] S. Boyd and L. Vandenberghe. *Convex Optimization*. Cambridge University Press, 2004.

[18] H. W. Braden. The equation $A^T X \pm X^T A = B$. *SIAM. J. Matrix Anal. Appl.*, 20:295–302, 1998.

[19] M. S. Branicky. Analyzing continuous switching systems: Theory and examples. In *Proc. Amer. Control Conf.*, pages 3110–3114, 1994.

[20] M. S. Branicky. *Studies in Hybrid Systems: Modeling, Analysis, and Control*. PhD thesis, Massachusetts Institue of Technology, 1995.

[21] M. S. Branicky. Multiple Lyapunov functions and other analysis tools for switched and hybrid systems. *IEEE Trans. Automat. Contr.*, 43(4):475 –482, 1998.

[22] B. Brogliato, S.-I. Niculescu, and P. Orhant. On the control of finite-dimensional mechanical systems with unilateral constraints. *IEEE Trans. Automat. Contr.*, 42(2):200–215, 1997.

[23] C. Canudas, K. Astrom, and K. Braun. Adaptive friction compensation in DC-motor drives. *IEEE J. Robot. Automat.*, 3(6):681–685, 1987.

[24] D. Cheng, A. Astolfi, and R. Ortega. On feedback equivalence to port controlled Hamiltonian systems. *Syst. Control Lett.*, 54(9):911–917, 2005.

[25] D. Cheng, G. Feng, and Z. Xi. Stabilization of a class of switched nonlinear systems. *IET Control Theory Appl.*, 4(1):53–61, 2006.

[26] G. Chesi, A. Garulli, A. Tesi, and A. Vicino. LMI-based computation of optimal quadratic Lyapunov functions for odd polynomial systems. *Int. J. Robust Nonlinear Control*, 15:35–49, 2005.

[27] H.-D. Chiang, C.-C. Chu, and G. Cauley. Direct stability analysis of electric power systems using energy functions: Theory, applications, and perspective. *Proc. IEEE*, 83(11):1497–1529, 1995.

[28] H. D. Chiang and L. Fekih-Ahmed. Quasi-stability regions of nonlinear dynamical systems: Optimal estimations. *IEEE Trans. Circuits Syst. I*, 43(8):636 –643, 1996.

[29] H.-D. Chiang, M. W. Hirsch, and F. F. Wu. Stability regions of nonlinear autonomous dynamical systems. *IEEE Trans. Automat. Contr.*, 33(1):16–27, 1988.

[30] H.-D. Chiang and J. S. Thorp. The closest unstable equilibrium point method for power system dynamic security assessment. *IEEE Trans. Circuits Syst.*, 36(9):1187–1200, 1989.

[31] H.-D. Chiang and J. S. Thorp. Stability regions of nonlinear dynamical systems: A constructive methodology. *IEEE Trans. Automat. Contr.*, 34(12):1229 –1241, 1989.

[32] P. Colaneri, J. Geromel, and A. Astolfi. Stabilization of continuous-time switched nonlinear systems. *Syst. Control Lett.*, 57(1):95 – 103, 2008.

[33] J. Cortés. Discontinuous dynamical systems. *IEEE Control Syst. Mag.*, 28(3):36–73, 2008.

[34] J. Daafouz and J. Bernussou. Robust dynamic output feedback control for switched systems. In *Proc. 41st IEEE Conf. Decision Control*, pages 4389–4394, 2002.

[35] J. Daafouz, P. Riedinger, and C. Iung. Stability analysis and control synthesis for switched systems: A switched Lyapunov function approach. *IEEE Trans. Automat. Contr.*, 47(11):1883 – 1887, 2002.

[36] A. Daasch. Abschätzung und Vergrößerung des Einzugsbereiches bei der passivitätsbasierten Regelung. Master's thesis, Technische Universität München, 2012. Supervisor: Tobias Kloiber.

[37] E. J. Davison and E. M. Kurak. A computational method for determining quadratic Lyapunov functions for non-linear systems. *Automatica*, 7:627–636, 1971.

[38] R. A. Decarlo, M. S. Branicky, S. Pettersson, and B. Lennartson. Perspectives and results on the stability and stabilizability of hybrid systems. *Proc. IEEE*, 88(7):1069 –1082, 2000.

[39] S. Devasia, C. Chen, and B. Paden. Nonlinear inversion-based output tracking. *IEEE Trans. Automat. Contr.*, 41(7):930–942, 1996.

[40] S. Devasia, B. Paden, and C. Rossi. Exact-output tracking theory for systems with parameter jumps. *Int. J. Control*, 67(1):117–131, 1997.

[41] M. di Bernardo, C. I. Hoyos Velasco, U. Montanaro, and S. Santini. Experimental implementation and validation of a novel minimal control synthesis adaptive controller for continuous bimodal piecewise affine systems. *Control Eng. Practice*, 20(3):269 – 281, 2012.

[42] M. di Bernardo, U. Montanaro, and S. Santini. Minimal control synthesis adaptive control of continuous bimodal piecewise affine systems. *SIAM J. Control Optim.*, 48(7):4242–4261, 2010.

[43] M. di Bernardo, U. Montanaro, and S. Santini. Canonical forms of generic piecewise linear continuous systems. *IEEE Trans. Automat. Contr.*, 56(8):1911–1915, 2011.

[44] M. di Bernardo, U. Montanaro, and S. Santini. Hybrid model reference adaptive control of piecewise affine systems. *IEEE Trans. Automat. Contr.*, 58(2):304–316, 2013.

[45] D. A. Dirksz and J. M. A. Scherpen. Power-based setpoint control: Experimental results on a planar manipulator. *IEEE Trans. Contr. Syst. Technol.*, 20:1384–1391, 2012.

[46] V. Duindam, A. Macchelli, S. Stramgioli, and H. Bruyninckx, editors. *Modeling and Control of Complex Physical Systems: The Port-Hamiltonian Approach*. Springer, 2009.

[47] H. Ehlich and K. Zeller. Schwankung von Polynomen zwischen Gitterpunkten. *Math. Zeitschr.*, 86:41–44, 1964.

[48] N. H. El-Farra, P. Mhaskar, and P. D. Christofides. Output feedback control of switched nonlinear systems using multiple Lyapunov functions. *Syst. Control Lett.*, 54(12):1163 – 1182, 2005.

[49] L. El Ghaoui, F. Oustry, and M. AitRami. A cone complementarity linearization algorithm for static output-feedback and related problems. *IEEE Trans. Automat. Contr.*, 42(8):1171–1176, 1997.

[50] G. Feng. Controller design and analysis of uncertain piecewise-linear systems. *IEEE Trans. Circuits Syst. I*, 49(2):224–232, 2002.

[51] A. F. Filippov. *Differential Equations with Discontinuous Righthand Sides*. Kluwer Academic Publishers, 1988.

[52] M. Fliess, J. Levine, P. Martin, and P. Rouchon. Flatness and defect of non-linear systems: introductory theory and examples. *Int. J. Control*, 61(6):1327–1361, 1995.

[53] O. Föllinger. Design of time varying systems by pole assignment. *Regelungstechnik*, 26(6):189–196, 1978. (in German).

[54] E. Francini. Starshapedness of level sets for solutions of nonlinar elliptic equations. *Math. Nachr.*, 193:49 – 56, 1998.

[55] L. Freidovich, A. Robertsson, A. Shiriaev, and R. Johansson. LuGre-model-based friction compensation. *IEEE Trans. Contr. Syst. Technol.*, 18(1):194–200, 2010.

[56] K. Fritzsche and H. Grauert. *From Holomorphic Functions to Complex Manifolds*. Springer, 2002.

[57] F. Fuchshumer, W Kemmetmüller, and A. Kugi. Nonlinear control of variable-displacement self-supplied axial piston pumps. *at - Automatisierungstechnik*, 55(2):58–68, 2007. (in German).

[58] K. Fujimoto, K. Sakurama, and T. Sugie. Trajectory tracking control of port-controlled Hamiltonian systems via generalized canonical transformations. *Automatica*, 39(12):2059 – 2069, 2003.

[59] K. Fujimoto and T. Sugie. Canonical transformation and stabilization of generalized Hamiltonian systems. *Syst. Control Lett.*, 42(3):217 – 227, 2001.

[60] M. Galaz. *Nonlinear control of power systems*. PhD thesis, De l'Université Paris XI Orsay, 2003.

[61] M. Galaz, R. Ortega, A. S. Bazanella, and A. M. Stankovic. An energy-shaping approach to the design of excitation control of synchronous generators. *Automatica*, 39(1):111 – 119, 2003.

[62] S. Galeani, L. Menini, and A. Potini. Robust trajectory tracking for a class of hybrid systems: An internal model principle approach. *IEEE Trans. Automat. Contr.*, 57(2):344–359, 2012.

[63] J. Gallier. *Geometric Methods and Applications: For Computer Science and Applications*. Springer, 2011.

[64] F. R. Gantmacher. *The Theory of Matrices*, volume 1. Chelsea Publishing Company, 1960.

[65] E. García-Canseco, D. Jeltsema, R. Ortega, and J. M. A Scherpen. Power-based control of physical systems. *Automatica*, 46(1):127 – 132, 2010.

[66] Ute Gärtel. *Fehlerabschätzung für vektorwertige Randwertaufgaben zweiter Ordnung, insbesondere für Probleme aus der chemischen Reaktions-Diffusions-Theorie*. PhD thesis, Universität Köln, 1987.

[67] C. Gaviria, E. Fossas, and R. Griñó. Robust controller for a full-bridge rectifier using the IDA approach and GSSA modeling. *IEEE Trans. Circuits Syst. I*, 52(3):609–616, 2005.

[68] R. Genesio, M. Tartaglia, and A. Vicino. On the estimation of asymptotic stability regions: State of the art and new proposals. *IEEE Trans. Automat. Contr.*, 30(8):747 – 755, 1985.

[69] S. Gnutzmann. *Stückweise lineare Approximation implizit definierter Mannigfaltigkeiten*. PhD thesis, Universität Hamburg, 1988.

[70] R. Goebel, R. G. Sanfelice, and A. R. Teel. Invariance principles for switching systems via hybrid systems techniques. *Syst. Control Lett.*, 57:980–986, 2008.

[71] J. W. Grizzle, M. D. Di Benedetto, and F. Lamnabhi-Lagarrigue. Necessary conditions for asymptotic tracking in nonlinear systems. *IEEE Trans. Automat. Contr.*, 39(9):1782–1794, 1994.

[72] Y. Guo and D. Cheng. Stabilization of time-varying Hamiltonian systems. *IEEE Trans. Automat. Contr.*, 14:871 – 880, 2006.

[73] P.-O. Gutmann and P. Hagander. A new design of constrained controllers for linear systems. *IEEE Trans. Automat. Contr.*, AC-30(1):22–33, 1985.

[74] W. M. Haddad, S. G. Nersesov, and V. Chellaboina. Energy-based control for hybrid port-controlled Hamiltonian systems. *Automatica*, 39(8):1425–1435, 2003.

[75] P. Hartman. *Ordinary Differential Equations*. SIAM, 2002.

[76] W. P. M. H. Heemels. *Linear Complementarity Systems: A Study in Hybrid Dynamics*. PhD thesis, Technische Universiteit Eindhoven, 1999.

[77] M. Heller, R. David, and J. Holmberger. Falling leaf motion supression in the F/A-18 Hornet with revised flight control software. In *42nd AIAA Aerospace Sciences Meeting and Exhibit*, 2004.

[78] J. P. Hespanha. Uniform stability of switched linear systems: extensions of LaSalle's invariance principle. *IEEE Trans. Automat. Contr.*, 49(4):470–482, 2004.

[79] J. P. Hespanha and A. S. Morse. Switching between stabilizing controllers. *Automatica*, 38(11):1905 – 1917, 2002.

[80] M. Hilairet, M. Ghanes, O. Béthoux, V. Tanasa, J-P. Barbot, and D. Normand-Cyrot. A passivity-based controller for coordination of converters in a fuel cell system. *Control Eng. Practice*, 21(8):1097 – 1109, 2013.

[81] D. Hill and P. Moylan. The stability of nonlinear dissipative systems. *IEEE Trans. Automat. Contr.*, 21(5):708–711, 1976.

[82] R. M. Hirschorn. Invertibility of nonlinear control systems. *SIAM J. Control Optim.*, 2(2):289–297, 1979.

[83] R. M. Hirschorn and E. Aranda-Bricaire. Global approximate output tracking for nonlinear systems. *IEEE Trans. Automat. Contr.*, 43(10):1389–1398, 1998.

[84] H. Hoang, F. Couenne, C. Jallut, and Y. Le Gorrec. The port Hamiltonian approach to modeling and control of continuos stirred tank reactors. *J. Process Contr.*, 21(10):1449–1458, 2011.

[85] John Hodges. Some matrix equations over a finite field. *Ann. Mat.*, 44:245–250, 1957.

[86] I. M. Horowitz. *Synthesis of feedback systems*. Academic Press, New York, 1963.

[87] J. Imura and A. J. van der Schaft. Characterization of well-posedness of piecewise-linear systems. *IEEE Trans. Automat. Contr.*, 45(9):1600–1619, 2000.

[88] I. V. Ionova and E. A. Carter. Ridge method for finding saddle points on potential energy surfaces. *J. Chem. Phys.*, 98(8):6377–6386, 1993.

[89] A. Isidori. *Nonlinear Control Systems*. Springer, 1995.

[90] D. Jeltsema and J. M. A Scherpen. Multidomain modeling of nonlinear networks and systems. *IEEE Control Syst. Mag.*, 29(4):28–59, 2009.

[91] T. Kailath. *Linear Systems*. Prentice-Hall, 1980.

[92] D. Karagiannis and A. Astolfi. Nonlinear observer design using invariant manifolds and applications. In *Proc. 44th IEEE Conf. Decision Control Eur. Control Conf.*, pages 7775–7780, 2005.

[93] D. Karagiannis, A. Astolfi, R. Ortega, and M. Hilairet. A nonlinear tracking controller for voltage-fed induction motors with uncertain load torque. *IEEE Trans. Contr. Syst. Technol.*, 17(3):608–619, 2009.

[94] W. Kemmetmüller, F. Fuchshumer, and A. Kugi. Nonlinear pressure control of self-supplied variable displacement axial piston pumps. *Control Eng. Practice*, 18(1):84–93, 2010.

[95] H. K. Khalil. *Nonlinear Systems*. Prentice-Hall, 2nd edition, 1996.

[96] S.-J. Kim, S.-Y. Kim, and I.-J. Ha. An efficient identification method for friction in single-dof motion control systems. *IEEE Trans. Contr. Syst. Technol.*, 12(4):555–563, 2004.

[97] T. Kloiber and P. Kotyczka. Estimating and enlarging the domain of attraction in IDA-PBC. In *Proc. 51st Conf. Decision Control*, pages 1852–1858, 2012.

[98] T. Kloiber and P. Kotyczka. Passivity-based design of switching controllers for nonlinear systems. In *Proc. Amer. Control Conf.*, pages 2431–2436, 2012.

[99] T. Kloiber and P. Kotyczka. Passivity-based control of switched nonlinear systems. *at - Automatisierungstechnik*, 60(8):487–498, 2012 (in German).

[100] G. Koch and T. Kloiber. Driving state adaptive control of an active vehicle suspension system. *IEEE Trans. Contr. Syst. Technol.*, 22(1):44–57, 2014.

[101] P. Kotyczka. Passivity based trajectory tracking control with predefined local linear error dynamics. In *Proc. Amer. Control Conf.*, pages 3429–3434, 2010.

[102] P. Kotyczka. *Transparent Dynamics Assignment for Nonlinear State Feedback Control*. PhD thesis, Technische Universität München, 2010. (in German).

[103] P. Kotyczka. Local linear dynamics assignment in IDA-PBC. *Automatica*, 49:1037–1044, 2013.

[104] A. Kugi. *Non-linear Control Based on Physical Models*. Springer, 2001.

[105] P. Lancaster and P. Rosza. On the matrix equation $AX + X^*A^* = C$. *SIAM J. Alg. Disc. Meth.*, 4:432–436, 1983.

[106] J. P. LaSalle. Some extensions Liapunov's second method. *IRE Trans. Circuit Theory*, CT-7:520–527, 1960.

[107] J. Lee. Dynamic gradient approaches to compute the closest unstable equilibrium point for stability region estimate and their computational limitations. *IEEE Trans. Automat. Contr.*, 48(2):321 – 324, feb. 2003.

[108] J. M. Lee. *Introduction to Smooth Manifolds*. Springer, 2006.

[109] T. C. Lee and Z. P. Jiang. Uniform asymptotic stability of nonlinear switched systems with an application to mobile robots. *IEEE Trans. Automat. Contr.*, 53(5):1235–1252, 2008.

[110] J. Lévine. *Analysis and Control of Nonlinear Systems*. Springer, 2009.

[111] Q.-K. Li, J. Zhao, and G. M. Dimirovski. Tracking control for switched time-varying delays systems with stabilizable and unstabilizable subsystems. *Nonlinear Anal. Hybrid Syst*, 3:133–142, 2009.

[112] Z.G. Li, C.Y. Wen, and Y.C. Soh. Stabilization of a class of switched systems via designing switching laws. *IEEE Trans. Automat. Contr.*, 46(4):665–670, 2001.

[113] D. Liberzon. *Switching in Systems and Control*. Birkhäuser, 2003.

[114] D. Liberzon and A. S. Morse. Basic problems in stability and design of switched systems. *IEEE Control Syst. Mag.*, 19(5):59 –70, 1999.

[115] H. Lin and P. J. Antsaklis. Stability and stabilizability of switched linear systems: A survey of recent results. *IEEE Trans. Automat. Contr.*, 54(2):308 –322, 2009.

[116] C.-W. Liu and J.S. Thorp. A novel method to compute the closest unstable equilibrium point for transient stability region estimate in power systems. *IEEE Trans. Circuits Syst. I*, 44(7):630 –635, 1997.

[117] L. Long and J. Zhao. Global stabilization for a class of switched nonlinear feedforward systems. *Syst. Control Lett.*, 60(9):734 – 738, 2011.

[118] R. Ma and J. Zhao. Backstepping design for global stabilization of switched nonlinear systems in lower triangular form under arbitrary switchings. *Automatica*, 46:1819–1823, 2010.

[119] J. L. Mancilla-Aguilar and R. A. García. A converse Lyapunov theorem for nonlinear switched systems. *Syst. Control Lett.*, 41(1):67–71, 2000.

[120] J. L. Mancilla-Aguilar and R. A. García. An extension of LaSalle's invariance principle for switched systems. *Syst. Control Lett.*, 55(5):376–384, 2006.

[121] J. L. Mancilla-Aguilar and R. A. García. Some results on the stabilization of switched systems. *Automatica*, 49(2):441 – 447, 2013.

[122] C. D. Meyer. *Matrix Analysis and Applied Linear Algebra*. SIAM, 2000.

[123] P. Mhaskar, N. H. El-Farra, and P. D. Christofides. Predictive control of switched nonlinear systems with scheduled mode transitions. *IEEE Trans. Automat. Contr.*, 50(11):1670 – 1680, 2005.

[124] W. Mielczarski and A. M. Zajaczkowski. Nonlinear field voltage control of a synchronous generator using feedback linearization. *Automatica*, 30(10):1625–1630, 1994.

[125] V. F. Montagner, Leite V. J. S., R. C. L. F. Oliveira, and P. L. D. Peres. State feedback control of switched linear systems: An LMI approach. *J. Comput. Appl. Math.*, 194:192–206, 2006.

[126] P. J. Mosterman and G. Biswas. Towards procedures for systematically deriving hybrid models of complex systems. In N. Lynch and B. H. Krogh, editors, *Hybrid Systems: Computation and Control*, Lecture Notes in Computer Science, pages 324–337. Springer, 2000.

[127] F. Natterer. *The Mathematics of Computerized Tomography*. SIAM, 2001.

[128] H. Nijmeier and A. J. van der Schaft. *Nonlinear Dynamical Control Systems*. Springer Verlag New York Inc., 1990.

[129] J. Nocedal and S. Wright. *Numerical Optimization*. Springer, 2006.

[130] Y. Orlov. Extended invariance principle for nonautonomous switched systems. *IEEE Trans. Automat. Contr.*, 48(8):1448 – 1452, August 2003.

[131] R. Ortega, M. Galaz, A. Astolfi, Y. Sun, and T. Shen. Transient stabilization of multimachine power systems with nontrivial transfer conductances. *IEEE Trans. Automat. Contr.*, 50(1):60–75, 2005.

[132] R. Ortega and E. Garcia-Canseco. Interconnection and damping assignment passivity-based control: A survey. *Eur. J. Control*, 10(5):432–450, 2004.

[133] R. Ortega, D. Jeltsema, and J. M. A. Scherpen. Power shaping: A new paradigm for stabilization of nonlinear RLC-circuits. *IEEE Trans. Automat. Contr.*, 48:1762–1767, 2003.

[134] R. Ortega, A. Loría, P. J. Nicklasson, and H. Sira-Ramírez. *Passivity-based Control of Euler-Lagrange Systems*. Springer, 1998.

[135] R. Ortega and J. G. Romero. Robust integral control of port-Hamiltonian-systems: The case of non-passive outputs with unmatched disturbances. *Syst. Control Lett.*, 61:11–17, 2012.

[136] R. Ortega and M. Spong. Adaptive motion control of rigid robots: A tutorial. *Automatica*, 25(6):877–888, 1989.

[137] R. Ortega, M.W. Spong, F. Gomez-Estern, and G. Blankenstein. Stabilization of a class of underactuated mechanical systems via interconnection and damping assignment. *IEEE Trans. Automat. Contr.*, 47(8):1218–1233, 2002.

[138] R. Ortega, A. J. van der Schaft, F. Castanos, and A. Astolfi. Control by interconnection and standard passivity-based control of port-Hamiltonian systems. *IEEE Trans. Automat. Contr.*, 53(11):2527–2542, 2008.

[139] R. Ortega, A. J. Van Der Schaft, I. Mareels, and B. Maschke. Putting energy back in control. *IEEE Control Syst. Mag.*, 21(2):18 –33, apr. 2001.

[140] R. Ortega, A. J. van der Schaft, B. Maschke, and G. Escobar. Interconnection and damping assignment passivity-based control of port-controlled Hamiltonian systems. *Automatica*, 38(4):585–596, 2002.

[141] A. Ostrowski and H. Schneider. Some theorems on the inertia of general matrices. *J. Math. Anal. Appl*, 4:72–84, 1962.

[142] M.A. Pai. *Energy function analysis for power system stability*. Kluwer Academic Publishers, 1989.

[143] A. Pavlov, A. Pogromsky, N. Van De Wouw, and H. Nijmeijer. On convergence properties of piecewise affine systems. *Int. J. Control*, 80(8):1233–1247, 2007.

[144] Philippos Peleties and Raymond DeCarlo. Asymptotic stability of m-switched systems using Lyapunov-like functions. In *Proc. Amer. Control Conf.*, pages 1679 –1684, 1991.

[145] W. H. Press, S. A. Teukolsky, W. T. Vetterling, and Flannery B. P. *Numerical Recipes in C: The Art of Scientific Computing*. Cambridge University Press, 2002.

[146] L. Rodrigues and S. Boyd. Piecewise-affine state feedback for piecewise-affine slab systems using convex optimization. *Syst. Control Lett.*, 54(9):835 – 853, 2005.

[147] L. Rodrigues and J. P. How. Observer-based control of piecewise-affine systems. *Int. J. Control*, 76(5):459–477, 2003.

[148] K. Sakurama and T. Sugie. Trajectory tracking control of bimodal piecewise affine systems. *Int. J. Control*, 78(16):1314–1326, 2005.

[149] A. Saleme, B. Tibken, S. A. Warthenpfuhl, and C. Selbach. Estimation of the domain of attraction for non-polynomial systems: A novel method. In *Proc. 18th IFAC World Congress*, pages 10976–10981, 2011.

[150] S. Sastry. *Nonlinear Systems*. Springer, 1999.

[151] R. Sepulchre, M. Janković, and P. V. Kokotović. *Constructive Nonlinear Control*. Springer-Verlag, London, 1997.

[152] T. Shen, R. Ortega, Q. Lu, S. Mei, and Tamura K. Adaptive L_2 disturbance attenuation of Hamiltonian systems with parametric perturbation and application to power systems. *Asian J. Control*, 5:143 – 152, 2003.

[153] A. Shiriaev, A. Robertsson, and R. Johansson. Friction compensation for passive systems based on the LuGre model. In *Proc. 2nd IFAC Workshop Lagrangian Hamiltonian Methods Nonlinear Control*, pages 183 –188, 2003.

[154] R. Shorten and F. Ó Caibre. A proof of global attractivity for a class of switching systems. *IMA J. Math. Control Inform.*, 18:341–353, 2001.

[155] R. Shorten, F. Wirth, O. Mason, and K. Wulff. Stability criteria for switched and hybrid systems. *SIAM Review*, 49(4):545–592, 2007.

[156] R. N. Shorten and K. S. Narendra. Investigating the stability of a class of hybrid system. *Comput. Control Eng.*, 9(2):81 –88, 1998.

[157] S. Solmaz. *Topics in automotive rollover prevention: Robust and adaptive switching strategies for estimation and control.* PhD thesis, Hamilton Institute, National University of Ireland-Maynooth., 2007.

[158] S. Solmaz, R. Shorten, K. Wulff, and F. Ó Caibre. A design methodology for switched discrete time linear systems with applications to automotive roll dynamics control. *Automatica*, 44(9):2358 – 2363, 2008.

[159] E. D. Sontag. Nonlinear regulation: The piecewise linear approach. *IEEE Trans. Automat. Contr.*, 26(2):346–358, 1981.

[160] E. D. Sontag. Remarks on piecewise-linear algebra. *Pacific J. Math*, 98(1):183–201, 1982.

[161] M. Spivak. *A Comprehensive Introduction to Differential Geometry.* Publish or perish, Inc., 1999.

[162] G. W. Stewart. *Afternotes on Numerical Analysis.* SIAM, 1996.

[163] H. J. Sussmann. Subanalytic sets and feedback control. *J. Diff. Equations*, 31:31–52, 1979.

[164] K. Swamy. On Sylvester's criterion for positive-semidefinite matrices. *IEEE Trans. Automat. Contr.*, 18(3):306 – 306, 1973.

[165] P. Tabuada and G. J. Pappas. From nonlinear to Hamiltonian via feedback. *IEEE Trans. Automat. Contr.*, 48(8):1439 – 1442, 2003.

[166] M. Takegaki and A. Arimoto. A new feedback method for dynamic control of manipulators. *ASME J. Dyn. Syst. Meas. Control.*, 103:119–125, 1981.

[167] W. Tan and A. Packard. Stability region analysis using polynomial and composite polynomial Lyapunov functions and sum-of-squares programming. *IEEE Trans. Automat. Contr.*, 53(2):565–571, 2008.

[168] Y. Tian. Equalities and inequalities for inertias of hermitian matrices with applications. *Linear Algebra Appl.*, 433(1):263 – 296, 2010.

[169] Y. Tian and Y. Liu. Extremal ranks of some symmetric matrix expressions with applications. *SIAM J. Matrix Anal. Appl.*, 28(3):890–905, 2006.

[170] B. Tibken and O. Hachicho. Estimation of the domain of attraction for polynomial systems using multidimensional grids. In *Proc. 39th Conf. Decision Control*, pages 3870–3874, 2000.

[171] U. Topcu, A. Packard, and P. Seiler. Local stability analysis using simulations and sum-of-squares programming. *Automatica*, 44:2669–2675, 2008.

[172] M. Valášek and N. Olgat. Efficient eigenvalue assignments for general linear MIMO systems. *Automatica*, 31(11):1605 – 1617, 1995.

[173] N. van de Wouw and A. Pavlov. Tracking and synchronisation for a class of PWA systems. *Automatica*, 44:2909–2915, 2008.

[174] A. J. van der Schaft. *L_2 - Gain and Passivity Techniques in Nonlinear Control*. Springer-Verlag, London, 2 edition, 2000.

[175] A. Venkatraman, R. Ortega, I. Sarras, and A. J. van der Schaft. Speed observation and position feedback stabilization of partially linearizable mechanical systems. *IEEE Trans. Automat. Contr.*, 55(5):1059–1074, 2010.

[176] M. Vidyasagar. *Nonlinear Systems Analysis*. SIAM, 2002.

[177] A. Volf. Transparente Parametrierung der Trajecktorienfolgeregelung mit IDA-PBC. Master's thesis, Technische Universität München, 2009. Supervisor: P. Kotyczka.

[178] Y. Wang, G. Feng, and D. Cheng. Simultaneous stabilization of a set of nonlinear port-controlled Hamiltonian systems. *Automatica*, 43(3):403 – 415, 2007.

[179] J. C. Willems. Dissipative dynamical systems part i: General theory. *Arch. Rational Mech. Anal.*, 45:321 – 350, 1972.

[180] J.-L. Wu. Feedback stabilization for multiinput switched nonlinear systems: Two subsystems case. *IEEE Trans. Automat. Contr.*, 53(4):1037 –1042, 2008.

[181] J.-L. Wu. Stabilizing controllers design for switched nonlinear systems in strict-feedback form. *Automatica*, 45(4):1092 – 1096, 2009.

[182] Z. Wu and F. Ben Amara. Regulation in bimodal systems. *Int. J. Robust Nonlin. Control*, 18(11):1115–1141, 2008.

[183] Z. Wu and F. Ben Amara. Adaptive regulation in bimodal linear systems. *Int. J. Robust Nonlin. Control*, 20(1):59–83, 2010.

[184] Z. Wu and F. Ben Amara. Adaptive regulation in switched bimodal systems: An experimental evaluation. *IEEE Trans. Contr. Syst. Technol.*, 18(4):885–895, 2010.

[185] Z. Wu and F. Ben Amara. Regulator synthesis for bimodal linear systems. *IEEE Trans. Automat. Contr.*, 56(2):390–394, 2011.

[186] K. Wulff, F. Wirth, and R. Shorten. A control design method for a class of switched linear systems. *Automatica*, 45(11):2592 – 2596, 2009.

[187] Z. Xi. Adaptive stabilization of generalized Hamiltonian systems with dissipation and its applications to power systems. *Int. J. Syst. Sci.*, 33:839 – 846, 2002.

[188] X. Xu and P. J. Antsaklis. Optimal control of switched systems based on parameterization of the switching instants. *IEEE Trans. Automat. Contr.*, 49(1):2–16, 2004.

[189] H. Yang, V. Cocquempot, and B. Jiang. On stabilization of switched nonlinear systems with unstable modes. *Syst. Control Lett.*, 58(10-11):703 – 708, 2009.

[190] G. Zames. On the input-output stability of time-varying nonlinear feedback systems. Part i: Conditions derived using concepts of loop gain, conicity, and positivity. *IEEE Trans. Automat. Contr.*, AC-11:228–238, 1966.

[191] M. Zefran, F. Bullo, and M. Stein. A notion of passivity for hybrid systems. In *Proc. 40th Conf. Decision Control*, pages 768 –773, 2001.

[192] J. Zhao and D. J. Hill. On stability, L_2-gain and H_∞ control for switched systems. *Automatica*, 44(5):1220 – 1232, 2008.

[193] J. Zhao and D. J. Hill. Passivity and stability of switched systems: A multiple storage function method. *Syst. Control Lett.*, 57(2):158 – 164, 2008.

[194] Jun Zhao and D.J. Hill. Dissipativity theory for switched systems. *IEEE Trans. Automat. Contr.*, 53(4):941 –953, 2008.